Pediatric Radiology (2019) 49 (Suppl 1):S1–S245
https://doi.org/10.1007/s00247-019-04376-7

The Society for Pediatric Radiology introduced its new logo August 15, 2013. The logo communicates both the warmth of the Society community and the strength of the members' commitment to excellent and thoughtful care of the pediatric patient.

The first official logo for the SPR was designed by Tamar Kahane Oestreich of Cincinnati, Ohio in 1985. Thank you, Mrs. Oestreich.

Founded in 1959
The Society for Pediatric Radiology

62nd Annual Meeting & Postgraduate Course
April 30 – May 4, 2019

Hilton San Francisco Union Square
San Francisco, California, United States

Pediatric Imaging Technologist Program
May 2 – May 3, 2019

Jointly provided by the American College of Radiology

This supplement was not sponsored by outside commercial interests; it was funded entirely by the Society's own resources.

TABLE OF CONTENTS

WELCOME MESSAGE

I am pleased to welcome you to the 62nd meeting of The Society for Pediatric Radiology in San Francisco, California. This year's SPR meeting planning team (THE TEAM) consists of Pinar Karakas-Rothey and Janet Reid (Postgraduate Course Co-directors), Sarah Bixby and Paul Guillerman (Sunrise and Midday Workshop Co-directors), myself (Scientific Program Chair), and the entire SPR administrative staff led by Angela Davis, Jennifer Boylan, Kasey O'Dea, Jennifer Raju and Leah Gearheart. The theme of our meeting is **"Learn from the Past; Innovate for the Future".**

Following the theme and designing the program, Pinar and Janet have constructed two equally practical and creative tracks for you to choose from in the Postgraduate Course. They are, "Tricks of the Trade: Imaging Updates with How to Do, Interpret & Report" and "Emergency Radiology: What Not to Miss & What Surgeon Wants to Know - Case Based". Most importantly, all of the content of the **Postgraduate Course will be recorded** and made available for registrants after the course. Therefore, you should not feel that you will be missing out on some great talks!

Similarly, Sarah and Paul have also put together nine sessions of specific topics for the Sunrise and Midday Workshops during the Scientific Meeting. Some provocative titles of these sessions include, "What's New that Radiation Can Do for You", "Incidentalomas", and "Heartless Vascular Imaging", to name a few. These sessions will be also be recorded so you can relax and enjoy sessions without feeling like you are missing out on others!

For the Annual Meeting program, I want to emphasize **Artificial Intelligence…**or should I have used the term **Machine Learning**, or maybe **Deep Learning**? Do we really know what AI, ML, or DL really mean? To educate all of us, our **Neuhauser Lecturer, Professor Jitendra Malik** of the Department of Electrical Engineering & Computer Science (EECS) at the University of California at Berkeley, will introduce AI to us in his talk "Deep Visual Understanding from Deep Learning". In addition, I have tasked **Shreyas Vasanawala** of Lucile Packard Children's Hospital to organize a special session on the applications of AI in Radiology **"AI: A Real Assistant for Imagers",** to immediately follow the Neuhauser Lecture**.** Artificial Intelligence is here to stay and we should not be afraid of it; let's understand it, and embrace it; let's innovate together with the help of AI and make an even brighter future for pediatric radiology with us directing it! I urge you to attend this year's Neuhauser Lecture by Prof. Malik. I trust that it will be one of many Neuhauser lectures that you will remember for a long time!

This year we will also have a new unopposed session on Thursday early afternoon: **Research & Education Foundation (REF) Symposium** showcasing our grant recipients' works followed immediately by the popular **Jeopardy session** with our dynamic new host**, Richard Heller.** The REF Symposium will start off with a keynote talk by **Miki Lustig** from EECS Department of UC Berkeley. Those of you who are familiar with magnetic resonance will have heard of Miki and his seminal work on Compressed Sensing. Miki is the only MR physicist I have been acquainted with in the past 25 years who is wholly committed to improving pediatric MR. He will show us his vision in his talk: **"Towards Pediatric Body MR without Anesthesia".** It will be an amazing talk and he might even sing[1]!

There will be several keynote speakers in the various scientific oral presentation sessions by experienced clinicians and pediatric radiologists. They all deserve special mentions. Please check the program[2] for additional information. I will just point out a few world-renowned individuals such as cardiovascular surgeon **Shunji Sano,** who invented the Sano Shunt procedure, speaking on stem cell research in patients with single ventricle; pediatric urologist **Larry Baskin** speaking on how imaging helps in clinical urologic cases; pediatric neuroradiologist **Jim Barkovich** speaking about "How Alterations of Normal Brain Development Results in Malformations" as he believes that we need to know how the brain forms before we can understand how it 'malforms'; vascular malformation specialist / pediatric interventional radiologist, **Pat Burrows**, speaking on the novel topic of "Angioarchitecture" and she is supposedly retired! All kidding aside, we are so fortunate that Pat agreed to emerge from retirement to deliver this talk to us. We will also get to hear the story behind the world's first total body PET/CT scanner[3] from its co-inventor, **Ramsey Badawi.** I am also most excited to learn about "The Sacred Work of Caring for Children" from writer, philosopher, and pediatric radiologist, **Richard Gunderman**; how advanced imaging can help in Sports Medicine by pediatric orthopedic surgeon, **Nirav Pandya,** and in gastrointestinal disorder by pediatric gastroenterologist, **Zachary Sellers**; how fetal imaging changes fetal/perinatal surgical decisions by fetal surgeon, **Darrell Cass;** how pediatric neurosurgeon, **Kurtis Auguste**, is utilizing Virtual Reality in his practice; learn about whether we should worry about Gadolinium deposition in children from **Alexander Radbruch**, radiologist from Essen, Germany; and last but not least, how can we can standardize the imaging and interpretation of post-natal bronchopulmonary malformation from pediatric radiologist, **Bev Newman**.

Finally, on Saturday May 4th, we will have six different 1/2-day courses for you to choose from including the **new Cardiac CT Course** incorporating cloud-based case-studies accessible on your laptop. The **Hands-on Ultrasound** session will also be back by popular demand. "May the 4th be with you!!!" "Much to learn we still have!!"

I hope you can also take advantage of the San Francisco Bay Area and come early and/or leave later to enjoy Napa Valley/Wine Country in the north and/or Carmel/Pebble Beach/17-mile Drive in the south. Of course, there is plenty to do in the city itself with the iconic cable cars, Fisherman's Wharf, Pacific Coast, Alcatraz Island, etc.

The TEAM is looking forward to seeing you in San Francisco!

Taylor Chung

Taylor Chung, MD
President & Program Director
The Society for Pediatric Radiology

1. https://www.youtube.com/watch?v=hWQiwIkWRU0
2. https://www.pedrad.org/Portals/5/SPR%202019%20Brochure_3_15_1.pdf
3. https://www.ucdavis.edu/news/human-images-worlds-first-total-body-scanner-unveiled/

SPR 2019 ORGANIZATION

2019 MEETING CURRICULUM COMMITTEE

Taylor Chung, MD (Program Director and Paper Committee Chair)
Sarah D. Bixby, MD (Poster Committee Vice Chair, Workshop Director)
Leah E. Braswell, MD (Interventional Radiology Session)
Lorna P. Browne, MD, FRCR (Cardiac Session)
Kassa Darge, MD, PhD (Hands-On Ultrasound Session)
Monica Epelman, MD (Hands-On Ultrasound Session)
J. Damien Grattan-Smith, MBBS (REF Session)
Laura A. Gruber, MBA, RT(R), RDMS, RVT (Technologist Program Director)
R. Paul Guillerman, MD (Workshop Director)
Christine Harris, RT (MR) MRSO (Technologist Program Director)
Richard E. Heller, III, MD, MBA (Jeopardy Session)
Thierry A. G. M. Huisman, MD (Neuroradiology Session)
S. Pinar Karakas, MD (Postgraduate Course Director)
Prakash M. Masand, MD (Cardiac Session)
Sarah S. Milla, MD, FAAP (Poster Committee Chair)
Helen R. Nadel, MD, FRCPC (Nuclear/Oncology Session)
Manish N. Patel, DO (Interventional Radiology Session)
Janet R. Reid, MD, FRCPC (Postgraduate Course Director and Education Session)
Cynthia K. Rigsby, MD, FACR (Cardiac Session)
Victor J. Seghers, MD, PhD (Nuclear/Oncology Session)
Dennis W. W. Shaw, MD (Neuroradiology Session)
Mahesh M. Thapa, MD (Education Session)
Shreyas S. Vasanawala, MD, PhD (AI Session)

ABSTRACT REVIEW COMMITTEE – PAPERS

Taylor Chung, MD, Chair
Christopher I. Cassady, MD, FAAP, Vice Chair
Dianna M. E. Bardo, MD
Sarah D. Bixby, MD
David A. Bloom, MD, FACR
Heather Bray, MD
Alan Brody, MD
Lorna P. Browne, MD, FRCR
Michael J. Callahan, MD
Nancy A. Chauvin, MD
Govind Chavhan, MD
Kassa Darge, MD, PhD
Jonathan R. Dillman, MD, MSc
James S. Donaldson, MD, FACR
Mark R. Ferguson, MD
Donald P. Frush, MD, FACR
Michael S. Gee, MD, PhD
J. Damien Grattan-Smith, MBBS
R. Paul Guillerman, MD
Roger K. Harned, MD, FACR
Mark J. Hogan, MD
Bamidele Kammen, MD
S. Pinar Karakas, MD
Beth M. Kline-Fath, MD
Rajesh Krishnamurthy, MD
Tal Laor, MD
John D. MacKenzie, MD
M. Beth McCarville, MD
Beverly Newman, MD, FACR
Susan Palasis, MD
John M. Racadio, MD
Janet R. Reid, MD, FRCPC
Cynthia K. Rigsby, MD, FACR
Caroline Robson, MD
Victor J. Seghers, MD, PhD
Dennis W. W. Shaw, MD
Ethan A. Smith, MD
Mahesh Thapa, MD
Andrew T. Trout, MD
Teresa Victoria, MD, PhD
Stephan D. Voss, MD, PhD
Jason P. Weinman, MD

ABSTRACT REVIEW COMMITTEE – POSTERS

Sarah S. Milla, MD, FAAP, Chair
Sarah D. Bixby, MD, Vice Chair
Anjum N. Bandarkar, MD
Madhan Bosemani, MD
Kiery A. Braithwaite, MD
Micheal A. Breen, MD
Maria A. Calvo-Garcia, MD
Gulraiz A. Chaudry, MBChB, MRCP, FRCR
Kassa Darge, MD, PhD
Nilesh Desai, MD
Paula Dickson, MD
Steven Don, MD
Eric Eutsler, MD
Judith A. Gadde, DO, MBA
Anne Gill, MD
Leslie E. Hirsig, MD
Thierry A.G.M. Huisman, MD
J. Herman Kan, MD

Neha S. Kwatra, MD
Maria F. Ladino-Torres, MD
Shailee V. Lala, MD
Jonathan M. Loewen, MD
Adeka D. McIntosh, MD
Craig S. Mitchell, DO, MA
Jonathan G. Murnick, MD
Helen R. Nadel, MD, FRCPC
Srikala Narayanan, MD
Hansel J. Otero, MD
Daniel J. Podberesky, MD
Sanjay P. Prabhu, MD
Janet R. Reid, MD, FRCPC
Susan E. Sharp, MD
Manrita K. Sidhu, MD
Bruno P. Soares, MD
Aylin Tekes-Brady, MD
Paul G. Thacker, MD, MHA
Stephanie B. Theut, MD
Alexander J. Towbin, MD
Jason Tsai, MD
Jennifer Vaughn, MD
Nghia (Jack) Vo, MD
Ewa M. Wasilewska, MD
Arash R. Zandieh, MD

IMAGING TECHNOLOGIST PROGRAM & ABSTRACT COMMITTEE

Christine Harris, RT (MR) MRSO (Co-Chair)
Laura A. Gruber, MBA, RT(R), RDMS, RVT (Co-Chair)
Stuart Brice
Brian Fox, MBA
Charles R. Fritz, RT, MBA
Lynne Hamer, MEd., RT
Todd Lehkamp
M. Craig Morriss, MD
Stephen F. Simoneaux, MD, FACR, Advisor
R. Daniel Smock, BHS RT(R)(MR)(CT), MRSO (MRSC)

CASE OF THE DAY ORGANIZERS

Neil D. Johnson, MBBS
Christopher Sternal-Johnson

MEETING INFORMATION TECHNOLOGY

Safwan S. Halabi, MD, Meeting IT Co-Director
Alexander J. Towbin, MD, Meeting IT Co-Director

CONTINUING MEDICAL EDUCATION

ACCREDITATION STATEMENT:

This activity has been planned and implemented in accordance with the accreditation requirements and policies of the Accreditation Council for Continuing Medical Education through the joint sponsorship of The American College of Radiology and the Society for Pediatric Radiology. The American College of Radiology is accredited by the ACCME to provide continuing medical education for physicians.

CREDIT DESIGNATION STATEMENT:

The American College of Radiology designates this live activity for a maximum of 37.75 *AMA PRA Category 1 Credits* ™. Physicians should claim only the credit commensurate with the extent of their participation.

TECHNOLOGIST:

The American College of Radiology is approved by the American Registry of Radiologic Technologists (ARRT) as a Recognized Continuing Education Evaluation Mechanism (RCEEM) to sponsor and/or review CME programs for Radiologic Technologists and Radiation Therapists. The American College of Radiology designates this educational activity as meeting the criteria for up to 37.75 *Category A* credit hours.

MAINTENANCE OF CERTIFICATION

Qualified on January 29, 2019, select sessions from this activity meet the American Board of Radiology criteria for a self-assessment (SAM) activity and is designated for up to 17.75 SAM credits toward the ABR Maintenance of Certification Program.

LEARNING OBJECTIVES

The 2019 62nd Annual Meeting & Postgraduate Course will provide pediatric and general radiologists with an opportunity to do the following:

1. Summarize the most current information on state-of-the-art pediatric imaging and the practice of pediatric radiology.
2. Describe and apply new technologies and imaging findings for pediatric imaging.
3. Discuss trends in research and education concerning the care and imaging of pediatric patients.
4. Identify common challenges facing pediatric radiologists, and possible solutions.
5. Describe and apply basic principles for implementing quality and safety programs in pediatric radiology.
6. Evaluate and apply means of managing radiation exposure and the need for sedation/anesthesia during diagnostic imaging and image-guided therapy.

At the conclusion of the experience, participants should have an improved understanding of the technologies discussed, increased awareness of the benefits and costs of diagnostic imaging in children and of ways to minimize risks, and an improved general knowledge of pediatric radiology.

DISCLOSURE STATEMENT

In compliance with ACCME requirements and guidelines, the ACR has developed a policy for review and disclosure of potential conflicts of interest, and a method of resolution if a conflict does exist. The ACR maintains a tradition of scientific integrity and objectivity in its educational activities. In order to preserve this integrity and objectivity, all individuals participating as planners, presenters, moderators and evaluators in an ACR educational activity or an activity jointly sponsored by the ACR must appropriately disclose any financial relationship with a commercial organization that may have an interest in the content of the educational activity.

The following planners, presenters, staff and evaluators have disclosed that neither they nor their spouse/partner has any financial interests, arrangements or affiliation in the context of this activity:

PROGRAM PLANNERS/FACULTY

Adina L. Alazraki, MD
Ahmad I. Alomari, MD
Alan Daneman, MD
Alan E. Schlesinger, MD
Alexander Radbruch, MD
Allison S. Aguado, MD
Ami Gokli, MD
Amie S. Robinson, BSRT, (R)(MR) CCRP
Amy R. Mehollin-Ray, MD
Andrea Rossi, MD
Andrew S. Phelps, MD
Andrew Schapiro, MD
Andy Tsai, MD, PhD
Angela Quintello
Anjum N. Bandarkar, MD
Anne Gill, MD
Aparna Joshi, MD
Apeksha Chaturvedi, MBBS, MD
Arun Rangaswami, MD
Ashok Panigrahy, MD
Asim F. Choudhri, MD
Aylin Tekes, MD
Bamidele F. Kammen, MD
Benjamin Thompson, DO
Beverley Newman, MD, FACR
Boaz Karmazyn, MD
Brandi Kozak, RDMS
Brandon P. Brown, MD, MA, FAAP
Brandy Bales, RPA, RT(R)(M)
Brian D. Coley, MD, FACR, FAIUM
Brooke S. Lampl, DO
Bruce R. Parker, MD, FACR
Bruno P. Soares, MD
Camilo Jaimes, MD
Carlos F. Ugas Charcape, MD
Carol E. Barnewolt, MD
Charles Stanley
Christine Harris, RT (MR) MRSO
Christina Sammet, PhD
Christopher I. Cassady, MD, FAAP
Christopher Lam, MD
Christopher Newton, MD
Cicero T. Silva, MD
Cory M. Pfeifer, MD, MS, FAAP
Cynthia K. Rigsby, MD, FACR
D. Gregory Bates, MD
J. Damien Grattan-Smith, MBBS
Darrell L. Cass, MD
David B. Larson, MD
David Saul, MD
Delma Y. Jarrett, MD
Dennis W. W. Shaw, MD

Diego Jaramillo, MD, MPH
Donald P. Frush, MD, FACR
Dorothy I. Bulas, MD, FACR
Douglas C. Rivard, DO
Edward R. Oliver, MD, PhD
Elad Nevo, M.S., RT(MR)(N)(CT), CNMT
Elizabeth Silvestro, MSc
Ellen M. Chung, MD
Ellen S. Park, MD, MS
Emily S. Orscheln, MD
Eric Hoggard, MD
Erica Gates
Erica L. Riedesel, MD
Evan J. Zucker, MD
Francisco Perez, MD, PhD
Gabe Linke, BSRT (R)(MR)
Gary L. Hedlund, DO
Gary R. Schooler, MD
Geetika Khanna, MD, MS
George A. Taylor, MD, FACR
George S. Bisset, MD, FACR
Georgina Prevett, MS, RT(R)(N) (CT)(MR), CNMT
Giridhar Shivaram, MD
Giulio Zuccoli, MD
HaiThuy N. Nguyen, MD
Harriet J. Paltiel, MD
Heather Bray, MD
Heike E. Daldrup-Link, MD, PhD
Helen R. Nadel, MD, FRCPC
Hisham Dahmoush, MBBCh
Houchun Harry Hu, PhD
Hyun Woo Goo, MD, PhD
Jaishree Naidoo, FCRad
James E. Crowe, MD
Jane C. Cook, DO
Janet Mar, RDMS
Janet R. Reid, MD, FRCPC
Jason N. Wright, MD
Jeanne "Mei-Mei" S. Chow, MD
Jeannie K. Kwon, MD
Jennifer E. Lim-Dunham, MD, FACR
Jennifer Nicholas, MD
Jerry R. Dwek, MD
Jie C. Nguyen, MD, MS
Jitendre Malik, PhD
John D. Mackenzie, MD
Jonathan G. Murnick, MD, PhD
Joseph Cheng, MD
Joseph MacLean, CNMT
Joshua Nickerson, MD
Judith A. Gadde, DO, MBA
Kara Groom, RDMS
Kara Meister
Karen Lyons, MB, BCh, BAO
Karun Sharma, MD
Kassa Darge, MD, PhD
Katie Busher
Keith J. Strauss, MSc, FACR
Kevin Shoaf, ARRT RT
Kieran J. Frawley, MBBS
Kirsten Ecklund, MD
Korgun Koral, MD
Kristen Yeom, MD
Kurtis Auguste, MD
Lacey Gander, RDMS
Ladonna J. Malone, MD
Lamont Hill, RT, ARDMS
Laura Gruber, MBA, RT(R), RDMS, RVT
Laura L. Hayes, MD
Laura Poznick, RDMS
Laura Z. Fenton, MD, FACR
Lauren W. Averill, MD
Leah E. Braswell, MD
Lindsay Griffen, MD
Lisa J. States, MD
Lorna P. Browne, MD, FRCR
Luis F. Goncalves, MD
Lydia Bajno, MD
Lynn A. Fordham, MD, FACR
M. Beth McCarville, MD
M. Ines Boechat, MD, FACR
Maggie Zhong, MD
Mahesh M. Thapa, MD
Manish Patel, DO
Manohar Shroff, MD, FRCPC
Maria G. Smith, BS, RDMS, RVT
Mariana L. Meyers, MD
Marielle Fortier, MD
Mark Goce, RDMS
Mark R. Ferguson, MD
Marta Hernanz-Schulman, MD, FACR
Martha M. Munden, MD
Maryam Ghadimi Mahani, MD
Matthew A. Zapala, MD, PhD
Matthew R. Hammer, MD
Matthias Wagner, MD
Merima Karastanovic, MS, RT(R)(MR)
Merlye Eklund, MD
Michael J. Callahan, MD
Michael M. Moore, MD
Michael R. Acord, MD
Michael S. Gee, MD, PhD

Micheal A. Breen, MBBCh BAO
Misun Hwang, MD
Molly E. Dempsey, MD
Monica Atalabi, MD
Monica Epelman, MD
Nadia F. Mahmood, MD
Nalin Gupta, MD
Neha S. Kwatra, MD
Nghia (Jack) Vo, MD
Nicholas Rubert, PhD
Nicholas V. Stence, MD
Nikki Butler, BMSc, RT(R)(QM)
Olivier Gavaert, PhD
Oscar M. Navarro, MD
Pamela M. Ketwaroo, MD
Parker Stanley
Patricia E. Burrows, MD
Patricia T. Acharya, MD
Patrick Waren, MD
Paul G. Thacker, MD, MHA
Pek-Lan Khong, MBBS, FRCR
R. Paul Guillerman, MD
Rajesh Krishnamurthy, MD
Rama S. Ayyala, MD
Raymond W. Sze, MD
Ricardi Faingold, MD
Richard B. Gunderman, MD, PhD, FACR
Richard E. Heller III, MD, MBA
Richard Southard, MD
Robert C. Orth, MD, PhD
Ronald A. Cohen, MD
Roxanne Munyon
S. Pinar Karakas, MD
Safwan Halabi, MD
Sarah D. Bixby, MD
Sarah Desoky, MD
Sarah J. Menashe, MD
Sarah S. Milla, MD, FAAP
Scott R. Dorfman, MD
Sherwin S. Chan, MD
Shireen Hayatghaibi, MA, MPH
Shreyas Vasanwala, MD, PhD
Shunji Sano, MD, PhD
Sjirk J. Westra, MD, FACR
Skorn Ponrartana, MD
Spencer Behr, MD, PhD
Stephan D. Voss, MD, PhD
Stephanie Suller, RDMS
Steven Don, MD
Sudha A. Anupindi, MD
Sumit Pruthi, MBBS, DNB
Summer L. Kaplan, MD, MS
Susan E. Sharp, MD
Susan Palasis, MD
Talissa Altes, MD
Tara Cielma
Teresa Victoria, MD, PhD
Theirry A. G. M. Huisman, MD
Timothy N. Booth, MD
Timothy R. Singewald, MD
Todd Abruzzo, MD
Trista Raymer Maule, RT, (R)(CT)(MR)
Trudy Morgan, RDMS
Unni K. Udayasankar, MD
Victor J. Seghers, MD, PhD

The planners and faculty listed below have disclosed the following relevant financial relationships. Potential conflicts have been resolved.

PROGRAM PLANNERS/FACULTY WITH DISCLOSURES

A. James Barkovich, MD	NIH – Research Grant
A. Carl Merrow, MD	Elsevier - Consultant, Honoraria, Royalties
Akshay Chaudhari, PhD	Brain Key - Advisory Board, Subtle Medical - Deep Learning Research Scientist, LVIS Corporation - Equity, Subtle Medical - Deep Learning Research Scientist, Skope MR Technologies - ex Technology and Application Specialist
Alan S. Brody, MD	Vertex Pharmaceuticals, Consultant
Alexander J. Towbin, MD	IBM Watson Health; Applied Radiology - Consultant, Honoraria, Siemens; Guerbet; Cystic Fibrosis Foundation - Research Grants
Andrew T. Trout, MD	Guerbet - Consultant, Honoraria, iiCME - Speakers Bureau, Elsevier, Wolters Kluwer - Royalties, JRCNMT - Officer, Siemens, Canon - Research Grants
Arthur B. Meyers, MD	Amirsys, Elsevier – Royalties
Birgit B. Ertl-Wagner, MD, MHBA	Siemens - Spouse Stock, Springer - Royalty
Dianna M.E. Bardo, MD	Koninklijke Philips, NV - Consultant, Honoraria, Speakers Bureau
David M. Biko, MD	Wolters Kluwer - Royalty

Erika Rubesova, MD	Clementia Pharmaceuticals - Consultant
Ethan A. Smith, MD	Elsevier – Royalties
Govind B. Chavhan, MD	Bayer Inc. - Consultant, Honoraria
Henry J. Baskin, MD	UpToDate - Consultant
Jesse Courtier, MD	HoloSurg3D, Inc – Equity
Jonathan R. Dillman, MD, MSc	Canon Medical Systems, Siemens Medical Solutions USA, Bracco Diagnostics - Research Grants
Juan Santos, PhD	HeartVista, Inc. - Equity, Officer
Judy H. Squires, MD	Elsevier - Royalty
Laurence C. Baskin, MD	UpToDate - Consultant, NIH - Research Grants
Mai-Lan Ho, MD	RSNA Scholar Grant, SPR Pilot Award, ASHNR Hanafee Grant - Research Grants
Matthew P. Lungren, MD	Nines Inc - Consultant, Honoraria
Michael Aquino, MD	Elsevier - Royalty
Michael "Miki" Lustig, PhD	InkSpace Imaging - Equity Interest/Stock Options, GE Healthcare - Research Grants
Nirav Pandya, MD	Orthopediatrics - Consultant, Honoraria
Prakash M. Masand, MD	Canon Medical Systems, Phillips Medical Systems - Consultant; Canon Medical Systems, Speakers Bureau; Amirsys - Royalty
Ramsey D. Badawi, MD, PhD	United Imaging Healthcare - Research Grant
Ramesh Iyer, MD	Wolters Kluwer - Royalty
Ricardo Restrepo, MD	Elsevier - Royalty
Sandy Napel, PhD	Fovia Inc., Carestream Inc, and Radlogics Inc. - Consultant, Honoraria
Susan J. Back, MD	Siemens - Research Grant, Philips - Research Grant, Bracco - Education Grant
Steven J. Kraus, MD, MS	Elsevier - Royalty
Teresa Chapman, MD, MA	Wolters Kluwer - Royalty
Zachary M. Sellers, MD	Cystic Fibrosis Foundation, NIH - Research Grants

ACKNOWLEDGEMENTS *– As of March 14, 2019*

The Society for Pediatric Radiology gratefully acknowledges the support of the of the following companies in presenting the 62nd Annual Meeting & Postgraduate Course.

PLATINUM LEVEL SUPPORTER
Canon Medical Systems USA, Inc.
GE Healthcare
Philips Healthcare
Siemens Healthineers

SILVER LEVEL SUPPORTER

United Imaging Healthcare

BRONZE LEVEL SUPPORTER

Bayer HealthCare LLC

EXHIBITORS

Advocate Children's Hospital
Agfa Radiology Solutions
Arterys
Bracco Diagnostics Inc
Children's Hospital of Philadelphia
ChiRhoClin
Circle Cardiovascular Imaging
Elsevier, Inc.
FUJIFILM Medical Systems USA, Inc.
Guerbet LLC
Illuminate
KindVR
KinetiCor, Inc
LocumTenens.com
MEDNAX Radiology Solutions
Mindray North America
Samsung
ScImage
SealCath, LLC
SpellBound
St. Jude Children's Research Hospital
SuperSonic Imagine
Wolters Kluwer

SPR GENERAL INFORMATION

MISSION STATEMENT

The Society for Pediatric Radiology is dedicated to fostering excellence in pediatric health care through imaging and image-guided care.

DIVERSITY & INCLUSION STATEMENT

The Society for Pediatric Radiology actively promotes diversity and inclusion at all levels of training, practice and leadership for the benefit of our patients, our profession and for the Society as a whole.

SPR OFFICERS, DIRECTORS AND COMMITTEES 2018–2019

BOARD OF DIRECTORS

Peter J. Strouse, MD, FACR, Chair, Board of Directors and Editor
Taylor Chung, MD, President
Christopher I. Cassady, MD, FAAP, President-Elect
J. Damien Grattan-Smith, MBBS, 1st Vice President and President, SPR Research and Education Foundation
Cynthia K. Rigsby, MD, FACR, 2nd Vice President
Michael J. Callahan, MD, Secretary
Laura Z. Fenton, MD, FACR, Secretary-Elect and Director
Stephen F. Simoneaux, MD, FACR, Treasurer
Jonathan R. Dillman, MD, MSc, Director
Josée Dubois, MD, Director
Beth M. Kline-Fath, MD, Director
Susan Palasis, MD, Director
Teresa Victoria, MD, PhD, Director
James. S. Donaldson, MD, FACR, Past President
Diego Jaramillo, MD, MPH, Past President
Brian D. Coley, MD, FACR, FAIUM, Past President
Richard A. Barth, MD, FACR, FAAP, ACR Commission on Pediatric Radiology Liaison
Donald P. Frush, MD, FACR, Image Gently Liaison
Benjamin H. Taragin, MD, Web Editor
Sarah S. Milla, MD, FAAP, AAP Liaison
Molly E. Dempsey, MD, SCORCH President
M. Ines Boechat, MD, FACR, WFPI Liaison

ABDOMINAL IMAGING COMMITTEE

Jonathan R. Dillman, MD, MSc, Chair
Sudha A. Anupindi, MD, Vice Chair
Govind B. Chavhan, MD
Ellen M. Chung, MD
Meryle Eklund, MD
Hansel J. Otero, MD
Daniel J. Podberesky, MD
Brian S. Pugmire, MD
Anil G. Rao, DMRD, DNB
Gary R. Schooler, MD
Ethan A. Smith, MD
Andrew T. Trout, MD

BYLAWS COMMITTEE

Peter J. Strouse, MD, FACR, Chair
Taylor Chung, MD
Michael J. Callahan, MD
Laura Z. Fenton, MD, FACR
Susan Palasis, MD

CARDIAC IMAGING COMMITTEE

Lorna P. Browne, MD, FRCR, Chair
Maryam Ghadimi Mahani, MD, Vice Chair
David M. Biko, MD
Joo Y. Cho, MD
Joseph Davis, MD
Mark R. Ferguson, MD
Jamie Frost, DO
Preetam Gongidi, MD
Brian Handly, MD
Eric Hoggard, MD
Siddharth P. Jadhav, MD
Christopher Keup, MD
Ramkumar Krishnamurthy, PhD
Christopher Lam, MD
Karen Lyons, MB, BCh, BAO
Ladonna J. Malone, MD
Prakash M. Masand, MD
Erin Opfer, MD
Cynthia K. Rigsby, MD, FACR, Advisory
Mike Seed, MBBS
Laureen M. Sena, MD, Advisory
Ting Y. Tao, MD, PhD
Smyrna Tuburan, MD

CHILD ABUSE COMMITTEE

Sabah Servaes, MD, Chair
Arabinda K. Choudhary, MBBS, MRCP, FRCR, Vice Chair
David A. Bloom, MD
Karen Blumberg, MD, FACR
Tejaswini K. Deshmukh, MD
Michael F. Fadell, II, MD
Laura L. Hayes, MD
Gary L. Hedlund, DO
Muhammad N. Khan, MD
Jeannie K. Kwon, MD
Shailee V. Lala, MD
Megan B. Marine, MD
Bradley A. Maxfield, MD
Kenneth L. Mendelson, MD
David M. Mirsky, MD
Joelle Moreno, JD
Michael A. Murati, MD

Sandeep Narang, MD
Susan Palasis, MD
Ashishkumar K. Parikh, MD
Jeannette M. Perez-Rossello, MD, FACR
Cory Pfeifer, MD, FAAP
Veronica J. Rooks, MD
Daniel M. Schwartz, MD
Dana S. Schwartz, MD
V. Michelle Silvera, MD
Heba S. Takrouri, MBBS
Chido Vera, MD
Gregory A. Vorona, MD
Matthew A. Zapala, MD, PhD
Stephen D. Brown, MD, Advisory
Richard I. Markowitz, MD, FACR, Advisory
Peter J. Strouse, MD, FACR, Advisory

CONTRAST-ENHANCED ULTRASOUND COMMITTEE

M. Beth McCarville, MD, Chair
Susan J. Back, MD, Vice Chair
Patricia T. Acharya, MD
Carol E. Barnewolt, MD
Joo Y. Cho, MD
Kassa Darge, MD, PhD, Advisory
Reza Daugherty, MD
Lynn A. Fordham, MD, FACR
Ami Gokli, MD
Preetam Gongidi, DO
Misun Hwang, MD
Jeannie K. Kwon, MD
Annie Lim, DO
Martha M. Munden, MD
Harriet J. Paltiel, MD
Judy H. Squires, MD
Abhay S. Srinivasan, MD

CT COMMITTEE

John D. MacKenzie, MD, Chair
Prakash M. Masand, MD, Vice Chair
Sheila C. Berlin, MD, Advisory
Tushar Chandra, MBBS, MD
Apeksha Chaturvedi, MD
Joo Y. Cho, MD
Kara G. Gill, MD
Aparna Joshi, MD
Grace S. Phillips, MD
Karuna V. Shekdar, MD
Richard Southard, MD
Jason P. Weinman, MD
Sjirk J. Westra, MD

DIVERSITY AND INCLUSION COMMITTEE

Ashok Panigrahy, MD, Co-Chair
Stephanie E. Spottswood, MD, MSPH, Co-Chair
Adebunmi Adeyiga, MD
Aparna Annam, DO
Christopher I. Cassady, MD, FAAP, President-Elect
Taylor Chung, MD, President
Gregory L. Compton, MBBS
Sarah Desoky, MD
Marta Hernanz-Schulman, MD, FACR
Katrina Hughes, MD
Melanie B. Levin, MD
Maria-Gisela Mercado-Deane, MD
Cindy R. Miller, MD
Kristi Bogan Oatis, MD
Tina Young Poussaint, MD, FACR
Sheena Saleem, MD
Amit S. Sura, MD, MBA
Philip Teitelbaum, MD
Adrienne F. Thompson, MD
Chido Vera, MD
Valerie L. Ward, MD, MPH
Lisa Wheelock, MD
Ammie M. White, MD
Sonia Wright, MD

EDUCATION-CURRICULUM COMMITTEE

Christopher I. Cassady, MD, FAAP, Chair
Sarah S. Milla, MD, FAAP, Vice Chair
Michael J. Callahan, MD
Monica Epelman, MD
Laura Z. Fenton, MD
Liliane H. Gibbs, MD
J. Damien Grattan-Smith, MBBS
Safwan S. Halabi, MD
Daniel J. Podberesky, MD
Sanjay P. Prabhu, MBBS FRCR
Janet R. Reid, MD, FRCPC
Michele Retrouvey, MD
Cynthia K. Rigsby, MD, FACR
Peter J. Strouse, MD, FACR
Benjamin H. Taragin, MD
Mahesh M. Thapa, MD
Smyrna Tuburan, MD
Laura J. Varich, MD
Kevin Wong, DO

EMERGENCY RADIOLOGY & TRAUMA COMMITTEE

Susan D. John, MD, FACR, Chair
Michael R Aquino, MD, Vice Chair
Sandra M. Allbery, MD
Joseph T. Davis, MD
Tejaswini K. Deshmukh, MD
David Dinan, MD
Michael P. George, MD
Ashwin Hegde, MD, FRCPC
Jeanne G. Hill, MD
Victor M. Ho-Fung, MD
Tara L. Holm, MD
James D. Ingram, MD, FACR
Paul J. Iskander, MD
Jennifer H. Johnston, MD
Summer L. Kaplan, MD, MS
George C. Koberlein, MD
Jonathan M. Loewen, MD
Michael A. Murati, MD
Michael P. Nasser, MD
Jennifer Veltkamp, MD

FELLOWSHIP PROGRAM DIRECTOR COMMITTEE

Paula N. Dickson, MD, Co-Chair
Sabah Servaes, MD, Co-Chair

FETAL IMAGING COMMITTEE

Teresa Victoria, MD, PhD, Chair
Mariana L. Meyers, MD, Vice Chair
Rama S. Ayyala, MD
Richard A. Barth, MD, FACR, FAAP
Micheal A. Breen, MBBCh
Brandon P. Brown, MD, FAAP
Dorothy I. Bulas, MD, FACR, FAAP
Christopher I. Cassady, MD, FAAP
Gabrielle C. Colleran, MD
Patricia Cornejo, MD
Nilesh Desai, MD
Ryne A. Didier, MD
Michael S. Gee, MD, PhD
Luis Goncalves, MD
Carolina V. Guimaraes, MD
Camilo Jaimes Cobos, MD
Pamela M. Ketwaroo, MD
Paggie Kim, MD
Beth M. Kline-Fath, MD
Amy B. Kolbe, MD
Jennifer Kucera, MD
Leann E. Linam, MD
David M. Mirsky, MD
Usha D. Nagaraj, MD
Edward R. Oliver, MD
Erika Rubesova, MD

FINANCE COMMITTEE

Avrum N. Pollock, MD, FRCPC, Chair
Narendra S. Shet, MD
Amit S. Sura, MD, MBA
Neil Vachhani, MD
Shannon G. Farmakis, MD
Stephen F. Simoneaux, MD, FACR
Christopher I. Cassady, MD, FAAP
J. Damien Grattan-Smith, MBBS
Cynthia K. Rigsby, MD, FACR

HISTORY COMMITTEE

Alan E. Schlesinger, MD, Historian

HONORS COMMITTEE

Brian D. Coley, MD, FACR, FAIUM, Chair
James S. Donaldson, MD, FACR
Diego Jaramillo, MD, MPH

INFORMATICS COMMITTEE

Safwan S. Halabi, MD, Chair
Jeannie K. Kwon, MD, Vice Chair
Steven L. Blumer, MD
Brian D. Handly, MD
Mai-Lan Ho, MD
Neil U. Lall, MD
Annie Lim, DO
Morgan McBee, MD
Saad A. Ranginwala, MD
Marla BK Sammer, MD
Uygar Teomete, MD
Alexander J. Towbin, MD, Advisory
Esben S. Vogelius, MD
Evan J. Zucker, MD

INTERVENTIONAL COMMITTEE

Manish N. Patel, DO, Chair
Leah E. Braswell, MD, Vice Chair
Raja Shaikh, MD
Joseph T. Davis, MD
Matthew P. Lungren, MD
Anne Gill, MD
Radu Nicolaescu, MD
Abhay S. Srinivasan, MD
Timothy R. Singewald, MD
Ranjith Vellody, MD
Fabiola C. Weber, MD

MR COMMITTEE

Michael S. Gee, MD, PhD, Chair
Govind B. Chavhan, MD, Vice Chair
Sudha A. Anupindi, MD
Sherwin S. Chan, MD
Tushar Chandra, MBBS, MD
Apeksha Chaturvedi, MD
Taylor Chung, MD, Advisory
Jesse Courtier, MD
Jorge H. Davila-Acosta, MD
Shahnaz Ghahremani Koureh, MD
Mai-Lan Ho, MD
Camilo Jaimes Cobos, MD
Hee-Kyung Kim, MD
Amy B. Kolbe, MD
Archana Malik, MD
Michael M. Moore, MD
Hansel J. Otero, MD
Skorn Ponrartana, MD
Anil G. Rao, DMRD, DNB
Gary R. Schooler, MD
Mitchell L. Simon, MD
Susan Sotardi, MD
Gayathri Sreedher, MD
Unni K. Udayasankar, MD
Shreyas S. Vasanawala, MD, PhD, Advisory
Teresa Victoria, MD, PhD
Esben Vogelius, MD

MUSCULOSKELETAL IMAGING COMMITTEE

Jerry R. Dwek, MD, Chair
Arthur B. Meyers, MD, Vice Chair
Sebastien Benali, MD
Sarah D. Bixby, MD
Tushar Chandra, MBBS, MD
Nancy A. Chauvin, MD
Andrew J. Degnan, MD
Kirsten Ecklund, MD
Eric Eutsler, MD
R. Paul Guillerman, MD
Matthew R. Hammer, MD
Siddharth P. Jadhav, MD
Shawn E. Kamps, MD
Hee-Kyung Kim, MD
Archana Malik, MD
Tracey R. Mehlman, MD
Jie C. Nguyen, MD, MS
Allison K. Person, MD
Jonathan Samet, MD
Amisha J. Shah, MD
Mahesh M. Thapa, MD
Andy Tsai, MD
Jennifer Veltkamp, MD

NEONATAL IMAGING COMMITTEE

Rama S. Ayyala, MD, Chair
Emily M. Janitz, DO, Vice Chair
Krista L. Birkemeier, MD
Judy A. Estroff, MD
Kara G. Gill, MD
Mai-Lan Ho, MD
Tara L. Holm, MD
Misun Hwang, MD
Shailee V. Lala, MD
Brooke S. Lampl, DO
David W. McDonald, MD
Richard Parad, MD
Pallavi Sagar, MD
Cassandra M. Sams, MD
Mitchell L. Simon, MD
Jennifer L. Williams, MD

NEURORADIOLOGY COMMITTEE

Dennis W. W. Shaw, MD, Chair
Thierry A. G. M. Huisman, MD, Vice Chair
Mariaem M. Andres, MD
Ravi Bhargava, MD
Timothy N. Booth, MD
Shankar Srinivas Ganapathy, MD
Carolina V. Guimaraes, MD
Mai-Lan Ho, MD
Susan Palasis, MD
Sumit Pruthi, MD
Gaurav Saigal, MD
Rupa Radhakrishnan, MBBS
Raghu H. Ramakrishnaiah, MD
Caroline D. Robson, MBChB
Nancy K. Rollins, MD
Matthew T. Whitehead, MD
Jason N. Wright, MD
Charles R. Fitz, MD, Advisory

NOMINATING COMMITTEE

Peter J. Strouse, MD, FACR, Chair
Judy A. Estroff, MD
Richard E. Heller, III, MD, MBA
Tara L. Holm, MD
Sabah Servaes, MD
Raymond W. Sze, MD
Stephan D. Voss, MD, PhD

NUCLEAR MEDICINE COMMITTEE

Helen R. Nadel, MD, FRCPC, Chair
Victor J. Seghers, MD, PhD, Vice Chair
Adina L. Alazraki, MD, FAAP
Deepa R. Biyyam, MB BS
Sachin Kumbhar, MD
Neha S. Kwatra, MD
Hollie A. Lai, MD
Maria R. Ponisio, MD
Sabah Servaes, MD
Summit H. Shah, MD, MPH
Barry L. Shulkin, MD, MBA
Lisa J. States, MD
S. Ted Treves, MD
Stephan D. Voss, MD, PhD
Jennifer L. Williams, MD

ONCOLOGY COMMITTEE

Adina L. Alazraki, MD, FAAP, Chair
Susan E. Sharp, MD, Vice Chair
Govind B. Chavhan, MD
Kelly R. Dietz, MD
Meryle Eklund, MD
Anne Gill, MD
Sue C. Kaste, DO
Muhammad N. Khan, MD
Geetika Khanna, MD, MS
Arzu Kovanlikaya, MD
Irit R. Maianski, MD
M. Beth McCarville, MD
Erika Pace, MD
Marguerite T. Parisi, MD, MS
Edward J. Richer, MD
Judy H. Squires, MD
Lisa J. States, MD
Stephan D. Voss, MD, PhD
Sireesha Yedururi, MD

PHYSICIAN RESOURCES COMMITTEE

Rebecca L. Hulett-Bowling, MD, Chair
Kristen B. Thomas, MD, Vice Chair
Ellen M. Chung, MD
Shannon G. Farmakis, MD
Brooke S. Lampl, DO
Janice D. McDaniel, MD

Debbie J. Merinbaum, MD
Melinda Jane Morris, MD
Unni K. Udayasankar, MD

POST-MORTEM IMAGING COMMITTEE

Mary P. Harty MD, Chair
Pierre J. Schmit, MD, Vice Chair
Mutaz Alassar, MD
Lucia Carpineta, MD
William R. Carter, MD
Kristin Fickenscher, MD
Sharon W. Gould, MD
Timothy Higgins, MD
Jeanne G. Hill, MD
Tatum S. Johnson, MD
Vinay V.R. Kandula, FRCR, MRCP
Muhammad N. Khan, MD
Amy R. Mehollin-Ray, MD
Elka Miller, MD
Melinda J. Morris, MD
Nina Stein, MD

PROFESSIONALISM COMMITTEE

Brandon P. Brown, MD, FAAP, Chair
R. Paul Guillerman, MD, Vice Chair
Patricia Acharya, MD
Rama Ayyala, MD
Micheal A. Breen, MBBCh
Stephen D. Brown, MD
Dorothy I. Bulas, MD, FACR, FAAP
Teresa Chapman, MD, MA
Jeanne G. Hill, MD
Anastasia Hryhorczuk, MD
Susan D. John, MD, FACR
Craig M. Johnson, DO
Pamela M. Ketwaroo, MD
Sarah S. Milla, MD, FAAP
Tina Young Poussaint, MD, FACR
Sabah Servaes, MD
Raymond W. Sze, MD

PUBLICATIONS COMMITTEE

Ethan A. Smith, MD, Chair
Andrew T. Trout, MD, Vice Chair
Michael J. Callahan, MD, *Ex Officio*
Johan G. Blickman, MD, PhD
Sarah J. Menashe, MD
Ashok Panigrahy, MD
Sumit Pruthi, MD
Pooja D. Thakrar, MD
Peter J. Strouse, MD, FACR, Editor
Brian D. Coley, MD, FACR, FAIUM, Assistant Editor
Geetika Khanna, MD, MS, Assistant Editor
Cynthia K. Rigsby, MD, FACR, Assistant Editor

PUBLIC POLICY COMMITTEE

David W. Swenson, MD, Chair
Aparna Annam, DO, Vice Chair
Patricia T. Acharya, MD
Neil Anand, MD
Richard A. Barth, MD, FACR, FAAP
Richard M. Benator, MD, FACR, Advisory
Andrew J. Degnan, MD
Michael L. Francavilla, MD
Marta Hernanz-Schulman, MD, FACR, Advisory
Susan D. John, MD, FACR
Michael E. Katz, MD, FACR
Asef B. Khwaja, MD
Beth M. Kline-Fath, MD
Annie Lim, DO
Lauren Y. Peng, MD
Anil G. Rao, DMRD, DNB
Erica L. Riedesel, MD
Summit H. Shah, MD
Susan Sotardi, MD
Jonathan Swanson, MD

QUALITY AND SAFETY COMMITTEE

Ramesh S. Iyer, MD
Raymond W. Sze, MD, Vice Chair
Neil Anand, MD
Einat Blumfield, MD
Tushar Chandra, MBBS, MD
Govind B. Chavhan, MD
Thomas R. Goodman, MBBCh
Muhammad N. Khan, MD
Michael M. Moore, MD
Christina L. Sammet, PhD
Arta-Luana Stanescu, MD
David W. Swenson, MD
Chido Vera, MD
Amy C. Danehy, MD
Aparna Joshi, MD
Ammie M. White, MD

SPR REPRESENTATIVES

Richard A. Barth, MD, FACR, ARR and ACR Commission on Pediatric Radiology
Stephen F. Simoneaux, MD, FACR, ABR
Beverley Newman, MD, FACR, ACR
Sarah Milla, MD, FAAP, AAP

THORACIC IMAGING COMMITTEE

Paul G. Thacker, MD, MHA, Chair
Sarah Desoky, MD, Vice Chair
David M. Biko, MD
Alan S. Brody, MD
Matthew Cooper, MD
Monica Epelman, MD
Robert Fleck, MD
Maryam Ghadimi Mahani, MD
Paul J. Iskander, MD
Manisha Jana, MBBS, MD, FRCR
Arzu Kovanlikaya, MD
David Manson, MD
Beverley Newman, MD, FACR
Pallavi Sagar, MD

Jason P. Weinman, MD
Evan J. Zucker, MD

ULTRASOUND COMMITTEE

Monica Epelman, MD, Chair
Andrew S. Phelps, MD, Vice Chair
Angela J. Beavers, MD
Richard D. Bellah, MD, Advisory
Christian L. Carlson, MD
Tushar Chandra, MBBS, MD
Paul Clark, DO
Harris L. Cohen, MD, FACR
Ricardo Faingold, MD
Rachelle Goldfisher, MD
Kerri Highmore, MD
Vinay VR Kandula, FRCR, MRCP
Arzu Kovanlikaya, MD
Sosamma T. Methratta, MD
HaiThuy N. Nguyen, MD
Rodrigo V. Ozelame, MD
Harriet J. Paltiel, MD
Michele Retrouvey, MD
Erica L. Riedesel, MD
Henrietta Kotlus Rosenberg, MD, FACR
Cicero T. Silva, MD
Judy H. Squires, MD
Neil Vachhani, MD
Dayna M. Weinert, MD
Jonathan R. Wood, MD

WEBSITE EDITORIAL COMMITTEE

Benjamin H. Taragin, MD, Chair and Web Editor
Kiery A. Braithwaite, MD
Matthew R. Hammer, MD
Peter A. Marcovici, MD, Assistant Web Editor
Amy R. Mehollin-Ray, MD, Assistant Web Editor
Anh-Vu H. Ngo, MD, Assistant Web Editor – Social Media
Mahesh M. Thapa, MD, Assistant Web Editor – Education
Lincoln M. Wong, MD

SPR RESEARCH AND EDUCATION FOUNDATION

J. Damien Grattan-Smith, MBBS, President
Taylor Chung, MD, Vice President
Michael J. Callahan, MD, Secretary
Laura Z. Fenton, MD, FACR, Secretary-Elect
Stephen F. Simoneaux, MD, FACR, Treasurer
Sudha Anupindi, MD
R. Paul Guillerman, MD
Joseph J. Junewick, MD
William H. McAlister, MD
John D. Mackenzie, MD
Stuart A. Royal, MS, MD
Andrew T. Trout, MD
Thierry A.G.M. Huisman, MD

SPR PAST PRESIDENTS, PREVIOUS & FUTURE MEETING SITES, AWARDEES & EDWARD B. D. NEUHAUSER LECTURERS

PAST PRESIDENTS & PREVIOUS MEETING SITES

1958	Edward B. D. Neuhauser, MD	Washington, D.C.
1959	Frederic N. Silverman, MD	Cincinnati, Ohio
1960	John F. Holt, MD	Atlantic City, New Jersey
1961	Arthur S. Tucker, MD	Miami Beach, Florida
1962	John W. Hope, MD	Washington, D.C.
1963	R. Parker Allen, MD	Montreal, Quebec, Canada
1964	Edward B. Singleton, MD	Minneapolis, Minnesota
1965	J. Scott Dunbar, MD	Washington, D.C.
1966	Harvey White, MD	San Francisco, California
1967	M.H. Wittenborg, MD	Washington, D.C.
1968	David H. Baker, MD	New Orleans, Louisiana
1969	John A. Kirkpatrick, Jr., MD	Washington, D.C.
1970	Norman M. Glazer, MD	Miami Beach, Florida
1971	Bertram R. Girdany, MD	Boston, Massachusetts
1972	Donald H. Altman, MD	Washington, D.C.
1973	Hooshang Taybi, MD	Montreal, Quebec, Canada
1974	John L. Gwinn, MD	San Francisco, California
1975	Lawrence A. Davis, MD	Atlanta, Georgia
1976	Marie A. Capitanio, MD	Washington, D.C.
1977	John P. Dorst, MD	Boston, Massachusetts
1978	John P. Dorst, MD	Denver, Colorado
1979	Bernard J. Reilly, MB, FRCP (C)	Toronto, Ontario, Canada
1980	Walter E. Berdon, MD	Salt Lake City, Utah
1981	Andrew K. Poznanski, MD	San Francisco, California
1982	N. Thorne Griscom, MD	New Orleans, Louisiana
1983	Virgil R. Condon, MD	Atlanta, Georgia
1984	Jerald P. Kuhn, MD	Las Vegas, Nevada
1985	Lionel W. Young, MD	Boston, Massachusetts
1986	John C. Leonidas, MD	Washington, D.C.
1987	Derek C. Harwood Nash, MD, DSc & Denis Lallemand, MD (ESPR, IPR'87)	Toronto, Ontario, Canada
1988	Beverly P. Wood, MD	San Diego, California
1989	John F. O'Connor, MD	San Antonio, Texas
1990	E.A. Franken, Jr., MD	Cincinnati, Ohio
1991	Donald R. Kirks, MD & Hans G. Ringertz, MD, PhD (ESPR, IPR '91)	Stockholm, Swedan
1992	William H. McAlister, MD	Orlando, Florida
1993	M. B. Ozonoff, MD	Seattle, Washington
1994	Joanna J. Seibert, MD	Colorado Springs, Colorado
1995	Eric L. Effmann, MD	Washington, D.C.
1996	Kenneth E. Fellows, MD & Paul S. Thomas, MD (ESPR, IPR '96)	Boston, Massachusetts
1997	Diane S. Babcock, MD	St. Louis, Missouri
1998	Charles A. Gooding, MD	Tucson, Arizona
1999	Robert L. Lebowitz, MD	Vancouver, British Columbia, Canada
2000	Thomas L. Slovis, MD	Naples, Florida
2001	Janet L. Strife, MD & Francis Brunelle, MD (ESPR, IPR'01)	Paris, France
2002	Bruce R. Parker, MD	Philadelphia, Pennsylvania
2003	Richard B. Towbin, MD	San Francisco, California
2004	David C. Kushner, MD	Savannah, Georgia
2005	Stuart A. Royal, MS, MD	New Orleans, Louisiana
2006	George A. Taylor, MD & Richard Fotter, MD (ESPR, IPR'06)	Montreal, Quebec, Canada
2007	Marilyn J. Goske, MD	Miami, Florida
2008	Marta Hernanz-Schulman, MD	Scottsdale, Arizona
2009	M. Ines Boechat, MD, FACR	Carlsbad, California

2010	Neil D. Johnson, MBBS	Boston, Massachusetts
2011	Dorothy I. Bulas, MD & Catherine M. Owens, MD (ESPR, IPR'11)	London, England
2012	Donald P. Frush, MD	San Francisco, California
2013	Sue C. Kaste, DO	San Antonio, Texas
2014	Richard A. Barth, MD	Washington, D.C.
2015	Brian D. Coley, MD	Bellevue, Washington
2016	James S. Donaldson, MD, FACR & Karen Rosendahl, MD, PhD (ESPR, IPR' 16)	Chicago, Illinois
2017	Diego Jaramillo, MD, MPH	Vancouver, British Columbia, Canada
2018	Peter J. Strouse, MD, FACR	Nashville, Tennessee
2019	Taylor Chung, MD	San Francisco, California

FUTURE MEETINGS

2020	May 12 – May 16, 2020	TBD
2021	June 15 - June 19, 2021 (IPR)	Rome, Italy
2022	April 27 – May 1, 2022	Denver, Colorado

GOLD MEDALISTS

1988	Frederic N. Silverman, MD
1989	John L. Gwinn, MD
1990	John F. Holt, MD
1991	John A. Kirkpatrick, Jr., MD
1991	Bernard J. Reilly, MB, FRCP
1992	Edward B. Singleton, MD
1993	Hooshang Taybi, MD
1994	Walter E. Berdon, MD
1994	J. Scott Dunbar, MD
1995	Guido Currarino, MD
1995	Derek C. Harwood Nash, MD, DSc
1996	Andrew K. Poznanski, MD
1996	Beverly P. Wood, MD
1997	N. Thorne Griscom, MD
1997	John F. O'Connor, MD
1998	William H. McAlister, MD
1999	E. A. Franken, MD
2000	Eric L. Effmann, MD
2001	Giulio J. D'Angio, MD
2002	David H. Baker, MD
2003	Brinton B. Gay, Jr., MD
2003	William H. Northway, Jr., MD
2004	Diane S. Babcock, MD
2004	Virgil R. Condon, MD
2005	Jerald P. Kuhn, MD
2005	Thomas L. Slovis, MD
2006	Robert L. Lebowitz, MD
2006	John C. Leonidas, MD
2007	Leonard E. Swischuk, MD
2008	Barry D. Fletcher, MD
2009	Charles A. Gooding, MD
2010	Janet L. Strife, MD
2011	Carol M. Rumack, MD
2012	Marilyn J. Goske, MD
2013	Stuart A. Royal, MS, MD
2014	David C. Kushner, MD
2015	George A. Taylor, MD
2016	Jennifer K. Boylan, MA
2017	M. Ines Boechat, MD
2017	Paul K. Kleinman, MD
2018	Dorothy I. Bulas, MD, FACR, FAAP
2018	Neil D. Johnson, MBBS
2019	Donald P. Frush, MD, FACR
2019	Marta Hernanz-Schulman, MD, FACR, FAAP

PIONEER HONOREES

1990	John P. Caffey, MD
1991	M. H. Wittenborg, MD
1992	Edward B. Singleton, MD
1993	Frederic N. Silverman, MD
1994	John P. Dorst, MD
1995	Edward B. D. Neuhauser, MD
1996	E. A. Franken, MD
1996	Kazimierz Kozlowski, MD
1996	M. Arnold Lassrich, MD
1997	Arnold Shkolnik, MD
1998	Heidi B. Patriquin, MD
1998	William H. Northway, Jr., MD
2000	Jerald P. Kuhn, MD
2001	Diane S. Babcock, MD
2001	Fred E. Avni, MD, PhD
2003	Walter E. Berdon, MD
2004	G. B. Clifton Harris, MD
2005	Rita L. Teele, MD
2006	Robert L. Lebowitz, MD
2007	Carol M. Rumack, MD
2008	Paul S. Babyn, MD
2009	Kenneth E. Fellows, MD
2010	David K. Yousefzadeh, MD
2011	Massoud Majd, MD
2012	George S. Bisset, III, MD
2013	Barry D. Fletcher, MD
2014	Diego Jaramillo, MD, MPH
2015	William E. Shiels, DO
2016	Mary R. Wyers, MD
2017	H. Theodore Harcke, Jr., MD
2018	Richard B. Towbin, MD, FACR
2019	Michael DiPietro, MD, FACR

PRESIDENTIAL RECOGNITION AWARDS

1999	David C. Kushner, MD
2000	Paul K. Kleinman, MD
2001	Neil D. Johnson, MBBS
2001	Christopher Johnson
2002	Jennifer K. Boylan, MA
2002	Thomas L. Slovis, MD
2003	Danielle K.B. Boal, MD
2003	Marta Hernanz-Schulman, MD
2004	Kenneth L. Mendelson, MD
2005	Taylor Chung, MD
2005	J. A. Gordon Culham, MD
2005	Shi-Joon Yoo, MD
2006	L. Christopher Foley, MD
2007	Donald P. Frush, MD
2008	Mary K. Martel, PhD
2008	Connie L. Mitchell, MA, RT(R)(CT)
2008	Harvey L. Neiman, MD
2009	Karen S. Schmitt
2010	Richard A. Barth, MD
2011	Kimberly E. Applegate, MD, MS
2011	Keith Strauss, MS, FACR
2012	David C. Kushner, MD, FACR
2012	Stuart A. Royal, MS, MD
2013	Alan E. Schlesinger, MD
2014	Richard M. Benator, MD
2015	Cynthia K. Rigsby, MD
2016	Vicente Gilsanz, MD, PhD

2017	Tal Laor, MD
2018	Joëlle A. Moreno, JD
2018	Patricia Vario
2019	A. James Barkovich, MD
2019	Patricia E. Burrows, MD

HONORARY MEMBERS

1985	Jacques Sauvegrain, MD
1987	Bryan J. Cremin, MD
1987	Ole A. Eklof, MD
1987	Clement C. Faure, MD
1987	Andres Giedion, MD
1987	Denis Lallemand, MD
1987	Arnold Lassrich, MD
1987	Ulf G. Rudhe, MD
1998	Frederic N. Silverman, MD
1989	John L. Gwinn, MD
1990	John F. Holt, MD
1990	Richard G. Lester, MD
1991	Gabriel L. Kalifa, MD
1991	Javier Lucaya, MD
1991	John P. Masel, MD
1991	Noemi Perlmutter Cremer, MD
1991	Hans G. Ringertz, MD
1991	John A. Kirkpatrick, Jr., MD
1991	Bernard J. Reilly, MB, FRCP(C)
1992	Edward B. Singleton, MD
1992	Donald R. Kirks, MD
1992	Beverly P. Wood, MD
1992	Walter E. Berdon, MD
1993	Hooshang Taybi, MD
1994	Marie A. Capitanio, MD
1994	E. A. Franken, Jr., MD
1994	John C. Leonidas, MD
1994	William H. McAlister, MD
1994	Andrew K. Poznanski, MD
1994	J. Scott Dunbar, MD
1995	David H. Baker, MD
1992	Derek C. Harwood Nash, MD, DSc
1995	N. Thorne Griscom, MD
1995	Guido Currarino, MD
1996	Francis O. Brunelle, MD
1996	Lloyd L. Morris, MD
1996	Heidi B. Patriquin, MD
1997	John F. O'Connor, MD
1997	Theodore E. Keats, MD
1998	Rita L. Teele, MD
1998	H. Ted Harcke, MD
1999	J. Bruce Beckwith, MD
2000	Joseph Volpe, MD
2001	Ulrich V. Willi, MD
2001	Henrique M. Lederman, MD
2001	Mutsuhisa Fujioka, MD
2002	Eric J. Hall, DSc, FACR, FRCR
2002	Walter Huda, PhD
2003	Michael R. Harrison, MD
2004	Lee F. Rogers, MD
2005	Carden Johnston, MD
2006	Alan B. Retik, MD
2007	Robert R. Hattery, MD
2008	Professor Hassen A. Gharbi
2009	Dolores Bustelo, MD
2009	Pedro A. Daltro, MD, PhD

2009	Cristian Garcia, MD
2009	Antônio Soares de Souza, MD
2010	Stephen Chapman, MD
2011	Catherine M. Owens, MBBS
2011	Madan M. Rehani, PhD
2012	Harvey L. Neiman, MD, FACR
2013	Savvas Andronikou, MBBCh, FCRad, FRCR, PhD
2014	Timothy M. Cain, MBBS
2015	In-One Kim, MD
2015	Professor Guy Sebag (posthumously)
2016	Bernard F. Laya, DO
2017	Gloria Soto Giordani, MD
2018	Fred E. Avni, Jr., MD, PhD
2018	Karen Rosendahl, MD, PhD
2019	Omolola (Monica) Atalabi, MD
2019	Kushaljit S. Sodhi, MD, PhD, MAMS, FICR, PIMER

EDWARD B. SINGLETON-HOOSHANG TAYBI AWARD

2006	Corning Benton, Jr., MD
2007	Michael P. D'Alessandro, MD
2007	Janet R. Reid, MD
2008	Dorothy I. Bulas, MD
2009	Lane F. Donnelly, MD
2010	Wilbur L. Smith, Jr., MD
2011	Ralph S. Lachman, MD, FACR
2012	Alan Daneman, MD
2013	Lisa H. Lowe, MD
2014	Robert H. Cleveland, MD
2015	Stephen F. Simoneaux, MD
2016	Michael A. DiPietro, MD
2017	Shi-Joon Yoo, MD
2018	John D. Strain, MD, FACR

JOHN A. KIRKPATRICK YOUNG INVESTIGATOR AWARD

This award is given to the author of the best paper presented by a resident or fellow at the SPR meeting. Beginning in 1995, the award became known as the John A. Kirkpatrick Young Investigator Award.

1993	Philipp K. Lang, MD
1993	Stephanie P. Ryan, MD
1994	Sara O'Hara, MD
1995	Philipp K. Lang, MD
1996	Fergus V. Coakley, MB, FRCR
1997	Ronald A. Alberico, MD
1998	Laura J. Varich, MD
1999	A. E. Ensley, BS
1999	R.W. Sze, MD
2000	S. H. Schneider, MD
2001	Valerie L. Ward, MD
2002	Ricardo Faingold, MD
2003	Andrea Doria, MD
2004	Nina M. Menezes, PhD
2005	Lena Naffaa, MD
2006	Courtney A. Coursey, MD
2007	Ashley J. Robinson, MBChB
2008	Hee Kyung Kim, MD
2009	Conor Bogue, MD
2010	Albert Hsiao, MD, PhD
2011	Ethan A. Smith, MD
2012	Saivivek Bogale, MD
2013	Emma Raver, BA
2014	Aarti Luhar, MD
2015	Ashish Parikh, MD

2016	Sila Kurugol, PhD
2017	Ezekiel Maloney, MD
2018	Arleen Li

WALTER E. BERDON AND THOMAS L. SLOVIS AWARDS - 2018

The Walter E. Berdon Award recognizes the best clinical research paper submitted to the journal of ***Pediatric Radiology*** in the year preceding the meeting. This award was established to honor Walter E. Berdon who served as the North American Editor of Pediatric Radiology for 30 years and who stepped down as editor on June 30, 2003.

The Thomas L. Slovis Award recognizes the best basic scientific paper submitted to the journal of ***Pediatric Radiology*** in the year preceding the meeting. This award was established to honor Thomas L. Slovis who served as the North American Editor of Pediatric Radiology following Dr. Berdon and who stepped down as editor on December 31, 2012.

Prior to 2012, Walter E. Berdon Awards recognized both the best clinical research paper and the best basic scientific paper.

2018 recipients will be announced at the meeting.

2017

Best Clinical Paper (Walter E. Berdon Award):
Jennifer E. Lim-Dunham, MD, FACR, Iclal Erdem Toslak, MD, Khalid Alsabban, MD, Amany Aziz, MD, Brendan Martin, PhD, Gokcan Okur, MD, Katherine C. Longo, MD. Ultrasound risk stratification for malignancy using the 2015 American Thyroid Association Management Guidelines for Children with Thyroid Nodules and Differentiated Thyroid Cancer.

Best Basic Science Paper (Thomas L. Slovis Award):
Monwabisi Makola, PhD, M. Douglas Ris, PhD, E. Mark Mahone, PhD, Keith Owen Yeates, PhD, Kim M. Cecil, PhD. Long-term effects of radiation on white matter of the corpus callosum: a diffusion tensor imaging study

2016

Best Clinical Paper (Walter E. Berdon Award):
Rothman S, Gonen A, Vodonos A, Novack V, Shelef I (2016) Does preparation of children before MRI reduce the need for anesthesia? Prospective randomized control trial. Pediatr Radiol 46:1599-1605

Best Basic Science Paper (Thomas L. Slovis Award):
Jarvis K, Schnell S, Barker AJ, Garcia J, Lorenz R, Rose M, Chowdhary V, Carr J, Robinson JD, Rigsby CK, Markl M (2016) Evaluation of blood flow distribution asymmetry and vascular geometry in patients with Fontan circulation using 4-D flow MRI. Pediatr Radiol 46:1507-1519

2015

Best Clinical Paper (Walter E. Berdon Award):
Choudhary AK, Bradford R, Dias MS, Thamburaj K, Boal DK (2015) Venous injury in abusive head trauma. Pediatr Radiol 45:1803-1813

Best Basic Science Paper (Thomas L. Slovis Award):
Back SJ, Edgar JC, Canning DA, Darge K (2015) Contrast-enhanced voiding urosonography: In vitro evaluation of a second generation ultrasound contrast agent for in vivo optimization. Pediatr Radiol 45:1496-1505

2014

Best Clinical Paper (Walter E. Berdon Award):
Tyson ME, Bohl DD, Blickman JG. (2014) A randomized controlled trial: child life services in pediatric imaging. Pediatr Radiol 44:1426-1432

Best Basic Science Paper (Thomas L. Slovis Award):
Tsai A, McDonald AG, Rosenberg AE, Gupta R, Kleinman PK (2014) High-resolution CT with histopathological correlates of the classic metaphyseal lesion of infant abuse. Pediatr Radiol 44:124-140

2013

Best Clinical Paper (Walter E. Berdon Award):
Punwani S, Cheung KK, Skipper N, Bell N, Bainbridge A, Taylor SA, Groves AM, Hain SF, Ben-Haim S, Shankar A, Daw S, Halligan S, Humphries PD (2013) Dynamic contrast enhanced MRI improves accuracy for detecting focal splenic involvement in children and adolescents with Hodgkin disease. Pediatr Radiol 43:941-949

Best Basic Science Paper (Thomas L. Slovis Award):
Hanquinet S, Rougemont AL, Courvoisier D, Rubbia-Brandt L, McLin V, Tempia M, Anooshiravani M (2013) Acoustic radiation force impulse (ARFI) elastography for the non-invasive diagnosis of liver fibrosis in children. Pediatr Radiol 43:545-551

2012

Best Clinical Paper (Walter E. Berdon Award):
Swanson JO1, Vavilala MS, Wang J, Pruthi S, Fink J, Jaffe KM, Durbin D, Koepsell T, Temkin N, Rivara FP (2012) Association of initial CT findings with quality-of-life outcomes for traumatic brain injury in children. Pediatr Radiol 42:974-981

Best Basic Science Paper (Thomas L. Slovis Award):
Tkach JA, Hillman NH, Jobe AH, Loew W, Pratt RG, Daniels BR, Kallapur SG, Kline-Fath BM, Merhar SL, Giaquinto RO, Winter PM, Li Y, Ikegami M, Whitsett JA, Dumoulin CL (2012) An MRI system for imaging neonates in the NICU: initial feasibility study. Pediatr Radiol 412:1347-1356

2011

Best Basic Science Paper:
Castaneda RT1, Boddington S, Henning TD, Wendland M, Mandrussow L, Liu S, Daldrup-Link H (2011) Labeling human embryonic stem-cell-derived cardiomyocytes for tracking with MR imaging. Pediatr Radiol 41:1384-1392

Best Clinical Research Paper:
Schachar JL, Zampolin RL, Miller TS, Farinhas JM, Freeman K, Taragin BH (2011) External validation of the New Orleans Criteria (NOC), the Canadian CT Head Rule (CCHR) and the National Emergency X-Radiography Utilization Study II (NEXUS II) for CT scanning in pediatric patients with minor head injury in a non-trauma center. Pediatr Radiol 41:971-979

2010

Best Basic Science Paper:
Goo HW (2010) Initial experience of dual energy lung perfusion CT using a dual source CT system in children. Pediatr Radiol 40:1536-1544

Best Clinical Research Paper:
Raissaki M, Perisinakis K, Damilakis J, Gourtsoyiannis N (2010) Eye-lens bismuth shielding in paediatric head CT: artefact evaluation and reduction. Pediatr Radiol 40:1748-1754

2009

Best Basic Science Paper:
Helm EJ, Silva CT, Roberts HC, Manson D, Seed MT, Amaral JG, Babyn PS (2009) Computer-aided detection for the identification of pulmonary nodules in pediatric oncology patients: initial experience. Pediatr Radiol 39:685-693

Best Clinical Research Paper:
Ben Saad M, Rohnean A, Sigal-Cinqualbre A, Adler G, Paul JF (2009) Evaluation of image quality and radiation dose of thoracic and coronary dual-source CT in 110 infant with congenital heart disease. Pediatr Radiol 39:668-676

2008

Best Basic Science Paper:
Wang ZJ, Boddington S, Wendland M, Meier R, Corot C, Daldrup-Link H (2008) MR imaging of ovarian tumors using folate-receptor-targeted contrast agents. Pediatr Radiol 38:529-537

Best Clinical Research Paper:
Hallowell LM, Stewart SE, de Amorim E Silva CT, Ditchfield MR (2008) Reviewing the process of preparing children for MRI. Pediatr Radiol 38:271-279

2007

Best Basic Science Paper:
Maree GJ, Irving BJ, Hering ER (2007) Paediatric dose measurement in a full-body digital radiography unit. Pediatr Radiol 37:990-997

Best Clinical Research Paper:
Silva CT, Daneman A, Navarro OM, Moore AM, Moineddin R, Gerstle JT, Mittal A, Brindle M, Epelman M (2007) Correlation of sonographic findings and outcome in necrotizing enterocolitis. Pediatr Radiol 37:274-282

2006

Best Basic Science Paper:
Goo HW, Suh DS (2006) The influences of tube voltage and scan direction on combined tube current modulation: a phantom study. Pediatr Radiol 36:833-840

Best Clinical Research Paper:
Lee T, Tsai IC, Fu YC, Jan SL, Wang CC, Chang Y, Chen MC (2006) Using multidetector-row CT in neonates with complex congenital heart disease to replace diagnostic cardiac catheterization for anatomical investigation: initial experiences in technical and clinical feasibility. Pediatr Radiol 36:1273-1282

2005

Best Basic Science Paper:
Nield LE, Qi XL, Valsangiacomo ER, Macgowan CK, Wright GA, Hornberger LK, Yoo SJ (2005) In vivo MRI measurement of blood oxygen saturation in children with congenital heart disease. Pediatr Radiol 35:179-185

Best Clinical Paper:
Jones A, Granger S, Brambilla D, Gallagher D, Vichinsky E, Woods G, Berman B, Roach S, Nichols F, Adams RJ (2005) Can peak systolic velocities be used for prediction of stroke in sickle cell anemia? Pediatr Radiol 35:66-72

2004

Best Basic Science Paper:
Peng SS, Lee WT, Wang YH, Huang KM (2004) Cerebral diffusion tensor images in children with tuberous sclerosis: a preliminary report. Pediatr Radiol 34:387-392

Best Clinical Paper:
Babyn PS, Chu WC, Tsou IY, Wansaicheong GK, Allen U, Bitnun A, Chee TS, Cheng FW, Chiu MC, Fok TF, Hon EK, Gahunia HK, Kaw GJ, Khong PL, Leung CW, Li AM, Manson D, Metreweli C, Ng PC, Read S, Stringer DA (2004) Severe acute respiratory syndrome (SARS): chest radiographic features in children. Pediatr Radiol 34:47-58

2003

Best Basic Science Paper:
Xiang J, Holowka S, Sharma R, Hunjan A, Otsubo H, Chuang S (2003) Volumetric localization of somatosensory cortex in children using synthetic aperture magnetometry. Pediatr Radiol 33:321-327

Best Clinical Paper:
Grattan-Smith JD, Perez-Bayfield MR, Jones RA, Little S, Broecker B, Smith EA, Scherz HC, Kirsch AJ (2003) MR imaging of kidneys: functional evaluation using F-15 perfusion imaging. Pediatr Radiol 33:293-304

2002

Best Basic Science Paper:
Nield LE, Qi X, Yoo SJ, Valsangiacomo ER, Hornberger LK, Wright GA (2002) MRI-based blood oxygen saturation measurements in infants and children with congenital heart disease. Pediatr Radiol 32:518-522

Best Clinical Paper:
Lamer S, Dorgeret S, Khairouni A, Mazda K, Brillet PY, Bacheville E, Bloch J, Penneçot GF, Hassan M, Sebag GH (2002) Femoral head vascularisation in Legg-Calvé-Perthes disease: comparison of dynamic gadolinium-enhanced subtraction MRI with bone scintigraphy. Pediatr Radiol 32:580-585

SPR RESEARCH AND EDUCATION FOUNDATION AWARDS

The SPR Research and Education Foundation is dedicated to promoting research and scholarship and education in pediatric radiology. In 2019, the REF Board of Directors announced that the Jack Haller Award for Excellence in Pediatric Radiology Education has been renamed to be, The Jack O. Haller – Thomas L. Slovis, Award for Excellence in Pediatric Radiology Education.

As background, in 2004 Jack Haller passed away and his friend Tom Slovis asked the SPR Foundation Board of Directors to establish an award in Jack's memory to recognize excellence in pediatric radiology education. The Foundation Board approved the request and Tom seeded the fund with the inaugural donation of $10,000. Tom continued to support the Haller fund in subsequent years. We hope you agree that it is fitting that the award that celebrates excellence in pediatric radiology education, also through this renaming, now also celebrates the lasting impact of friendship and goodwill.

THE JACK O. HALLER AWARD FOR EXCELLENCE IN PEDIATRIC RADIOLOGY EDUCATION

2005	Alan Daneman, MD
2006	William R. Cranley, MD
2006	John F. O'Connor, MD
2007	Cindy R. Miller, MD
2008	Sara J. Abramson-Squire, MD
2009	Michael A. DiPietro, MD
2010	George A. Taylor, MD
2011	Paul K. Kleinman, MD
2012	Richard I. Markowitz, MD
2013	Gary L. Hedlund, DO
2014	Tal Laor, MD
2014	Carrie B. Ruzal-Shapiro, MD
2015	Laura Z. Fenton, MD
2016	Melvin Senac, MD
2017	Janet R. Reid, MD, FRCPC
2018	Veronica J. Rooks, MD
2018	Yukata Sato, MD, PhD

THE JACK O. HALLER – THOMAS L. SLOVIS AWARD FOR EXCELLENCE IN PEDIATRIC RADIOLOGY EDUCATION

2019	Mahesh M. Thapa, MD

THE HEIDI PATRIQUIN INTERNATIONAL FELLOWSHIP

2005	Luy Lyda, MD, Angkor Hospital for Children, Siem Reap, Cambodia
2006	Hakima Al-Hashimi, MD Salmaniya Medical Complex, Manama, Bahrain
2006	Pannee Visrutaratna, MD, Chiang Mai University, Chiang Mai, Thailand
2006	Juana Maria Vallejo, MD, Clinica del Country, Bogota, Colombia
2007	Nathan David P. Concepcion, MD, St. Luke's Medical Center, Quezon City, Philippines
2008	Rolando Reyna Lopez, MD, Hospital Santo Tomas, Panama City, Panama
2009	Ahmed Mussa Jusabani, MD, Kilimanjaro Christian Medical Centre, Moshi Town, Tanzania
2010	Omolola Mojisola Atalabi, MD, College of Medicine, University of Ibadan, Nigeria
2011	Kushaljit Singh Sodhi, MD, Postgraduate Institute of Medical Education and Research
2012	Wambani Sidika Jeska, MBchB, Kenyatta National Hospital, Nairobi, Kenya
2012	Yocabel Gorfu, MD, Addis Ababa University, Addis Ababa, Ethiopia
2013	Regina Nava, MD, St. Luke's Medical Center, Quezon City, Philippines
2013	Olubukola Abeni Omidiji, MBBS, University of Lagos, Lagos, Nigeria
2014	Nneka I. Iloanusi, MBBS, University of Nigeria Teaching Hospital, Enugu, Nigeria
2014	Beatrice Mulama, MBChB, M. Med, Kenyatta National Hospital, Nairobi, Kenya
2015	Nasreen Mahomed, MBBCh, University of the Wiwatersand, Johannesburg, Gauteng
2015	Waseem Akhtar Mirza, MBBS, The Aga Khan University, Karachi, Pakistan
2016	Daniel Zewdneh Solomon, MD, Addis Ababa University, Addis Ababa, Ethiopia
2016	Vikas Yadav, MD, Christian Medical College, Vellore, Tamilnadu, India
2017	Hatíce Ariöz Habíbí, MD, Cerrahpasa Medical, Istanbul University, Turkey
2017	Faizah Mohd Zaki, MD, Universiti Kebangsaan Malaysia Medical Centre, Kuala Lumpur, Malaysia
2018	Bernadette Wambui Muthee, MD, Aga Khan University Hospital, Nairobi, Kenya
2019	Fathia Omer Salah, MD, Black Lion Hospital, Addis Ababa, Ethiopia
2019	Sunder Suwal, MD, University Teaching Hospital, Maharajgunj, Kathmandu, Nepal

SPR RESEARCH AND EDUCATION FOUNDATION GRANTS

The 2018 grant recipients are listed. 2019 grant recipients will be announced at the meeting. For grants from prior years, please see the SPR website.

EDUCATION PROJECT AWARD

"Child Abuse Radiology: Report, Research and Teaching Tool – CAR3T2" **-** Jeannette M. Perez-Rossello MD, Boston Children's Hospital

JOHN DORST-FELIX FLEISCHNER SEED GRANT AWARDS

"Utility of Respiratory Gated Dynamic Volumetric CTA in the Awake State Compared to Non-Gated Dynamic Volumetric CTA and Bronchoscopy in Pediatric Patients With Suspected Proximal Airway Obstruction"- Anna Lillis, MD, Nationwide Children's Hospital, Columbus, OH

"Automated Image Quality Assessment Utilizing Machine Learning in Clinical Chest Projection Imaging in Young Children"
- Gary Schooler, MD, Duke University, Durham, North Carolina

MULTI-INSTITUTIONAL PILOT AWARD

"Contrast-Enhanced Brain Ultrasound in Extreme Premature Fetal Lambs Maintained by the EXTra-uterine Environment for Neonatal Support (EXTEND): Evaluation of Perfusion Parameters and Assessment of Intracranial Pressure" - Ryne A Didier, MD, Children's Hospital of Philadelphia

"A Pilot Study to Assess if fMRI is a Potential Radiological Biomarker in Youth with Persistent Concussion Symptoms"
- Jessie Aw-Zoretic, MBChB, Lurie Children's Hospital, Chicago

"Zero Echo-Time MRI for Radiation Free Pediatric Bone Imaging" - Mai-Lan Ho, MD, Mayo Clinic, Rochester, Minnesota

SEED GRANT

"Integrative Imaging Biomarker Assessment of Hepatic Involvement and Severity in Gaucher Disease to Tailor Personalized Therapy"
- Andrew Degnan, MD, MPhil, Children's Hospital of Philadelphia

YOUNG INVESTIGATOR

"High Performance Engine for Dose-Reduced CT Imaging System" - Xiao Wang, PhD, Boston Children's Hospital; Mentor: Simon Warfield

PREVIOUS EDWARD B. D. NEUHAUSER LECTURES

1971- John Caffey, MD, Pittsburgh, Pennsylvania: "The Radiologist and Unexplained Injury to Infants: Early History and Current Status"
1972- M. Judah Folkman, MD, Boston, Massachusetts: "Patterns of Discovery Fundamental to Radiology and Biology"
1973- Josef Warkany, MD, Cincinnati, Ohio: "Pediatric Radiology and Syndromology"
1974- Benjamin H. Landing, MD, Los Angeles, California: "Syndromes of Congenital Heart Disease with Tracheobronchial Anomalies"
1975- Frederic N. Silverman, MD, Cincinnati, Ohio: "Viral Diseases of Bone Do They Exist?"
1976- Lynne M. Reid, MD, Boston, Massachusetts: "The Lung Its Growth and Remodeling in Health and Disease"
1977- John F. Holt, MD, Ann Arbor, Michigan: "Neurofibromatosis in Children"
1978- Helen B. Taussig, MD, Baltimore, Maryland: "The Tetralogy of Fallot"
1979- Robert B. Salter, MD, Toronto, Ontario, Canada: "Legg Perthes Disease: The Scientific Basis for the Various Methods of Treatment and Their Indications"
1980- C. John Hodson, MD, New Haven, Connecticut: "Reflux Nephropathy and the Pediatric Radiologist"
1981- Stanley M. Garn, Ph.D., Ann Arbor, Michigan: "Contributions of the Radiographic Image to the Understanding of Human Growth"
1982- Duncan V. B. Neuhauser, Ph.D., Cleveland, Ohio: "Careful Thinking"
1983- J. Bruce Beckwith, MD, Seattle, Washington: "Renal Tumors of Children Pathologic Considerations Relevant to Diagnostic Imaging"
1984- J. Scott Dunbar, MD, Cincinnati, Ohio: "The Accessory Nasal Sinuses"
1985- John A. Kirkpatrick, Jr., MD, Boston, Massachusetts: "The Neuhauser Legacy"
1986- Kurt Hirschhorn, MD, New York, New York: "Recent Advances in Prenatal Diagnosis of Genetic and Congenital Disease"
1987- Andres Giedion, MD, Zurich, Switzerland: "Radiological Syntax of Genetic Bone Disease"
1988- Joseph J. Volpe, MD, St. Louis, Missouri: "Brain Injury in the Premature Infant"
1989- David H. Baker, MD, New York, New York: "Personal Reflections on Men and Machines from Red Goggles to Spin Wobbles"
1990- William H. Northway, Jr., MD, Stanford, California: "Bronchopulmonary Dysplasia and Research in Diagnostic Radiology"
1991- Derek C. Harwood Nash, MD, DSc, Toronto, Canada: "Pediatric Neuroimaging: The Evolution and Revolution of a Sub Specialty"
1992- Walter E. Berdon, MD, New York, New York: "Diseases of the Bone Marrow: MRI Observations"
1993- Morrie E. Kricun, MD, Philadelphia, Pennsylvania: "Paleoradiology: A Look into the Past"
1994- Beverly Wood, MD, Los Angeles, California: "Acute Pulmonary Disease in the Compromised Child"
1995- Frances S. Collins, MD, PhD, Washington, DC: "The Human Genome Project and the Future of Medicine"
1996- M. Judah Folkman, MD, Boston, Massachusetts: “Clinical Applications of Angiogenesis Research”
1997- S. Steven Potter, PhD, Cincinnati, Ohio: “Homeobox Genes and Pattern Formation (Master Genes)”
1998- Roy A. Filly, MD, San Francisco, California: “Fetal Thoracic Surgery”
1999- Harold A Richman, PhD, Chicago, Illinois: “Child Abuse: From a Radiologist’s Discovery to a Major Issue of Public Policy. What Have We Wrought?”
2000- William D. Lyman, PhD, Detroit, Michigan: “Prenatal Molecular Diagnosis and Fetal Therapy”
2001- Jerry R. Dwek, MD, Columbus, Ohio: “Médecins Sans Frontiéres/The Doctors Without Borders Experience – Afghanistan”
2002- Eric J. Hall, DSc, FACR, FRCR, New York, New York: “Lessons We Have Learned From Our Children: Cancer Risks From Diagnostic Radiology”
2003- Jeffrey A. Towbin, MD, Houston, Texas: “Molecular Cardiology: Laboratory to Bedside”
2004- Bruce R. Rosen, MD, PhD, Boston, Massachusetts: “New Advances in MRI: A Guide for the Practicing Pediatric Radiologist”
2005- Bruce R. Korf, MD, PhD, Birmingham, Alabama: “Pathobiology and Management of NF1 in the ‘Genomic Era’”
2006- Richard M.J. Bohmer, MD, MPH, Boston, Massachusetts: “Evolution, Innovation and the Changing Nature of Healthcare Delivery”
2007- Nogah Haramati, MD, Bronx, New York: “21st Century Radiology: Growth and Development of Our Workflows and Processes”
2008- Emanuel Kanal, MD, FACR, FISMRM, AANG, Pittsburg, Pennsylvania: “MR Technology: Where Are We, Where Are We Going?
2009- Roberta G. Williams, MD, Los Angeles, California: “Cardiology and Radiology: Partners in Producing Healthy Adults with Congenital Heart Disease”
2010- Regina E. Herzlinger, PhD, Boston, Massachusetts: “The Economic Basis of Change in Healthcare”
2011- Sanjiv Gambhir, MD, PhD, Stanford, California: “Molecular Imaging”
2012- William R. Hendee, PhD, Milwaukee, Wisconsin: “Past and Future Patient Benefits of Radiologist/Physicist Collaboration”
2013- James R. Downing, MD, Memphis, Tennessee: “The Pediatric Cancer Genome Project – Implications for Clinical Medicine
2014- Robert Pearl, MD, Oakland, California: “The Future of American Medicine – The Impact of Health Care Reform”
2015- Robert J. Gillies, PhD, Tampa, Florida: “Radiomics and Radiogenomics”
2016- Scott E. Fraser, PhD, Los Angeles, California: "Multimodal Imaging of the Molecular, Cellular and Tissue Events Underlying Embryonic Development”
2017- James H. Thrall, MD, FACR, Boston, Massachusetts: “Roles for Imaging in the Age of Precision Medicine”
2018- Paul K. Kleinman, MD, FAAP, Boston, Massachusetts: Curious Bones: Sustaining Discovery in the Face of Doubt

SPR 2019 HONOREES

SPR 2019 GOLD MEDALIST

The Gold Medal of The Society for Pediatric Radiology is our most distinguished honor. The SPR Gold Medal is awarded to pediatric radiologists who have contributed greatly to the SPR and our subspecialty of pediatric radiology as a scientist, teacher, personal mentor and leader.

Donald P. Frush, MD, FACR

"Don is a compelling visionary. His focus on radiation dose many years ago has been transformative to the practice of pediatric radiology."
- George Bissett, MD

The Society for Pediatric Radiology is most fortunate to have unusually dedicated and talented members who speak on behalf of children. One of these individuals is Donald P. Frush, MD, who through his passion and scientific achievements has been one of the leading voices for our Society both nationally and internationally since joining the SPR in 1992. Don's voice is always calm and substantive, and he has represented our specialty with the highest of ethics and humility.

Don was born in upstate New York in 1958. He had an idyllic childhood in the small community of Los Gatos, California where his family moved when he was 5 years old. His father was an IBM engineer and his mother was dedicated to raising their four children. He describes his parents as "very progressive, enlightened about the environment and dedicated to diversity and inclusiveness"." As a boy, he loved camping and sports (tennis, basketball…really any sport) with his three siblings (one older sister and two younger brothers). As an undergraduate at the University of California- Davis, he majored in psychology but found himself drawn to working with children. He decided to enter medical school at Duke University where he met his wife Karen. They married his senior year of medical school. During a two-year pediatric residency at University of California- San Francisco, pediatric radiologists Charles Gooding, Robert Brasch and Hooshang Taybi were influential in Don's ultimate career choice of Pediatric Radiology. By serendipity, the Duke Radiology residency had an unmatched position and Don started his radiology training there in 1987. Eric Effmann, MD, past-President of the SPR remembers Don and Karen well upon their return to their medical alma mater in Durham. Eric says, "Now, more than 30 years after meeting them, they stand as role models as academic physicians…their life and their work is inextricably linked."

Don is driven by "doing what needs to be done". He believes his success (when you can get him to talk about it!) has been "fortuitous" and due to his being surrounded by great people. During his fellowship at Cincinnati Children's Hospital Medical Center, "there was a sense that you do the right thing for the patient that is right in front of you." He found critical colleagues in Lane Donnelly and George Bissett, two other innovative pediatric radiology leaders. George describes Don as "a leader, he has great strength in building consensus. If leadership is defined by results, Don is at the top of the class!"

In 2001, an article was published on the front page of the newspaper USA TODAY, with the headline "CT scans in children linked to cancer". The same year, Don and Dr. Annie Paterson looked at pediatric CT scans performed at outside hospitals and found that the radiation dose for children was not reduced compared to adults. This pivotal publication was published alongside a second article by Donnelly, Frush and colleagues from Cincinnati on strategies to minimize radiation dose at a large children's hospital, with an accompanying editorial by AJR Editor Dr. Lee Rogers. Dr. Rogers later told Don that publishing those two articles was one of the most significant contribution he had made as editor. These two frequently cited articles provided quantifiable evidence that change was needed to improve patient safety in pediatric CT. In 2002, Dr. Tom Slovis, one of Don's mentors, organized a revolutionary conference that included radiologists, medical physicists, industry and government and published the proceedings in the journal, *Pediatric Radiology*. Don says that, "through these events, I was literally thrown into the field of radiation protection".

In 2000, he and Dr. Ehsan Samei, Professor of Medical Physics at Duke began performing translational research in pediatric CT dose reduction utilizing MOSFET technology that while basic was "always grounded in kids". Ehsan tells us "Don is an outstanding human being! In spite of how good he is as a clinician and as a scientist, he cares deeply and passionately about each person. This is what makes him exceptional."

During his 26 years of faculty at Duke, Don has been Professor of Radiology and Pediatrics, Chief of the Division of Pediatric Radiology and the John Strohbehn Distinguished Professor of Radiology. He has written over 300 scientific articles, 43 book chapters and 14 grants. To highlight just several of his honors, Don received the SPR Young Investigator award, the Caffey award, the SPR Presidential Recognition award, an RSNA Editorial Fellowship and was an Associate Editor of *Radiology* and an Assistant Editor of *Pediatric Radiology*. He is past-President of the SPR. He has been a consultant to the International Atomic Energy Agency, the World Health Organization, Trustee and Chair of the American Board of Radiology and is Chair of the Image Gently Alliance.

When I asked Don what he was most proud of in his career, he did not speak of his accomplishments in medicine; rather he spoke of his wife and four children. "By far, my wife and my children are my legacies." His wife Karen is the Chief Quality Officer at Stanford Healthcare in California, where she and Don recently moved. In her words "It's the *combination* of things he's accomplished—he is a global leader in radiation reduction in kids, an award-winning teacher and scholar, a dedicated radiologist and mentor, a committed and loving husband, and a father who's been very involved in the lives of all four of our kids." All four of their children, (Sarah, Ben, Jack and Jenna) will or have graduated from Duke or UNC Medical School. The oldest, Sarah, admires "his integrity, his graciousness". Jack, a radiology intern, said his Dad taught him about "patience". Karen elaborated on this trait, telling us that this 'over the top' sports fan waited 27 years for Pittsburgh Steelers football tickets!

Don has many outside interests. Don is a farmer and loves tractors. A medical meeting had to be cut short because Don had to go home for a farming emergency…some of their cows broke through a fence and were having a "drive" down the local road.
Don, yes, your family is your legacy, but you have also given us in pediatric radiology the strongest of legacies…to be the voice for quality care for children. For this lasting message from you to our Society, we thank you and are grateful to you for all of your work, compassion and contributions to our specialty and are so pleased to honor you with the Society's highest honor, the Society for Pediatric Radiology's Gold Medal.

Marilyn J. Goske, MD, FACR

SPR 2019 GOLD MEDALIST

Marta Hernanz-Schulman, MD, FACR, FAAP

The Gold Medal of The Society for Pediatric Radiology is our most distinguished honor. The SPR Medal is awarded to pediatric radiologists who have contributed greatly to the SPR and our subspecialty of pediatric radiology as a scientist, teacher, personal mentor and leader.

"Leadership is the capacity to translate vision into reality"
– Warren Bennis

Marta Hernanz-Schulman, MD, FAAP, FACR, Professor of Radiology and Pediatrics, Chief of Pediatric Radiology at the Monroe Carell Jr. Children's Hospital at Vanderbilt has had a remarkable career as a leader, researcher and mentor. Her path to the field of medicine was challenging, but she took advantage of each curve that eventually led her to her success as a leader in quality and safety as well as a renowned expert in pediatric GI and GU imaging.

Marta was born in Cuba and came to the United States during the time of the Peter Pan airlift, between the Bay of Pigs invasion and the 1962 missile crisis. She was fortunate in being able to travel with her aunt who was able to join her two grown children in New York City; as others who left Cuba in similar circumstances, they were allowed to bring no physical possessions. Thus, at the young age of 10 speaking no English, Marta began her new life in the US with her aunt and cousins in Brooklyn, who worked several jobs in order to make ends meet. She attended fifth grade as an auditor, graduating from grammar school with a good command of the English language and a grade point average of 98+. Marta never saw her father again and was separated from her mother for over 8 years.

Coincident with Marta's start of High School at Bishop McDonnell Memorial, her cousins moved to Spain to continue their dreams of finishing medical school that they had begun in Cuba. At the end of her sophomore year, Marta left her school to spend a year in Salamanca with her aunt and cousins. She spent that year studying Spanish and French classics. That year her mother was able to leave Cuba for Spain and finally was reunited with her daughter.

Marta returned to Brooklyn after a year in Spain, and with the help of a teacher/mentor was able to complete her High School work within a three-year time span, and graduate with her classmates. The same mentor encouraged her to work toward her dream to become a physician and broaden her horizons beyond the immediate neighborhood by applying to the Ivy Leagues. Marta was accepted to Princeton in the first class of women. Upon graduation from Princeton, she attended medical school at NYU. As a freshman, she met her beloved husband Gerald Schulman, a fellow student. They married at graduation and stayed in NYC for residency – he to complete internal medicine and she to complete pediatrics at Mt Sinai Hospital. She finished her Pediatric residency and became Pediatric Board certification.

Marta began looking for options for specialization in Boston, as Gerry had accepted a fellowship in Nephrology at the Brigham. After weighing other options, she interviewed with the Radiology Chair at Boston University, Jerome H. Shapiro, who, impressed with her clinical credentials, accepted her on the spot, indicating that she could subspecialize in Pediatric Radiology at Boston Children's Hospital after her residency. She became Chief Resident at Boston University, and was subsequently chosen as Chief Fellow by John Kirkpatrick when she began her fellowship at Boston Children's. Her classmates included George Taylor, Fred Hoffer, and Stephen Done. Rita Teele, Ken Fellows, Thorne Griscom, Roy Strand, John Kirkpatrick and Bob Lebowitz were among her mentors and role models.

Gerry and Marta moved back to NYC, where Marta worked at NYU with Nancy Genieser and Mike Ambrosino, whom she considers colleagues and friends for life. During that time, Marta was responsible for radiology at Bellevue Hospital and integrated ultrasound into the Pediatric Radiology department. During her first year there, she received new faculty teacher award, and in the second year was named Teacher of the Year by the Pediatric house staff.

In 1988, Marta and Gerry were recruited to Vanderbilt, where Gerry became the Director of Dialysis and End Stage Renal Disease. The Chief of Pediatric Radiology at Vanderbilt, Richard M. Heller, welcomed Marta as a faculty member. She later became Chief of Pediatric Radiology, helping lead the department into a full service multimodality Department in a freestanding children's hospital. She helped build pediatric subspecialists in all areas, including Neuroradiology, MSK and IR, because "children deserve the best that we can provide." At

Vanderbilt within two years, she was promoted to Associate Professor with tenure, and became a full Professor five years later.

Marta's work with the SPR began early in her career. Bob Lebowitz and Joanna Siebert asked Marta to join the Publications Committee of the Society for Pediatric Radiology in 1994. Marta did a superb job renegotiating contracts with Springer and as Chair of the committee for two terms helped direct the searches that led to Tom Slovis and subsequently Peter Strouse to become Editors of *Pediatric Radiology*. She served as a member of the SPR Board of Directors from 1999-2002. Marta's work ethic and organizational skills resulted in numerous committee appointments including the Practice Standards, Bylaws, Finance, Program, and Corporate Relations, and was elected to a second term on the Board as Second Vice President in line to the presidency. During David Kushner's presidency she helped to reorganize the committee structures, and became the leader of the Clinical Practices Initiative from 2004-2007. She served as Vice President of the SPR Research and Education Foundation and as President and Chair of the Board of the SPR from 2007-2009.

Through her long career in the ACR, Marta has always worked towards the welfare of the pediatric patient, espousing the mission of the SPR. Marta began her ACR career on the Ultrasound committee at the invitation of Carol Rumack, and later worked with Marilyn Siegel on the DXIT In-Service examination, where she continues to chair the Pediatric section. As a member of the Pediatric Commission of the ACR, she chaired the Pediatric Committee on Guidelines and Standards (now Parameters) and in that role helped to develop the mechanism for the collaborative ACR-SPR guidelines used today. She has served in the Executive Committee of the Intersociety Conference, and the Ultrasound Accreditation Committee. During her time in the ACR she worked with other members, including the members of the Ultrasound Accreditation Committee and the Pediatric MR committee, to ensure that work done for children in pediatric hospitals is recognized during the accreditation process. She was a member of the Commission on Education and chaired the Skills Assessment Committee, of which the In-Service examination is a part. She succeeded Don Frush as the second Chair of the Pediatric Commission of the ACR, serving on its Board of Chancellors for six years. During that time, she contributed the perspective of the pediatric radiologists to the deliberations of the Board, and worked with pediatric radiologists, such as Richard Barth, in Advocacy for pediatric patients and pediatric radiologists through the ACR. She also served in the Fellowship Committee, the Honors Committee and the Audit committee of the ACR. As Chair of the Pediatric Commission, she also started and chaired the Pediatric Rapid Response Committee, which has created over 300 pediatric Appropriate Use Criteria (AUC) for use in pediatric computerized decision support. She currently serves as the elected Vice-President of the ACR within the Board of Chancellors, and as a member of its Executive Committee.

Marta has also been active in the ABR over the years, serving as a Board Examiner, contributing to exam development, and serving as the Chair of the Pediatric MOC Committee, receiving a Lifetime Achievement Award.

Marta was one of the first critical members of the Image Gently Campaign and its Steering Committee and led the incredibly successful "Pause and Pulse" fluoroscopy campaign. Marta understood the power and concept of Image Gently right away. Her campaign was well conceived, using marketing techniques (Pause and Pulse on radiation badges…her idea!) and organizing and creating web content, scientific papers, presentations and numerous collaborations. She spoke vividly and passionately at an FDA meeting on the need for radiation protection in fluoroscopy for children. This resulted in that campaign receiving recognition from an online publication for its reach and efficacy; the campaign and the pediatric radiologists who worked with Marta received the Minnies Award for Most Effective Philanthropy campaign in 2011. Marta was also one of the original founding members of the Image Wisely Campaign, asked by Dr. Richard Baron to represent the RSNA in the original discussions that resulted in Image Wisely.

Marta's energies have not been limited to committee leadership. As a researcher and scholar she has authored or co-authored over 140 peer reviewed articles, served as co-editor of Caffey's Pediatric Diagnostic Imaging, authored over 50 book chapters, clinical tapes and web courses, and given nearly 200 scientific presentations and invited lectures. She is currently a member of the Editorial Board of the journal *Pediatric Radiology*, and served for ten years in the Editorial Board of Radiology. She has been the recipient of 13 grants and has received awards for her work including the Caffey Award for Best Research in Pediatric Radiology.

Marta lost her beloved husband of 39 years, Gerald Schulman in 2016 to an unexpected illness. A Professor of Medicine he served as co-director of the Vanderbilt Clinical Trials Center. His compassionate and thoughtful care led to the establishment of the Gerald Schulman Lectureship by his trainees in his honor. Their son Alan in her own words "is her greatest personal achievement." They love to travel and remain close as he continues with his career in computer science.

"If you work hard enough and assert yourself, and use your mind and imagination, you can shape the world to your desires."
– Malcolm Gladwell

Through the many years of service, challenges and opportunities, Marta has never lost sight of her primary mission: "to provide the best possible care to all patients, to advance medical knowledge with the North Star of advancing and improving patient care, and placing the welfare of the patient above all other concerns." A true star, she serves as a unique role model for excellence, service, diversity and advocacy inspiring our specialty to reach for the stars as she has done so successfully.

Dorothy I. Bulas, MD, FACR, FAAP

SPR 2019 PIONEER AWARD

Pioneer Honorees were first acknowledged in 1990 as a means to honor certain physicians who made special contributions to the early development of our specialty. The Pioneer Award now honors individuals who have advanced pediatric radiology through innovation, forethought and leadership.

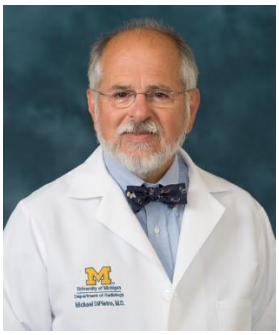

Michael DiPietro, MD, FACR

Meet Michael DiPietro the 2019 Pioneer Awardee of the SPR.

In 1984, while a junior staff member at The University of Michigan, CS Mott Children's Hospital, Mike introduced ultrasound of the spinal canal to the SPR and received the Caffey Silver Award. His subsequent contributions to neurosonography have led to our knowledge of Periventricular Leukomalacia (PVL), sonography of white matter including first report of the peri-trigonal echogenic blush and use of intraoperative ultrasound to evaluate Chiari I and II malformation. One of his most cited papers is the 1993 Radiology article "The conus medullaris: normal US findings throughout childhood". After decades of clinical experience and investigation including extensive presentations and publications, his accumulation of knowledge led to the co-authorship of the 2006 ACR Practice Guideline for Performance of an Ultrasound Examination of the Neonatal Spine. In 2007, he was part of the initiative to merge ACR/AIUM guidelines to the combined Guideline for Performance of Neurosonography. His work has had significant impact on the way neurosonography is practiced throughout the world. In fact, in 2012, he received one of two annual University of Michigan Medical School Dean's Lifetime Achievement Awards for Excellence in Clinical Care; the nomination was proposed by Neurosurgery.

But wait, isn't Mike DiPietro the Educator who received the SPR 2016 Singleton-Taybi Excellence in Education Award? And in 2009, the Jack O. Haller Award for Excellence in Teaching? He certainly is that person, known at the University of Michigan Medical School and Mott Children's Hospital for dedication to radiology education at all levels, including the pediatricians to whom he relates so effectively since he was one at Pittsburg Children's before coming to Pediatric Radiology by way of Yale (Residency) and Boston Children's (Fellowship). Among numerous awards and recognitions at Michigan was his 2005 naming as the Inaugural John F. Holt Collegiate Professor of Radiology.

Surely, you will want to meet Mike DiPietro the Producer/Director who as Co-Director of the Musculoskeletal Ultrasound Society has staged courses around the world. From Abu Dhabi to Singapore and Brazil to Israel the society's programs have fostered the development of musculoskeletal ultrasound for adults and children. MSUS courses are known for their balance of lecture and student "hands-on" scanning under the eyes of expert instructors. The dual projection of video patient scan and real time image display has become a standard for teaching musculoskeletal ultrasound.

Before you are finished, you should meet Mike DiPietro the musician. Lest you think this was not connected to his medical career, he once lectured on "Brains, bassoons, and other interesting things" as Visiting Professor at Boston Children's. His fascination with the double reed began after being "drafted" in elementary school. A love of music continued through high school and college (Union) but went through a hiatus in his early medical career. Pediatric radiologist Jack Lawson challenged him to return to the bassoon in 1987 and from then on lessons, practice and performance have been an important part of his life. U of M affiliated symphonies (including the University of Michigan Life Sciences Orchestra where he was the principal bassoonist and a founding member) benefit from his dedication to performing. Mike notes that whether teaching or presenting a lecture, one is communicating, just as one does when performing music or a play.

The many Mike DiPietros blend together to produce a man of academic competence, dedication to our subspecialty and most importantly to the children and families we serve. While small in physical stature and quietly humble in manner, Mike stands shoulder-to-shoulder with his mentors, who include such familiar names as Girdany, Oh, Young, Kirkpatrick and Holt. In addition, his education included contact with Drs. Caffey and Neuhauser, a claim few can make. How does he handle the many facets of his busy multi-persona life? … By talking and traveling with Alice, his wife of 45 years, and walking his often-photographed West Highland Terriers (Howie, Bertie and Robin).

H. Theodore Harcke, MD, FACR, FAIUM

SPR 2019 PRESIDENTIAL RECOGNITION AWARD

The Society bestows Presidential Recognition Awards on members or other individuals whose energy and creativity have made a significant impact on the work of the Society and its service to its members.

A. James Barkovich, MD

The SPR Presidential Recognition is awarded to A. James A Barkovich. This award recognizes his fantastic career and life-long contribution to the development and advancement of the subspecialty of pediatric neuroradiology. Numerous patients have benefited from his insightful and timely diagnoses. Our Society and our membership have benefited from all his teachings in prior SPR meetings and all his academic publications. His clinical and research works epitomize the mission of SPR: to foster excellence in the imaging care for pediatric patients.

James (Jim) grew up in the Bay area of San Francisco during the tumultuous time of the Vietnam War. He graduated from Redwood High School where he was an outstanding athlete as well as a student. He continued his education at U.C. Davis where he not only graduated Magna Cum Laude with a major in Chemistry but also was a two-year starter at point guard on the Division 1 varsity basketball team and a decathlete on the track team. Following graduation, Jim began work on a Ph.D. in Organic Chemistry at University of California at Berkeley. It was here that Jim met his future wife Karen. After less than 3 years, Jim had already passed his Oral Defense and had only to write up his dissertation. By then, however, he had been accepted to George Washington University School of Medicine and his career changed course.

Jim was accepted for an Army scholarship (rising to the rank of Major); and following graduation at GW, he began his Post Graduate training in Radiology at Letterman Army Medical Center in San Francisco. It was during his residency, which included rotations at UCSF Medical Center that he fell in love with Neuroradiology. In 1984, Jim began a two-year fellowship in Neuroradiology at the Walter Reed Medical Center in Washington, D.C. During his second year, Jim focused on Pediatric Neuroradiology; he spent time at The Johns Hopkins Hospital, Children's Hospital National Medical Center, and The Hospital for Sick Children in Toronto.

Following the completion of his fellowship, Jim returned to Letterman Army Medical Center to head up Neuroradiology while also having a joint appointment at UCSF in the section of Neuroradiology. Once his Army commitment had been fulfilled, Jim accepted a full-time faculty position at UCSF in 1989.

Jim brought the science to Pediatric Neuroimaging. He utilized the emerging imaging technology of magnetic resonance and his background as a scientist to combine the science of neurobiology and neuroembryology with imaging. He helped us to understand not just how the normal and abnormal pediatric brain and spine appear on imaging, but also how the brain and spine develop and why they appear the way they do.

Jim has achieved an exhaustive list of honors and awards over his distinguished career. Among them: the Founder, the President, and the first Gold Medal awardee of the American Society of Pediatric Neuroradiology, the President of the American Society of Neuroradiology, and the Chairman of the Board of Trustees, Neuroradiology Education and Research Foundation. He has served on numerous Editorial Boards and served on and chaired numerous international, national, regional, and local committees.

Jim has an astounding 465 publications. His paper titled, **CT and MR of profound perinatal and infantile asphyxia**, published in 1992 in the *American Journal of Neuroradiology* was named one of the 10 best neuroradiology papers of the century in 2000. His landmark textbook Pediatric Neuroimaging is in its sixth addition, a testament to the role it continues to play in our specialty. Jim has also won a number of teaching awards and has been an invited speaker in every continent of the globe. By a quick count on his CV, he has lectured in 28 different countries. As if all of this were not enough, Jim has somehow managed to find the time to coach Jr. League basketball and High School track. Some of his most enjoyable times came coaching the teams in which Karen and Jim's three sons played on.

Steven K. Sargent, MD
Taylor Chung, MD

SPR 2019 PRESIDENTIAL RECOGNITION AWARD

Patricia E. Burrows, MD

This SPR Presidential Recognition is awarded to Patricia E. Burrows. This award recognizes her fantastic career and life-long dedication to the image-guided treatment of patients, in particular, with vascular malformations and hemagiomas, and patients with cardiovascular and neurovascular diseases. Besides numerous patients whom she has positively altered their lives, our Society and our membership have also benefited from all her teachings at past SPR meetings and her numerous academic publications. Her clinical and research works epitomize the mission of SPR: to foster excellence in pediatric health care through imaging and image-guided care.

Pat grew up in southern Manitoba, Canada, and received her MD at the University of Manitoba Faculty of Medicine in 1976. She started in a pediatric residency but switched to radiology after 1 year and completed her residency in Winnipeg, Manitoba in 1981. She completed a fellowship in pediatric radiology at Winnipeg Children's Hospital, under the mentorship of Martin Reed and Rod McPherson. She enjoyed doing extra angiography during her residency, as well as a rotation in the cardiac Cath Lab at Children's Hospital. This led to a second fellowship in what was called "pediatric special procedures" including congenital heart disease, angiography, and neuroradiology at Children's Hospital Boston, Harvard Medical School in 1982. She was assigned a research project correlating angiographic findings with John Mulliken's new classification of vascular anomalies.

After her fellowship, she moved with a group of cardiovascular surgeons to Arkansas Children's Hospital in Little Rock. This was short-lived because of her immigration status and she took a position at The Hospital for Sick Children's Hospital in Toronto in 1983, as head of cardiac radiology. She performed pediatric cardiac catheterizations and cardiac interventions and developed pediatric cardiac MRI locally. She continued practicing general pediatric radiology and angiography and then became involved in pediatric neuroimaging. While in Toronto, she met Pierre Lasjaunias, a French neuro- interventionalist who was recruited to train the neuroradiologists at the Toronto Western Hospital in neuro-interventional techniques. Lasjaunias agreed to train Pat in Paris and she spent seven months with him in 1985 to 86 where she learnt learned even more about vascular anomalies, neurovascular anatomy and interventional techniques. In this pre-micro catheter era, she modified the adult techniques for the pediatric patients including embolization of arteriovenous fistula using detachable balloons, coils and glue, as well as ethanol and sodium tetradecyl sulfate sclerotherapy for venous and lymphatic malformations. She also had the opportunity to work with Dr. Colapinto and subsequently published the first series of pediatric trans-jugular liver biopsies and the first case report of embolization for pediatric traumatic priapism. She was also the first person to use platinum fiber micro coils in Canada and the first to perform renal artery stenting (with Chet Rees) in a child.

In 1994, Pat was recruited to Boston Children's Hospital as chief of Pediatric Interventional Radiology. With this move, she decided to give up cardiac imaging in order to focus on vascular anomalies. With John Mulliken, plastic surgeon, and Judah Folkman, vascular scientist, Pat was a cofounder and subsequent codirector of the Vascular Anomalies Center [VAC] at Boston Children's Hospital. She realized very early on the importance of a multidisciplinary team for optimizing both the work-up and the therapeutic alternatives in the field of vascular congenital anomalies. This VAC became the model for many other institutions for the treatment of patients with vascular anomalies. Her motto in congenital vascular anomalies was straight forward "you cannot treat if you don't understand the lesion".

She became a member of the International Society for the Study of Vascular Anomalies [ISSVA] in 1994, and served on the Board of Directors from 2006 to 2014, and as president from 2010 to 2012. While in Boston, Pat began using doxycycline to treat cystic lymphatic malformations and subsequently showed that it was safe and effective to use in infants. She trained many fellows and residents, and two of them, Ahmad Alomari and David Lord, went on to direct Vascular Anomalies programs themselves.

In 2006, Pat left Boston Children's after 13 years and joined Alejandro Berenstein at his vascular anomalies center in Roosevelt Hospital in New York City. This was a very fruitful relationship. Missing the pediatric culture of large children's hospitals, Pat decided to relocate to Houston, Texas, as chief of pediatric interventional radiology at Texas Children's Hospital, Baylor College of Medicine in 2009. She also spent one year at Memorial Hermann Hospital in Houston, University of Texas. In 2012, Pat relocated to Children's Hospital of Wisconsin, Medical College of Wisconsin in Milwaukee, with plans to be more involved in translational research. During the her six years in Milwaukee, Pat joined forces with Kelleigh's Cause to carry out some basic research. The organization ultimately funded a Pediatric

Radiology based postdoctoral fellowship in vascular anomalies research under the direction of Dr. Ramani Ramchandran, head of developmental vascular biology. This program resulted in new observations of the role of endothelial cilia in vasculogenesis which were recently published, as well as a zebrafish model for AVM being used for drug screening. Pat retired on August 31, 2018 and has relocated to St. Petersburg, Florida. Upon retirement, Pat received Congressional tribute for all her contributions in advancement and discovery of new knowledge in the field of vascular malformations from the 8th Congressional district of Michigan. Besides numerous visiting professorships and keynote addresses which she cherishes, Pat is most proud of her many key publications in vascular anomalies and also of her namesake for the chair in Pediatric Interventional Radiology and Vascular Anomalies at Children's Hospital Boston.

She enjoys spending her time with her spouse, Jay, sharing their passion for sailing. When she is on land, she enjoys gardening and has become an excellent potter in the past 7 years! From handling and steering that tracker catheter anywhere in all large and small vessels from head to toe, Pat is bringing her concentration and dexterity to pottery and may all potters beware!!!

Taylor Chung, MD
Joséee Dubois, MD

SPR 2019 HONORARY MEMBER

The Society extends Honorary Membership to individuals outside of the SPR who have made outstanding contributions to the care of children.

Omolola (Monica) Atalabi, MD

"I had a destiny to fulfill"

Dr. Omolola Mojisoloa Atalabi (Monica) is one of only a few pediatric radiologists practicing in Africa. Her remarkable story begins in Nigeria where she was born and raised. Through sheer will and the support of family and mentors, she has become a strong advocate and leader shining a light on the vast imaging needs of the children she serves.

The eldest of a family of six children, Monica's father, David Daramola, was a typist in a hospital in Akure, Nigeria while her mother, Agnes, despite no formal education, encouraged her daughter to complete school. Being the eldest, Monica was initially sent to her paternal grandmother to be raised. There she was happily doted on, but was also told by her grandmother that she must study hard. Unbeknown to Monica, years prior, her father broke his arm when growing up. Her grandmother saw his X-ray and was fascinated with the technology. She hoped her son (Monica's father) would one day become a pediatric radiologist. Not aware of this story until years after she already had chosen radiology as a specialty, Monica truly believes she had a destiny to fulfill!

Her grandmother died when Monica was 7 and she returned to her parents' home. While her father assumed she would marry and did not need to complete high school, her mother continued to push her to continue her studies.

At 18, Monica met her soon to be husband Femi Atalabi, a physician. Unusual for that time, he supported her interest in schooling. She had her first son at age 20 and second son at age 21. Femi was accepted to an OB GYN residency in Edinburgh and they moved to the United Kingdom. Her mother helped support caring for her children while she went back full time to Cranley School for Girls in Edinburgh Scotland. There she completed her physics requirements. Following the birth of her daughter, she applied to medical school and returned to Nigeria to begin her 6 years of training at the University of Ibadan. When asked what specialty she was interested in she stated she had a burning desire to enter radiology. She hoped to focus on breast imaging but to her dismay, there was only an opening in pediatrics. It was then that she learned of her deceased grandmother's fascination in pediatric radiology so her destiny was set.

Eager to be the best, she applied for an RSNA Derek Harwood Nash International Fellowship. In 2007, Dr. Atalabi was accepted to go for three months to Boston Children's Hospital. There she met many inspiring radiologist particularly George Taylor who took her under his wing. She wrote several papers with Drs. Taylor and Ed Lee and returned to Nigeria motivated to focus on pediatrics and inspire others to share her enthusiasm for this specialty.

Understanding the importance of growing radiology expertise in Nigeria, Monica became active in numerous societies including leadership roles in the Medical Women Association of Nigeria, Association of Radiologists of West Africa, AAWR, SPR, Pediatric Oncology Society of Nigeria, West African College of Surgeons, RSNA International Advisory Committee, and RSNA Committee for Middle East and Africa. She developed a curriculum for pediatric radiology and serves as an examiner for the National Post Graduate Medical College of Nigeria and West African College of Surgeons.

Dr. Atalabi helped found the Society of Pediatric Imaging in Nigeria (SPIN) and became President of the African Society of Pediatric Imaging in 2015 with the encouragement of Savvas Andronikou. She became a member in council of the World Federation of Pediatric Imaging in 2012 and currently serves as its President.

Dr. Atalabi is a cherished teacher and mentor, encouraging her students to travel and take every opportunity to learn. She has published over 66 articles and 2 chapters including many of her trainees as coauthors. A wonderful role model, she teaches the importance of stretching

oneself, pushing forward against all odd s, recognizing opportunities rather than limitations. She was promoted to the post of Professor of radiology in the Premier University of Ibadan in Nigeria in September 2018.

Monica lost her husband 20 years ago. Her mother, Agnes, remained a staunch advocate helping care for her children throughout her career, and is deeply missed since her passing in 2014. Monica's children Tola, Tomoye and Tutu are successfully independent with two grandchildren thriving in the UK.

Monica has received many awards for her multiple accomplishments and inspiring work ethic. Invited to come to the SPR in San Francisco in 2010 as a Heidi Patriquin International Fellow, she got a standing ovation for her presentation on the limited imaging resources children face in Africa. This moving talk helped galvanize support for WFPI outreach, which was in its infancy. It is very fitting that Dr. Atalabi will be awarded the SPR Honorary Membership in San Francisco this year for her wonderfully effective advocacy.

Dorothy I. Bulas, MD, FACR, FAAP

SPR 2019 HONORARY MEMBER

Kushaljit S. Sodhi, MD, PhD, MAMS, FICR

Professor Dr. Kushaljit Singh Sodhi is a pediatric radiologist and a leader among Indian radiologists. He is a Professor of Radiology at the Postgraduate Institute of Medical Education and Research (PGIMER) in Chandigarh, India, which is one of Asia's premier medical institutions.

Dr. Sodhi received his medical degree from Government Medical College, Patiala in India in 1996, and he did his Radiology residency at Dayanand Medical College Hospital in Ludhiana, India. He joined PGIMER following his residency as a senior resident/fellow, and was subsequently appointed as a faculty member in 2003, and promoted to Associate Professor at the institute in 2006. Following this, in 2007, Dr. Sodhi completed a fellowship at the renowned Royal Children's Hospital in Melbourne, Australia.

After his return to India, he started to accelerate the pace of his research and education endeavors in the field of pediatric radiology. His prolific research output has resulted in more than 190 papers in peer-reviewed journals and 12 chapters in leading pediatric radiology textbooks. His most prominent work is in establishing use of MRI of the lungs for pediatric patients, which was also the focus of his PhD. He is a member of several editorial committees of Indian and international medical journals. He has received multiple national and international awards recognizing his work including the Young Investigators Scholarship from the Asia Oceania Congress of Radiology in 2008 and the very prestigious Heidi Patriquin Fellowship Award in 2011 from the SPR.

Dr. Sodhi has worked tirelessly to ensure safer imaging of children in the Indian subcontinent and is a staunch proponent of the Image Gently campaign. He has furthered pediatric radiology education and research in India, the Asia Oceania region and other parts of the world for the last decade. He helped establish a pediatric radiology fellowship in his institute, which was amongst the first in the Indian subcontinent. More recently, he worked with the WFPI to establish a new three-month fellowship in India starting in April 2019.

His leadership and organizational skills have been carefully honed over the years organizing several radiology conferences in India and the Asia Oceania region. Most recently, this was evident in his role as the organizing secretary of the Asian Oceanic Society of Pediatric Radiology annual meeting in Chandigarh last year, which had an attendance of more than 750 delegates, the largest number in its history.

Dr. Sodhi currently serves as executive committee member of the World Federation of Pediatric imaging (WFPI). He is regarded as a world leader in the campaign against pediatric tuberculosis and he recently took over as the leader of the tuberculosis group at the WFPI. He serves as the current Treasurer for the Asian and Oceanic Society for Paediatric Radiology (AOSPR) and as the Secretary of the Indian Society of Paediatric Radiology (ISPR).

Dr. Sodhi has lectured as an invited visiting professor at hospitals around the world including leading North American institutions like Lurie Children's Hospital in Chicago and the world-renowned Hospital of Sick Children in Toronto.

At home, Dr. Sodhi is happily married to Dr. Shanujeet Kaur, an obstetrician, and they are blessed with a set of multi-talented teenager twin sons, Arhanjit and Arnavjit.

We are proud to recognize Dr. Sodhi's many academic, educational and organizational contributions to our field, his work as an ambassador for pediatric imaging in the Asia Oceania region, and bestow him with an honorary membership of the SPR.

Sanjay P. Prabhu, MD

SPR 2019 JACK O. HALLER – THOMAS L. SLOVIS AWARD

This award is given in memory of Jack O. Haller and Thomas L. Slovis who both excelled as educators, and mentors. Their abilities and enthusiasm stimulated many young medical students and residents to pursue pediatric radiology. This award is given to an individual who has demonstrated evidence of outstanding ability to educate trainees (medical student, resident and fellow) who has shown sustained substantial excellence in mentorship skills.

Mahesh M. Thapa, MD

Mahesh Thapa attended the University of Las Vegas as an undergraduate, earning a degree in Biological Chemistry. He then obtained his M.D. at the Keck School of Medicine at USC in Los Angeles.

After a year of internship in Las Vegas, he began a Diagnostic Radiology Residency at the University of Washington in 2000. This was followed by a Fellowship in Pediatric Radiology at Seattle Children's Hospital, then led by Eric Effmann. He was heavily influenced by the faculty, especially David Brewer and Ed Weinberger, and opted to join the group in 2006.

Once on faculty, Mahesh quickly established himself as an enthusiastic creative medical educator. He took part in the University of Washington Teaching Scholar program in 2008. Over five years, Mahesh acted as the chair of the first year Medical Student Radiology/Anatomy Correlation course at the University of Washington, working with John Clark, the Chair of the Department of Biological Structure, providing classroom instruction to first year medical students using software such as Osirix, Keynote, PowerPoint, and QuickTime. He enlisted many of the younger pediatric radiology faculty in this effort, and the course was extremely well received by the medical students while simultaneously introducing the discipline of pediatric radiology to entire medical student classes at the earliest stages of their careers.

The ability to blend a wide variety of technologic advances into educational innovation has always been a hallmark of Dr. Thapa's success. Early on, he developed an obsession with digital photography as a hobby, with his Instagram skills competing with and complementing his abilities as a radiology educator, (@starvingphotographer; 270,000 followers). He continues to provide invited talks at the RSNA, AUR, and SPR on the effective use of technology in education. In 2008, he helped to develop a PowerPoint plug-in to facilitate image stack scrolling and demonstrated how to use common tools such as PhotoShop and Podcasting in the pursuit of greater educational impact. He also initiated a monthly SPR multi-site conference along with Carl Merrow at Cincinnati Children's Hospital; focused on pediatric musculoskeletal imaging, providing subspecialists worldwide an opportunity to consult on challenging cases and learn from their peers (https://www.pedrad.org/Specialties/MSK/Multi-site-Pediatric-MSK-Conference).

Mahesh has extended his influence by serving as an active visiting faculty in California, New York, Ohio, Georgia, and Massachusetts, also travelling internationally to Mexico, Australia, and Canada to speak on pediatric musculoskeletal techniques and educational technology. At times, this includes hands-on workshops in ultrasound-guided musculoskeletal procedures. His easy confidence and positive attitude are highly infectious and lends to his great success and popularity as an instructor.

He thrives on mentoring his colleagues, including our junior faculty, all while working with clinical colleagues on challenging cases and research projects. For many years, he has served our department as a member of the Faculty-Residency Mentorship Committee and for several years as the Program Director for our Pediatric Radiology Fellowship.

Over his career, he has authored 48 peer-reviewed publications, served as co-editor for several books, and given 65 invited educational and scientific talks. Mahesh is a reviewer for multiple journals - *Pediatric Radiology*, *Radiology Case Reports*, the *American Journal of Roentgenology*, and serves on the Editorial Board and as Deputy Editor for *Academic Radiology*.

Dr. Thapa has been a member of the ABR, authoring questions for graduating trainees and CAQ certification. Nationally, he has served on the RSNA and SPR Education Committees, the SPR Website and Musculoskeletal Committees, and over the past decade he has been very active in the Alliance of Clinician-Educators in Radiology (ACER), serving as president in 2014-2015, and receiving the ACER Achievement Award in 2017.

Mahesh also recently served as a Co-Director for the Postgraduate Courses during the 2018 Society for Pediatric Radiology Annual Meeting. He frequently serves as a Committee Co-Chair for the University of Washington's Annual Emergency Radiology Course and will also be part of the Organizing Committee for the Sunrise Sessions for IPR 2020 in Rome.

The Jack O. Haller Award is a tremendous honor that appropriately acknowledges Dr. Thapa's unmatched enthusiasm, creativity, and genuine interest in fostering the next generation of pediatric radiologists.

Randolph K. Otto, MD

HEIDI PATRIQUIN AWARD

In recognition of Dr. Patriquin's commitment to international education, this fellowship is designed to subsidize the expenses of one Pediatric Radiologist per year who practices outside of North America.

Fathia Omer Salah, MD
Black Lion Hospital, Addis Ababa, Ethiopia

HEIDI PATRIQUIN AWARD

Sundar Suwal, MD
University Teaching Hospital, Maharajgunj, Kathmandu, Nepal

JOHN P. CAFFEY AWARDS

John P. Caffey, MD, 1895-1978

Dr. John P. Caffey was regarded throughout the world as the father of pediatric radiology. His classic textbook, "Pediatric X-Ray Diagnosis", which was first published in 1945, has become the recognized bible and authority in its field. The seventh edition of this book was completed several months before his death in 1978. It has been among the most successful books of its kind in the medical field.

Dr. Caffey was born in Castle Gate, Utah on March 30, 1895. It is interesting that he was born in the same year that Roentgen discovered the x-ray. Dr. Caffey was graduated from University of Michigan Medical School in 1919, following which he served an internship in internal medicine at Barnes Hospital in St. Louis. He spent three years in Eastern Europe with the American Red Cross and the American Relief Administration, and returned to the United States for additional training in medicine and in pediatrics at the Universities of Michigan and Columbia, respectively.

While in the private practice of pediatrics in New York City at the old Babies Hospital of Columbia University College of Physicians and Surgeons, he become interested in radiology and was charged with developing a department of pediatric radiology in 1929. He frequently expressed appreciation and admiration for Ross Golden, Chairman of Radiology at Columbia Presbyterian Hospital, who allowed him to develop a separate department of diagnostic radiology without undue interference, and who was always available to help and advise him.

Dr. Caffey's keen intelligence and inquiring mind quickly established him as the leader in the fields of pediatric x-ray diagnosis, which recognition became worldwide almost instantaneously with the publication of his book in 1945.

Dr. Caffey received many awards in recognition of his achievements. Outstanding among these were the Mackenzie Davidson Medical of the British Institute of Radiology in 1956, the Distinguished Service Award of the Columbia Presbyterian Medical Center in 1962, the Outstanding Achievement Award of the University of Michigan in 1965, the Howland Award of the American Pediatric Society in 1967, the Jacobi Award of the American Medical Association in 1972, and the Gold Medal Award of the American College of Radiology in 1975. He had been a member of the American Journal of Roentgenology. He was a counselor of The Society for Pediatric Radiology and was an honorary member of the European Society of Paediatric Radiology.

Dr. Caffey's contributions to the pediatric radiologic literature were many. He was instrumental in directing attention to the fact that a prominent thymic shadow was a sign of good health and not of disease, an observation that literally spelled the end to the practice of thymic irradiation in infancy. Infantile cortical hyperostosis was described by him and is called "Caffey's Disease". Dr. Caffey in 1946 first recognized the telltale radiographic changes that characterize the battered child, and his students helped disseminate his teachings about these findings. It was Dr. Caffey who first recognized and descried the characteristic bony changes in vitamin A poisoning. He recognized and described the findings associated with prenatal bowing of the skeleton.

In 1963, 3 years after his retirement from Babies Hospital, he joined the staff of the Children's Hospital of Pittsburgh as associate radiologist and as Visiting Professor of Radiology and Pediatrics at the University of Pittsburgh School of Medicine. Although Dr. Caffey came to Children's Hospital and the University of Pittsburgh in an emeritus position, he worked daily and on weekends throughout the years he was there. In Pittsburgh, he made four major new contributions to the medical literature. He described the entity, "idiopathic familial hyperphosphatasemia". He recognized and described the earliest radiological changes in Perthes' Disease. He called attention to the potentially serious effects of shaking children, and used this as a subject of his Jacobi Award lecture. He described, with the late Dr. Kenny, a hitherto unrecognized form of dwarfism, which is now known as the Caffey-Kenny dwarf. The John Caffey Society, which includes as its members pediatric radiologists who have been intimately associated with Dr. Caffey, or who have been trained by his students, was established in 1961. This society is now among the most prestigious in the field of radiology. His book and the society named in his honor will live on as important memorials to this great man.

His greatness was obvious to all who worked with him. He was warm, kind, stimulating, argumentative, and above all, honest in his approach to medicine and to x-ray diagnoses. His dedication to the truth was expressed in his abiding interest in the limitations of x-ray signs in pediatric diagnosis and in his interest in normal variation in the growing skeleton. He was concerned with the written and spoken word and was a skilled semanticist. His book and his articles are masterpieces of language and construction. He stimulated and was stimulated and loved by all who had the privilege of working with him. Radiology and Pediatrics have lost a great man, but they shall ever have been enriched by his presence.

Bertram R. Girdany, MD

JOHN P. CAFFEY AWARD PAPERS (1969-1998)

1969- Pneumonia of Atypical Measles: Residual Nodular Lesions; Young LW, Smith DI, Glasgow LA.

1970- Plain Skull Roentgenograms in Children with Head Trauma; Roberts F, Shopfner CE.

1971- Vascular Thromboembolism Complicating Umbilical Artery Catheterization; Williams HJ, Jarvis CW, Neal WA, Reynolds JW.

1972- Hydrometrocolpos in Infancy; Reed MH, Griscom NT.

1973- Various Radionuclide Patterns of Cerebral Inflammation in Infants and Children; Gilday DL.

1974- The Tethered Filum; Fitz CR, Harwood-Nash DC.

1975- B-Mode Ultrasound and the Nonvisualizing Kidney in Pediatrics; Shkolnik A.

1976- The Pediatric Tracheostomy: Roentgen Signs of Normal Healing and Complications-The Value of Xerography; Scott JR, Kramer SS.

1977- A Prospective Study of Intraventricular Hemorrhage in Premature Newborns Using Computed Tomography; Burstein J, Papile L, Burstein R.

1978- Chemotherapy-Induced Inhibition of Compensatory Renal Growth in the Immature Mouse; Moskowitz PS, Donaldson SS.

1979- Lithiasis Due to Interruption of the Enterohepatic Circulation of Bile Salts; Kirks DR.

1980- Cranial Ultrasound Findings in Patients with Meningomyelocele; Babcock DS, Han BK.

1981- Effect of Contrast Agents in the Lungs of Animals; McAlister WH, Siegel MJ, Shackelford GD, Glasier CH, Askin FB.

1982- Real-Time Ultrasonographic Detection of Vesicoureteral Reflux in Children; Kessler RM, Altman DH.

1983- Ultrasonic Evaluation of Caudal Spine Anomalies in Children; Naidich TP, Fernbach SK, McLone DG, Shkolnik A.

1984- Experimental Neonatal Intraventricular Hemorrhage: Clinical Radiographic and Pathologic Features; Goske MJ, Morin FC, Eskin TA.

1985- The Metaphyseal Lesion in Abused Infants: A Radiologic? Histopathologic Study; Kleinman PK, Marks SC, Blackbourne BD.

1986- Magnetic Resonance Appearance of Blood and Blood Products; Cohen MD, Smith JA, Cory DA.

1987- Intussusception Reduction by Rectal Insufflation of Air; Gu L, Alton DJ, Daneman A, Stringer DA, Liu P, Wilmot DM, Reilly BJ.

1988- MR Imaging Determination of the Location of the Conus Medullaris in Normal Children and in Children with Tethered Cord Syndrome; Wilson DA, Prince JR.

1989- Early Avascular Necrosis: MRI and Histological Examination in an Animal Model; Brody AS, Strong M, Babikian G, Seidel FG, Kuhn JP.

1990- Determination of Functional Residual Capacity from Digital Radiography in an Animal Model of the Neonatal Chest; White KS, Muelenaer AA, Beam CA, Effmann EL.

1991- Juvenile Colonic Perforation: Experimental Results and Clinical Applications; Shiels II WE, Keller GL, Ryckman FR, Daugherty CC, Specker BL, Kirks DR, Summa DW.

1992- Pulmonary oxygen toxicity: Experimental assessment of capillary leakiness using contrast-enhanced MRI; Brasch RC, Berthezene Y, Vexler V, Shames DM, Jerome H, Clément O, Mühler AR, Kuwatsuru R.

1993- High Resolution CT Assessment of Bronchoconstriction: Differential Effects of Methacholine and Histamine; Kramer SS, Hoffman EA, Amirav I.

1994- Inhibition of Neutrophil Phagocytosis by Barium Sulfate; Hernanz-Schulman M, Hakim RM, Schulman G, Vanholder R.

1995- Evaluation of Perfusion of the Normal and Ischemic Cartilaginous Epiphysis by Using Gadolinium-enhanced MR Imaging; Jaramillo D, Shapiro F, Villegas OL, Mulkern RV, Doty D, Dwek J.

1996- The Detection of Pulmonary Metastases with Pathological Correlation: Effect of Breathing on the Accuracy of Spiral CT. Coakley FV, Cohen MD, Waters D, Davis MM.

1997- MR Imaging Microvessel Permeability Correlates with Pathologic Tumor Grade; Brasch RC, Daldrup HE, Shames DM, Rosenau W, Okuhata Y, Wendland, MF.

1998- Imaging Acute Heart and Lung Transplant Rejection in Rats by Using Tc-99m -radiolabeled Annexin V; Blankenberg FG, Vriens, P, Robbins RC, Ohtusuki K, Tait JF, Strauss HW.

JOHN P. CAFFEY AWARD FOR BEST BASIC SCIENCE RESEARCH PAPER

1999- Changes in Renal Blood Flow Depicted with Contrast-enhanced Harmonic Imaging During Acute Urinary Obstruction; Claudon, M, Barnewolt, CE, Taylor, GA, Dunning, PS, Gobet, R, MD; Badawy, A.

2000- Detection of Early Atherosclerosis with Radiolabeled Monocyte Chemoattractant Protein-1 in Prediabetic Zucker Rats; Blankenberg FG, Tait, JF, Strauss, HW, Valentine HA.

2001- Computer-Simulated Radiation Dose Reduction For Pediatric Abdominal Helical CT, Frush, D, Slack,CC, Hollingsworth, CL, Bisset III,GS, Donnelly, LF, Hsieh,Jl

2002- Understanding the Functional Angiogenic Process in an Antigen-Induced Arthritis Model: Correlative BOLD MR Imaging (fMRI) of the Stages of Synovitis along the Time Course of the Disease; A. S. Doria, MD , Diagnostic Imaging, Hospital for Sick Children, Ontario, P.S. Babyn, MD, A. Crawley, PhD, M. Noseworthy, PhD, K. Pritzker, MD, R. B. Salter, MD, et al

2003- A Novel Method for Non-Viral Gene-Therapy: Transcatheter Hydrodynamic Delivery Using Isolated Liver as a Depot Organ In a Rabbit Model; Kevin Baskin, MD, Children's Hospital of Philadelphia, PA, Simon J. Eastman, PhD; Ronald K. Scheule, PhD; Bradley L. Hodges, PhD; Qiuming Chu, MS; Richard B. Towbin, MD

2004- Site-Specific Induction of Lymphatic Malformations in a Rat Model for Image-Guided Therapy; Robert F. Short, MS, Department of Radiology, Children's Radiological Institute, Children's Hospital, Columbus, OH; William E. Shiels, DO; Thomas J. Sferra, MD; Katherine Nicol, MD; Minka Schofield, MD; Gregory Wiet, MD

2005- Quantitative Measurement of Microbubble Ultrasound Contrast Agent Flow To Assess the Efficacy of Angiogenesis Inhibitors In Vivo; Beth McCarville, MD, Dept of Rad Sciences, St. Jude Children's Research Hosp, Memphis, TN; Christian Streck, MD; Chin-Shang Li, PhD; Andrew Davidoff, MD

2006- 4Cu-Immuno-PET Imaging of Neuroblastoma with Bioengineered Anti-GD2 Antibodies; Stephan D Voss, MD, PhD, Radiology, Children's Hospital Boston, Harvard Medical School, Boston, MA; Suzanne V Smith, PhD; Nadine M Di Bartolo, PhD; Lacey J McIntosh; Erika M Cyr; Ali A Bonab, PhD, et. al.

2007- MR Imaging of Adenocarcinomas with Folate-Receptor Targeted Contrast Agents; Heike E Daldrup-Link, MD, PhD, Radiology, University of California San Francisco, San Francisco, CA; Zhen J Wang, MD; Reinhard Meier, MD; Claire Corot, PhD

2008- Evaluation of Quality Assurance Quality Control Phantom for Digital Neonatal Chest Projection Imaging; Steven Don, MD, Mallinckrodt Institute of Radiology, Washington University School of Medicine

2009- Faster Pediatric MRI Via Compressed Sensing - Shreyas Vasanawala, Stanford University, Marcus Alley, Richard Barth, Brian Hargreaves, John Pauly, Michael Lustig

2010- Clinical Evaluation of Readout-Segmented-EPI for Diffusion-Weighted Imaging – Roland Bammer, PhD, Stanford University, Palo Alto, CA, Samantha J Holdsworth, PhD;Stefan Skare, PhD; Kristen Yeom, MD; Patrick D Barnes, MD

2010- High-Resolution Motion-Corrected Diffusion-Tensor Imaging (DTI) in Infants – Stefan T Skare, PhD, Stanford University, Stanford, CA; Samantha J Holdsworth, PhD; Kirsten Yeom, MD; Patrick D Barnes, MD; Roland Bammer, PhD

2010- 3D SAP-EPI in Motion-Corrected Fast Susceptibility Weighted Imaging (SWI) – Roland Bammer, PhD, Stanford University, Palo Alto, CA, Samantha J Holdsworth, PhD; Stefan Skare, PhD; Kristen Yeom, MD; Patrick D Barnes, MD

2010- T1-Weighted 3D SAP-EPI for Use in Pediatric Imaging – Roland Bammer, PhD, Stanford University, Palo Alto, CA, Samantha J Holdsworth, PhD; Stefan Skare, PhD; Kristen Yeom, MD; Patrick D Barnes, MD

2011- An MR System for Imaging Neonates in the NICU, Jean Tkach, Randy Giaquinto, Wolfgang Loew, Ronald Pratt, Barret Daniels, Blaise Jones, Lane Donnelly, Charles Dumoulin, Cincinnati Children's Hospital Medical Center

2012- Advantages of a Nanoparticle Blood Pool Contrast Agent Over Conventional Intravascular Glomerular-Filtered Contrast Agents for Pulmonary Vascular Imaging; Ananth Annapragada, Texas Children's Hospital, R. Paul Guillerman, Eric Hoffman, David Kaczka, Ketan Ghaghada, Cristian Badea

2013- Psychometric Function: A Novel Statistical Analysis Approach to Optimize CT Dose: Steven Don, MD, Mallinckrodt Institute of Radiology, St. Louis, MO,Bruce Whiting, David Politte, Parinaz Massoumzadeh, Charles Hildebolt

2014- No longer a holiday: Improving the pediatric radiology elective for medical students and pediatric housestaff Eddie Hyatt, Vanderbilt University, Department of Radiology and Radiological Sciences, Nashville, TN, Cody Penrod, Sudha Singh, Jayne Seekins, DO, Amy Fleming, Melissa Hilmes, MD

2015- Gonad Shields: Good or Bad for Patient Radiation Exposure?; Summer L. Kaplan, MD, Department of Radiology, The Children's Hospital of Philadelphia, Philadelphia, PA, Dennise Magill, MS, Marc A. Felice, MS, Sayed Ali, MD, Xiaowei Zhu, MS

2016- In vivo Profiling of Folate Receptor Expression in Rat Placenta Using MR Molecular Imaging; Ketan Ghaghada, PhD, Zbigniew Starosolski, PhD, Eric Tanifum, PhD, Haijun Gao, PhD, Igor Stupin, MD, PhD, Saakshi Bhayana, BS, Chandresh Patel, BS, Chandrasekhar Yallampalli, DVM, PhD, Ananth Annapragada, PhD, Texas Children's Hospital, Houston, TX

2017- Performance of a Deep Neural Network Learning Model in Assessing Skeletal Maturity on Pediatric Hand Radiographs; David B. Larson, MD, MBA, Matthew C. Chen, Matthew P. Lungren, MD, MPH, Safwan S. Halabi, MD, Nicholas V. Stence, MD, Curtis P. Langlotz, MD, PhD Radiology, Stanford University, Stanford, CA University of Colorado, Aurora, CO

2018- Feed and Wrap MRU; Sila Kurugol, PhD, Radiology, Boston Children's Hospital and Harvard Medical School, Onur Afacan, PhD, Catherine Seager, MD, Reid Nichols, Richard S. Lee, MD, Simon K. Warfield, PhD, Jeanne S. Chow, MD

JOHN P. CAFFEY AWARD FOR BEST CLINICAL RESEARCH OR EDUCATION PAPER

1999 - Triangular Cord Sign in Biliary Atresia: A Gold Standard for the Millennium? Tan Kendrick AP, Phua, KB, Subramaniam, R.

2000 - Cisterna Magna Thrombus and Subsequent Posthemorrhageic Hydrocephalus. Cramer BC, Walsh EA.

2001 - Aneurysmal Bone Cysts In Children: Percutaneous Sclerosing Therapy, An Alternative To Surgery. Dubois J, Garel LA, Rypens FF, Grimard G, Isler, M, Mercier C

2002 - MR Imaging of Kidneys: Functional Evaluation Using F-15 Perfusion Imaging, Grattan-Smith D, Jones RA; Little S, Perez M, Kirsch A

2003 - Differential Regurgitation in Branch Pulmonary Arteries after TOF Repair. Yoo SJ, Kang IS, Redington A, Benson LN; Macgowan CK; Valsangiacomo ER

2004 - Feasibility of a Free-Breathing SSFP Sequence for Dymanic Cardiac Imaging in Pediatric Patients. Krishnamurthy, R, Muthupillai R, Vick G, Su J, Kovalchin J, Chung T; Diagnostic Imaging, Texas Children's Hospital, Houston, TX

2005 - Evaluation of High Resolution Cervical Spine CT In 529 Cases of Pediatric Trauma: Value Versus Radiation Exposure. Shiran, D, Jimenez, R, Altman, D, DuBose, M, Lorenzo, R

2006 - Alterations in Regional O2 Saturation (StO2) and Capillary Blood Volume (HbT) with Brain Injuries and ECMO. P Ellen Grant, MD, Pediatric Radiology, Massachusetts General Hospital, Boston, MA; George Themelis; Kara Arvin, MD; Sonal Thaker; Kalpathy K Krishnamoorthy, MD; Maria Angela Franceschini, PhD

2007 - Evaluation of Single Functioning Kidneys Using MR Urography. Damien Grattan-Smith, MBBS, Department of Radiology, Children's Healthcare of Atlanta, Atlanta, GA; Richard Jones, PhD; Stephen Little, MD; Andrew Kirsch, MD; Adina Alazraki, MD

2008 - Evaluating the Effects of Childhood Lead Exposure with Proton MR Spectroscopy & Diffusion Tensor Imaging Neuroradiology; Kim M Cecil PhD, Cincinnati Children's Hospital Medical Center

2009 - Improving Patient Safety: Effects of a Safety Program on Performance and Culture in a Department of Radiology at a Children's Hospital - Lane Donnelly, Cincinnati Children's Hospital Medical Center, Julie Dickerson, Martha Goodfriend, Stephen Muething

2010 - Juvenile Osteochondritis Dissecans (JOCD): Is It a Growth Disturbance of the Secondary Physis of the Epiphysis? Tal Laor, MD, Cincinnati Children's Hospital Medical Center, Cincinnati, OH, Eric J Wall, MD; Andrew M Zbojniewicz, MD

2011 - Quantitative Assessment of Blood Flow with 4D Phase-Contrast MRI and Autocalibrating Parallel Imaging Compressed Sensing, Albert Hsiao, Stanford University, Micheal Lustig, Marcus Alley, Mark Murphy, Shreyas Vasanawala

2012 - Multidetector CT Pulmonary Angiography in Children with Suspected Pulmonary Embolism: Thromboembolic Risk Factors and Implications for Appropriate Use; Edward Lee, MD, MPH, Children's Hospital, Boston, Sunny K. Tse, David Zurakowski , Victor M. Johnson, Tracy A. Donald, Phillip M. Boiselle

2013 - Prospective Comparison of MRI and Ultrasound for the Diagnosis of Pediatric Appendicitis; Robert Orth, MD, PhD, Texas Children's Hospital, Houston, TX, R. Paul Guillerman, Prakash Masand, MD, Wei Zhang, George Bisset

2014 - Ultrasound-Derived Shear Wave Speed Correlates with Liver Fibrosis in Children; Jonathan Dillman, M.D., Department of Radiology, Section of Pediatric Radiology, University of Michigan C.S. Mott Children's Hospital, Ann Arbor, MI, Ethan Smith, Amer Heider, Nahid Keshavarzi, Jacob Bilhartz, Jonathan Rubin

2015 - Contrast Enhanced Ultrasound in the Assessment of Pediatric Solid Tumor Response to Anti-Angiogenic Therapy; Beth McCarville, MD, Department of Radiological Sciences, Division of Diagnostic Imaging, St. Jude Children's Research Hospital, Memphis, TN, Jamie Coleman, MD, Junyu Guo, PhD, Yimei Li, PhD, Xingyu Li, PhD, Fariba Navid, MD

2016- Intra-operative MRI guided, laparoscopic-assisted anorectoplasty in the treatment for imperforate anus; Damien Grattan-Smith, MBBS, Children's Healthcare of Atlanta, Atlanta, GA, George Raschbaum, John Bleacher, Joseph Williams, Edwin Smith, Stephen Little, Richard Jones

2017- CXR Reduction Protocol in the Neonatal Intensive Care Unit (NICU) – Lessons Learned; Michelande Ridore, MS, Dorothy Bulas, MD, William Pastor, MS, MPH, Sarah McKenney, PhD, Lamia Soghier, MD, Billie Lou Short, MD, CNMC, Washington DC

2018- Association of T2 Lymphatic Imaging in Single Ventricle Patients After Superior Cavopulmonary Connection with Acute Post-Fontan Outcomes; David Biko, MD, Department of Radiology, The Children's Hospital of Philadelphia, Aaron Dewitt, MD, Michael O'Byrne, MD, Mark Fogel, MD, Matthew Harris, MD, Sara Partington, MD, Kevin Whitehead, MD, PhD, David Saul, MD, David Goldberg, Jack Rychik, Andrew Glatz, MD, Matthew Gillespie, MD, Jonathan Rome, MD, Yoav Dori

JOHN P. CAFFEY AWARD FOR POSTERS

1994- Wilms Tumor: Unusual Manifestations. Navoy JF, Royal SA, Vaid YN, Mroczek EC.

1995- Evaluation of Suspected Air Trapping with Dynamic CT Densitometry. Johnson JL, Kramer SS, Mahboubi S.

1996- MR Imaging in the Diagnosis of Experimental Pyelonephritis in Piglets. Pennington, Lonergan GJ, Flack CE, Waguespack L, Jackson CB.

1997- Sensorineural Hearing Loss in Children. Lowe LH, Vezina GL.

1998- Primary Immunodeficiencies: An Immunology Primer for Radiologists. Manson DE, Sikka BS, Cohen S, Reid B, Roifman CM.

1999- Retinoblastoma: US Findings with Pathologic Correlation Kaste, SC, Jenkins, III, JJ, Pratt, CB; Langston, JW, Haik, BG

2001- Mitochondrial Disorders Of Oxidative Phosphorylation In Children: Patterns Of Disease Palasis S, Grattan-Smith JD, Shoffner JM, Neish AS, Stewart S.

2002- Volumetric Localization of Somatosensory Cortex in Children Using Synthetic Aperture Magnetrometry. Xiang J, MD, PhD, The Hospital for Sick Children, Toronto, ON, Canada Chuang S., MD; Holowka S; Babyn P, Otsubo H, Sharma R

2003- Assessing the Use of Magnetic Resonance Imaging in Determining the Age of Closure of Growth Plates. Rajwani T, Huang EM, Secretan C, Bhargava R, Lambert R, Bagnall K

2004- Outstanding Basic Science Research Poster - Imaging of the Diaphragm in Neonates and Young Infants, with Special Emphasis on Diaphragmatic Motion. Epelman M, Navarro O, Miller S Department of Diagnostic Imaging, Hospital for Sick Children, Toronto, ON, Canada

2004- Outstanding Clinical Research Poster - The Spectrum of Renal Cystic Disease in Children. Restrepo R, Ranson M, Sookman J, Jacobson E, Daneman A, Fontalvo L, Department of Radiology, Miami Children's Hospital, Miami, FL

2005- 3D MRI and CT in the Evaluation of Congenital Anomalies of the Aortic Arch. Dehkharghani S, Olson K, Richardson, R

2006- Diffusion Weighted Imaging in Pediatric Neuroradiology: A Primer. Pallavi Sagar, MD, Pediatric Radiology, Massachusetts General Hospital, Boston, MA; P Ellen Grant, MD

2006- Imaging of Suprarenal Fossa in Children: Radiological Approach and Clinico-Pathological Correlation. Kamlesh Kukreja, MD, Radiology, Miami Children's Hospital, Miami, FL; Ricardo Restrepo, MD; Maria D'almeida, MD

2007- Neuroimaging of Nonaccidental Trauma: Pitfalls and Controversies. Lisa H Lowe, MD, Radiology, Children's Mercy Hospitals and Clinics and The University of Missouri-Kansas City, Kansas City, MO; Ruby E Obaldo, MD; Kristin A Fickenscher, MD; Irene Walsh, MD

2008- Estimation of Cumulative Effective Doses from Diagnostic and Interventional Radiological Examinations in Pediatric Oncology Patients. KE Thomas, BA Ahmed, P Shroff, B Connolly, A Lee Chong, C Gordon, The Hospital for Sick Children – Toronto

2009- Case Report: Multi-Modality Imaging Manifestations of the Meckel's Diverticulum in Pediatric Patients. Manish K Kotecha, MD, Richard D Bellah, MD, Andres H Pena, MD, Peter Mattei, MD

2009- Educational: MR Urography: Functional Analysis – Made Simple! Dmitry Khrichenko, BSc, Kassa Darge, MD, PhD

2009- Scientific: MRI Findings in the Term Infant with Neonatal Seizures. An Etiologic Approach - Monica Rebollo Polo,Julie Hurteau-Miller, Eoghan Laffan, Hazar Tabban, Husein Naser, Khaldoun Koujok

2010- Scientific: Dual Phase Intravenous Contrast Injection in Pediatric Body CT Erika Mann, MD, Hospital for Sick Children,Toronto, ON, CA, Amin Alzahrani; Nancy Padfield; Liane Farrell; Guila BenDavid; Karen Thomas, MD

2010- Educational: Hemangiomas Revisited: The Useful, the Unusual and the New Ricardo Restrepo, MD, Miami Children's Hospital, Miami, FL, Rajaneeshankar Palani, MD; Umamahesh Matapathi, MD; Nolan Altman, MD; Luisa Cervantes, MD; Ana-Margarita Duarte, MD; Ibrahim Amjad, MD

2010- Case Report: MRI of Congenital Urethroperineal Fistula Maryam Ghadimi Mahani, MD, University of Michigan Health System, C.S. Mott Children's Hospital, Ann Arbor, MI, Jonathan R Dillman, MD; Deepa Pai, MD; John M Park, MD; Michael A Dipietro, MD; Maria F Ladino Torres, MD

2011- Scientific: Updated Estimated Radiation Dose for Pediatric Nuclear Medicine Studies, Frederick Grant, Children's Hospital, Boston, Laura Drubach, S. Ted Treves, Fred Fahey

2011- Educational: Button Battery Ingestion in Children: What the Radiologist Must Know, Mariam Kappil, Children's Memorial Hospital, Chicago, Cynthia Rigsby, Martha Saker, Emma Boylan

2011- Case Report: MR Imaging Features of Fetal Mediastinal and Intrapericardial Teratomas, Eva Rubio, Children's National Medical Center, Washington, DC, Beth Kline-Fath, Maria Calvo-Garcia, Carolina Guimaraes

2012- Case Report: Neuroimaging in Hemiplegic Migraine: Cases and Review of the Literature, Nicholas V. Stence, Children's Hospital Colorado, Sita Kedia, John A. Maloney, Jennifer Armstrong-Wells, Timothy Bernard

2012- Educational: Primary and Secondary Amenorrhea in Pediatric Patients: From the Beginning to the End, Cesar Cortes, Miami Children's Hospital, Yanerys Ramos, Ricardo Restrepo, Alejandro Diaz, Lorena Sequeira, Edward Lee

2012- Scientific: Prenatal Evaluation of Limb Body Wall Complex with Emphasis on MRI, Elisa Aguirre-Pascual, Hospital Universitario de Getafe, Teresa Victoria, Ann Johnson, Nancy Chauvin, Beverly Coleman, Monica Epelman

2013- Case Report: Percutaneous trans-splenic embolization of Roux limb varices in children with chronic portal vein occlusion (PVO) post orthotopic liver transplant (OLT) Sheena Pimpalwar,MD, Texas Children's Hospital- Interventional radiology, Houston, TX; Aparna Annam, Ponraj Chinnadurai, Alberto Hernandez

2013- Educational: MR imaging of coronary arteries in children: Case Based Teaching File, Roy Jacob, MD, Children's Medical center, Dallas, TX; Shannon Blalock, Jeanne Dillenbeck

2013- Scientific Exhibit: Phantom Iterative Reconstruction Technique (PIRT)-a quantitative ALARA method to test iterative reconstructions effect on image quality and dose in the pediatric population Anne McLellan, DO, Medical, Radiology, Phoenix Children's Hospital, Phoenix, AZ; James Owen, MS, Robyn Augustyn, BSRT (R)(CT), John Egelhoff, DO, John Curran, MD Jeffrey Miller, MD, Richard Southard, MD William Pavlicek, PhD, Richard Towbin, MD

2013- Scientific Exhibit: Morbidity associated with delayed treatment of cholelithiasis in pediatric patients with sickle cell disease Heather Imsande, MD, Boston Medical Center, Boston, MA

2014- Case Report: Contrast-enhanced Ultrasound of Pediatric Abdominal Visceral Trauma: Initial Data; Beatrice Dionigi, Carol Barnewolt, Jill Zalieckas, David Mooney, Harriet Paltiel, MD, Department of Surgery, Boston Children's Hospital, Boston, MA

2014- Educational Poster: The Pediatric Breast: What to do with Lumps and Bumps; Natalie Burns, University of Washington Medical Center, Seattle, WA, Habib Rahbar, Teresa Chapman

2014- Scientific Poster: Towards radiation dose reduction in MDCT with iterative reconstruction for the prenatal diagnosis of skeletal dysplasia: the minimum radiation dose required to evaluate the normal fetal bones?; Chihiro Tani, Hiroshima University Hospital, Hiroshima, Japan, Yoshinori Funama, Chikako Fujioka, Kazuo Awai

2015- Case Report: Congenital Portocaval Shunt: A Rare Entity, Arash Zandieh, MD, Georgetown University Hospital, Washington, DC, Christabel Lee, Frank Volberg

2015- Educational Poster: Pediatric Radiology Economics and Politics in Jeopardy: A Primer, David Swenson, MD, The Alpert Medical School of Brown University, Providence, RI, Cassandra Sams

2015- Scientific Poster: Infant Bone Age Estimation Based on Fibular Shaft Length: A Validation Study, Andy Tsai, MD, PhD, Boston Children's Hospital, Boston, MA, Catherine Stamoulis, Sarah Bixby, Michael Breen, Susan Connolly, Paul Kleinman

2016- Case Report: Imaging Appearances of Crayons; Aaron McAllister, MD, MS, Radiology, Cincinnati Children's Hospital, Cincinnati, OH, Neil Lall, MD, Radiology, Cincinnati Children's Hospital, Cincinnati, OH

2016- Educational Poster: Pediatric Thyroid Cancer: Common Sonographic Appearances and Pitfalls; Claudia Martinez-Rios, MD, Diagnostic Imaging, The Hospital for Sick Children, Toronto, ON, Canada, Lydia Bajno, Alan Daneman, Rahim Moineddin, Danielle CM van der Kaay, Jonathan Wasserman

2016- Scientific Poster: Ultrasound Diagnosis of Median Arcuate Ligament Syndrome (MALS): A Single Institutional Experience; Anjum Bandarkar, Children's National Health System, Washington, DC, Hansel Otero, MD

2017- Case Report: Cutaneous Metastases of Infantile Choriocarcinoma can Mimic Infantile Hemangioma both Clinically and Radiographically; Logan Dance, MD; Patricia Cornejo, MD; Mittun Patel, MD, Phoenix Children's Hospital, Phoenix, AZ

2017- Educational Poster: Sonographic Evaluation of Diaphragmatic Motion: A Practical Guide to Performance and Interpretation; Benjamin D. Smith, MD, Hansel Otero, MD, Tara Cielma, Anjum Bandarkar, MD, Children’s National Medical Center, Washington, DC

2017- Educational Poster: Nuts and Bolts: A Radiologist’s Guide to Orthopedic Hardware Utilized in the Lower Extremities of Children; Hailey Allen, MD, Radiology University of Wisconsin, Madison, WI, Kirkland Davis, MD, Kenneth Noonan, MD, Jie Nguyen, MD

2017- Scientific Poster: Sinusoidal Obstruction Syndrome Causes Increased Liver Stiffness; Naresh Reddivalla, MD, Erin Opfer, DO, Amie Robinson, BSRT(R)(MR) CCRP, Kimberly J Reid, MS, Mohamed Radhi, MD, & Sherwin Chan, MD, PhD, The Children’s Mercy Hospital, Kansas City, MO

2018- Case Report: Calcifying Nested Stromal-Epithelial tumor of the liver: Case report of a rare primary liver tumor; Deepa Biyyam, MD, Mostafa Youssfi, MD, Gerald Mandell, MD, Steve Taylor, MHS, PA and Mittun Patel, MD

2018- Educational Poster: Optimizing Pediatric Leptomeningeal Metastasis Detection: Technical Considerations; Julie H. Harreld, MD, Muhammad Ayaz, PhD, Claudia M. Hillenbrand, PhD; Ralf B. Loeffler, PhD, Zoltan Patay, MD, PhD

2018- Scientific Poster: 3D T1-Weighted Post-Contrast Spine and Abdomen 3 Tesla MRI Using a Golden Angle Radial Acquisition; H. Harry Hu, PhD, Thomas Benkert, PhD, Ramkumar Krishnamurthy, PhD, Mark Smith, MS, Jerome Rusin, MD, Aaron McAllister, MD, Jeremy Jones, MD, Brent Adler, MD, Cody Young, MD, Kathryn Milks, MD, Rajesh Krishnamurthy, MD, and Kai Tobias Block, PhD

2019 EDWARD B. D. NEUHAUSER LECTURER

Jitendra Malik, PhD

Deep Visual Understanding from Deep Learning

Jitendra Malik received the B.Tech degree in Electrical Engineering from Indian Institute of Technology, Kanpur in 1980 and the PhD degree in Computer Science from Stanford University in 1985. In January 1986, he joined the University of California at Berkeley, where he is currently the Arthur J. Chick Professor in the Department of Electrical Engineering and Computer Sciences. He is also on the faculty of the department of Bioengineering, and the Cognitive Science and Vision Science groups. During 2002-2004, he served as the Chair of the Computer Science Division and as the Department Chair of EECS during 2004-2006 as well as 2016-2017. Since January 2018, he is also Research Director and Site Lead of Facebook AI Research in Menlo Park.

Prof. Malik's research group has worked on many different topics in computer vision, computational modeling of human vision, computer graphics and the analysis of biological images. Several well-known concepts and algorithms arose in this research, such as anisotropic diffusion, normalized cuts, high dynamic range imaging, shape contexts and R-CNN. He has mentored more than 60 PhD students and postdoctoral fellows. His publications have received numerous best paper awards, including five test of time awards - the Longuet-Higgins Prize for papers published at CVPR (twice) and the Helmholtz Prize for papers published at ICCV (three times). He received the 2013 IEEE PAMI-TC Distinguished Researcher in Computer Vision Award, the 2014 K.S. Fu Prize from the International Association of Pattern Recognition, the 2016 ACM-AAAI Allen Newell Award, and the 2018 IJCAI Award for Research Excellence in AI. He is a fellow of the IEEE and the ACM. He is a member of the National Academy of Engineering and the National Academy of Sciences, and a fellow of the American Academy of Arts and Sciences.

2019 SOCIAL EVENTS

SPR RESEARCH AND EDUCATION FOUNDATION FUN RUN

Wednesday, May 1, 2019
6:00 a.m. – 7:45 a.m.
Join us for a three-mile run through Downtown San Francisco and get your day off to a great start!
Runners and walkers are all welcome. Entrance fee is $25 and includes a T-shirt.
Runners/walkers should meet in the Hotel lobby at 5:45 a.m.
Underwritten by Texas Children's Hospital

EXHIBIT HALL KICK-OFF PARTY

Wednesday, May 1, 2019
3:30 p.m. – 4:00 p.m.
Hilton San Francisco Union Square, Golden Gate Ballroom
Join us as we welcome the 2019 SPR Exhibitors.

WELCOME RECEPTION

Wednesday, May 1, 2019
7:00 p.m. - 8:00 p.m.
Hilton San Francisco Union Square, Plaza Room
Hors d'oeuvres and Refreshments will be served. Business Casual Attire

RECEPTION AND ANNUAL BANQUET

Friday, May 3, 2019
7:00 p.m.-10:30 p.m.
Hilton San Francisco Union Square, Vista Room
Reception, Dinner and Dancing. Business Casual Attire.
Registration fees apply.

SPR XCHANGE LOUNGE

Come kick back and relax at the SPR XChange Networking Lounge!
Hilton San Francisco Union Square, Golden Gate Ballroom
The lounge will be open throughout the meeting during Exhibit Hall hours.

SAN FRANCISCO ACTIVITIES

The Hilton San Francisco Union Square employs concierge staff who are happy to share their detailed knowledge of San Francisco, California and the surrounding area. You may contact them by email at SFOFH-Concierge@hilton.com.

Additional information is included on the SPR website.

2019 SCHEDULE OF EVENTS

POSTGRADUATE COURSE PROGRAM
TUESDAY, APRIL 30

7:00 AM – 8:00 AM **Continental Breakfast** – *East Lounge*
7:00 AM – 5:00 PM **Registration** – *East Lounge*
7:00 AM – 5:00 PM **ePoster Viewing** – *East Lounge*
8:00 AM – 11:59 PM **Cases of the Day Online Activity**

8:00 AM – 10:00 AM **Postgraduate Course Track I (SAM) – Newborn and Young Infant**
Continental Ballroom 4&5

8:00-8:20 a.m. **Welcome & Introduction**
Janet R. Reid, MD, FRCPC & Taylor Chung, MD, SPR President

8:20-8:30 a.m. **NEC Ultrasound/X-ray – How To**
Janet R. Reid MD, FRCPC

8:30-8:40 a.m. **NEC – Complicated Cases**
Nadia F. Mahmood, MD

8:40-8:50 a.m. **Newborn Bowel Obstruction – How To**
D. Gregory Bates, MD

8:50-9:00 a.m. **Newborn Bowel Obstruction – Cases**
Boaz Karmayzn, MD

9:00-9:10 a.m. **UTD Classification System – Pros and Cons**
Jeanne "Mei-Mei" S. Chow, MD

9:10-9:20 a.m. **UTD Cases on MRI and US**
Andrew T. Trout, MD

9:20-9:30 a.m. **Radiologic Approach: Neonate with Disorder of Gender Development**
Heather Bray, MD

9:30-9:40 a.m. **Challenging Cases of Infant Lung Disease**
R. Paul Guillerman, MD

9:40-10:00 a.m. **Discussion**

8:00 AM – 10:00 AM **Postgraduate Course Track II (SAM) – Body Non-Trauma**
Continental Ballroom 6

8:00-8:20 a.m. **Welcome & Introduction**
S. Pinar Karakas, MD & Taylor Chung, MD, SPR President

8:20-8:30 a.m. **Radiologic Approach: Scrotal Pain with Positive Flow**
S. Pinar Karakas, MD

8:30-8:40 a.m. **MRI in Acute Abdomen – How To**
Jesse Courtier, MD

8:40-8:50 a.m. **MRI in Acute Abdomen – Cases (Adnexal/Mullerian/Other)**
Unni K. Udayasankar, MD

8:50-9:00 a.m. **Intussusception – How To**
Sudha A. Anupindi, MD

9:00-9:10 a.m. **Intussusception – Complicated Cases**
Oscar M. Navarro, MD

9:10-9:20 a.m. **Child with Chest Pain - Cases**
David Saul, MD

9:20-9:30 a.m. **Child with Stridor - Cases**
Evan J. Zucker, MD

9:30-9:40 a.m. **Challenging X-rays – Cases from the Emergency Room**
James E. Crowe, MD

9:40-10:00 a.m. **Discussion**

10:00 AM – 10:20 AM **Break**

10:20 AM – 12:00 PM **Postgraduate Course Track I (SAM) – Body**
Continental Ballroom 4&5

10:20-10:30 a.m. **Diffuse Liver Disease – How To (US & MRI Elastography)**
Jonathan R. Dillman, MD, MSc

10:30-10:40 a.m. **Diffuse Liver Disease - Cases**
Prakash M. Masand, MD

10:40-10:50 a.m. **Crohn's Disease Standardized Nomenclature/Reporting – How To**
Michael S. Gee, MD, PhD

10:50-11:00 a.m. **Crohn's Disease Standardized Nomenclature/Reporting – Cases**
Ethan A. Smith, MD

11:00-11:10 a.m. **Esophageal Disease – How To**
Steven J. Kraus, MD, MS

11:10-11:20 a.m. **Esophageal Disease – Cases**
Lynn A. Fordham, MD, FACR

11:20-11:30 a.m. **Radiologic Approach: Teenager with Amenorrhea**
Laura Z. Fenton, MD, FACR

11:30-11:40 a.m. **Challenging Cases of Pancreatitis**
Michael J. Callahan, MD

11:40 a.m.-12:00 p.m. **Discussion**

10:20 AM – 12:00 PM **Postgraduate Course Track II (SAM) – Body Trauma**
Continental Ballroom 6

10:20-10:30 a.m. **Pros and Cons of American Association for the Surgery of Trauma (AAST) Classifications**
Christopher Newton, MD

10:30-10:40 a.m. **Chest Trauma: Lung and Diaphragm**
Paul G. Thacker, MD, MHA

10:40-10:50 a.m. **Abdomen Trauma: Liver, Spleen and Pancreas**
Michael Aquino, MD

10:50-11:00 a.m. **Abdomen Trauma: Bowel and Mesentery**
Ramesh S. Iyer, MD

11:00-11:10 a.m. **Abdomen Trauma: Renal, Ureter and Bladder**
Henry J. Baskin, MD

11:10-11:20 a.m. **Abdomen Trauma: Shock Abdomen**
Emily S. Orscheln, MD

11:20-11:30 a.m. **Radiologic Approach: Child with Straddle Injury (Perineal, Urethral, Scrotal Injury)**
Summer L. Kaplan, MD, MS

11:30-11:40 a.m. **Challenging Cases of Ingested, Aspirated and Penetrated Foreign Bodies**
Beverly Newman, MD, FACR

11:40 a.m.-12:00 p.m. **Discussion**

12:00 PM – 1:30 PM **Lunch on Own**

12:00 PM – 1:30 PM **jSPR Luncheon** *(pre-registration required)*
Continental Ballroom 2&3
Panel Presentation: Mentorship: Sharing Mentees and Mentors Experiences

1:30 PM – 3:00 PM **Postgraduate Course Track I (SAM) – Oncology**
Continental Ballroom 4&5

1:30-1:40 p.m. **Neuroblastoma Imaging Update on IDRF - How To**
M. Beth McCarville, MD

1:40-1:50 p.m. **Neuroblastoma Imaging Update on IDRF - Cases**
Meryle Eklund, MD

1:50-2:00 p.m. **Imaging of Liver Masses – How to (Including PRETEXT)**
Alexander J. Towbin, MD

2:00-2:10 p.m. **Imaging of Liver Masses - Cases**
Ellen M. Chung, MD

2:00-2:10 p.m. **Lymphoma/Leukemia – How To**
Lisa J. States, MD

2:10-2:20 p.m. **Lymphoma/Leukemia - Cases**
Stephan D. Voss, MD, PhD

2:20-2:30 p.m. **Radiologic Approach: Post Oncologic Treatment Complications**
Geetika Khanna, MD, MS

2:30-2:40 p.m. **Challenging Cases of Oncologic Emergencies**
Heike E. Daldrup-Link, MD, PhD

2:40-3:00 p.m. **Discussion**

1:30 PM – 3:00 PM **Postgraduate Course Track II (SAM) – Neuro Non-Trauma**
Continental Ballroom 6

1:30-1:40 p.m. **Radiologic Approach: Child with Acute Lower Extremity Weakness**
Korgun Koral, MD

1:40-1:50 p.m. **Increased Intracranial Pressure – How To**
Jason N. Wright, MD

1:50-2:00 p.m. **Increased Intracranial Pressure - Cases**
Jonathan G. Murnick, MD, PhD

2:00-2:10 p.m. **Stroke and Look-alikes – How To**
Aylin Tekes, MD

2:00-2:10 p.m. **Stroke and Look-alikes - Cases**
Dennis W. W. Shaw, MD

2:10-2:20 p.m. **Acute Encephalopathy – How To**
Manohar Shroff, MD, FRCPC

2:20-2:30 p.m.	**Acute Encephalopathy - Cases** Bruno P. Soares, MD
2:30-2:40 p.m.	**Challenging Cases of Complicated Sinusitis/Mastoiditis** Sumit Pruthi, MBBS, DNB
2:40-3:00 p.m.	**Discussion**
3:00 PM – 3:20 PM	**Break**
3:20 PM – 5:00 PM	**Postgraduate Course Track I (SAM) – MSK** *Continental Ballroom 4&5*
3:20-3:30 p.m.	**Joint Disease – How To** Sarah D. Bixby, MD
3:30-3:40 p.m.	**Joint Disease - Cases** Apeksha Chaturvedi, MBBS, MD
3:40-3:50 p.m.	**Imaging of FAI- How To** Jerry R. Dwek, MD
3:50-4:00 p.m.	**Imaging of FAI - Cases** Molly E. Dempsey, MD
4:00-4:10 p.m.	**Bone Marrow Imaging – How To** Andrew Schapiro, MD
4:10-4:20 p.m.	**Bone Marrow Imaging - Cases** Kirsten Ecklund, MD
4:20-4:30 p.m.	**Radiologic Approach: Child with Multifocal Bone Lesions** A. Carl Merrow, MD
4:30-4:40 p.m.	**Challenging Cases of Peripheral Neuropathy (US-MRI)** Ricardo Restreppo, MD
4:40-5:00 p.m.	**Discussion**
3:20 PM – 5:00 PM	**Postgraduate Course Track II (SAM) – Neuro Trauma** *Continental Ballroom 6*
3:20-3:30 p.m.	**Challenging Cases of NAT** Gary L. Hedlund, DO
3:30-3:40 p.m.	**Child with Severe Head Trauma – How To** Laura L. Hayes, MD
3:40-3:50 p.m.	**Child with Severe Head Trauma - Cases** Hisham Dahmoush, MBBCh
3:50-4:00 p.m.	**C-Spine Trauma – How To** Camilo Jaimes, MD
4:00-4:10 p.m.	**C-Spine Trauma - Cases** Judith A. Gadde, DO, MBA
4:10-4:20 p.m.	**Facial and Orbital Trauma – How To** Timothy N. Booth, MD
4:20-4:30 p.m.	**Facial and Orbital Trauma - Cases** Asim F. Choudhri, MD
4:30-4:40 p.m.	**Challenging Cases of Thoracic Spine Trauma** Nicholas V. Stence, MD
4:40-5:00 p.m.	**Discussion**
5:00 PM	**Adjourn**

WEDNESDAY, MAY 1

6:00 AM	**SPR/REF Fun Run** Meet in the hotel lobby at 5:45 a.m..
7:00 AM – 8:00 AM	**Continental Breakfast & Exhibit Hall Opens** – *Golden Gate Ballroom*
8:00 AM – 11:59 PM	**Cases of the Day Online Activity**
7:00 AM – 7:45 AM	**Siemens Breakfast Session (Non-CME)** *Continental Ballroom 6*
8:00 AM – 9:40 AM	**Postgraduate Course Track I (SAM) – Fetal** *Continental Ballroom 4&5*
8:00-8:10 a.m.	**Twin-Twin Complications – How To** Amy R. Mehollin-Ray, MD
8:10-8:20 a.m.	**Twin-Twin Complications – Cases** Edward R. Oliver, MD, PhD
8:20-8:30 a.m.	**Fetal Bowel – Imaging Updates and How to Do, Interpret & Report** Teresa Victoria, MD, PhD

8:30-8:40 a.m. **Fetal Bowel – Cases**
Brandon P. Brown, MD, MA, FAAP

8:40-8:50 a.m. **Placental Invasion Disorders – How To**
Luis F. Goncalves, MD

8:50-9:00 a.m. **Placental Invasion Disorders – Cases**
Mariana L. Meyers, MD

9:00-9:10 a.m. **Radiologic Approach: Fetal Ventriculomegaly**
Sarah S. Milla, MD, FAAP

9:10-9:20 a.m. **Challenging Cases in the Fetal Abdomen**
Christopher I. Cassady, MD, FAAP

9:20-9:40 a.m. **Discussion**

8:00 AM – 9:40 AM **Postgraduate Course Track II (SAM) – MSK in the ED**
Continental Ballroom 6

8:00-8:10 a.m. **Radiologic Approach: Child with Acute and Painful Limping**
Kieran J. Frawley, MBBS

8:10-8:20 a.m. **Pelvis Fractures: How To**
Arthur B. Meyers, MD

8:20-8:30 a.m. **Pelvis Fractures: Cases**
Matthew R. Hammer, MD

8:30-8:40 a.m. **Sickle Cell Patient with Bone Pain – How To**
Mahesh M. Thapa, MD

8:40-8:50 a.m. **Sickle Cell Patient with Bone Pain - Cases**
Bamidele F. Kammen, MD

8:50-9:00 a.m. **Soft Tissue – Trauma vs. Infection – How To**
Andrew S. Phelps, MD

9:00-9:10 a.m. **Soft Tissue – Trauma vs. Infection - Cases**
Delma Y. Jarrett, MD

9:10-9:20 a.m. **Challenging Extremity Trauma Radiographs**
Erika Rubesova, MD

9:20-9:40 a.m. **Discussion**

9:40 AM – 10:20 AM **Break** – *Golden Gate Ballroom*

10:20 AM – 12:00 PM **Postgraduate Course Track I (SAM) – Updates on Ultrasound**
Continental Ballroom 4&5

10:20-10:30 a.m. **Contrast-enhanced US of Solid Mass – How To**
Susan J. Back, MD

10:30-10:40 a.m. **Contrast-enhanced US of Solid Mass - Cases**
Judy H. Squires, MD

10:40-10:50 a.m. **Liver Transplant Doppler – How To**
Rama S. Ayyala, MD

10:50-11:00 a.m. **Liver Transplant Doppler - Cases**
Michael R. Acord, MD

11:00-11:10 a.m. **Lung US – How To**
Monica Epelman, MD

11:10-11:20 a.m. **Lung US - Cases**
Brian D. Coley, MD, FACR, FAIUM

11:20-11:30 a.m. **Radiologic Approach to Renal Doppler – When Is It Helpful?**
Harriet J. Paltiel, MD

11:30-11:40 a.m. **Challenging Cases of Thyroid Sonography (TI-RADS)**
Jennifer E. Lim-Dunham, MD, FACR

11:40 a.m.-12:00 p.m. **Discussion**

10:20 AM – 12:00 PM **Postgraduate Course Track II (SAM) – NAT**
Continental Ballroom 6

10:20-10:30 a.m. **Radiologic Approach: Young Child with Healing Fractures**
Ellen S. Park, MD, MS

10:30-10:40 a.m. **Warning Signs of NAT in Infant Head Trauma**
Teresa Chapman, MD, MA

10:40-10:50 a.m. **Differential Diagnosis of NAT in Infant Head Trauma**
Giulio Zuccoi, MD

10:50-11:00 a.m. **Skeletal Trauma in NAT: Common and Uncommon Skeletal Injuries in NAT**
Lydia Bajno, MD

11:00-11:10 a.m. **Skeletal Trauma in NAT: How Old is the Injury?**
Andy Tsai, MD, PhD

11:10-11:20 a.m. **Abdominal and Pelvic Injuries in NAT – How To**
HaiThuy N. Nguyen, MD

11:20-11:30 a.m.	**Abdominal and Pelvic Injuries in NAT - Cases** Aparna Joshi, MD
11:30-11:40 a.m.	**Radiologic Approach: Child with Skull Base Trauma** Mai-Lan Ho, MD
11:40 a.m.-12:00 p.m.	**Discussion**
12:00 PM	**Postgraduate Course Adjourns**
12:00 PM – 1:30 PM	**Lunch on Your Own**

ANNUAL MEETING PROGRAM

12:00 PM – 1:30 PM	**3D Read with the Experts (Non-CME)** *Continental Ballroom 2&3* *Moderators: Dianna M. E. Bardo, MD & Mark Ferguson, MD*
12:00 PM – 1:30 PM	**CT Protocol Session (Non-CME)** *Continental Ballroom 7&8* *Moderators: Prakash Masand, MD & John D. MacKenzie, MD & Grace Phillips, MD*
12:00-12:05 p.m.	**Welcome & Introduction**
12:05-12:13 p.m.	**Physics of Dual Energy CT** Robert MacDougall, MSc
12:13-12:21 p.m.	**Dual Energy for Oncology – Initial Diagnosis** Grace Phillips, MD
12:21-12:29 p.m.	**Spectral dual-energy CT in a Pediatric Department: How, Why and at What Cost?** Richard Southard, MD
12:29-12:37 p.m.	**Ultrafast Chest CT Obviating the Need for Sedation** Sjirk J. Westra, MD, FACR
12:37-12:45 p.m.	**Enteric Contrast Optimization for CT Enterography** Joo Y. Cho, MD
12:45-12:53 p.m.	**Tips and Tricks for a Successful Pediatric CTA – Part I** Jason P. Weinman, MD
12:53-1:01 p.m.	**Tips and Tricks for a Successful Pediatric CTA – Part II** Tushar Chandra, MBBS, MD
1:01-1:30 p.m.	**Discussion/Vendor Q&A**
1:30 PM – 2:30 PM	**Annual Meeting Welcome & Neuhauser Lecture** *Continental Ballroom 4&5*
1:30-1:35 p.m.	**2019 Welcome Address** Taylor Chung, MD, SPR President
1:35-2:30 p.m.	**Edward B. D. Neuhauser Lecture – Deep Visual Understanding from Deep Learning** Jitendra Malik, PhD, Professor, Department of Electrical Engineering & Computer Science, University of California at Berkeley
2:30 PM – 3:30 PM	**Artificial Intelligence: A Real Assistant for Imagers** *Continental Ballroom 4&5* *Moderator: Shreyas S. Vasanawala, MD, PhD, Radiologist & Scientist, Stanford University*
2:30-2:40 p.m.	**Landscape & Introduction** Shreyas S. Vasanawala, MD, PhD, Radiologist & Scientist, Stanford University
2:40-2:55 p.m.	**Learning to Create Images** Joseph Cheng, PhD, Senior Scientist, Stanford University
2:55-3:10 p.m.	**Speeding up Imaging Segmentation** Akshay Chaudhari, PhD, Post-doctoral Scholar, Stanford University
3:10-3:25 p.m.	**Autonomous Image Acquisition (Non-CME)** Juan Santos, PhD, Scientist & Founding CEO HeartVista
3:25-3:30 p.m.	**Discussion**
3:30 PM – 4:00 PM	**Exhibit Hall Kick-off Party** *Golden Gate Ballroom* Join us as we welcome the 2019 SPR Exhibitors!

4:00 PM – 5:15 PM **Scientific Session I-A: Gastrointestinal**
Continental Ballroom 4&5
Moderators: Michael S. Gee, MD, PhD & Sudha A. Anupindi, MD

4:00 p.m.	Paper #: 001	Karmazyn, Boaz	Pilot study on contrast enhanced ultrasound in children post liver transplant
4:10 p.m.	Paper #: 002	Khanna, Geetika	To evaluate rates of gadoxetate disodium induced transient severe respiratory motion artifact in children
4:20 p.m.	Paper #: 003	Gilligan, Leah	Comparison of Navigator-Gated and Breath-Held Image Acquisition Techniques for Multi-echo Quantitative Dixon Imaging of the Liver in Children and Young Adults
4:30 p.m.	Paper #: 004	Grasparil, Angela Don II	Low b-value diffusion-weighted images detect significantly more hyperintense liver lesions in children than T2-weighted images.
4:40 p.m.	Paper #: 005	McCleary, Brendan	Normal Pancreatic Parenchymal Volume in Heathy Children
4:50 p.m.	Paper #: 006	McCleary, Brendan	Assessment of Normative Cut-offs for Pancreas Thickness and T1 Signal Ratios in the Pediatric Pancreas
5:00 p.m.	Paper #: 007	Gilligan, Leah	Magnetic Resonance Imaging T1 Relaxation Times for the Liver, Pancreas, and Spleen in Healthy Children at 1.5 and 3T

4:00 PM – 5:15 PM **Scientific Session I-B: Interventional**
Continental Ballroom 6
Moderators: Leah E. Braswell, MD & Timothy R. Singewald, MD

4:00 p.m.	Paper #: 008	Sharma, Karun	Development of MRI-compatible Robots for MRI-Guided Procedures in Pediatric Interventional Radiology
4:10 p.m.	Paper #: 009	Dao, Kimberly	Sclerotherapy of Aneurysmal Bone Cysts: MRI Imaging Findings and Clinical Outcomes
4:20 p.m.	Paper #: 010	Shah, Jay	Long-term Results and Durability of Cryoablation of Osteoid Osteoma in the Pediatric and Adolescent Population
4:30 p.m.	Paper #: 011	Jain, Neil	Image-guided biopsy for suspected pediatric osteomyelitis: analysis of experience
4:40 p.m.	Paper #: 012	Pezeshkpour, Paymum	Ultrasound-Guided Synovial Biopsy in Children
4:50 p.m.	Paper #: 013	Escobar, Fernando	Complex Cystic Thyroid Nodule Fine Needle Biopsies in Chidlren – Experience in a Tertiary Pediatric Center
5:00 p.m.	Paper #: 014	Durand, Rachelle	Novel Approach to Increase Technical Success during Pediatric Percutaneous Gastrostomy/Gastrojejunostomy Tube Placement using Transgastric Balloon Occlusion

4:00 PM – 5:15 PM **Scientific Session I-C: Informatics, Education, Policy**
Continental Ballroom 2&3
Moderators: Scott R. Dorfman, MD & Alexander J. Towbin, MD

4:00 p.m.	Paper #: 015	Kwon, Jeannie	Bridging the Barriers for Better Team-Based Patient Care by Incorporating NICU Radiology Tele-rounds
4:10 p.m.	Paper #: 016	Kirby, Courtney	Implementing the “What-Where-When” approach to improve patient history availability at the time of radiograph interpretation
4:20 p.m.	Paper #: 017	White, Ammie	Effect of a Double-Interpretation Skeletal Survey Program on Child Abuse Evaluations
4:30 p.m.	Paper #: 018	Utama, Evelyn Gabriela	Effectiveness of showing an interactive animated video vs regular animated video in improving children’s cooperativeness during MRI scan: a prospective, randomized, non-inferiority trial
4:40 p.m.	Paper #: 019	Gokli, Ami	Improved Workflow with MRI Protocol Optimization and Technologist Education
4:50 p.m.	Paper #: 020	Zumberge, Nicholas	Wait Time Reduction for Sedated MRIs
5:00 p.m.	Paper #: 021	Khwaja, Asef	Pediatric Emergency Medicine Point of Care Ultrasound Impact on Radiology Ultrasound Volume

5:15 PM **Sessions Adjourn**

5:15 PM – 7:00 PM **Awards Ceremony**
Continental Ballroom 4&5

7:00 PM – 8:00 PM **2019 Annual Meeting Welcome Reception**
East Lounge

THURSDAY, MAY 2

6:45 AM – 8:00 AM **Continental Breakfast & Exhibit Hall** – *Golden Gate Ballroom*
8:00 AM – 11:59 PM **Cases of the Day Online Activity**

7:00 AM – 8:20 AM **Sunrise Session I - Creating a Research Infrastructure**
Continental Ballroom 2&3
Moderators: Amie S. Robinson, BSRT, (R) (MR) CCRP & Shireen Hayatghaibi, MA, MPH

7:00-7:15 a.m. **Chief's Perspective/Providing Value through Research**
Rajesh Krishnamurthy, MD

7:15-7:30 a.m. **Research Types**
Raymond W. Sze, MD

7:30-7:40 a.m. **Administrative Do's and Don'ts**
Amie S. Robinson, BSRT, (R)(MR)CCRP & Sherwin S. Chan, MD

7:45-7:55 a.m. **Developing a Curriculum for Trainees**
Andrew T. Trout, MD

7:55-8:05 a.m. **Measuring Success with Key Metrics**
Shireen Hayatghaibi, MA, MPH

8:05-8:20 a.m. **Leveraging Your Resources and Talents**
Douglas C. Rivard, DO

7:00 AM – 8:20 AM **Sunrise Session II – WFPI**
Continental Ballroom 7&8
Moderator: Dorothy I. Bulas, MD, FACR

7:00-7:05 a.m. **Introduction**
M. Ines Boechat, MD, FACR

7:05-7:25 a.m. **Pediatric Radiology Education & Innovation in China**
Yumin Zhong, MD, PhD

7:25-7:35 a.m. **Innovation in Africa using Artificial Intelligence as a Sustainable Solution for Healthcare**
Jaishree Naidoo, FCRad

7:35-7:45 a.m. **Challenges of Ensuring Radiation Safety in Low Resource Settings**
Monica Atalabi, MD

7:45-7:50 a.m. **Update in WFPI Fellowship Initiatives**
Jaishree Naidoo, FCRad

7:50-8:10 a.m. **Innovation Outreach Initiatives – Top 5 Recommendations**
Dorothy I. Bulas, MD, FACR, FAAP
Rwanda Experience – George A. Taylor, MD, FACR
Mozambique Experience – Ricardi Faingold, MD
Tanzania Experience – Sjirk J. Westra, MD, FACR

8:10-8:20 a.m. **Discussion**

7:00 AM – 8:20 AM **Sunrise Session III – Professionalism**
Continental Ballroom 1
Moderator: Brandon P. Brown, MD, MA, FAAP

7:00-7:15 a.m. **Burnout in Pediatric Radiology**
Rama S. Ayyala, MD

7:15-7:30 a.m. **Customer Service in Radiology**
Alexander J. Towbin, MD

7:30-7:50 a.m. **What Your Hospital/Chief Wants From You**
George S. Bisset, MD, FACR

7:50-8:05 a.m. **The Changing Workforce in Radiology**
Jane C. Cook, DO

8:05-8:20 a.m. **Building a Culture of Professionalism**
Brandon P. Brown, MD, MA, FAAP

7:00 AM – 8:20 AM **Sunrise Session IV – What's New That Radiation Can Do For You**
Continental Ballroom 6
Moderator: Steven Don, MD

7:00-7:20 a.m. **Spectral CT – Applications in Pediatric Radiology**
Nicholas Rubert, PhD

7:20-7:35 a.m. **Clinical Case Utilization of Spectral CT Applications**
Richard Southard, MD

7:35-7:50 a.m. **DECT in Clinical Practice**
Erica L. Riedesel, MD

7:50-8:05 a.m. **Update on Digital Radiography: What's New?**
Steven Don, MD

8:05-8:20 a.m. **3D and Videofluoroscopy Techniques in Pediatric Radiology**
Benjamin Thompson, DO

7:00 AM – 8:20 AM **Sunrise Session V – Learn From the Experts**

Continental Ballroom 6

Moderators: George A. Taylor, MD, FACR & Alan S. Brody, MD

7:00-7:15 a.m. **What Were We Thinking?**
James E. Crowe, MD

7:15-7:30 a.m. **Career Lessons – Thoughts on Leadership**
George A. Taylor, MD, FACR

7:30-7:45 a.m. **Keeping Things in Perspective**
Alan E. Schlesinger, MD

7:45-8:00 a.m. **Lessons: The Good, The Bad and The Ugly**
Alan S. Brody, MD

8:00-8:15 a.m. **Retirement Starts at 30**
Bruce R. Parker, MD, FACR

8:15-8:20 a.m. **Q&A**

8:30 AM – 10:20 AM **Scientific Session II-A: Genitourinary**

Continental Ballroom 4&5

Moderators: Ronald A. Cohen, MD & Patricia T. Acharya, MD

8:30 a.m.	n/a	Keynote Presentation	**Interesting Pediatric Urology Cases** – **How Imaging Can Help** - Laurence Baskin, MD, Oakland-San Francisco
8:50 a.m.	Paper #: 022	Shapira – Zaltsberg, Gali	Non-visualization of the ovaries on pediatric transabdominal Ultrasound with a non-distended bladder: can adnexal torsion be excluded?
9:00 a.m.	Paper #: 023	Wishah, Fidaa	Introduction of Contrast enhanced voiding urosonography into clinical practice: Assessment of Clinical Indications, Imaging results, and Urologist Acceptance.
9:10 a.m.	Paper #: 024	Shellikeri, Sphoorti	3D printed anatomic contrast enhanced voiding urosonography (ceVUS) teaching phantoms: bringing pediatric vesicoureteral reflux (VUR) to life
9:30 a.m.	Paper #: 026	Chow, Jeanne	Comparison of glomerular filtration rate estimated by motion-robust high spatiotemporal resolution dynamic contrast enhanced MRI and plasma clearance of 99mTc-DTPA
9:40 a.m.	Paper #: 027	Grehten, Patrice	Correlation of MR-Urography and intravoxel incoherent motion MRI based estimation of split renal function in the pediatric clinical population
9:50 a.m.	Paper #: 028	Calle Toro, Juan	Identifying Calyceal Diverticula at Magnetic Resonance Urogram in Children
10:00 a.m.	Paper #: 029	Sandberg, Jesse	Distinguishing clinical and imaging characteristics of nephrogenic rest vs. small Wilms tumor: a report from the Children's Oncology Group
10:10 a.m.	Paper #: 030	Silvestro, Elizabeth	Enhancing Presurgical 3D Modeling and Printing: Multiphase MRI Technique

8:30 AM – 10:20 AM **Scientific Session II-B: Cardiovascular/Education**

Continental Ballroom 6

Moderators: Rajesh Krishnamurthy, MD & Karen Lyons, MD

8:30 a.m.	n/a	Keynote Presentation	**Stem Cell Therapy for Patients with Single Ventricle** - Shunji Sano, MD, PhD, San Francisco-Oakland
8:50 a.m.	Paper #: 031	Mercado, Maria-Gisela	Adolescents With Obesity:Carotid Intima Media Thickness (cIMT) and Cardiovascular (CV) Risk Factors
9:00 a.m.	Paper #: 032	Cohen, Sara	Longitudinal Assessment of Imaging Features of Generalized Arterial Calcification of Infancy
9:10 a.m.	Paper #: 033	Jadhav, Siddharth	Value of emergent pediatric cardiac computed tomographic angiography service: Initial experience at a large children's hospital.
9:20 a.m.	Paper #: 034	Cervantes, Luisa	Intravenous Contrast Material Injection Protocol for Coronary CTA in Children: Changing The Paradigm From Contrast Volume To Injection Duration
9:30 a.m.	Paper #: 035	Barrera, Christian	Contrast extravasation using power injectors for contrast-enhanced computed tomography in children: Safety profile and injury severity assessment
9:40 a.m.	Paper #: 036	Barrera, Christian	Diagnostic performance of CT Angiography to detect pulmonary vein stenosis in children
9:50 a.m.	Paper #: 037	Zucker, Evan	Feasibility and Utility of Dual-Energy Chest CTA for Preoperative Planning in Pediatric Pulmonary Artery Reconstruction

10:00 a.m.	Paper #: 038	Jadhav, Siddharth	Correlation of ductus arteriosus length and morphology between computed tomographic angiography and catheter angiography and their relation to ductal stent length
10:10 a.m.	Paper #: 039	Caro Domínguez, Pablo	Blood flow redistribution in fenestrated and completed Fontan circulations: With special emphasis on abdominal flow

8:30 AM – 10:20 AM **Scientific Session II-C: Interventional Radiology**
Continental Ballroom 7&8
Moderators: Ahmad L. Alomari, MD & Anne Gill, MD

8:30 a.m.		Keynote Presentation	**Angioarchitecture and the Imaging of Vascular Malformations** - Patricia E. Burrows, MD, St. Petersburg
8:50 a.m.	Paper #: 040	Durand, Rachelle	Sirolimus treatment for complex lymphatic malformations in children
9:00 a.m.	Paper #: 041	Vatsky, Seth	Three-dimensional (3D) printed pediatric endovascular phantom for simulating vascular interventions - A feasibility study
9:10 a.m.	Paper #: 042	Srinivasan, Abhay	Percutaneous transluminal angioplasty in children with Reno vascular hypertension, experience in a tertiary pediatric institution.
9:20 a.m.	Paper #: 043	Srinivasan, Abhay	Adjunctive Cutting Balloon Angioplasty in Children with Resistant Renal Artery Stenosis – Experience on a Tertiary Pediatric Institution.
9:30 a.m.	Paper #: 044	Shah, Jay	Catheter-directed pharmacologic thrombolysis for acute submassive and massive pulmonary emboli in children and adolescents.
9:40 a.m.	Paper #: 045	Bertino, Frederic	Technical feasibility and clinical efficacy of common iliac vein stenting in adolescent patients with May-Thurner Syndrome
9:50 a.m.	Paper #: 046	Cleveland, Heather	Split Liver vs Whole Liver OLT: Technical Demands of Pediatric Portal Vein Recanalization
10:00 a.m.	Paper #: 047	Kim, Yu Jin	Comparison of Modified Single Puncture Technique for Tunneling Short-term Central Venous Catheter with Peripherally Inserted Central Catheter in Pediatric Group: A Preliminary Study.
10:10 a.m.	Paper #: 048	Yen, Christopher	Outcomes of tunneled internal jugular venous catheters in children younger than 6 months of age

8:30 AM – 10:20 AM **Technologist Program – Session I**
Continental 9
Moderator: Laura Gruber, MBA, RT(R), RDMS, RVT

8:30-8:50 a.m.	**Ice Breaker** Nikki D. Butler, BmSc, RT(R)(QM), HACP
8:50-9:05 a.m.	**Transitioning From Adults to Pediatrics** Gabe Linke, BSRT (R)(MR)
9:05-9:20 a.m.	**Strategies for Imaging Patients with Special Needs** Merima Karastanovic, MS, RT(R)(MR)
9:20-9:35 a.m.	**Why Do I Need to Look at Other Imaging Studies Prior to Performing Exams?** Patricia Lacy Gander, BS, RDMS, RVT, RT
9:35-9:50 a.m.	**Struggles of Anesthesia** Christine Harris, RT (MR) MRSO
9:50-10:05 a.m.	**Slight of the Hand Scheduling Magic** Angela Quintello, AAS
10:05-10:20 a.m.	**Gad Dep in the Pediatric Population** Charles Stanley

10:20 AM – 10:50 AM **Break in Exhibit Hall –** *Golden Gate Ballroom*

10:50 AM – 12:00 PM **Midday Session I – Heartless Vascular Imaging**
Continental 4&5
Moderator: Prakash M. Masand, MD

10:50-11:05 a.m.	**Ferumoxytol/Feraheme Contrast for MRA** Dianna M.E. Bardo, MD
11:05-11:20 a.m.	**Contrast-enhanced Body MRA in Children: Techniques and Indications** Ladonna J. Malone, MD
11:20-11:30 a.m.	**Blood Pool Contrast for Abdominal MRA Post Ablavar** Lindsay Griffen, MD
11:30-11:45 a.m.	**Contrast and Non-contrast Extremity MRA** Michael A. Breen, MBBCh

11:45 a.m.-12:00 p.m. **MR Lymphangiography**
Govind B. Chavhan, MD

10:50 AM – 12:00 PM **Midday Session II – Incidentalomas**
Continental 7&8
Moderator: R. Paul Guillerman, MD

10:50-11:05 a.m. **Neuroradiology**
Laura Hayes, MD

11:05-11:20 a.m. **Musculoskeletal**
Lauren W. Averill, MD

11:20-11:30 a.m. **Chest**
Paul G. Thacker, MD, MHA

11:30-11:45 a.m. **Gastrointestinal**
Martha M. Munden, MD

11:45 a.m.-12:00 p.m. **Genitourinary**
R. Paul Guillerman, MD

10:50 AM – 12:00 PM **Midday Session III – Pearls in Neonatal Ultrasound**
Continental Ballroom 2&3
Moderator: Monica Epelman, MD & Rama S. Ayyala, MD

10:50-11:05 a.m. **US for Necrotizing Entercolitis: Utility and Pitfalls**
Cicero T. Silva, MD

11:05-11:20 a.m. **Head US in HIE in Term Infants**
Monica Epelman, MD

11:20-11:35 a.m. **Utility of Supplemental Views for Head US in Preterm Infants**
Rama S. Ayyala, MD

11:35-11:45 a.m. **US of Diaphragm**
Brooke S. Lampl, DO

11:45 a.m.-12:00 p.m. **US of Brachial Plexus**
Ramesh S. Iyer, MD

10:50 AM – 12:00 PM **Midday Session IV – Noninterpretive Skills**
Continental Ballroom 1
Moderator: Richard E. Heller III, MD, MBA

10:50-11:05 a.m. **Communication**
George S. Bisset, MD, FACR

11:05-11:20 a.m. **Presentation Skills**
Richard E. Heller III, MD, MBA

11:20-11:30 a.m. **Time Management**
Jonathan R. Dillman, MD, MSc

11:30-11:40 a.m. **Faculty Development**
Brian D. Coley, MD, FACR, FAIUM

11:40 a.m.-12:00 p.m. **Leading As a Pediatric Radiologist**
Richard B. Gunderman, MD, PhD, FACR

10:50 AM – 12:00 PM **Midday Session V – CEUS Technique and Applications**
Continental Ballroom 6
Moderators: Kassa Darge, MD, PhD & M. Beth McCarville, MD

10:50-11:00 a.m. **Contrast US of the Brain**
Misun Hwang, MD

11:00-11:10 a.m. **Contrast US of the Liver**
Jeannie K. Kwon, MD

11:10-11:20 a.m. **Contrast US of the Spleen, Kidney and Co.**
Patricia T. Acharya, MD

11:20-11:30 a.m. **CEUS Bowel**
Ami Gokili, MD

11:30-11:40 a.m. **Contrast US of the Hip Joint**
Susan J. Back, MD

11:40-11:50 a.m. **Contrast enhanced Voiding Urosonography**
Jeanne “Mei-Mei” S. Chow, MD

11:50 a.m.-12:00 p.m. **Contrast US for Interventional Radiology**
Michael R. Acord, MD

10:50 AM – 12:00 PM **Technologist Program – Session II**
Continental Ballroom 9
Moderator: Trista Raymer Maule, RT(R)(CT)(MR)MRSO

10:50-11:10 a.m. **MRI Imaging of Cochlear Implants**
Christina Sammet, PhD

11:10-11:30 a.m. **US TCD in Ages 1-4**
Brandi Kozak, BS, RDMS

11:30 a.m.-12:00 p.m. **Interesting Uses of Imaging (Mummy Experience and Cadaver Imaging)**
Gabe Linke, BSRT (R)(MR)

12:00 PM – 1:30 PM **Lunch on Your Own**

12:00 PM – 1:30 PM **MR Protocol Session (Non-CME)**
Continental Ballroom 7&8
Moderators: Michael S. Gee, MD, PhD, Govind Chavhan, MD &
Shreyas S. Vasanawala, MD, PhD

1:30 PM – 2:40 PM **REF Research in Action**
Continental Ballroom 4&5
Moderator: J. Damien Grattan-Smith, MBBS

1:30-1:50 p.m. **Keynote Presentation: Towards Pediatric Body MR without Anesthesia**
Michael "Miki" Lustig, PhD, Associate Professor, Department of Electrical Engineering & Computer Science, UC Berkeley

1:50-1:58 p.m. **Education Project Grant – "Facilitating a Pediatric Radiology Curriculum in the Global Health Setting Using Tablet Computers"**
Jennifer L. Nicholas, MD, MHA

1:58-2:06 p.m. **Education Project Grant – "Pediatric Cardiovascular CT: A Faculty Development Initiative"**
Lorna P. Browne, MD, FRCR

2:06-2:14 p.m. **Seed Grant – "Feasibility of contrast-enhanced Transfontanelle Ultrasound: Comparison with Magnetic Resonance Imaging in the Neonate"**
Judy H. Squires, MD

2:14-2:22 p.m. **Young Investigator Award – "In vivo Tau Imaging using 18F-AV-1451 PET Radioligand in a Swine Model of Closed Head Injury"**
Neha S. Kwatra, MD

2:22-2:30 p.m. **Multi-Institutional Pilot Award – "Determination of Normal Liver Stiffness by MR Elastography in Children"**
Andrew T. Trout, MD

2:30-2:40 p.m. **Wrap-up & Announcements**
J. Damien Grattan-Smith, MBBS

2:40 PM – 3:30 PM **Pediatric Radiology Jeopardy**
Continental Ballroom 4&5
Host - Richard E. Heller III, MD, MBA

Hall of Fame Team – Captain - Dorothy I. Bulas, MD, FACR, FAAP
Marta Hernanz-Schulman, MD, FACR, George Taylor, MD, FACR
& Brian D. Coley, MD, FACR, FAIUM

All-Star Team – Captain - Jonathan R. Dillman, MD
Rama Ayyala, MD, Sarah Milla, MD, FAAP & R. Paul Guillerman, MD

1:30 PM – 3:30 PM **Technologist Program – Session III**
Continental Ballroom 9
Moderator: Christine Harris, RT (MR) MRSO

1:30-2:15 p.m. **Hot Topics**
2:15-3:30 p.m. **Scientific Abstract Presentations**

2:15 p.m.	Paper #: 001(T)	Moore, Theresa	Upper gastrointestinal studies indeterminate for malrotation: Are there opportunities for improvement?
2:25 p.m.	Paper #: 002(T)	Munyon, Roxanne	The Importance of Proper Patient Positioning and Immobilization in Suspected Non-Accidental Trauma Cases
2:35 p.m.	Paper #: 003(T)	Silvestro, Elizabeth	Running a Hospital in-house3d printing lab: Challenges and Considerations
2:45 p.m.	Paper #: 004(T)	Silvestro, Elizabeth	Application of 3D Printing and Mold Making to construct custom Phantoms and Task Trainers
2:55 p.m..	Paper #: 005(T)	Prevett, Georgina	Innovating Change in Imaging for Patient Care
3:05 p.m.	Paper #: 006(T)	Goehner, Melissa	Staff Engagement and the Correlation with Increasing Customer Service
3:15 p.m.	Paper #: 007(T)	Shipp, Rozalon	Regulartory Readiness: Preparing Diaganostic Imaging for Joint Commission Accreditation

3:30 PM – 4:00 PM **Exhibit Hall Break –** *Golden Gate Ballroom*

4:00 PM – 5:40 PM **Scientific Session III-A: Neuroradiology/Cardiology**

Continental Ballroom 4&5

Moderators: Susan Palasis, MD & Skorn Ponratana, MD, MPH

4:00 p.m.	Paper #: 049	Zafer, Rizwan	Evaluation of Automated Extraction of Velocity Envelope for Transcranial Doppler Ultrasound
4:10 p.m.	Paper #: 050	El-Ali, Alexander	Shear Wave Elastography in Brain Ultrasonography: Initial Experience and Utility in Detecting White Matter Disease
4:20 p.m.	Paper #: 051	Choi, Jungwhan	Review of Neck CTA Examinations for Soft Palate Injury and Proposal of a New Targeted CTA Protocol
4:30 p.m.	Paper #: 052	Little, Stephen	Fissures of the annulus fibrosus and cervical cord anterior spinal artery infarcts in children: telltale signs of fibrocarilaginous disc emboli?
4:40 p.m.	Paper #: 053	Bhatia, Aashim	Clinical benefit of ferumoxytol whole body vascular imaging including the central nervous system in pediatric patients
4:50 p.m.	Paper #: 054	McAllister, Aaron	Comparison of 2D Turbo-Spin-Echo BLADE and Spin-Echo Echo-Planar Diffusion Weighted Brain MRI at 3 Tesla: Preliminary Experience in Children
5:00 p.m.	Paper #: 055	Tabari, Azadeh	Evaluation of Highly Accelerated Wave-CAIPI Susceptibility-Weighted Imaging (SWI) in the Non-Sedated Pediatric Setting: Initial Clinical Experience
5:10 p.m.	Paper #: 056	Tabari, Azadeh	Comparison of Ultrafast Wave-CAIPI Magnetization-Prepared Rapid Acquisition Gradient-Echo (Wave-MPRAGE) and Standard MPRAGE in Non-Sedated Children:Initial Clinical Experience
5:20 p.m.	Paper #: 057	Little, Stephen	Bridging vein evaluation in suspected abusive head trauma: beyond tadpoles and lollipops
5:30 p.m.	Paper #: 058	Proisy, Maïa	Facial hemangioma: risk of PHACE syndrome and associated anomalies.

4:00 PM – 5:40 PM **Scientific Session III-B: Musculoskeletal**

Continental Ballroom 6

Moderators: John D. MacKenzie, MD & Jie C. Nguyen, MD, MS

4:00 p.m.	Paper #: 059	Bowden, Jonathan	Validation of Automated Analysis of Bone Age from Hand Radiograph
4:10 p.m.	Paper #: 060	Khandwala, Nishith	Multi-institutional Implementation of an Automated Tool to Predict Pediatric Skeletal Bone Age: How We Did It
4:20 p.m.	Paper #: 061	Starosolski, Zbigniew	Cross-validation of two Convolutional Neural Networks for radiographic fracture detection
4:30 p.m.	Paper #: 062	Starosolski, Zbigniew	Improved accuracy for tibial fracture identification by a convolutional neural network and transfer learning
4:40 p.m.	Paper #: 063	Starosolski, Zbigniew	Improved accuracy for recognition of pediatric long-bone fractures in the setting of variable open growth plates by Convolutional Neural Networks
4:50 p.m.	Paper #: 064	Degnan, Andrew	Underappreciated Elbow Fractures: Pediatric Radial Head and Neck Fractures and Additional Fracture Associations
5:00 p.m.	Paper #: 065	Edwards, Emily	Utilizing 3D-Printed Models to Optimize Digital Tomosynthesis for Pediatric Medial Epicondyle Elbow Fractures
5:10 p.m.	Paper #: 066	Tsai, Andy	Long Bone Growth and Skeletal Maturation Patterns of Children with Progeria
5:20 p.m.	Paper #: 067	Maza, Noor	Can Ultrasound be reliably used to evaluate infants with DDH after age 6 months without the use of plain film radiography?
5:30 p.m.	Paper #: 068	Prince, Jeffrey	Outcomes Measures Related to Care Process Models in the Evaluation of Infants for Developmental Dysplasia of the Hips

4:00 PM – 5:40 PM **Scientific Session III-C: ALARA/Gastrointestinal**

Continental Ballroom 2&3

Moderators: Gary R. Schooler, MD & Heather Bray, MD

4:00 p.m.	Paper #: 069	Benali, Sébastien	Comparative dose and image quality evaluation for scoliosis follow-up exams: assessment of standard and low-dose modes of a slot-scan radiographic system
4:10 p.m.	Paper #: 070	Snyder, Elizabeth	Comparing Image Quality and Exposure Rates Between Flat Panel Detectors and Image Intensifiers in Fluoroscopy
4:20 p.m.	Paper #: 071	Ross, Steven	Novel Use of Optical Video for Reducing Radiation Dose in Pediatric Fluoroscopy
4:30 p.m.	Paper #: 072	Don, Steven	Efficient ALARA Determination using Adaptive Simulated Low-Dose Pediatric Appendicitis CT and a Psychometric Function

4:40 p.m.	Paper #: 073	Finkle, Joshua	Radiation burden associated with imaging of suspected appendicitis-related abscess: Pathway to a radiation free MR appendicitis imaging protocol
4:50 p.m.	Paper #: 074	Southard, Richard	Implementation of Single-Source Dual-Layer Spectral CT in a Pediatric Imaging Department: Addressing Dose Neutrality and Maintenance of Image Quality in Abdominal-Pelvic CT in Children
5:00 p.m.	Paper #: 075	Siegel, Marilyn	Size-specific dose estimate reference levels for pediatric abdominopelvic examinations using single and dual-energy dual-source CT
5:10 p.m.	Paper #: 076	Richer, Edward	Plain film findings in ileocolic intussusception. Why should we care?
5:20 p.m.	Paper #: 077	Ma, Grace	Recurrent Intussusceptions in Children
5:30 p.m.	Paper #: 078	Tshuma, Makabongwe	Piriform Fossa Sinus Tract - A 15 year retrospective review of cases from birth to adolescence presenting to a Children's Hospital

4:00 PM – 5:40 PM **Technologist Program – Session IV**

Continental Ballroom 9

Moderator: Laura Poznick, AAS, RDMS

4:00-4:20 p.m. **MR Cardiac Pacemakers**
Georgina Prevett, MS, RT(R)(N) (CT)(MR), CNMT(CT)

4:20-4:40 p.m. **Innovation Meets Operations: Strategies in Building Interventional Labs**
Kevin R. Shoaf ARRT RT(R)

4:40-5:00 p.m. **MRI Safety Initiatives and Improvements**
Katherine Busher, BS,RT(R)MR,MRSO

5:00-5:40 p.m. **Scientific Abstract Presentations**

5:00 p.m.	Paper #: 008(T)	Wilson, Justine	MR Imaging of the Forgotten Circulation: Intrahepatic Dynamic Contrast MR Lymphangiography (IH-DCMRL) to Evaluate the Liver and Central Lymphatics
5:10 p.m..	Paper #: 009(T)	Johnson, Maggie	Move over wearable and embedded devices there a new MRI safety challenge today call ingestible
5:20 p.m.	Paper #: 010(T)	Carson, Robert	MRI Safety and the MRSO
5:30 p.m.	Paper #: 011(T)	Maule, Trista	MRI Safety: Getting the FTEs You Need

5:40 PM **Sessions Adjourn**

FRIDAY, MAY 3

6:45 AM – 8:00 AM **Continental Breakfast & Exhibit Hall** – *Golden Gate Ballroom*

8:00 AM – 11:59 PM **Cases of the Day Online Activity**

7:00 AM – 8:20 AM **WFPI Breakfast Get Together: Pediatric Radiology Outreach FAQ (Non-CME)**

Continental Ballroom 1

Interested in outreach? Interested in learning what your colleagues in the World Federation of Pediatric Imaging, an alliance of Pediatric Radiology organizations across the globe, are doing and, if interested, how you could jump in? Pick up your breakfast from the hallway and join us for an informal gathering of WFPI volunteers and supporters!

7:00 AM – 8:20 AM **Sunrise Session VI – Thoracic Imaging**

Continental Ballroom 4&5

Moderator: Alan S. Brody, MD

7:00-7:15 a.m. **Dynamic Airway Imaging**
Pamela M. Ketwaroo, MD

7:15-7:35 a.m. **What is Pneumonia and What Should We Do about It?**
Alan S. Brody, MD

7:35-7:50 a.m. **Pediatric Chest CTA**
Karen Lyons MD, BCh, BAO

7:50-8:05 a.m. **Functional Lung MRI: From Research Tool to Clinical Application**
Talissa Altes, MD

8:05-8:20 a.m. **Strategies for Optimizing Thoracic CT and MRI in Children**
Sarah Desoky, MD

7:00 AM – 8:20 AM **Sunrise Session VII – Hybrid Imaging**
Continental Ballroom 6
Moderator: Stephan D. Voss, MD, PhD

7:00-7:20 a.m. **Hybrid Imaging in Pediatrics**
Stephen D. Voss, MD, PhD

7:20-7:35 a.m. **SPECT/CT ONC**
Susan E. Sharp, MD

7:35-7:50 a.m. **PET CT in Lymphoma**
Pek-Lan Khong, MBBS, FRCR

7:50-8:05 a.m. **PET and SPECT CT in Epilepsy**
Jason N. Wright, MD

8:05-8:20 a.m. **PET MR Oncology**
Heike E. Daldrup-Link, MD, PhD

7:00 AM – 8:20 AM **Sunrise Session VIII – Safety**
Continental Ballroom 2&3
Moderator: Michael J. Callahan, MD

7:00-7:15 a.m. **Here's Looking at You, CT**
Donald P. Frush, MD, FACR

7:15-7:30 a.m. **MRI Safety**
Cory M. Pfeifer, MD, MS, FAAP

7:30-7:45 a.m. **Gadolinium Deposition: Update**
Alexander Radbruch, MD

7:45-8:00 a.m. **Anesthesia Safety**
Joshua Nickerson, MD

8:00-8:20 a.m. **Putting It Together: Risk/Benefit of Abdominal MRI vs. CT in Young Pediatric Patients**
Michael J. Callahan, MD

7:00 AM – 8:20 AM **Sunrise Session IX – Radiogenomics**
Continental Ballroom 7&8
Moderator: Matthew A. Zapala, MD, PhD

7:00-7:15 a.m. **Radiogenomics: A Primer and Initial Applications to Pediatric Radiology**
Matthew A. Zapala, MD, PhD

7:15-7:30 a.m. **Practical Radiomics and Radiogenomics Using Computational Pipelines**
Sandy Napel, PhD

7:30-7:45 a.m. **Radiogenomics in Pediatric Neuroradiology**
Kristen Yeom, MD

7:45-8:00 a.m. **Radiogenomics in the World of Nuclear Medicine**
Spencer Behr, MD, PhD

8:00-8:20 a.m. **Imaging Genomics in the Age of Bioinformatics, a Computational Perspective**
Olivier Gavaert, PhD

8:30 AM – 10:20 AM **Scientific Session IV-A: Nuclear/Oncology**
Continental Ballroom 4&5
Moderators: Stephan D. Voss, MD, PhD & Adina L. Alazraki, MD

8:30 a.m.	n/a	Keynote Presentation	**Total-Body PET/CT: Simultaneous Imaging of the Entire Body with EXPLORER** - Ramsey Badawi, MD, PhD, Davis
8:50 a.m.	Paper #: 079	Sher, Andrew	Ultrafast PET/CT: A qualitative and quantitative analysis of reduced imaging times using Digital PET/CT
9:00 a.m.	Paper #: 080	Gillum, Jason	Utility of 18F-FDG PET/CT following ketogenic diet in detecting endocarditis in children and adult congenital heart disease patients.
9:10 a.m.	Paper #: 081	Muehe, Anne	Standardized Uptake Values on PET/MR scans are not affected by iron oxide nanoparticles
9:20 a.m.	Paper #: 082	Zapala, Matthew	Radiomic analysis of staging CT scans for neuroblastoma: An initial investigation of correlations with tumor histology, MYCN status, INRG stage, relapse and death
9:30 a.m.	Paper #: 083	Devkota, Laxman	Monitoring Response to Immunotherapies in Neuroblastoma Using Nanoparticle Contrast-Enhanced CT
9:40 a.m.	Paper #: 084	Hasweh, Reem	Gadolinium-based contrast media improve detection of image defined risk factors at diagnosis of neuroblastoma
9:50 a.m.	Paper #: 085	Grassi, Daphine	The Structured Report for Oncology – An Important Tool for Oncologists and Radiologists
10:00 a.m.	Paper #: 086	Siedek, Florian	Are Ferumoxytol-enhanced MRI scans equally suitable to evaluate tumor size and extension of pediatric bone tumors compared to Gadolinium-enhanced MRI scans?
10:10 a.m.	Paper #: 087	Doria, Andrew	Diagnostic Accuracy of Imaging Approaches for Early Tumor Detection in Patients with Li-Fraumeni Syndrome

8:30 AM – 10:20 AM **Scientific Session IV-B: Neonatal/Fetal/Neuroradiology**
Continental Ballroom 6
Moderators: Misun Hwang, MD & Rama S. Ayyala, MD

8:30 a.m.	n/a	Keynote Presentation	**How Alterations of Normal Brain Development Results in Malformations** -James Barkovich, MD, Oakland-San Francisco
8:50 a.m.	Paper #: 088	Rubesova, Erika	Doppler imaging in hypoxic ischemic encephalopathy: What is the value of the resistivity index with and without compression of the fontanel?
9:00 a.m.	Paper #: 089	Zheng, Qiang	Region-Specific Perfusion Alterations in Neonatal Hypoxic Ischemic Injury Evaluated with Arterial Spin Labeling MRI
9:10 a.m.	Paper #: 090	Proidy, Maïa	Changes in brain perfusion in successive arterial spin labelling MRI scans in neonates with hypoxic-ischemic encephalopathy
9:20 a.m.	Paper #: 091	Zheng, Qiang	Quantitative ASL Perfusion Method for Detection of Neonatal Hypoxic Ischemic Injury as Reference Standard for Developing Contrast-Enhanced Ultrasound
9:30 a.m.	Paper #: 092	Cort, Kayla	Contrast-enhanced ultrasound for the evaluation of neonatal brain injury: Interpretation and implementation
9:40 a.m.	Paper #: 093	Didier, Ryne	Contrast-Enhanced Brain Ultrasound Perfusion Metrics in the EXTra-uterine Environment for Neonatal Development (EXTEND): Correlation with Hemodynamic Parameters
9:50 a.m.	Paper #: 094	Parakh, Anushri	Artificial Intelligence Detection of Germinal Matrix Hemorrhage on Head Ultrasound Examinations Using Convolutional Neural Networks
10:00 a.m.	Paper #: 095	Kralik, Stephen	The Frontal Temporal and Frontal Occipital Horn Ratios in Pediatric Hydrocephalus: Comparison and Validation of Head Ultrasound with Volumetric Analysis via MRI
10:10 a.m.	Paper #: 096	Didier, Ryne	Incidence and Concordance of Suspected Intraventricular Hemorrhage (IVH) on Fetal US and MRI in Open Spinal Dysraphism with Postnatal Follow-Up

8:30 AM – 10:20 AM **Scientific Session IV-C: Thoracic**
Continental Ballroom 2&3
Moderators: Paul G. Thacker, MD, MHA & Ladonna J. Malone, MD

8:30 a.m.	n/a	Keynote Presentation	**Standardization of Postnatal CT Imaging and Interpretation of Bronchopulmonary Malformations**- Beverley Newman, MD, Stanford
8:50 a.m.	Paper #: 097	Cort, Kayla	Chest ultrasound for the screening and diagnosis of pulmonary lymphangiectasia
9:00 a.m.	Paper #: 098	Biko, David	Contrast Enhanced Ultrasound (CEUS) Evaluation of Thoracic Duct Outlet Patency After Percutaneous Injection of Intranodal Contrast
9:10 a.m.	Paper #: 099	Wallace, Andrew	Dual and Single Energy Pediatric Thoracic Computed Tomographic Angiography: Effects on Radiation Dose and Imaging Quality
9:20 a.m.	Paper #: 100	Agahigian, Donna	Preoperative Visualization of the Artery of Adamkiewicz in Pediatric Patients on Dynamic 4D airway CT angiograms
9:30 a.m.	Paper #: 101	Shin, Su-Mi	CT Angiographic Findings of Pulmonary Arteriovenous Malformations (PAVM) in Children with Hereditary Hemorrhagic Telangiectasia (HHT): Spectrum of PAVM and Correlation with Graded Transthoracic Contrast Echocardiography (TTCE)
9:40 a.m.	Paper #: 102	Mong, David	Predictive model for pediatric pulmonary embolism risk utilizing semantic data mapping, neural embedding technique, and recurrent neural network
9:50 a.m.	Paper #: 103	Zeng, David	Artificial Intelligence Correction of Image Artifacts for Faster Pediatric Lung MRI
10:00 a.m.	Paper #: 104	Ibrahim, Ala'	Imaging evaluation for thoracic spine fractures in pediatric trauma patients: a single center experience at an academic children's hospital
10:10 a.m.	Paper #: 105	Grey, Neil	Imaging Findings Following Button Battery Ingestions

8:30 AM – 10:20 AM **Technologist Program – Session V**
Continental Ballroom 9
Moderator: Tara Cielma, RDMS, RDCS, RVT, RT(S)

8:30-8:50 a.m. **MSK Ultrasound**
Parker Stanleym MHA, RDMS

8:50-9:10 a.m. **LEAN in Nuclear Medicine**
Joseph MacLean, MHA, CNMT

9:10-9:30 a.m. **CT Dynamic Imaging**
Erica Gates

9:30-10:20 a.m. **Scientific Abstract Presentations**

9:30 a.m.	Paper #: 012(T)	Riemann, Monique	Ultrasound Imaging of Orthopedic Magnetically controlled Spinal Rods

9:40 a.m.	Paper #: 013(T)	Silvestro, Elizabeth	Fabrication and utilization of an Ultrasound Phantom for young patient engagement and understanding
9:50 a.m.	Paper #: 014(T)	Silvestro, Elizabeth	Design and construction of an infant phantom for hip ultrasound education and training
10:00 a.m.	Paper #: 015(T)	Morgan, Trudy	Pulmonary Lymphangiectasia (PL) - Diagnosing with Ultrasound Instead of MRI
10:10 a.m.	Paper #: 016(T)	Brondell, Ashley	IVUS for Venous Compression Syndromes

10:50 AM – 12:00 PM **Midday Session VI – Image Gently**
Continental Ballroom 2&3
Moderator: Donald P. Frush, MD, FACR

10:50-11:10 a.m. **From Abbey Road to the Digital Highway: Update on Medical Radiation Exposure to Children in the US**
Donald P. Frush, MD, FACR

11:10-11:30 a.m. **Help: Decision Support for Pediatric CT**
Marta Hernanz-Schulman, MD, FACR

11:30-11:50 a.m. **Get Back: Recommendations for Gonadal Shielding in Children**
Keith J. Strauss, MSc, FACR

11:50 a.m.-12:00 p.m. **Come Together: AI/Machine Learning in Radiology**
Matthew P. Lungren, MD, PhD

10:50 AM – 12:00 PM **Midday Session VII – Cardiac MR**
Continental Ballroom 4&5
Moderator: Lorna P. Browne, MD, FRCR

10:50-11:10 a.m. **Crash Course in the Common Congenital Cardiac Surgeries**
Lorna P. Browne, MD, FRCR

11:10-11:20 a.m. **How Do I Start Incorporating T1 and T2 Mapping in to my Clinical Practice?**
Christopher Z. Lam, MD

11:20-11:30 a.m. **How Do I Start Scanning Pacemakers in my Clinical Practice?**
Maryam Ghadami Mahani, MD

11:30-11:40 a.m. **How Do I Start Incorporating 4D Flow into my Clinical Practice?**
Cynthia K. Rigsby, MD, FACR

11:40-11:50 a.m. **How Do I Image a Failing Fontan?**
David M. Biko, MD

11:50 a.m.-12:00 p.m. **Q&A**

10:50 AM – 12:00 PM **Midday Session VIII – Advanced Topics in Pediatric MRI**
Continental Ballroom 6
Moderator: Sarah D. Bixby, MD

10:50-11:05 a.m. **Accelerated MSK MRI**
Sarah D. Bixby, MD

11:05-11:20 a.m. **Accelerated Body MRI**
Michael S. Gee, MD, PhD

11:20-11:40 a.m. **Accelerated Neuro MRI**
Mai-Lan Ho, MD

11:40 a.m.-12:00 p.m. **High Value MRI: What Does the Future Look Like?**
Houchun H. Hu, PhD

10:50 AM – 12:00 PM **Midday Session IX – Diagnostic Dilemmas/Questions**
Continental Ballroom 1
Moderator: Kirsten Ecklund, MD

10:50-11:05 a.m. **Whole Body MRI vs. PET**
Govind B. Chavhan, MD

11:05-11:20 a.m. **When Do Cartilage Maps Actually Help**
Diego Jaramillo, MD, MPH

11:20-11:35 a.m. **Developments in Lung MRI**
Shreyas S. Vasanawala, MD, PhD

11:35-11:50 a.m. **Options for Scoliosis Imaging**
Kirsten Ecklund, MD

11:50 a.m.-12:00 p.m. **MRE – Do I Really Need 25 Sequences?**
Prakash M. Masand, MD

10:50 AM – 12:00 PM **Midday Session X – Value-Added Radiology**
Continental Ballroom 7&8
Moderator: David B. Larson, MD

10:50-11:00 a.m. **Adding Value as a Consultant**
Brandon P. Brown, MD, MA

11:00-11:15 a.m.	**Measuring the Value of Consultation** Nghia (Jack) Vo, MD
11:15-11:25 a.m.	**Time-Driven Activity-Based Costing** Robert C. Orth, MD, PhD
11:25-11:45 a.m.	**The Role of Technologist Education in Practice Reform** David B. Larson, MD
11:45 a.m.-12:00 p.m.	**Using Radiology Extenders to Add Value** Brandy Bales, RPA, RT(R)(M)

10:50 AM – 12:00 PM **Technologist Program – Session VI**
Moderator: Patricia Lacy Gandor, BS, RDMS

10:50-11:10 a.m.	**PET/MR How to Decrease Overall Scan Time** Elad Nevo, MS, RT(MR)(N)(CT), CNMT
11:10-11:30 a.m.	**Comparison of Standard VCUG, ceVcug, Nuclear VCUG** Roxanne M. Munyon, BS/AS Joseph Maclean, CNMT Laura Poznick, AAS, RDMS
11:30 a.m.-12:00 p.m.	**Imaging Jeopardy** Nikki D. Butler, BMSc, RT(R)(QM)

12:00 PM – 1:30 PM **Lunch on Your Own**

12:00 PM – 1:30 PM **SPR Business Meeting –** *SPR Members Only*
Continental Ballroom 4&5

1:30 PM – 3:30 PM **Scientific Session V-A: Fetal/Musculoskeletal**
Continental Ballroom 4&5
Moderators: Carol E. Barnewolt, MD & Sarah J. Menashe, MD

1:30 p.m.	n/a	Keynote Presentation	**Fetal Imaging: Key to Fetal/Peri-natal Surgical Management in 2019?** – Darrell L. Cass, MD, Cleveland
1:50 p.m.	Paper #: 106	Estroff, Judy	Unreliability of standard fetal imaging biomarkers for prediction of lethal pulmonary hypoplasia (PH)
2:00 p.m.	Paper #: 107	Atluri, Mahesh	Attention-Aware Deep Learning Networks for Predicting Gestational Brain Age Using Fetal MRI
2:10 p.m.	Paper #: 108	Choi, Jungwhan	Inner and external ear malformations as assessed on fetal ultrasound and MRI
2:20 p.m.	Paper #: 109	Barrera, Christian	Comparison of SAR and SED between fetal MR imaging at 1.5T and 3T: Our experience with 3247 examinations
2:30 p.m.	Paper #: 110	Badachhape, Andrew	Determination of Placental Fractional Blood Volume in a Pregnant Mouse Model
2:40 p.m.	Paper #: 111	Spiller, Lisa	Growth Recovery Lines: A Specific Indicator of Child Abuse and Neglect?
2:50 p.m.	Paper #: 112	Karmazyn, Boaz	Establishing signs for acute and healing phases of classic metaphyseal lesions
3:00 p.m.	Paper #: 113	Messer, Diana	A Systematic Review of Radiographic Time Since Injury Methods for Pediatric Healing Fractures

1:30 PM – 3:30 PM **Scientific Session V-B: Cardiovascular**
Continental Ballroom 6
Moderators: Houchun Harry Hu, PhD & Christopher Z. Lam, MD

1:30 p.m.	n/a	Keynote Presentation	**Gadolinium Deposition in Children: Should we Worry?** – Alexander Radbruch, MD, Essen, Germany
1:50 p.m.	Paper #: 115	Kelly, John	Morphometry of a tissue engineered vascular graft (TEVG) by multimodality imaging including MRI, intravascular ultrasound and angiography in a translational sheep model
2:00 p.m.	Paper #: 116	Biko, David	Intrahepatic Dynamic Contrast Enhanced MR Lymphangiography: A New Technique for Visualization of the Central Lymphatics
2:10 p.m.	Paper #: 117	Pednekar, Amol	Evaluation of Cumulative Perimetric Ratio as Quantitative Index for Degree of Left ventricular Myocardial Trabeculations in Adolescents and Young Adults
2:20 p.m.	Paper #: 118	Pednekar, Amol	Circumventing Anesthesia in Pediatric Cardiac Patients Considered High-Risk for Anesthesia using Free Breathing CMR
2:30 p.m.	Paper #: 119	Ponrartana, Skorn	Non-contrast Flow-independent Relaxation-Enhanced MR Angiography Using Inversion Recovery and T2-Prepared 3D mDIXON Gradient-Echo DIXON Technique: Applications in the Pediatric Population

2:40 p.m.	Paper #: 120	Diaz, Eric	Image Quality Assessment of Cardiothoracic Respiratory Motion Compensated Relaxation Enhanced 3D Non-Contrast MRA with Reference to Dynamic Contrast-Enhanced 3D MRA: A Pilot Study
2:50 p.m.	Paper #: 121	Sandino, Christopher	Highly accelerated cardiorenal 4D flow MRI using 3D cones trajectory
3:00 p.m.	Paper #: 122	Bush, Adam	Multi Echo fLow-encoded Rosette (MELROSE) for Quantitative Assessment of Cardiac and Intravascular T2* and Blood Oxygen Saturation Determination
3:10 p.m.	Paper #: 123	Bush, Adam	Contigious Rosette Echoes iN Single Highly Accelerated Acquistion (CRENSHAA) for Motion Robust and Time Resolved Cardiac and Abdominal T2* Assessment
3:20 p.m.	Paper #: 124	Sandino, Christopher	Deep learning-based reconstruction of 2D cardiac CINE MRI data

1:30 PM – 3:30 PM **Scientific Session V-C: Neuroradiology**
Continental Ballroom 2&3
Moderators: Ashok Panigrahy, MD & Hisham M. Dahmoush, MBBCh

1:30 p.m.	n/a	Keynote Presentation	**Immersive Virtual Reality Imaging in Pediatric Neurosurgery** – Kurtis Auguste, MD, Oakland – San Francisco
1:50 p.m.	Paper #: 125	Chan, Alex	The utility of the ASL sequence in parenchymal injury of the brain in abusive head trauma (AHT).
2:00 p.m.	Paper #: 126	Maleki, Maryam	ASL Perfusion Imaging of the Frontal Lobes Predicts the Occurrence and Resolution of Posterior Fossa Syndrome
2:10 p.m.	Paper #: 127	Sarma, Asha	Neuroimaging findings in infants with human parechovirus infection
2:20 p.m.	Paper #: 128	Riotti, Jessica	Longitudinal Brain MRI Characterization of Normal Appearing Zika-exposed children using advanced MRI techniques and Correlations with Neurodevelopmental Outcomes
2:30 p.m	Paper #: 129	Chu, Zili	Brain Network Architecture Correlates with Seizure-Free Outcome in Children Undergoing Epilepsy Surgery
2:40 p.m.	Paper #: 130	Coblentz, Ailish	Using Connectome Mapping to Define a Target for Deep Brain Stimulation in Paediatric Dystonia
2:50 p.m.	Paper #: 131	Maloney, Ezekiel	In the era of mTOR inhibitors for treatment of tuberous sclerosis complex, is MRI surveillance of subependymal giant cell atrocytoma growth reliable without gadolinium?
3:00 p.m.	Paper #: 132	Maloney, Ezekiel	Non-inferiority of a non-gadolinium-enhanced MRI follow up protocol for isolated optic pathway gliomas – interim analysis from a multi-reader-multi-case study
3:10 p.m.	Paper #: 133	Ugas Charcape, Carlos	Primary intracranial sarcoma in pediatrics: MRI findings
3:20 p.m.	Paper #: 134	Teixeira, Sara	Thalamic lesion in Leigh syndrome: An unusual finding mimicking Percheron artery infarct

3:30 PM – 3:45 PM **Break** – *East Lounge*
3:45 PM – 5:45 PM **Scientific Session VI-A: Musculoskeletal**
Continental Ballroom 4&5
Moderators: Bamidele F. Kammen, MD & Mahesh M. Thapa, MD

3:45 p.m.	n/a	Keynote Presentation	**How Advanced Imaging Has Changed Surgical Practice in the Age of Sports Specialization** – Nirav Pandya, MD, Oakland
4:05 p.m.	Paper #: 135	Tamir, Jon	Introduction of Targeted Rapid Knee MRI exam using T2 Shuffling into Clinical Practice: Retrospective Analysis on Image Quality, Cost and Scan Time
4:15 p.m.	Paper #: 136	Sandberg, Jesse	Silent and Distortionless Diffusion MRI
4:25 p.m.	Paper #: 137	Pezeshkpour, Paymun	Novel Functional BOLD MR Imaging Techniques for Assessment of Juvenile Dermatomyositis: Preliminary Results
4:35 p.m.	Paper #: 138	Shet, Narendra	MR-HIFU: What the Pediatric Radiologist Should Know
4:45 p.m.	Paper #: 139	Matheney, Travis	Intra-Operative Contrast-Enhanced Ultrasound of Infant Hips: A Comparison with Post-Operative MRI and Correlation with Development of Femoral Head Avascular Necrosis
4:55 p.m.	Paper #: 140		***Withdrawn***
5:05 p.m.	Paper #: 141	Hammer, Matthew	A Multidisciplinary Approach Leads to More Efficient Magnetic Resonance Imaging, Less Use of Contrast Material, and Improved Clinical Outcomes During Musculoskeletal Infection Evaluation
5:15 p.m.	Paper #: 142	Doria, Andrea	Value of Functional T2 Map MRI in the Assessment of Early Cartilage Degeneration of Pediatric Patients with Hemophilia
5:25 p.m.	Paper #: 143	Xu, Lin	Role of DWI in detecting early satage of sacroiliac joint lesions in children with enthesitis related arthritis

5:35 p.m.	Paper #: 144	Nguyen, Jie	Stable versus unstable osteochondral lesions of the elbow: Performance of MR imaging criteria for instability

3:45 PM – 5:45 PM **Scientific Session VI-B: Gastrointestinal**
Continental Ballroom B
Moderators: Govind Chavhan, MD & Ethan A. Smith, MD

3:45 p.m.	n/a	Keynote Presentation	**Advanced Imaging is Integral to the Clinical Care of Pediatric Gastrointestinal, Hepatologic, and Pancreatic Diseases** – Zachary Sellers, MD, PhD, Stanford
3:55 p.m.	Paper #: 145	Harris, Lisa	Abdominal Wall Thickness in Children Correlates with Hepatic Steatosis
4:05 p.m.	Paper #: 146	Gee, Michael	Automated Sonographic Assessment of Fatty Liver in Pediatric Patients
4:15 p.m.	Paper #: 147	Barrera, Christian	Biexponential T2* relaxation model for estimation of liver iron concentration in children: A better fit for high liver iron concentrations
4:25 p.m.	Paper #: 148	Calle Toro, Juan	R2-Relaxometry MRI for estimation of Liver Iron Concentration. A comparison between two methods.
4:35 p.m.	Paper #: 149	Thompson, Benjamin	Magnetic Resonance Elastography of the Liver in Children: Variations in Regional Stiffness
4:45 p.m.	Paper #: 150	Northern, Nathan	Technical Success Rate of Two-Dimensional Ultrasound Shear Wave Elastography in a Large Pediatric and Young Adult Population: A Clinical Effectiveness Study
4:55 p.m.	Paper #: 151	Sandberg, Jesse	Biliary atresia versus other causes of neonatal jaundice: What is the value of Shear Wave Elastography complementing grayscale findings?
5:05 p.m.	Paper #: 152	Shin, Hyun Joo	Quantitative assessment of liver stiffness and perfusion using shear wave elastography and dual energy computed tomography in hepatic veno-occlusive disease in rabbit model
5:15 p.m.	Paper #: 153	Trout, Andrew	Normal Liver and Pancreas Shear Wave Stiffness in Healthy Children
5:25 p.m.	Paper #: 154	Gilligan, Leah	Use of Clinical and Quantitative Magnetic Resonance Cholangiopancreatography Parameters for Differentiating Autoimmune Liver Diseases
5:35 p.m.	Paper #: 155	Marie, Eman	How Can Criteria for Interpretation of MRI Examinations of Appendicitis Influence Diagnostic Accuracy?

3:45 PM – 5:45 PM **Scientific Session VI-C: Informatics/Educational**
Continental Ballroom 2&3
Moderators: David B. Larson, MD, MBA & Michael M. Moore, MD

3:45 p.m.	n/a	Keynote Presentation	**The Sacred Work of Caring for Children** – Richard B. Gunderman, MD, PhD, FACR, Indianapolis
4:05 p.m.	Paper #: 156	Hailu, Tigist	Walk in My Shoes: Interdepartmental Role Shadowing to Develop Workplace Wellness at a Large Pediatric Radiology Department
4:15 p.m.	Paper #: 157	Ayyala, Rama	Assessment of Factors Associated with Burnout and Wellness in Pediatric Radiologists
4:25 p.m.	Paper #: 158	Gokli, Ami	Gender Representation in Recent SPR-Sponsored Events
4:35 p.m.	Paper #: 159	Sammer, Marla	Review of Learning Opportunity Rates: Correlation with Radiologist Assignment, Patient Type, and Exam Priority
4:45 p.m.	Paper #: 160	Gokli, Ami	Teaching File: An Extensive Revision to Optimize Integration and Educational Value
4:55 p.m.	Paper #: 161	Gokli, Ami	Multifaceted Educational Scaffolding Supports Sub-Specialization in Pediatric Radiology
5:05 p.m.	Paper #: 162	Reid, Janet	RADIAL Learning Management System - One Year Later
5:15 p.m.	Paper #: 163	Otero, Hansel	Cost-Effectiveness Analysis in Pediatric Radiology: How the Evidence (or, the Lack Thereof) Can Lead Future Research
5:25 p.m.	Paper #: 164	Mesi, Erin	Tackling the “black hole” of encounter specific quality improvement data in imaging
5:35 p.m.	Paper #: 165	Koci, Martin	Comparison of Different Weight Groups in Pediatric Trauma Using Split-bolus Single-pass Contrast CT protocol.

5:45 PM **Sessions Adjourn**

7:00 PM – 10:30 PM **Reception & Annual Banquet** – *separate fee applies*
Plaza Room

SATURDAY, MAY 4

7:00 AM – 8:00 AM — **Continental Breakfast** – *Golden Gate Ballroom*
8:00 AM – 11:59 PM — **Cases of the Day Online Activity**

7:00 AM – 8:00 AM — **US Protocol Session (Non-CME)**
Golden Gate Ballroom
Moderators: Monica Epelman, MD & Andrew S. Phelps, MD
Ultrasound for necrotizing enterocolitis: protocol, pearls and pitfalls
Monica Epelman, MD
Ultrasound Technical Tips
Andrew S. Phelps, MD
Q&A with Vendors

8:00 AM – 12:00 PM — **Cardiac CT** – *Pre-registration required, Non-CME*
Continental Ballroom 6

8:00-8:10 a.m. — **Welcome & Introductions**
Lorna P. Browne, MD, FRCR

8:10-8:25 a.m. — **Cardiac CT – Technical Aspects**
Prakash M. Masand, MD

8:25-8:40 a.m. — **Cardiac CT Dose & Pitfalls**
Lorna P. Browne, MD, FRCR

8:40-8:55 a.m. — **Cardiac CT for Anomalous Pulmonary Venous Connections**
Mark R. Ferguson, MD

8:55-9:10 a.m. — **Neonatal and Infantile Coronary Artery CT**
Eric Hoggard, MD

9:10-9:25 a.m. — **Anomalous Aortic Origin of the Coronary Arteries and Myocardial Bridge Evaluation**
Dianna M. E. Bardo, MD

9:25-9:40 a.m. — **Approach to Heterotaxy on Cardiac CT**
Rajesh Krishnamurthy, MD

9:40-9:55 a.m. — **Cardiac CT for Ductal Dependent Anatomy**
David M. Biko, MD

9:55-10:20 a.m. — **Wrap-up/Break**
10:20-10:30 a.m. — **Case Review Session Introduction & Buttonology with Arterys**
10:30-11:00 a.m. — **Independent Case Review**
11:00-11:10 a.m. — **Mentored Case Review – Anomalous Pulmonary Venous Connections**
Marielle Fortier, MD

11:10-11:20 a.m. — **Mentored Case Review – Coronary Arteries**
Hyun Woo Goo, MD, PhD

11:20-11:30 a.m. — **Mentored Case Review - Heterotaxy**
Maryam Ghadimi Mahani, MD

11:30-11:40 a.m. — **Mentored Case Review – Ductal Dependent Anatomy**
Cynthia K. Rigsby, MD, FACR

11:40 a.m.-12:00 p.m. — **Interesting Case Review**
Carlos F. Ugas Charcape, MD

8:00 AM – 12:00 PM — **Interventional Radiology (SAM)**
Continental Ballroom 4&5
Moderator: Manish Patel, DO

8:00-8:05 a.m. — **Welcome, Introductions & SAM Overview**
Leah E. Braswell, MD

8:05-8:30 a.m. — **HIFU**
Karun Sharma, MD

8:30-8:55 a.m. — **Complex Vascular Access IJ & Beyond**
Allison S. Aguado, MD

8:55-9:20 a.m. — **Management of Biliary Strictures**
Giridhar Shivaram, MD

9:20-9:45 a.m. — **Discussion & SAM Questions**
9:45-10:00 a.m. — **Break**
10:00-10:05 a.m. — **Welcome Back & SAM Reminder**
10:05-10:30 a.m. — **Artificial Intelligence in IR**
Matthew P. Lungren, MD

10:30-10:55 a.m. — **Retinoblastoma Intra-arterial Chemotherapy**
Todd Abruzzo, MD

10:55-11:20 a.m. — **Pediatric Thrombolysis with Update on Management for May-Thurner**
Patrick Warren, MD

11:20 a.m.-12:00 p.m. — **Discussion & SAM Questions**

8:00 AM – 12:00 PM **Best Practices: Collaboration & Innovation for Pediatric Nuclear Medicine & Hybrid Imaging (SAM)**
Continental Ballroom 2&3
Moderators: Helen Nadel, MD, FRCPC & Victor J. Seghers, MD, PhD

8:00-8:05 a.m. **Welcome, Introductions & SAM Overview**
Helen Nadel, MD, FRCPC

8:05-8:30 a.m. **How Nuclear Medicine is Practiced at Children's Hospitals**
Victor J. Seghers, MD, PhD

8:30-8:55 a.m. **Brain PET/MRI for Epilepsy – Best Practices**
Hisham Dahmoush, MBBCh

8:55-9:20 a.m. **Considerations of Pediatric Nuclear Medicine Including PET/MRI**
Derrick Gillan, BS, CNMT PET, RT (N)(CT)(MR)

9:20-9:45 a.m. **Discussion & SAM Questions**

9:45-10:00 a.m. **Break**

10:00-10:05 a.m. **Welcome Back & SAM Reminder**
Victor J. Seghers, MD, PhD

10:05-10:35 a.m. **Multidisciplinary Approach to Thyroid Cancer – Two Centers' Experience**
Kara D. Meister, MD & Adina L. Alazraki, MD

10:35-11:00 a.m. **Clinical Update on Liver Tumors**
Arun Rangaswami, MD

11:00-11:20 a.m. **Lymphoscintigraphy**
Adina L. Alazraki, MD, FAAP

11:20-11:40 a.m. **NAT**
Sabah Servaes, MD

11:40-11:50 a.m. **Discussion & SAM Questions**

11:50 a.m.-12:00 p.m. **Wrap-up**

8:00 AM – 12:00 PM **Education: Advanced Skills in Translational Teaching (SAM)**
Continental Ballroom 1

8:00-8:15 a.m. **Welcome, Introductions & SAM Overview**
Sarah Milla, MD, FAAP

8:15-8:30 a.m. **Teaching Dynamically**
Sarah Milla, MD, FAAP

8:30-9:15 a.m. **Technology That Works in Teaching**
Janet R. Reid, MD, FRCPC

9:15-10:00 a.m. **Hands-on: Two Minute PowerPoint & Panel**
Sarah Milla, MD, FAAP

10:00-10:30 a.m. **Break**

10:30-10:45 a.m. **The Complete Scope of Teaching**
Janet R. Reid, MD, FRCPC

10:45-11:00 a.m. **Building and Maintaining a Teaching Portfolio**
Mahesh M. Thapa, MD

11:00-11:45 a.m. **Hands-on: Teaching Portfolio**
Sarah Milla, MD, FAAP

11:45-12:00 p.m. **Discussion & SAM Questions**

8:00 AM – 12:00 PM **Neuroradiology (SAM)**
Continental Ballroom 7&8

8:00-8:05 a.m. **Welcome, Introductions & SAM Overview**

8:05-8:35 a.m. **Pediatric Leukodystrophies**
Andrea Rossi, MD

8:35-9:05 a.m. **Metabolic Disorders in Newborns**
Theirry A. G. M. Huisman, MD

9:05-9:30 a.m. **Pediatric Vascular Imaging in 2019**
Francisco Perez, MD, PhD

9:30-9:45 a.m. **Discussion & SAM Questions**

9:45-10:00 a.m. **Break**

10:00-10:35 a.m. **Imaging of Hydrocephalus**
Birgit B. Ertl-Wagner, MD, MHBA

10:35-11:05 a.m. **Hydrocephalus Treatment – Neurosurgery Perspective**
Nalin Gupta, MD

11:05-11:35 a.m. **Basics of Artificial Intelligence in Pediatric Neuroimaging**
Matthias Wagner, MD

11:35 a.m.-12:00 p.m. **Discussion & SAM Questions**

8:00 AM – 12:00 PM **Hands-On Ultrasound**

Golden Gate Ballroom

Moderators: Kassa Darge, MD, PhD & Monica Epelman, MD

8:00-8:45 a.m. **Session I: Intravesical Contrast Enhanced Ultrasound**
Presentation: Susan J. Back, MD
Station 1: Preparation of Ultrasound Contrast Agents – Laura Poznick, RDMS & Brandi Kozak, RDMS
Station 2: Imaging of Microbubbles: A Teach Yourself Session – Lamont Hill, RT, ARDMS & Kassa Darge, MD, PhD
Station 3: Imaging of Microbubbles: A Teach Yourself Session – Trudy Morgan, RDMS
Station 4: Simulation of Contrast Enhanced Voiding Urosonography – Susan J. Back, MD & Elizabeth Silvestro, MSc

8:45-8:50 a.m. **Break**

8:50-9:20 a.m. **Session II: Ultrasound Elastography**
Presentation: Jonathan R. Dillman, MD, MSc
Station 1 – Jonathan R. Dillman, MD, MSc
Station 2 – Andrew S. Phelps, MD
Station 3 - Trudy Morgan, RDMS & Brandi Kozak, RDMS
Station 4 – Monica Epelman, MD & Maria G. Smith, BS, RDMS, RVT
Station 5 – Kara Groom, RDMS

9:20-9:35 a.m. **Break**

9:35-10:20 a.m. **Session III: Ultrasound of the Appendix**
Presentation: Andrew S. Phelps, MD
Station 1 – Andrew S. Phelps, MD & Janet Mar, RDMS
Station 2 – Monica Epelman, MD & Kara Groom, RDMS
Station 3 – Maria G. Smith, BS, RDMS, RVT & Stephanie Suller, RDMS
Station 4 – Lamont Hill, RT, ARDMS & Mark Goce, RDMS
Station 5 – Trudy Morgan, RDMS & Kassa Darge, MD, PhD

10:20-10:25 a.m. **Break**

10:25-10:55 a.m. **Session IV: Ultrasound of the Knee**
Presentation: Jie C. Nguyen, MD, MS
Station 1 – Jie C. Nguyen, MD, MS & Lamont Hill, RT, ARDMS
Station 2 – Trudy Morgan, RDMS & Laura Poznick, RDMS
Station 3 – Brandi Kozak, RDMS
Station 4 – Monica Epelman, MD & Kara Groom, MD
Station 5 – Mahesh M. Thapa, MD & Maria G. Smith, BS, RDMS, RVT

10:55-11:00 a.m. **Break**

11:00-11:30 a.m. **Session V: Ultrasound of the Ankle**
Presentation: Mahesh M. Thapa, MD
Station 1 – Mahesh M. Thapa, MD
Station 2 – Jie C. Nguyen, MD, MS & Lamont Hill, RT, ARDMS
Station 3 – Trudy Morgan, RDMS & Laura Poznick, RDMS
Station 4 – Monica Epelman, MD & Maria G. Smith, BS, RDMS, RVT
Station 5 – Kara Groom, RDMS & Brandi Kozak, RDMS

11:30-11:35 a.m. **Break**

11:35 a.m.-12:00 p.m. **Session VI: Ultrasound of the Tonsils**
Presentation: Anjum N. Banarkar, MD
Station 1 – Anjum N. Banarkar, MD
Station 2 – Kara Groom, RDMS
Station 3 – Maria G. Smith, BS, RDMS, RVT
Station 4 – Monica Epelman, MD & Brandi Kozak, RDMS
Station 5 – Lamont Hill, RT, ARDMS & Trudy Morgan, RDMS

SCIENTIFIC PAPERS

Authors are listed in the order provided. An author listed in bold identifies the presenting author.

Paper #: 001

Pilot study on contrast enhanced ultrasound in children post liver transplant

Dilek Saglam, MD[3], Richard S. Mangus, MS FACS[2], **Boaz Karmazyn, MD[1]**, *bkarmazy@iupui.edu*; [1]Indiana University, Riley Hospital for Children, Indianapolis, IN, [2]Indiana university school of medicine, Department of Surgery, Indianapolis, IN, [3]Malatya Education and Research Hospital, Malatya, Turkey

Disclosures: All authors have disclosed no financial interests, arrangements or affiliations in the context of this activity.

Purpose or Case Report: Assessing the added value of contrast enhanced US in detecting the vascular complications of liver transplantation in children.
Methods & Materials: We retrospectively evaluated all Doppler US and contrast enhanced ultrasound (ceUS) performed since 8/2017 when we started to routinely use ceUS. For the first 5 post-operative days (POD) All patients had twice a day Doppler US. ceUS was performed as a baseline in the first POD and to confirm any suspected vascular complications. Demographic, clinical and imaging findings were recorded and were correlated with surgery.
Results: 14 children (9 females) had 15 liver transplants during this period. The mean age was 4.1 years old (range 6 months-16.1 years). Indications of the liver transplants were as follows; biliary atresia (n=9), alpha 1 antityripsin deficiency (n=1), metabolic liver disease (n=2), cystic fibrosis (n=1) and cryptogenic cirrhosis (n=1). Three patients had split liver and 11 patients had whole liver transplantation.ceUS was successfully performed in all patients. There were no complications related to the ceUS. In three patients CEUS was performed to evaluate for vascular complications following abnormal Doppler US. In two patients ceUS demonstrated vascular thrombosis confirmed in surgery: In a six month old male post whole liver transplant, initial ceUS in POD 1, confirmed portal vein thrombosis (PVT) seen on Doppler US. Surgery confirmed PVT but also hepatic artery (HA) thrombosis. Marked HA narrowing in the initial ceUS could be seen retrospectively when compared with a post thrombectomy follow-up ceUS. In a one year old female post whole liver transplant, initial ceUS was normal. On POD 3, Doppler showed tardus parvus flow in intrahepatic arteries this followed immediately by ceUS that demonstrated marked HA stenosis. This led to seven hours follow-up ceUS that showed progression to complete HA occlusion confirmed in surgery. In a 16 year-old female, POD 1 ceUS excluded right hepatic vein thrombosis suggested by Doppler and Color US.
Conclusions: Our pilot study shows that ceUS can provide definite bed side diagnosis of vascular complications in the immediate post liver transplant period. Use of ceUS has the potential to provide earlier diagnosis of liver vascular complications and obviate the need to perform contrast enhanced CT and reduce unnecessary exploratory surgeries.

Paper #: 002

To evaluate rates of gadoxetate disodium induced transient severe respiratory motion artifact in children

Michael H. Lanier, MD PhD, Andrew B. Wallace, **Geetika Khanna, MD, MS**, *khannag@mir.wustl.edu*; Washington University, Mallinckrodt Institute of Radiology, St Louis, MO

Disclosures: Geetika Khanna, MD, MS: Financial Interest: Elsevier - Royalty: Independent contractor. All other authors have disclosed no financial interests, arrangements or affiliations in the context of this activity.

Purpose or Case Report: Gadoxetate disodium (Eovist ®) is the preferred MR contrast agent for pediatric hepatobiliary imaging. It is known to cause arterial phase transient severe breathing motion artifacts in 5-22% of adults, and adult studies have raised caution against its use for evaluation of arterial enhancing lesions.This study seeks to evaluate the frequency of transient severe respiratory motion secondary to gadoxetate disodium in a pediatric cohort.
Methods & Materials: This is a retrospective, IRB approved study with informed consent waiver. The radiology information system of a children's hospital was searched to identify all MRI studies performed with gadoxetate disodium during January 2016- June 2018. Exclusion criterion was MRI studies with incomplete set of dynamic post contrast imaging. Two readers independently evaluated the pre-contrast, arterial, portal and equilibrium phase of dynamic liver imaging for respiratory motion artifact on a 5 point scale (1 no motion, 2 mild motion, 3 moderate motion, 4 severe motion- still diagnostic, 5 extreme motion- not diagnostic). Average scores of the 2 readers for each phase were used for analysis. Transient severe respiratory motion was defined as an increase in breathing motion score of ≥ 1.5 from pre contrast to arterial phase that returned to < 3 in equilibrium phase of imaging.
Results: The study cohort consisted of 140 cases (60% female), age range: 1 month - 23 years (median 13 years). 102/140 scans were performed non-sedated. 98 scans were performed on 1.5T scanners and 42 on 3T scanners. Mean respiratory motion score for each phase of scan for the entire cohort was: pre-contrast: 2.23, arterial: 2.56, portal venous: 2.39, equilibrium: 2.31. Breathing motion score increased by a factor of ≥ 1.5 in 15/140 (10.71%) cases after injection of gadoxetate disodium. The score remained at ≥ 3 in 7/15 cases, and returned to < 3 in 8 cases resulting in a transient severe respiratory motion rate of 5.71 % (8/140 cases).
Conclusions: The rate of transient severe respiratory motion artifacts in the pediatric population is estimated at 5.7%, similar to reported rates in the adult population. Pediatric radiologists should be aware of this potential limitation of gadoxetate disodium when performing hepatobiliary MRI in children.

Paper #: 003

Comparison of Navigator-Gated and Breath-Held Image Acquisition Techniques for Multi-echo Quantitative Dixon Imaging of the Liver in Children and Young Adults

Leah A. Gilligan, MD, *leah.gilligan@cchmc.org*; Jonathan R. Dillman, MD. MSc, Jean A. Tkach, PhD, Andrew T. Trout; Radiology, Cincinnati Children's Hospital Medical Center, Cincinnati, OH

Disclosures: Jonathan R. Dillman, MD, MSc: Research Grants: Canon Medical Systems; Siemens Healthineers; Perspectum Diagnostics; Bracco Diagnostics, Other: Travel Support (Philips Healthcare, GE Healthcare); **Andrew T. Trout, MD:** Consultant, Honoraria: Guerbet Group, Royalty: Elsevier, Wolters-Kluwer, Research Grants: Canon Medical, Siemens Medical Solutions, National Pancreas Foundation, In-Kind Support: ChiRhoClin Inc., Perspectum Diagnostics. All other authors have disclosed no financial interests, arrangements or affiliations in the context of this activity.

Purpose or Case Report: To compare hepatic proton density fat fraction (PDFF), R2* values, and respiratory motion between navigator-gated and breath-held multi-echo Dixon (mDixon) magnetic resonance imaging (MRI) acquisition techniques in children and young adults with suspected liver disease.
Methods & Materials: This retrospective study was approved by the institutional review board with a waiver of informed consent. Patients who underwent liver MRI with breath-held and navigator-gated mDixon sequences between January 2017 and July 2018 were included. One reviewer, blinded to sequence, placed free-hand regions of interest, inclusive of as much liver as possible, on four images from each PDFF and R2* parametric map. Another blinded reviewer graded respiratory motion using a 5-point Likert scale. Pearson correlation (r), Lin's concordance coefficients (r_c), and Bland-Altman analyses were used to assess agreement between techniques. Frequency of clinically-liming motion (score≥3) was compared with Fisher's exact test.
Results: 42 patients were included (15F:27M; mean age:15.7±4.6 years). Mean PDFF and R2* were 16.6±13.1% and 29.3±4.7 sec^{-1} on breath-held images vs. 17.0±13.2% and 29.6±5.2 sec^{-1} on navigator-gated images. PDFF demonstrated almost perfect agreement between sequences (r_c=0.997, 95%CI:0.994-0.998; mean bias:0.3%; 95% limits of agreement:-2.4 to +1.7%), while R2* values demonstrated very strong correlation but poor agreement (r=0.837, r_c=0.832, 95%CI:0.716-0.910). Navigator-gated images exhibited significantly higher frequency of clinically-limiting respiratory motion (88% vs. 48%, p=0.0001).
Conclusions: Despite greater respiratory motion artifact, a free-breathing navigator-gated mDixon sequence produces PDFF values with almost perfect agreement to a breath-held sequence and thus may be an option in patients with limited breath-holding capacity.

Paper #: 004

Low b-value diffusion-weighted images detect significantly more hyperintense liver lesions in children than T2-weighted images.

Angelo Don Grasparil, *angelodon.grasparil@sickkids.ca*; Hemali Solanki, Elizabeth Sheybani, Govind B. Chavhan, MD, DABR; Hospital for Sick Children, Toronto, Ontario, Canada

Disclosures: Govind B. Chavhan, MD, DABR: Consultant, Honoraria: Bayer, Inc. All other authors have disclosed no financial interests, arrangements or affiliations in the context of this activity.

Purpose or Case Report: Applying lower diffusion gradient eliminates signal from all the vessels thereby improving visibility of T2-hyperintense lesions on image with low b-value of 50-100 s/mm2 (LBV). LBV have been shown to be superior to T2-weighted fast spin echo sequence (T2W) in detection of liver lesions in adults. There are no such studies assessing this in children. The purpose of the study is to compare the sensitivity of LBV images and T2W images in the detection of focal liver lesions in children.
Methods & Materials: A retrospective review of liver MRI performed for assessment of focal liver lesions in 50 children (22 males, 28 females; age 2 months to 17 years (mean 10.88 years)) was done. Two radiologists reviewed both LBV and T2W sequences independently at different occasions to note number of lesions, smallest lesion size, and location. A consensus reading of the entire MRI examination and correlation with follow-up, other imaging modalities, and pathology in available cases, was used to determine final number of lesions as a reference standard. Inter-observer agreement between 2 sequences for each reader for detection of number of lesions was assessed using intra-class correlation coefficient (ICC). The average number of lesions per patient detected by both readers on each sequence was compared with each other and with the reference standard using ICC and Signed-Rank test. The smallest lesions detected by each sequence were compared using paired t-test.
Results: A total of 170 hyperintense lesions were identified on consensus review to serve as reference standard. The average number of lesions identified by both readers on LBV was 134 (79%) and on T2W were 95 (56%). There was excellent inter-observer agreement for detection of lesions on LBV (ICC=0.96 (0.93-0.98)) and T2W (ICC=0.85 (0.75-0.91)), with slightly better agreement on LBV. Both readers identified significantly more lesions on LBV compared to T2W (reader 1 p=0.0036, reader 2 p=0.0001). Compared to the reference standard (mean number of lesions=3.45), T2W detected significantly less lesions (mean number of lesions=1.91; p=0.0000) while there was no significant difference in lesion detection on LBV (mean number of lesions-2.68; p=0.1527). LBV and T2W were not significantly different in identifying the smallest lesion size (reader 1 p=0.50, reader 2 p=0.53).
Conclusions: Low b-value DWI images are more sensitive than T2-weighted sequences in detecting hyperintense focal liver lesions in children.

Paper #: 005

Normal Pancreatic Parenchymal Volume in Heathy Children

Brendan McCleary, MD[1], *bmccleary@gmail.com*; Andrew T. Trout[1], Maisam Abu-El-Haija, MD[1], Lin Fei, PhD[1], Qin Sun, MPH[1], Suraj Serai[2], Jonathan R. Dillman, MD. MSc[1]; [1]Radiology, Cincinnati Children's Hospital Medical Center, Cincinnati, OH, [2]Children's Hospital of Philadelphia, Philadelphia, PA

Disclosures: Andrew T. Trout, MD: Consultant, Honoraria: Guerbet Group, Royalty: Elsevier, Wolters-Kluwer, Research Grants: Canon Medical, Siemens Medical Solutions, National Pancreas Foundation, In-Kind Support: ChiRhoClin Inc., Perspectum Diagnostics; **Jonathan R. Dillman, MD, MSc:** Research Grants: Canon Medical Systems; Siemens Healthineers; Perspectum Diagnostics; Bracco Diagnostics, Other: Travel Support (Philips Healthcare, GE Healthcare). All other authors have disclosed no financial interests, arrangements or affiliations in the context of this activity.

Purpose or Case Report: Pancreatic atrophy, a finding of chronic pancreatitis, has traditionally been defined qualitatively. Volumetric measurements of the pancreas may provide a means to define atrophy more quantitatively but an understanding of normal volume is required. The purpose of this study was to define normal pancreatic parenchymal volume in children, its relationship with demographic and anthropometric factors and its relationship to volume of fluid secreted after secretin administration.
Methods & Materials: This study was IRB-approved and compliant with HIPAA. A single observer manually segmented (Vitrea, Vital Images) the pancreas on axial MR images prospectively obtained in 50 children (6-16 years) without pancreatic disease. Parenchymal volumes were correlated (Pearson) with age, height, weight, body surface area (BSA) and with previously calculated volume of fluid secreted in response to secretin. Student's t-test was used to compare means. Quantile regression was used to define $5^{th}/95^{th}$ percentiles for parenchymal volume by BSA.
Results: Mean (±SD) parenchymal volume for our 50 healthy children was 46.0±18.8mL. There was no significant difference in parenchymal volume by sex. There were statistically significant correlations between parenchymal volume and age ($r = 0.51$, $p=0.002$), height ($r=0.67$, p<_0.0001), weight ($r=0.75$, $p<0.0001$) and BSA ($r=0.75$, $p<0.0001$). The 5^{th} percentile for parenchymal volume by BSA could be calculated by: = -4.97+24.66xBSA.Parenchymal volume was statistically significantly correlated with secreted fluid volume in response to secretin ($r=0.51$, $p=0.0002$).
Conclusions: In this study we have defined normal pancreatic volumes for children, and shown that these values vary with patient age and size. We have also defined the 5^{th} percentile for parenchymal volume by BSA, below which atrophy might be considered to be present as a feature of chronic pancreatitis. We have also shown that pancreatic parenchymal volume was moderately correlated with volume of fluid secreted by the pancreas in response to secretin.

Paper #: 006

Assessment of Normative Cut-offs for Pancreas Thickness and T1 Signal Ratios in the Pediatric Pancreas

Brendan McCleary, MD, *bmccleary@gmail.com*; Andrew T. Trout, Jonathan R. Dillman, MD. MSc, Maisam Abu-El-Haija, MD; Radiology, Cincinnati Children's Hospital Medical Center, Cincinnati, OH

Disclosures: Andrew T. Trout, MD: Consultant, Honoraria: Guerbet Group, Royalty: Elsevier, Wolters-Kluwer, Research Grants: Canon Medical, Siemens Medical Solutions, National Pancreas Foundation, In-Kind Support: ChiRhoClin Inc., Perspectum Diagnostics; **Jonathan R. Dillman, MD, MSc:** Research Grants: Canon Medical Systems; Siemens Healthineers; Perspectum Diagnostics; Bracco Diagnostics, Other: Travel Support (Philips Healthcare, GE Healthcare). All other authors have disclosed no financial interests, arrangements or affiliations in the context of this activity.

Purpose or Case Report: Normal values for linear thickness of the pancreas in children have recently been established on CT, but have not been validated for MRI. Additionally, a normal T1 ratio (pancreas:spleen) has been defined in adults but this has not been validated in children. The purposes of this study were: 1) To validate previously defined normal pancreatic thickness measurements for MRI and in a distinct pediatric population. 2) To validate the previously defined T1 ratio (pancreas:spleen) for adults in a pediatric population and assess its relationship to demographic factors.
Methods & Materials: This study was IRB approved and HIPAA compliant. A single observer measured linear thickness of the pancreas in the four previously defined segments (head, neck, body and tail) on axial images from 50 MRI exams prospectively obtained in children (6-16 years old) without pancreatic disease. ROIs were also placed in each the pancreas and spleen (on the same slice, if possible) on T1-weighted gradient recalled echo (GRE) images to measure the T1 ratio. Linear measurements were compared to previously defined norms. T1 ratios were summarized with means and standard deviations and assessed for their relationship to age, sex, height, weight and body surface area (BSA) using t-tests and linear regression, as appropriate.
Results: Using previously defined normal values for pediatric pancreatic thickness, 34 healthy participants (68%) had "atrophy" of one segment and 14 (28%) had "atrophy" of two or more segments.Mean (±SD) T1 ratio for the study population was 1.33±0.15. There was a statistically significant correlation between T1 ratio and age and height ($r=-0.44$, $p=0.0015$ and $r=-0.38$, $p=0.0069$, respectively). but not with weight or BSA. There was no significant difference in T1 ratio based on sex. 11 participants (22.4%) had a T1 signal ratio <1.2, a threshold previously determined to correspond with exocrine insufficiency in an adult population.
Conclusions: We demonstrate that previously defined normal pancreas thickness values for children are likely too restrictive and that better measures of pancreas bulk in children are needed. Mean T1 ratio in children is related to age and height and is above the normal threshold of 1.2 previously described in adults but >20% of children have T1 ratios below the adult cut-off suggestive of exocrine insufficiency. Specific cut-offs for disease identification by T1 ratio in children are needed.

Paper #: 007

Magnetic Resonance Imaging T1 Relaxation Times for the Liver, Pancreas, and Spleen in Healthy Children at 1.5 and 3T

Leah A. Gilligan, MD, *leah.gilligan@cchmc.org*; Jonathan R. Dillman, MD. MSc, Jean A. Tkach, PhD, Stavra A. Xanthakos, MD, MS, Jacqueline K. Gill, MPA, Andrew T. Trout; Radiology, Cincinnati Children's Hospital Medical Center, Cincinnati, OH

Disclosures: Jonathan R. Dillman, MD, MSc: Research Grants: Canon Medical Systems; Siemens Healthineers; Perspectum Diagnostics; Bracco Diagnostics, Other: Travel Support (Philips Healthcare, GE Healthcare). **Andrew T. Trout, MD:** Consultant, Honoraria: Guerbet Group, Royalty: Elsevier, Wolters-Kluwer, Research Grants: Canon Medical, Siemens Medical Solutions, National Pancreas Foundation, In-Kind Support: ChiRhoClin Inc., Perspectum Diagnostics. All other authors have disclosed no financial interests, arrangements or affiliations in the context of this activity.

Purpose or Case Report: Magnetic resonance imaging (MRI) T1 relaxation time is altered by fibrosis and inflammation and is a potential marker for diseases of the solid abdominal organs. The purpose of this study was to measure T1 values of the liver, pancreas, and spleen in healthy children.
Methods & Materials: This cross-sectional IRB-approved study prospectively recruited healthy children aged 7 to 17 years with BMI in the 5th to 85th percentile to undergo abdominal MRI at 1.5 or 3T, including T1 mapping with a variant Modified Look-Locker (MOLLI) sequence between February 2018 and August 2018. A single reviewer placed free-hand regions of interest on the T1 parametric maps in the liver, pancreas, and spleen, inclusive of as much parenchyma as possible and on up to four axial images per organ. Student t-tests were used to identify differences in T1 values by gender. Linear regression was performed to assess associations between T1 values and age.
Results: 32 patients were included in the study (16F:16M; mean age:12.2±3.1 years; n=16 at 1.5T; n=16 at 3T). Median T1 relaxation times per organ at 1.5T were: 1) liver: 569±39 ms; 2) pancreas: 576±55 ms; and 3) spleen: 1172±71 ms and at 3T were 1) liver: 767±63 ms; 2) pancreas: 730±30 ms; and 3) spleen: 1356±87 ms. T1 values were not significantly different between males and females at either field strength. Linear regression showed no significant association between age and T1 values of the liver, pancreas, and spleen at 1.5T (r=0.66, p=0.30; r=0.48, p=0.094; and r=0.49, p=0.057; respectively) and 3T (r=0.50, p=0.12; r=0.56, p=0.15; and r=0.40, p=0.12; respectively).
Conclusions: We report normal MRI T1 values for the liver, pancreas, and spleen at 1.5 and 3T in a cohort of healthy children and observed no significant association between age or sex and T1 values. While these values might be used to exclude disease, a larger cohort will likely be needed to establish cut-off values to allow future comparisons with disease states.

Paper #: 008

Development of MRI-compatible Robots for MRI-Guided Procedures in Pediatric Interventional Radiology

Karun Sharma, MD, Ph.D[1], *kvsharma@cnmc.org*; Dan Stoianovici, PhD[2], Reza Monfaredi[1], Bhupender, Yadav[1] Ranjith, Vellody[1], Kevin Cleary, PhD[1]; [1]Radiology, Childrens National Medical Center, McLean, VA, [2]Johns Hopkins Medical Center, Baltimore, MD

Disclosures: All authors have disclosed no financial interests, arrangements or affiliations in the context of this activity.

Purpose or Case Report: Percutaneous needle placement relies on image guidance using X-ray, CT, US, or MRI. MRI-guided interventions are ideal for pediatric patients to eliminate ionizing radiation while providing superior imaging of the nervous and musculoskeletal systems. However, performing procedures within a closed-bore MRI scanner is challenging because of the ergonomics of limited patient access. We are developing small, MRI-compatible robotic systems that will enable MRI-guided interventions.
Methods & Materials: Three systems are being developed for bone biopsy, arthrography, and nerve block/ablation. For bone biopsy, a table-mounted robot with bone drill guide was developed and tested in a cadaveric leg to evaluate feasibility and accuracy. For arthrography, a patient-mounted four degree of freedom robotic positioning and orienting stage was developed and tested in cadaveric shoulder and hip joints. For nerve block/ablation, a two degree of freedom needle driving and rotation stage will allow remote needle advancement under real-time MRI guidance. A software interface allows the physician to select the target and skin entry point which define the safest needle trajectory.
Results: The bone biopsy robot study shows feasibility and clinically acceptable bone drill accuracy in a cadaver leg (Figure 1). A total of 10 biopsy targets were sampled using MRI guidance, 5 from the femur and 5 from the tibia. All of the targets were successfully reached with an average targeting accuracy of 1.43 mm. The arthrography robot study in Thiel embalmed cadavers shows feasibility and good success for intra-articular injection during MR arthrography (Figure 2). In one male and one female cadaver, a total of 13 robotically-targeted joint injections were performed (10 shoulder, 3 hip). All were successful with an average procedure time of 20 minutes. The next step is a pilot clinical trial.
Conclusions: The robotic devices presented here are being developed to enable radiation-free MRI-guided procedures. Clinical application in bone biopsy of suspicious lesions, joint injection for MR arthrography, and nerve block/ablation for pain management are pertinent to pediatric patients. The patient-mounted design minimizes challenges of patient motion and MR-compatibility allows safe use in the scanner bore without degradation of image quality. These devices have the potential to enable physicians to perform MR interventions with high accuracy and safety and also shorten procedure duration.

Paper #: 009

Sclerotherapy of Aneurysmal Bone Cysts: MRI Imaging Findings and Clinical Outcomes

Kimberly Dao, MD, *kimberlyanhdao@gmail.com*; Patrick Johnston, MMath, Msc, Raja Shaikh, MBBS, MD; Boston Children's Hospital, Boston, MA

Disclosures: All authors have disclosed no financial interests, arrangements or affiliations in the context of this activity.

Purpose or Case Report: To investigate the long-term MRI imaging findings and clinical outcomes of pediatric patients with aneurysmal bone cysts treated by sclerotherapy at a large tertiary children's hospital.
Methods & Materials: An IRB-approved retrospective review was performed on patients who completed sclerotherapy for aneurysmal bone cyst from 2007 through 2018. Patients were excluded if they had no pre-treatment MRI, post-treatment MRI, or received surgery between sclerotherapy treatments, yielding a total number of 38 patients. Pre-treatment and final post-treatment MRI imaging and reports were reviewed. The sclerotherapy treatment(s) and surgical history were recorded. Electronic medical records were also reviewed for clinical symptoms prior to initial presentation and preceding the final MRI study. The data analysis for this study was generated using SAS software.
Results: Pre-treatment MRI and biopsy results confirmed the presence of aneurysmal bone cysts. 95% (36/38) of patients had lesions showing fluid-fluid levels on pre-treatment MRI (95% confidence interval (CI) 0.84-0.99). All subjects (38/38) had lesions that were thin-walled, sclerotic rimmed, expansile locular, and showed internal hyperintense T2 signal (CI 0.94-0.99 for all 4 variables).The mean number of sclerotherapy treatments was 3.6, the mean time between the last sclerotherapy treatment and the final MRI was 158 days, and the average interval between sclerotherapy treatments was 118 days. The mean total follow-up time was 438 days.On post-treatment MRI imaging, 74% (28/38) showed a decreased number of cystic spaces (CI 0.58-0.86); 68% (26/38) demonstrated cortical thickening (CI 0.53-0.81); 84% (32/38) showed decreased fluid-fluid levels (CI 0.7-0.93); 87% (33/38) had decreased internal T2 signal (CI 0.74-0.95); and 89% (34/38) showed remodeling deformity (CI 0.77-0.96).Prior to treatment, 94% (33/35) of the patients reported pain (CI 0.84-0.99), while by the final MRI, only 17% (6/35) of the patients reported pain. The difference was -77 percentage points ($p<0.001$). Data for 3 patients was not available regarding pain. 9/38 patients went on to receive additional surgery after sclerotherapy.
Conclusions: There is little information about the evolution of MRI imaging findings following successful sclerotherapy of aneurysmal bone cysts. This study provides a summary of common MRI findings in aneurysmal bone cysts and clinical outcomes for these patients after sclerotherapy.

Paper #: 010

Long-term Results and Durability of Cryoablation of Osteoid Osteoma in the Pediatric and Adolescent Population

Jay Shah, MD, *jay.interventionalradiology@gmail.com*; Anne Gill, MD, Jennifer Laporte, Morgan Whitmore, Frederic Bertino, MD, John David Prologo, Kelley W. Marshall, MD, Jorge Fabregas, Nickolas Reimer, C. Matthew Hawkins, MD; Interventional Radiology / Pediatric Radiology, Emory University Hospital / Children's Hospital of Atlanta, Atlanta, GA

Disclosures: John David Prologo, MD: Consultant, Honoraria: Galil, Research Grants: Galil, Endocare. All other authors have disclosed no financial interests, arrangements or affiliations in the context of this activity.

Purpose or Case Report: To confirm technical feasibility and clinical efficacy of osteoid osteoma (OO) cryoablation in a large, pediatric/adolescent cohort with short and long term follow-up.
Methods & Materials: An electronic medical record and imaging archive review was performed to identify all cryoablations performed for OOs between 2011 and 2018 at a single tertiary care pediatric hospital. The analysis included 63 patients with suspected OOs treated by cryoablation (age range, 3-18 y; mean age, 11.7 y; 37 boys; 26 girls). Conventional CT guidance was used in 22 procedures; cone-beam CT needle guidance was used in the remaining procedures. Follow-up data were obtained via a standardized telephone questionnaire and clinical notes.
Results: Technical success, defined as placement of cryoprobes in the desired location, was achieved in 100% of the 63 patients.Immediate clinical success (cessation of pain and nonsteroidal antiinflammatory drug [NSAID] use within 1 mo after the procedure) was achieved in 61/63 (96.8%) of patients. There were 2/63 (3.2%) clinical failures, both in small bones of the feet. 5/63 (7.9%) patients had clinical recurrence with repeat ablation and subsequent complete response. Furthermore, long-term clinical success (cessation of pain and NSAID use for > 12 mo after the procedure) was achieved in 54/57 patients (94.7%) at the time of this submission. There were no major complications. Two patients (3.2%) were admitted overnight for pain control after the procedure (minor complications). There were no other minor complications.
Conclusions: Image-guided cryoablation is a known technically feasible, clinically efficacious, and safe therapeutic option for children and adolescents with symptomatic OO. Long-term results in this study provide confirmation of a definitive treatment paradigm.

Paper #: 011

Image-guided biopsy for suspected pediatric osteomyelitis: analysis of experience

Neil K. Jain, *jainn@email.chop.edu*; Sulman Mahmood, Victor Ho-Fung, MD, James Edgar, Sphoorti Shellikeri, Master's in Biomedical Engineering, Anne Marie Cahill, Ganesh Krishnamurthy, MD, Abhay Srinivasan, MD; Pediatric Interventional Radiology, Children's Hospital of Philadelphia, Philadelphia, PA

Disclosures: All authors have disclosed no financial interests, arrangements or affiliations in the context of this activity.

Purpose or Case Report: Biopsy is often performed to aid in diagnosis and to clarify optimum management of children with suspected osteomyelitis. We describe our experience with bone biopsy for pediatric osteomyelitis and analyze yield with regard to imaging features on MRI and procedure technique.
Methods & Materials: This was a retrospective review of patients with suspected osteomyelitis who underwent percutaneous bone biopsy in interventional radiology. Review parameters included MRI features, technical aspects of the procedure, and clinical data, including details of clinical presentation and microbiology and pathology results.
Results: Forty patients (mean age 9.5y, range 0.4-25.8y) underwent biopsy. Fluoroscopy was used in 29 cases. CT guidance was used in 9 and US guidance was used in 2. Additional US guidance for adjacent soft tissue biopsy was used in 15 cases. A 16G bone biopsy cannula was utilized in 34 cases; 13G in 5; and an 11G in 1 case. The mean number of bone cores obtained was 3.6 (range 1-10). There were no procedure-related complications.Biopsy culture yielded a pathogen in 4 of 40 cases, and culture yield did not show significant correlation with fever, leukocytosis/blood culture, ESR/CRP, number of cores, instrument gauge, or acquisition of liquid aspirate or soft tissue. Based on culture and/or pathology results, 23 patients were diagnosed with infectious osteomyelitis (17 acute and 6 chronic). One patient was diagnosed with a stress fracture and one with Hodgkin lymphoma. Chronic recurrent multifocal osteomyelitis (CRMO) was diagnosed in 15 patients; CRMO was supported on pathology in 9 cases. Biopsy results, therefore, did not directly inform diagnosis in 6 (15%)

patients.On MRI, 74% of lesions were in the appendicular skeleton and 26% in the axial skeleton. An axial location demonstrated a significant association with a positive bacterial culture (p=0.04). There was also a statistically significant association between a lesion size ≤20 mm on MRI and negative bacterial culture (p<0.01). There was no association between culture yield with interosseous/subperiosteal fluid or myositis.
Conclusions: Results support bone biopsy as a safe and effective procedure in the management of pediatric osteomyelitis. Although culture yield from bone biopsy was low, overall biopsy results aided in diagnosis in a majority (85%) of patients with suspected osteomyelitis. On MRI, lesion size ≥20 mm and an axial location demonstrated association with positive culture.

Paper #: 012

Ultrasound-Guided Synovial Biopsy in Children

Paymun Pezeshkpour, B.Sc.,
*paymun.pezeshkpour@mail.utoronto.ca;*Catherine Chung, Shirley Tse, Afsaneh Amirabadi, Simal Goman, Michael Temple; Hospital for Sick Children, Toronto, Ontario, Canada

Disclosures: All authors have disclosed no financial interests, arrangements or affiliations in the context of this activity.

Purpose or Case Report: To determine technical success, complication and diagnostic rates of ultrasound-guided synovial biopsy (USGSB) in pediatric patients at a pediatric tertiary referral center.
Methods & Materials: This retrospective single center study was approved by the research ethics board and included all patients who underwent USGSB at a tertiary referral center. Patients were identified using the GE Centricity Picture Archiving and Communication System (PACS), the Interventional Radiology EST-IGT database and Surgical Information Systems software (SIS). Patient demographics, clinical information (history and physical exam), clinical investigations including pathology reports, procedure details and complications were collected. A Microsoft Excel 2016 database was used to compile data for descriptive analysis. All statistical analyses were performed by SPSS.
Results: Between May 2000 to March 2017, 22 patients (4M:18F) underwent 25 USGSBs. Median age was 11 years (range 1.6–17) & median weight was 40.2 kg (range 10–83). Presenting symptoms were pain, mobility issues and joint effusion (n=15, 10, 9 respectively) with use of analgesics (14/22 patients), antibiotics (1/22) & immune modulators (2/22). Synovial thickening ranged between 1.5–15mm with a mean of 5mm. 21/25 biopsies had effusion measured and it was detected in 12/21. 18/25 biopsies measured doppler signal and 7/18 were subjectively increased. A total of 105 passes (median 4, range 2-8) yielded 95 cores (median 4; range, 1-8). All procedures were technically successful. 8/25 samples did not contain synovium ((5/8 were referred by orthopedics, 3/8 from rheumatology, p=0.06); 1/8 diagnosis of underlying reparative process made). Based on multivariable logistic regression analysis, the number of cores/passes, ultrasound probe type and biopsy orientation did not predict the absence of synovium. Only 1 patient with a non-diagnostic biopsy underwent subsequent surgical biopsy. In the remaining 17, pathology showed no pathological abnormality (n=2), synovitis (n=6), reparative changes (n=5), neoplastic process (n=2) & other (n=3; 1 lymphoplasma synovitis, 1 necrotic bone and 1 hemosiderin-laden macrophage infiltration). 3 mild procedure related adverse events considered rarely preventable.
Conclusions: USGSB is a technically feasible and safe procedure in the diagnosis of synovial thickening of unknown etiology or with inconclusive aspiration results and/or serologic findings. A trend towards nondiagnostic samples was found in orthopedic patients.

Paper #: 013

Complex Cystic Thyroid Nodule Fine Needle Biopsies in Children – Experience in a Tertiary Pediatric Center

Fernando Escobar, MD, *escobarf@email.chop.edu*; Madiha Aslam, MBBS, Abhay Srinivasan, MD, Anne Marie Cahill; The Children's Hospital of Philadelphia, Philadelphia, PA

Disclosures: All authors have disclosed no financial interests, arrangements or affiliations in the context of this activity.

Purpose or Case Report: Complex cystic lesions of the thyroid can be challenging to biopsy even with fine needle technique especially if intralesional hemorrhage during biopsy partially obscures the lesion.The purpose of this study is to review our experience with fine needle biopsy of complex cystic and simple cystic thyroid nodules in children and assess the rate of intralesional hemorrhage.
Methods & Materials: An IRB approved database of patients who underwent ultrasound guided fine needle biopsies for simple cystic and complex cystic thyroid nodules was queried for diagnostic accuracy. Correlation of intra-lesional hemorrhage with risk factors such as age, size and vascularity of nodule, needle gauge and number of passes.
Results: One hundred and seven patients with 196 thyroid nodules US guided fine needle aspiration biopsy procedures, (85 F, 22M), mean age 15.4 yrs. (7-25yrs). Nodules were as follows; 169/196 (86%) complex cystic and 27/196 (14%) were simple cystic. Technical success was 195/196 (99%) one procedure aborted due to patient discomfort. Needle gauge was; 27g in 120/195 nodules, 25g in 67/195 and both in 9/195 nodules. Number of passes were as follows; 2 passes in 9/195 nodules, 3 in 139/195, 4 in 41/195, 5 in 4/195, 6 in 1/195, 8 in 1/195 nodules. Intralesional hemorrhage was seen in 84/195 nodules (43%); of those 60/84 (71%) were complex cystic nodules, 24/84 (29%) were simple cystic nodules. Number of passes in these nodules were; 3 passes in 61/84 nodules, 4 passes in 18/84, 5 passes in 5/84 nodules. Diagnosis was achieved in 189/195 nodules (97%). Histological diagnoses were as follows; benign hyperplastic focus in nodular goiter in 157/195 nodules, follicular lesion of undetermined significance in 11/195, papillary thyroid carcinoma 9/195, follicular neoplasm 7/195, atypia of undetermined significance 4/195, benign squamous cyst in 1/195 and unsatisfactory specimen in 6/195 nodules. The intralesional hemorrhage rate was 89 % (24/27) for simple cystic lesions and 36% (60/169) for complex cystic nodules. Pathological surgical correlation was available in 51/107 patients (48%) and 5/51 (10%) patients had a divergent malignant diagnosis from FNA biopsy with papillary microcarcinoma diagnosed on surgical pathology.
Conclusions: In our experience the diagnostic yield for FNA of complex and simple cystic lesions of the thyroid (97%) was very high compared to other published studies with the number of unsatisfactory diagnoses too low to correlate with lesion or biopsy technique characteristics.

Paper #: 014

Novel Approach to Increase Technical Success during Pediatric Percutaneous Gastrostomy/Gastrojejunostomy Tube Placement using Transgastric Balloon Occlusion

Rachelle Durand, DO, *durandr@email.chop.edu*; Sphoorti Shellikeri, Master's in Biomedical Engineering, Anne Marie Cahill, Michael Acord, MD; Radiology, Children's Hospital of Philadelphia, Philadelphia, PA

Disclosures: All authors have disclosed no financial interests, arrangements or affiliations in the context of this activity.

Purpose or Case Report: Adequate gastric distension via insufflation is a key step in creating a safe percutaneous window during gastrostomy/gastrojejunostomy (G/GJ) placement. However, this may be limited due to rapid egress of air from the stomach into the duodenum, despite the use of glucagon. Herein, we describe an adjunctive novel technique of transgastric balloon occlusion to maximize gastric insufflation and assess the outcome of this technique during G/GJ placement in children.
Methods & Materials: A single-center, IRB-approved, retrospective review of 15 patients (6 female and 10 males) with a mean age of 4.8±5.6 years (range 0-16 years) and mean weight of 20.9±18.9 kg (range 3-54.2 kg) who had G/GJ placement utilizing transgastric balloon occlusion over a 2 year period. The standard technique was antegrade placement with administration of glucagon. After initial percutaneous failure, more recently the practice of positioning a balloon in the proximal duodenum was adopted to temporarily obstruct the gastric outlet. Clinical history, patient demographics, procedure reports, balloon type, technical success, and outcomes were reviewed.
Results: The addition of a transgastric balloon occlusion was successful in salvaging G/GJ tube placement in 10/15 (67%) patients (3 G, 7 GJ) which likely would have been unsuccessful using standard practice. Most common underlying disorders included cardiac (5), neurologic (3), and oncologic (2). Of 5 unsuccessful placements, 3 were attributed to persistent colonic interposition/high position, 2 to high stomach position. Subsequently, 4 of 5 underwent surgical gastrostomy placement. No procedure-related complications were reported.
Conclusions: The technical success of G/GJ placement in children with challenging percutaneous access may be improved by the novel use of transgastric balloon occlusion to prevent rapid egress of air out of the stomach. A larger cohort is needed to assess the technical efficacy and to identify ideal balloon characteristics and insufflation location based on patient and disease characteristics.

Paper #: 015

Bridging the Barriers for Better Team-Based Patient Care by Incorporating NICU Radiology Tele-rounds

Susan E. Schmidt, MD, Joseph Cao, Kate Louise M. Mangona, MD, Thomas O'Neill, **Jeannie Kwon**, *kwonjk@gmail.com*; UTSW, Lucas, TX

Disclosures: All authors have disclosed no financial interests, arrangements or affiliations in the context of this activity.

Purpose or Case Report: Pediatric radiologists have provided valuable daily on-site consultation for two separate neonatal intensive care units (NICU), located at the university hospital (UH) and the public county hospital. This historically required travel to three separate physical locations throughout the day. Additional challenges to the workflow included the addition of a third location for daily consultation rounds at the children's hospital NICU and the elimination of a campus shuttle route. While the pediatric radiology department's goal was to maintain the high level of service, availability, and communication with the neonatology team, concerns regarding time and movement energy waste due to travel threatened to make this untenable.
Methods & Materials: A reliable process for conducting patient care rounds with participants physically located in different institutions across the medical campus was established using a web-based teleconferencing tool. Requirements of the application were that connectivity should be (nearly) instantaneous across the networks of three different hospitals, reliable, and user-friendly, with two-way audio and video, including screen sharing to facility discussion of interesting radiology findings. Schedule, daily electronic meeting apointments were sent to the assigned pediatric radiologist and the NICU conference room at the UH, where clinical team rounds occurred over a two-hour period daily. On-site rounds were preserved at the two larger NICUs which were also in closer proximity to one another.
Results: Travel times were significantly reduced following implementation of remote consultation at the UH NICU facility, with an estimated savings of 4940 minutes, 113.1 miles, and 225,420 steps over a six month timeframe. Feedback from pediatric radiology faculty and NICU treatment teams was widely positive following the implementation of telerounds. We demonstrated the ability to provide a similar level of quality of communication, ability to entertain dialogue regarding exams, and timeliness of rounds and a significant increase in satisfaction after implementation across all metrics.
Conclusions: The implementation of tele-radiology NICU rounds resulted in savings in time and travel and improved satisfaction with communication for both radiology and NICU providers.

Paper #: 016

Implementing the "What-Where-When" approach to improve patient history availability at the time of radiograph interpretation

Aaron S. McAllister, MD, **Courtney M. Kirby, MBA**, *Courtney.Kirby@nationwidechildrens.org*; Julee Eing, RT, Erin L. Mesi, RT(R), Phillip McGonagill, LSSBB, Benjamin Thompson, DO, Nicholas A. Zumberge, MD, Rajesh Krishnamurthy; Nationwide Children's Hospital, Columbus, OH

Disclosures: Aaron S. McAllister, MD: Equity Interest/Stock Option: GE, MMM, CHD, JNJ. All other authors have disclosed no financial interests, arrangements or affiliations in the context of this activity.

Purpose or Case Report: Nonexistent/incomplete clinical information at the time of radiographic exam is an impediment to efficient and accurate radiological interpretations. We aim to improve the relevant information at point of care interpretation for radiologists. Technologists were utilized to gather relevant clinical information at the point of care to supplement the available clinical information utilizing a previously described "What-Where-When" approach (Hawkins et al., 2013).
Methods & Materials: Histories were considered complete when they contained all of the following 3 elements: what (reason for the study, mechanism of injury, etc.,) where (location - lateral, diffuse, etc.,) and when (element of time: acute, chronic, etc.) A baseline measure was obtained by evaluating a random sampling (n=213) of histories accompanying radiographs by awarding 1 point for each element present in the history (max =3) acquired via the hospital's EMR in April 2018.Subsequently, technologists were asked to fill in missing data elements from the ordering provider's clinical history at point of care. Clinical histories

were rescored in October 2018 (n=232), this time including the supplemental history acquired by the technologist. Balance measures were considered by sampling 100 exams to verify the accuracy of the technologist supplemented clinical histories and additional analysis was conducted to measure any negative effect on exam turnaround time. Additionally, a technologist survey assessed participation and ideas for improvement. A radiologist survey assessed perceived usefulness of the available history before and after technologist augmentation as well as impact on diagnostic confidence, accuracy, and efficiency.
Results: Exams with complete patient histories increased from 22% to 56%. The exam history, on average, saw an increase in elements present. The accuracy of the supplemented exam history was 97%. There was no increase in technologist turnaround time following the addition of this task. Radiologist's rated impact of the completed histories on their imaging interpretation using a scale of 1-5 (low-high): interpretation efficiency: 5.0, accuracy: 5.0, frequency of use: 4.3, altered search pattern or thought process: 3.7.
Conclusions: Radiograph technologists have proven capable and successful at gathering the what, when, and where at point of care with no significant negative impact. This targeted clinical information collected by x-ray technologist's results in improved diagnostic confidence, efficiency, and accuracy.

Paper #: 017

Effect of a Double-Interpretation Skeletal Survey Program on Child Abuse Evaluations

M Katherine Henry, MD, MSCE, **Ammie M. White, MD**, *whitea@email.chop.edu*; Sabah Servaes, Andrew J. Degnan, MD, MPhil, Michael L. Francavilla, MD, Victor Ho-Fung, MD, Ann Johnson, Summer Kaplan, MD MS, Richard Markowitz, Hansel J. Otero, MD, David Saul, Lisa States, Raymond Sze, Joanne Wood, Philip Scribano; Children's Hospital of Philadelphia, Philadelphia, PA

Disclosures: All authors have disclosed no financial interests, arrangements or affiliations in the context of this activity.

Purpose or Case Report: Child protection teams (CPTs) rely on skeletal surveys (SS) to identify young children with occult fractures who may be victims of abuse. Little is known about the utility of double interpretation SS programs. The goals of this project are to (1) quantify disagreement between radiologists regarding fractures and (2) evaluate whether second interpretations alter management of children undergoing evaluation for abuse.
Methods & Materials: Our institution's CPT and Department of Radiology established a quality improvement collaboration to pilot a double interpretation SS program. During this ongoing pilot, SSs are first interpreted by pediatric radiologists, and later, CPT requests a second interpretation from a core group of second readers, with an option to ask a question for clarification. The second radiologist documents whether the second interpretation: (a) has a different interpretation regarding fracture presence, absence, or certainty (b) a different interpretation regarding another aspect of the SS, (c) whether additional views or modalities were reviewed, and then (d) answers CPT's question. CPT reviews the second reader's responses and determines: (e) whether the second read process changed concern for abuse; (f) whether medical management changed; and, (g) degree (Likert scale) to which this process was helpful in increasing confidence in SS interpretation.
Results: To date, 129 SS double interpretations were completed, 93 (72.1%) initial and 36 (27.9%) follow up. Median age was 7.2 months; 58.9% were male. The proportion of second reads with a different interpretation (disagreement) regarding fracture presence, absence, or certainty was 7.0% (95% CI 3.6, 12.9; N=9). As a result of the second read process, CPT concern for abuse changed in 8 cases (6.2%; 95% CI 3.1,12.0), increased in 5 and decreased in 3. After consideration of the constellation of clinical findings, CPT concern rarely changed from abuse to non-abuse (N=1) or from non-abuse to abuse (N=1). CPT medical management changed in 11.6% (95% CI 7.1, 18.5). CPT reported that the second read process was helpful in increasing confidence in SS interpretation in over 90% of cases.
Conclusions: Our pilot identified agreement in fracture presence, absence, or certainty in >90% of cases. The second read process resulted in a change in the level of concern for abuse in <10% of cases. Additional data are needed to understand if certain SS findings are at higher risk for disagreement to understand the utility of targeted second read programs.

Paper #: 018

Effectiveness of showing an interactive animated video vs regular animated video in improving children's cooperativeness during MRI scan: a prospective, randomized, non-inferiority trial

Evelyn Gabriela Utama, Doctor of Medicine (MD Candidate)[1] *evelynutama@gmail.com*; Seyed Ehsan Saffari, PhD[2], Phua Hwee Tang, FRCR[3]; [1]Duke-NUS Medical School , Singapore, Singapore, [2]Duke-NUS Medical School, Centre for Quantitative Medicine, Singapore, Singapore, [3]Department of Diagnostic & Interventional Imaging, KK Women's and Children's Hospital, Singapore, Singapore

Disclosures: All authors have disclosed no financial interests, arrangements or affiliations in the context of this activity.

Purpose or Case Report: Magnetic resonance imaging (MRI) can cause considerable anxiety in children due to the unfamiliar environment, loud noises, confined space, and the need to lie still. They can become un-cooperative and move during the scan, resulting in non-diagnostic images due to motion artefacts. We previously reported in a prospective, randomized controlled trial that animated educational videos shown to children before their MRI scan reduced the percentage of children needing repeated MRI sequences and improved children's confidence of staying still for at least 30 minutes. However, it is unknown which video (regular or interactive) had a bigger influence on the outcomes. A greater number of children were found to enjoy the interactive video more than the regular video as well. In this study, we seek to investigate whether the use of an interactive educational animated video is non-inferior to showing two videos (regular and interactive) in improving children's cooperativeness during MRI scans.
Methods & Materials: In this Institutional Review Board-approved prospective, randomized, non-inferiority trial, 462 children aged 3 to 20 years old scheduled for elective MRI scan during the period of June 2017 to October 2018 at the Singapore KK Women's and Children's Hospital were randomized into interactive animated video only, and regular cum interactive animated videos groups. Children were surveyed and shown the videos before they went in for their MRI scan. Three outcomes were assessed across the two groups: repeated MRI sequences, general anesthesia (GA), and improvement in children's confidence of staying still for at least 30 minutes.
Results: In the interactive video only group (n = 229), 76 (33.2%) patients needed repeated MRI sequences, 2 (0.9%) needed GA, and 64 (27.9%) became more confident of staying still for at least 30 minutes. In the combined videos group (n = 233), 89 (38.2%) patients needed repeated MRI sequences, 4 (1.7%) needed GA, and 66 (28.3%) became more confident of staying still for at least 30 minutes. The three outcomes are not significantly different between the two groups using Chi-squared test at 0.05 significance level.

Conclusions: The interactive animated video group demonstrated non-inferiority to the combined videos group by showing a comparable repeated MRI sequences and GA proportions, and the increase in confidence level of staying still for at least 30 minutes.

Paper #: 019

Improved Workflow with MRI Protocol Optimization and Technologist Education

Ami Gokli, *aag298@nyu.edu*; Janet R. Reid, MD, FRCPC, Suraj Serai; Children's Hospital of Philadelphia, Philadelphia, PA

Disclosures: All authors have disclosed no financial interests, arrangements or affiliations in the context of this activity.

Purpose or Case Report: There has been recent increasing interest in imaging protocol standardization. At our institution, challenges to standardization stem from being a large hospital system with multiple sites and 10 MRI scanners at our facility alone. Scanners are different ages, designed by different manufacturers and vary by type. Posted protocols were not standardized by name and would often not match those within the MRI scanners. Finally, sequence names on MRI scanners varied by manufacturer and type of scanner, and these names would not match posted protocol names. We aim to optimize imaging protocols by standardizing the MRI naming system, making protocols readily available, and continuing to maintain image quality. Our goal is to avoid communication breakdown between technologists, radiologists and referring physicians and to add value by providing consistency.
Methods & Materials: A multidisciplinary team including technologists, radiologists and physicists was assembled and a standard sequence naming system was agreed upon. The process of updating the online posted protocols was re-evaluated and representative “thumbnail” images were associated with each sequence in a protocol to avoid confusion. A soft launch of the new system was implemented with the most frequently used MRI MSK protocol in September 2018. An electronic survey was distributed in October to identify challenges and acceptance by technologists.
Results: 22 MRI technologists completed the survey. Of all respondents, 95.5% (n=21) found the new naming convention easier to understand with 81% also adding that it positively affected their workflow (n=18). 57.1% of respondents utilized the new protocol (n=13) since the soft launch the month prior. Of those who utilized it, 100% found the new thumbnail images helpful during the workday (n=13), and 100% also noted that it should be adopted for all protocols (n=13). 90.9% of responding technologists noted they would refer to the posted protocols more often if thumbnail images were included in all protocols (n=20). Individual suggestions for improvement included indicating anatomic coverage on thumbnail photos, including unusual scanning angles, and demonstrating preferred patient positioning.
Conclusions: MRI protocol optimization including standardization of protocols, sequences, coverage and a reference article supporting protocol design was well received by technologists and improves their daily workflow.

Paper #: 020

Wait Time Reduction for Sedated MRIs

Nicholas A. Zumberge, MD, *Nicholas.Zumberge@nationwidechildrens.org*; Brian Schloss, MD, Rajesh Krishnamurthy, Phillip McGonagill, BA, Lean Six Sigma Black Belt, Ramkumar Krishnamurthy, PhD, Akila Sankaran; Radiology, Nationwide Children’s Hospital, Columbus, OH

Disclosures: All authors have disclosed no financial interests, arrangements or affiliations in the context of this activity.

Purpose or Case Report: Large hospitals are facing increased pressure from free standing imaging facilities for timely sedate imaging services. Meanwhile, wait times have traditionally been long due to resource constraints. This study takes a multifactorial approach to improving wait times for patients that require an MRI under sedation. Our aim is to apply focused interventions in reducing wait times at Nationwide Children's Hospital from 56 days down to 15 days.
Methods & Materials: To reduce sedated MRI (SMRI) wait times, we looked at 4 key drivers; the first, sedation capacity (SC). The goal here was to increase sedation resources. The second key driver we looked at was education. The goal was to educate patients on the risks of sedation. This approach might aid in reducing the demand for SMRI slots. We also wanted to recruit the help of ordering clinicians to share with patients our information sheet on sedation, and child life contact information, if families chose to go the non-sedation route. The third key driver was MRI simulation. With the help of Child Life, divert more patients to our MRI simulator and/or Virtual Reality (VR) goggles, then, if successful, on to an unsedated scan. Finally, reduce MRI scan times. Towards this effort, we set out to reduce protocol standards to the minimum necessary for quality scans; as well as reduce sequencing times in order to further abbreviate scans.
Results: In Aug 2017, we introduced simulator Fridays. With the aid of Child Life services, eligible patients were offered the opportunity to try the MRI simulator. Once successful, the child would then be scheduled for an immediate unsedated MRI. By Dec 2017, we saw a dip in SMRI wait time from 62 days to 52 days, a 16% improvement. On 01 Feb 2018, we added a third sedation room on Mondays. The additional sedation resource achieved the greatest impact. By 30 Sep 2018, wait times had fallen to a low of 18 days, a 71% reduction from Jul 2017.
Conclusions: By far our most dramatic gains have been from the increase in sedation resources. We continue to push for Child Life support for sim MRI and soon the MRI VR goggles. We are also working with ordering clinics, in an effort to divert more patients to unsedated scans. We are diligently working to shorten protocols and sequencing times for scans to further reduce the SMRI burden. This future abbreviated approach, with the aid of VR scans, will allow for our Child Life team to further stratify patients towards non-sedate slots.

Paper #: 021

Pediatric Emergency Medicine Point of Care Ultrasound Impact on Radiology Ultrasound Volume

Asef Khwaja, MD, *asef.khwaja@gmail.com*; Sandra Saade-Lemus, MD, Rachel Rempell, MD, Aaron Chen, MD, James Edgar, Summer Kaplan, MD MS; The Children's Hospital of Philadelphia, Philadelphia, PA

Disclosures: All authors have disclosed no financial interests, arrangements or affiliations in the context of this activity.

Purpose or Case Report: Point of care ultrasound(POCUS) use is growing in pediatric emergency medicine(PEM). At our institution, POCUS was implemented in the emergency department(ED) in March of 2013. POCUS is used for teaching, procedure guidance, and for directing selection of radiology(RAD) performed exams. POCUS may even replace RAD ultrasound(US). For example, US evaluation of skin and soft tissue infections(SSTI) may be performed by RAD or PEM at our institution. To our knowledge, no studies have assessed the impact of PEM POCUS on RAD US volume. We investigated the impact of PEM POCUS at our institution on RAD US exam volumes in total and for SSTI.
Methods & Materials: In this IRB-exempt study we retrospectively reviewed monthly US exam volume for RAD and PEM 60 months before and after existence of an organized POCUS program in the ED. Exams were identified by exam type and patient location. SSTI RAD US were identified by key word search for "soft tissue". Volume of digital radiography (DR) in the ED was assessed as control unaffected by POCUS. A descriptive inspection of exam growth rate using linear regression was performed. Secondary analysis was performed while normalizing for total number of ED visits and ED patients with ICD-10 codes indicating soft tissue infection. Graphical inspection of data showed a sudden increase in US and DR volumes preceding POCUS by 28 months, so this period was excluded from analysis.
Results: Mean monthly US volume after POCUS was 616 exams for RAD and 32 exams for PEM. Rate of RAD US increased from 2.0-fold per month ($p < 0.05$) to 4.0-fold per month ($p < 0.001$) after POCUS, while POCUS increased at a rate of 1.2-fold per month ($p < 0.001$). For SSTI US, RAD orders from ED were similar before and after POCUS, increasing at a rate of 0.5-fold per month ($p < 0.01$), while POCUS exams for SSTI increased 0.2-fold per month ($p < 0.001$). Growth rate of RAD US per ED visit was 3x higher than for POCUS. Growth rate of RAD SSTI US per SSTI diagnosis was 2.4x higher than for POCUS SSTI, similar to difference in absolute growth rate for these exams.
Conclusions: Our results suggest that PEM POCUS does not impair growth of RADS US from the ED. More work is needed to determine if PEM POCUS for SSTI impaired growth for RAD US for SSTI, but the small growth in POCUS SSTI exams suggests lack of growth in RAD US for SSTI is due to nearing maximum capacity. Results suggest that radiologists should not fear loss of referrals due to ED POCUS, but should collaborate with PEM to improve patient care.

Paper #: 022

Non-visualization of the ovaries on pediatric transabdominal Ultrasound with a non-distended bladder: can adnexal torsion be excluded?

Gali Shapira - Zaltsberg, MD, *Shapira.gali1979@gmail.com*; Fleming Nathalie, Anna Karwowska, Maria Esther Perez Trejo, Gerald Guillot, Elka Miller, MD; Pediatric radiology, CHEO, Ottawa, Ontario, Canada

Disclosures: All authors have disclosed no financial interests, arrangements or affiliations in the context of this activity.

Purpose or Case Report: The purpose of this study was to retrospectively investigate if clinically suspected adnexal torsion can be excluded based on non-visualization of the ovaries on transabdominal ultrasound (TUS) with a non-distended bladder in pediatric patients.
Methods & Materials: This retrospective study comprised 340 girls (4-18 years) who were referred to TUS to assess for adnexal torsion and/or appendicitis, and the ovaries were initially not visualized on TUS. Their bladders were subsequently filled and were rescanned with a distended bladder showing the ovaries. Ovarian volumes and time between TUS scans were documented. The ratio of the volume of the larger ovary to the smaller one was calculated. If ovarian abnormalities were noted on imaging, the medical record was reviewed for clinical correlation. A sample size of 340 participants was selected based on a margin of error (MOE) between 0.75% and 2.3% for an assumed probability of a girl testing negative for adnexal torsion in the TUS with a full bladder in the range 0.95-0.995.
Results: None of the girls (0/340) who had a TUS study done with a non-distended bladder in which the ovaries were not visualized, had a positive diagnosis of adnexal torsion, confirming the hypothesis that non-visualization of ovaries on TUS can help exclude adnexal torsion. Nonetheless, 0.6% (2/340) of the girls had significantly enlarged ovarian volume when subsequently visualized after bladder filling, that radiologically may be concerning for adnexal torsion. The mean and median time difference between the scans was 105.1 (65.8) and 89.0 (59.0, 130.5) minutes respectively.
Conclusions: In the right clinical setting, non-visualization of the ovaries on TUS study can be just as helpful as a negative study, alleviating the need for bladder filling and prolonging the wait time in the emergency department. Inclusion of non-visualization of the ovaries as one of the features in a predictive score for adnexal torsion should be considered.

Paper #: 023

Introduction of Contrast enhanced voiding urosonography into clinical practice: Assessment of Clinical Indications, Imaging results, and Urologist Acceptance.

Fidaa Wishah, MD[1], *fidaaw@stanford.edu*; Erika Rubesova, MD[1], Safwan Halabi, MD[1], Jesse Sandberg, M.D.[1], Edward Diaz, M.D.[2], William A. Kennedy II[2], Richard Barth, MD[1]; [1]Department of Pediatric Radiology Lucile Packard Children's Hospital, Stanford, CA, [2]Department of Pediatric Urology Lucile Packard Children's Hospital, Stanford, CA

Disclosures: Edward Diaz, M.D.: Research Grants: Bracco Diagnostics as lead PI investigator**.** All other authors have disclosed no financial interests, arrangements or affiliations in the context of this activity.

Purpose or Case Report: Prior studies have validated contrast enhanced voiding urosonography (ceVUS) to be as accurate as fluoroscopic VCUG for the diagnosis of vesicoureteral reflux (VUR). Our purpose is to assess performance of ceVUS in clinical practice including clinical indications, imaging results (including adequacy of urethral visualization), and urologist acceptance.
Methods & Materials: A retrospective review was performed on 170 consecutive patients (mean age 17.1 months, 91 males, 79 females) referred for ceVUS between 8/4/2017 and 9/14/2018. We used a GE- Logiq E9 machine with a C2-9 probe in high resolution mode, mechanical index (MI) range (0.06-0.18), average 0.13. We reviewed clinical indications, duration of examination, imaging results and follow up VCUG for inadequate ceVUS. Image evaluation by 4 radiologists included grading of urethral visualization (0/poor,1/good.,2/excellent). Urologist acceptance was assessed via questionnaire.
Results: Clinical indications included: hydronephrosis (34%), UTI (29%),VUR followup (13%), other (24%). Ordering providers were pediatric urologists in 90%. In 41/170 (24%) ceVUS was follow-up to fluoroscopic VCUG (22%) or CeVUS (2%). ceVUS was inadequate in 1/170 (0.6%) and was converted to VCUG. Average ceVUS examination time was 22 minutes. VUR was found in 25 patients and 83 kidneys(K) - grade 1 (7K), grade 2 (28K), grade 3 (29/K), grade 4 (15K), grade (4K). Consensus review graded anterior/posterior urethra visualization in males as excellent in 52%/40%, good in

19%/21% and poor in 24%/32%. Urethral visualization in females as excellent in 58%,good in 10%, poor in 9%. 23/170 patients did not void while imaging. Referring urologists' online questionnaire results: Is CeVUS satisfactory for detecting VUR? (100%), Would you order fluoroscopic VCUG? sometimes/rarely (66.7/33.3%).VCUG indications included suspected UPJ obstruction, complex anatomy, posterior urethral valves, and bilateral grade 4 prenatal hydronephrosis. 66.7/33.3% felt somewhat/very confident in interpreting a CeVUS without a radiologist. 66.7/33.3% thought that CeVUS is very/extremely adequate in urethral visualization. 66.7/33.3% felt definite patient preference/no preference to CeVUS over fluoroscopic VCUG. Should ceVUS replace fluoroscopic VCUG nationwide? 66.7% agreed, 33.3% neither agreed or disagreed
Conclusions: ceVUS was readily integrated into clinical practice and well-accepted by urologists for diagnosis of VUR as an alternative to VCUG. Urethra visualization may be suboptimal and require a VCUG.

Paper #: 024

3D printed anatomic contrast enhanced voiding urosonography (ceVUS) teaching phantoms: bringing pediatric vesicoureteral reflux (VUR) to life

Sphoorti Shellikeri, Master's in Biomedical Engineering, *sphoortishellikeri@gmail.com*; Elizabeth Silvestro, MSE, Laura Poznick, AAS, ARDMS, Trudy Morgan, Kassa Darge, MD, PhD, Raymond Sze, Susan J. Back, MD; Radiology, Children's Hospital of Philadelphia, Philadelphia, PA

Disclosures: Kassa Darge, MD, PhD: Research Grants: Bracco, Lantheus, Siemens, Philips, NIH, Thrasher Society, Helfer Society, ITMAT, Foerderer, MTR, RSNA, SPR; **Susan J. Back, MD:** Research Grant: Siemens, Philips, Educational Grant: Bracco. All other authors have disclosed no financial interests, arrangements or affiliations in the context of this activity.

Purpose or Case Report: Vesicoureteral reflux (VUR) is the most frequently detected problem of the pediatric urinary tract. Contrast enhanced voiding urosonography (ceVUS) is a highly sensitive examination to diagnose VUR. Following FDA approval for the use of an ultrasound contrast agent for ceVUS in children, there is increasing interest in learning how to do the ceVUS examination. Ultrasound (US) phantoms that depict VUR are not available. We created 3D-printed phantoms as teaching tools to simulate the grades of VUR during the ceVUS examination.
Methods & Materials: MR urograms that depicted varying degrees of urinary tract dilation in infants were identified and segmented to represent the four highest grades of VUR, one kidney for each grade. The segmented kidneys were connected to a CAD generated bladder, urethra, and ureter. Kidneys were paired to create two models to simulate the 4 grades of reflux that involved the upper urinary tract. The renal models were printed in polyvinyl alcohol (PVA) and embedded into a silicon (smooth-on eco flex 30) mold of an infantile abdomen and pelvis. The PVA parts were dissolved leaving behind cavities of the renal anatomy in the silicon. Printed posts were added to open and close the ureters to simulate grade 1 reflux. A catheter was placed in the urethra to enable filling.
Results: GE LOGIQ E9 US system with a C2-9 contrast enabled transducer was used to image the models. One operator administered the contrast-saline solution in the urethral catheter while the other obtained US images. The US transducer was placed on the anatomic regions of the flanks, abdomen and pelvis with US coupling gel. Still and cine US images were obtained. Each kidney was easily visualized, as were the ureters and bladder including visualization of all anatomic structures in a single image. Images highly resembled clinical examinations.
Conclusions: These ceVUS phantoms are reusable and can be used as a versatile teaching tool to demonstrate and practice the ceVUS procedure while depicting the appearance of different grades of VUR in children.

Paper #: 025 - ***Withdrawn***

Paper #: 026

Comparison of glomerular filtration rate estimated by motion-robust high spatiotemporal resolution dynamic contrast enhanced MRI and plasma clearance of 99mTc-DTPA

Sila Kurugol, PhD[1], Onur Afacan, PhD[1], Reid Nichols[1], Monet Dugan[1], Richard Lee, M.D.[2], Simon K. Warfield, Ph.D.[1], **Jeanne S. Chow, MD[1]**, *jeanne.chow@childrens.harvard.edu*; [1]Radiology, Boston Children's Hospital and Harvard Medical School, Boston, MA, [2]Boston Children's Hospital and Harvard Medical School, Boston, MA

Disclosures: All authors have disclosed no financial interests, arrangements or affiliations in the context of this activity.

Purpose or Case Report: The purpose of our study was to assess the accuracy of measuring glomerular filtration rate (GFR) using motion-robust high spatiotemporal resolution 3D dynamic contrast enhanced MRI, by comparison of MRI-GFR to GFR from 99mTcDTPA nuclear medicine study (NM-GFR).
Methods & Materials: This IRB approved study enrolled children, between 0-20 years, undergoing both a clinically indicated contrast enhanced MRI, and a nuclear medicine GFR study within 2 weeks of each other. Each patient consented for the study underwent an additional 6-minute dynamic contrast enhanced MRI scan using the motion-robust high spatiotemporal resolution dynamic radial VIBE sequence (Siemens 3T). The images were reconstructed offline using compressed sensing image reconstruction including regularization in temporal dimension to improve image quality and reduce streaking artifacts due to fast imaging. Images were then automatically post processed using in-house developed software. Post processing steps included segmentation of kidney parenchyma and aorta using a convolutional neural network technique and tracer kinetic model fitting using the Sourbron's two-compartment tracer kinetic model to calculate the magnetic resonance based GFR (MRI-GFR). The MRI-GFR results were compared to the glomerular filtration rate measured by 99mTcDTPA nuclear medicine study (NM-GFR).
Results: 18 children (average age 5.9, 8 female:10 male) were enrolled between July 2017- present. The method was technically feasible in all patients. The results showed that the MRI-GFR correlated with NM-GFR with r-square value of 0.94. We also performed Bland Altman analysis (i.e. difference of MRI-GFR and NM-GFR versus mean of NM-GFR and MR-GFR), which showed a reproducibility coefficient (RPC) of 22 with 95% confidence interval, and the coefficient of variation (CV) of 8.2% with values between -21 (-1.96 standard deviation) and 24 (+1.96 standard deviation).
Conclusions: MR-GFR is a reliable method of measuring glomerular filtration rate and is comparable to the GFR measured by plasma clearance of 99mTcDTPA.

**Work supported by the SPR Research and Education Foundation*

Paper #: 027

Correlation of MR-Urography and intravoxel incoherent motion MRI based estimation of split renal function in the pediatric clinical population

Patrice Grehten, MD[1], *patrice.grehten@kispi.uzh.ch*; Christian J. Kellenberger, MD[1], Andras Jakab, MD, PhD[2]; [1]Diagnostic Imaging, University Children's Hospital Zurich, Zurich, Switzerland, [2]Center for MR-Research, University Children's Hospital Zurich, Zurich, Switzerland

Disclosures: All authors have disclosed no financial interests, arrangements or affiliations in the context of this activity.

Purpose or Case Report: To evaluate the usability of intravoxel incoherent motion MRI (IVIM) for predicting split renal function in the pediatric population undergoing clinically indicated functional MR-Urography
Methods & Materials: We retrospectively analyzed data of 41 children (age: 38.8 ± 33 months) with morphologically normal kidneys or urinary tract dilation. High-resolution 3D T2-CUBE, dynamic MR urography and IVIM were acquired with free breathing on a 1.5T MRI scanner. IVIM was co-registered to T2-CUBE and an in-house developed tool was used for motion correction. We utilized the IVIM model to separate diffusion and perfusion in the renal cortex, medulla and pelvis after manually delineating in largest coronal cross-section and 2 further slices from coronal mid-plane. Split renal function was evaluated with the volume adjusted Patlak method based on the post contrast dynamic MR-Urography.
Results: After correcting for age and sex, we found a moderate correlation between renal transit time and the cortex perfusion fraction (f) (Pearson partial correlation coefficient, r=0.315, p=0.006), medulla f (r=0.270, p=0.025), pelvis pseudo-diffusion coefficient (r=0.383, p=0.0001) and a negative correlation with pelvis f (r=-0.292, p=0.012) as well as negative correlation of split kidney function with the cortex f (r=-0.270, p=0.037).
Conclusions: Our results provide evidence that IVIM imaging is useful to evaluate split renal function. We propose that the separation of perfusion and diffusion processes is necessary to estimate renal function in children using diffusion MRI. Image processing and statistical models adjusting for patient age were necessary to reveal correlations between microvascular perfusion and function, however, we did not find similar correlation with the diffusion coefficient.

Paper #: 028

Identifying Calyceal Diverticula at Magnetic Resonance Urogram in Children

Juan S. Calle Toro, MD, *ctjuans@gmail.com*; Susan J. Back, MD, Kassa Darge, MD, PhD, Hansel J. Otero, MD; Radiology, Children's Hospital of Philadelphia, Philadelphia, PA

Disclosures: Susan J. Back, MD: Research Grant: Siemens, Philips, Educational Grant: Bracco; **Kassa Darge, MD, PhD:** Research Grants: Bracco, Lantheus, Siemens, Philips, NIH, Thrasher Society, Helfer Society, ITMAT, Foerderer, MTR, RSNA, SPR. All other authors have disclosed no financial interests, arrangements or affiliations in the context of this activity.

Purpose or Case Report: To report the frequency of calyceal diverticula (CD) as seen at functional MR urography (fMRU) and determine the ability of fMRU to diagnose calyceal diverticulum in a pediatric cohort.
Methods & Materials: This is an IRB-approved retrospective study of all patients with suspected CD that underwent fMRU at our institution. Two-pediatric radiologists reviewed each fMRU, blinded to clinical information and other imaging, to determine the presence, morphology and contrast accumulation in cystic lesions suspected of being CD. Each radiologist made a determination of cyst or CD solely based on the presence of contrast within the lesion. Size and location were also recorded. The timing at which the contrast was first seen within the lesion and the pattern of contrast within the lesion (i.e. complete filling versus layering contrast) were also recorded. The diagnosis of CD was confirmed by either surgery, retrograde pyelogram or acknowledgement of fMRU results in the urologic clinical note. Chi-square was used to examine differences between characteristics of cysts versus diverticula. Inter-reader agreement was also calculated with kappa.
Results: A total of 66 lesions from 52 studies in 50 children (29 girls and 21 boys; mean age 10.9 ± 5.7 years) were included. Nineteen (28.8%) lesions demonstrated contrast filling, hence characterized as diverticula; while the remaining 47 (71.2%) were cysts. The overall frequency of CD in our sample was 18 cases per 1000 patients. The average size of CD was 2.3 cm (+/- 1.2 cm). CD were more common in the right side (58% versus 42% in the left) and in the upper pole (42% versus 32% and 26% in the interpolar and lower pole, respectively); all of the CD were medullary. Contrast filling was observed on average at 4.0 minutes (SD +/- 2.4; range 1.5-13 minutes). There was complete opacification of the CD in the majority (n=12, 63%) of cases. The agreement between radiologists was 91% (kappa=0.78). 18 cysts and 6 CD were confirmed invasively with a 100% match between fMRU and invasive technique diagnosis.
Conclusions: Calyceal diverticula, as seen at fMRU, are at least three times more frequent that previously reported during intravenous urograms. Moreover, fMRU is an accurate diagnostic tool to differentiate calyceal diverticula from renal cysts. In our sample, all diverticula were identified within a 15 minute delay cut-off, which allows to perform shorter examinations. Delays of over 30 minutes are hence unnecessary.

Paper #: 029

Distinguishing clinical and imaging characteristics of nephrogenic rest vs. small Wilms tumor: a report from the Children's Oncology Group

Jesse Sandberg, MD[4], *jesseksandberg@gmail.com*; Ethan A. Smith, MD[1], Fredric Hoffer, MD[11], Sabah Servaes, MD[2], Yueh-Yun Chi[10], Elizabeth Mullen, MD, FAAP[3], Elizabeth Perlman, MD[5], Peter Ehrlich, MD[6], James Geller, MD[7], Jeffrey Dome, MD/PhD[8], Conrad V. Fernandez, MD[9], Geetika Khanna[4]; [1]Section of Pediatric Radiology, Cincinnati Children's Hospital, Cincinnati, OH, [2]Department of Radiology, Children's Hospital of Philadelphia, Philadelphia, PA, [3]Department of Pediatric Oncology, Children's Hospital Boston/Dana-Farber Cancer Institute, Boston Children's Hospital, Boston, MA, [4]Mallinckrodt Institute of Radiology, Washington University School of Medicine, St. Louis, MO, [5]Department of Pathology and Laboratory Medicine, Ann & Robert H. Lurie Children's Hospital of Chicago and Northwestern University Feinberg School of Medicine, Chicago, IL, [6]Section of Pediatric Radiology, Department of Radiology, C.S. Mott Children's Hospital, University of Michigan Health System, Ann Arbor, MI, [7]Division of Pediatric Oncology, Cincinnati, Children's Hospital Medical Center, University of Cincinnati, Cincinnati, OH, [8]Division of Pediatric Oncology, Children's National Medical Center, Washington, DC, [9]Department of Pediatrics, Dalhousie University & IWK Health Centre, Halifax, Nova Scotia, Canada, [10]Department of Biostatistics, College of Public Health & Health Professions College of Medicine, University of Florida, Gainesville, FL, [11]Department of Radiology, University of Washington, Seattle, WA

Disclosures: Geetika Khanna, MD, MS: Financial Interest: Elsevier - Royalty: Independent contractor. All other authors have disclosed no financial interests, arrangements or affiliations in the context of this activity.

Purpose or Case Report: Nephrogenic rests (NR) are known precursors for Wilms tumor (WT). Distinguishing between NR and small WT can be challenging and relies on pathological identification of capsule around the WT. Prior publications have suggested that homogeneity of lesion and elliptical shape favor the diagnosis of NR over WT. Interpretation of these studies was limited by small sample sizes or pre-biopsy chemotherapy. The purpose of this study was to identify if clinical and/or imaging findings robustly distinguish NR from WT.
Methods & Materials: All cases of pathologically diagnosed NRs and a comparison group of WT (< 5 cm) in patients <5 year of age were identified from the Children's Oncology Group renal tumor biology, banking and classification study (AREN03B2) (July 2006-Aug 2016). Exclusion criteria: chemotherapy prior to pathological evaluation and >30days between imaging and surgical sampling. Two radiologists blindly assessed all lesions on available CT/MR images for size, shape, interface (lesion margin) and, location and homogeneity. All cases underwent central pathology review. Two-sample t-test was used for continuous variables, and Fischer's exact test for categorical variables. Receiver operating characteristic (ROC) analysis was performed to determine size cutoff for differentiating rests vs. WT.
Results: 31 cases with rests (20 perilobar, 11 intralobar) and 29 WT were identified. History of a predisposition syndrome (46% rests, 11.5% WT, p 0.03) and younger age (median age rest 1.10, range 0.22-4.04 years, WT 3.28, range 0.36-5.57 years, p <0.001) were more common in NR cases. Median diameter of NR was 1.3 cm (0.7-3.4) vs. WT 3.2 cm (1.8-4.9) (p < 0.001). Imaging findings supportive of WT included a round, exophytic lesion (p <0.001). Imaging assessment of interface was not predictive of NR vs. WT (p 0.20). Perilobar rests (83%) were more likely to be homogeneous compared to intralobar rests (30%) or WT (10%) (p <0.001). ROC analysis showed that in lesions <5cm, optimal cutoff between rest vs. WT was 1.75 cm (p <0.001). The size cutoff remained the same at 1.75cm after excluding WT 4-5cm in size (p<0.001).
Conclusions: In children <5 years of age, diagnosis of WT should be favored over NR when a renal mass is round and exophytic. Homogeneity favors the diagnosis of perilobar NRs. Imaging is not effective in identifying capsule (a key pathological discriminator of NR vs WT). We suggest 1.75 cm as the optimal cutoff for differentiating between NR vs. small WT.

Paper #: 030

Enhancing Presurgical 3D Modeling and Printing: Multiphase MRI Technique

Elizabeth Silvestro, MSE, *silvestro@email.chop.edu*; Thomas Kolon, MD, Douglas Canning, MD, Robert H. Carson, B.S.R.T. R,MR, Suraj Serai, Raymond Sze, Susan J. Back, M.D.; Radiology, Children's Hospital of Philadelphia, Philadelphia, PA

Disclosures: Susan J. Back, MD: Research Grant: Siemens, Philips, Educational Grant: Bracco. All other authors have disclosed no financial interests, arrangements or affiliations in the context of this activity.

Purpose or Case Report: The process of anatomic 3D modeling and printing conventionally is done from one imaging set, inherently limiting the visibility and detail of some structures. Multiphase post contrast image acquisition and intracavitary contrast instillation allows construction of composite models using sequences optimized for specific anatomic detail. This technique is ideal for renal tumor or genitourinary modeling. Applications include preoperative oncologic and reconstructive imaging.
Methods & Materials: Multiphase gadolinium enhanced sequences were obtained as part of a preoperative MRI examination. Delayed phase imaging detailed the renal collecting system and ureters when applicable. Direct instillation of dilute gadolinium into the urinary bladder and vagina facilitated defining cavitary anatomy. Following acquisition, images were reviewed and selected for segmentation. A sequence was selected as an anatomic reference to alignall required structures. Images detailing arterial, venous, renal collecting system and cavitary anatomy were selected. Each structure was segmented independently using threshold and contouring tools. The desired structures were exported and overlaid together on the reference scan. If there was variation in size or orientation of a scan an unrelated structure, such as the spine, was segmented and used to resize and orient the regions of interest. Finally, posting and coloration were added to the model to illustrate any focus of the surgery or diagnosis depending on the capability of the available additive manufacturing machine, or 3D printer.
Results: The process of acquiring and modeling anatomy can be applied to numerous surgical and diagnostic applications. The most promising uses thus far have been to model the relationships of renal arteries, veins and collecting system in Wilmstumor. Urologist(s) remarked that 3D models aided comprehension and conceptualization of the imaging anatomy. Furthermore, one model was used to plan a multidisciplinary surgical approach as well as educate the patient and family.
Conclusions: Multiphase scan segmentation technique can produce a complexmodel without compromising structural detail. The composite model aids preoperative planning for complex surgeries. This process can be extended to merging of any temporally related images.

Paper #: 031

Adolescents With Obesity:Carotid Intima Media Thickness (cIMT) and Cardiovascular (CV) Risk Factors

Suzanne E. Cuda, MD, **Maria-Gisela Mercado-Deane, MD**, *gmercad01@yahoo.com*; Children's Hospital of San Antonio, San Antonio, TX

Disclosures: All authors have disclosed no financial interests, arrangements or affiliations in the context of this activity.

Purpose or Case Report: Atherosclerosis begins in childhood and progresses throughout life. Current management of adolescents with obesity (AWO) is not directly linked to CV risk. Instead, we use surrogate measures such as the components of the metabolic syndrome (MS) or biomarkers. Noninvasive imaging using carotid ultrasound is used in other at risk pediatric populations but has not been used among AWO except to note that it is increased as compared to normal weight controls. In this pilot study we investigate associations between CV risk factors (%BMIp95, lipid profile, HbA1c, blood pressure, fasting blood glucose and insulin, liver function tests and high sensitivity C reactive protein) and cIMT in AWO between the ages of 13-17 years. The normal increase in cIMT is 0.009 mm per year.
Methods & Materials: 77 AWO, ages 13-17(45M/32F) were enrolled on their baseline visit to a pediatric weight management clinic. Criteria for inclusion: BMI>95th percentile for age, and no type 2 diabetes mellitus prior to presentation. Baseline laboratories for CV risk factors and cIMT were compared across increasing %BMIp95. cIMT was measured by taking the average of the common carotid artery measurements (Avg CCA).

Results: Mean age 15.16 years, mean BMI 38.27 kg/m2. Both age (P=0.0265) and systolic blood pressure (SBP) (P=0.0179) were significantly associated with Avg CCA using a simple linear regression model. No other variables were significantly associated with Avg CCA. After simultaneously adjusting for age and SBP in a multiple linear regression model, Avg CCA increased by 0.0125 mm per year increase in age (95% CI:-0.002, 0.027;P=0.10). Avg CCA increased by 0.0168 mm per 10 mm Hg increase in SBP (95% CI: -0.001,0.035;P=0.064).
Conclusions: CIMT significantly increases with age and systolic blood pressure in AWO. The rate of increase of Avg CCA per year of age exceeds the expected rate. No other CV risk factors were significantly associated with increases in Avg CCA. There was no significant increase in Avg CCA with increase in %BMIp95.

Paper #: 032

Longitudinal Assessment of Imaging Features of Generalized Arterial Calcification of Infancy

Sara Cohen, MD, *cohens10@email.chop.edu*; Christian A. Barrera, M.D., David M. Biko, MD, David Saul, MD, Ammie M. White, MD, Hansel J. Otero, MD; Children's Hospital of Philadelphia, Philadelphia, PA

Disclosures: David M. Biko, MD: Financial Interest: Wolters Kluwer - Royalty: Editor of Review Book. All other authors have disclosed no financial interests, arrangements or affiliations in the context of this activity.

Purpose or Case Report: Generalized arterial calcification of infancy (GACI), also known as idiopathic infantile arterial calcification, is a rare genetic disorder characterized by calcifications and injury to large and medium size vessels. We aim to describe the imaging findings of GACI in children.

Methods & Materials: This is a retrospective review of initial and follow up CT, CTA, MRA, and vascular ultrasound imaging in children with confirmed GACI at a single institution. All initial imaging studies were reviewed for the presence and distribution of arterial calcifications, stenosis, and wall thickening/irregularity within the chest, abdomen, and pelvis. Available follow up studies were compared to initial imaging findings. A chart review was performed for clinical history.
Results: A total of 8 patients (5 boys) from 6 families (2 sets of siblings) were identified. Patients presented prenatally (n=4); or with cardiac failure (n=2), seizures (n=1), or hypertension (n=1). Average follow up was 37 months (range 0 – 11 years). A single death occurred at 2 months of age.5 patients underwent imaging at birth and all had arterial calcifications as follows: aorta (n=4), pulmonary (n=3), mesenteric (n=3), renal (n=3), iliac (n=3), subclavian (n=2), brachiocephalic (n=1), common carotid (n=1), coronary (n=1), and splenic (n=1) arteries. 1 patient had main pulmonary artery stenosis and 1 had bilateral renal artery stenosis.4 of the newborn patients underwent follow up imaging between 1 month and 3 years of age. Calcifications were: decreased (n=2), resolved (n=1), or stable (n=1). Stenosis was new or progressed in these 4 patients as follows: renal (n=3), pulmonary (n=2), aorta (n=2), mesenteric (n=2), and iliac (n=1) arteries. Vessel wall irregularity/thickening developed in the pulmonary (n=1), aorta (n=1), mesenteric (n=1) and renal (n=1) arteries. 1 patient in this age group underwent initial imaging and was found to have renal artery stenosis and no calcifications.5 patients over 3 years of age underwent imaging (3 follow up and 2 initial), none of which had calcifications. Both initial studies in older siblings were normal. The follow up studies showed: stable infrarenal aortic, mesenteric and renal artery stenosis (n=1); progressive renal artery stenosis (n=1); and improved renal artery stenosis (n=1).
Conclusions: Patients with GACI have characteristic vascular calcifications at birth. While calcifications may decrease or disappear with treatment, disease progression may occur in terms of stenosis and wall irregularity.

Paper #: 033

Value of emergent pediatric cardiac computed tomographic angiography service: Initial experience at a large children's hospital.

Siddharth P. Jadhav, MD[1], *spjadhav@texaschildrens.org*; Pamela Ketwaroo[1], Snehal R. More[2], Gilbert Rizarri[1], Prakash M. Masand, MD[1]; [1]Radiology, Texas Children's Hospital, Houston, TX, [2]vRad, Eden Prairie, MN

Disclosures: Prakash M. Masand, MD: Consultant, Honoraria: Canon Medical Systems, Phillips MRI Users Meeting 2018, Daiichi Sankyo, Speakers Bureau: Canon Medical Systems, Royalty: Amirsys. All other authors have disclosed no financial interests, arrangements or affiliations in the context of this activity.

Purpose or Case Report: With newer generation scanners providing free-breathing, high-resolution cardiac imaging at sub milli-Sievert radiation dose, demand for pediatric cardiac computed tomography angiography (CTA) is increasing. It is only a matter of time before sub-specialized emergent cardiac CTA service during weekends and after-hours on weekdays will become an expectation for optimal patient care. The purpose of this study is to describe our experience of providing this service and its effect on patient care.
Methods & Materials: We retrospectively identified all patients that underwent after-hours weekday or weekend emergent cardiac CTA between January 2017 and August 2018. Sub-specialized cardiac CTA in the setting of congenital heart disease and coronary imaging were included. Routine vascular imaging in patients without structural heart disease, such as for aortic dissection, is commonly handled by non-cardiac trained radiologists and was therefore excluded. Data collected included day and time of CTA, patient age, indication, patient location, post-op status, need for anesthesia, need for surgery, intervention and/or change in medical management based on the emergent CTA.
Results: A total of 47 studies were identified, 26 (55%) of which were performed on a weekend or holiday and 21(45%) after 5 PM on a weekday. These were performed under direct supervision of a cardiac imager (1 of 3 FTE's). 28 (60%) were male. 34 (72%) were in infants out of which 19 (40%) were neonates. 16 (34%) patients were imaged for coronary artery evaluation, 9 (19%) for post-op conduit and shunt evaluation and 8 (17%) for aortic arch. Only 7 (15%) patients needed sedation with breath-holding for CTA, all of which were infants needing evaluation of coronaries. One patient was already intubated prior to CTA. 27 (57%) patients were from the ICU, 9 (19%) from intermediate care unit and 11 (23%) from the emergency room. Half (n=24, 51%) had at least 1 surgery for congenital heart disease at time of imaging. 29 (62%) CTA's had positive findings explaining patient's symptoms. Following CTA, 20 (43%) patients underwent either surgery or an interventional procedure, and 9 (19%) had change in medical management based on CTA findings. Surgery/intervention delay from CTA ranged from 0 days to 29 days with median of 3.5 days.
Conclusions: Emergent pediatric cardiac CTA is a valuable service leading to a change in management in 62% of our cases. Larger multi-institutional studies will be needed to ascertain if outcomes are affected by this service.

Paper #: 034

Intravenous Contrast Material Injection Protocol for Coronary CTA in Children: Changing The Paradigm From Contrast Volume To Injection Duration

Luisa F. Cervantes[1], *luisa.cervantes@mch.com*; Juan C. Infante, MD[2], Viky Loescher, MD[3], Juan Carlos Muniz, MD[1], Joshua B. Gruber, MSPH[1]; [1]Nicklaus Children's Hospital, Miami, FL, [2]University of Miami, Miami, FL, [3]Mount Sinai Medical Center, Miami Beach, FL

Disclosures: All authors have disclosed no financial interests, arrangements or affiliations in the context of this activity.

Purpose or Case Report: Optimal coronary artery opacification in pediatric coronary artery CTA (CCTA) is highly dependent on appropriate administration of contrast material. There is no standard prescription for contrast volume, injection duration (ID), injection rate (IR), and timing in pediatric CCTA. We sought to assess the efficacy of an intravenous contrast administration protocol based on a fixed ID and either a weight-based IR (< 50kg) or fixed IR (>50kg) to achieve optimal coronary enhancement in pediatric CCTA.
Methods & Materials: Patients who underwent CCTA at our institution from 2015 to 2018 were retrospectively evaluated. Studies with a fixed ID (14 or 16 sec) and a weight-based or fixed IR were included. Timing bolus was utilized in all studies. Age, weight, indication, contrast administration parameters (ID, IR, contrast volume, additional delay from timing bolus peak enhancement), and acquisition parameters (kV, scan time, CTDI volume, and DLP) were recorded. Vascular enhancement was measured as mean attenuation in Hounsfield units (HU) at the aortic root, proximal right and left coronary arteries, distal right coronary artery (RCA), and descending aorta. Optimal enhancement was defined as > 350 HU. The presence and location of artifact from the incoming contrast bolus was noted.
Results: 109 CCTAs were performed in 108 patients. Median age was 13.5 years (range 4 - 20). Median weight was 51.5 kg (range 20.5 - 118). Injection duration was 14 sec in 50% and 16 sec in 50%. Median injection rate for patients <50 kg was 0.1 mL/kg/sec. For patients >50 kg, the injection rate was 5 mL/sec in 58% and 5.5 mL/sec in 35%. Median contrast volume (including the timing bolus) was 1.9 mL/kg (range 1.0 - 2.6). No patient had significant bolus artifact in the superior vena cava or right heart obscuring the coronary arteries. In 5%, there was mild or moderate bolus artifact at the level of the right pulmonary artery. Optimal enhancement in the aorta and proximal coronary arteries was achieved in 95% of the patients. Suboptimal enhancement of the distal RCA was seen in 11% of patients with optimal opacification of the proximal coronary arteries. Enhancement was higher in patients scanned at lower kV.
Conclusions: Optimal coronary artery opacification can be achieved in pediatric patients utilizing a fixed injection rate and an injection duration protocol of 14 or 16 seconds.

Paper #: 035

Contrast extravasation using power injectors for contrast-enhanced computed tomography in children: Safety profile and injury severity assessment

Christian A. Barrera, M.D.,*barreracac@email.chop.edu*; Ammie M. White, MD, Ashley M. Shepherd, Patricia Mecca, BSRT, R,CT, MR, David M. Biko, MD, David Saul, MD, Hansel J. Otero, MD; The Children's Hospital of Philadelphia, Philadelphia, PA

Disclosures: David M. Biko, MD: Financial Interest: Wolters Kluwer - Royalty: Editor of Review Book. All other authors have disclosed no financial interests, arrangements or affiliations in the context of this activity.

Purpose or Case Report: To evaluate the safety of power injector use in contrast-enhanced CT in children
Methods & Materials: We searched our institution's medical records for patients age 0 - 18 years old who received intravenous contrast agent for a computed tomography between the dates of April 2015 - April 2018. The inclusion criteria were an IV contrast injection performed using a power injector. Data collected included patient demographic information, power injector information, catheter gauge, injection site and contrast agent. Then, we identified all confirmed cases of contrast extravasation in our sample. Contrast extravasations are classified at our institution according to our Peripheral Intravenous Infiltration and Extravasation (PIVIE) system into mild, moderate, severe and severe with an injury. T-test and Chi-square for gross analysis. For a sub-analysis, non-parametric tests were used. A p-value of < 0.05 was considered significant.
Results: 2,429 contrast-enhanced CTs performed with a power injector were identified. 18 contrast extravasation cases were confirmed, for a prevalence of 0.7%. 1,496 cases (823 boys and 673 girls) had complete information from the power injector. The mean contrast dose was 59.3 ± 34.5 mL. Iohexol was the most commonly used contrast medium (98.6%) followed by Iodixanol (1.3%). The mean peak pressure was 68.9 ± 62.3 psi and the flow rate was 1.7 ± 0.9 mL/s. Regarding patients with extravasation, the mean age was 11.2 ± 6.2 years; the most common peripheral IV access site was the antecubital fossa (n = 12). The most common catheter size was 22 gauge (n = 8) and the median catheter dwelling time was between 0 – 3 days. The contrast agents used were Iohexol 350 mg/dL (n = 12) and Iohexol 300 mg/dL (n = 6). The PIVIE score observed were seven mild, six moderate and five severe. There is no difference in PIVIE score with respect to flow rate, peak pressure, catheter dwelling time, catheter size, catheter injection site, ultrasound guidance and contrast agent ($p > 0.05$). Cases with extravasation had significantly higher peak pressure ($p < 0.001$) and flow rate ($p < 0.001$) compared to those without extravasation. Patients who received Iohexol 350 had a significantly higher incidence of contrast extravasation compared to those who used Iohexol 300 ($p = 0.03$).
Conclusions: The use of power injectors in children undergoing contrast-enhanced CT is safe under current standards. However, a significantly higher rate of extravasation was seen in patients receiving contrast with a higher viscosity.

Paper #: 036

Diagnostic performance of CT Angiography to detect pulmonary vein stenosis in children

Christian A. Barrera, M.D., *barreracac@email.chop.edu*; Hansel J. Otero, MD, Jordan B. Rapp, MD, David Saul, Ammie M. White, MD, David M. Biko, MD; Radiology, The Children's Hospital of Philadelphia, Philadelphia, PA

Disclosures: All authors have disclosed no financial interests, arrangements or affiliations in the context of this activity.

Purpose or Case Report: To assess the diagnostic accuracy of CT Angiography (CTA) to detect pulmonary vein stenosis in newborns, infants and toddlers
Methods & Materials: We retrospectively identify patients younger than 4 years who have undergone cardiac CTA and had either conventional angiography or surgery confirming or excluding a diagnosis of pulmonary vein stenosis. We excluded patients with previous surgery involving the pulmonary veins, exclusively right-heart conventional angiography or insufficient data in the operation note to confirm the presence or absence of

pulmonary vein stenosis. Demographic information, CT parameters and radiation dose were recorded. Two pediatric radiologists, blinded to clinical data, evaluated each case independently, determine the presence of stenosis and the pulmonary veins affected. Disagreement between the readers were solved by consensus with a third senior reader. The sensitivity, specificity, positive predictive value (PPV), negative predictive value (NPV), and accuracy of CTA and their 95% CI were calculated. Inter-observer agreement was evaluated with kappa statistics. Scores of 0.41 – 0.60, 0.61 – 0.80 and ≥ 0.80 were regarded as moderate, good, and excellent agreement, respectively. Descriptive values were reported as mean ± SD.
Results: 28 patients (11 girls, 17 boys) were included in the final sample. The mean age, weight, height and BSA were 4.9 ± 6.7 months, 4.5 ± 2.1 kg, 55.2 ± 8.7 cm and 0.25 ± 0.09 m^2, respectively. The mean effective dose was 0.5 ± 0.4 mSv. The pulmonary veins status was confirmed by conventional angiography in 22 patients and during surgery in 6 patients. The mean time between the gold standard and CTA was 0.7 ± 1.0 month (range: 1 day - 3 months). Thirteen cases with confirmed pulmonary vein stenosis were identified and evaluated. The interobserver agreement was moderate (k = 0.70). Six cases were resolved in consensus. The diagnostic performance at patient level showed the sensitivity, specificity, PPV and NPV were 78.5% (49.2%–95.3%), 87.5% (61.6%–98.4%), 84.2% (59.3%–95.4%), 82.3% (62.7%–92.8%) and 82.3% (62.7%–92.8%). The performance at the pulmonary vein level showed sensitivity of 73.3% (54.1%– 87.7%), specificity of 98.8% (93.9%– 99.9%), PPV of 95.6% (75.6%–99.4%) and NPV of 91.6% (85.8%–95.2%).
Conclusions: CTA is a reliable image technique with a high specificity, PPV and NPV to identify pulmonary vein stenosis in young children performing better when analyzed at the individual vein level.

Paper #: 037

Feasibility and Utility of Dual-Energy Chest CTA for Preoperative Planning in Pediatric Pulmonary Artery Reconstruction

Evan J. Zucker, MD[1], *zucker@post.harvard.edu*; Aya Kino, MD[1], Heiko Schmiedeskamp, PhD[2], Virginia Hinostroza, BS, BA[1], Dominik Fleischmann, MD[1], Frandics P. Chan, MD, PhD[1]; [1]Stanford University, Stanford, CA, [2]Siemens Healthineers, Forchheim, Germany

Disclosures: Heiko Schmiedeskamp, PhD: Salary: Siemens Medical Solutions USA; **Dominik Fleischmann, MD:** Research Grants: Siemens Healthineers. All other authors have disclosed no financial interests, arrangements or affiliations in the context of this activity.

Purpose or Case Report: To assess the added value of preoperative dual-energy (DE) chest CTA for pulmonary artery (PA) reconstruction planning.
Methods & Materials: Pediatric PA reconstruction candidates were prospectively recruited for a new dose-neutral DE CTA protocol (rather than anatomy-only) from Feb 2017-Oct 2018. Studies were performed in end-inspiration on a Siemens Flash (parameters- tube A: 80 kVp/150-200 ref mAs; tube B: Sn140 kVp/64-85 ref mAs; pitch: 0.7), using main PA bolus timing and 2 mL/kg IV contrast. For each case, the severity of anatomic PA obstruction was graded by two pediatric cardiovascular radiologists in consensus using a modified Qanadli index (each segment scored for stenosis as- 0: none, 1: <50%, 2: 50-69%, 3: >=70%). Pulmonary blood volume (PBV)/iodine maps were qualitatively reviewed and auto-segmented using Siemens syngo.via software, providing mean Hounsfield unit (HU) attenuation of each lung to the lobar level. Associations between Qanadli scores (QSs) and PBV were assessed with Spearman correlation (r) and ROC analysis. Effective radiation doses (EDs) were estimated from scan DLP and ICRP 103 k-factors, using cubic Hermite spline interpolation for age gaps.
Results: 16 patients were recruited with mean (SD) age of 6.4 (5.4) years (range: 1.1-18.8 years), 10 (62.5%) female, 11 (68.8 %) anesthetized. Indications were: redo unifocalization (7, 43.8%), TOF with PA stenosis (3, 18.8%), primary PA stenosis (6, 37.5%), and 1 post-op CPAM (6.3%), as a normal-PA control. Mean (SD) scan time, ED, and total QS were 2.2 (0.8) sec, 1.7 (0.5) mSv, and 35.7 (12.9), respectively. Higher QS correlated with lower PBV (normalized in each case to the average HU of the combined lungs), both on a whole lung ($r = -0.57$, $p = 0.001$) and lobar ($r = -0.50$, $p < 0.001$) basis. In addition, the lung with lowest normalized PBV was predictive of the highest %Qanadli obstruction (assigned score/total possible points), with AUC of 0.72 (95% CI: 0.47-0.97). Qualitatively, PBV maps were heterogeneous, corresponding to multifocal PA stenoses, with visually decreased iodine content in areas of most severe obstruction (e.g., unilateral absent PA). All scans were anatomically diagnostic.
Conclusions: DE chest CTA is feasible for pediatric PA reconstruction candidates, and PBV deficits correlate with more severe anatomic obstruction. PBV maps facilitated by DE CTA may improve identification of the most heavily diseased PA segments and serve as a novel biomarker in this population.

Paper #: 038

Correlation of ductus arteriosus length and morphology between computed tomographic angiography and catheter angiography and their relation to ductal stent length

Siddharth P. Jadhav, MD[1], *spjadhav@texaschildrens.org*; Varun Aggarwal[2], Prakash Masand[1], Wei Zhang[1], Athar Qureshi[1]; [1]Radiology, Texas Children's Hospital, Houston, TX, [2]Baylor College of Medicine, Houston, TX

Disclosures: Prakash Masand, MD: Consultant, Honoraria: Canon Medical Systems, Phillips MRI Users Meeting 2018, Daiichi Sankyo, Speakers Bureau: Canon Medical Systems, Royalty: Amirsys. **Athar Qureshi, MD:** Consultant: W.L Gore and Associates and Edwards Lifesciences Corp. All other authors have disclosed no financial interests, arrangements or affiliations in the context of this activity.

Purpose or Case Report: Patent ductus arteriosus (PDA) stent placement in infants with ductal dependent pulmonary blood flow is being increasingly adopted in clinical practice. PDA stenting can be challenging due to variable anatomy. The purpose of this study is to correlate computed tomographic angiographic (CTA) morphology and length of the PDA with catheter angiography (CA) and its relation to eventual PDA stent length.
Methods & Materials: We retrospectively identified all pediatric patients that underwent PDA stenting at our institute from 2004-2017. Patients who had CTA prior to stenting were included. PDA length was measured by a radiologist blinded to the CA data, using Syngo-via post-processing software (Siemens, Germany). Vessel centerline technique was used. The actual length of the duct as well as straight length between aortic and pulmonary ends was measured. The PDA morphology was classified as straight (type I), mildly tortuous with 1 turn (II) and tortuous with >1 turn (III). The PDA was also measured and morphology classified on catheter angiography by an interventional cardiologist blinded to the CTA findings. The CTA and CA lengths, straight lengths and stent length were compared using scatter plots and Pearson correlation.

Results: A total of 83 patients that had PDA stenting were identified of which 17 had prior CTA. 15 of these were neonates. There was agreement between CTA and CA regarding the PDA morphology in 94% cases. There was good agreement between CTA and CA actual and straight PDA lengths with Pearson correlation coefficients of 0.71 and 0.80 respectively. There was good agreement between CTA actual length, CTA straight length, CA actual length, CA straight length and eventual stented PDA length with Pearson correlation coefficients of 0.61, 0.75, 0.73 and 0.72 respectively. The correlation was higher for CTA straight length that CTA actual length presumably reflecting straightening of some of the tortuous ducts post-stenting.
Conclusions: PDA length and morphology description on CTA correlates well with CA and can be a reliable guide for the interventional cardiologist in decision-making regarding appropriate choice of PDA stent length.

Paper #: 039

Blood flow redistribution in fenestrated and completed Fontan circulations: With special emphasis on abdominal flow

Pablo Caro Domínguez, *pablocaro82@hotmail.com*; Govind B. Chavhan, MD, DABR, Lars Grosse-Wortmann, Mike Seed, Deane Yim, Prashob Porayette, Christopher Lam, Shi-Joon Yoo; The Hospital for Sick Children, Toronto, Ontario, Canada

Disclosures: Govind B. Chavhan, MD, DABR: Consultant, Honoraria: Bayer, Inc. All other authors have disclosed no financial interests, arrangements or affiliations in the context of this activity.

Purpose or Case Report: The aim was to assess the blood flow distribution in the fenestrated and completed Fontan statuses as compared to normal using phase contrast magnetic resonance and to correlate them with abdominal MR imaging findings.
Methods & Materials: We identified 39 children with fenestrated or completed Fontan circulation in whom phase-contrast velocity mapping of major thoracic and abdominal vessels was a part of the magnetic resonance (MR). The patients were divided into 3 groups: fenestrated Fontan group with MR under general anesthesia (GA) (15 patients, average age 5.87 years), completed Fontan group with MR under GA (6 patients, average age 8.74 years) and completed Fontan group with MR without GA (18 patients, average age 12.52 years). Patients' flow data were compared with the previously published flow data obtained in heathy control (average age, 13.58 years) at fasting status and after a meal.
Results: As compared to healthy controls, Group 1 (fenestrated Fontan) showed normal or marginally increased cardiac output (3.92 ± 0.40 vs 3.72 ± 0.69 L/min/m^2, $p<0.30$), while Groups 3 (completed Fontan) showed decreased cardiac output (3.24 ± 0.71 vs 3.96 ± 0.64 L/min/m^2, $p=0.003$). Both Group 1 and Group 3 showed reduced abdominal blood flow. Reduced abdominal flow was mainly due to diversion of a large part of cardiac output to aortopulmonary collaterals in Group 1 and reduced cardiac output in Group 3. Superior mesenteric and portal venous flows were more profoundly reduced in Group 3 than in Group 1. On the contrary, the hepatic arterial flow was mildly increased in Group 1 and markedly increased in Group 3. Group 2 showed flow data similar to Group 1 except for the tendency toward decreased cardiac output and superior vena caval flow. Hepatic parenchymal changes were more severe in complete Fontan than in fenestrated Fontan group. There was no significant correlation between the hepatic flow and imaging findings.
Conclusions: Fenestrated and completed Fontan circulations showed distinctly different pattern of flow distribution among body parts. Further prospective study in a larger cohort is required to correlate the flow redistribution in Fontan physiology with imaging and laboratory findings as well as the long term outcome.

Paper #: 040

Sirolimus treatment for complex lymphatic malformations in children

Rachelle Durand, DO, *durandr@email.chop.edu*; Anne Marie Cahill, Janet R. Reid, MD, FRCPC, Jean Belasco, MD, Sphoorti Shellikeri, Master's in Biomedical Engineering, Juan S. Calle-Toro, MD, Abhay Srinivasan, MD; Radiology, Children's Hospital of Philadelphia, Philadelphia, PA

Disclosures: All authors have disclosed no financial interests, arrangements or affiliations in the context of this activity.

Purpose or Case Report: Complex lymphatic malformations can be very extensive and cause significant morbidity. They are often refractory or not amenable to extant treatment options such as surgical resection, sclerotherapy and ablation. Sirolimus acts through the mTOR signaling pathway and may downregulate cell proliferation and angiogenesis. It is a promising agent for treatment of vascular anomalies. We assess the effect of sirolimus on complex lymphatic malformations in children.
Methods & Materials: This was a retrospective review of patients administered sirolimus for refractory lymphatic malformations over a 5 year period. MRI studies performed at the initiation of therapy and the most recent available study were reviewed. Lesion volume was measured to determine change over the treatment period. Tissue composition was also evaluated for change in fluid content.
Results: Sirolimus (daily dose range 0.18-3.2 mg, mean duration 24±12 m) was administered to 23 patients, mean age 6±4.9 y (range 0-17 y; 12 female). No serious adverse effects were encountered. No patients underwent surgery or sclerotherapy after initiation of sirolimus. The average time between MR studies was 774±375 d (range 160-1519 d). There was a significant decrease in lymphatic malformation volume ($p=0.0001$), with a mean decrease of 39±25%. Four of 23 patients (17%) saw an apparent increase in lesion size, however the volume increase was relatively small (median 12%). When normalized to body mass index, 20/23 patients (87%) showed a mean 44% reduction in lesion volume. There was no correlation between percent volume decrease and age, sex or dose duration. Lesions demonstrated a change in tissue composition (lower relative fluid content) in 14 patients (64%), while unchanged in 8 patients (36%). Notably, 75% of increasing lesions (3/4) also had a change in tissue composition, whereas patients with volume reduction had a composition change in only 39% (7/18, $p<0.005$).
Conclusions: Sirolimus therapy produced a significant reduction in lesion volume and relative fluid content in a majority of patients, suggesting efficacy in treatment of complex lymphatic malformations. Our results support consideration of sirolimus in the treatment of lymphatic malformations, but additional data that better predict responders, durability of effect, and long-term adverse effects would be beneficial in further characterizing its efficacy.

Paper #: 041

Three-dimensional (3D) printed pediatric endovascular phantom for simulating vascular interventions - A feasibility study

Sphoorti Shellikeri, Master's in Biomedical Engineering, **Seth Vatsky**, vatskys@email.chop.edu; Elizabeth Silvestro, MSE, Sean Trahan, BSE, Abhay Srinivasan, MD, Rachelle Durand, DO, Raymond Sze, Anne Marie Cahill; Radiology, Children's Hospital of Philadelphia, Philadelphia, PA

Disclosures: All authors have disclosed no financial interests, arrangements or affiliations in the context of this activity.

Purpose or Case Report: To assess the feasibility of performing multiple complex vascular interventions on an anatomically accurate 3D-printed pediatric endovascular phantom.
Methods & Materials: The phantom consists of three anatomic sections, chest, neck, and thigh with arterial and venous vasculature created from CT angiography images of 15-year-old patients. The vasculature was aligned with chest, neck and thigh regions segmented from CT images of a teenager in Materialise Mimics and 3-Matic. Rubber tube connections inserted between the anatomic regions together with pumps simulate circulatory flow. Vascular access points were created at the neck and thigh region, covered with a replaceable "skin patch" for reusability. The vasculature mold and breakaway cavities were 3D printed on a Stratasys Fortus 450mc in ABS plastic. Smooth-On Ecoflex 30 silicone was used for molding simulating body texture and DragonSkin10 used for the skin patches.Three pediatric interventional radiologists and a trainee successfully performed the following procedures under fluoroscopic guidance: renal angiography, cavography, femoral and jugular supra and infra-renal IVC filter placement and retrieval, non-target coil embolization and snare retrieval, and iliac stent placement. Post simulation, all operators completed a questionnaire, consisting of 13 questions, rating their experience with the phantom using a 5-point Likert scale (1-Strongly disagree, 2-Disagree, 3-Neutral, 4-Agree and 5-Strongly agree).
Results: All operators reported that the 3D printed phantom and vasculature were anatomically accurate, and sheath placement, catheter/wire manipulation, supra/infrarenal filter placement and retrieval, and iliac stent placement were realistic. Three operators reported that the aortography and cavography compared favorably to live patients. All operators recommended the 3D printed phantom for basic vascular interventional training for fellows and for training in complex/infrequent pediatric vascular interventions for attendings.
Conclusions: To our knowledge this is the first pediatric endovascular multiuse phantom providing capability of simulating complex/uncommon procedures in one model with "soft tissue" consistency. The next iteration will involve prospective enrollment of IR trainees and formal assessment of technical skill development with repeatability possible by replacing anatomic phantom segments (stenting). Initial feedback from operators validates the importance of the utility of the 3D printed medical model for training purposes.

Paper #: 042

Percutaneous transluminal angioplasty in children with Reno vascular hypertension, experience in a tertiary pediatric institution.

Abhay Srinivasan, MD, srinivassa@email.chop.edu; Madiha Aslam, MBBS, Kevin Meyers, MD, Sphoorti Shellikeri, Master's in Biomedical Engineering, Anne Marie Cahill; Interventional Radiology, The Children's Hospital of Philadelphia, Philadelphia,, PA

Disclosures: All authors have disclosed no financial interests, arrangements or affiliations in the context of this activity.

Purpose or Case Report: Renal artery stenosis is an important cause of hypertension in children. The aim of this study is to assess the technical and clinical outcome of percutaneous transluminal angioplasty in children with RVHN
Methods & Materials: An IRB approved database of patients undergoing percutaneous renal angioplasty for RVHN was retrospectively queried. Technical success was defined as the ability of the angioplasty balloon to cross the stenosis. Angioplasty success was defined as angiographic improvement in lesion stenosis per procedure. Clinical patient outcomes were defined as normal BP off medications, normal BP with reduced or same medications, no improvement in BP despite technical success, deterioration in BP and technical failure per patient.
Results: 58 patients diagnosed with RVH underwent 73 percutaneous transluminal angioplasties (28F, 30M), mean age 8.8yrs (1-18yrs), mean weight 37.6kgs (12.8-105kgs). Diagnoses included; FMD (43), MAS (4), NF-MAS (1) and NF-1 (10). Technical success was achieved in 67 out of 73 angioplasties (91.7%), 81 of 86 lesions (94.1%). Angiographic success was achieved in 69 of 73 angioplasties (94.5%); residual stenosis was <30% in 55/73 (75.3%), 31-50% in 6/73 (8.2%), 51-70% in 5/73 (6.8%) and angiographic failure in 4/73 (5.4%). Mean follow up was 39 months (mode 100m). Clinical outcome was as follows; normal BP, off medication (cure) in 23/58 patients (40%), normal BP on reduced medications in 18/58 patients (31%), normal BP on same medications in 5/58(8.6%), no improvement in BP despite technical success in 8/58 (13.7%), patient lost to follow up 4/58(6.8%). Cure and improvement was seen in 35/43 patients (81.3%) with FMD, 7/10 patients (70%) with NF-1, 3/4 patients (75%) with MAS. Procedure related complication rate was 8.2% (6/73);mild flow limiting dissection in 1(1.3%), dissection with pseudo aneurysm in 1(1.3%), Left brachial artery pseudo aneurysm at site of puncture in 1 (1.3%), segmental branch thrombus with perfusion defect in 2(2.7%), stable occlusive thrombus in right common femoral artery in 1(1.3%).Cutting balloon was used after failure to efface with conventional angioplasty in 20 patients and was successful in 17/20 (85%) patients.
Conclusions: Renal artery angioplasty plays a significant role in blood pressure modulation in children with renovascular hypertension. In our experience clinical improvement (normal BP, off meds and normal BP on reduced meds) was observed in 79.2% patients with cure observed in 40%**.**

Paper #: 043

Adjunctive Cutting Balloon Angioplasty in Children with Resistant Renal Artery Stenosis – Experience in a Tertiary Pediatric

Abhay Srinivasan, MD, srinivasaa@email.chop.edu; Madiha Aslam, MBBS, Kevin Meyers, MD, Sphoorti Shellikeri, Master's in Biomedical Engineering, Anne Marie Cahill; Interventional Radiology, The Children's Hospital of Philadelphia, Philadelphia,, PA

Disclosures: All authors have disclosed no financial interests, arrangements or affiliations in the context of this activity.

Purpose or Case Report: Renal artery stenosis in children tends to have an angiographic pattern similar to intimal fibroplasia/hyperplasia which can be resistant to conventional angioplasty. The aim of this study is to assess the outcome of adjunctive cutting balloon angioplasty in children with RVHN.
Methods & Materials: An IRB approved database of patients undergoing renal angioplasty for RVHN was retrospectively queried. The criteria for cutting balloon use was a lack of response to conventional angioplasty. Technical success was defined as the ability of the cutting balloon to cross the stenosis. Angioplasty success was defined as angiographic improvement in lesion stenosis per procedure. Clinical patient outcomes were defined as normal BP off medications, normal BP with reduced or same medications, no improvement in BP despite technical success, deterioration in BP and technical failure per patient.
Results: Twenty of 58 children diagnosed with RVH undergoing renal angioplasty were identified as having 25 cutting balloon angioplasty procedures (13M, 7F), mean age 8.3yrs (3-15yrs), mean weight 36.2kgs, (17.5-105kgs). Diagnoses included; FMD (14), MAS (3) and NF-1 (3). Technical success was achieved in 21/25 angioplasties (84%) and 22/25 lesions (88%), 1 lesion having repeat angioplasty. Angioplasty success was achieved in 23/25 angioplasties (92%); residual stenosis was <30% in 16/25 (64%), 31-50% in 2/25 (8%), 51-70% in 3/25 (12%) and angiographic failure in 2/25 (8%). All 25 lesions were main renal artery, 9/25 ostial and 16/25 were non ostial. Mean follow up 40 months. Clinical outcome was as follows; normal BP, off medication in 6/20 patients (30%), normal BP on reduced medications in 11/20 patients (55%) of which 2/11 also had intra parenchymal disease, no improvement in BP despite technical success in 2/20 (10%), both also having intra parenchymal disease, technical failure in 1/20 (5%). Procedure related complication rate was 12% (3/25); mild flow limiting dissection in 1(4%), segmental branch thrombus with perfusion defect in 1(4%), both treated with systemic heparin and dissection with pseudo aneurysm in 1(4%) treated with coil embolization.
Conclusions: This is the largest series of cutting balloon angioplasty to date in children with RVH. It can be used as an adjunctive technique to improve angioplasty response in children with resistant RAS. Complication rates are not insignificant and need to be considered.

Paper #: 044

Catheter-directed pharmacologic thrombolysis for acute submassive and massive pulmonary emboli in children and adolescents.

Jay Shah, MD, *jay.interventionalradiology@gmail.com*; Anne Gill, MD, Dabin Ji, Wesley Durrence, Kavita Patel, MD, MSc, Matthew Paden, C. Matthew Hawkins, MD; Interventional Radiology/Pediatric Radiology, Emory University Hospital / Children's Hospital of Atlanta, Atlanta, GA

Disclosures: Kavita Patel, MD, MSc: Consultant, Honoraria: Daiichi Sankyo. All other authors have disclosed no financial interests, arrangements or affiliations in the context of this activity.

Purpose or Case Report: The standard of care for pulmonary embolism (PE) in adults and children is anticoagulation and systemic intravenous thrombolysis inferring an associated risk of major hemorrhage. Catheter-directed-thrombolysis (CDT) is a relatively safe and effective alternative to systemic thrombolysis in adults with massive/submassive PE while delivering lower doses of thrombolytics; however, existing medical literature assessing safety and efficacy of pulmonary artery (PA) CDT for PE in children is limited.
Methods & Materials: A 16-month retrospective review of EMR and PACS was performed of patients < 21 years-old who presented with massive or submassive PE and were treated with PA-CDT at a tertiary care children's hospital. Multiple parameters were analyzed including indications, technical success, clinical efficacy, and safety of CDT.
Results: Nine-patients (mean 13.9 years-old; range 6-19) with massive/submassive PE who underwent PA-CDT were included. PE was diagnosed by CT-angiography and CDT was technically successful in all cases. At cessation of CDT, follow-up pulmonary-angiography revealed complete thrombus resolution in 4-patients, partial resolution in 5-patients. Mean PA pressures decreased in all patients (mean pre-CDT PA pressure=36.5 mmHg; mean post-CDT PA pressure=28.0 mmHg). CDT alone was clinically successful in 7-patients (78%). One-patient with acute-on-chronic PE with severe pulmonary hypertension required surgical thrombectomy of chronic-thrombus after CDT of acute-thrombus. One-patient died following cessation of CDT for reasons unrelated to CDT procedure. There were no immediate bleeding complications from CDT therapy. All patients who survived were maintained on anticoagulation treatment following CDT.
Conclusions: PA-CDT is a technically feasible and relatively safe therapeutic option for children and adolescents with submassive and massive pulmonary emboli.

Paper #: 045

Technical feasibility and clinical efficacy of common iliac vein stenting in adolescent patients with May-Thurner Syndrome

Frederic Bertino, MD, *fbertin@emory.edu*; Anne Gill, MD, Jay Shah, MD, C. Matthew Hawkins, MD; Radiology and Imaging Sciences, Division of Interventional Radiology, Emory University School of Medicine, Atlanta, GA

Disclosures: All authors have disclosed no financial interests, arrangements or affiliations in the context of this activity.

Purpose or Case Report: To define the technical feasibility and clinical efficacy of common iliac vein stenting in adolescents with thrombosed and non-thrombosed May-Thurner syndrome (MTS)
Methods & Materials: IRB approved retrospective review identified 20 (Female = 13, mean age 15.7 (13-19), mean weight = 72.4kg) patients who underwent endovascular stenting of the common iliac vein for symptoms of thrombosed MTS (T-MTS) and non-thrombosed MTS (NT-MTS) between 2014-2016. Clinical presentations included NT-MTS (n=3) and T-MTS (n=17). NT-MTS clinical presentation ranged from lower extremity swelling, pain, and/or venous congestion. All patients underwent pre-and-post stent intravascular ultrasound (IVUS) and venography. All T-MTS had stent placement performed at the time of pharmacomechanical rheolysis. Catheter directed thrombolysis with pharmacomechanical rheolysis was performed in all cases of TMTS. All patients were treated with

self-expanding stents, ranging from 14-22mm in diameter, and 4-9cm in length. Patients with residual thrombus after pharmacomechanical thrombolysis were placed on our institution's catheter directed thrombolysis protocol using weight-based dosing of tPA; repeat venography and IVUS were performed the following day to evaluate for residual clot burden. Clinical follow up was conducted at 1-6 month time points. Patients with residual or chronic thrombus or persistent/recurrent symptoms received follow-up lower extremity Doppler sonography. All patients with T-MTS were treated with at least 6 months of anticoagulation by the hematology service. All patients with NT-MTS were treated with 6 months of anti-platelet therapy.
Results: Technical success was 100%. Clinical success (defined as improvement/elimination of symptoms) = 90%. Overall patency at 6, 12, 18, and 24 months was 100%. No patients had recurrence of symptoms. One periprocedural complication included histaminergic reaction to paparavine given for venospasm.
Conclusions: Endovascular stenting of the common iliac vein in thrombotic and nonthrombotic MTS is technically feasible and clinically efficacious with excellent patency and low complication rates in adolescent patients. Continued retrospective analysis of patients in our database is ongoing.

Paper #: 046

Split Liver vs Whole Liver OLT: Technical Demands of Pediatric Portal Vein Recanalization

Heather Cleveland, BSRS, PA-S[2], *hcleveland@mghihp.edu*; Daniel Ashton[1], Alex Chau, MD[1], Ryan Himes, MD[1], DON R. TURNEY, BA[1], Alberto j. Hernandez[1]; [1]Radiology, Texas Children's Hospital, Houston, TX, [2]Massachusetts General Hospital Institute of Health Professionals, Boston, MA

Disclosures: All authors have disclosed no financial interests, arrangements or affiliations in the context of this activity.

Purpose or Case Report: Compare technical details and clinical success of chronically occluded portal vein (PV) recanalization in pediatric patients with split liver vs whole liver orthotopic liver transplant (OLT).
Methods & Materials: IRB approval was obtained to retrospectively review PV recanalization (42 procedures) in 18 OLT patients (12 female) with chronic PV occlusion between 10/2011- 9/2018. Patient demographics, procedure details, technical and clinical success as well as complications and follow-up were recorded from chart review.
Results: Technically successful PV recanalization and reduction of PV pressure gradient to ≤ 5 mmHg was performed in 17/18 patients (94%). Technical success in split liver vs whole liver was 64% (9/14) and 86% (12/14) in the 28 attempted and successful recanalization procedures respectively. PV Recanalization success was higher at first attempt in the whole liver group (10/12, 83%) in comparison to the split liver group (3/6, 50%). There was improvement in signs and symptoms of portal hypertension in 16/18 (89%) patients. Both procedure time (median: 4.3, range: 2.3-9.9 hours) and fluoroscopy time (median: 36.9, range: 7.4-153 minutes) were markedly greater in the split liver group, while the whole liver group was a median of 3.1 hours (range: 1.4-6.8) and 24.8 minutes (range: 5.2-113.9) respectively. . The procedure time (median: 5.9, range: 4.3-9.9 hours) and fluoroscopy time (median: 66.1, range: 38.6-153 minutes) were also both higher in the split liver group during the time of successful recanalization in comparison to the whole liver procedure (median:3.5, range: 1.8-6.1 hours) and fluoroscopy time (median:46.9, range: 8.4-75.5 minutes). Age (median: 3, range: 2-16 years) and weight (median: 17, range: 13-47 kg) are both reported lower in the split liver group in comparison to whole liver with median age of 5 years (range: 1-17) and weight of 28 kg (range: 21-71) respectively.There were 7 (17%) major complications (SIRC) total. In split liver vs whole liver there were 4 (20%) and 3 (22%) complications respectively. These included perisplenic hematoma (n=2), hemoperitoneum (n=4), and hepatic artery pseudo aneurysm (n=1) managed with pain medication and blood product replacement. Median follow-up was 17 months (range: 2-84 months).
Conclusions: Technical challenges requiring longer procedure and fluoroscopy times could be contingent upon the anatomy of the patient based on the type of OLT. Though small sample, technical and clinical success were comparable.

Paper #: 047

Comparison of Modified Single Puncture Technique for Tunneling Short-term Central Venous Catheter with Peripherally Inserted Central Catheter in Pediatric Group: A Preliminary Study.

Yu Jin Kim[1], *youkio97@gmail.com*; Young Hun Choi[2]; [1]Department of Radiology, Chungbuk National University Hospital , Cheongju-si, Chungcheongbuk-do, Korea (the Republic of), [2]Seoul National University Hospital, Seoul, Seoul, Korea (the Republic of)

Disclosures: All authors have disclosed no financial interests, arrangements or affiliations in the context of this activity.

Purpose or Case Report: Tunneling is known to be less prone to infection. To compare utility between single puncture technique for tunneling short-term central venous catheter targeting internal jugular vein (tunneled C-line) and peripherally inserted central catheter (PICC) in the pediatric group.
Methods & Materials: From October 2017 to July 2018, consecutive 32 cases of 25 in-patients (11 boys and 14 girls) were underwent tunneled C-line or PICC insertion. Both techniques were performed by a single pediatric radiologist. The procedure time and catheter lifespan between the two techniques were compared using the Mann-Whitney test. The rate of bedside procedure and catheter-related bloodstream infection (CRBSI) between the two techniques was calculated.
Results: 24 cases (mean age 5 years, range 0-15) of tunneled C-line insertion and 8 (means age 6 years, range 2-18) cases of PICC insertion were performed. The procedure time was significantly shorter in tunneled C-line insertion than PICC insertion (13±5 min Vs. 19±6 min, p=0.030). The catheter lifespan showed no significant difference between tunneled C-line and PICC (12±11 days Vs. 24±21 days, p=0.192). The bedside procedure was performed for poor patient's condition in 88% and 0% of cases of tunneled C-line and PICC, respectively. The rate of CRBSI of tunneled C-line and PICC were 6.7 and 10.6 per 1,000 catheter-days, respectively.
Conclusions: Tunneled C-line was associated with shorter procedure time, no significant difference in catheter lifespan and a lower rate of CRBSI compared with PICC. Tunneled C-line can be an alternative to PICC in severely ill young children at the bedside.

Paper #: 048

Outcomes of tunneled internal jugular venous catheters in children younger than 6 months of age

Christopher J. Yen, MD[1], *cjyen@bcm.edu*; Wei Zhang[2], Daniel Ashton[2]; [1]Radiology, Baylor College of Medicine, Houston, TX, [2]Texas Children's Hospital, Houston, TX

Disclosures: All authors have disclosed no financial interests, arrangements or affiliations in the context of this activity.

Purpose or Case Report: There is limited data on complications of central lines in younger infants. The purpose of this study is to identify factors which may affect complication rates of tunneled internal jugular (IJ) venous catheters placed in neonates and infants under 6 months of age.
Methods & Materials: This is a retrospective review of patients 180 days of age and younger who underwent tunneled IJ venous catheter placements in the pediatric interventional radiology department at a single institution over a 4 year period. Patient demographics, device characteristics, procedural factors, and clinical follow-up were collected for each catheter placed. Complication rates, fluoroscopy times, and procedural times were analyzed based on patient age, weight at time of placement, side of placement, and technique (single-incision or conventional). Complication types (line malfunction, malpositioning, or infection) were analyzed based on duration of placement and method of resolution.
Results: 146 lines were placed in 128 patients with a total dwell time of 6,467 line days. A total of 49 complications were observed which required either replacement over a wire or removal (total complication rate 33%, or 132 line days per complication). Complications included 14 infections, 27 malpositioned lines, and 8 line malfunctions. As expected, lines which ultimately required exchange or removal had a higher average dwell time compared to lines without complications (33.2 days vs 66.2 days, $p < 0.0001$). For dwell times less than 50 days, Cox regression analysis showed a statistically significant higher rate of complication-free line survival in patients greater than 5 kg compared to those less than or equal to 5 kg (hazard ratio 5.12 for <=5kg, $p = 0.002$). Although not statistically significant, patients 90 days of age and younger tended to have higher line survival rates compared to patients older than 90 days of age (hazard ratios 0.55-0.86). Side of placement, procedure time, and fluoroscopy time did not have a statistically significant association with complication rate.
Conclusions: When caring for patients less than 6 months of age who require tunneled internal jugular venous access, providers should be aware that dwell time, weight and age may affect complication risk. Longer dwell times result in greater risk of complication. In patients weighing less than 5 kg, there is a higher risk of complication compared to heavier patients for the first 50 line days. Overall, infants older than 90 days may have a higher risk of complication.

Paper #: 049

Evaluation of Automated Extraction of Velocity Envelope for Transcranial Doppler Ultrasound

Justin Baraboo, BS MS[1], **Rizwan Zafer[2]**, *rmzafer@gmail.com*; Sherwin S. Chan, MD PhD[1]; [1]Radiology, Children's Mercy Hospital, Kansas City, MO, [2]Kansas City University of Medicine and Biology, Kansas City, MO

Disclosures: Rizwan Zafer: Financial Interest: Jazz Pharmaceuticals - Medical advisory board: Consultant; **Sherwin S. Chan:** Consultant, Honoraria: Jazz Pharmaceuticals, Research Grant: GE Healthcare. All other authors have disclosed no financial interests, arrangements or affiliations in the context of this activity.

Purpose or Case Report: The purpose of our study was to test our custom software program's ability to estimate the blood flow velocity envelope for transcranial spectral Doppler ultrasound waveforms.
Methods & Materials: Our group has programmed a custom algorithm that uses image contrast and neighboring data to estimate the envelope of a spectral Doppler waveform. Our algorithm was implemented in java and uses image-based extraction methods: region of interest reductions, preprocessing, and a novel envelope extraction technique. To test this method against industry standards, we performed a retrospective review on pediatric patients who underwent transcranial Doppler between 1/1/2008 to 7/15/2017 at a single pediatric center on Philips IU-22 machines. Ultrasound images of these waveforms formed three groups: waveforms with manufacturer envelopes, waveforms with technologist drawn envelopes and waveforms without envelopes. The manufacturer and manual envelopes were removed from those images and a human drew the ideal waveform envelope on each waveform. The average absolute pixel difference between the human gold standard and another technique (custom software, manufacturer, and technologist) was the metric of comparison and was also scaled to the region's size. The entire waveform and a single manufacturer determined wave region were compared across techniques. Correlation analysis was also performed on the average pixel error between our algorithm and the manufacturer algorithm for each waveform.
Results: 230 patients were included with 3810 unique waveforms. Our approach outperformed the manufacturer or technologist by average pixel error compared to the gold standard ($p<.01$). For entire waveforms, our algorithm was on average 2 pixels more accurate than the manufacturer; for single waves, our algorithm was on average 2.9 pixels more accurate than the manufacturer and 1 pixel more accurate than the technologist. For entire waveforms unable to be processed by the manufacturer, our algorithm was on average 18 pixels different from the gold standard. Error correlation was low between our approach and manufacturer ($r^2 <.32$). Artifacts and resizing seemed to have little effect on our technique, with waveform quality impacting measurement more than artifacts or scaling.
Conclusions: Our custom algorithm outperforms manufacturer techniques and technologists' manual tracing in determining accurate waveform envelopes for TCD images. This work is a precursor to using these waveforms for input into machine learning algorithms.

Paper #: 050

Shear Wave Elastography in Brain Ultrasonography: Initial Experience and Utility in Detecting White Matter Disease

Alexander M. El-Ali, MD[1], *alexander.elali@gmail.com*; Subramanian Subramanian[2], Lisa Krofchik, RDMS[2], Morie Kephart, RDMS[2], Judy H. Squires, MD[2]; [1]Radiology, University of Pittsburgh Medical Center, Pittsburgh, PA, [2]Children's Hospital of Pittsburgh, Pittsburgh, PA

Disclosures: All authors have disclosed no financial interests, arrangements or affiliations in the context of this activity.

Purpose or Case Report: Grayscale and color imaging can assess a range of intracranial pathology in neonates and young infants; however, there are recognized limitations in the evaluation of symmetric bilateral white matter abnormalities. Early reports suggest that Ultrasound (US) Shear Wave Elastography (SWE) is a feasible method in neonatal brain imaging. We describe our initial experience with brain SWE and report preliminary data suggesting its utility in detecting white matter disease.
Methods & Materials: SWE has been a part of the standard head US protocol at our institution since September 2018. SWE velocity measurements were obtained using a GE Logiq E9 machine with a C1-6 transducer and were recorded in meters per second (m/s). Regions of Interest (ROI) were placed by an US technologist with additional measurements by the supervising doctor, for consistency. In order to establish normal anatomic stiffness, ROIs were attempted for each patient in the following areas: periventricular white matter (pWM), lateral ventricular cerebrospinal fluid, and basal ganglia (thalamus and/or caudate head). All ROIs were included for analysis.

Statistics were performed in the R software package.
Results: A total of 33 SWE studies were attempted and 22 (67%) were successfully performed. The most common reason for failure was excessive patient motion. Most patients were less than 30 days old (n=16, 73%) with an age range of 0-197 days. All patients were born at >33 weeks gestational age.19 patients (86%) had normal head ultrasounds or only minor intracranial pathology that did not affect SWE analysis. 3 patients (14%) demonstrated significant WM abnormalities including extensive bilateral venous infarction. SWE demonstrated reliable differences in mean velocity between the lateral ventricle (0.83 m/s), pWM (1.17 m/s), and basal ganglia (1.56 m/s) (ANOVA, $p<0.001$). Direct comparison between pWM and basal ganglia was also statistically significant (t-test, $p<0.001$). Mean velocity for normal pWM (1.17 m/s) significantly differed from abnormal pWM (2.49 m/s) (t-test, $p<0.001$). Basal ganglia measurements did not differ significantly between these groups (t-test, $p = 0.52$).
Conclusions: Results from our prospective study demonstrate that SWE is a feasible technique for evaluation of brain parenchyma as it can reliably differentiate various normal intracranial structures. Additionally, our preliminary data suggest the utility of SWE in the evaluation of white matter disease.

Paper #: 051

Review of Neck CTA Examinations for Soft Palate Injury and Proposal of a New Targeted CTA Protocol

Jungwhan J. Choi, MD,
jungwhan.choi@childrens.harvard.edu; Christiane Burton, Ph.D., Amy Danehy, M.D., Stephan Voss; Boston Children's Hospital, Boston, MA

Disclosures: All authors have disclosed no financial interests, arrangements or affiliations in the context of this activity.
Purpose or Case Report: Neck CTA is commonly requested for patients with soft palate trauma to exclude vascular injury. Debate exists regarding which imaging studies are indicated in this setting and standard neck CTA protocols, extending from thoracic inlet to skull base, result in considerable radiation. The purpose of this study is to review the yield of neck CTA following oropharyngeal trauma and to propose a new reduced dose targeted CTA protocol for this indication.
Methods & Materials: Neck CTA's obtained between 2008-2018 for evaluation of soft palate injury were retrospectively reviewed. Study variables included age; mechanism of injury; presence of vascular or neurologic injury; and other clinically significant findings.All CTA exams were performed from the thoracic inlet to skull base per standard institutional protocol. Effective dose was estimated using CTDIvol and tissue weighting conversion factors from ICRP 60 with calculations based on sagittal reconstructions, using the z-axis of the patient from skull base to thoracic inlet (full CTA) and to hyoid bone (targeted CTA) to estimate organs at risk. Dose reduction for the targeted CTA was defined as the % decrease in effective dose compared to full CTA.
Results: Between 2008-2018, 98 neck CTA's were ordered in the setting of soft palate trauma. Average patient age was 5.1 ± 3.3 yrs. The most common indication was fall with toothbrush in mouth. 1 study was excluded due to contrast extravasation.No studies were positive for either neurologic or carotid artery injury. 1 study was positive for minor small vessel injury. Clinically significant nonvascular findings were present in 5/97 cases and included: phlegmonous change (n=2); retained toothbrush foreign body; retropharyngeal/upper mediastinal air; and nondisplaced medial pterygoid process fracture. With exception of mediastinal air, all vascular and non-vascular findings would have been included in a targeted CTA extending from hyoid bone to skull base.Mean effective dose was 8.63 ± 3.98 mSv per ICRP 60 for standard neck CTA. For the proposed targeted CTA extending only from skull base to the hyoid bone, the effective dose estimate was 2.25 ± 0.96 mSv, resulting in significant dose reduction of 72% ± 8% ($p<0.01$).
Conclusions: Based on the low yield of routine neck CTA for evaluation of vascular injury following oropharyngeal trauma, a new targeted neck CTA protocol is proposed that results in significantly less dose to the neck, while preserving the diagnostic yield for both vascular and non-vascular findings.

Paper #: 052

Fissures of the annulus fibrosus and cervical cord anterior spinal artery infarcts in children: telltale signs of fibrocarilaginous disc emboli?

Stephen Little, M.D., *stephen.little@choa.org*; Damien Grattan-Smith, MBBS, Susan Palasis, Richard Jones, Andrew Reisner; Children's Healthcare of Atlanta, Atlanta, GA

Disclosures: All authors have disclosed no financial interests, arrangements or affiliations in the context of this activity.

Purpose or Case Report: To determine if there is an association between fissures of the annulus fibrosus and anterior spinal artery (ASA) infarcts of the cervical cord in children.
Methods & Materials: We retrospectively reviewed the sagittal T2 or STIR images from 145 MRIs of the cervical spine (870 disc levels), including 103 consecutive examinations and 42 examinations performed for acute myelopathy (male 76, female 69; ages 0.2 to 20.7 years). Acute myelopathy patients were collected from the radiology database using keywords 'spinal cord infarct', 'transverse myelitis', 'acute disseminated encephalomyelitis', and 'neuromyelitis optica'. Images were transferred to an independent workstation and de-identified. Masks were placed over the spinal cords to reduce potential bias. Following a training session, two experienced pediatric neuroradiologists independently graded the C2-C3 through C7-T1 discs for annular tear and nuclear degeneration. Six weeks later, the readers independently reviewed the sagittal T2 or STIR, axial T2 or STIR and diffusion images (if available) of the 42 acute myelopathy patients. For this review, masks were placed over the anterior vertebral column to reduce potential bias. Patients were classified as ASA infarct, not ASA infarct or uncertain based on typical imaging characteristics described in published reports. The frequency of findings and reliability of observations were calculated.
Results: Cervical anterior spinal artery infarcts were identified in 7 children (2 male, 5 female) age 3 to 17 years. Type 2 annular fissures were seen in 43-57% of patients with ASA infarcts, in 3% of myelopathy patients without ASA infarct and in 2-5% of non-myelopathy patients. Odds ratio for ≥1 type 2 or 3 annular fissure in ASA infarct vs. non ASA infarct was 25.1, 95% CI [2.6, 204.4], $p<0.002$ for examiner B and 32.0, 95% CI [4.3, 354.1], $p<0.001$ for examiner A.
Conclusions: Type 2 annular fissures are associated with cervical cord ASA infarct in children and are uncommon in children without ASA infarct (2-5%). Disc dessication is somewhat more common in children with ASA infarct but is commonly seen in children without ASA infarct (41-54%). Interestingly, annular fissures associated with ASA infarct typically do not enhance at presentation but may develop enhancement on follow up. Non-enhancing type 2 annular fissures may be acute and are a potential pathway for fibrocartilaginous disc emboli to reach the ASA and cord.

Paper #: 053

Clinical benefit of ferumoxytol whole body vascular imaging including the central nervous system in pediatric patients

Aashim Bhatia, *aashimbhatia@gmail.com*; Alexandra Jane Borst, MD, Jessica Duis, MD, Josephine M. Ndolo, MBChB, James D. Phillips, MD, Christopher Baron, MD; Vanderbilt Children's Hospital, Nashville, TN

Disclosures: All authors have disclosed no financial interests, arrangements or affiliations in the context of this activity.

Purpose or Case Report: Ferumoxytol, an iron oxide nanoparticle coated by a carbohydrate shell, is increasingly reported as an off-label blood pool contrast agent for MR angiography (MRA). We explore the imaging quality and clinical utility of central nervous system (CNS) and whole-body vascular MR imaging with ferumoxytol in pediatric patients.
Methods & Materials: Use of ferumoxytol for MRA was approved by the pharmacy and therapeutics committee. We retrospectively reviewed all pediatric patients 0-18 years of age undergoing MRI with ferumoxytol from September 2016-Sepetember 2018.A blinded radiologist independently scored imaging quality to determine the results of clinical investigation using a five-point subjective score, where a score > 3 was considered diagnostic. The five-point scale was as follows: 1=excellent image quality: no limitations, 2=good image quality: minimal limitations, 3=sufficient image quality: moderate limitations, 4=restricted image quality: relevant limitations, 5=poor image quality: non-diagnostic.
Results: Fourteen children aged 1-17 years of age (mean age 10.7 years) underwent MRA examinations on a 3.0 T MRI after administration of ferumoxytol at a dose of 3 mg/kg. Whole body vascular imaging focused on the brain, neck, chest, abdomen, and selected extremities based on clinical history.In all patients, the MRI studies were diagnostic with imaging quality demonstrating excellent signal-to-noise ratio. The average of the scores was 4.7 (standard deviation of 0.47). Eight of the fourteen indications were to exclude vascular malformations or aneurysms. Four studies were performed to evaluate systemic vasculitides (Takayasu Arteritis and Loeys-Dietz Syndrome). Two studies were performed for thoracic outlet syndrome. In multiple cases, findings on MRI with ferumoxytol were confirmed with biopsy and conventional angiogram. None of the patients had an adverse reaction to the ferumoxytol.
Conclusions: Ferumoxytol-enhanced MRA is a commonly used contrast agent at our institution to diagnose vascular abnormalities in the brain or whole body. Use of ferumoxytol allows the radiologist to interrogate multiple territories in one study due to its highly stable intravascular time. We were able to confidently detect and characterize vascular abnormalities and exclude vascular malformations. No infusion reactions were noted in our cohort. Therefore, ferumoxytol is a beneficial and safe alternative to gadolinium-based contrast agents for high resolution CNS and whole body MR angiography.

Paper #: 054

Comparison of 2D Turbo-Spin-Echo BLADE and Spin-Echo Echo-Planar Diffusion Weighted Brain MRI at 3 Tesla: Preliminary Experience in Children

Aaron S. McAllister, MD[1], *aaron.mcallister@nationwidechildrens.org*; Bhavani Selvaraj, MS[1], Lacey J. Lubeley, BS[1], Ning Jin, PhD[2], Kun Zhou[3], Mark Smith[1], Ramkumar Krishnamurthy, PhD[1], Houchun Hu, PhD[1]; [1]Radiology, Nationwide Children's Hospital, Columbus, OH, [2]Siemens Medical Solutions, Cleveland, OH, [3]Siemens Shenzhen Magnetic Resonance Ltd., Shenzhen, China

Disclosures: Aaron S. McAllister, MD: Equity Interest/Stock Option: GE, MMM, CHD, JNJ. **Ning Jin, PhD:** Salary: Siemens Medical Solutions. **Kun Zhou, PhD:** Salary: Siemens Healthineers, Employment. All other authors have disclosed no financial interests, arrangements or affiliations in the context of this activity.

Purpose or Case Report: To compare a 2D turbo-spin-echo (TSE) non-Cartesian BLADE diffusion-weighted MRI with a conventional SE echo-planar imaging (SE-EPI).
Methods & Materials: All data obtained on a 3T Siemens clinical scanner. 53 patients (10.4±7.9 years) underwent both SE-EPI diffusion imaging and the prototype BLADE sequence.A neuroradiologist evaluated the severity of image artifacts and whether their presence affected diagnostic image quality (IQ). The radiologist answered whether BLADE or SE-EPI was preferred in each case. A 4-point score was given for each sequence based on the presence of artifacts and signal pile-up near air tissue interfaces or presence of shunts/orthodontia: 1: none, 2: mild-diagnostic IQ not affected, 3: moderate-IQ partially affected, and 4: significant-IQ heavily affected. Anterior-posterior and right-left dimensions of the brain were measured at co-registered locations on both DWI sequences and compared to reference measurements obtained from a 3D T1-weighted inversion-recovery Cartesian scan.Parameters for SE-EPI were: 1.5mm resolution, 4mm slices, TR/TE=4100/81ms, fat suppression, GRAPPAx2 with 40 references lines, partial Fourier readout, 1446Hz/pixel bandwidth, 0.8ms echo spacing, an EPI factor=192, four diffusion directions, and two signal averages for b=0 and three signal averages for b=1000, scan time ~ 2min. For the prototype BLADE, 1.3mm resolution, 4mm slices, TR/TE=5200/41ms, fat suppression, no GRAPPA and partial Fourier, no signal averaging, 520Hz/pixel bandwidth, 11ms echo spacing, EPI factor of 3, and a turbo factor of 11, scan time ~4min.
Results: In 46% of the cases, BLADE was preferred; in 45% of the cases, both sequences were preferred equally. Average scores for SE-EPI was 2.4±0.7 vs. BLADE 1.1±0.3 ($p<0.01$). In the A/P direction, the percent geometric distortion varied from -38.8% to 70.1% for SE-EPI (0.4%±16.4%), whereas for BLADE it was significantly lower, from -8.6% to 17.5%, while the average was similar 0.8%±5.12%. However, in the R/L direction, the distortion varied from -27.5% to 59.5% for SE-EPI (average: 7.0%±15.7%), whereas for BLADE it was significantly lower, from -7.6% to 20.9% (1.3%±4.8%). Overall, SE-EPI exhibited more edge distortions, more signal pile-up, but had slightly better signal centrally and more visually pleasing ADC maps than BLADE. Motion artifacts were minimal on both sequences.
Conclusions: BLADE DWI is feasible in pediatric patients at 3T, and exhibits less distortion near air tissue interfaces and in the presence of shunts/orthodontia.

Paper #: 055

Evaluation of Highly Accelerated Wave-CAIPI Susceptibility-Weighted Imaging (SWI) in the Non-Sedated Pediatric Setting: Initial Clinical Experience

John Conklin, **Azadeh Tabari, MD**, *atabari@mgh.harvard.edu*; Maria Gabriela Figueiro Longo, MD, Camilo Jaimes, Kawin Setsompop, Steve Cauley, John E Kirsch, Susie Yie Huang, Otto Rapalino, MD, Michael S. Gee, Paul A Caruso; Radiology, Massachusetts General Hospital, Boston, MA

Disclosures: All authors have disclosed no financial interests, arrangements or affiliations in the context of this activity.

Purpose or Case Report: To compare highly accelerated SWI using Wave Controlled Aliasing in Parallel Imaging (Wave-

CAIPI SWI) to conventional 3D SWI in the awake pediatric outpatient clinical setting.
Methods & Materials: This study was IRB approved and HIPAA compliant. Twenty-three patients (9 girls, 14 boys; mean age 134.3±55 months, range 1-214 months) underwent awake outpatient 3T clinical brain MRI (Siemens Healthcare, Erlangen) using commercially available 32-channel and 20-channel RF coils. All studies included a conventional 3D SWI sequence (R=2, acquisition time TA=4.3 minutes) and a highly accelerated Wave-CAIPI SWI sequence (R=9, TA=1.0 minute for the 32-channel head coil; R=6, TA=1.5 minutes for the 20-channel head coil). Two blinded neuroradiologists independently rated both sequences in terms of artifacts, noise (central and peripheral), anatomic contrast (ability to delineate normal structures) and pathologic contrast (ability to delineate the clinical pathology, when present). The images (standard SWI and Wave-CAIPI SWI) were anonymized and presented side-by-side on two adjacent monitors. A predefined 5-points scale was used, where negative numbers favor standard SWI and positive numbers favor Wave-CAIPI SWI: 0 indicates that the sequences were equivalent, -1 or 1 indicates that one sequence was subjectively preferred but the difference would not have changed the diagnosis, and -2 or 2 indicates that one sequence was superior and the difference would impact the diagnosis. Wilcoxon signed-rank test was used to evaluate the difference between sequences for each variable.
Results: There were no failed exams (e.g., due to excessive motion or inability to tolerate scanning). The most common indications for MRI included tumor, epilepsy, and headache. Standard and Wave-CAIPI SWI had similar performance for evaluation of pathologic findings, normal anatomic structures, noise within the peripheral brain, and artifacts. There was subjectively more noise within the central brain (n = 15, P <0.001) using the Wave-SWI sequence, however there were no cases where this difference would have impacted the final diagnosis (no scores of +/-2). The inter-reader agreement for these parameters was moderate to good (kappa 0.45 – 0.75).
Conclusions: Highly accelerated Wave-CAIPI SWI of the brain is feasible in non-sedated children and can be achieved without significant impact on overall diagnostic quality. The accelerated sequence was associated with a subjective increase in central (but not peripheral) image noise.

Paper #: 056

Comparison of Ultrafast Wave-CAIPI Magnetization-Prepared Rapid Acquisition Gradient-Echo (Wave-MPRAGE) and Standard MPRAGE in Non-Sedated Children:Initial Clinical Experience

Azadeh Tabari, MD, *atabari@mgh.harvard.edu*; John Conklin, Maria Gabriela Figueiro Longo, MD, Camilo Jaimes, Kawin Setsompop, Steve Cauley, John E Kirsch, Susie Yie Huang, Otto Rapalino, MD, Michael S. Gee, MD, PhD, Paul A Caruso; Massachussets General Hospital, Boston, MA

Disclosures: All authors have disclosed no financial interests, arrangements or affiliations in the context of this activity.

Purpose or Case Report: The prolonged scan times of MRI can be uncomfortable for children, increase the potential for motion artifacts, limit clinical availability and increase cost. This study evaluated the feasibility of an ultrafast Wave-MPRAGE sequence for brain imaging of awake pediatric patients
Methods & Materials: IRB approved and HIPPA compliant. Twenty-one patients scheduled for clinical brain MRI were scanned on a 3T scanner (Siemens Healthcare, Erlangen) using commercially available 32-channel and 20-channel RF coils. In addition to the clinical protocol, each MRI included a standard MPRAGE sequence (R=2, acquisition time TA=5.2 min) and an ultrafast Wave-MPRAGE sequence (R=9, TA = 1.15 min for the 32-channel RF coil; R=6, TA=1.75 min for the 20-chanel RF coil). Pre-contrast (n=8) and post-contrast (n=13) exams were included. Two blinded neuroradiologists independently evaluated Wave-MPRAGE and standard MPRAGE in terms of artifacts, noise (central and peripheral), anatomic contrast (ability to delineate normal structures) and pathologic contrast (ability to delineate the clinical pathology, when present). A predefined 5-points scale was used, where negative numbers favor standard MPRAGE and positive numbers favor Wave-MPRAGE: (0) sequences are equivalent, (-1 or 1) one sequence is subjectively preferred but the difference would not impact the diagnosis, and (-2 or 2) one sequence is superior and the difference would impact the diagnosis.Wilcoxon signed-rank test was used to evaluate the difference between sequences for each variable
Results: Twenty-one patients (10:11 F:M; mean age 143±48 months, range 1-214 months) were included. The most common clinical indications were: tumor(9), epilepsy(3), adrenoleukodystrophy(2), headache(2) and other(5). Wave-CAIPI MPRAGE provided an 80% reduction in scan time using the 32-channel coil and a 67% reduction using the 20-channel coil. Standard MPRAGE was subjectively preferred for evaluation of normal anatomic findings (18/21). Pathologic findings and artifacts were similar for both sequences (P>0.05). Image noise was subjectively increased with Wave-MPRAGE for both the central and peripheral brain (P<0.01), but there were no cases (0/21) where this difference would have impacted the final diagnosis.
Conclusions: Ultrafast brain imaging with Wave-MPRAGE is feasible in awake pediatric patients, providing a dramatic reduction in scan time at a cost of subjectively increased image noise. Diagnostic performance was comparable to standard MPRAGE in this initial clinical evaluation

Paper #: 057

Bridging vein evaluation in suspected abusive head trauma: beyond tadpoles and lollipops

Stephen Little, M.D., *stephen.little@choa.org*; Damien Grattan-Smith, MBBS, Richard Jones; Children's Healthcare of Atlanta, Atlanta, GA

Disclosures: All authors have disclosed no financial interests, arrangements or affiliations in the context of this activity.

Purpose or Case Report: Traumatic subdural hematomas in abusive head trauma are most often due to bridging vein disruption. Indeed, the pattern of injured veins may be helpful in distinguishing minor from major and direct (impact) from indirect (shaking) trauma. Bridging vein thrombosis (tadpole or lollipop sign) may accompany acute vein disrupution but can be difficult to distinguish from extra-axial hemorrhage and may not be seen if imaging is delayed or in cases of repeated trauma. Selection and optimization of magnetic resonance venography (MRV) pulse sequences and post processing techniques is required for reliable cortical and bridging vein evaluation in infants and young children.
Methods & Materials: We reviewed 32 MRV examinations in 24 subjects (8 female, 16 male; age 2-44 months, mean 8.5 months, median 5 months). Examinations were perfomed for suspected abusive head trauma, macrocephaly, vomiting, infantile spasms, developmental regression and ventriculomegaly. Techniques included 2D TOF (coronal or sagittal), 3D PC, contrast enhanced MRV (CE-MRV), CE-MRV with subtraction and post Gd 2D TOF (axial). Post-processing techniques included whole volume MIP, whole volume weighted MIP, volume-rendered and thin slab MIP. Pulse sequences and post processing techniques providing optimal visualization of cortical and bridging veins were selected by

consensus.
Results: First pass contrast enhanced MRV with subtraction provided the best visualization of cortical and briding veins, even in infants as young as 2-3 months. 3D phase contrast MRV was nearly as good, but image quality was scanner dependent. Sagittal 2D TOF MRV was moderately good at demonstrating cortical and bridging veins near the sagittal sinus, but suffered from in-plane flow saturation and poor spatial resolution in coronal or axial reconstructions. Coronal 2D TOF MRV was the least desireable for briding vein evaluation. Weighted MIP images provided the best (and easiest) overall visualization of the superficial venous system. Thin-slab MIP and volume-rendered techniques were useful in selected cases.
Conclusions: Selection and optimization of MR venography pulse sequences and post-processing techniques allows for the reliable demonstration of cortical and bridging veins in infants and young children with suspected abusive head trauma. Improved characterization of bridging vein injury may distinguish traumatic from atraumatic SDH and provide valuable insight into the nature and magnitude of head injury.

Paper #: 058

Facial hemangioma: risk of PHACE syndrome and associated anomalies.

Maïa Proisy, M.D[1], *maia.proisy@chu-rennes.fr*; Frederic Thomas-Chausse, MD[1], Julie Powell, MD[2], Francoise Rypens, MD[1], Chantale Lapierre, MD[1], Josée Dubois, MD[1]; [1]CHU Sainte-Justine, Medical Imaging Department, Montreal, Quebec, Canada, [2]CHU Sainte-Justine, Department of Pediatrics, Montreal, Quebec, Canada

Disclosures: Maïa Proisy, M.D.: Research Grants: Société Francaise de Radiologie, Région Bretagne (France). All other authors have disclosed no financial interests, arrangements or affiliations in the context of this activity.

Purpose or Case Report: PHACE syndrome is defined as a large segmental infantile hemangioma (IH) larger than 5 cm, posterior fossa malformations, cerebral arterial anomalies, aortic coarctation, eye anomalies and sternal defect. Cerebrovascular anomalies are estimated at 55% and cardiovascular anomalies at 42%. Cerebral artery anomalies were reported to be on the same side as the facial IH. The objective of our study is to review facial hemangioma and the risk of cerebral or cardiovascular anomalies in PHACE or non-PHACE patients.
Methods & Materials: We reviewed all patients seen in our vascular anomalies group with the diagnosis of facial IH and who have clinical photos and MRI. The clinical photos were reviewed to determine the localization of the lesion by segment and the right or left lateralization. Cerebrovascular, posterior fossa or cerebral anomalies were reviewed. The presence of cardiovascular anomalies, sternal defect, eye anomalies or intracranial hemangioma was recorded. Two experienced paediatric radiologists scored brain MRI. Clinical data was reviewed by dermatologists using the consensus statement on diagnostic criteria for PHACE syndrome.
Results: One hundred twenty-six children (93 girls and 33 boys, mean age 16.8 months) with facial hemangioma and brain MRI scan were included. Twenty-one patients out of 126 had PHACE syndrome. Thirty-eight (30%) children had a segmental hemangioma larger than 5 cm and 88 (70%) smaller than 5 cm. Cerebrovascular anomalies were seen in 18/126 (14%). Of them, 17/18 (94%) were PHACE. Brain anomalies were seen in 9/21 PHACE patients (42%) whereas only one non-PHACE patient had brain anomalies ($p<0.001$). Seventeen of 38 patients with hemangioma larger than 5 cm had an associated cerebrovascular anomaly whereas only one patient with a hemangioma smaller than 5 cm had cerebrovascular anomaly ($p<0.001$). Eight of those 38 patients (30%) had associated brain anomalies whereas only 2 patients with hemangioma of less than 5 cm had associated brain anomalies ($p<0.001$). The laterality of the cutaneous hemangioma and the underlying cerebrovascular anomalies was concordant in 61% (11/18). Cardiovascular anomalies were seen in 6 patients and ocular anomalies in 8 patients. All of them had a PHACE syndrome.
Conclusions: In patient with facial segmental hemangioma of more than 5 cm, brain MR, MRA and cardiovascular MR have to be performed. The ipsilaterality of the cerebrovascular anomalies was seen in only 61% of our cases. Long-term follow-up is recommended.

Paper #: 059

Validation of Automated Analysis of Bone Age from Hand Radiograph

Jonathan Bowden, *bowdenjon01@gmail.com*; Sasigarn Bowden, Brent Adler, MD, Houchun Hu, PhD, Rajesh Krishnamurthy, Ramkumar Krishnamurthy, PhD; Radiology, Nationwide Children's Hospital, Columbus, OH

Disclosures: All authors have disclosed no financial interests, arrangements or affiliations in the context of this activity.

Purpose or Case Report: Bone Age (BA) is the measurement of the skeletal maturity of an individual using hand radiograph. Manual BA assessment, performed by a trained radiologist, is the current gold standard and has high inter observer variability (IOV). BoneXpert is an automated machine learning algorithm (software) with zero IOV, and generates results in 5 seconds. The aims of this study are to compare the BA analysis by BoneXpert with the radiologists' manual readings in a cross-sectional cohort, as well as a longitudinal cohort. manual readings.
Methods & Materials: A total of 614 BA studies from 473 patients, assessed by three radiologists from 2013-2018 were identified for automatic determination of BA by BoneXpert (Visiana, Holte, Denmark). BA readings by BoneXpert were compared with those by radiologists' manual readings based on the Greulich and Pyle Method. Spearman's correlation coefficients were used to assess the association between BoneXpert and manual readings.
Results: A total of 583 BA studies were included in the cross-sectional analysis comparing the manual readings and the BoneXpert's assessment. BA data from a subset of 119 patients that had two or more BA studies were analyzed for a longitudinal study to compare the change in skeletal maturation between these 2 methods. BA analyses by BoneXpert and manual reports showed a strong correlation ($r = .9786$; $P < 0.0001$) with the mean difference of BA between these 2 methods being 0.12 ± 0.76 years. When stratified to male and females groups, BA analyses by BoneXpert and manual method remained strongly correlated ($P<0.0001$) in each gender group. In the longitudinal study, there was also a strong correlation between BoneXpert and manual readings ($r = .7852$; $P < 0.01$).
Conclusions: BoneXpert can analyze the hand radiographs quickly and effectively, and produce a BA assessment that is comparable to the manual readings. Other future research will determine the clinical utility of Bone Health Index assessed by radiogrammetry of BoneXpert and how it is correlated with bone density measurement and bone health in pediatric patients with various metabolic bone disorders.

Paper #: 060

Multi-institutional Implementation of an Automated Tool to Predict Pediatric Skeletal Bone Age: How We Did It

Nishith Khandwala[1], *nishith@stanford.edu*; David Eng[1], Sarah S. Milla, MD[2], Nadja Kadom, MD[2], Naomi Strubel[3], Shailee Lala[3], Nancy Fefferman[3], Ross Filice[4], Sanjay P. Prabhu, MBBS, FRCR[5], Michael L. Francavilla, MD[6], Summer Kaplan, MD MS[6], Susan E. Sharp, MD[7], Alexander J. Towbin, MD[7], Mac Everist[8], Neville Irani[8], Safwan Halabi, MD[1]; [1]Radiology, Stanford University, Stanford, CA, [2]Emory University, Atlanta, GA,[3]NYU Langone Health, New York, NY, [4]MedStar Georgetown University Hospital, District of Columbia, DC, [5]Boston Children's Hospital, Boston, MA, [6]Children's Hospital of Philadelphia, Philadelphia, PA, [7]Cincinnati Children's Hospital and Medical Center, Cincinnati, OH, [8]University of Kansas Health System, Kansas City, KS

Disclosures: All authors have disclosed no financial interests, arrangements or affiliations in the context of this activity.

Purpose or Case Report: Skeletal bone age assessment is a common clinical practice to investigate endocrinology, genetic and growth disorders of children. Clinical interpretation and bone age analyses are time-consuming, labor intensive and often subject to inter-observer variability. Bone age prediction models developed with deep learning methodologies can be leveraged to automate bone age interpretation and reporting. The bone age model developed at our institution was offered to interested health systems and institutions to implement and validate the model. This study discusses the logistical, technical, and clinical issues encountered with this model implementation.
Methods & Materials: After IRB approval, multiple U.S. based radiology departments were solicited to adopt and validate the Stanford University bone age model. A total of 8 institutions (4 standalone pediatric hospitals and 4 academic radiology departments) agreed to partner with the primary investigators. IRBs at each institution were required in addition to registration with ClinicalTrials.gov registry. Standardization of the data use agreements was performed. Patient data and protected health information data was retained at each institution. Technical requirements included model hosting at each institution and integration to send images to the model server and results to the interpreting radiologists.
Results: Multiple logistical, technical, and clinical issues were encountered. IRBs at the various institutions had different requirements including waiving patient consent. Technical differences between institutions included model hosting, PACS integrations, interfaces with the reporting system, and image preprocessing. Clinical differences included report templates, calculation of bone age standard deviation, use of Brush foundation, and ability to directly send bone predictions to the reporting system (versus displaying the results as a separate interface). The bone age model was successfully implemented at 7 institutions and approximately 190 studies have been evaluated.
Conclusions: There are myriad challenges to implementing and validating models developed with deep learning methodologies. As models are developed for various clinical use cases including bone age assessment, it will be incumbent on radiology practices and health information systems to integrate these models into clinical practice.

Paper #: 061

Cross-validation of two Convolutional Neural Networks for radiographic fracture detection

Zbigniew A. Starosolski, PhD, *zastaros@texaschildrenshospital.org;* J. H. Kan, MD, Ananth Annapragada; Pediatric Radiology, Texas Childern's Hospital, Houston, TX

Disclosures: All authors have disclosed no financial interests, arrangements or affiliations in the context of this activity.

Purpose or Case Report: We evaluate the hypothesis that Convolutional Neural Networks (CNNs) well-trained for detection of a certain class of fractures can be cross-applied to a different class of fractures and long bone anatomy in children. We tested a network trained for detection of acute distal tibia fractures (CNN-DTF) on generalized long bone fractures of the upper and lower extremity (CNN-LBF) and conversely, a CNN-LBF network on only tibial fractures.
Methods & Materials: Both CNNs (CNN-DTF and CNN-LBF) were based on the Xception network with additional five fully convoluted reasoning layers and a drop-off layer. Network training was performed with 50/50 class balance of positive and negative exams. CNN-DTF (mean age 6.4 years, male 54.6%) was trained on 980 radiographs of acute distal tibia fractures with accuracy of 97.8% for detection of DTF. CNN-LBF (mean age 8.6 years, male 58.2%) was trained on 521,000 patches generated from 1444 long bone radiographs of fractures that included both upper and lower extremities with an 86% accuracy for detection of LBF. These networks were then cross applied and their accuracy measured.
Results: CNN-DTF which was trained to find nondisplaced distal tibial fractures only, had an accuracy 58.5%, sensitivity 92.9%, specificity 24.2 % in identifying any acute fracture when given a mixture of pediatric upper and lower extremity multi-orthogonal long bone radiographs (correct identification of 29721/32000 positive exams, correct identification of 7730/32000 negative exams). CNN-DTF algorithm was unable to correctly differentiate normal physes and apophyses, as well as overlaying bones of the forearm from pathology. CNN-LBF trained to find fractures in any pediatric upper and lower extremity long bones, had an accuracy 66.7%, sensitivity 43.4%, specificity 89.8% in identifying any pediatric acute tibia fracture (correct identification of 145/256 positive exams, correct identification of 26/256 negative exams). CNN-LBF was not able to find small nondisplaced fractures and buckle type fractures typical in distal tibia fractures in younger children, resulting in a high false negative rate.
Conclusions: Both networks undergo a loss of accuracy when utilized for fracture identification of anatomy that they were not trained to evaluate. These results show the importance of proper utilizing anatomy specific training sets which is a significant limitation of current CNN's.

Paper #: 062

Improved accuracy for tibial fracture identification by a convolutional neural network and transfer learning

Zbigniew A. Starosolski, PhD, *zastaros@texaschildrenshospital.org*; J. H. Kan, MD, Ananth Annapragada; Pediatric Radiology, Texas Childern's Hospital, Houston, TX

Disclosures: All authors have disclosed no financial interests, arrangements or affiliations in the context of this activity.

Purpose or Case Report: CNN's trained for automated radiologic imaging interpretation using large datasets are highly

accurate. However, such large training sets are often not available. The purpose of this study is to determine whether a partly pre-trained CNN network with a limited number of specific cases may achieve high accuracy for tibial fractures.
Methods & Materials: An extended text search within the electronic medical records at a children's hospital was performed on all radiographic exams conducted between 2009 and 2017 with 490 acute tibial fractures and 490 normal leg exams with a total of 2118 radiographs (mean age 6.4 years, with 54.6% boys). All images were cropped to a standard size of 299x299 pixels and rotated to a standard orientation. The images were then randomly divided into a training set/validation-set/test-set in an approximately 80/10/10 ratio: The training set contained 784 images, while the Validation set and the Test set each included 98 images. A pre-trained CNN with 136 layers was augmented with an additional two segments with fully convoluted reasoning layers and a drop-off layer for robust feature preservation. After training, a test set containing 49 radiographs with fractures and 49 without fractures was classified by the CNN. Both the test and training set contained leg radiographs in multiple orthogonal views (AP, oblique, and lateral).
Results: CNN automated radiologic interpretation correctly classified 47 of the 49 positive radiographs, and correctly identified the 49 normal radiographs, corresponding to sensitivity, specificity, and accuracy of 95.9%, 100%, and 97.8%, respectively. There were no false positive studies. Retrospective examination of the 2/49 false negative results were subtle fractures that would had probably been missed by most radiologists.
Conclusions: Our feasibility study on the use of CNN for CAD of tibial fractures has the promise to automate and improve workflow for radiologists. Our partly-trained CNN network using a limited dataset, similar to the numbers a typical radiology trainee will see, was robust and able to multi-orthogonally identify fractures and distinguish these fractures from normal physes. This pilot exam on tibial fractures will serve as a basis and foundation for future CNN training for long bone fractures elsewhere in the skeletally immature child.

Paper #: 063

Improved accuracy for recognition of pediatric long-bone fractures in the setting of variable open growth plates by Convolutional Neural Networks

Zbigniew A. Starosolski, PhD,
zastaros@texaschildrenshospital.org; J. H. Kan, MD, Ananth Annapragada; Pediatric Radiology, Texas Childern's Hospital, Houston, TX

Disclosures: All authors have disclosed no financial interests, arrangements or affiliations in the context of this activity.

Purpose or Case Report: Convolutional neural networks (CNNs) show promise for automatic facilitated radiologic diagnosis. Fracture morphology heterogeneity in the setting of skeletal immaturity with variable appearances of physes and apophyses are a challenge for traditional automatic classification techniques. The purpose of this study was to evaluate the effect of CNN architecture and training set generation methods on the accuracy of computer-aided diagnosis (CAD) of upper and lower extremity long-bone fractures in children.
Methods & Materials: This IRB approved study was performed with a dataset obtained at a children's hospital from 2015-18 that included 1444 pediatric acute fractures and 1147 normal radiograph of the upper and lower extremity long bones (mean age 8.6 years, 58.2% male). Abnormal exams with casts, implants, healing, or other pathology were excluded. Fracture locations were recorded in image coordinates for further dataset generation. Radiographs were patched into 512x512 image sets from the raw DICOM images. Patches were randomly generated in an automated fashion. Training set including 512000 patches was created with 50/50 fracture-to-normal ratio. The validation set and test set each had 64000 images with exact class balance. The previously trained Xception network was chosen for this task due to its high overall accuracy for image classification. A transfer learning approach with five additional fully connected layers on the top of the Xception network and one drop-off layer for robust feature preservation, was used for the classification task. To further improve the classification, the classification threshold - the critical value that divides positive form negative predictions was optimized.
Results: A classification threshold of 0.2 was selected to minimize false negative results. The CNN correctly classified 27816 of the 32000 fracture cases and 27603 of the 32000 normal cases, corresponding to sensitivity, specificity, and accuracy of 86.93%, 86.62%, and 86.6%, respectively. The area under ROC curve was 0.93
Conclusions: Acute pediatric long bone fracture identification is possible with high accuracy using an automated patch approach with well parameterized CNN's using transfer learning. The automated patch approach eliminates image scaling and allows localization of the classified fracture within a relatively narrow spatial domain. Our optimized CNN performs similarly to adult long bone fracture algorithms despite the presence of variable growth plates in the skeletally immature child.

Paper #: 064

Underappreciated Elbow Fractures: Pediatric Radial Head and Neck Fractures and Additional Fracture Associations

Andrew J. Degnan, MD, MPhil, *degnana@email.chop.edu*; Victor Ho-Fung, MD, Jie C. Nguyen, John T. Lawrence, Summer Kaplan, MD MS; Radiology, Children's Hospital of Philadelphia, Philadelphia, PA

Disclosures: John T. Lawrence: Royalty: Sawbones. All other authors have disclosed no financial interests, arrangements or affiliations in the context of this activity.

Purpose or Case Report: Radial head and neck fractures represent a small fraction of all pediatric elbow fractures but are often associated with significant long-term morbidity. Various mechanisms can cause these radius fractures; however, the constellation of associated injuries is poorly understood in the pediatric population. The goal of this study is to assess the frequency of additional fractures in the setting of proximal radial head and neck fractures.
Methods & Materials: This IRB-approved study reviewed 600 consecutive cases with reports suggesting a proximal radius fracture obtained during a five-year period (2013-2017). Pathologic and non-radial head or neck fractures were excluded. Initial and follow-up radiographs were re-reviewed to assess the presence and type of fracture as well as the presence of elbow joint effusion on initial presentation. Fracture types and properties were analyzed using ANOVA and independent samples t-tests.
Results: 334 radial head and neck fractures were identified (50% female; mean age: 9.6 years, SD 3.9). 37% were noted to have one or more additional fracture about the elbow. Olecranon fractures were most common (23% of all cases), followed by additional medial epicondyle fractures (4%), coronoid fractures (3%), ulnar diaphyseal fractures (3%), and olecranon with medial epicondyle fractures (2%) and others (1-2%). Approximately one-third (33%) of additional fractures were missed by the initial interpreting radiologist. Most (68%) of the missed fractures were visible on the initial radiographs, but 32% were only visible on follow-up radiographs because of

a healing response.Presence of a complete fracture (OR: 2.6, CI:1.6-4.1, p<0.001) and joint effusion (OR: 2.2, CI:1.2-4.0, p<0.001) both increased the likelihood of secondary fracture. Isolated radius fractures occurred in older patients compared with those with additional associated fractures (mean age: 9.3 years, SD 3.9 vs. 7.6 years, SD 3.6; p<0.001).
Conclusions: Proximal radius fractures are often associated with additional fractures, most commonly olecranon fractures. These additional fractures are frequently missed. Presence of joint effusion and complete radius fracture may suggest greater likelihood of an additional elbow fracture and prompt additional investigation.

Paper #: 065

Utilizing 3D-Printed Models to Optimize Digital Tomosynthesis for Pediatric Medial Epicondyle Elbow Fractures

Emily A. Edwards, *famousamose@gmail.com*; Kristin S. Livingston, MD, Michael Griffith, RT, Andrew Phelps, MD, Jesse Courtier, MD, John D. MacKenzie, MD, Matthew A. Zapala, MD, PhD; Radiology and Biomedical Imaging, University of California, San Francisco, San Francisco, CA

Disclosures: All authors have disclosed no financial interests, arrangements or affiliations in the context of this activity.

Purpose or Case Report: Pediatric elbow fractures rely heavily on imaging for clinical evaluation and determination of operative versus non-operative management, specifically for medial epicondyle fractures. Standard radiographic views are often suboptimal for visualizing maximal medial epicondyle displacement, and orthopedic surgeons may require elbow computed tomography (CT) for definitive characterization. Digital tomosynthesis (DT) is an imaging technique that creates multiple radiographs with high in-plane resolution. The hypothesis of this study is that DT can assess displacement of medial epicondyle fractures with similar accuracy to CT and lower radiation dose. Radiopaque 3D-printed models were used to optimize positioning and DT technique.
Methods & Materials: Three 3D-printed models were generated based on CT data of pediatric patients with medial epicondyle fractures using at least 20% polylactic acid fill. DT was performed in thirteen projections/sweeps to determine optimal visualization of fracture fragment displacement. Two pediatric radiologists independently reviewed all projections/sweeps and measured maximal displacement. CT of the 3D-printed models was performed as the gold standard with consensus agreement by the two radiologists on maximal displacement. Estimated radiation dose for pediatric elbow DT was calculated using phantoms. Non-contrast upper extremity CT dose estimates were extracted from dose reports at the authors' institution between July 1, 2015 and June 30, 2018 (N=52).
Results: Absorbed dose estimates for DT were 0.15-0.21 mGy, compared to 0.02-0.04 mGy for 2-view elbow radiographs and median CT upper extremity dose 3.9 mGy. Six projections were excluded for poor fracture visualization and inter-reader measurement variation >1 mm. The remaining seven projections had good inter-reader agreement (both readers <1 mm variance from each other, Pearson coefficient 0.93). The lateral transverse and oblique longitudinal DT projections were closest to consensus CT maximal displacement (2.9 and 3.4% measurement variance from CT, respectively).
Conclusions: 3D-printed models help to optimize DT technique for ideal visualization of displacement of pediatric medial epicondyle fractures. The lateral transverse and oblique longitudinal DT projections had high inter-reader agreement and high correlation with CT measurement of fracture displacement, at approximately 1/20th the absorbed radiation dose.

Paper #: 066

Long Bone Growth and Skeletal Maturation Patterns of Children with Progeria

Andy Tsai, MD, PhD[1], *andy.tsai@childrens.harvard.edu*; Patrick Johnston, MMath, Msc[1], Michele Walters, MD[1], Leslie Gordon, MD, PhD[2], Monica Kleinman, M.D.[1], Tal Laor, MD[1]; Boston Children's Hospital, Boston, MA, [2]Rhode Island Hospital, Providence, RI

Disclosures: All authors have disclosed no financial interests, arrangements or affiliations in the context of this activity.

Purpose or Case Report: Hutchinson Gilford progeria syndrome (HGPS or Progeria) is a rare sporadic genetic disorder (1 in 20 million) that uniformly is fatal, with most deaths attributed to myocardial infarction between 7-21 years of age. Due to the disease rarity and short patient life-span, there are only ~400 children with Progeria alive worldwide at any given time. One early clinical manifestation in Progeria is abnormal skeletal growth, yet this has not been fully characterized. The objective of this study is to characterize the longitudinal long bone growth and skeletal maturation pattern of children with Progeria.

Methods & Materials: Skeletal survey radiographs of children with Progeria performed at a large tertiary hospital (1/1/2009-7/31/2018) were reviewed. The protocol for the surveys varied over time, but the majority included PA radiographs of the left hand/wrist, and AP radiographs of each humerus, radius, ulna, tibia, and fibula. No femur radiographs were obtained. Using the left hand/wrist radiographs, bone ages of these children were estimated by the standards of Greulich and Pyle. Following methodology established in the literature for studying long bone growth, the study cohort was separated into 2 overlapping age groups: childhood (≤12 years-old) and adolescence (≥10 years-old). For those in the childhood cohort, bone length measurements were made between physes along the midline long axis of the bone. For those in the adolescence cohort, bone length measurements were made along the midline long axis of the bone from the upper margins of the proximal to the lower margin of the distal ossified epiphyses. These long bone length measurements (humerus, radius, ulna, tibia, and fibula) and bone age estimates were plotted against patient chronologic ages and compared to published normal reference standards.
Results: Eighty-six children (M:F=46:40) with 253 skeletal surveys (M:F=121:132; age range=2 months-22 years) were included. Bone age estimates showed a skeletal maturation pattern that is comparable to normal. However, longitudinal long bone lengths from these children began to significantly deviate from normal by age 1-2. The growth curves of these long bones plateau at around age 10. At adulthood, long bone lengths ranged from 48-61% of normal.
Conclusions: Our study establishes reference standards for long bone growth and skeletal maturation of children with Progeria. These 2 outcome measures may offer objective assessments to evaluate the efficacy and response of these children undergoing treatment.

Paper #: 067

Can Ultrasound be reliably used to evaluate infants with DDH after age 6 months without the use of plain film radiography?

Noor M. Maza, BS[1], *noor.maza@icahn.mssm.edu*; Stanley Ewala[1], Christopher Ferrer[1], Abigail Allen, MD[2], Sheena Ranade, MD[2], Joy Masseaux, MD[2], Henrietta K. Rosenberg, MD, FACR, FAAP[2]; [1]Icahn School of Medicine, New York, NY, [2]Mount Sinai Hospital, New York, NY

Disclosures: All authors have disclosed no financial interests, arrangements or affiliations in the context of this activity.

Purpose or Case Report: DDH occurs in 1.5/1000 births and requires prompt diagnosis and treatment as well as interval clinical and imaging surveillance for assessment of healing and complications. Current screening and monitoring guidelines recommend the use of US for evaluation of the hip in infants <6 months of age, and XR imaging in patients >6 months. The purpose of this study is to determine whether US is a reliable surrogate for XR for evaluation for DDH in patients >6 months.
Methods & Materials: This is an IRB approved retrospective study of a series of 22 at risk patients >6 months of age who had both US and XR for assessment of DDH. All of the imaging studies of potential patients were reviewed by 1-2 experienced pediatric radiologists with all the studies having been performed by an experienced pediatric radiologist. 30 patients >6 months were identified who had both US and XR studies of which 8 patients with a time difference between modalities greater than 4 months were excluded. Dynamic hip US was performed (transverse flexion and longitudinal flexion views without stress and with stress and during the Ortolani maneuver were obtained; Graf angles measured), except when patient was in a Pavlik harness or brace at which time adynamic hip sonography was performed. When it was determined that alignment was normal without stress, dynamic hip US was added. Size, configuration, and symmetry of the femoral capital epiphyseal ossification centers was assessed when present. All of the studies were performed using Philips IU22 US units (L12-5 and/or L9-3 probes with a few of the earlier images obtained with a C5-2 or 9-4 probe). The US reports included descriptions of the hip morphology (including Graf angles), alignment, and stability. AP supine XR included either a neutral projection or both neutral and frog lateral views. The shape of the acetabulum, alignment of the hips, and the presence, size and symmetry of the femoral capital epiphyses was assessed, and the acetabular angles were measured on neutral views. Alignment was also assessed on frog lateral views.
Results: In all 22 patients, there was excellent correlation between the US and XR finding.
Conclusions: US may be used as a first line imaging modality in babies >6 months of age presenting with clinical suspicion of DDH as well as those who were diagnosed with DDH prior to 6 months and are due for follow up surveillance, as long as the operator is appropriately experienced and the probe technology allows for visualization of all pertinent landmarks.

Paper #: 068

Outcomes Measures Related to Care Process Models in the Evaluation of Infants for Developmental Dysplasia of the Hips

Jeffrey Prince, MD,*jeffreysprince@gmail.com*; Department of Medical Imaging, Primary Children's Hospital, Salt Lake City, UT

Disclosures: All authors have disclosed no financial interests, arrangements or affiliations in the context of this activity.

Purpose or Case Report: Care process models (CPM) give guidance for the use of imaging in clinical scenarios and can be effective in screening processes.A CPM needs to be supported by and modified based on outcomes measures. We evaluate 2 CPM's associated with screening for developmental dysplasia of the hip (DDH) in infants to see if the outcomes measures support or improve the CPM. One model gives guidance regarding timing of initial ultrasound evaluation for possible DDH in an attempt to avoid multiple ultrasound studies as part of the evaluation. The second model involves the methods used in evaluated patients with a breech risk factor for DDH.
Methods & Materials: All patients evaluated with ultrasound for possible DDH in a 27 month period were retrospectively reviewed. Age at the first ultrasound exam, result of that exam, number of follow-up exams, referral to orthopedics, and ultimate outcome for the patient were recorded. Additionally in patients evaluated because of breech presentation, the use of a follow-up radiograph between 6 and 12 months of age and the outcome of that study was also recorded.
Results: Over the review period, 1830 patients were evaluated for the possibility of DDH. 143 were diagnosed with DDH. 1289 were felt to be normal. 398 were placed in an immature category. Immature categorization was given in 38.4% of patients under the age of 6 weeks at initial evaluation, in 29.4% of patients between the ages of 6 and 7 weeks, and in 7.3% of patients at 8 weeks of age or greater. Patients in the immature category required on average 0.92 additional ultrasound examinations. 97.9% of immature patients normalized without therapy.592 were evaluated initially because of breech presentation as a risk factor over a one year period. 203 of these patients had a follow-up radiograph as part of their evaluation as was recommended in the CPM. 98.0% of these patients were normal at the time of the radiograph. 12 patients were referred to orthopedics because of an abnormal radiograph. 4 of these required therapy and 8 were observed and remained normal clinically.
Conclusions: Outcomes measures support the recommendation that an initial hip ultrasound for risk factors should not be performed until the patient is 6 weeks of age. If this recommendation had been followed, 111 unnecessary ultrasound examinations could have been avoided. Outcomes measures do not support the recommendation of a follow-up radiograph for patients screened for a risk factor of breech presentation. These patients rarely develop hip dysplasia.

Paper #: 069

Comparative dose and image quality evaluation for scoliosis follow-up exams: assessment of standard and low-dose modes of a slot-scan radiographic system

Sébastien Benali, MD, *sebastien.benali.hsj@ssss.gouv.qc.ca*; Sylvain Deschenes, Ph.D., Stefan Parent, MD, Marjolaine Roy-Beaudry, Veronika Syzonenko, Josée Dubois, MD; Medical Imaging, CHU Sainte-Justine, Montreal, Quebec, Canada

Disclosures: All authors have disclosed no financial interests, arrangements or affiliations in the context of this activity.

Purpose or Case Report: We compare standard and low-dose modes of an X-Ray slot-scanner through a wide-ranging evaluation of dose and image quality for scoliosis exams.
Methods & Materials: The EOS^{TM} slot-scanner is a bi-planar system that can acquire simultaneously two orthogonal x-ray images. The patient is scanned vertically by fan beams coupled with linear gaseous detectors. The system offers high quality images using radiation dose several times lower than DR due to a better management of scatter radiation.Recently, a new low dose mode was introduced for the system. The goal is to offer images of diagnostic quality using less radiation dose. This is achieved by lowering the tube tension and current while applying adapted image post-processing.In this work, we compare images acquired on 28 pediatric patients and their respective dose. Patients underwent two scoliosis follow-up examinations, both consisting in the acquisition of lateral and posteroanterior x-ray images, once with standard dose parameters and once in low-dose mode. Dose-Area product for each examination was collected and OSL dosimeters were placed near radiosensitive regions on the patient before each scan. Two radiologists evaluated the images in a randomized order using a questionnaire targeting anatomic landmarks. Visibility of the structures was rated on a 4 degrees scale. Image

quality assessment was analyzed using a Wilcoxon signed ranks test.
Results: Dose-Area Products show decrease in dose ranging from 3 to 5 times when imaging in low-dose mode. These reductions are consistent with direct measurements obtained with OSL.All images meet diagnostic quality standards. Assessment of global image quality and visibility of a large majority of musculoskeletal landmarks showed no statistically significant bias when comparing standard and low-dose images. Few landmarks, such as femoral heads in lateral view, were better seen in standard mode (p=0.013), while other, like cervicothoracic junction in posteroanterior view, scored better in low-dose mode (p=0.002).
Conclusions: We established that the low-dose mode offers diagnostic image quality while decreasing drastically the dose to the patient.This dose reduction is crucial for scoliosis follow-ups since they involve repeated X-rays that can increase the risk of detrimental effects due to ionizing radiation.

Paper #: 070

Comparing Image Quality and Exposure Rates Between Flat Panel Detectors and Image Intensifiers in Fluoroscopy

Elizabeth Snyder, MD, *elizabeth.j.snyder@gmail.com*; Marta Hernanz-Schulman, MD, Kenneth Lewis, Diana Carver; Vanderbilt University Medical Center, Nashville, TN

Disclosures: All authors have disclosed no financial interests, arrangements or affiliations in the context of this activity.

Purpose or Case Report: Flat panel detectors (FPD) have increasingly replaced image intensifiers (IIs) with the aim of providing high image quality and potentially lower patient radiation doses. As limiting radiation exposure is particularly important in our pediatric patients, our objective was to compare exposure rates and image quality between FPD and II fluoroscopes.
Methods & Materials: Exposure rates were measured for the FPD in both medium- and low-dose modes and for the II in low-dose mode at three magnification levels for both continuous and pulsed fluoroscopy at 7.5 frames/sec. All measurements were recorded at 1 cm above the fluoroscopy table. Image quality was evaluated using the 19.3 cm CIRS Rad Fluoro phantom, with the detector positioned 50 cm above the table on both the FPD and II to compare spatial and contrast resolution at the same 3 magnification levels.
Results: For pulsed fluoroscopy in low-dose mode, exposure rates (R/min) were lower for the FPD than the II at all mag levels:At 7.5 fps, mag factors 1, 2, 3, FPD values were: 0.79, 1.18 and 1.62 R/min.II values were: 1.36, 2.32 and 3.90 R/min.In medium-dose mode, measured similarly, FPD exposure rates were slightly higher than the II at the first mag level, but lower at the second and third levels: 1.44, 1.78 and 2.10.For continuous fluoroscopy at low-dose, exposure rates were lower in the FPD at all 3 mag levels: FPD 1.99, 3.11 and 3.8 vs II 2.78, 3.48 and 4.42.At medium-dose, FPD rates were lower than the II at the first mag level, but higher at the second and third levels: 2.55, 4.26 and 5.74.Spatial resolution between low-dose II to low-dose FPD was better on the II (4 objects vs 3 well-delineated). Between low-dose II to medium-dose FPD, resolution was better on FPD especially for mag 3 (4 objects vs 3 at mag 1; 5 vs 3 at mag 3).Contrast resolution between low-dose II to low-dose FPD was better on II (3.5-4 objects vs 2.5-3); between low dose II to medium-dose FPD, contrast was equivalent (3-4 objects for both).
Conclusions: Use of state-of-the-art fluoroscopy FPD equipment over the traditional II results in radiation dose savings when operating in low-dose mode, although this comes at the expense of some image quality. Changing to medium dose mode eradicates some of the radiation savings and results in modest gain in image quality which may not be commensurate. Our findings indicate that care must be taken in initial equipment calibration, physicist input is important, and image quality should be tailored to the needs of the specific examination.

Paper #: 071

Novel Use of Optical Video for Reducing Radiation Dose in Pediatric Fluoroscopy

Steven Ross, MD, *rossification@gmail.com*; Radiology, El Paso Children's Hospital, El Paso, TX

Disclosures: Steven Ross, MD: Financial Interest: Personal Ownership of Provisional Patent - Intellectual Rights: Inventor and Patent Holder. All other authors have disclosed no financial interests, arrangements or affiliations in the context of this activity.

Purpose or Case Report: Fluoroscopic exams are a significant contributor to pediatric patient radiation dose. Innovations such as “last image hold”, pulsed fluoroscopy, and digital fluoroscopy have reduced the patient dose; however, development of new technology to further reduce dose has been largely absent in the last decade. A source of dose during fluoroscopy is “fluoro hunting” which is the use of fluoroscopy to center the image over the site of interest. The purpose of this study is to determine if the use of optical video to position the image before using fluoroscopy can reduce the dose from the exam.
Methods & Materials: An optical video device was designed and placed on the fluoroscopy unit used at El Paso Children’s Hospital. The device was used on 20 consecutive voiding cystourethrograms (VCUG) and 20 consecutive upper GI (UGI) exams performed on children ages 2 weeks to 15 years by one pediatric radiologist. The device was used to center the fluoroscopy machine in relation to the site of interest prior to using radiation during these exams. The cumulative air-kerma area products (KAP) and fluoroscopy times (FT) were recorded for these exams. This data was compared to the same operator’s KAP and FT from UGIs and VCUGs performed prior to the development of this study. A student’s independent sample t-test was used to compare the KAP and FT from the exams using the device and those performed without the device.
Results: FT was used as the primary indicator of effectiveness since KAP also depended on patient sizes. These FTs were compared to the retrospective control group. The average FT using the device for UGI was 3 seconds. The average FT from 115 UGIs without the device was 20.7 seconds. This was an 85.5% decrease in FT when using the device. The average FT using the device for VCUG was 4.5 seconds. The average FT from 78 VCUGs without the device was 22.8 seconds. This is an 80.0% decrease in FT when using the device. The student t-test revealed a statistically significant decrease in FT and KAP using the device.
Conclusions: This study revealed that using an optical video device to align patients for fluoroscopic imaging significantly lowers the FT of both UGI and VCUG. While at least a portion of the time reduction is likely due to the elimination of “fluoro hunting”, the reduction was larger than expected. Since the device allows the use of fluoroscopy to be limited to actual diagnostic rather than alignment imaging, it also likely increases the radiologist’s awareness of when radiation is being used.

Paper #: 072

Efficient ALARA Determination using Adaptive Simulated Low-Dose Pediatric Appendicitis CT and a Psychometric Function

Steven Don, MD[1], *dons@mir.wustl.edu*; Michael F. Lin, M.D.[1], Eric P. Eutsler, M.D.[1], David Politte, D.Sc.[1], Ruth Holdener, R.T.R. (M) (CT)[1], Craig K. Abbey, Ph.D.[2], Bruce Whiting, Ph.D.[3]; [1]Mallinckrodt Institute of Radiology, St. Louis, MO, [2]University of California, Santa Barbara, Santa Barbara, CA, [3]University of Pittsburgh Medical Center, Pittsburgh, PA

Disclosures: Steven Don, MD: Financial Interest: Vantage Medical Imaging - Stock: Clinical lead; Fujifilm - Honorarium: Speaker; **Craig Abbey, MD:** Consultant, Honoraria: Canon Medical Research, USA; All other authors have disclosed no financial interests, arrangements or affiliations in the context of this activity.

Purpose or Case Report: Evaluate a method to efficiently characterize the effect of noise on CT readers of pediatric appendicitis, combining adaptively simulated low-dose images with a novel parameterized observer response function.
Methods & Materials: CT scans from 201 pediatric patients (0.27-21.2 years; 115 male-86 female; 84 nonperforated appendicitis and 117 without appendicitis) acquired on Siemens Sensation 16, AS 64, or Flash scanners, were used for image simulation based on 1 mm thick slices. Simulated low-dose scans formatted in the axial and coronal planes as 3 mm reconstructions were presented to 3 observers (2 pediatric radiologists, 1 adult abdominal radiologist). The amount of added noise was selected based on prior responses of the individual (adaptive simulation). They marked the location of the appendix, rated the likelihood for appendicitis on a 6-point scale (1–definitely normal to 6–definitely appendicitis). The full-dose study was then presented to the observer, who again marked the appendix, rated the likelihood for appendicitis and the visualization of the appendix. The in situ noise in the appendiceal region was estimated using variance propagation methods. The intraobserver agreement of readers, matching between low dose and full dose, was fit to a parameterized psychometric function (agreement versus noise level) by maximizing the log-likelihood probability. This function can be used to analytically compute a noise shoulder N_{Σ}, which characterizes a reader's sensitivity to noise. Readers' responses for appendicitis and normal cases were also separately analyzed.
Results: At full dose the observers had an area under the curve (AUC) of 0.973(0.018, stdev) and selected locations had a mean noise of 9.9 (4.3) HU. Individual readers had a range of noise tolerances (shoulder location), with mean tolerated noise of 23.6 HU (range 18.9-30.3). This equates to an 85% dose reduction. In general, appendicitis cases were less tolerant of noise reduction than normal cases.
Conclusions: The adaptive psychometric function is a promising tool to efficiently determine ALARA for task-specific CT diagnosis, providing an order of magnitude reduction in cases needed compared with receiver operating characteristic curves. These results indicate that estimated CT dose decreases of 85% or a noise ceiling of 23.6 HU could be tolerated without affecting agreement.

Paper #: 073

Radiation burden associated with imaging of suspected appendicitis-related abscess: Pathway to a radiation free MR appendicitis imaging protocol

Joshua H. Finkle, MD, *jfinkle@luriechildrens.org*; Cynthia K. Rigsby, MD, Timothy Lautz, MD, Nicole Murphy, Christina L. Sammet, PhD, DABR; Radiology, Ann & Robert H. Lurie Children's Hospital of Chicago, Chicago, IL

Disclosures: All authors have disclosed no financial interests, arrangements or affiliations in the context of this activity.

Purpose or Case Report: Abscess formation is a common appendicitis complication both pre- and post-operatively. At our institution, MR is exclusively used to evaluate for acute appendicitis after an equivocal or non-diagnostic US study, and contrast-enhanced CT is the test of choice only when abscess is suspected clinically or following US. Our aims are to 1) assess the radiation burden of patients who undergo CT for suspected appendicitis-related abscess and 2) determine the frequency of abscess detection and positive predictive value (PPV) for abscess detection of non-contrast appendicitis MR including diffusion weighted imaging in the setting of suspected appendicitis.
Methods & Materials: We performed an IRB approved retrospective review of all children who between 2015 and 2018 underwent CT after an US study suspicious for abscess in the setting of either suspected appendicitis or to evaluate for abscess post-appendectomy. CT effective dose was calculated using Monte Carlo simulation software (Radimetrics, Bayer Healthcare). We also reviewed all MR studies performed after an equivocal US for acute appendicitis to determine the frequency of abscess detection and the positive predictive value (PPV) of MR for abscess evaluation. Clinical course including surgery or interventional (IR) drainage was recorded for patients with abscesses by CT or MR.
Results: 220 CT studies in 165 patients (mean 9.3+/-3.8 years, 58% male) were performed for abscess evaluation with a mean CT effective dose of 9.8 mSv per exam or 13.1 mSv per patient. 35% of patients (57/165) had CT imaging related to initial appendicitis presentation of which 70% (40/57) were positive for abscess; 48% (19/40) went on to IR drainage, 45% (18/40) to surgery. 65% of patients (108/165) had CT imaging post-appendectomy of which 66% (71/108) were positive for abscess; 76% (54/71) went on to IR drainage and 7% (5/70) to surgery. The patients who did not have IR drainage or surgery were treated conservatively with antibiotics. Of 893 MR exams for appendicitis, 20 were read as positive for abscess and all had proven abscess by operative or IR drainage, PPV of 100%. Additional ongoing MR data collection will be presented in detail.
Conclusions: There is a substantial CT radiation burden with an average of 13 mSv per patient to evaluate for abscess in the setting of appendicitis. MR has a high PPV for abscess detection suggesting it is a viable alternative to CT and allows for a radiation-free appendicitis imaging pathway.

Paper #: 074

Implementation of Single-Source Dual-Layer Spectral CT in a Pediatric Imaging Department: Addressing Dose Neutrality and Maintenance of Image Quality in Abdominal-Pelvic CT in Children

Richard Southard, MD, *rsouthard@phoenixchildrens.com*; Nicholas Rubert, PhD, Robyn Augustyn, BSRT RT(R)(CT), M'hamed Temkit, PhD, Mittun Patel, MD, Dianna M. Bardo, MD; Department of Medical Imaging, Phoenix Children's Hospital, Phoenix, AZ

Disclosures: Dianna M. Bardo, MD: Consultant, Honoraria; Speakers Bureau: Koninklijke Philips, NV. All other authors have disclosed no financial interests, arrangements or affiliations in the context of this activity.

Purpose or Case Report: To assess the effect of single-source dual-layer (SSDL) CT on radiation exposure and image quality in pediatric patients undergoing contrast-enhanced abdominal-pelvic CT examinations.
Methods & Materials: We reviewed 395 consecutive abdominal-pelvic CT examinations between December 2017 and April 2018: 152 patients (123 months, 2-268 months) imaged on SSDL using 120 kVp compared with 243 patients (119 months, 0.8-270 months) imaged on single-energy CT (SECT) using weight-based protocols (80 kVp/100kVp/120 kVp), matching automatic exposure control, hybrid-iterative reconstruction and image quality indices. Image quality (IQ) metrics included SNR, CNR and subjective radiologist scores. Dose calculations included $CTDI_{vol}$ and size-specific dose estimates (SSDE).
Results: Comparing all SSDL and SECT patients, there was $CTDI_{vol}$ dose parity (4.0 mGy vs. 3.6 mGy, p=0.0840), with individual weight subgroup dose increase of 5%-11% for $CTDI_{vol}$ and 2-12% for SSDE. SNR, CNR and IQ scores were maintained or improved in all SSDL weight groups with the exception of 15% reduced CNR in the 0-30 kg subgroup. We present representative cases which demonstrate how CNR can be recovered with low-energy virtual mono-energetic (mono-E) images (VMI) following material decomposition of the spectral data. Our measured SSDL doses were comparable or lower than those reported for children imaged using other dual-energy scanners and compared to the ACR national dose index registry for pediatric body CT, would rank in the lower quartiles of reported $CTDI_{vol}$. Minor dose increase observed in patients despite matching AEC and dose index are likely secondary to machine differences in filters, collimation and a softer beam spectrum.
Conclusions: SSDL can be safely implemented in a pediatric department with overall dose neutrality and maintained image quality; however, there may be increased dose observed in the smallest patients despite matching AEC and dose index likely secondary to differences in filters, collimation and softer beam spectrum. Spectral CT offers many benefits by virtue of material-specific information in addition to diagnostic anatomic detail, and VMI low mono-E reconstruction can recover CNR potentially lost with use of higher kVp. To our knowledge, we are the first to explore dose-neutrality in children undergoing abdominal-pelvic CT examinations using single-source dual-layer spectral CT.

Paper #: 075

Size-specific dose estimate reference levels for pediatric abdominopelvic examinations using single and dual-energy dual-source CT

Marilyn J. Siegel, MD[1], *siegelm@wustl.edu*; Juan Carlos Ramirez Giraldo, PhD[2]; [1]Mallinckrodt Institute of Radiology, Washington University St Louis, St Louis, MO, [2]Computed Tomography R&D, Siemens Healthineers, Malvern, PA

Disclosures: Marilyn J. Siegel, MD: Financial Interest: JCRG is an employee of Siemens Healthineers - Salary: JCRG is a senior key expert scientist working for Siemens; **Juan Carlos Ramirez Giraldo, PhD**: JCRG is scientist employed by Siemens. All other authors have disclosed no financial interests, arrangements or affiliations in the context of this activity.

Purpose or Case Report: To present size-specific dose estimate (SSDE) reference levels for pediatric abdominopelvic single-energy CT (SECT) and dual-energy CT (DECT) examinations
Methods & Materials: This single-center HIPPA-compliant study was approved by institutional review board. Retrospective CT dose data were collected in pediatric patients (mean age 9.3±5.9 years) from September 2014 until March 2018) using dose tracking software. Contrast-enhanced abdominopelvic CT studies were sorted into two categories: single energy CT (SECT) (N=1719) and DECT (N=375) CT. Clinical indications included abdominal pain, mass, bowel diseases. Size-specific dose estimates (SSDEs) based on body circumference and volume CT dose index ($CTDI_{vol}$) were calculated. All examinations were performed on a dual-source CT system (Somatom Flash, Siemens Healthineers). Both SECT and DECT acquisitions used automatic exposure control and iterative reconstruction. SECT was performed using kilovoltages ranging from 70 to 120 kVp. Patient data were grouped into one of five body circumferences. The median, 25^{th} and 75^{th} quartile of the SSDEs within each circumference group was calculated. Statistical unpaired comparisons were made between groups. Subjective image quality (scale 1, excellent, to 4, non-diagnostic) of 25 DECT and SECT scans from each circumference group was assessed.
Results: For the five effective diameters (< 15cm, 15-19cm, 20-24cm, 25-30 cm and > 30cm), the median SSDE [25^{th}-75^{th} quartile] for DECT and SECT were 6.3[5.9-6.7] mGy and 7.8 [6.5-8.2] mGy ($P > .05$); 6.7[6.3-7.4] mGy and 7.5 [6.6-7.8] mGy ($P > .05$); 7.8[7.3-8.7]mGy and 7.9 [6.7-9.7] mGy ($P > .05$); 8.9[8.2-9.6] and 9.9[8.7-10.7] mGy ($P < .01$) ; 10.8[9.9-12.6] and 12.2[11.0-14.3] ($P < .05$), respectively. The SSDE for DECT was statistically lower than that of SECT in patients with circumferences $\geq$ 25 cm ($P < .01$). SSDE for DECT and SECT were not significantly different in smaller patients. Image quality was also similar for both DECT and SECT.
Conclusions: The SSDE diagnostic references levels in this study as a function of body circumference can provide guidance to establish reference radiation exposures in clinical practice for contrast-enhanced DECT and SECT in pediatric abdominopelvic CT on a dual-source CT scanner. The SSDEs of DECT are comparable or lower than those of SECT.

Paper #: 076

Plain film findings in ileocolic intussusception. Why should we care?.

Dhruv Patel, MD, Jonathan M. Loewen, MD, Kiery Braithwaite, MD, Sarah Milla, MD, **Edward Richer, MD**, *richerej@gmail.com*; Radiology, Emory University, Atlanta, GA

Disclosures: All authors have disclosed no financial interests, arrangements or affiliations in the context of this activity.

Purpose or Case Report: Determine the spectrum of plain film findings encountered in ileocolic intussusceptions and assess their predictive value in reducibility by therapeutic enema, and in surgical outcomes in patients with failed reductions.
Methods & Materials: An IRB approved, retrospective study was performed. The radiology information system at our institution was queried for the keyword "intussusception" in fluoroscopic reports from September 2012 – August 2017. Two authors then reviewed plain films obtained prior to therapeutic enema, when available, for the following findings: normal, paucity of bowel gas, soft tissue mass, meniscus sign, or obstruction. When plain films were not available, the scout image from the therapeutic enema was reviewed. Disagreements were resolved by consensus. The medical record was then reviewed for each patient to determine success of therapeutic enema, and surgical outcome in cases of failed reduction. Complicated surgical cases were defined as those that required more extensive surgery than a standard laparoscopic reduction, such as conversion to open laparotomy.
Results: 182 total cases of intussusception reduction were identified and reviewed. A normal bowel gas pattern was seen in 14%, paucity of bowel gas in 65%, soft tissue mass in 26%, meniscus sign in 12%, and obstruction in 10%. Percentages total > 100% due to more than one finding in some patients. A normal bowel gas pattern was associated with the highest therapeutic enema success rate (83%) and lowest rates of complicated surgery (4%) and bowel resection (4%). Conversely, bowel obstruction was associated with the lowest enema success rate (21%), and highest rates of complicated surgery (47%) and bowel resection (42%). Patients with bowel obstruction had a significantly higher likelihood of needing surgical reduction (OR 9.0, 95% CI 2.84-28.47) and bowel resection (OR 11.1, 95% CI 3.66-33.86) than those without obstruction. Paucity of bowel gas, presence of soft tissue mass, and meniscus sign showed enema success rates and surgical outcomes intermediate between normal and obstruction.
Conclusions: In most cases of ileocolic intussusception, plain films show an abnormality, with paucity of bowel gas being the most common finding. Plain film findings can provide important prognostic information to both the radiologist and the surgeon, with significantly lower enema reduction rates and higher rates of complicated surgeries in patients with bowel obstruction.

Paper #: 077

Recurrent Intussusceptions in Children

Grace M. Ma, MD[1], *gracemy.ma@gmail.com*; Craig Lillehei, MD[2], Michael J. Callahan, MD[2]; [1]Radiology, The Hospital for Sick Children, Toronto, Ontario, Canada, [2]Boston Children's Hospital, Boston, MA

Disclosures: All authors have disclosed no financial interests, arrangements or affiliations in the context of this activity.

Purpose or Case Report: Air-contrast enema (ACE) is an effective treatment for ileocolic intussusception (ICI). There is currently no consensus on the number of ACE attempts for multiple ICI prior to surgery. The purpose of this study is to review the patterns of ICI and ACE success rates in patients with and without recurrence and to determine the number of ACE attempts to be considered for recurrent ICI that may obviate the need for surgery.
Methods & Materials: Retrospective review of 683 children (≤ 18 years) with ACE for ICI between January 2000-May 2018. Recurrent ICI were separated into mutually exclusive categories: short-term (ST, ≤7 days between episodes) and long-term (LT, > 7 days between episodes) ICI. ACE success rates and rates of pathologic lead point (PLP) were calculated.
Results: 606/683 (89%) patients had at least 1 successful ACE ICI reduction. 115/606 (19%) patients had ≥1 recurrent ICI. The success rate after the initial successful ACE for those with recurrent ICI was 96% (110/115), with only 5 patients undergoing surgery for failed ACE on the recurrent ICI. 9/115 (7.8%) patients underwent subsequent surgery despite successful ACE for multiple recurrences (n=7), and PLP seen on ultrasound (n=2). Overall, 101/115 (88%) patients with recurrent ICI underwent successful ACE without subsequent surgery. PLP was identified in 3.5% and 4.3% of patients with 1 ICI and >1 ICI, respectively. Of those with >1 ICI (recurrence), PLP was identified in 11% (2/19) of patients with only LT ICI, and none of the 77 patients with only ST ICI. In those with ≤4 ST only ICI, 96% (67/70) of patients underwent successful ACE without surgery. Of the 3 patients who underwent subsequent surgery, 2 were related to failed ACE during the first recurrence and 1 was related to recurrence after successful reduction on ACE.
Conclusions: The majority of recurrent ICI are successfully treated by repeat ACE. Patients with LT ICI are more likely to need surgery due to higher PLP rates. Nevertheless, most patients with ≤4 ST ICI underwent successful ACE without surgery. In the correct clinical context, we propose that ACE could be attempted at least 4 times in patients with ST recurrent ICI.

Paper #: 078

Piriform Fossa Sinus Tract - A 15 year retrospective review of cases from birth to adolescence presenting to a Children's Hospital

Makabongwe Tshuma, MBChB (Hons); FRCR, *drtshuma@doctors.org.uk*; Heather Bray, MD, Anna Lee, MD, Neil Chadha, MD, Jim Potts, MD; BC Children's Hospital / University of British Columbia, Vancouver, British Columbia, Canada

Disclosures: All authors have disclosed no financial interests, arrangements or affiliations in the context of this activity.

Purpose or Case Report: An underlying Piriform Fossa Sinus Tract (PFST) may be overlooked in children presenting with cystic neck mass or suppurative thyroiditis, leading to recurrent infection possibly life threatening. We aim to determine the pattern of presentation, imaging findings and management of PFST in children and define the most appropriate imaging investigations.
Methods & Materials: A retrospective analysis of the clinical presentation, imaging findings and management of 16 cases of PFST presenting to our tertiary children's hospital between 2003 and 2018. Cases were identified by medical records and PACS search using relevant ICD-10 coding. Statistical analyses with SAS Statistical Software® version 9.4
Results: Age at presentation ranged from prenatal to 16 years with a male to female ratio of 2:1. All patients presented with neck swelling, 13(81%) had neck infection/suppurative

thyroiditis at initial presentation. Two patients had severe thyroiditis/mediastinitis requiring ICU admission. Three neonates presented with non-infected cystic neck masses; two had been detected prenatally. Two neonates were presumed to have lymphatic malformations, with spontaneous clinical resolution by three months of age later re-presenting with evidence of PFST. PFST was left-sided in 94%. Eight patients were initially diagnosed with branchial cleft cyst and underwent cyst resection ± hemithyroidectomy without consideration for PFST. These patients re-presented with multiple episodes of recurrent neck abscess. All patients had neck imaging prior to definitive diagnosis. Imaging studies included radiographs, ultrasound, CT, MRI and Upper GI contrast studies. No single modality was diagnostic of PFST in all patients with 75% undergoing multimodality imaging prior to diagnosis. PFST was identified on upper GI study in 6/12 patients. All cases were confirmed by endoscopic visualization. The interval from presentation to endoscopy was 2.6-174 months.Management of PFST was via endoscopic cauterization in 13 patients, surgery in 2, and 1 patient did not require either.
Conclusions: This study highlights the complex nature of PFST. This anomaly is uncommon, has variable clinical and imaging presentations and may have a lengthy, complicated course if not considered at initial presentation. An episode of suppurative thyroiditis in a child should prompt investigation for a PFST. We are the first group to describe the atypical presentation of a neonatal cystic neck mass undergoing spontaneous clinical resolution but re-presenting as a PFST.

Paper #: 079

Ultrafast PET/CT: A qualitative and quantitative analysis of reduced imaging times using Digital PET/CT

Andrew Sher, MD, *acsher@texaschildrens.org*; Raymond B. Pahlka, PhD., Wei Zhang, Victor J. Seghers, M.D.; Pediatric Radiology, Texas Children's Hospital, Houston, TX

Disclosures: All authors have disclosed no financial interests, arrangements or affiliations in the context of this activity.

Purpose or Case Report: Analyze the feasibility of a performing an ultrafast Digital PET/CT on pediatric patients by comparing image quality and SUV quantification of normal structures using multiple simulated time-per-bed position protocols.
Methods & Materials: This HIPAA compliant retrospective study had IRB approval. 10 patients ranging in age from 3 to 17 years old had an ^{18}F-FDG PET/CT performed on a digital PET/CT scanner at a tertiary academic hospital. In addition to the clinical standard 120-seconds per bed position scan, simulated PET images were generated using list mode data to create PET data sets at 30-, 60-, and 90-seconds per bed position. Two readers blinded to time-per-bed position assessed the data evaluating image quality using a 5-point Likert scale (1: extremely poor quality study with major artifacts that is not clinically useful, 2: poor quality study with major artifacts, whose clinical use is not advised, 3: average study with moderate artifacts, probably affecting clinical use, 4: good study with only minor artifacts not affecting clinical use, 5: excellent study without artifacts). SUVmax was calculated on seven regions of interest placed on physiologic structures for each data set. Spearman correlation and relative median and interquartile ranges were calculated.
Results: 40 reconstructed data sets from 10 patients were analyzed. Mean Likert scores for the 30-second, 60-second, 90-second and 120-second images were 3.7, 4.3, 4.6 and 4.7 for Reader 1 and 4.1, 4.9, 4.8, and 4.9 for Reader 2, respectively. Reader 1 found three 30-seconds per bed position scans below clinical acceptance, Reader 2 found all images clinically acceptable. For the 70 regions of interest per data set, there was near perfect SUVmax correlation with the standard 120-seconds per bed position exam (ρ = .98, .994 and .997 respectively for 30, 60 and 90 seconds per bed position, $p<.00001$). The median and interquartile ranges of the relative SUVmax differences for the 30-, 60- and 90-seconds per bed position exams compared to the clinical standard were 15% (7-27%), 6% (1-14%) and 3% (-1- 7%) respectively.
Conclusions: Our study demonstrates the feasibility of performing ultrafast PET/CT in pediatric patients on a digital PET/CT. Reduction in scan times of up to 50% (60 seconds) are attainable without adversely affecting the SUVMax measurements or image interpretability. Digital PET/CT using an ultrafast protocol is a promising technology that may result in decreased imaging times and improved patient compliance.

Paper #: 080

Utility of ^{18}F-FDG PET/CT following ketogenic diet in detecting endocarditis in children and adult congenital heart disease patients.

Jason Gillum, MD, *jason.gillum@childrens.harvard.edu*; Neha Kwatra, MD, Laura Drubach, MD, Douglas Y. Mah, MD, Stephan Voss; Radiology, Boston Children's Hospital, Boston, MA

Disclosures: All authors have disclosed no financial interests, arrangements or affiliations in the context of this activity.

Purpose or Case Report: Congenital heart disease patients are at increased risk of infective endocarditis, related to implantable devices such as prosthetic valves and pacemarkers. With standard PET/CT protocols, physiologic myocardial glucose uptake limits the assessment of the heart and related cardiac structures. The objective of the present study is to evaluate the utility of ^{18}F FDG PET/CT following ketogenic diet preparation in children and adult congenital heart disease patients in confirming suspected endocarditis.
Methods & Materials: Congenital heart disease patients who had undergone FDG PET/CT for suspected endocarditis were identified using a database search. A total of 25 individual patients were identified. Of these, 22 had undergone PET/CT specifically for evaluation of suspected endocarditis. Patients who underwent PET/CT for non-endocarditis indications were excluded from the remainder of the analysis. At the time of their index PET/CT scans, the ages of the 22 evaluated patients ranged from 11 months to 65 years of age, with a median age of 24 years. PET/CT findings were correlated with peripheral blood cultures, surgical findings, explant cultures and histopathology, and clinical course.
Results: Ketogenic dietary preparation was successful (myocardial uptake visually suppressed) in 16 of 22 patients. The majority of the patients (18/22) had focal FDG PET/CT findings suspicious for endocarditis, while 4 had negative or nonspecific scans. 14 of 22 patients subsequently were managed surgically; 13 of these patients had explant specimens with histologic evidence of infection and/or positive cultures. The remainder of the patients received antibiotic therapy; five of these clinically managed patients were followed to symptom and/or imaging resolution. Clinically significant non-cardiac PET findings were identified in six patients (e.g. osteomyelitis) that potentially changed management.
Conclusions: Given an adequate index of clinical suspicion, ^{18}F-FDG PET/CT is a sensitive and specific imaging modality for diagnosing infective endocarditis in the congenital heart disease population, particularly in patients with prosthetic valves or other device implants in whom other imaging modalities such as echocardiography are limited by hardware-associated acoustic artifacts. In certain patients in whom endocarditis is not diagnosed other sites of remote spread of infection may also be identified.

Paper #: 081

Standardized Uptake Values on PET/MR scans are not affected by iron oxide nanoparticles

Anne M. Muehe, MD, *amuehe@stanford.edu*; Ashok J. Theruvath, MD, Jayne M. Seekins, MD, Heike E. Daldrup-Link, MD, PhD; Radiology, Stanford University, Palo Alto, CA

Disclosures: All authors have disclosed no financial interests, arrangements or affiliations in the context of this activity.

Purpose or Case Report: Treatment response assessment of pediatric cancer patients relies on accurate measurement of standardized uptake values (SUV) of tumors and normal organs on positron emission tomography (PET). Ferumoxytol is an iron oxide nanoparticle compound that can be used "off label" as a contrast agent for integrated PET/MR scans. However, ferumoxytol tissue enhancement could affect MR-based attenuation correction (AC) of PET data. The purpose of our study was to evaluate if SUV values generated from either ferumoxytol-enhanced and unenhanced MRAC maps were significantly different.
Methods & Materials: 30 children (6-18 years) with malignant tumors underwent ^{18}F-FDG PET/MR scans (dose 3 MBq/kg) with (n=15) or age- and sex-matched to patients without (n=15) intravenous injection of ferumoxytol (5 mg Fe/kg). MRAC was obtained by a two-point Dixon LAVA sequence accounting for fat, air/background, lung, and soft tissue. We compared the signal to noise ratio (SNR), SUVmean and SUVmax, calculated based on body weight (bw) and body surface area (bsa) of blood, brain and normal organs on enhanced and unenhanced MRAC and PET images using a mixed effects linear model. In addition, we compared the number of tissue misclassifications on ferumoxytol-enhanced and unenhanced AC-maps by Poisson regression model. All comparisons were performed assuming alpha of 0.05.
Results: The SNR of the blood, brain, and visceral organs on ferumoxytol-enhanced scans was significantly higher compared to unenhanced scans ($p<0.001$). The SUVmean and SUVmax values of different organs based on bw or bsa on ferumoxytol-enhanced and unenhanced AC-maps were not significantly different (all $p>0.05$). Ferumoxytol-enhanced AC-maps showed no significant difference in tissue misclassifications ($p=0.09$).
Conclusions: Ferumoxytol administration does not affect SUV measurements on ^{18}F-FDG PET/MR scans. Therefore, unenhanced scans can be omitted, and the acquisition of PET/MR scans can be accelerated by obtaining all images after primary contrast agent injection.

Paper #: 082

Radiomic analysis of staging CT scans for neuroblastoma: An initial investigation of correlations with tumor histology, MYCN status, INRG stage, relapse and death

Matthew A. Zapala, MD, PhD, *mzapala@hotmail.com*; William Temple, MD, Mimi Poon, MD, Kieuhoa Vo, MD, Katherine Matthay, MD, Andrew Phelps, MD, Spencer Behr, MD/PhD, Benjamin Franc, MD, Youngho Seo, PhD; Radiology, UCSF Benioff Children's Hospital, San Francisco, CA

Disclosures: All authors have disclosed no financial interests, arrangements or affiliations in the context of this activity.

Purpose or Case Report: To correlate computer-generated radiomic features from staging CT scans of neuroblastoma with clinical and histopathological features.

Methods & Materials: A retrospective cohort study of patients enrolled on the Children's Oncology Group study ANBL00B1 at a tertiary care academic pediatric hospital from 2000-2015 with pathology-proven neuroblastoma. Clinical data collected included relapse and death, MYCN copy number, histopathology, and International Neuroblastoma Risk Group (INRG) stage. A total of 35 pediatric patients (age range 0-14.6 years, mean age 2.9 years, 17 males and 18 females) met inclusion criteria. Primary tumor foci were hand-segmented from initial staging CT scans using the freely available open source 3D-slicer (https://www.slicer.org). A CAQ-qualified pediatric radiologist with 8 years experience independently reviewed the hand-segmented primary tumors for accuracy. Radiomic feature extraction was performed using the Pyradiomics library, an extension of 3D-slicer, with a total of 105 quantitative features. Spearman rank correlations were performed between radiomic features and clinical and histopathological features (sorted rho > 0.4 and p-value < 0.05).
Results: Shape features, as opposed to first and second order quantitative statistical features, were the most correlated with histology (8 of the top 10), MYCN status (7 of the top 10), INRG stage (6 of the top 10), and death (8 of the top 10). Only relapse had a minority of shape features in the top 10 (3 of 10), however no other radiomic feature had more than 2 in the top 10 for relapse. Most statistically significant radiomic features demonstrated moderate agreement at best (rho = 0.4-0.59, p-value < 0.05). The highest correlation was strong agreement between 2D diameter and INRG stage (rho = 0.65 p-value = < 0.0001).
Conclusions: While this initial study has a small sample size of 35 patients, it is the first study to look at the radiomic features of neuroblastoma and attempt to identify relationships with histopathology and clinical outcomes. Interestingly, the majority of radiomic features that demonstrated at least a moderate statistically significant correlation with histopathology and clinical outcome were shape features that can be visually identified by radiologists.

Paper #: 083

Monitoring Response to Immunotherapies in Neuroblastoma Using Nanoparticle Contrast-Enhanced CT

Laxman Devkota, PhD[1], *Laxman.Devkota@BCM.edu*; Charlotte H. Rivas[1], Andrew A. Badachhape, Ph.D.[1], Igor Stupin[2], Mayank Srivastava[2], Zbigniew A. Starosolski, PhD[2], Ananth Annapragada[2], Robin Parihar, MD, PhD[1], Ketan B. Ghaghada, PhD[2]; [1]Pediatric Radiology, Baylor College of Medicine, Houston, TX, [2]Texas Children's Hospital, Houston, TX

Disclosures: All authors have disclosed no financial interests, arrangements or affiliations in the context of this activity.

Purpose or Case Report: The tumor microenvironment (TME) in neuroblastoma (NB) is a key regulator of treatment resistance and disease relapse. Myeloid-derived suppressor cells (MDSCs) play a central role in maintaining the TME in NB by suppressing host immunity, driving angiogenesis, and remodeling tissue. Since MDSCs play a central role in angiogenesis, we hypothesized that MDSC-targeted therapies will alter the architecture of tumor vasculature. In this pre-clinical study, we investigated contrast-enhanced CT (CECT) using a long circulating liposomal-iodine (Lip-I) nanoparticle contrast agent for monitoring changes in tumor vasculature in response to MDSC-targeted immunotherapy.
Methods & Materials: *In vivo* studies were performed in three groups of humanized mice: 1) NB tumor cells (*Tumor group*); 2) NB tumor cells + human MDSCs (*Tumor+MDSC group*) and 3) NB tumor cells + MDSC cells + Immunotherapy (*MDSC-directed Therapy group*). For the Therapy group, MDSC-

directed natural killer (NK) cells were intravenously administered 10 days prior to CT imaging. CECT was performed at 2 and 4 weeks post-tumor implantation. Lip-I was injected four days prior to CT. On the day of imaging, non-contrast CT was performed to determine tumor vascular permeability. A second dose of Lip-I agent was administered and CT angiogram acquired to determine tumor vascularity. Tumors were segmented to study 3D spatial variations in vascular structure. Animals were then euthanized to determine MDSC burden and peri-vascular localization using flow cytometry and immunohistochemistry (IHC).
Results: Quantification of CT signal demonstrated a 2.2-fold increase in vascularity for Tumor+MDSC group compared to Tumor group. Further, IHC analysis revealed a higher vascular density and a predominant perivascular distribution of MDSCs in Tumor+MDSC group, indicating a role for MDSCs in tumor angiogenesis. The MDSC-directed Therapy group showed a 4-fold reduction in tumor vascularity compared to Tumor+MDSC group, suggesting a reduction in MDSC burden. Flow cytometry analysis corroborated with CECT findings and demonstrated a 6-fold reduction of MDSC burden in MDSC-directed Therapy group compared to Tumor+MDSC group.
Conclusions: Contrast-enhanced CT using a nanoparticle contrast agent enabled assessment of changes in tumor vasculature in response to MDSC burden. The imaging methodology could facilitate monitoring acute response to MDSC-targeted therapies in neuroblastoma and other solid tumors.

Paper #: 084

Gadolinium-based contrast media improve detection of image defined risk factors at diagnosis of neuroblastoma

Reem Hasweh, *drreemng@hotmail.com*; Christopher G. Anton, MD, Andrew T. Trout, Ethan A. Smith, MD, Jonathan R. Dillman, MD. MSc, Emily Orscheln, MD, Bin Zhang, Alexander J. Towbin, MD; Department of Radiology, Cincinnati Children's Hospital Medical Center, Cincinnati, OH

Disclosures: Andrew T. Trout, MD: Consultant, Honoraria: Guerbet Group, Royalty: Elsevier, Wolters-Kluwer, Research Grants: Canon Medical, Siemens Medical Solutions, National Pancreas Foundation, In-Kind Support: ChiRhoClin Inc., Perspectum Diagnostics; **Jonathan R. Dillman, MD. MSc:** Research Grants: Canon Medical Systems; Siemens Healthineers; Perspectum Diagnostics; Bracco Diagnostics, Other: Travel Support (Philips Healthcare, GE Healthcare). All other authors have disclosed no financial interests, arrangements or affiliations in the context of this activity.

Purpose or Case Report: MRI with gadolinium-based contrast material (GBCM) is one of the modalities used to diagnose and characterize neuroblastoma. However, the use of GBCM is not without risk. Recent data have shown variable retention of GBCM in the brain, bones, and other organs. In addition, GBCM adds cost and time to the imaging study. The purpose of our study was to determine if GBCM are needed to identify image-defined risk factors (IDRF) in patients with neuroblastoma.
Methods & Materials: A retrospective case-control study was performed. All patients who received an abdominal MRI at the time of diagnosis of intra-abdominal neuroblastoma were included. Each exam was duplicated with the contrast-enhanced images removed from one copy of the exam. A single pediatric radiologist blinded to study purpose reviewed the separated imaging exams in a random order on our research PACS measuring three dimensions of the tumor (width x length x height), reporting the presence or absence of each potential abdominal IDRF and the presence or absence of metastatic disease. Considering the exam including contrast-enhanced images as the reference-standard, Kappa coefficient, sensitivity and specificity were calculated for the detection of IDRF and metastases. A paired t-test was used to compare differences in tumor measurements.
Results: 50 patients were included in the study. There was no significant difference between groups for any diameter measurement (p-values: 0.82-0.9). However, there was a statistically significant difference in the detection of each IDRF as well as for the detection of metastatic disease. The kappa value ranged from 0.46 to 0.94 for IDRF detection (p-value range 0.007 to <0.001) and from 0.23 to 1 for the detection of metastatic disease (p-value range 0.01 to <0.001). The sensitivity of IDRF detection ranged from 0.81 to 1 while specificity ranged from 0.33-1. The highest sensitivity of the non-contrast images was for detection of lower mediastinal invasion, superior mesenteric artery encasement, and lung metastasis while the highest specificity was for infiltration of the porta hepatis, encasement of the iliac vessels, invasion to the liver, and detection of lung metastases.
Conclusions: GBCM does not significantly improve a radiologist's ability to measure neuroblastoma size. However, use of GBCM is associated with a significant difference in the detection of IDRFs at diagnosis.

Paper #: 085

The Structured Report for Oncology – An Important Tool for Oncologists and Radiologists

Daphine Grassi, MD, *grassid@email.chop.edu*; Summer Kaplan, MD MS, Janet R. Reid, MD, FRCPC, Lisa States; CHOP, Philadelphia, PA

Disclosures: All authors have disclosed no financial interests, arrangements or affiliations in the context of this activity.

Purpose or Case Report: Determine radiologists' and oncologists' perceived impact of the structured report on clinical workflow, point of care teaching, and research in a large academic pediatric institution.
Methods & Materials: Fellows and attending radiologists from both radiology and oncology departments at our institution completed an online survey regarding their perceptions of the impact of the structured report on workflow, teaching and research. Surveys were sent to 42 radiologists and 51 oncologists.Two different surveys were created with specific directed questions for radiology and oncology; there were 7 questions in the oncology survey and 10 in the radiology survey. The structured report template was included with the survey to serve as a convenient reference.
Results: The survey was completed by 50% of the radiologists and 27% of the oncologists. All oncologists claimed their preference of structured over free text reports. 70% of oncologists reported fewer questions for the radiologists after implementation of structured reporting. 64.3 % reported improved workflow efficiency and improved clinical management of their patients. 75% of radiologists preferred structured reporting, with 70% claiming improved accuracy of their reports and a more efficient process when asked to review cases with the referring clinicians. Of interest, 80% of radiologists considered using structured reports as a teaching tool while 50% of the oncologists used them for this purpose
Conclusions: Our results show that radiologists and oncologists perceive a significantly positive impact of the structured report for pediatric tumors on workflow and efficiency of initiating care. In addition the structured report provides a teaching tool to enhance the current educational experience for trainees in both radiology and oncology programs.

Paper #: 086

Are Ferumoxytol-enhanced MRI scans equally suitable to evaluate tumor size and extension of pediatric bone tumors compared to Gadolinium-enhanced MRI scans?

Florian Siedek, MD, *siedek@stanford.edu*; Anne M. Muehe, MD, Ashok J. Theruvath, MD, Raffi S. Avedian, MD, Sheri Spunt, Jarrett Rosenberg, Crystal R. Farrell, MD, Heike E. Daldrup-Link, MD, PhD; Department of Radiology, Stanford University School of Medicine, Stanford, CA

Disclosures: All authors have disclosed no financial interests, arrangements or affiliations in the context of this activity.

Purpose or Case Report: To investigate if Ferumoxytol (Fe)-enhancement in MRI scans influences assessment of tumor size and extension in pediatric bone tumors compared to Gadolinium (Gd)-enhancement in a clinically relevant manner. We hypothesized that tumor size and extension can be equally assessed on Fe-MRI scans and Gd-MRI scans.
Methods & Materials: In this retrospective, IRB-approved study, we compared quantitative and qualitative image parameter of bone tumors in 13 patients (11 osteosarcomas, 2 Ewing sarcomas; 9m/4f; 15.9 ± 4.7y/o) that received a Fe- and a Gd-MRI scan within one month of each other and before treatment initiation. One investigator measured the maximum tumor length in 3 orientations and the tumor volume on T1w-LAVA, T1w-SE and T2w-FSE sequences. Results were compared using Bland Altman analysis. In addition, 3 radiologists independently evaluated tumor involvement of the diaphysis, metaphysis and epiphysis using a Likert-scale. Results were pooled across readers and then analyzed according their agreement on tumor assessment (affected – yes/no/uncertain) and confidence (uncertain/probably/definitely).
Results: Tumor lengths were not significantly different on Fe-MRI and Gd-MRI scans with mean differences of 0.13±0.72cm (axial-short axis), 0.28±0.59cm (axial-long axis) and 0.29±0.79cm (coronal) with 95% limits of agreement (95%LoA) of -1.27–1.53cm, -0.88–1.43cm and -1.84–1.26cm respectively and high concordance correlation coefficients (CCC) of 0.97 (axial-la) and 0.98 (axial-sa/cor). The tumor volume also showed a strong similarity with a mean difference of 5.86±43.81 mm^2 with 95%LoA of -80.0 – 91.7 mm^2 and an even higher CCC of 0.99. The assessment of tumor presence in the metaphysis and the associated confidence showed perfect agreement for all sequences (1.0, 1.0) of the Fe- and Gd-scans. For the diaphysis, the assessment and confidence, respectively, showed highest agreement for T1-LAVA (0.99, 0.98) and lower agreement for both T2-FSE (0.87, 0.85) and T1-SE (0.87, 0.85). For the epiphysis, the assessment and confidence showed the highest agreement for T2-FSE (0.94, 0.90), slightly lower for T1-LAVA (0.91, 0.85) and the lowest for T1-SE (0.77, 0.73).
Conclusions: Our results suggest that Fe-enhanced MRI scans can be equally used for assessment of tumor size and extension in pediatric bone tumors compared to Gd-enhanced MRI scans.

Paper #: 087

Diagnostic Accuracy of Imaging Approaches for Early Tumor Detection in Patients with Li-Fraumeni Syndrome

Thitiporn Junhasavasdikul, MD, Sanuj Panwar, Armin Abadeh, Anita Villani, MD, David Malkin, **Andrea Doria, MD**, *andrea.doria@sickkids.ca*; The Hospital for Sick Children, Toronto, Ontario, Canada

Disclosures: All authors have disclosed no financial interests, arrangements or affiliations in the context of this activity.

Purpose or Case Report: To assess the accuracy of imaging techniques currently used in practice for early detection of tumors in patients with Li-Fraumeni syndrome (LFS).
Methods & Materials: Two radiologists retrospectively reviewed all available imaging data from patients with LFS (January 1999 to September 2017). Based on the results from the imaging analysis, lesions were categorized into benign, malignant and indetermined. Histopathological and clinical information were also obtained and independently reviewed. Reference standard measures were (1) findings in dedicated cross-sectional imaging obtained within 6 months from index scan; (2) histopathologic diagnosis; or (3) clinical outcomes obtained at least 3 years from the index scan. Imaging accuracy was defined by the true positive (TP), true negative (TN), false positive (FP) and false negative (FN) results.
Results: Out of 1430 imaging studies, 16 FP and 12 FN results were identified, yielding an average delay of 235 days in diagnosis. Most cases of inaccurate diagnosis of tumors were noted in whole body magnetic resonance imaging (WB-MRI) examinations. Sensitivity and specificity of tumor diagnosis respectively were 0.96 and 1.0 for abdominal ultrasound, 1.0 and 0.85 for brain MRI, and 0.57 and 0.89 for skeletal lesions identified by WB-MRI, respectively.
Conclusions: WB-MRI had relatively low sensitivity in early tumor detection in patients with LFS. FN results were responsible for delay in the diagnosis of tumors in specific cases. Double reading by radiologists and understanding potential sources of misdiagnosis may compensate for perceptual inconsistencies in the detection of small tumors and possibly increase diagnostic accuracy of WB-MRI by minimizing FN results.

Paper #: 088

Doppler imaging in hypoxic ischemic encephalopathy: What is the value of the resistivity index with and without compression of the fontanel?

Erika Rubesova, MD[1], *rubesova@stanford.edu*; Tuva Sandgren[2], Anton Flink Elmfors[2], Valerie Chock, MD[1], Alexis S. Davis, MD[1], Hans Ringertz, MD, PhD[1]; [1]Stanford University, Stanford, CA, [2]Linköping University, Linköping, Sweden

Disclosures: All authors have disclosed no financial interests, arrangements or affiliations in the context of this activity.

Purpose or Case Report: Ultrasound diagnosis of hypoxic ischemic encephalopathy (HIE) remains challenging. Grayscale diagnosis is limited by nonspecific findings such as increase of echogenicity or loss of gray-white matter differentiation. Previous studies have shown that the resistivity index (RI) value is of poor reliability to predict outcome, especially in early phases of HIE or under hypothermia treatment. Measurements of the RI with gentle compression of the fontanel have been suggested to stress the brain autoregulation in neonates with abnormal intracranial compliance. We compared RI with compression (wi/c) and without compression (wo/c) in babies with and without HIE to define whether RI with compression correlates better with HIE status.
Methods & Materials: 53 babies with clinically, cord and blood PH and EEG proven HIE and 174 babies with normal head ultrasound (GA 34-42 weeks) had head ultrasound with measure of peak systolic and diastolic velocities, RI wi/c and wo/c and RI delta (% difference in RI between wo/c and wi/c) of the pericallosal artery. Ultrasound grayscale findings were recorded. The RI was adjusted for GA, gender, and type of delivery. Relationship between RI wi/c and wo/c with severity of HIE was established and compared to normal values. RI for each of HIE severity (mild, moderate,severe) were compared. Ansari-Bradley and Fligner-Policello tests were used for statistical analyses with a significance level of 0.05.

Results: 40/53 grayscale US of HIE babies were reported normal. There was no significant effect of gender, gestational age on RI. Mean RI and dispersion of values of RI was significantly different between HIE (mean=0.63, SD=0.13) and normal babies wo/c (mean RI=0.66, SD=0.08), p=0.002 and wi/c, HIE (mean=0.64, SD=0.12), normal (mean=0,68, SD=0.09) Moderate and severe grades had significantly higher variability in RI wo/c compared to mild grade (p=0.017). RI wi/c was not significantly different among grades (p=0.32). There was no significant effect on RI delta when comparing the normal with HIE babies (p=0.45). RI delta was not significantly different between the three groups of grades of HIE (p=0.30).
Conclusions: We report values of RI of the pericallosal artery in babies with HIE and normal, for comparison. Babies with HIE have different mean and a wider range of RI values than normal babies whether the RI is performed with or without gentle compression of the fontanel. The change of RI with compression doesn't help to differentiate HIE from normal brain.

Paper #: 089

Region-Specific Perfusion Alterations in Neonatal Hypoxic Ischemic Injury Evaluated with Arterial Spin Labeling MRI

Qiang Zheng, Ph.D, *zhengq@email.chop.edu*; Juan S. Martin-Saavedra, MD, Minhui Ouyang, Sandra Saade-Lemus, MD, Qinlin Yu, Hao Huang, Raymond Sze, Misun Hwang, MD; Department of Radiology, Children's Hospital of Philadelphia, Philadelphia, PA

Disclosures: All authors have disclosed no financial interests, arrangements or affiliations in the context of this activity.

Purpose or Case Report: To evaluate region-specific perfusion alterations in neonatal hypoxic ischemic injury (HII) based on pulsed arterial spin labeling (ASL) magnetic resonance imaging (MRI) data as compared to controls.
Methods & Materials: The ASL perfusion data of 19 normal neonates (10 male/9 female, 12 ± 6 days) and 31 HII neonates with positive MRI findings (14 male/17 female, 9 ± 7 days) were retrospectively evaluated. The cerebral blood flow (CBF) maps were first calculated using the ASL data processing toolbox (ASLtbx). From the CBF calculation results, averaged region-specific perfusion values were extracted for comparison. Specifically, the JHU neonate atlas was used to specify 130 brain regions for perfusion quantification. For accurate comparison of each brain region, both CBF image and JHU atlas were aligned to the subject-specific T2-contrast structural image space. Permutation test was used to identify brain regions with significant perfusion alterations between the control and HII group with positive MRI findings.
Results: The experimental results identified 10 brain regions significantly different in perfusion between the control and HII groups based on the permutation test with p<=0.01.The brain regions with the most significant perfusion alterations included left/right precuneus (p=0.005/0.007), left/right superior occipital gyrus (p=0.002/0.004), left/right cuneus (p=0.001/0.001), left/right lingual gyrus (p=0.005/0.005), left/right cerebellar hemisphere (p=0.001/0.003). Other than the region-specific perfusion comparison, the whole brain comparison was also implemented between the two groups by stacking all 130 average values of each brain region according to the JHU atlas. The results also showed the significant difference in whole brain perfusion (p<0.0001) with the average and standard deviation value (ml/100g/min) to be 11.5±4.7 and 17.1±7.3 for the control and HII groups, respectively.
Conclusions: The region-specific perfusion analysis based on the brain ASL data can help identify brain regions most significantly affected by the hypoxic ischemic injury. Further studies are warranted to explore the prognostic implications of perfusion alterations in these regions.

Paper #: 090

Changes in brain perfusion in successive arterial spin labelling MRI scans in neonates with hypoxic-ischemic encephalopathy

Maïa Proisy, M.D[1], *maia.proisy@chu-rennes.fr*; Isabelle Corouge[2], Antoine Legouhy[2], Valerie Charon[1], Amelie Nicolas[1], Nadia Mazille[3], Stéphanie Leroux[3], Bertrand Bruneau[1], Christian Barillot[2], Jean-Christophe Ferré[1]; [1]CHU Rennes, Radiology Department, Rennes, France, [2]Univ Rennes, Inria, CNRS, INSERM, IRISA, VISAGES ERL U-1228, Rennes, France, [3]CHU Rennes, Neonatology Department, Rennes, France

Disclosures: Maïa Proisy, M.D.: Research Grants: Société Francaise de Radiologie, Région Bretagne (France). All other authors have disclosed no financial interests, arrangements or affiliations in the context of this activity.

Purpose or Case Report: The primary objective of this study was to evaluate changes in cerebral blood flow (CBF) using arterial spin labeling MRI between day 3 of life (DOL3) and day 10 of life (DOL10) in neonates with hypoxic-ischemic encephalopathy (HIE) treated with hypothermia. The secondary objectives were to compare CBF values between the different regions of interest (ROIs) and between infants with ischemic lesions on MRI and infants with normal MRI findings.
Methods & Materials: We prospectively included all consecutive neonates with HIE admitted to the neonatal intensive care unit of our institution who were eligible for therapeutic hypothermia. Each neonate systematically underwent two MRI examinations as close as possible to day 3 (early MRI) and day 10 (late MRI) of life. A custom processing pipeline of morphological and perfusion imaging data adapted to neonates was developed to perform automated ROI analysis.
Results: Twenty-eight neonates were included in the study between April 2015 and December 2017. There were 16 boys and 12 girls. Statistical analysis was finally performed on 37 MRIs, 17 early MRIs and 20 late MRIs. Eleven neonates had both early and late MRIs of good quality available. Eight out of 17 neonates (47%) had an abnormal early MRI and 7/20 neonates (35%) had an abnormal late MRI. CBF values in the basal ganglia and thalami (BGT) and temporal lobes were significantly higher on DOL3 than on DOL10 ($p<0.05$). There were no significant differences between DOL3 and DOL10 for the other ROIs. CBF values were significantly higher in the lobe grey matter (GM) vs. the brain and in the BGT vs. the cortical GM, on both DOL3 and DOL10 ($p<0.05$). On DOL3, the mean CBF was significantly higher in the cortical GM, the BGT, and the frontal and parietal lobes in subjects with an abnormal MRI compared to those with a normal MRI ($p<0.05$). The perfusion differences between subjects with an injury and those without an injury on MRI had disappeared on the DOL10 scan.
Conclusions: This study is, to our knowledge, the first to evaluate CBF on two successive scans within the first 15 days of life in the same subjects in this clinical setting. ASL imaging in asphyxiated neonates therefore seems more relevant when used relatively early, in the first days of life. The correlation with neurodevelopmental outcome warrants investigation in a large cohort, to determine whether CBF values can provide prognostic information beyond that provided by visible structural abnormalities on conventional MRI.

Paper #: 091

Quantitative ASL Perfusion Method for Detection of Neonatal Hypoxic Ischemic Injury as Reference Standard for Developing Contrast-Enhanced Ultrasound

Qiang Zheng, Ph.D, *zhengq@email.chop.edu*; Juan S. Martin-Saavedra, MD, Minhui Ouyang, Sandra Saade-Lemus, MD, Qinlin Yu, Hao Huang, Raymond Sze, Misun Hwang, MD; Department of Radiology, Children's Hospital of Philadelphia, Philadelphia, PA

Disclosures: All authors have disclosed no financial interests, arrangements or affiliations in the context of this activity.

Purpose or Case Report: To develop a quantitative method for detection of neonatal hypoxic ischemic injury (HII) based on pulsed arterial spin labeling (PASL) magnetic resonance imaging (MRI) perfusion data which can be served as a reference standard for brain contrast enhanced ultrasound (CEUS), a perfusion based ultrasound technique.
Methods & Materials: The ASL perfusion data of 19 controls (10 male/9 female, 12 ± 6 days) and 31 neonates with HII and positive findings on MRI imaging (14 male/17 female, 9 ± 7 days) were identified for retrospective analysis. After calculating the cerebral blood flow (CBF) map from the ASL data using the ASL data processing toolbox (ASLtbx), the quantitative ASL perfusion ratios of central gray nuclei to white matter (GNW) and central gray nuclei to cortex (GNC) were compared between the control and HII groups by permutation test. The perfusion ratios were calculated on the mid-coronal plane as defined by the plane in which maximum cross sectional area of the central gray nuclei is visualized. The mid-coronal slice has previously been used for the wash-in time intensity curve on brain CEUS, and the selection of this slice for ASL quantification was based on the premise of developing a reference standard for developing brain CEUS for diagnosis of neonatal HII.
Results: Our results demonstrate that quantitative perfusion ratios of GNW and GNC are significantly different between the control and HII groups. Based on the permutation test, the white matter of cingulum hippocampal part (p=0.013) and cerebral peduncle (p=0.004) showed significant difference by GNW comparison, and the cortex of superior temporal gyrus (p=0.045), middle temporal gyrus (p=0.010), inferior temporal gyrus (p=0.043), parahippocampal gyrus (p=0.006), hippocampus (p=0.016), and insular cortex (p=0.008) showed significant difference by GNC comparison. The ratios of central gray nuclei to entire white matter, entire cortices, and all brain regions on the middle coronal plane excluding gray nuclei were also extracted for comparison, and the results revealed significant group differences with p values of 0.035, 0.017, and 0.013, respectively.
Conclusions: Quantitative perfusion ratios can be used to detect the presence of brain injury, which has critical implications for developing perfusion-based ultrasound techniques including brain CEUS. The utilization of quantitative perfusion ratios also minimizes inter-subject and technical variability while allowing subject's own perfusion as internal control.

Paper #: 092

Contrast-enhanced ultrasound for the evaluation of neonatal brain injury: Interpretation and implementation

Kayla Cort, DO, *kayla.cort12@gmail.com*; James Edgar, Jie C. Nguyen, Hansel J. Otero, MD, Ann Johnson, Teresa Victoria, MD, PhD, Ammie M. White, MD, Misun Hwang, MD; Children's Hospital of Philadelphia, Philadelphia, PA

Disclosures: All authors have disclosed no financial interests, arrangements or affiliations in the context of this activity.

Purpose or Case Report: Contrast-enhanced ultrasound (CEUS) is a new and promising modality for evaluating neonatal brain injury through the detection of alterations in perfusion. Qualitative and quantitative evaluation of perfusion can be performed for diagnostic interpretation of brain CEUS scans. As brain CEUS is a novel application, there are challenges in implementing this into the clinical setting. We explored whether a brief didactic session on the normal brain CEUS perfusion pattern can improve radiologists' interpretation of brain CEUS scans.
Methods & Materials: Four attending pediatric radiologists evaluated 6 CEUS mid coronal view cine clips of neonatal brains demonstrating either normal perfusion or various patterns of perfusion abnormalities over a two-day period. Findings on all brain CEUS scans were confirmed by magnetic resonance imaging. On a provided questionnaire, evaluators indicated if each example was normal or abnormal (diagnosis). If an abnormality was deemed present, evaluators specified the distribution (focal, multifocal, diffuse), location (right hemisphere, left hemisphere, bilateral hemispheres) and perfusion characteristics (hypoperfused, hyperperfused). After initial evaluation, a brief didactic session was provided, demonstrating the normal neonatal brain perfusion pattern. On the following day, participants reevaluated the same cases, using the same questionnaire. Distribution of error pre and post education was analyzed using McNemar testing for responses in each of the following categories: diagnosis, distribution, location and perfusion.
Results: The perfusion category showed 10 incorrect responses pre education and 4 incorrect responses post education, p=0.07. The diagnosis category showed 8 incorrect responses pre education and 2 incorrect responses post education, p=0.07. The location category showed 11 incorrect responses pre education and 6 incorrect responses post education, p=0.18. The distribution category showed 13 incorrect responses pre education and 9 incorrect responses post education, p=0.22.
Conclusions: Preexisting familiarity with intravenous contrast use and education on the normal neonatal brain perfusion pattern on CEUS was insufficient to significantly alter exam interpretation, although a trend toward improvement in all areas was observed. This suggests that more familiarity with the concept is warranted and that there is a potential benefit in developing quantitative methods to be used in addition to qualitative methods for detecting injury on brain CEUS.

Paper #: 093

Contrast-Enhanced Brain Ultrasound Perfusion Metrics in the EXTra-uterine Environment for Neonatal Development (EXTEND): Correlation with Hemodynamic Parameters

Ryne A. Didier, *didierr@email.chop.edu*; Anush Sridharan, PhD, Kendall Lawrence, Barbara E. Coons, Marcus G. Davey, Beverly G. Coleman, MD, Alan W. Flake; Children's Hospital of Philadelphia, Philadelphia, PA

Disclosures: All authors have disclosed no financial interests, arrangements or affiliations in the context of this activity.

Purpose or Case Report: Advancements in contrast-enhanced ultrasound (CEUS) have allowed analysis of perfusion metrics in various organs, including the brain. The influence of hemodynamic parameters such as heart rate (HR), mean arterial pressure (MAP), and blood flow have not been delineated. The goal of this study was to assess for correlation between hemodynamic parameters and perfusion metrics in CEUS of the brain in fetal sheep maintained on the EXTra-uterine Environment for Neonatal Development (EXTEND) system.
Methods & Materials: Following IACUC-approved protocols, 9 premature fetal lambs were transferred from placental support to the EXTEND system. 0.1-0.3 mL Lumason® ultrasound contrast was administered into the pumpless umbilical arterial to umbilical venous oxygenator circuit at varying gestational ages (93-133 days). Images were acquired as 90 second cine clips using a GE Logiq E9 ultrasound system and C2-9 transducer with settings optimized for contrast visualization. Clips were analyzed with VueBox™ post-processing software and time-intensity-curves (TICs) were generated. Hemodynamic parameters including HR, MAP, blood flow through the oxygenator, pre-oxygenator oxygen level, oxygen delivery, pre- and post-oxygenator pressure differential, and sweep requirements across the oxygenator were recorded continuously and averaged over the 90 seconds of imaging.
Results: A total of 86 CEUS examinations were performed, 72 of which were quantifiable and included in analysis. A multilevel mixed-effects linear regression was performed with random intercepts by subject. Hemodynamic parameters had no effect on mean transit time (MTT), rise time (RT), fall time (FT), or time-to-peak (TTP) ($p>0.06$). Sweep requirement and oxygen delivery demonstrated an association with wash-in rate (WIR), wash-out rate (WOR), wash-in area-under-the-curve (WiAUC), wash-out AUC (WoAUC), wash-in-wash-out AUC (WiWoAUC), and wash-in-perfusion-index (WiPi) ($p<0.03$).
Conclusions: CEUS perfusion metrics dependent on time including MTT, RT, FT, and TTP are not correlated with systemic hemodynamic data and any detectable changes in these perfusion parameters reflects differences in localized blood flow. None of the parameters need to be corrected for HR or MAP. Perfusion parameters dependent on AUC quantification including WiAUC, WoAUC, WiWoAUC, and WiPi are correlated with sweep requirement and oxygen delivery and these associations should be taken into consideration when interpreting TIC results in future studies.

Paper #: 094

Artificial Intelligence Detection of Germinal Matrix Hemorrhage on Head Ultrasound Examinations Using Convolutional Neural Networks

Anushri Parakh, MD[1], *aparakh1@mgh.harvard.edu*; Chao Huang[1], Camilo Jaimes[2], Hyunkwang Lee[1], Synho Do[1], Michael S. Gee[1]; [1]Radiology, MGH, Boston, MA, [2]Boston Children's Hospital, Boston, MA

Disclosures: All authors have disclosed no financial interests, arrangements or affiliations in the context of this activity.

Purpose or Case Report: To evaluate the feasibility of artificial intelligence detection of germinal matrix hemorrhage (GMH) on neurosonograms using convolutional neural networks (CNN).
Methods & Materials: In this HIPAA-compliant, institutional review board-approved study, a single-institution radiology report database was queried to identify neonatal head ultrasounds (US) performed between January 2016-July 2018, which were then categorized according to presence/absence as well as the grade (I-IV based on the Papile classification) and side of GMH. Static US images (gray-scale coronal and sagittal views from the anterior fontanelle) from these exams were used to train, validate, and test the CNN. From a total of 1000 images, 800 (n=400 each) served as the training dataset, 100 (n=49 for normal and n=51 for abnormal) as the validation dataset, and 100 (n=51 for normal and n=49 for abnormal) as the test dataset. Performance of the CNN was determined by calculating sensitivity, specificity and accuracy based on the clinical radiology report reference. Area under the receiver-operating curve (AUC) was also obtained.
Results: A total of 387 US exams were identified, including 325 normal exams and 62 that were positive for GMH. The mean corrected gestational age at the time of imaging for normal studies was 38 weeks 3 days, compared with 30 weeks 6 days for studies positive for GMH. In the 100 case test set, the overall accuracy of CNN was 72% for GMH detection with an AUC of 0.79. 44/51 normal cases were correctly classified (specificity=86.3%). However, sensitivity was low (57.1%) with a high false negative rate (28/49).
Conclusions: Artificial intelligence is currently not able to detect GMH on head ultrasound examinations with acceptable accuracy, primarily due to low sensitivity. This suggests that ultrasound images may be less amenable to CNN training than CT or radiographs due to decreased image contrast, and reaffirms the primary role of human radiologists in head ultrasound interpretation.

Paper #: 095

The Frontal Temporal and Frontal Occipital Horn Ratios in Pediatric Hydrocephalus: Comparison and Validation of Head Ultrasound with Volumetric Analysis via MRI

Rupa Radhakrishnan, MBBS MS[1], **Stephen F. Kralik, MD[1]**, *steve.kralik@gmail.com*; Brandon P. Brown, MD, MA[1], Danielle Monn, MD[2], Scott A. Persohn[2], Paul R. Territo[2], Andrew Jea, MD[1], Boaz Karmazyn, MD[1]; [1]Radiology, Riley Hospital for Children at Indiana University Health, Carmel, IN, [2]Indiana University School of Medicine, Indianapolis, IN

Disclosures: All authors have disclosed no financial interests, arrangements or affiliations in the context of this activity.

Purpose or Case Report: Accurate measurement of ventricular dimensions is crucial in infantile ventriculomegaly to guide treatment. Although multiple methods of HUS ventricular measurements exist, it is unclear if linear HUS measurements are concordant with other imaging modalities and how they correlate with ventricular volumes.Therefore, the purpose of this study was to assess correlation between Frontal Occipital Horn Ratio (FOHR) and Frontal Temporal Horn Ratio (FTHR) indices obtained from HUS, with that of MRI, and to correlate FOHR and FTHR with ventricular volumes.
Methods & Materials: We retrospectively included 100 infants at < 3 months of age with ventriculomegaly who had head ultrasound (HUS) and head MRI in a 3 day period without interval intervention. Each study, HUS and MRI was reviewed by 2 independent and blinded observers. Each observer measured the FOHR (bifrontal horn dimension + bioccpital horn dimension/ 2*biparietal diameter) and FTHR (bifrontal horn dimension + bitemporal horn dimension/ 2*biparietal diameter). MR images were used to calculate true ventricular and intracranial volumes and the ratio of the ventricular to intracranial volume (Vetricular volume ratio - VVR) was calculated using Analyze software. Intraclass correlation coefficients (ICC) and Bland Altman analyses were generated to evaluate inter-observer concordance between a) the 2 HUS observations, b) the 2 MRI observations, and c) between the HUS and MRI observations for the FOHR and FTHR. Correlation between the HUS and MRI FOHR and FTHR with the VVR was assessed using Pearson correlation analysis.
Results: ICC showed excellent correlation between the two reviewers in HUS FOHR (r=0.91), MRI FOHR (r=0.96) and

HUS FTHR (r=0.91) and good correlation for the MRI FTHR index (r=0.86). ICC showed excellent correlation between the HUS FOHR and MRI FOHR (r=0.84). ICC showed good correlation between the mean HUS FTHR and MRI FTHR (r=0.85). Bland Altman plots of the FOHR and FTHR between mean observations of HUS and MRI showed excellent agreement in both cases. VVR had high correlation with HUS FHOR (r=0.87), MRI FOHR (r=0.85), HUS FTHR (r=0.83) and MRI FTHR (r=0.79).
Conclusions: Frontal occpital horn ratio and frontal temporal horn ratio indices obtained from ultrasound in infants with ventriculomegaly show excellent inter-observer correlation, correlate with MRI derived indices, and correlate with ventricular volumes. This is therefore a promising tool for future studies on management strategies in infantile ventriculomegaly.

Paper #: 096

Incidence and Concordance of Suspected Intraventricular Hemorrhage (IVH) on Fetal US and MRI in Open Spinal Dysraphism with Postnatal Follow-Up

Ryne A. Didier, *didierr@email.chop.edu*; Juan S. Martin-Saavedra, MD, Edward R. Oliver, MD, PhD, Suzanne E. DeBari, RDMS, RVT, RT, Julie S. Moldenhauer, MD, Nahla Khalek, Lori J. Howell, DNP, MS, RN, Gregory G. Heuer, N. Scott Adzick, Beverly G. Coleman, MD; Children's Hospital of Philadelphia, Philadelphia, PA

Disclosures: All authors have disclosed no financial interests, arrangements or affiliations in the context of this activity.

Purpose or Case Report: Ependymal nodularity, layering debris, or susceptibility artifact can suggest intraventricular hemorrhage (IVH) by fetal ultrasound (US) or magnetic resonance imaging (MRI) in suspected open spinal dysraphism. However, imaging findings overlap with grey matter heterotopia (GMH). The goal of this study was to assess US and MRI in the prenatal detection and characterization of IVH in open spinal dysraphism and determine potential predictive factors that may suggest IVH over GMH.
Methods & Materials: A retrospective, IRB-approved review of pregnant patients referred to our institution for suspected open spinal dysraphism from 1/2013-4/2018 was conducted. Prenatal and postnatal US and MRI reports were reviewed for findings of suspected IVH or GMH. Neonatal chart review was performed to determine fetal or postnatal surgical intervention.
Results: 482 cases were confirmed to have open spinal dysraphism by US with 467 corresponding fetal MRIs and 216 postnatal MRIs. Ependymal nodularity was seen in 133/467 (23.4%) and 130/467 (27.8%) of fetal US and MRIs, respectively (κ=0.5). Suspected IVH was reported in 57/467 (12.2%) and 99/467 (21.2%) of fetal US and MRIs, respectively (κ=0.5). Suspected GMH was reported in 73/467 (15.6%) and 88/467 (18.8%) of fetal US and MRIs, respectively (κ=0.56). Increased lateral and third ventricular size as continuous variables were both associated with suspected IVH by both US and MRI ($p<0.05$) but not with IVH on postnatal MRI ($p>0.07$). Even after excluding postnatal MRIs performed > 21 days of age or after an intracranial intervention, IVH was seen in only 6/17 (35.3%) suspected by fetal US and 13/28 (46.4%) suspected by fetal MRI. In this patient subset, when IVH was seen on both US and MRI prenatally (n=11), subjects with IVH on postnatal MRI demonstrated increased incidence of persistent hindbrain herniation when compared to those without IVH postnatally [83.3% (5/6) vs. 0% (0/5); p=0.02] despite similar rates of fetal surgical intervention [67% (4/6) vs. 80% (4/5); p=1.0].
Conclusions: Fetal US and MRI reported similar rates of IVH, agreement between modalities was moderate, and concordance with postnatal MRI findings was fair. Increased lateral and third ventricular size may suggest IVH over GMH in the setting of ependymal nodularity although evidence of IVH is infrequently present on postnatal MRI. IVH may cause decreased cerebrospinal fluid resorption leading to persistent hindbrain herniation and continued evidence of blood products postnatally.

Paper #: 097

Chest ultrasound for the screening and diagnosis of pulmonary lymphangiectasia

Kayla Cort, DO, *kayla.cort12@gmail.com*; Hansel J. Otero, MD, Christian A. Barrera, M.D., Erin Pinto, NP, Trudy Morgan, Ammie M. White, MD, David Saul, Yoav Dori, MD, PhD, David M. Biko, MD; Children's Hospital of Philadelphia, Philadelphia, PA

Disclosures: David M. Biko, MD: Royalty: Wolters Kluwer. All other authors have disclosed no financial interests, arrangements or affiliations in the context of this activity.

Purpose or Case Report: Dynamic contrast enhanced MR lymphangiography (DCMRL) is being increasingly used in clinical practice to image the lymphatic system. However, DCMRL is expensive, invasive and often requires sedation. Recently, high resolution chest ultrasound of the lung surface has been proposed as a bedside method for diagnosing pulmonary lymphangiectasia (PL). We compare high resolution chest ultrasound of the pleural surface to DCMRL in patients with suspected PL.
Methods & Materials: We retrospectively reviewed the high resolution chest ultrasound in children with suspected PL who also had DCMRL. Transverse and coronal images in the upper, middle and lower lung surfaces along the mid-axillary and midclavicular lines were acquired on each side using a high frequency (15mHz) linear transducer. The presence or absence of lung surface irregularity, sub-pleural cysts, and pleural effusions was documented. Correlation was made with intranodal lymphatic contrast perfusion to the lung interstitium or pleural space on DCMRL and the presence of interstitial edema and pleural effusion on heavily T2 weighted imaging.
Results: 5 children (4 boys) between the ages of 1 month and 4 years old underwent both high resolution chest ultrasound and DCMRL. Chest ultrasound and DCMRL were performed in average 4.4 days apart (range 1 to 7 days). Four patients had congenital heart disease and one had a primary lymphatic disorder.4 of 5 patients had sonographic findings of PL including lung surface irregularity (3 bilateral, 1 unilateral, 1 absent) and sub-pleural cystic spaces (1 bilateral, 2 unilateral, 2 absent). All 5 patients had pleural effusions (3 bilateral, 2 unilateral) on ultrasound. Similarly, at DCMRL 4 of 5 had abnormal pulmonary lymphatic perfusion (3 bilateral, 1 unilateral, 1 absent). Interstitial edema (5 bilateral) and pleural effusions (4 bilateral, 1 unilateral) were present on T2 weighted imaging. US and DCMRL findings were in agreement in all 5 patients. Lung surface irregularity and sub-pleural cysts on ultrasound correlated with abnormal pulmonary lymphatic perfusion on DCMRL
Conclusions: High resolution chest ultrasound of the pleural surface shows sonographic findings that correlate with findings on DCMRL in patients with pulmonary lymphangiectasia. US seems to be a promising modality for the screening of PL in children to avoid invasive DCMRL.

Paper #: 098

Contrast Enhanced Ultrasound (CEUS) Evaluation of Thoracic Duct Outlet Patency After Percutaneous Injection of Intranodal Contrast

David M. Biko, MD, *bikod@email.chop.edu*; Erika J. Mejia, MD, Hansel J. Otero, MD, Christopher L. Smith, MD, PhD, Molly Shipman, Mandi Liu, Erin Pinto, NP, Aaron G. Dewitt, Jonathan J. Rome, MD, Yoav Dori, MD, PhD; Department of Radiology, The Children's Hospital of Philadelphia, Philadelphia, PA

Disclosures: David M. Biko, MD: Financial Interest: Wolters Kluwer - Royalty: Editor of Review Book. All other authors have disclosed no financial interests, arrangements or affiliations in the context of this activity.

Purpose or Case Report: To evaluate the diagnostic accuracy of contrast enhanced ultrasound (CEUS) for the evaluation of thoracic duct (TD) patency following percutaneous intranodal ultrasound contrast injection into the groin.
Methods & Materials: CEUS examinations of the left neck following intranodal injection of ultrasound contrast (sulfur hexafluoride lipid-type A microspheres) were retrospectively evaluated for TD outlet patency by 2 blinded and independent pediatric radiologists with experience in both lymphatic and CEUS imaging. Inguinal lymph node access was obtained under ultrasound guidance. CEUS exams were performed concurrently with intranodal inguinal injection of contrast and imaged continuously for 3-5 minutes or until contrast appeared. The TD outlet was classified as patent or not patent by visualization of lymphatic contrast passage into the venous system. Results were correlated with conventional lymphangiography (when available) which was reviewed independently and blinded by a lymphatic interventionalist.
Results: 11 patients (9 male) who presented for lymphatic evaluation were identified for the present study. Mean age was 4.4 years (range 2 months to 13.8 years). Of the 11 cases, the TD outlet was patent on CEUS in 10 patients and not patent in one. There was agreement between both CEUS readers on all cases. 9 of 11 patients also had conventional lymphangiography (8 of 9 on the same day, 1 within 6 months of CEUS). Of these 9 cases, the TD outlet was patent in 8 patients and not patent in one on conventional lymphangiography. These patency results matched the CEUS findings for each patient, thereby demonstrating agreement in all 9 cases.
Conclusions: CEUS of the neck following intranodal inguinal ultrasound contrast injection can accurately determine TD outlet patency and can thus eliminate the need for conventional lymphangiography when no percutaneous intervention is needed.

Paper #: 099

Dual and Single Energy Pediatric Thoracic Computed Tomographic Angiography: Effects on Radiation Dose and Imaging Quality

Andrew B. Wallace, MD[1], *wallaceab@wustl.edu*; Juan Carlos Ramirez Giraldo, PhD[2], Marilyn J. Siegel, MD[1]; [1]Mallinckrodt Institute of Radiology, Saint Louis, MO, [2]Siemens Healthineers, Malvern, PA

Disclosures: Juan Carlos Ramirez Giraldo, PhD: JCRG is scientist employed by Siemens. **Marilyn J. Siegel, MD**: Financial Interest: JCRG is an employee of Siemens Healthineers - Salary: JCRG is a senior key expert scientist working for Siemens All other authors have disclosed no financial interests, arrangements or affiliations in the context of this activity.

Purpose or Case Report: The benefits of dual energy computed tomography (DECT) over single energy computed tomography (SECT) in thoracic computed tomographic angiography (CTA) include automated bone removal, perfused blood volume, and iodine mapping in patients with congenital heart disease, arteriovenous malformations, trauma, and thromboembolic disease; however, the radiation dose of DECT must be considered. This study compares the image quality and size-specific dose estimates (SSDE) of DECT and SECT in pediatric thoracic CTA.
Methods & Materials: This institutional review board approved, retrospective study included 109 children (median age 7.5 years, 1 day to 17 years) who underwent DECT (n=53) or SECT (N=56) thoracic CTA between September 2014 and March 2018. DECT was performed on a Somatom Flash dual-source scanner (Siemens) with 80 and 140 kVp. SECT was performed at 80 kVp. Both DECT and SECT were performed with automatic exposure control and iterative reconstruction. SSDE was calculated based on effective chest diameter determined by the patient's age. Image quality was subjectively scored on a scale of 1 to 4 (1 excellent, 4 non-diagnostic). For analysis, data were divided into four groups based on the effective diameter, and two-sample t and Kruskal-Wallis tests were performed.
Results: For the four size ranges of <15cm (group 1), 15-19cm (group 2), 20-24cm (group 3), and >24cm (group 4); the median (25^{th}-75^{th} quartiles) SSDE values for DECT were 2.2 (1.9-2.3), 2.1 (1.8-2.5), 3.4 (2.5-3.5), and 4.2 (3.6-5.1) mGy; respectively. For SECT, the values were 2.2 (2.0-2.6), 2.1 (1.7-2.4), 2.0 (1.7-2.3), and 4.1 (3.4-5.3) mGy, respectively. Doses were not significantly different in groups 1, 2, and 4. In group 3, the median SSDE was statistically higher for DECT ($p<0.1$). Median patient age was similar between DECT and SECT in all four groups. Subjective image quality was diagnostic in all studies.
Conclusions: We have shown that in smaller children, DECT thoracic CTA can be performed with a radiation dose that does not exceed that of SECT while maintaining image quality. Though dose was higher for DECT in some larger patients, this may be due to small sample size. Regardless, DECT has several advantages over SECT, which may outweigh a potential small increase in radiation dose on a case by case basis. We suggest that DECT can be introduced into routine practice for pediatric thoracic CTA.

Paper #: 100

Preoperative Visualization of the Artery of Adamkiewicz in Pediatric Patients on Dynamic 4D airway CT angiograms

Donna Agahigian, RT(R)(CT), *Donna.agahigian@childrens.harvard.edu*; Russell Jennings, MD, Sanjay P. Prabhu, MBBS, FRCR; Boston Children's Hospital, Boston, MA

Disclosures: All authors have disclosed no financial interests, arrangements or affiliations in the context of this activity.

Purpose or Case Report: Preoperative artery of Adamkiewicz (AoA) visualization is requested prior to surgery for tracheobronchomalacia and thoracoabdominal tumors in children as AoA injury can result in spinal cord injury. Unlike in adults, MRA & CTA have not been successful in identifying the AoA in pediatric patients, thereby necessitating more invasive digital subtraction angiography (DSA) in some of these patients.Purpose of this study was to determine whether the AoA could be identified on dynamic 4D airway CT angiogram studies in pediatric patients being performed for evaluation of airway and esophageal anomalies.
Methods & Materials: We evaluated multiple phases of the free breathing (sedated/non-sedated) dynamic 4D airway CT angiograms performed for investigation of tracheobronchomalacia on a dual energy CT scanner with extended craniocaudal dynamic phase coverage below L1. Image acquisition was initiated with peak descending aortic enhancement (425 HU). Qblique coronal 1.3-1.5 mm thick maximum intensity projections were reconstructed from the phase where the AoA was identified as a hairpin curved vessel in the anterior midsagittal surface of the spine. The AoA was considered visualized if the "hairpin loop" of the artery within the spinal canal was visible in addition to the anterior spinal artery and the vessel could be traced to the intercostal artery by paging through oblique coronal reformats. The vertebral body above the level at which the spinal branch of the segmental artery entered the spinal canal and continued as the AoA was considered the level of AoA origin. The study radiologist blinded to the official report reviewed all scans.
Results: Dynamic 4D airway CTs in 79 patients (43 male, 5 months-18 years) who underwent preoperative imaging for airway anomalies were evaluated. Continuity between AoA and aorta through intercostal or lumbar artery was confirmed in 67 (84%) patients. Level of origin of AoA was most frequent at T10 and T11 (19 and 24 patients, respectively) but was also found as high as C7. AoA was most commonly seen on 3rdacquisition (56%). Of 12 patients in whom all the criteria for AoA were not fulfilled, the anterior spinal artery was visualized in the lower spinal canal in 5 patients.
Conclusions: AoA can be identified in pediatric patients on dynamic 4D airway studies with greater craniocaudal coverage, optimal timing of scan acquisition and tailored multiphase data processing. This information is valuable to surgeons and helps avoid more invasive procedures like DSA.

Paper #: 101

CT Angiographic Findings of Pulmonary Arteriovenous Malformations (PAVM) in Children with Hereditary Hemorrhagic Telangiectasia (HHT): Spectrum of PAVM and Correlation with Graded Transthoracic Contrast Echocardiography (TTCE)

Su-Mi Shin[1], *susemi513@gmail.com*; Hee K Kim, MD[2], Katherine Wusik Healy[2], Adrienne M. Hammill, MD, PhD[2]; [1]Radiology, SMG-SNU Boramae Medical Center, Seoul, Korea (the Republic of), [2]Cincinnati Children's Hospital Medical Center, Cincinnati, OH

Disclosures: All authors have disclosed no financial interests, arrangements or affiliations in the context of this activity.

Purpose or Case Report: Hereditary hemorrhagic telangiectasia (HHT) is a genetic disorder. Pulmonary AVM (PAVM) is one of the classic manifestations and may be progressive in nature.The purpose of this study is to characterize CT angiographic (CTA) findings of PAVM in children with HHT and to correlate these with graded transthoracic contrast echocardiography (TTCE).
Methods & Materials: A total of 40 patients (median age 14.9 years) with a diagnosis of HHT who had undergone both CTA and TTCE were included. With CTA, PAVM was evaluated based on location, distribution, and size. Each PAVM was scored with a grading system being applied to conventional and maximum intensity projection (MIP) images as follows:0 = nodule, but unlikely AVM, 1 = ground glass opacity (GGO), 2 = GGO with increased vascular network, 3 = GGO or nodule with single draining vein, 4 = GGO or nodule with equally sized afferent and efferent vessels, 5 = GGO or nodule with afferent and asymmetrically enlarged efferent vessels, 6 = true AVM with aneurysmal sac without the nodule or GGO. Total number of PAVM, cumulative PAVM grading (adding up individual PAVM grades), the highest grade given, total volume, and age were recorded for each patient. TTCE was graded as per Gazzaniga et al based on the number of bubbles (0 to 3) from pulmonary right to left shunt and then correlated with the variables of CTA and patient's age (Pearson correlation).
Results: A total of 124 pulmonary lesions were identified on CTA, including; peripheral (n=112), central (n=10), and both (n=2); all the lesions were localized without diffuse form. The CTA grading was increased on MIP images in 39 out of 124 PAVMs on conventional CT. The distribution of grades on MIP included grade 0 (n=9), grade 1 (n=16), 2 (n=9), 3 (n=42), 4 (n=34), 5 (n=2), and 6 (n=12). The median size and volume were 3.9mm and 31.1mm^3 respectively. A statistically significant correlation was seen between all variables of CTA and TTCE ($p<0.05$), with the strongest correlation seen in those with the CTA highest grading (*$r=0.79$,* $p<0.0001$*).* Age did not correlate with any variables of CTA or TTCE grading.
Conclusions: In children with HHT, GGO or nodule with single (grade 3) or two vessels (grade 4) were seen in two thirds of cases. MIP images enabled more precise detection of the afferent or efferent vessels. The highest grade in each patient had the strongest correlation with the severity of pulmonary right to left shunt. Unlike in adults, age was not an important factor in determining the severity of PAVM in children.

Paper #: 102

Predictive model for pediatric pulmonary embolism risk utilizing semantic data mapping, neural embedding technique, and recurrent neural network

David A. Mong, MD[1], *david.mong@childrenscolorado.org*; Imon Banerjee, PhD[2], Matthew Lungren, MD MPH[3]; [1]Children's Hospital Colorado, Denver, CO, [2]Stanford University, Palo Alto, CA

Disclosures: Matthew Lungren, MD MPH: Consultant, Honoraria: Nines, Inc. All other authors have disclosed no financial interests, arrangements or affiliations in the context of this activity.

Purpose or Case Report: Risk factors and clinical presentation of pediatric pulmonary embolism (PE) do not necessarily align with adult populations, and standardized clinical likelihood models have not been developed for children. Despite increasing CTA utilization for evaluation of pediatric PE, the rate of positive cases remains low, increasing exposure to ionizing radiation secondary to lack of evidence-based clinical imaging support guidelines. We propose a deep learning model for estimating risk of PE in pediatric patients analyzing free-text clinical notes.
Methods & Materials: After IRB approval, a retrospective data base was collected including 5189 pediatric patients (1 month – 18 years, 2387 female, 2799 male, 1 unknown**)** seen at a tertiary care pediatric hospital between 1/1/98 and 2/1/17 who had at least one contrast enhanced chest CT exam in their electronic medical record (EMR). EMR data collected up to one year before CT included heterogeneous clinical notes (H&P, ED notes, discharge), with temporal sequence maintained in the data base. Semantic data mapping and neural embedding technique were integrated in a single framework to produce an unsupervised text summarization method for handling the clinical notes. A many-to-one stacked recurrent neural network (RNN) was designed to model temporal dependency of patient visits with weighted categorical cross entropy loss function. The RNN model was trained with Adam optimizer (learning rate = 0.001) and 100 batch size.
Results: The studied population had a total of 11744 chest CTs and between 5 - 1400 clinical notes/patient. The database contained 4% positive PE cases (545). 80% of reports were randomly selected for training the neural network model and 20% for hold-out testing while maintaining patient-level separation. Our model achieved 0.81 AUC-ROC on the 20% hold-out test set.
Conclusions: The model predicts PE risk accurately with high sensitivity, as well as returning most of positive PE cases (high recall).

Paper #: 103

Artificial Intelligence Correction of Image Artifacts for Faster Pediatric Lung MRI

David Y. Zeng, *davidyzeng@stanford.edu*; Dwight G. Nishimura, Shreyas Vasanawala, MD/PhD, Joseph Y. Cheng, PhD; Electrical Engineering, Stanford University, Stanford, CA

Disclosures: David Y. Zeng: Financial Interest: GE Healthcare-Research Funding: Research; **Dwight G. Nishimura:** Research Grants: GE Healthcare, Salary: GE Healthcare (spouse); **Shreyas Vasanawala, MD/PhD:** Arterys, Royalty: Arterys, GE Healthcare, Siemens, Philips, Research Grants: GE Healthcare. **Joseph Y. Cheng, PhD:** Consultant, Honoraria: HeartVista, Inc., Research Grant: GE Healthcare.

Purpose or Case Report: Pediatric MRI often involves sedation or general anesthesia (S/GA) to minimize bulk and respiratory motion to improve image quality, especially for uncooperative patients. To minimize the duration and intensity of S/GA and to potentially eliminate S/GA completely, rapid imaging is essential. In this work, we enable rapid pediatric chest imaging with a time-efficient 3D cones trajectory and deep-learning off-resonance artifact correction.
Methods & Materials: A prospective study of 30 pediatric chest magnetic resonance angiography exams (16 female; mean age, 5.9 years; range, 0-17 years) was performed to train and validate a residual convolutional neural network to correct off-resonance artifacts (Off-ResNet). Each exam acquired a short-readout scan (1.18msec ±0.38) and a long-readout scan (3.35msec ±0.74) at 3T. Short-readout scans, with longer scan times but negligible off-resonance blurring, were used as reference images and augmented with additional off-resonance for supervised training examples. Long-readout scans, with greater off-resonance artifacts but shorter scan time, were corrected by autofocus and Off-ResNet and compared to short-readout scans by normalized root-mean-square error (NRMSE), structural similarity index (SSIM), and peak signal-to-noise ratio (PSNR). Scans were also compared by scoring on eight anatomical features by two radiologists, using analysis of variance with post-hoc Tukey's test. Reader agreement was determined with intraclass correlation.
Results: Long-readout scans were on average 59.3% shorter than short-readout scans ($P<0.001$). The proposed method had superior NRMSE, SSIM, and PSNR compared to uncorrected images across ±1kHz off-resonance ($P<0.01$). The proposed method had superior NRMSE over -677Hz to +1kHz and superior SSIM and PSNR over ±1kHz compared to autofocus ($P<0.01$). Radiologic scoring demonstrated that long-readout scans corrected with Off-ResNet were non-inferior to short-readout scans ($P<0.01$).
Conclusions: The proposed method enabled scan time reduction by 59.3% with longer readout durations, while maintaining non-inferior image quality to diagnostically-standard scans, suggesting viability of accelerating 3D cones trajectories for pediatric imaging. Additional acceleration can be achieved by combining parallel imaging and compressed sensing, both of which pair well with acceleration from longer readout durations.

Paper #: 104

Imaging evaluation for thoracic spine fractures in pediatric trauma patients: a single center experience at an academic children's hospital

Ala' Y. Ibrahim, *ala.ibrahim@sickkids.ca*; Michael R. Aquino, MD; Radiology, Hospital for Sick Children, Toronto, Ontario, Canada

Disclosures: All authors have disclosed no financial interests, arrangements or affiliations in the context of this activity.

Purpose or Case Report: Review epidemiology and imaging work-up of thoracic spine fractures in pediatric trauma patients over a 16-year period at an academic children's hospital. Determine the diagnostic performance of radiographs for identifying thoracic spine fractures in the setting of trauma
Methods & Materials: This was a retrospective review of all trauma patients ≤18-year-old that presented to an academic children's hospital between January 1, 2000 and December 31, 2016. A trauma patient database was used to identify all patients with thoracic spine fractures. Recorded data included: patient demographics, modality and results of imaging performed, mechanism of injury, injury severity score(ISS), associated injuries, management details, and patient's outcome
Results: There were 3,265 trauma patients identified. Of these, 90 (3%) had thoracic spine fractures. The most common

mechanism of injury was "fall", 39/90 (43%). Management for thoracic spine fracture was required in 26/90 (29%) patients, 7/26 (27%) surgical. Thoracic spine fracture was significantly associated with 1) the presence of a fracture at another spinal level, 2) soft tissue spine injury, and 3) ISS. ISS as a predictor of thoracic spine fracture resulted in sensitivity 77.6% (63.4 - 88.2) and specificity 57.1% (53.9-60.4) using a score >10 on the receiver-operator curve. Radiographs were obtained in 85/90 patients with thoracic spine fractures. Of these, 75/85 had additional imaging: 46/75 (61%) CT, 10/75 (13%) MRI, and 19/75 (25%) both CT and MRI. Three patients had both CT and MRI only, and 1 patient had only CT. A total of 276 thoracic fractures were detected in the 90 patients. The most common fracture was simple compression fracture followed by transverse process fracture. A total of 140/276 (51%) thoracic spine fractures in 46/75 (61%) patients were not identified on radiographs including 4/9 unstable fractures that required surgical fusion (1/4) and brace (3/4). Three simple compression fractures were missed by CT. MRI identified all fractures seen on radiographs and CT.
Conclusions: Thoracic spine fractures are significantly associated with the presence of other spine fractures and soft-tissue injuries and increasing ISS. Radiographs have poor sensitivity and can miss clinically significant fractures that require surgical management.

Paper #: 105

Imaging Findings Following Button Battery Ingestions

Neil Grey, *neil.grey@ucdenver.edu*; Peter E. DeWitt, Robert E. Kramer, Lorna Browne, Angie L. Miller, LaDonna Malone, MD; Pediatric Radiology, University of Colorado, Aurora, CO

Disclosures: All authors have disclosed no financial interests, arrangements or affiliations in the context of this activity.

Purpose or Case Report: The severity of button battery ingestion (BBI) in children has been increasing since the early 2000s with outcomes ranging from mild localized inflammation to fatal aortoesophageal fistula. Severe damage can occur in as little as 2 hours after ingestion, and complications can have a latency period of more than 2 weeks. Given the potentially for severe outcomes, beginning in 2012 the authors' institution began performing serial MRI/MRAs of the chest on all BBI patients after retrieval.
Methods & Materials: Following approval by IRB, we conducted a retrospective review of all BBI cases between April 2012 and September 2018. Clinical history and endoscopic findings were collected and all imaging studies were re-reviewed. The degree and location of mediastinal inflammatory change was graded and the presence of complications was recorded: periesophageal, peritracheal and periaortic inflammation as well as fistula, fluid collection, and vascular injury.
Results: 23 patients with BBI had at least one MRI/MRA chest for a total of 51 MRI/MRAs. The cohort was 70% male with median age 2 years [0.94-17 y]. Severe complications were encountered in 13 patients (57%) and included fluid collection (n=11), tracheoesophageal fistula (TEF) (n=3), vocal cord paralysis(n=1), and discitis(n=1). There were no patients with vascular injury (0). TEF on MRI was graded as negative/possible/probable with a sensitivity of 100% and specificity of 85% vs. bronchoscopy. Location of the battery was cervical esophagus in all but 1 patient with severe complications (92%). Time from ingestion of BB did not correlate with complications (p=0.65). All complications were visualized on initial MRI performed in first 3 days following retrieval. Subsequent serial examinations did not demonstrate new latent complications (>1 week post retrieval) with a trend to decreased mediastinal inflammation on serial imaging.
Conclusions: MRI after BBI demonstrates a high diagnostic ability to identify the common associated complications including fistula, fluid collection, and TEF. No conclusion can be drawn regarding vascular injury risk as no patients in this cohort had vascular injury. However, in clinical practice, the detection of inflammation receding from the vascular structures on serial MRIs provides invaluable information utilized to make important management decisions. To our knowledge, this is the first paper to report specifically on the MR findings after BBI.

Paper #: 106

Unreliability of standard fetal imaging biomarkers for prediction of lethal pulmonary hypoplasia (PH)

Richard B. Parad, MD[2], Deborah Stein, MD[1], Ali Gholipour, PhD[1], **Judy A. Estroff, MD[1]**,
judy.estroff@childrens.harvard.edu; [1]Radiology, Boston Children's Hospital, Boston, MA, [2]Brigham and Women's Hospital, Boston, MA

Disclosures: All authors have disclosed no financial interests, arrangements or affiliations in the context of this activity.

Purpose or Case Report: Assess survival and pulmonary outcomes in a cohort of fetuses with severe oligohydramnios who underwent maximal neonatal resuscitative efforts.
Methods & Materials: We evaluated 33 fetuses with severe oligohydramnios, from any cause, seen in the prior 5 years at either the Boston Children's Hospital Advanced Fetal Care Center or Brigham and Women's Hospital Center for Fetal Medicine, whose parents were counseled on risk of lethal pulmonary hypoplasia based on prenatal sonographic findings and who chose to have maximal neonatal resuscitative efforts at birth. These efforts included immediate intubation, high frequency ventilation, chest tube evacuation of pneumothoraces and inhaled nitric oxide for pulmonary hypertension. A retrospective medical record review compared fetal imaging biomarkers associated with pulmonary hypoplasia (including gestational age (GA) at onset of oligohydramnios, AFI, presence/appearance of kidneys, presence of urine in the bladder, appearance of lungs on MRI) in surviving and non-surviving newborns.
Results: Standard imaging biomarkers did not reliably predict poor outcome. Oligohydraminos was defined as AFI ≤ 5 cm or deepest vertical pocket (DVP) < 2 cm; anhydramnios was defined as absent amniotic fluid. Median GA at birth was 35.5 weeks. Intubation in the delivery room was required in 50% and pneumothorax occurred in 50% of subjects. 77% of the cohort survived to discharge home. Only 3/8 fetuses with anhydramnios survived. Mean GA at onset and duration of oligohydramnios did not differ significantly between survivors and non-survivors. 6/7 deaths occured in the delivery room; 1 NICU death occured at 12 days. 6/7 subjects who died had autosomal recessive polycystic kidney disease (ARPKD), all of whom had large echogenic kidneys; however, 9/16 other fetuses in this cohort also had ARPKD with large echogenic kidneys and survived. 6/7 subjects who eventually had a renal transplant did not require peritoneal dialysis. One subject is on dialysis awaiting transplant. Of 2 infants with a prenatal diagnosis of renal agenesis, one was found postnatally to have tiny dysplastic kidneys, and survived to transplant. Of 7 infants with no fluid in the bladder *in utero*, only 1 survived.
Conclusions: Standard imaging biomarkers did not reliably predict survival. Fetuses can survive what is predicted to be "lethal" oligohydraminios if aggressive neonatal resuscitation takes place and renal replacement therapy is initiated. More hopeful counseling than is currently presented may be warranted.

Paper #: 107

Attention-Aware Deep Learning Networks for Predicting Gestational Brain Age Using Fetal MRI

Mahesh Atluri, DO[2], *matluri@stanford.edu*; Katie Shpanskaya[2], Lily H. Kim[2], Quin Lu[3], Safwan Halabi, MD[2], Beth M. Kline-Fath, MD[1], Kristen W. Yeom, M.D.[2]; [1]Cincinnati Children's Hospital Medical Center, Cincinnati, OH, [2]Stanford University, Palo Alto, CA, [3]Philips Healthcare NA, Gainesville, FL

Disclosures: Quin Lu, PhD: Salary: Philips. All other authors have disclosed no financial interests, arrangements or affiliations in the context of this activity.

Purpose or Case Report: Given the dramatic structural changes of fetal neurodevelopment, precise knowledge of gestational age and the associated neuroanatomical hallmarks is key to the accurate interpretation of the fetal brain MRI. In this study, we aim to develop and validate a novel deep learning approach to accurately predict gestational age from fetal brain MRI.
Methods & Materials: We retrospective reviewed all fetal MRIs acquired by our institution from 2004-2017. Normal brain development was assessed by a rigorous review of each study firstly by review of the initial radiology report followed by further evaluation of the fetal brain images by an expert pediatric neuroradiologist. Gestational age was calculated using the current obstetric standard of care approach that references the estimated date of delivery recorded at the first-trimester ultrasound. The robust database of 855 normal fetal brain MRIs was distributed across training (70%), validation (10%) and testing (20%) sets for experimental evaluation. We developed a novel attention-aware deep learning network consisting of two convolutional neural networks (CNNs) working in parallel to combine whole slice image features with brain-specific features, derived from engineered attention maps. This innovative approach mimics the expert neuroradiologists' behavior, allowing a rotation-invariant auto-detection of the fetal brain and thus boosting the prediction outcomes. Regression model performance was evaluated by the R2 statistic.
Results: Our attention-aware model achieved strong predictive performance (R2 = 0.93, Mean error = 7.4 days) of gestational age using multi-plane fetal MRI. Single-plane prediction of gestational age achieves an R2 of 0.88 (axial), 0.87 (coronal), and 0.83 (sagittal) with attention-map guidance. A standard CNN without attention enhancement was able to retain high R2 of 0.83, 0.84, and 0.81 for the corresponding axial, coronal, and sagittal MRI planes, respectively.
Conclusions: Deep neural networks can accurately characterize healthy in utero brain development from fetal MRI. Clinical translation of such insights has the potential to improve early detection of normal and abnormal fetal brain maturation. The proposed deep learning algorithm could serve as an adjunct diagnostic tool in evaluating appropriate fetal neurodevelopment on MRI.

Paper #: 108

Inner and external ear malformations as assessed on fetal ultrasound and MRI

Jungwhan J. Choi, M.D., *jungwhan.choi@childrens.harvard.edu*; Caroline Robson, MB ChB, Judy A. Estroff, MD; Radiology, Boston Children's Hospital, Boston, MA

Disclosures: All authors have disclosed no financial interests, arrangements or affiliations in the context of this activity.

Purpose or Case Report: Previous literature has documented associations between external ear abnormalities with syndromes as assessed on ultrasound. The purpose of this study is to review abnormalities of the inner and external ears as assessed on ultrasound and 3T fetal MRI and to document their association with syndromes, thus better informing patients, clinicians, genetic counseling and workup.
Methods & Materials: An IRB approved retrospective review was performed of fetal ultrasound and MRI examinations performed between 8/1/2013-8/1/2018. Examinations were reviewed for the presence of malformations of the inner and /or external ears. When available, genetic testing and postnatal clinical documents and imaging were also reviewed.
Results: From the dates of 8/1/2013-8/1/2018, 41 pregnant females were imaged in whom ear malformations were observed in their fetuses. The most commonly observed external ear malformations included malformed pinnae (n = 20) including microtia (n = 9); low set ears (n = 17); external auditory canal malformation or atresia (n = 9); mass involving or abutting the external ear (n = 4, most commonly lymphatic malformations); preauricular skin tags (n = 3); and anotia (n = 2). The most commonly observed inner ear malformations included cochlear malformation (n = 6); absence and / or malformation of the semicircular canals (n= 4); vestibular malformation (n = 3); malformed internal auditory canals (n = 3); and absence of the inner ear structures (n = 1). Ear abnormalities were associated with syndromes on the basis of additional imaging findings, genetic testing and / or postnatal examination in a large number of cases (18/41) with the most commonly observed syndromes including CHARGE (n = 4), Trisomy 18 (n = 3), Trisomy 13 (n = 3), 22q11.2 duplication (n = 2), Brachio-Oto-Renal syndrome (n = 1), Trisomy 21 (n = 1), Trisomy 22 (n = 1), Goldenhar syndrome (n = 1), Klinefelter Syndrome (n = 1), and Cat-Eye Syndrome (n = 1). Syndromic associations were suggested in 5/41 cases, but were not confirmed due to redirected care. Vascular anomalies counted for 4/41 cases involving the external ear. In the remainder of the ear malformations, no syndromic correlation, genetic abnormality or unifying diagnosis was made.
Conclusions: Our findings suggest that detailed evaluation of the inner and external ears should be performed in every evaluation of the fetus and malformation may suggest the presence of underlying syndromic condition.

Paper #: 109

Comparison of SAR and SED between fetal MR imaging at 1.5T and 3T: Our experience with 3247 examinations

Christian A. Barrera, M.D.[1], *barreracac@email.chop.edu*; Michael L. Francavilla, MD[1], Suraj Serai[1], James Edgar[1], Camilo Jaimes[2], Michael S. Gee[3], Teresa Victoria, MD, PhD[1]; [1]Radiology, The Children's Hospital of Philadelphia, Philadelphia, PA, [2]Boston Children's Hospital, Boston, MA, [3]Massachusetts General Hospital, Boston, MA

Disclosures: All authors have disclosed no financial interests, arrangements or affiliations in the context of this activity.

Purpose or Case Report: To compare and contrast the Specific Absorption Rate (SAR) and Specific Energy Dose (SED) of fetal MR examinations obtained at 1.5T and 3T magnet strength.
Methods & Materials: All fetal MRIs performed on 1.5T and 3T scanners from 2012 to 2016 were included. Patients with incomplete clinical information and with prematurely halted studies were excluded. Sequences performed include Steady State Free Precession (SSFP), Single Shot Fast Spin Echo (SSFSE), T1-weighted Spoiled Gradient Echo 2D (SPGR), SPGR 3D (SPGR-3D), SSFP 3D (SSFP - 3D) Echo Planar Imaging (EPI), and SSFP Cine. The SAR (W/kg) and acquisition time values were retrieved from the DICOM header. The SED (J/kg), which reflects the sum of energy absorbed by the patient in the course of the MRI examination, was calculated as the SAR multiplied by the acquisition time in seconds. The accumulated SED is the sum of energy absorbed by the patient in the course of the MRI examination. Descriptive data is presented as mean ± SD. Independent-sample t-test was used. Effect sizes (Cohen's *d*) were calculated and classified as: small between 0.20 – 0.50, medium between 0.5 – 0.8 and large at 0.80 or greater. A p-value < 0.05 was considered significant.
Results: 3247 fetal MRIs were included: 2784 at 1.5T and 463 at 3T. The mean maternal age, gestational age and weight were 29.8 ± 5.7 years, 24.4 ± 5.7 weeks and 78.1 ± 19.4 kg, respectively. In total, 93,764 sequences were retrieved for analysis: 81,535 performed at 1.5T and 12,229 at 3T. The mean acquisition time was shorter at 1.5T (25.1 ± 13.2 sec) than 3T (30.2 ± 13.9 sec), $p < 0.001$. Significantly higher SAR was observed at 3T (1.1 ± 0.6) than 1.5T (1.0 ± 0.6) ($d = 0.06$, $p < 0.001$). Mean SED per sequence was higher at 3T (37.7 ± 25.6) than 1.5T (32.9 ± 26.7) ($d = 0.17$, $p < 0.001$). Accumulated SED collectively did not show a difference between 1.5T and 3T (965.1 ± 408.1 vs 996.1 ± 365.6, $d = 0.07$, $p = 0.12$). The following sequences demonstrated a higher SAR at 3T than at 1.5T ($p < 0.001$): EPI (0.2 vs 0.1), SPGR (1.1 vs 0.4), SSFP-3D (1.5 vs 1.4) and SSFP Cine (1.6 vs 1.5). The following sequences demonstrated a higher SED at 3T than 1.5T ($p < 0.001$): EPI (8.3 vs 2.0), SSFSE (55.9 vs 50.8), SPGR (26.1 vs 9.5), SSFP (45.7 vs 35.7), SSFP-3D (27.0 vs 16.5) and SSFP Cine (58.2 vs 56.2).
Conclusions: Fetal MRI performed at 1.5T and 3T scanners share similar energy deposition metrics. Although some differences were observed between 1.5T and 3T, the effect sizes indicate that the differences were very small.

Paper #: 110

Determination of Placental Fractional Blood Volume in a Pregnant Mouse Model

Andrew A. Badachhape, Ph.D., *badachha@bcm.edu*; Laxman Devkota, PhD, Igor Stupin, M.D. / Ph.D., Mayank Srivastava, Ph.D., Poonam Sarkar, Ph.D., Ketan B. Ghaghada, PhD, Eric Tanifum, Ph.D., Ananth Annapragada; Radiology, Baylor College of Medicine / Texas Children's Hospital, Houston, TX

Disclosures: All authors have disclosed no financial interests, arrangements or affiliations in the context of this activity.

Purpose or Case Report: Greater than 60% of placentae from low birth weight infants show signs of hypoxic or ischemic injury from vascular hypo-perfusion. Placental fractional blood volume (FBV) is indicative of perfusion and may be used as a marker of local ischemia. Non-invasive methods for the estimation of placental FBV are therefore of interest in the study of placental pathologies. In this pre-clinical study, we investigated contrast-enhanced magnetic resonance imaging (MRI) for the estimation of placental FBV in a pregnant mouse model. A high T1 relaxivity blood-pool liposomal-gadolinium (liposomal-Gd) contrast agent, which does not permeate placental barrier in rodents, was used for the determination of placental FBV.
Methods & Materials: *In vivo* studies were performed in pregnant C57BL/6 mice (8-10 feto-placental units per dam). MRI was performed on a 1T scanner at day 18 of gestation. Pre-contrast and post-contrast images were acquired using a T1-weighted 3D gradient-recalled echo sequence. Post-contrast images were acquired following intravenous administration of liposomal-Gd (0.1 mmol Gd/kg). A variable flip-angle method was used to determine T1 relaxation time and relaxation rates in the placenta ($R1^{P}=1/T1^{P}$) and the inferior vena cava ($R1^{IVC}=1/T1^{IVC}$). Differences between pre-contrast and post-contrast R1 values were determined in the placenta ($\Delta R1^{P}$) and IVC ($\Delta R1^{IVC}$). MRI-derived placental FBV was calculated as a ratio of R1 differences in the placenta to IVC: $FBV^{MRI} = \Delta R1^{P}/\Delta R1^{IVC}$. Contrast-enhanced CT (CECT), where signal is proportional to concentration of iodine contrast agent, was used for validation of MRI-derived FBV. CT scans were performed on a small animal micro-CT scanner. CECT was performed after intravenous administration of a liposomal-iodinated agent (1.1 g I/kg). CT-derived placental FBV (FBV^{CT}) was calculated as the ratio of signal enhancement in placenta to IVC.
Results: The long circulating property of liposomal-Gd resulted in uniform vascular signal enhancement. T1 relaxation time reduced nearly four-fold in the IVC (pre-contrast $T1^{IVC} = 1230 \pm 50$ ms; post-contrast $T1^{IVC} = 310 \pm 25$ ms). In the placenta, T1 relaxation times decreased three-fold (pre-contrast $T1^{P} = 1870 \pm 150$ ms; post-contrast $T1^{P} = 540 \pm 70$ ms). MRI-derived placental FBV was computed as 0.55 ± 0.07 and showed good agreement with values derived from CT ($FBV^{CT} = 0.52 \pm 0.03$).
Conclusions: Contrast-enhanced MRI using a liposomal-Gd blood-pool contrast agent enables accurate determination of placental fractional blood volume.

Paper #: 111

Growth Recovery Lines: A Specific Indicator of Child Abuse and Neglect?

Lora Spiller, MD[1], *spillerl@uthscsa.edu*; Nancy Kellogg, MD[1], Maria-Gisela Mercado-Deane, MD[2], Anthony I. Zarka, D.O.[2], Jonathan Gelfond, MD, PhD[1]; [1]University of Texas Health San Antonio, San Antonio, TX, [2]Children's Hospital of San Antonio, San Antonio, TX

Disclosures: All authors have disclosed no financial interests, arrangements or affiliations in the context of this activity.

Purpose or Case Report: The purpose of this study was to gain an understanding of the distribution, quantity, and associations of growth recovery lines (GRLs) in children from 0 to 24 months of age with high and low risk for child maltreatment.
Methods & Materials: We performed a retrospective cohort study of children from 0 to 24 months who had skeletal surveys and an assessment regarding the level of concern for maltreatment. Two pediatric radiologists blinded to the abuse likelihood independently counted the number of GRLs at each proximal and distal bone site of the extremities. A GRL was defined as a radiodense band traversing parallel to the metaphysis involving at least 50% of the width of the metaphysis. Subjects were classified into 1 of 3 groups: low risk (no findings of abuse or neglect on examination), physical abuse, and neglect. Assessments were conducted by at least one child abuse pediatrician prior to the radiologists' review. The demographic data (age in months and gender) and the key outcomes (total number of GRLs in each subject and number of bone sites with GRLs) were tested for association with the risk group variable using Chi-squared and ANOVA.
Results: Of the 135 children in this study, 58 were in the low risk group, 26 were in the neglect group, and 51 were in the physical abuse group. Children in the neglected and physically

abused groups had 1.73 ($p = 0.007$) times and 1.84 ($p < 0.001$) times more GRLs than the low risk group, respectively. The specificity for maltreatment in subjects with at least 10 GRLs in the long bones was greater than 84% [range 84% to 95%], while the sensitivity was less than 35% [range 25% to 35%]. The most common location for GRLs in abused children was the distal radius, followed by the proximal and distal tibia.
Conclusions: The presence of at least 10 GRLs in the long bones of children between 0 and 24 months of age is highly specific for maltreatment in the absence of another identified stressor. It is important to note that these findings most likely represent previous episodes of unidentified maltreatment, rather than the incident that resulted in their identification as a victim. This was the first study to identify the distal radius as the bone site most likely to have GRLs in physically abused children. X-rays with multiple growth recovery lines should raise concern for child abuse and neglect.

Paper #: 112

Establishing signs for acute and healing phases of classic metaphyseal lesions

Dilek Saglam, MD[2], Megan B. Marine, MD[1], Matthew R. Wanner[3], Roberta Hibbard, MD[1], Greg Jennings[3], **Boaz Karmazyn, MD[1]**, *bkarmazy@iupui.edu*; [1](3) Department of Pediatrics, Indiana University School of Medicine, Riley Hospital for Children, Section of Child Protection Programs, Indianapolis, IN, [2]Malatya Education and Research Hospital, Malatya, Turkey, Turkey, [3]Department of Radiology and Imaging Sciences, Indiana University School of Medicine, Indianapolis, IN

Disclosures: All authors have disclosed no financial interests, arrangements or affiliations in the context of this activity.

Purpose or Case Report: To analyze changes in distal tibial CMLs within 2 weeks follow-up to establish stages of healing.
Methods & Materials: From 2009 to 2018 we identified all skeletal surveys with a diagnosis of distal tibia CML with 2 week follow-up survey. Our routine skeletal survey includes AP and lateral radiographs of the long bones. The surveys were reviewed independently by two pediatric radiologists. Likert score from 1 to 5 (1=no CML, 5=definite CML) was used. Only cases with a Likert score of 4 or 5 by both radiologists were selected.Demographic, clinical, and imaging findings were recorded. One radiologist reviewed all CMLs at initial and 2 week follow-up skeletal survey for presence of the following signs: corner fracture, thin bucket handle fracture (BHF), thick BHF, BHF with endochondral bone filling the gap (BHFG), subphyseal lucency (SPL), increased metaphyseal density (IMD), deformed corner (DC), and subperiosteal bone formation (SPBF).We hypothesized that findings seen only on initial surveys represent acute phase signs. Any signs seen on 2 week follow-up represent healing phase.
Results: The study group included 25 children (12 females) with age range 1-12 months (mean 3 months). 22/25 (88%) children had other fractures.34 distal tibia CMLs were analyzed (right 18, left 16). Thin BHF (n=19, 56%) and isolated corner fractures (n=2, 6%) were only seen on initial skeletal survey and therefore were determined to represent signs of acute phase (n=21). On follow-up, most (n=11, 52%) had thick BHF and others had BHFG (n=3, 14%), DC (n=6, 29%), or were normal (n=1, 5%).12 cases of thick BHF (n=7) or BHFG (n=5) were noted on initial surveys. six of them had corner fractures. On follow-up, 3 (25%) had DC and 7 (58%) were normal. None of these demonstrated thin BHF on follow-up.The following signs of healing CMLs were seen in the initial (n=12) and follow-up (n=34) series; IMD (n=7, 15%), DC (n=6, 13%), and SPL (n=4, 9%). SPBF was not evaluated in five patients with concomitant other tibial fractures and was seen in 49% (20/41) of the fractures in the healing phase.
Conclusions: Our findings suggest that thin BHF is the most common finding of acute CML fractures. Acute CMLs most commonly progress to thick BHF. SPBF is seen in about half of the healing CMLs. Other findings of healing CML are BHF with endochondral bone filling the gap, increased metaphyseal density, corner deformity and subphyseal lucency. Normal metaphysis on 2-week follow up does not exclude CML as it was seen in about one-fifth of cases.

Paper #: 113

A Systematic Review of Radiographic Time Since Injury Methods for Pediatric Healing Fractures

Diana L. Messer, MS[1], *dianamesser@gmail.com*; Brent Adler, MD[2], Farah Brink, MD[2], Henry Xiang, MPH, PhD, MD[2], Amanda Agnew, PhD[1]; [1]The Ohio State University, Columbus, OH, [2]Nationwide Children's Hospital, Columbus, OH

Disclosures: All authors have disclosed no financial interests, arrangements or affiliations in the context of this activity.

Purpose or Case Report: In physically abused children, fractures often go undetected; in such cases, time since injury (TSI) estimation may be essential for identification of abuse as well as prevention of continued violence. The present study was designed to systematically review empirical studies of radiographic methods to assess TSI of healing fractures in pediatric patients. These methods were evaluated for their utility in clinical as well as forensic settings, with particular concern for child protection.
Methods & Materials: A systematic literature search was performed of EBSCO, Embase, MEDLINE (PubMed), and Web of Science for scientifically-based radiographic methods to assess TSI published from the earliest available through August 6, 2018. After screening 4,549 articles, this search identified eleven empirical studies of pediatric fracture healing that met study inclusion criteria.
Results: Of eleven articles, seven were based on samples of patients less than one year old while four articles combined patients of varying ages. Seven articles based their timelines on pooled fracture locations, of which six included fractures of the upper and lower limb; only two examined differences in healing based on fracture location. Two articles focused on abuse-related fractures while many articles failed to exclude abuse-related fractures. Inconsistencies in fracture healing variables exist across articles, which limits many direct associations. When comparisons can be made, healing timelines vary between articles, potentially in part due to the retrospective nature of the research. Though several articles mentioned that the methods and associated timelines could be applied to fracture locations other than those used in their study, few validation studies exist. In addition, the appropriateness of applying fracture healing timelines derived from accidental fractures to abuse-related fractures has not yet been explored.
Conclusions: TSI methods applied to fracture locations and patients with ages other than those the method was developed from could provide inaccurate estimates of fracture healing. Research into patient age, fracture location, and abuse status on fracture healing must be further examined before new methods are developed. It is suggested that methods derived from pooled patient age populations as well as pooled fracture locations (especially those derived from combined upper and lower limb fractures) be used with caution until otherwise substantiated for broader use.

Paper #: 114 - ***Withdrawn***

Paper #: 115

Morphometry of a tissue engineered vascular graft (TEVG) by multimodality imaging including MRI, intravascular ultrasound and angiography in a translational sheep model

John M. Kelly, MD, *john.kelly@nationwidechildrens.org*; Ramkumar Krishnamurthy, PhD, Houchon Hu, Jason Zakko, Kevin Blum, Jacob Zbinden, Yuichi Matsuzaki, Kejal Shah, Toshiharu Shinoka, Christopher Breuer, Rajesh Krishnamurthy, Kan Hor, M.D.; Pediatric Cardiology, Nationwide Children's Hospital, Columbus, OH

Disclosures: All authors have disclosed no financial interests, arrangements or affiliations in the context of this activity.

Purpose or Case Report: First-in-human studies by our group have demonstrated the successful implantation of a biodegradable polymer based tissue engineered vascular graft for use in the treatment of children with complex congenital heart disease. However, widespread adoption is limited by potential complications including aneurysmal dilatation, infection, calcification and stenosis. In this translational study on sheep, we utilized MRI, intravascular ultrasound (IVUS) and conventional angiography (CA) to evaluate graft morphometry and blood flow properties across the graft in the near-term.
Methods & Materials: 2 cm long TEVGs, assembled by seeding autologous bone marrow derived mononuclear cells onto a biodegradable tubular scaffold of polyglycolic acid and a 50:50 copolymer of poly(actide-co-glycolid), were implanted in the intrathoracic inferior vena cava of juvenile sheep (n=8). Animals were evaluated at 1 week and 6 weeks post implantation with CA, IVUS, black blood TSE MRI, contrast enhanced 3D radial MR angiography (MRA), MR 2D and 3D flow velocity mapping, and delayed enhancement imaging for fibrosis. In each subject, native IVC before and after the graft, proximal and distal graft anastomotic sites, and the mid graft were analyzed on all 3 modalities, and compared between weeks 1 and 6. Patterns of luminal distortion were assessed, and characterized using flow velocity changes, turbulence, energy loss, and tissue response as demonstrated on dynamic early contrast enhancement (DCE), and delayed enhancement (DE).
Results: MRA yielded excellent morphometric definition of the native and grafted vasculature for luminal caliber and distortion when compared to angiography. There was good correlation between measurements of graft thickness obtained by IVUS and TSE. Some degree of stenosis was noted in all subjects with anastomotic and whole graft involvement, while there were no cases of rupture, aneurysm formation or infection. Unique information obtained from MRI included area deformation of the TEVG throughout the cardiac cycle, flow alterations and collateralization related to stenosis, estimates of wall shear stiffness and power loss, and estimate of host response at 1 and 6 weeks based on DCE and DE of the graft wall.
Conclusions: MRI/MRA provides comprehensive assessment of TEVG by providing information on luminal architecture, wall thickness, graft integrity, flow perturbations and energy loss, which will be used to develop computational models to predict tissue engineered graft remodeling and stenosis.

Paper #: 116

Intrahepatic Dynamic Contrast Enhanced MR Lymphangiography: A New Technique for Visualization of the Central Lymphatics

David M. Biko, MD, *bikod@email.chop.edu*; Christopher L. Smith, MD, PhD, David Saul, Hansel J. Otero, MD, Ammie M. White, MD, Mandi Liu, Molly Shipman, Erin Pinto, NP, Aaron G. Dewitt, Jonathan J. Rome, MD, Yoav Dori, MD, PhD; Dept. of Radiology, The Children's Hospital of Philadelphia, Philadelphia, PA

Disclosures: David M. Biko, MD: Financial Interest: Wolters Kluwer - Royalty: Editor of Review Book. All other authors have disclosed no financial interests, arrangements or affiliations in the context of this activity.

Purpose or Case Report: Dynamic contrast enhanced MR lymphangiography (DCMRL) is a well described technique of imaging the central lymphatics following intranodal contrast injection. Intrahepatic dynamic contrast enhanced MR lymphangiography (IH-DCMRL) involves ultrasound guided injection of a gadolinium contrast agent into the intrahepatic lymphatic ducts followed by MRI of the chest and abdomen with dynamic time resolved and delayed imaging. We aim to describe the MRI findings of IH-DCMRL.
Methods & Materials: Imaging of all patients less than 20 years of age who underwent an IH-DCMRL over 6 months was retrospectively and independently reviewed by 2 blinded pediatric radiologists who subspecialize in lymphatic imaging. Initially, success of intrahepatic lymphatic access and injection was evaluated. Imaging finds such as pericholecystic enhancement, mesenteric and retroperitoneal reflux, and visualization of the thoracic duct (TD) was assessed. Presence or absence of abnormal lymphatic perfusion to the peritoneal cavity, bowel, and lung and hila was determined. Images were also evaluated for hepatic vein contamination and peritoneal contamination. Disagreements between the 2 readers were solved by consensus. A chart review was performed for demographics and history.
Results: A total of 21 patients (10 male) with a mean age of 7.4 years (range 4 months to 16.9 years, interquartile range 13.1 years) were identified. Clinical indications included pleural effusion (n=11), ascites (n= 7), protein losing enteropathy (PLE,n=6), anasarca (n=2), and intestinal lymphangiectasia (n=1). Two (10%) IH-DCMRLs were technically unsuccessful due to needle displacement. Pericholecystic enhancement (n=7) and reflux into the mesenteric (n=17) and retroperitoneal lymphatics (n=17) was present. Abnormal lymphatic perfusion to the peritoneal cavity (n=7), bowel (n=7), and lung (n=11) was seen. Readers were in agreement on the presence or absence of lymphatic perfusion to the peritoneal cavity in all cases, in 18/19 cases of perfusion to the bowel, and in 17/19 cases of perfusion to the lung and hila. The TD was visualized in 15/19 patients (79%). Hepatic vein contamination was common (n=14). Peritoneal contamination occurred in 3 patients, 2 of which were unsuccessful IH-DCMRLs.
Conclusions: IH-DCMRL is a promising technique to evaluate the liver and central lymphatics which may be advantageous when lymphatic imaging via an intranodal approach is ineffective in demonstrating these lymphatic pathways.

Paper #: 117

Evaluation of Cumulative Perimetric Ratio as Quantitative Index for Degree of Left ventricular Myocardial Trabeculations in Adolescents and Young Adults

Amol Pednekar, PhD, *aspednek@texaschildrens.org*; Siddharth P. Jadhav, MD, Cory Noel, MD, Prakash M. Masand, MD; Radiology, Texas Children's Hospital, Houston, TX

Disclosures: Prakash M. Masand, MD: Consultant, Honoraria: Canon Medical Systems, Phillips MRI Users Meeting 2018, Daiichi Sankyo, Speakers Bureau: Canon Medical Systems, Royalty: Amirsys. All other authors have disclosed no financial interests, arrangements or affiliations in the context of this activity.

Purpose or Case Report: Cumulative perimetric ratio (CPR) serves as a quantitative index of irregularity and sparsity of the left ventricular (LV) trabecular structures in bright blood cine balanced steady-state free precession (bSSFP) MR images. The purpose of this abstract is to evaluate CPR as a 2D geometric measure complimentary to morphometric measures like non-compacted (NC) to compacted (C) length ratio (LR) and mass ratio (MR) in a pediatric population.
Methods & Materials: We retrospectively searched the cardiac MRI charts between August 2014 and September 2018 for clinical indications of myocardial hyper trabeculation, LV non-compaction, anomalous coronary origins, or Kawasaki disease. The inclusion criteria was normal cardiac anatomy, as well as normal preload and afterload. Epi and endocardial contours (EC) were drawn on the end-diastolic short-axis bSSFP images of the LV from mitral valve annulus to apex. These contours were used for automatic extraction of the trabecular edges (T). Following quantitative indices were computed using automated tool: 1) NC/C length ratio (LR) perpendicular to EC at each slice; 2) MR = percent NC of (NC+C) for entire LV; and 4) perimetric ratio (PR = length of T / perimeter of EC) for each slice. Global quantitative indices were derived as: 1) maximum of LR (MLR) across all slices; 2) MR; and 4) CPR over all slices. Combined criteria of MLR>2.3 and MR>35% was used to define patients with prominent trabeculations.
Results: A total of 80 patients (14.3±5.0 yrs) met the inclusion criteria. The values for MLR (1.99±0.88, 0.5-4), MR (31.7±12.1, 13.2-55.6), and CPR (1.67±0.31, 1.20-2.41) increased with degree of trabeculation as a continuous spectrum. There is a significant correlation between MR and MLR with correlation coefficient (r) of 0.85 (0.78-0.9). CPR has significant correlation with both MLR (0.73, 0.61-0.82) and MR (0.82, 0.73-0.88). Cut off value of CPR=1.6 yields 94% of area under the receiver operating characteristics curve with 86% sensitivity and 89% specificity.
Conclusions: CPR derived from epi and endocardial contours typically drawn for LV functional analysis correlated strongly with morphometric measures of NC/C length and mass ratios. CPR provides comprehensive measure of irregularity and extent of the LV trabeculations overcoming the inherent morphologic variability from base to apex by providing comprehensive measure of irregularity. CPR has potential to serve as a valuable marker for prominent trabeculations when used along with LR and MR.

Paper #: 118

Circumventing Anesthesia in Pediatric Cardiac Patients Considered High-Risk for Anesthesia using Free Breathing CMR

Amol Pednekar, PhD, *aspednek@texaschildrens.org*; Premal Trivedi, Siddharth P. Jadhav, MD, Cory Noel, MD, Prakash M. Masand, MD; Radiology, Texas Children's Hospital, Houston, TX

Disclosures: Prakash Masand, MD: Consultant, Honoraria: Canon Medical Systems, Phillips MRI Users Meeting 2018, Daiichi Sankyo, Speakers Bureau: Canon Medical Systems, Royalty: Amirsys. All other authors have disclosed no financial interests, arrangements or affiliations in the context of this activity.

Purpose or Case Report: General anesthesia (GA), while not always required, is frequently necessary in infants and children undergoing cardiac magnetic resonance imaging (CMR) based on risk-benefit of GA and breath-hold (BH) v/s the diagnostic value of the acquired cine images. Primarily, requirement of BH for cine imaging to evaluate ventricular volumes and function, a key prognostic measure in spectrum of congenital heart diseases, governs the necessity of GA. Herein we review our experience of completely free breathing (FB) CMR, including CArdio-REspiratory Synchronized (CARESync) cine imaging instead of multiple signal averaging (MSA) cine imaging, in unsedated pediatric population.
Methods & Materials: We retrospectively reviewed the anesthesia and MRI records for all patients who had undergone CMR between June 2017 and September 2018.
Results: Out of 1100 (17.1±7.8, 7.6-65.9 yrs) CMR studies performed a total of 77 (14.5±8.7, 7.6-63.0 yrs) unsedated patients were unable to hold their breath. All these 77 CMR studies were completed without anesthesia using FB-CMR and provided diagnostic image quality. Out of these 77 patients, 49 (14.9±12.5, 7.9-63.0 yrs) patients were considered high-risk (HR) for anesthesia: single ventricles (6: 11.1±1.3, 8.7-12.3 yrs), hypertrophic cardiomyopathy (HCM) (14: 14.0±5.9, 8.2-30.4 yrs), cardiomyopathy with moderate-to-severely depressed function (4: 20.6±9.6, 11.6-33.2 yrs), myocarditis (7: 14.7±3.5, 9.0 – 18.4 yrs), and atrioventricular valve diseases including, moderate-to-severe aortic insufficiency, aortic regurgitation, or mitral stenosis (18: 14.1±5.1, 7.6 – 24.2 yrs). Three (13.5±3.0, 10.3 – 16.1yrs) patients were indicated for left ventricular non-compaction (LVNC).

Conclusions: Our experience demonstrates that complete FB-CMR studies including (CARESync) cine imaging allow elimination of anesthesia while providing diagnostic morphologic, functional and pathophysiologic evaluation in young children, and adolescents considered high-risk for anesthesia. CARESync has been previously reported to improve image quality significantly over MSA and provide comparable ventricular volumes [1]. Furthermore, superior delineation of trabeculation and myocardium from blood pool allows accurate measurements of non-compacted and compacted myocardium critical for HCM and LVNC and overall better wall motion assessment. It may be worthwhile to explore increased utilization of FB-CMR to further reduce need for anesthesia.[1] Krishnamurthy R et al. J Cardiovasc Magn Reson. 2015;17.

Paper #: 119

Non-contrast Flow-independent Relaxation-Enhanced MR Angiography Using Inversion Recovery and T2-Prepared 3D mDIXON Gradient-Echo DIXON Technique: Applications in the Pediatric Population

Skorn Ponrartana, MD, MPH[1], *sponrartana@chla.usc.edu*; Michael Chiang, M.D.[1], Quin Lu[2]; [1]Radiology, Children's Hospital Los Angeles, Los Angeles, CA, [2]Philips Healthcare, Cleveland, OH

Disclosures: Quin Lu, PhD: Salary: Philips. All other authors have disclosed no financial interests, arrangements or affiliations in the context of this activity.

Purpose or Case Report: While Gadolinium-based contrast-enhanced MR Angiography (Gd-MRA) is a robust technique for evaluation of the vascular system, there are inherent limitations, such as the contraindication in renal failure and concern of intracranial Gadolinium deposition. This study exams the feasibility of flow-independent relaxation-enhanced MR Angiography without contrast and triggering (REACT) in various clinical indications and compares the sequence to corresponding Gd-MRA.
Methods & Materials: The REACT sequence is a combination of a two-point 3D chemical-shift water-fat separated mDIXON TFE pulse sequence, a non-volume selective adiabatic inversion pulse, and a four-refocusing-adiabatic-pulse T2-prep module, which suppresses signal from static tissues and enhances the long T1 and T2 native signal of unenhanced blood, thereby providing optimal vessel-to-background signal contrast.We retrospectively reviewed all cases where both the REACT sequence and Gd-MRA were available for comparison between June 2018 and October 2018. Imaging was performed on a 3 Tesla platform (Philips Ingenia, software R5.3) or a 1.5 Tesla platform (Philips Achieva, software R5.3). Two pediatric body radiologists in consensus qualitatively compared results from REACT with Gd-MRA to evaluate whether it was diagnostically useful either as a complement or potential replacement.
Results: We retrospectively reviewed a total 5 cases with both the REACT sequence and Gd-MRA. The clinical indications included pre-operative evaluation for vascular access, thoracic outlet syndrome, May-Thurner syndrome, deep venous thrombosis, and complex venolymphatic malformation. The REACT sequence was found to be equivalent at obtaining the diagnosis in all 5 cases. However, in 4 of the 5 cases, Gd-MRA provided improved contrast resolution and signal-to-noise compared with the REACT sequence. Only in the case of thoracic outlet syndrome were the images found to be non-inferior.
Conclusions: Our preliminary experience with REACT in children suggests that the sequence is robust and capable of providing diagnostic angiograms in a variety of clinical indications. One advantage of REACT is that it can be repeated as needed and is not constrained by timing of a contrast bolus. However, the major disadvantage of REACT is its lower contrast resolution and signal-to-noise ratio compared with Gd-MRA. Future studies with larger and more diverse sample sizes are needed to better validate whether REACT can obviate the need for Gd-MRA in more generalizable circumstances.

Paper #: 120

Image Quality Assessment of Cardiothoracic Respiratory Motion Compensated Relaxation Enhanced 3D Non-Contrast MRA with Reference to Dynamic Contrast-Enhanced 3D MRA: A Pilot Study

Eric Diaz, MD, *eric.diaz@gmail.com*; Siddharth P. Jadhav, MD, Pamela Ketwaroo, Amol Pednekar, PhD, Wei Zhang, Prakash M. Masand, MD; Texas Children's Hospital, Houston, TX

Disclosures: Prakash M. Masand, MD: Consultant, Honoraria: Canon Medical Systems, Phillips MRI Users Meeting 2018, Daiichi Sankyo, Speakers Bureau: Canon Medical Systems, Royalty: Amirsys. All other authors have disclosed no financial interests, arrangements or affiliations in the context of this activity.

Purpose or Case Report: This is a pilot study to evaluate image quality of relaxation-enhanced, non-contrast, MR angiography (RENC-MRA) in cardiothoracic vessels of children as compared to standard, contrast enhanced dynamic MRA (CE-dMRA). If RENC-MRA has similar or superior diagnostic quality to CE-dMRA, the costs, and potential risks of gadolinium (Gd) based contrast administration may be avoided.
Methods & Materials: A retrospective, cross-sectional study was performed on consecutive patients undergoing clinically indicated CE-dMRA on 1.5T clinical scanner (Ingenia, Philips) between Aug 1, 2018 and Sep 31, 2018. Prior to administration of Gd contrast, RENC-MRA was acquired with equivalent spatial resolution and coverage as CE-dMRA. Informed consent was waived.Patient age, sex, diagnosis, and multiple image quality metrics were recorded for 8 vessels in RENC-MRA and best phase CE-dMRA. Image quality was subjectively compared using a visual Likert scale from 1 to 5 for vascular edge clarity (EC). Quantitative metrics were computed based on vessel and background tissue ROI measures and included: 1) coefficient of variation (CV), 2) relative contrast (RC), and 3) signal to noise and contrast to noise ratios (SNR, CNR). Wilcoxon signed-rank test with alpha of 0.001, adjusted for multiple comparison, was performed for both averaged individual and average of all vessel metrics to assess for statistical significance.
Results: Fifteen patients met inclusion criteria (Ages:2-21, Male:10, Female:5). There was significantly lower vessel CV for averaged and all individual vessels in RENC-MRA ($p<0.001$), except in MPA and IVC ($p=0.05$), and SVC ($p=0.01$). There was no significant difference in EC, RC, background CV, SNR, and CNR for averaged vessel metrics. There was significantly increased RC, SNR, and CNR in IVC for RENC-MRA ($p<0.001$). There was a trend toward significance with lower RC in MPA and LPA for RENC-MRA ($p=0.005$), lower SNR and CNR in descending aorta for RENC-MRA ($p=0.01$), and higher RC, SNR, and CNR in SVC for RENC-MRA ($p=0.01$).
Conclusions: RENC-MRA sequence demonstrated similar image quality metrics to CE-dMRA with some exceptions. Although RENC-MRA cannot provide dynamic information, our data suggests that RENC-MRA has greater uniformity of image quality and superior characterization of systemic veins. Diagnostic accuracy of RENC-MRA must now be evaluated against post contrast equilibrium MRA, as similar accuracy of these would provide useful options, especially for patients in whom Gd-based contrast is contraindicated.

Paper #: 121

Highly accelerated cardiorenal 4D flow MRI using 3D cones trajectory

Christopher Sandino, M.S., *sandino@stanford.edu*; Joseph Y. Cheng, PhD, Marcus Alley, Shreyas Vasanawala, MD/PhD; Electrical Engineering, Stanford University, Menlo Park, CA

Disclosures: Christopher Sandino, M.S.: Financial Interest: General Electric Healthcare - Salary: Independent Contractor; **Marcus Alley, PhD:** Consultant, Honoraria: Arterys, Research Grant: GE Medical Systems. **Joseph Y. Cheng, PhD:** Consultant, Honoraria: HeartVista, Inc., Research Grant: GE Healthcare. **Shreyas Vasanawala, MD/PhD:** Arterys, Royalty: Arterys, GE Healthcare, Siemens, Philips, Research Grants: GE Healthcare. All other authors have disclosed no financial interests, arrangements or affiliations in the context of this activity.

Purpose or Case Report: Time-resolved, 3D phase-contrast (4D flow) MRI enables comprehensive cardiac evaluation, but long acquisition times and motion corruption limit pediatric abdominal clinical use. Here, we develop and integrate a time-efficient non-Cartesian 3D cones trajectory into 4D flow to reduce scan time while also increasing robustness to respiratory and bowel motion artifacts. We then assess whether the resulting non-Cartesian 4D flow is able to achieve high-quality, full-coverage cardiorenal evaluation in under 10 minutes.
Methods & Materials: We design a flow-encoded, golden-angle re-ordered 3D cones pulse sequence based on RF-spoiled gradient recalled echo (SPGR). Cones gradient waveforms are iteratively designed on-the-fly to enable arbitrary field of view and resolution prescription. Cardiac-resolved images are reconstructed using a combined parallel imaging and compressed sensing algorithm (l_1-ESPIRiT). To further improve motion-robustness, respiratory signals are estimated from each cone readout, and then used to suppress motion during reconstruction.With informed consent and IRB approval, 2 pediatric subjects (3-years-old and 7-years-old) referred for contrast-enhanced abdominal MRI were scanned using Cartesian 4D flow and cones 4D flow sequences on a 3T scanner (MR750, GE Healthcare) with a 32-channel cardiac coil. Cartesian and cones 4D flow scan parameters include spatial resolution: 1.0x1.0x1.5 mm^3, 8 cardiac phases, Venc: 100-150 cm/s, and scan durations: 5-7 minutes. All data was acquired with subjects freely breathing.
Results: Cones 4D flow reconstructions are feasible and show excellent delineation of renal vasculature in data acquired just under 5 minutes. By nature of the cones sampling trajectory, respiratory and bowel motion artifacts appear noise-like and incoherent. Similar image quality is observed after retrospectively undersampling data to simulate a 3-minute acquisition. Further, both aortic and renal arterial flow rates are conserved in the retrospectively undersampled acquisition. In a 7-minute acquisition, where the Cartesian and cones scan times are held constant, cones 4D flow provides superior image quality, but underestimates peak aortic flow by 26%. This difference is attributed to larger eddy current errors in the cones sequence, although, these can be corrected with more robust physical models.
Conclusions: We introduce the first 4D flow sequence with a 3D cones sampling trajectory. Cones can highly accelerate 4D flow acquisitions and reduce both flow and motion artifacts.

Paper #: 122

Multi Echo fLow-encoded Rosette (MELROSE) for Quantitative Assessment of Cardiac and Intravascular T2* and Blood Oxygen Saturation Determination

Adam Bush, Ph.D, *adambush@stanford.edu*; Christopher Sandino, M.S., Marcus Alley, Shreyas Vasanawala, MD/PhD; Radiology, Stanford University, South San Francisco, CA

Disclosures: Christopher Sandino, M.S.: Financial Interest: General Electric Healthcare - Salary: Independent Contractor; **Marcus Alley, PhD:** Consultant, Honoraria: Arterys, Research Grant: GE Medical Systems; **Shreyas Vasanawala, MD/PhD:** Arterys, Royalty: Arterys, GE Healthcare, Siemens, Philips, Research Grants: GE Healthcare. All other authors have disclosed no financial interests, arrangements or affiliations in the context of this activity.

Purpose or Case Report: Cardiac catheterization is an invasive albeit common procedure performed in children with congenital heart disease for intrathoracic oxygen saturation assessment that exposes patients to anesthesia and risk of infection and complication. Prior work with MRI based intrathoracic oxygenation methods have failed due to partial voluming of the blood pool and surrounding tissue. In this work we overcome this challenge, by using subtractive, velocity encoding for simultaneous flow, intravascular T2* and oxygen saturation determination using a Multi Echo fLowencoded ROSEtte (MELROSE) sequence. We validate flow and T2* values in a flow phantom and present preliminary results in a healthy subject.
Methods & Materials: TheoryRosette trajectories are flower-like k-space traversal patterns first described by Doug Noll [1]. We use a novel parameterization that's defines a rosette shape parameter, q [2]. MethodsAll scans were performed on a GE 750W with a 20 channel cardiac array. A MELROSE sequence with bipolar, tetrahedral, velocity encoding gradients of 100 cm/s, q= 2.2, FA = 15 and TR 34ms was constructed. A ferumoxytol doped water, gravity feed flow phantom was constructed. MELROSE assessment of flow and T2* quantification was compared to gold standard, Cartesian phase contrast for velocity measurements and gradient echo recalled multiecho for T2*. In Vivo: A 28 y/o male volunteer was imaged using a MELROSE sequence. All studies were IRB approved and conducted with informed consent.
Results: The average velocity in the flow phantom measured using Cartesian phase contrast was 45.3±12.6, 26.4±11.3 and 9.21 ±1.9 cm/s and 47.8±18.6, 27.7±12.0 and 8.48 ±2.6 cm/s using MELROSE. The static GRE measured T2* of the doped ferumoxytol solution was 21.9±1.0 ms and 18.6ms at an average velocity of 27.7 cm/s and 19.4ms at an average velocity of 8.5 cm/s using MELROSE. T2* and flow images were reconstructed in a volunteer subject.
Conclusions: DiscussionBoth quantitative flow and T2* estimates were in excellent agreement using both gold standard phase contrast and MELROSE in a constant flow phantom. These phantom data and preliminary results in a healthy volunteer demonstrate feasibility for time resolved blood flow and T2* estimates in healthy subjects with applications for noninvasive oxygenation assessment in children with congenital heart disease.[1] Noll, *IEEE Trans Med Imaging*, 1997[2] Bush, SPR 2019, Abstract #3110307

Paper #: 123

Contigious Rosette Echoes iN Single Highly Accelerated Acquistion (CRENSHAA) for Motion Robust and Time Resolved Cardiac and Abdominal T2* Assessment

Adam Bush, Ph.D[1], *adambush@stanford.edu*; Christopher Sandino, M.S.[1], Shreya Ramachandran[2], David Zeng, MS[1], Joseph Y. Cheng, PhD[1], Marcus Alley[1], Shreyas Vasanawala, MD/PhD[1]; [1]Radiology, Stanford University, South San Francisco, CA, [2]California Institute of Technology, Pasadena, CA

Disclosures: Christopher Sandino, M.S.: Financial Interest: General Electric Healthcare - Salary: Independent Contractor; **David Y. Zeng**: Financial Interest: GE Healthcare - Research Funding: Research; **Marcus Alley, PhD:** Consultant, Honoraria: Arterys, Research Grant: GE Medical Systems; **Joseph Y. Cheng, PhD:** Consultant, Honoraria: HeartVista, Inc., Research Grant: GE Healthcare; **Shreyas Vasanawala, MD/PhD:** Arterys, Royalty: Arterys, GE Healthcare, Siemens, Philips, Research Grants: GE Healthcare. All other authors have disclosed no financial interests, arrangements or affiliations in the context of this activity.

Purpose or Case Report: Multidimensional imaging approaches reduce total examination time by using a single acquisition to reconstruct several images contrast states, typically requiring several independent scans. In children, this scan reduction increases patient comfort and compliance while reducing the need for anesthesia. In this work, we introduce a novel multidimensional imaging approach that utilizes a rosette, or flower-like, k-space trajectory entitled Contiguous Rosette Echoes iN Single Highly Accelerated Acquisition (CRENSHAA). Using CRENSHAA, we demonstrate feasibility for self-gated, motion resolved T2* mapping for simultaneous cine imaging and iron quantification.
Methods & Materials: TheoryRosette trajectories employ oscillating gradient fields at two distinct frequencies to produce flower-like k-space traversal patterns first described by Doug Noll [1]. We extend this earlier work by using a novel rosette parameterization: If N is odd, q = { x | x = (2L-1)/N, L = (N+1+2m)/2, m Î Z^+} \ Z^+If N is even, q = { x | x = (2L)/N, L = (N-2+4m)/2, m Î Z^+} \ Z^+ where N represents the number of petals, L the number of layers, m is an incrementing variable and Z+ is the set of all positive integers. MethodsAll scans were performed on a GE 750W with a 20 channel cardiac array. Ex Vivo: T2* phantoms containing distilled water, MnCl2 and 3% carrageenan in 50ml falcon tubes were constructed for T2* validation. A CRENSHAA sequence with q=2.2, FA= 15 degrees and TR 34 ms produced echoes at 1.1, 4.1, 6.7, 9.3 and 11.9ms. 350 repetitions were acquired, each successively incremented by a rotation angle of 137.5° Exponential fitting was performed in MATLAB. Images were compared to a gold standard GRE multiecho sequence. In Vivo: A 31 y/o male volunteer was imaged using a CRENSHAA sequence. Self-gated, k-space magnitude CINE images were reconstructed at 30 phases with a 5 phase sliding window. All studies were IRB approved and conducted with informed consent.
Results: The measured T2 values using the gold standard GRE sequence were 70.4±8.3, 32.2±2.2, 28.5±2.0, 30.3±3.0, 7.8±0.51, 5.0±0.4 whereas the CRENSHAA measured T2* values were 64.9±19.6, 33.0±5.7, 28.5±7.6, 27.3±5.2, 10.0±0.7 and 6.4±0.5. CINE and T2* map reconstructions were performed in healthy volunteer subject.
Conclusions: CRENSHAA was successful in producing comparable T2* values to the gold standard in phantoms and reasonable values in a heathy subject. Future uses will explore motion resolved cardiac and liver iron assessment in children.

Paper #: 124

Deep learning-based reconstruction of 2D cardiac CINE MRI data

Christopher Sandino, M.S.[1], *sandino@stanford.edu*; Peng Lai, Ph.D.[2], Shreyas Vasanawala, MD/PhD[1], Joseph Y. Cheng, PhD[1] [1]Electrical Engineering, Stanford University, Menlo Park, CA, [2]General Electric Healthcare, Menlo Park, CA

Disclosures: Christopher Sandino, M.S.: Financial Interest: GE Healthcare - Salary: Independent contractor; **Shreyas Vasanawala, MD/PhD:** Arterys, Royalty: Arterys, GE Healthcare, Siemens, Philips, Research Grants: GE Healthcare; **Joseph Y. Cheng, PhD:** Consultant, Honoraria: HeartVista, Inc., Research Grant: GE Healthcare; **Peng Lai, PhD:** Salary: GE Healthcare. All other authors have disclosed no financial interests, arrangements or affiliations in the context of this activity.

Purpose or Case Report: Cardiac CINE is a common MRI technique for cardiac evaluation, but requires multiple breath-holds to acquire high quality images without respiratory motion artifacts. This in conjunction with rapid heart rate makes pediatric CINE imaging challenging. Neural networks can leverage previous exam data to learn how to reconstruct highly accelerated MRI data. Here we extend this to cardiac imaging, and present a deep learning-based reconstruction technique trained on fully-sampled healthy volunteer data. We show that our network outperforms combined parallel imaging and compressed sensing (PICS) reconstruction methods on 10x accelerated 2D CINE data with respect to common image quality metrics.
Methods & Materials: The proposed unrolled network iteratively applies 3D convolutional neural networks and data consistency updates to under-sampled input data. Data consistency layers enforce consistency with input k-space samples, and help the network generalize to data acquired from unhealthy patients. The network is trained to output fully-sampled complex images, preserving both magnitude and phase.With IRB approval, fully sampled 2D bSSFP cardiac CINE datasets were acquired from 12 healthy volunteers at different cardiac views and slice locations on 1.5T and 3.0T GE scanners. For training, ten volunteer datasets are split slice-by-slice into 155 slices, and then further augmented by random flipping, cropping, and variable-density undersampling (R=8-10). For evaluation, the remaining two volunteer datasets are retrospectively undersampled to simulate 10-fold acceleration with 25% partial echo. The same evaluation datasets are reconstructed using the proposed method and a PICS algorithm (l_1-ESPIRiT). Reconstruction quality is evaluated with respect to peak signal-to-noise ratio (PSNR) and structural similarity index (SSIM).
Results: The proposed method outperforms PICS with respect to both PSNR and SSIM metrics. The improvement of the proposed method over PICS is most apparent inside the heart with less spatiotemporal blurring of myocardium and papillary muscles in deep reconstructions. Deep reconstructions also depict systolic heart motion much more naturally, whereas PICS is susceptible to temporal staircasing artifacts due to strong regularization.
Conclusions: Preliminary results suggest that the proposed method can reconstruct 2D cardiac CINE data more accurately and robustly than compressed sensing. This technique can improve image quality for single breath-hold, and in the future, free-breathing scans.

Paper #: 125

The utility of the ASL sequence in parenchymal injury of the brain in abusive head trauma (AHT).

Alex Chan, D.O.[2], *alchan@christianacare.org*; Arabinda Choudhary, M.D.[1], Rahul Nikam, M.D.[1], Vinay V. Kandula, M.D.[1]; [1]Nemours/Alfred I. duPont Hospital for Children, Wilmington, DE, [2]Christiana Care Health System, Newark, DE

Disclosures: Arabinda Choudhary, M.D.: Consult, Honoraria: Child Abuse Lectures, Equity Interest/Stock Options: GE Shares. All other authors have disclosed no financial interests, arrangements or affiliations in the context of this activity.

Purpose or Case Report: To determine whether the ASL sequence can provide added value by demonstrating additional parenchymal abnormalities that are not easily identifiable on conventional MRI sequences.
Methods & Materials: In this IRB approved retrospective study, we reviewed MRI brain cases performed in children referred to child protective services at an US academic pediatric hospital between 2012-2018. The analysis was performed by an experienced Neuroradiologist and a senior Radiology Resident which assessed individual brain MRI exam for parenchymal changes identified on the ASL sequence and compared the findings with the other routine MRI sequences of the same exam. The ASL sequence was considered to provide added value if the ASL findings revealed additional parenchymal perfusion abnormalities not identified on routine sequences (T2WI, T1WI, FLAIR, SWAN, and DWI/ADC map) and with evidence of atrophy on either MRI or CT brain, if follow up imaging was performed. ASL was considered to not provide added value if the ASL findings did not reveal additional parenchymal perfusion abnormality. We excluded patients in which the imaging workup did not include an MRI study, ASL sequence, or uninterpretable ASL acquisition.
Results: A total of 54 patients were surveyed with an average age of 157.3 days. Of the 54 patients, 31/54 cases (57.4%) were excluded based on the described criteria. Of the included patients, 23/43 cases (42.6%), 9/23 cases (39.1%) demonstrated that ASL added value and 14/23 cases (60.9%) demonstrated no added value. Of the cases where ASL added value, 7/9 cases (77.8%) showed the sequela of brain parenchymal atrophy on follow up imaging within the previously identified areas of perfusion abnormalities, while the remaining 2/9 cases (22.2%) had no follow up imaging. Of the 9/23 cases where ASL demonstrated added value, 5/9 cases (55.6%) were male and 4/9 cases (44.4%) were female. Of the 14/23 cases where ASL demonstrated no added value, 9/14 (64.3%) cases were male and 5/14 (35.7%) cases were female.
Conclusions: Our study demonstrated that in cases of suspected abusive head trauma, evaluation of the ASL sequence in addition to other MRI sequences provided additional information regarding parenchymal injury as compared to routine MRI sequences alone. We propose that by adding the ASL sequence, in the setting of suspected AHT, to the evaluation brain parenchymal injury would add value by improving the detection of injury, assess long term prognosis, and may also help understand the mechanism of injury.

Paper #: 126

ASL Perfusion Imaging of the Frontal Lobes Predicts the Occurrence and Resolution of Posterior Fossa Syndrome

Maryam Maleki, M.D., *mmaleki@stanford.edu*; Derek W. Yecies, M.D., Katie Shpanskaya, Kristen W. Yeom, M.D.; Stanford University School of Medicine, Stanford, CA

Disclosures: All authors have disclosed no financial interests, arrangements or affiliations in the context of this activity.

Purpose or Case Report: Posterior fossa syndrome (PFS) is a common complication following the resection of posterior fossa tumors in children. The pathophysiology of PFS remains incompletely elucidated, however the wide-ranging symptoms of PFS suggest the possibility of wide-spread cortical dysfunction. In this study, we utilize arterial spin labeling (ASL), an MR perfusion imaging modality that provides quantitative measurements of cerebral blood flow without the use of intravenous contrast, to assess cortical blood flow in patients with PFS.
Methods & Materials: A retrospective review of pediatric medulloblastoma patients who underwent surgical tumor resection between 2004 and 2016 at our institution was performed. Postoperative ASL imaging was available for 14 patients who developed PFS and 10 age-matched controls. Bilateral frontal lobe perfusion measured was compared between PFS and control patients immediately after surgery. Additionally, in patients with PFS, ASL following the return of speech was compared with immediate postoperative ASL.
Results: On immediate postoperative ASL, patients who subsequently developed PFS had decreased right frontal lobe perfusion (37.00 ± 13.46 vs 49.7 ± 13.72, $p=0.046$) and a trend towards decreased perfusion in the left frontal lobe (41.00 ± 17.36 vs 53.5 ± 14.62, $p = 0.092$) compared to age-matched children who did not develop PFS after tumor resection. Patients with PFS had statistically significant increases in right (55.79 ± 18.34 vs 40.71 ± 15.27, $p=0.018$) and left 60.79 ± 21.75 vs 44.07 ± 17.25, $p =0.028$) frontal lobe perfusion after the resolution of symptoms compared to their immediate postoperative imaging.
Conclusions: ASL perfusion imaging identifies decreased frontal lobe blood flow as a strong physiologic correlate of PFS that is consistent with the symptomatology of PFS. This is also the first study to demonstrate that decreases in frontal lobe perfusion are present in the immediate postoperative period and resolve with the resolution of symptoms, suggesting a physiologic explanation for the transient symptoms of PFS.

Paper #: 127

Neuroimaging findings in infants with human parechovirus infection

Asha Sarma[2], *asha.sarma@vumc.org*; Emily Hanzlik[2], Rekha Krishnasarma[1], Lindsay Pagano[2], Sumit Pruthi[2]; [1]Boston Children's Hospital, Boston, MA, [2]Vanderbilt University Medical Center, Nashville, TN

Disclosures: All authors have disclosed no financial interests, arrangements or affiliations in the context of this activity.

Purpose or Case Report: To evaluate neuroimaging findings in patients with human parechovirus (HPeV) infection and review the current literature.
Methods & Materials: This retrospective review includes 6 cases from 2 children's hospitals. The electronic medical record was reviewed for parameters including patient age and sex, birth history and gestational age at birth, presenting symptoms, length of hospital/ICU stay, white blood cell count, cerebrospinal fluid

(CSF) analysis, and electroencephalography (EEG) results. MRI, US, and CT (if available) findings were assessed by two attending pediatric neuroradiologists. Technique and sequences acquired varied by case and institution.
Results: 6 infants presented at <60 days of life (DOL) with irritability, decreased PO intake and/or multifocal seizures. 4 full-term infants presented in the first 10 DOL, and 2 premature infants (33 and 35 weeks gestational age) presented on DOL 20 and 35. CSF showed no pleocytosis and was culture negative but was positive for HPeV by polymerase chain reaction-based testing. In 6/6, DWI demonstrated low ADC in the frontoparietal and temporal white matter, corpus callosum, internal and external capsules, optic radiations, frontal and atrial periventricular white matter, and thalami. 5/6 studies demonstrated low ADC in the occipital white matter and 2/6 cases demonstrated low ADC in occipital cortex. In 2/6 cases (from a single institution), T1-weighted imaging demonstrated hyperintensity in the corona radiata. Mild T2 prolongation was noted in involved white matter, and in 3/6 cases from a single institution, T2 shortening was observed along the distribution of deep medullary veins. 1/3 studies with MRS showed elevated lactate.
Conclusions: Brain MRI in HPeV infection tends to show a characteristic pattern of low diffusivity involving major supratentorial white matter tracts including the corpus callosum, and the thalami. Cortical involvement is unusual and the basal ganglia, brainstem, and cerebellum are spared. T2 shortening along the distribution of deep medullary veins in 3/6 cases (from a single institution obtained with similar MRI acquisition parameters) suggests perivenular invasion with venous ischemia as a potential etiology. This hypothesis is supported by histopathologic analysis provided by a case from the literature, which demonstrated the presence of HPeV in blood vessel walls.

Paper #: 128

Longitudinal Brain MRI Characterization of Normal Appearing Zika-exposed children using advanced MRI techniques and Correlations with Neurodevelopmental Outcomes

Jessica Riotti, MD[1], *jessica.riotti@jhsmiami.org*; Shanchita Ghosh[2], Amrutha Ramachandran[1], Fiama Reyes Avila[1], Ivan Gonzalez[1], Varan Govind[1], Gaurav Saigal[1]; [1]University of Miami, Miami, CA, [2]UC Davis, Sacramento, CA

Disclosures: All authors have disclosed no financial interests, arrangements or affiliations in the context of this activity.

Purpose or Case Report: Congenital Zika syndrome (CZS) is unique to fetuses infected with Zika virus (ZIKV) before birth and presents with distinct pattern of birth defects including characteristic brain abnormalities. The neurological manifestations in these infants with CZS have emerged lately and are well documented. However, the consequences of ZIKV exposure to fetuses of pregnant mothers and the neonates born to them were not thoroughly examined. Despite these ZIKV-exposed neonates demonstrating normal head circumference at birth [1], they may have subtle brain abnormalities and neurodevelopmental deficits that are possibly associated with congenital ZIKV [2,3]. Since these ZIKV-exposed infants represent a larger population as compared to those with CZS, it becomes all the more important to examine the brains of this group. The purpose of this prospective study is to compare the brain MRI volume measures of otherwise normal appearing ZIKV-exposed infants to matched controls, with neurodevelopmental correlates.
Methods & Materials: Volumetric MRI data of ZIKV-exposed infants (n = 9) and normal controls (n = 5), acquired from 1 to 6-months gestational age were scanned without sedation or contrast on a 3T MRI scanner. The MR protocol consists of T2, diffusion kurtosis imaging (DKI), susceptibility weighted imaging, and MR Spectroscopy (MRS) sequences. The images were hand contoured using Multitracer software to quantify the brain parenchymal and CSF volumes. The volumteric data of the above groups was compared, and the volume data of the ZIKV exposed group was correlated with outcomes of the NICU Network Neurobehavioral Scale administered at full-term equivalent gestation and the Bayley-III assessment performed at 6 months of age using the Student's T-test and Pearson's correlation test.
Results: The findings in the ZIKV-exposed neonates include a) significantly decreased brain parenchymal and supratentorial volumes and increased CSF volume as compared to matched controls, and b) a positive association between brain parenchymal volume and Bayley-III Language and Cognitive Composite Scores.
Conclusions: Our preliminary results demonstrate some of the neonates exposed to ZIKV show Zika-associated brain and neurobehavioral abnormalities. Further evaluation of the DKI and MRS sequences will allow for additional conclusions regarding subtle changes in tissue microstructure and metabolic activity, respectively. Longitudinal collection of brain imaging and behavioral data will further refine the clinical impact of Zika disease.

Paper #: 129

Brain Network Architecture Correlates with Seizure-Free Outcome in Children Undergoing Epilepsy Surgery

Zili D. Chu, PhD, *zdchu@texaschildrens.org*; Wei Zhang, Michael Paldino, MD; Texas Children's Hospital, Houston, TX

Disclosures: All authors have disclosed no financial interests, arrangements or affiliations in the context of this activity.

Purpose or Case Report: Surgery is an important option in the management of medically refractory epilepsy. Yet even in ideal surgical cohorts, a significant fraction of patients (typically 35-45%) do not achieve seizure freedom. This failure reflects in large part that pediatric focal epilepsy is a disorder of widespread cerebral cortical networks; some of these network alterations are epileptogenic and can drive recurrent seizures after resection. The goal of this study, therefore, was to define the relationship between global network architecture and seizure-free outcome in children selected for surgical management of focal epilepsy.
Methods & Materials: This is a retrospective, IRB approved study. Patients were identified who underwent surgical resection for seizure management and had 3Tesla-MR before surgery, including rs-fMRI. Surgical outcomes were assessed using the Engel classification: 1. free of disabling seizures; 2. rare disabling seizures; 3. some improvement; 4. no improvement. Resting state fMRI images were co-registered to a T1-weighted structural image, corrected for motion, and high-pass filtered (0.01 Hz). Networks for each child were defined using an anatomic parcellation technique with subdivision of whole brain gray matter into approximately 750 nodes. An undirected graph was constructed based on the pair-wise correlation of node BOLD time series. The following topological properties were calculated: clustering coefficient, modularity, path length and efficiency. A multivariate statistical learning technique was used to measure the independent contribution of each metric (adjusting for age, sedation during MR, gender, seizure duration and pathologic diagnosis) to surgical outcome.
Results: Fifty-two patients met inclusion criteria (21 female, mean age 10.3 ± 5.42 years). Diagnoses included primarily focal cortical dysplasia (n=21) and mesial temporal sclerosis (n=15). Global efficiency, clustering coefficient, and pathologic diagnosis each made an independent contribution to prediction

of Engel outcome by the learning algorithm. Prediction of Engel class 1 outcome was driven by global efficiency; Engel class 4 prediction by clustering coefficient.
Conclusions: We observed characteristic global network signatures of good/poor outcomes after epilepsy surgery. These findings support the potential clinical relevance of brain network metrics in children with refractory epilepsy.

Paper #: 130

Using Connectome Mapping to Define a Target for Deep Brain Stimulation in Paediatric Dystonia

Ailish Coblentz[1], *ailish.coblentz@sickkids.ca*; Alexandre Boutet[2], Musleh Algarni[2], Gavin Elias[2], Lais Oliveira[2], Elysa Widjaja[1], George Ibrahim[1], Alfonso Fasano[2], Andres Lozano[2]; [1]The Hospital for Sick Children, Toronto, Ontario, Canada, [2]Toronto Western Hospital, Toronto, Ontario, Canada

Disclosures: Alfonso Fasano: Consultant, Honoraria: Abbvie, Boston Scientific, Medtronic, Royalty: Springer, Research Grants: Abbvie, Boston Scientific, Medtronic; **Andres Lozano:** Consultant, Honoraria:Medtronic, St. Jude, and Boston Scientific. All other authors have disclosed no financial interests, arrangements or affiliations in the context of this activity.

Purpose or Case Report: Dystonia is one of the most common paediatric movement disorders, and often the most difficult to manage. Deep brain stimulation (DBS) is a surgical treatment that modulates dysregulated motor circuits, and has been used in 321 medically refractory cases, with mixed outcomes. Factors preventing maximal benefit may include: heterogeneous disease aetiologies, suboptimal lead placement, and difficulty in programming. Surgical insertion currently relies on adult-derived techniques and anatomic targeting. During programming, the clinician chooses which electrical settings, e.g. voltage, provide the greatest clinical benefit to an individual patient. Choosing these individualised parameters can be a tedious and often imprecise trial-and-error process. It requires multiple clinic visits, and reliance on difficult clinical observations. With appropriate targeting and stimulation programming, DBS can produce striking clinical benefits. We hypothesized that the imaging of our DBS-implanted paediatric dystonia patients could inform us on which neural networks and tracts should be modulated, resulting in improved clinical outcomes.
Methods & Materials: We conducted a retrospective analysis of 11 paediatric dystonia patients who underwent Globus Pallidus internus (GPi) DBS insertion at our institution. DBS electrodes were localized and transformed into a normative brain space. Volume of tissue activated (VTA) was estimated and weighted according to their associated clinical outcomes. Normative data were then used to identify functional and structural networks associated with optimal clinical benefits.
Results: The majority of our patients demonstrated clinical improvement. Using standardized neurosurgical coordinates, the optimal area of stimulation was located at 22, -8, -2, within the posterior GPi. This anatomical locale resulted in the best clinical benefit and lowest side effect profile, as determined clinically. The most closely associated neural network areas were the bilateral basal ganglia, cerebellum, and prefrontal cortex, all of known importance in motor circuitry. White matter tracts associated with the greatest clinical improvement were also involved in motor circuitry.
Conclusions: Paediatric dystonia patients responded better to DBS treatment engaging specific networks and tracts of the motor circuit. These findings could be used to improve surgical technique and post-operative empiric electrical titration, thereby benefiting patients and their families through better care and clinical outcomes.

Paper #: 131

In the era of mTOR inhibitors for treatment of tuberous sclerosis complex, is MRI surveillance of subependymal giant cell atrocytoma growth reliable without gadolinium?

Ezekiel Maloney, MD, *eze@uw.edu*; A. Luana Stanescu, MD, Francisco Perez, MD, Ramesh Iyer, MD, Stephanie Randle, MD, Randolph K. Otto, MD, Dennis W. Shaw, MD; Radiology, Seattle Children's Hospital, Seattle, WA

Disclosures: All authors have disclosed no financial interests, arrangements or affiliations in the context of this activity.

Purpose or Case Report: Subependymal giant cell astrocytomas (SEGAs) are low grade tumors, typically found in patients with tuberous sclerosis complex (TSC). SEGAs have slow growth potential and can cause ventricular obstruction. Key characteristics to support SEGA diagnosis are: 1) enlargement on serial MRIs and 2) hydrocephalus caused by a subependymal lesion. TSC patients often undergo annual MRI of the brain with gadolinium based contrast media (GBCM) until 25 years old. If a SEGA is identified, therapies include surgery or mTOR inhibitors (mTORi). Response to mTORi's is variable, and determined by changes in tumor volume on MRI. Life-long mTORi therapy with extended imaging monitoring may be required to maintain therapeutic benefit. In the setting of increasing concerns regarding gadolinium retention in the body, we aimed to preliminarily assess utilization of non-GBCM-enhanced MRI sequences for identification of clinically meaningful changes in SEGA volume.
Methods & Materials: Following IRB approval, the medical records and imaging for an internal database of TSC patients seen at our tertiary pediatric referral center in the last 2 years were reviewed. Patients with SEGAs demonstrating "clinically meaningful growth" (resulting in SEGA diagnosis or offer of tumor directed intervention) on serial MRI exams were identified. Paired exams were reviewed by a subspecialty board certified pediatric neuroradiologist to determine changes in tumor volume first on non-GBCM-enhanced sequences (T2W, T1W), and subsequently on GBCM-enhanced T1W sequences. Wilcoxon rank sum tests were performed in R.
Results: Of 68 patients in the TSC database, 9 (13%) had SEGAs. 6 of these patients had 7 SEGAs that demonstrated clinically meaningful growth on serial MRI exams. For these exam pairs, the distribution in measured changes in tumor volume was not significantly different when assessed with non-GBCM-enhanced sequences versus GBCM-enhanced sequences (p= 0.96), or between non-GBCM-enhanced sequence assessments (p= 0.88). Changes in tumor volume ranged from 148% to 115,050% increase.
Conclusions: TSC patients often undergo a large number of GBCM-enhanced MRI exams. In our study, assessments of changes in SEGA volume on MRI were not significantly different between GBCM-enhanced and non-GBCM-enhanced sequences. Given the lack of clinical benefit, it is prudent to limit GBCM administration for routine MRI follow up of subependymal nodules and known SEGAs in patients with TSC.

Paper #: 132

Non-inferiority of a non-gadolinium-enhanced MRI follow up protocol for isolated optic pathway gliomas – interim analysis from a multi-reader-multi-case study

Ezekiel Maloney, MD[1], *eze@uw.edu*; A. Luana Stanescu, MD[1], Francisco Perez, MD[1], Ramesh Iyer, MD[1], Randolph K. Otto, MD[1], Jason Wright, MD[1], Sarah Menashe, MD[1], Daniel Hippe, MS[2], Dennis W. Shaw, MD[1]; [1]Radiology, Seattle Children's Hospital, Seattle, WA, [2]University of Washington, Seattle, WA

Disclosures: Daniel Hippe: Research Grants: GE, Philips, Siemens, Toshiba**.** All other authors have disclosed no financial interests, arrangements or affiliations in the context of this activity.

Purpose or Case Report: Pediatric patients with optic pathway gliomas (OPGs) undergo a large number of follow-up MRI brain exams with gadolinium based contrast media (GBCM). Gadolinium retention in children has motivated parsimonious use of GBCM. We previously determined that increased OPG size was the only isolated finding on MRI that motivated changes in tumor directed therapies. In a pilot case series, change in tumor size was readily identifiable on non-GBCM enhanced MRI sequences. Our purpose was to investigate this result in a blinded, non-inferiority, multi-reader-multi-case study.
Methods & Materials: Following IRB approval, power calculations were performed with pilot data. The primary endpoint was intra-reader agreement for ≥25% increase in greatest axial diameter cross-product measurement. A denominator OPG population was derived from a regional cancer registry at our tertiary pediatric referral center. Consensus tumor board notes were reviewed for each patient, with attention to: (1) isolated OPG status, (2) change or (3) stability in OPG size between two specific MRI exams. All instances of criteria 1 & 2 were incorporated in the case set. Cases meeting criteria 1 & 3 were incorporated in order of most recent clinical follow up, maintaining a 50% ratio of NF1:non-NF1 exams. Exams were standardized with non-GBCM-enhanced and GBCM-enhanced versions. 7 pediatric radiologists were assigned to a randomized case panel for 3 blinded sessions, spaced by at least 1 week. The first session excluded GBCM-enhanced sequences, the others did not. Interim statistical analysis was performed in R for 4 readers.
Results: Power calculations revealed that a ≥80% probability of rejecting, at the $\alpha = 0.05$ level, the null hypothesis of -12% (non-inferiority margin) difference in intra-reader assessments beyond background variability could be achieved with an "n" of 60 exam pairs, each interpreted by at least 4 readers. Exam pairs were compiled from 42 patients with isolated OPG (19 with NF1), from a population of 104 patients with OPG. There were 8 "size change" exam pairs from 7 NF1 patients and 20 "size change" pairs from 18 non-NF1 patients. Tumors encompassed a diverse anatomic spectrum. Interim analysis demonstrated an overall -3% difference (95% CI: -9.9, 3.1%) in intra-reader agreement when using a non-GBCM-enhanced protocol.
Conclusions: Interim analysis suggests that a non-GBCM-enhanced protocol is non-inferior to a GBCM-enhanced protocol for assessment of change in size of isolated OPGs on follow-up MRI exams.

Paper #: 133

Primary intracranial sarcoma in pediatrics: MRI findings

Carlos Ugas Charcape, Radiologist[1] *,drugas2801@gmail.com* Claudia I. Lazarte, MD[2], Osmar A. Pillaca[3], Waldemar Mamani[4], Nella P. Baca[5]; [1]Cleveland Clinic Abu Dhabi, Abu Dhabi, United Arab Emirates; [2] Instituto del Nino San Borja; [3] Clinica Internacional San Borja [4]; Hospital Nacional Daniel Alcides Carrion; Hospital II Luis Negreiros[5]

Disclosures: All authors have disclosed no financial interests, arrangements or affiliations in the context of this activity.

Purpose or Case Report: ***Background:*** Primary brain sarcomas are rare, with an incidence reported ranging from 0.1 to 4.3% of all cerebral tumors and with a high mortality. There is a paucity of literature depicting radiologic features in children. ***Objective:*** Describe the most frequent MRI findings of pediatric intracranial sarcomas.
Methods & Materials: We retrospectively analyzed the data of 12 consecutive pediatric patients (7 boys and 5 girls; mean age: 8 years) referred to two national paediatric centres who underwent MRI imaging within a 48-month period.
Results: The most frequent MR feature were the presence of hemorraghe and necrosis, both in 92% (n=11); diffusion restriction and presence of cystic component, both in 83% (n= 10); regular borders and homogenous intense enhancement, in 75% (n= 9) ; and finally 67% (n=8) of tumors were supratentorial and showed extension to the meninges. Perfusion was performed in 7 patients, all of them with increased perfusion. 8 patients had spectroscopy, 50% (n= 4) of this cases showed increased lactate, lipids and choline and decreased NAA.
Conclusions: In the setting of pediatric brain tumor with regular edges, diffusion restriction, hemorrhage, cystic component, homogenous intense enhancement and increased perfusion, we must consider primary intracranial sarcoma in the differential diagnosis.In the setting of pediatric brain tumor with regular edges, diffusion restriction, hemorrhage, cystic component, homogenous intense enhancement and increased perfusion, we must consider primary intracranial sarcoma in the differential diagnosis.

Paper #: 134

Thalamic lesion in Leigh syndrome: An unusual finding mimicking Percheron artery infarct

Sara R. Teixeira, *teixeiras@email.chop.edu*; Cesar Augusto Alves, M.D, Fabricio G. Goncalves, Karuna Shekdar, MD, Juan S. Martin-Saavedra, MD, Colleen Muraresku, Amy Goldstein, Giulio Zuccoli, Children's Hospital of Philadelphia, Philadelphia, PA

Disclosures: All authors have disclosed no financial interests, arrangements or affiliations in the context of this activity.

Purpose or Case Report: Leigh syndrome (LS) (subacute necrotizing encephalopathy) is a rare mitochondrial cytopathy (MC) that commonly evolve in severe neurological impairment and death in childhood. LS is caused by different genetic mutations and, therefore, may yield variable imaging patterns. Classic imaging findings of LS are abnormal signal intensity of the basal ganglia and brainstem. However, unusual imaging findings can also be seen but have been rarely described in the literature. The purpose of this study is to describe the prevalence and the pattern of unusual lesions involving the thalami in patients with LS.
Methods & Materials: This is a retrospective study approved by the Institutional Review Board (IRB). Over a 19-year period

(2000-2018), a search for MC in the clinical and radiological database of a single academic children's hospital was performed. Inclusion criteria were: confirmed genetic mutation related to MC, available brain magnetic resonance imaging (MRI), and final diagnosis of LS. Diagnosis of LS was an according to the previous clinical described criteria retrieved from the medical notes. MRIs were reviewed on a standardized fashion by experienced pediatric neuroradiologists. Statistical analysis was performed accordingly.
Results: Out of 105 patients with confirmed genetic mutation of MC and available brain MRI, 34 met our inclusion criteria with a diagnosis of LS. Fifteen percent (N = 5) of the patients had bilateral thalamic lesions. Of these, 60 % (N = 3) had a stroke-like appearance similar to the Percheron artery infarction (selective bilateral medial thalamic involvement). All of the patients had oxidative phosphorylation deficiency involving the Complex I proteins. Specifically, underlying mutations were present in the genes NDUFS8, NDUFS4, ND3, and 2 patients with mutation in the gene ND5. All 3 patients with an imaging pattern mimicking the Percheron artery infarct had mitochondrial DNA defects in the ND3 and N5 genes. In all of the 5 patients, MRI showed at least one other lesion classically described in LS (brainstem and/or basal ganglia abnormalities).
Conclusions: Thalamic lesions may be present in LS. Our analysis demonstrated that lesions mimicking Percheron artery infarction may be seen in LS. This pattern must be considered in the differential diagnosis in the context of mitochondrial disorders.

Paper #: 135

Introduction of Targeted Rapid Knee MRI exam using T2 Shuffling into Clinical Practice: Retrospective Analysis on Image Quality, Cost and Scan Time

Jon Tamir, PhD[2], *jtamir@berkeley.edu*; Jesse Sandberg, M.D.[1] Fidaa Wishah, MD[1], Michael Lustig, PhD[2], Marcus Alley[3], Shreyas Vasanawala, MD/PhD[1]; [1]Radiology, Lucile Packard Children's Hospital - Stanford University, Palo Alto, CA, [2]University of California, Berkeley, Berkeley, CA, [3]Radiological Sciences Laboratory, Stanford University, Stanford, CA

Disclosures: Jon Tamir, PhD: Consultant, Honoraria & Equity Interest/Stock Option: Subtle Medical, Research Grants: GE Healthcare; **Marcus Alley, PhD:** Consultant, Honoraria: Arterys, Research Grant: GE Medical Systems; **Shreyas Vasanawala, MD/PhD:** Arterys, Royalty:Arterys, GE Healthcare, Siemens, Philips, Research Grants: GE Healthcare. All other authors have disclosed no financial interests, arrangements or affiliations in the context of this activity.

Purpose or Case Report: Volumetric fast spin echo (FSE) of the knee using T2 shuffle (T2Sh) technique has previously been described as being comparable to traditional 2D imaging. T2Sh has the added advantage of being a rapid single-scan 4D multiplane reformattable sequence for pediatric knee examinations. The purpose of this study is to investigate the feasibility and effectiveness of a targeted rapid pediatric knee MRI exam after introduction into clinical practice, with the goal of reducing cost and enabling same-day MRI access.
Methods & Materials: In an institutional review board approved study with informed consent/assent, we implemented a targeted pediatric knee MRI exam on three 3T scanners for assessing pediatric knee pain. The 10-minute protocol was based on T2 Shuffling, a four-dimensional acquisition that permits volumetric reconstruction of images with variable T2 contrast, and a single T1 2D FSE sequence. To enable a clinically feasible image reconstruction time, a distributed, compressed sensing-based iterative reconstruction was implemented on a local four-node high-performance compute cluster and integrated into the clinical scanner and PACS workflow. Pediatric patients were sub-selected for the exam based on insurance plan and clinical indication. Over a two-year period, 47 subjects were recruited for the study and 49 MRIs were ordered. Date and time information was recorded for MRI referral, registration, and completion. Descriptive statistics were also analyzed. Image quality was also assessed from 0 (non-diagnostic) to 5 (best anatomy delineation) by two radiologists, consensus was subsequently reached.
Results: Of the 47 subjects, 18 completed the exam on the same day as their referral. Median time from registration to exam completion was 18.7 minutes. Median end-to-end reconstruction time for the T2 Shuffling sequence was reduced from 18.8 minutes to 95 seconds using the distributed implementation. Technical fees charged for the targeted exam were one third that of the routine clinical knee exam. Image quality was assessed as 5/best delineation in 69.4% of cases, 4/very good in 16.3%, 3/good in 12.2% and 2/limited in 2.1%. No exams were deemed non-diagnostic or poor quality. No subject had to return for additional imaging.
Conclusions: The targeted knee MRI exam is feasible and reduces imaging time, cost, and barrier to same-day MRI access for pediatric patients.

Paper #: 136

Silent and Distortionless Diffusion MRI

Jesse Sandberg, MD[1], *jesseksandberg@gmail.com*; Jianmin Yuan, PhD[4], Yuxin Hu[5], Christopher Sandino[5], Anne Menini[2], Brian Hargreaves, PhD[3], Shreyas Vasanawala, MD/PhD[1]; [1]Department of Pediatric Radiology, Lucile Packard Children's Hospital, Stanford University, Stanford, CA, [2]Application Science Lab, GE Healthcare, Menlo Park, CA, [3]Department of Radiology, Stanford University, Stanford, CA, [4]Radiological Sciences Laboratory, Stanford University, Stanford, CA, [5]Department of Electrical Engineering, Stanford University, Stanford, CA

Disclosures: Christopher Sandino, M.S.: Financial Interest: General Electric Healthcare - Salary: Independent Contractor; **Shreyas Vasanawala, MD/PhD:** Arterys, Royalty: Arterys, GE Healthcare, Siemens, Philips, Research Grants: GE Healthcare. All other authors have disclosed no financial interests, arrangements or affiliations in the context of this activity.

Purpose or Case Report: Diffusion weighted (DW) imaging is a standard component of many MRI exams. However, with large diffusion encoding gradients and echo-planar imaging (EPI), DW-EPI is challenged in pediatrics by loud noise that distresses children and may cause motion artifacts. Further, DW-EPI suffers from image distortion, which is particularly problematic in children and extremity imaging. Thus we aim to develop and validate a novel silent and distortionless DWI method.
Methods & Materials: A multi-segmented Rotating Ultra-Fast Imaging Sequence (RUFIS) was modified with sinusoidal diffusion preparation gradients. The images were reconstructed with the total variation constraint. Phase cycling was used to reduce eddy current effects. Image contrast, apparent diffusion coefficient (ADC) and distortion were evaluated with a diffusion phantom (Model 128, High Precision Devices, Boulder, CO), with DW-EPI as gold standard (b50, b800). Acoustic noise levels with DW-RUFIS, standard DW-EPI, and no sequence were measured with a power monitor. With IRB approval and informed consent/assent, 80 consecutive pediatric patients (mean age 12.7 years, range 2-19) referred for extremity scans at 3T (MR750, GE Healthcare) were recruited (July 2018-October 2018) to undergo DW-RUFIS, and for comparison purposes 17 of those also underwent DW-EPI. DW-RUFIS parameters: FOV: 160x160 mm, matrix: 128x128, slice

thickness: 4mm, NEX: 2.5, b-values: 50 and 400. Scan time for two b-values for DW-EPI is 1 minute and DW-RUFIS is 6 minutes. ADC values of both sequences in knee exams (10 cases) were compared in bone and muscle (two-sample t-test). Artifacts were also compared.
Results: From the phantom scans, the diffusion contrast for DW-EPI and DW-RUFIS sequences are similar (visualization of pathology and anatomy). The ADC measurement of DW-RUFIS correlates well with DW-EPI ($R^2 = 0.99$). DW-EPI was louder than RUFIS-DWI (85±2.4dB vs 54±2.4dB) and ambient noise (51±2.8dB). In the cohort of sequential in-vivo knee examinations, DW-RUFIS and DW-EPI ADC values in both bone and muscle had no significant difference (p=0.88 and p=0.67 respectively). DW-EPI suffers from large image distortion near the skin surface; while DW-RUFIS is distortion free.
Conclusions: Silent distortionless diffusion is feasible and has comparable diffusion contrast and ADC measurements with conventional DW-EPI in cartilage and bone. Future work will be directed to incorporating acceleration to shorten scan time and assessment in other organs/applications.

Paper #: 137

Novel Functional BOLD MR Imaging Techniques for Assessment of Juvenile Dermatomyositis: Preliminary Results

Paymun Pezeshkpour, B.Sc.,
paymun.pezeshkpour@mail.utoronto.ca; Jessica Caterini, Greg Wells, Afsaneh Amirabadi, Carina Man, Tammy Rayner, Ruth Weiss, Brian Feldman, Andrea Doria, MD; Hospital for Sick Children , Toronto, Ontario, Canada

Disclosures: All authors have disclosed no financial interests, arrangements or affiliations in the context of this activity.

Purpose or Case Report: Juvenile dermatomyositis (JDM) causes diffuse vasculitis and proximal muscle inflammation. Searching for highly sensitive non-invasive methods for early diagnosis and treatment follow-up is key in this disease. We investigated blood-oxygen level-dependent (BOLD) MRI to detect physiologic changes at different levels of severity of JDM as compared to age-matched healthy control subjects.
Methods & Materials: Six JDM patients of 11-15 years (12.9 ± 1.6 years) and 6 age and sex-matched healthy controls (13.29 ± 1.50 years; 6 males and 6 females) completed the study. Participants performed 3 cycles of one-minute up-down exercise on a MRI-compatible cycle ergometer at 65 % of maximum workload, with 2 minutes of rest between each bout. BOLD MRI images were acquired immediately following exercise at 3T. Parameters of 10-min BOLD EPI gradient echo sequence were: TR/TE = 250/40 ms, flip angle = 90^0, FOV = 25 mm, matrix = 64x64 and slice thickness/gap = 10/0 mm. In addition, Childhood myositis assessment scale (CMAS) was collected as an indicator of disease progression. BOLD signal response in the vastus medialis (VM) and intermedius (VI) muscles during recovery were fitted to a sigmoid model with β, half-time point for recovery of intensity curve; α, response time and wash-out of deoxyhemoglobin; and κ, range of recovery from baseline. in JDM compared to healthy subjects following recovery from exercise.
Results: A comparison of BOLD signals between control and JDM subjects in VM and VI demonstrated a significant difference for the first half-time point for β of VM ($p = 0.04$). In addition, when adjusted for the CMAS score, the second recovery β for VI and the first for VM were significant ($p = 0.03$ and 0.02). However, all other variables showed no significant difference after adjusting for CMAS.
Conclusions: Our BOLD MRI sigmoid model at 3T allowed us to differentiate vascular and oxygenation changes in the quadriceps muscle between JDM and control cohorts in recovery re-oxygenation after exercise. Therefore, BOLD MRI may be useful to characterize early disease and monitor effects of therapy or exercise as adjuncts to conventional laboratory and clinical assessments of JDM.

Paper #: 138

MR-HIFU: What the Pediatric Radiologist Should Know

Narendra S. Shet, MD, *narendras@gmail.com*; jonathan Zember, MD, Pavel Yarmolenko, PhD, Caitlin Tydings, MD, AeRang Kim, MD, PhD, Karun Sharma; Children's National Medical Center, Washington, DC

Disclosures: All authors have disclosed no financial interests, arrangements or affiliations in the context of this activity.

Purpose or Case Report: Magnetic resonance imaging–guided high-intensity focused ultrasound (MR-HIFU) is a novel technology that integrates magnetic resonance imaging with therapeutic ultrasound. Although clinical experience in pediatrics is relatively small, the advantages of a completely noninvasive, precise, and radiation-free tumor therapy is especially attractive to growing children. Pediatric radiologists should be familiar with clinical applications of MR-HIFU, including pre- and post-procedure imaging protocols, treatment imaging, and post-treatment imaging assessment. To this end, we review applications of MR-HIFU in children and present cases from our institution to highlight the post-treatment MR-imaging findings and evolution of treated lesions over time.
Methods & Materials: Under IRB approved clinical protocols, 15 patients (age 7-21 years) with symptomatic benign (osteoid osteoma), locally aggressive (Desmoid tumor) and refractory malignant (Sarcoma) tumors have undergone MR-HIFU therapy at our institution since 2017. Pre-treatment diagnostic MRI scans, treatment imaging, and post-treatment follow-up MRI scans were reviewed. In addition to standard musculoskeletal MR sequences, volumetric 3D T2 weighted sequences as well as pre- and post-contrast axial fat-saturated T1 weighted sequences with subtraction imaging were obtained. Imaging findings were correlated with clinical history and follow-up course.
Results: We will present MRI findings from patients treated with MR-HIFU. Preprocedural, intraoperative, and postprocedural imaging findings will be discussed, and sample MRI protocols will be presented, detailing the purpose of essential sequences.
Conclusions: Our preliminary institutional experience with MR-HIFU has been educational for our pediatric radiology and oncology teams. There are currently ongoing studies for MR-HIFU therapy for a treatment of a variety of tumors as well as for enhanced local drug delivery. As use of this novel therapy expands in the pediatric population, it is important for diagnostic radiologists to have a basic understanding of the nature of the procedure as well as what to expect on imaging studies. Furthermore, close collaboration between radiologists and oncologists will be essential to determine the relationship between imaging findings and clinical response.

Paper #: 139

Intra-Operative Contrast-Enhanced Ultrasound of Infant Hips: A Comparison with Post-Operative MRI and Correlation with Development of Femoral Head Avascular Necrosis

Travis Matheney, MD,
travis.matheney@childrens.harvard.edu; Carol E. Barnewolt, MD, Harriet Paltiel, M.D.; Boston Children's Hospital, Boston, MA

Disclosures: All authors have disclosed no financial interests, arrangements or affiliations in the context of this activity.

Purpose or Case Report: Avascular necrosis (AVN) is a significant complication following surgical treatment of infant hip dislocation. One risk factor is post-operative decreased femoral enhancement on contrast-enhanced MRI (CEMRI). Ultrasound is the gold standard to evaluate infant hip dysplasia. Contrast-enhanced ultrasound (CEUS) has been utilized for over 20 years to assess tissue perfusion in real time. The goals of this study were to compare CEUS to CEMRI in assessing femoral head perfusion and to compare the ability of CEUS and CEMRI to predict AVN.
Methods & Materials: Institutional review board approval was obtained and retrospective analysis performed of cases undergoing closed or open reduction and intraoperative assessment by CEUS using Perflutren microspheres administered intravenously. This agent is currently FDA-approved for evaluation of focal liver lesions in children. CEUS was performed before and after hip reduction in planned casted position. CEMRI and CEUS appearance were graded as: fully enhancing, partially decreased or globally decreased enhancement. Four patients underwent a second CEUS assessment at a second procedure. Agreement between intra-operative CEUS and early post-operative CEMRI was analyzed; AVN was later graded following the most recent reduction at a minimum of one year.
Results: Twenty procedures were analyzed comparing CEUS and CEMRI. There were 16 patients, 38% male; average age 8 months (range 4-17). Sixty-eight percent were open reductions. Agreement between enhancement grade on US and MRI was good for normal versus partial/global decreased enhancement (k=0.73; 95% CI = 0.24 to 1.22). Fourteen hips (70%) were followed a minimum of 1 year post-reduction (12-45 months) and assessed for presence of AVN. Three hips developed AVN (21%; 95% CI = 6 to 51%). Based on ROC analysis, diagnostic utility was nearly the same for CEUS and CEMRI (= 0.74; 95% CI = 0.35 to 1.00 and AUC_{MRI} = 0.77; 95% CI = 0.39 to 1.00, respectively). AVN was diagnosed at follow-up where decreased enhancement was noted on CEUS in 71% (67% sensitivity; 73% specificity) and on CEMRI in 77% (67% sensitivity; 80% specificity). This is similar to previous CEMRI reports after closed reduction.
Conclusions: CEUS appears to be a viable method of assessing infant hip perfusion with overall good correlation with post-operative CEMRI. Further study is required to determine whether CEUS will provide adequate real-time feedback to aid in successful reduction while reducing the incidence of postoperative AVN.

Paper #: 140: ***Withdrawn***

Paper #: 141

A Multidisciplinary Approach Leads to More Efficient Magnetic Resonance Imaging, Less Use of Contrast Material, and Improved Clinical Outcomes During Musculoskeletal Infection Evaluation

Matthew R. Hammer, MD[1]
Matthew.Hammer@utsouthwestern.edu; Eduardo A. Lindsay, MD[2], Naureen G. Tareen, MPH[2], Jonathan R. Friedman, MD[1], Lawson A. Copley, MD[2]; [1]Children's Health / UTSW, Dallas, TX, [2]Children's Health, Dallas, TX

Disclosures: All authors have disclosed no financial interests, arrangements or affiliations in the context of this activity.

Purpose or Case Report: The diagnosis of musculoskeletal infection (MSI) in children frequently involves the use of magnetic resonance imaging (MRI), which often involves general anesthesia and the administration of intravenous contrast material. This study assesses the impact of a coordinated, inter-disciplinary approach to MRI efficiency as well as the use and utility of intravenous contrast material.
Methods & Materials: Children who underwent MRI for possible MSI between July 2012 and June 2018 were retrospectively studied under IRB approval. The MSI program involved many disciplines, including radiology and orthopaedics, which met before and during the scans for planning and immediate study interpretation to guide surgical decision making. Data collected included: MRI duration and parameters, use of intravenous contrast material, percentage of children taken to surgery immediately following MRI, and satisfaction with the hospital experience. Kruskal-Wallis test was used to periodically assess process improvement, followed by multiple comparisons using a Mann-Whitney test with Bonferroni Adjustment (alpha=0.017). A fisher's exact test was used to compare periodic improvement for categorical data ($p<0.05$).
Results: There were 526 children evaluated during the study period. MRI scan duration decreased from a mean of 81.7 minutes in 2012 to 24.4 minutes per study in 2018. This was attributed to scanning of fewer body areas (2.6 vs. 2.0) and obtaining fewer sequences per scan (8.2 vs. 3.9). In 2012, 87.8% of children received intravenous gadolinium-based contrast material compared to 8.5% in 2018. Contrast material administered was felt to be beneficial retrospectively in only 4.3% (15/346). Procedures were performed immediately after the MRI under continued anesthesia on 54.5% of children with indications in 2012, compared to 85.7%% in 2018. NRC Picker Satisfaction rating rose from 91% in 2012 to 100% in 2018. All differences were statistically significant ($p<0.05$).
Conclusions: A multidisciplinary team approach produced consistent improvement over time as evidenced by decreased MRI scan time, fewer sequences per scan, decreased use of intravenous contrast, and a higher rate of definitive procedures immediately following the MRI while under continued anesthesia. This study supports the practice of minimizing contrast use for children with suspected musculoskeletal infection with a team approach that improves patient care and satisfaction.

Paper #: 142

Value of Functional T2 Map MRI in the Assessment of Early Cartilage Degeneration of Pediatric Patients with Hemophilia

Haris Majeed, BSc[1], Marshall Sussman, PhD[2], Brian Feldman[1], Carina Man[1], Victor Blanchette[1], **Andrea Doria, MD[1]**, *andrea.doria@sickkids.ca*; [1]The Hospital for Sick Children, Toronto, Ontario, Canada, [2]Toronto General Hospital, Toronto, Ontario, Canada

Disclosures: All authors have disclosed no financial interests, arrangements or affiliations in the context of this activity.

Purpose or Case Report: Despite efforts of clinical research for hemophilia, evaluating internal cartilagederangement has been challenging. T2 map MRI enables identification of disarrangements in collagen fibers alignment prior to macroscopic cartilage degeneration in hemophilic arthropathy. Thus, recognizing relationships between cartilage maturation and degeneration by T2 map MRI is key in children/adolescents with hemophilia and age-matched control boys.
Methods & Materials: A cross-sectional study was conducted in ankles of males with hemophilia (n = 19) and of healthy controls (n = 16, aged 7-17 years), and in knees of males with hemophilia (n = 9) and of healthy controls (n = 7, aged 5-17 years) employing a multiecho spin-echo T2-weighted sequence at 3.0 T. T2 map relaxation times of pathologic ankle (tibia-talus) and knee (femur-tibia) cartilages were compared to that of age- and sex-matched healthy individuals and with a clinical structural MRI scale, the International Prophylaxis Study Group (IPSG) scale. An associational analysis was performed of pediatric age versus T2 relaxation times for ankle/knee cartilage.
Results: Predominantly significant differences were found between median T2 map relaxation times for hemophilia and healthy subjects' ankles/knees. Mean T2 map relaxation times in hemophilic and healthy ankles ranged from 36.6-59.4 ms, whereas 39.8-54.4 ms in the knees.Strong negative associations were found between pediatric age and T2 map relaxation times for the cartilage of hemophilia and healthy subjects' ankles/knees. Hence suggesting that T2 map relaxation times in ankle/knee cartilage decrease with increasing pediatric age, regardless of healthy or pathologic status of joints. We assessed the estimated mean of ankle/knee cartilage T2 map relaxation times by combining age, soft tissue, osteochondral, and total IPSG scores at 4 regions of interest in a multilinear regression model. Regression coefficients were found statistically significant for age for all regions in both ankles and knees. Mean mean regression coefficient for age was -1.5 ms/year ($P < 0.01$), while holding structural MRI joint scores constant.
Conclusions: T2 map MRI can be used as an adequate measure to study future cartilage degeneration in pediatric patients with hemophilia, allowing clinicians to better understand disease progression and manage treatment decisions.

Paper #: 143

Role of DWI in detecting early satage of sacroiliac joint lesions in children with enthesitis related arthritis

Lin Xu, *13482518105@163.com*; Yumin Zhong; Shanghai Children's Medicial Center, Shanghai, China

Disclosures: All authors have disclosed no financial interests, arrangements or affiliations in the context of this activity.

Purpose or Case Report: To investigate value of DWI in detecting early inflammation of sacroiliac joints in children with enthesitis related arthritis (ERA).
Methods & Materials: Totally 20 patients with clinical diagnosed ERA (ERA group) and 20 normal children (control group) were enrolled, all of them were aged 6-16 years old. The MRI were performed, including T1WI, spectral attenuated inversion recovery (SPAIR) T2WI and DWI (b value were 0 and 400 s/mm^2). The MRI feasures of sacroiliac joints were observed. The ADC value of all sacroiliac joints were measured and were compared between the two groups. The ROC curve was used to evaluate the diagnositc efficacy of ADC value on ERA.
Results: In ERA group, 17 patients showed high signal intensity at sacroiliac joints on SPAIR images and 3 were normal, and 16 patients showed high signal intensity on DWI and 4 were normal. In control group, 12 children were nornal on SPAIR images and 8 showed high signal intensity at sacroiliac joints, and15 children were nornal on DWI images and 5 showed high signal intensity. The ADC value in ERA group and control group was (1.24±0.32)×10-3 mm^2/s and (0.69±0.24)×10-3 mm^2/s, respectively (t=14.466, P=0.001). Taking ADC=0.87×10-3 mm^2/s as the threshold, the AUC of ROC curve in diagnosis of ERA were 0.834 (P=0.023), with the sensitivity, specificity and diagnostic accuracy, of 87.50%, 77.50% and 82.50%, respectively.
Conclusions: DWI is a sensitive method for displaying the inflammation of the sacroiliac joint in patiens with ERA. Quantitive analysis of ADC value shows high value in detecting the early inflammation in the sacroiliac joints.

Paper #: 144

Stable versus unstable osteochondral lesions of the elbow: Performance of MR imaging criteria for instability

Jie C. Nguyen, MD, MS[1], *nguyenj6@email.chop.edu*; Andrew J. Degnan, MD, MPhil[1], Theodore Ganley, MD[1], Christian A. Barrera, M.D.[1], Thor Perrin Hee[1], Richard Kijowski, MD[2]; [1]Radiology, Children's Hospital of Philadelphia, Philadelphia, PA, [2]University of Wisconsin, Philadelphia, PA

Disclosures: All authors have disclosed no financial interests, arrangements or affiliations in the context of this activity.

Purpose or Case Report: To retrospectively compare the performance of previously described magnetic resonance (MR) imaging criteria for the detection of instability in children with osteochondral lesions (OCL) of the elbow with clinical and arthroscopic findings as reference standards.

Methods & Materials: This IRB-approved, HIPAA compliant retrospective study included 45 elbow OCLs with MR studies from 43 children (mean age 13.1 years; range 9-17 years, 27 boys & 16 girls) diagnosed between April 1 2010 and May 31, 2018. Twenty-one lesions were stable, determined using arthroscopy or clinical assessment and 24 lesions were unstable, determined during arthroscopy. Two radiologists, blinded to clinical data, reviewed to determine the presence T2 high signal intensity rim, T2 dark signal intensity rim, surrounding cysts, subchondral disruption, overlying cartilage degeneration, fluid-filled osteochondral defect, and intra-articular fragments. The inter-observer agreement was evaluated with weighted-kappa. Kappa scores (k) of 0.41– 0.60, 0.61– 0.80 and ≥ 0.80 were regarded to be indicative of moderate, good, and excellent agreement, respectively. Fisher Exact and Mann Whitney U tests were used.
Results: Demographic characteristics of children with stable and unstable OCLs demonstrated no difference in age (p = 0.638) or symptom duration (p = 0.646). Fluid-filled osteochondral defects (k = 0.76, p = 0.02) and the presence of subchondral disruption (k = 0.81, p = 0.01), overlying cartilage degeneration (k = 0.79, p = 0.006), and intra-articular fragment (k = 0.66, p = 0.01) were significantly more common with

unstable OCLs. Lesion size ($p = 0.337$) and the presence of T2 high signal intensity rim ($k = 0.78$, $p = 0.28$), T2 dark signal intensity rim ($k = 0.65$, $p = 0.68$), and surrounding cysts ($k = 0.70$, $p = 0.19$) were not significantly different between stable and unstable OCLs. Although, unstable OCLs were more likely to have larger cysts (up to 7mm) and more cysts (up to 5 cysts) than stable OCLs (up to 5mm and up to 2 cysts, respectively).
Conclusions: Only some of the previously described MR imaging criteria for lesion stability for the knee joint can be applied to predict stability of lesions in the elbow joint. This may be due to the high prevalence of unstable lesions presenting with a displaced fragment at the time of diagnosis.

Paper #: 145

Abdominal Wall Thickness in Children Correlates with Hepatic Steatosis

Lisa K. Harris, MD[1], *lisa.katherine.harris@gmail.com*; Nicholas Dubay[2], Sandra M. Allbery, MD[1], Jihyun Ma[3]; [1]Children's Hospital and Medical Center, Omaha, NE, [2]Creighton University, Omaha, NE, [3]University of Nebraska Medical Center, Omaha, NE

Disclosures: All authors have disclosed no financial interests, arrangements or affiliations in the context of this activity.

Purpose or Case Report: Pediatric obesity is a serious health concern that affects 18.5% of US children and adolescents, but is significantly under reported by radiologists on imaging. The purpose of this study is to evaluate for any association of lateral abdominal wall thickness (LAWT) with histopathologic hepatic steatosis or other serious medical conditions. This may have implications on radiologic reporting of obesity.
Methods & Materials: IRB approval obtained. Retrospective imaging and chart review performed on all patients undergoing ultrasound guided liver biopsy at tertiary care children's hospital during a 5 year period (03-01-2013 to 03-01-2018). Images reviewed to record LAWT in the mid axillary line, obtained to gauge needle depth for the biopsy. LAWT was measured from the skin surface to the liver capsule. Medical records reviewed for age, sex, BMI, blood pressure, cholesterol levels, diagnosis of diabetes, and histopathologic biopsy result. Descriptive statistics included counts and percentages for categorical data and means, standard deviations, medians, minimums and maximums for continuous data. Pearson correlation coefficients were used to describe association of LAWT variable with other continuous variables. Two by two tables were presented to evaluate accuracy, sensitivity, specificity, positive predictive value, and negative predictive value for steatosis. ANOVA and Chi-square test were used to determine the dependency of the LAWT measure. $P<0.05$ was considered statistically significant.
Results: 166 liver biopsies in 151 patients, 95 male and 56 female, were reviewed. Hepatic steatosis with or without fibrosis was present in 67/166 (40.4%) of patients; 4/51 (7.8%) age 0-4, 6/16 (37.5%) age 5-9, and 57/99 (57.6%) age 10-19. There was a statistically significant association between LAWT and histopathologic hepatic steatosis ($p <0.001$), BMI independent of age ($p <0.0001$), systolic blood pressure in patients 10-19 ($p <0.0001$), and diagnosis of diabetes mellitus type 2 ($p < 0.002$). Sensitivity, Specificity, PPV, and NPV for LAWT predicting hepatic steatosis were 65.7%, 90.9%, 83%, 79.7% for >2 cm thickness and 37.3%, 99%, 96.2%, 70% for > 2.67 cm thickness, respectively.
Conclusions: Our results suggest that increasing lateral abdominal wall thickness correlates with statistically significant increased frequency of hepatic steatosis and other serious medical conditions; therefore, radiologists should consider reporting this finding.

Paper #: 146

Automated Sonographic Assessment of Fatty Liver in Pediatric Patients

Eugene Cheah[1], Theodore T. Pierce, M.D.[1], Arinc Ozturk, MD[1], Masoud Baikpour[1], Laura Brattain[1], **Michael S. Gee[2]**, *msgee@mgh.harvard.edu*; Anthony E. Samir, M.D.[1]; [1]Center for Ultrasound Research & Translation, Department of Radiology, Massachusetts General Hospital, Boston, MA, [2]Division of Pediatric Radiology, Department of Radiology, Massachusetts General Hospital, Boston, MA

Disclosures: Anthony E. Samir, M.D.: Consultant, Honoraria: General Electric, Pfizer, Bristol Myers Squibb, Research Grants: General Electric, Phillips. All other authors have disclosed no financial interests, arrangements or affiliations in the context of this activity.

Purpose or Case Report: To demonstrate the feasibility and accuracy of automatically extracted sonographic skin-to-liver-capsule distance (SCD) measurement as a biomarker for fatty liver in the pediatric population.
Methods & Materials: This institutional review board approved single-institution retrospective study evaluated consecutive pediatric patients, ages 2 to 18, who underwent abdominal ultrasound from February 2018 to September 2018. Diagnosis of fatty liver, obtained through the electronic medical record, was recorded on the basis of clinical notes, prior imaging tests, and liver biopsy pathology when available. Body mass indices (BMI) and normalized Z-scores using CDC's growth charts, were also extracted. Duplicate patients and those with absent clinical information or imaging were excluded. Using manually measured SCD as a reference standard, an image processing algorithm was developed to automatically extract the SCD measurement from manually selected B-mode images (one image per patient). Image processing steps included: 1) Region of Interest (ROI) placement, 2) image denoising (Gaussian filter), 3) contrast enhancement, 4) canny edge detection, 5) connected components detection using the binary image derived from step 4, 6) skin and Glisson capsule border detection, and 7) SCD calculation (distance between the detected skin and capsule). Receiver operating characteristic (ROC) curve analysis was performed to assess the diagnostic performance of BMI Z-scores and the SCD measurements for fatty liver.
Results: 174 patients, including 26 with hepatic steatosis, were analyzed (mean age 125.6±54.1 months, 74 males, 100 females). The root-mean-squared error (RMSE) between manually and automatically extracted SCD measurements was 5.06 mm. The area under the ROC curve (AUROC) for prediction of fatty liver was calculated to be 0.905 (95%CI: 0.856-0.954) for the BMI Z scores, 0.889 (95%CI: 0.818-0.961) for the manual SCD measurements, and 0.770 (95%CI: 0.668-0.873) for the algorithm-measured SCD.
Conclusions: In addition to BMI, sonographic SCD can be considered as a biomarker of hepatic steatosis. Measurement of SCD can be automated with acceptable accuracy. The benefits of using sonographic SCD rather than liver echogenicity as a biomarker are threefold: 1) it is faster, 2) can be performed at the point of care, and 3) reduces operator dependence compared with interpretation of B-mode ultrasound liver images.

Paper #: 147

Biexponential T2* relaxation model for estimation of liver iron concentration in children: A better fit for high liver iron concentrations

Christian A. Barrera, M.D., *barreracac@email.chop.edu*; Dmitry Khrichenko, Suraj Serai, Helge Hartung, David M. Biko, MD, Hansel J. Otero, MD; Radiology, The Children's Hospital of Philadelphia, Philadelphia, PA

Disclosures: David M. Biko, MD: Financial Interest: Wolters Kluwer - Royalty: Editor of Review Book. All other authors have disclosed no financial interests, arrangements or affiliations in the context of this activity.

Purpose or Case Report: To compare biexponential analysis of T2* relaxation of the liver in children with iron deposition disease to the more commonly used monoexponential model and establish its relation with different levels of iron overload in children.
Methods & Materials: All MRI studies performed for determination of liver iron concentration (LIC) performed in our institution between 2007 and 2017 that included T2* sequences were included. LIC was calculated using Monoexponential T2* (MonoExp) and Biexponential T2* (BiExp) models using both commercially available and an in-house developed software. The calculations were based on ROIs including the entire liver (ROI1), the periphery of the liver (excluding the major vessels) (ROI2) and the spleen (ROIcontrol). The LIC results were classified as normal (< 3.2 mg/dL), mild (3.2 - 7 mg/dL), moderate (7 - 15 mg/dL), and severe (> 15 mg/dL) as per commonly used treatment guidelines. Residuals and residuals ratios were calculated for each model (MonoExp and BiExp) in order to identify the best fitting model on each LIC category. A MonoE/BiExp residual ratio > 1.5 was considered to have a biexponential trend. Non-parametric tests and correlations were used, $p < 0.05$ was considered significant.
Results: 182 patients (110 boys, 71 girls) with a mean age of 12.3 years (range or SD) were included in the analysis. For both ROI1 and ROI 2, there was a near perfect agreement between MonoExp using the commercial and the in-house software ($r = 0.98$, $p < 0.001$, and $r = 0.99$, $p < 0.001$, respectively). According to the MonoExp/BiExp residual ratio, the BiExp model fits better in patients with a LIC > 15 mg/dL (ROI1: ratio = 11.5, $p < 0.001$ and ROI2: ratio = 2.3, $p < 0.001$). For those with a biexponential best fit (n = 38), the proportion of slow (second) component was 0.06 (range 0.01 - 0.11). In the internal control ROI (spleen), the MonoExp/BiExp ratio was not significantly different among different LIC categories ($p = 0.46$).
Conclusions: Biexponential T2* relaxation model for LIC estimation fits better than the monoexponential model in patients with severe iron overload (LIC > 15 mg/dL) and can be used to more accurately determine LIC in these patients. The proportion of slow (second) component of the model might be related to the intra-cellular iron in the liver.

Paper #: 148

R2-Relaxometry MRI for estimation of Liver Iron Concentration. A comparison between two methods.

Juan S. Calle Toro, MD, *ctjuans@gmail.com*; Christian A. Barrera, M.D., Kassa Darge, MD, PhD, Hansel J. Otero, MD, Suraj Serai; Radiology, Children's Hospital of Philadelphia, Philadelphia, PA

Disclosures: Kassa Darge, MD, PhD: Research Grants: Bracco, Lantheus, Siemens, Philips, NIH, Thrasher Society, Helfer Society, ITMAT, Foerderer, MTR, RSNA, SPR. All other authors have disclosed no financial interests, arrangements or affiliations in the context of this activity.

Purpose or Case Report: To assess the reproducibility and accuracy of R2-relaxometry MRI for estimation of liver iron concentration (LIC) between non-proprietary in-house-developed software and FDA-approved commercially available third party results.
Methods & Materials: All MR studies were performed in a 1.5T scanner. Multiple spin-echo scans with a fixed TR and increasing TE values of 6ms, 9ms, 12ms, 15ms and 18ms (spaced at 3ms intervals) were used based on methodology reported by St. Pierre et al. Post-processing of the images to calculate R2 included drawing of regions of interest (ROIs) to include the whole liver on mid-slice. The relationship between liver R2 values calculated with in-house nonproprietary software and values calculated by an external company (FerriScan®, Resonance Health, Australia) was assessed with correlation coefficient and Bland-Altman difference plot. Continuous variables are presented as mean ± standard deviation. Significance was set at p value < 0.05.
Results: 463 studies from 175 patients were included in the study (Mean age 10.44 ± 4.18 years (range 1 to 18 years); Girls 245, Boys 218). LIC ranged from 0.8-43 mg/g dry tissue, covering a broad range from normal levels to extremely high iron levels. Linearity between proprietary and non- proprietary methods was excellent across the observed range for R2 (31.5 to 334.8 s^{-1}). With the exception of borderline outliers on <30 studies, all other studies fell within 95% prediction limits (correlation coefficient for R2, $r = 0.8$, $p<0.001$). Bland-Altman R2 difference between the two methods show a mean bias of 17.8ms (range: -68.2 to 103.9ms between two standard deviations).
Conclusions: R2 Relaxometry MR imaging for liver iron concentration estimation is reproducible between FDA-approved commercially available and non-proprietary analysis methods.

Paper #: 149

Magnetic Resonance Elastography of the Liver in Children: Variations in Regional Stiffness

Anand Shankar, Ramkumar Krishnamurthy, PhD, Carol Potter, Cheryl Gariepy, Houchun Hu, PhD, Rajesh Krishnamurthy, **Benjamin P. Thompson**, *benpthompson@hotmail.com*; Radiology, Nationwide Children's Hospital, Columbus, OH

Disclosures: All authors have disclosed no financial interests, arrangements or affiliations in the context of this activity.

Purpose or Case Report: Liver Magnetic Resonance Elastography (MRE) is a non-invasive technique to measure the stiffness of hepatic tissue in vivo. In clinical practice MRE is used as an alternative to biopsy in evaluating liver stiffness. Many studies have demonstrated that liver stiffness directly correlates with liver fibrosis. Several studies of liver fibrosis in post mortem autopsies have proven that liver fibrosis is a heterogeneous process. There is an abundance of scientific literature evaluating global liver stiffness. Few studies have assessed regional liver stiffness variations in children using the eight Couinaud liver segments.
Methods & Materials: This retrospective IRB approved study involved 170 children who underwent MRE at 3T on a GE platform using a commercial 2D SE-EPI pulse sequence. Regional liver stiffness was measured at the locations of the Couinaud segments by a trained analyst. In each patient, the segment exhibiting maximum stiffness was recorded. The coefficient of variation (CoV=standard deviation/mean) across the eight segments was also computed. A higher CoV signifies

greater stiffness heterogeneity. Medical history was obtained from patient records and the cohort was stratified into five major disease groups, including: Nonalcoholic Fatty Liver Disease(NAFLD) (N=119), autoimmune disease (N=22), heart and cardiovascular conditions (N=4), genetic disorders (N=12) and "others", which included cystic fibrosis, portal vein thrombosis, ductal plate malformations and liver tumors (N=13). Statistical analysis was performed using R software.
Results: A wide range of regional variations in liver stiffness were observed (CoV=17.2 ± 7.3%, range =3.1-79.2%) across the cohort. Of the 170 patients, segments II and VII exhibited the highest stiffness, each in 29 patients. Patients with NAFLD displayed a significantly higher CoV (17.17±5.5%) compared to patients with autoimmune diseases (14.65±4.2%, p=0.019). No other significant differences in stiffness heterogeneity were observed.
Conclusions: We observed significant variations in liver stiffness across the eight Couinaud segments in 170 pediatric patients, with segments II and VII frequently exhibiting maximum stiffness. There were notable variations in stiffness heterogeneity between patients with NAFLD and autoimmune disease. Our results suggest that underlying disease conditions can potentially influence the degree of regional stiffness heterogeneity. Measuring regional stiffness may also better guide targeted biopsies and interventions for the patient.

Paper #: 150

Technical Success Rate of Two-Dimensional Ultrasound Shear Wave Elastography in a Large Pediatric and Young Adult Population: A Clinical Effectiveness Study

Nathan Northern, BS[2], *northena@mail.uc.edu*; Jonathan R. Dillman, MD. MSc[1], Andrew T. Trout[1]; [1]Department of Radiology, Cincinnati Children's Hospital Medical Center, Cincinnati, OH, [2]University of Cincinnati College of Medicine, Cincinnati, OH

Disclosures: Nathan Northern, BS: Financial Interest: Canon Medical Systems USA - Grant (unrelated to this research); **Jonathan R. Dillman, MD, MSc:** Research Grants: Canon Medical Systems; Siemens Healthineers; Perspectum Diagnostics; Bracco Diagnostics, Other: Travel Support (Philips Healthcare, GE Healthcare); **Andrew T. Trout, MD:** Consultant, Honoraria: Guerbet Group, Royalty: Elsevier, Wolters-Kluwer, Research Grants: Canon Medical, Siemens Medical Solutions, National Pancreas Foundation, In-Kind Support: ChiRhoClin Inc., Perspectum Diagnostics. All other authors have disclosed no financial interests, arrangements or affiliations in the context of this activity.

Purpose or Case Report: To determine the frequency of technical success of two-dimensional ultrasound (US) shear wave elastography (SWE) in a large pediatric and young adult cohort based on the interquartile range (IQR)/median of 10 shear wave speed (SWS) measurements.
Methods & Materials: This retrospective study was IRB approved, and the requirement for informed consent was waved. All patients that underwent 2D US SWE between February 2016 and March 2018 were identified. For each patient, records were reviewed for: age, sex, median liver stiffness (10 SWS measurements), mean liver stiffness (10 SWS measurements), IQR/median, anterior abdominal wall thickness, and serum alanine aminotransferase (ALT). The number of non-diagnostic examinations was calculated using three methods: 1) IQR/median >0.3; 2) IQR/median >95th percentile for our study population; and 3) identification of statistical outliers using the Tukey method. The effect of age, sex, median SWS, anterior abdominal wall thickness, BMI, and ALT on IQR/median was assessed using multivariable linear regression, with model selection based on the highest adjusted-R^2 value. The relationship between median and mean SWS was evaluated using Lin's concordance correlation coefficient (r_c).
Results: 573 patients underwent clinical US SWE. Mean age was 12.6 years; 274 (47.8%) patients were male. Average median liver stiffness was 1.75 ± 0.47 kPa, while the average mean liver stiffness was 1.75 ± 0.47 kPa (r_c=0.994 [95% confidence interval: 0.993-0.995]; p<0.0001). Based on methods 1, 2 and 3, 29/573 (5.1%), 28/573 (4.9%, IQR/median=0.303), and 30/573 (5.2%) exams were non-diagnostic. Significant predictors of IQR/median at regression included age (p=0.02), BMI (p=0.0011), median SWS (p<0.0001), and ultrasound transducer (p<0.0001).
Conclusions: Approximately 95% of US SWE exams are technically successful based on IQR/median. IQR/median is impacted by patient age, BMI, median SWS, and ultrasound transducer.

Paper #: 151

Biliary atresia versus other causes of neonatal jaundice: What is the value of Shear Wave Elastography complementing grayscale findings?

Jesse Sandberg, MD[1], *jesseksandberg@gmail.com*; Yinghua Sun, MD[2], Zhaoru Ju, MD[2], Shaoling Liu, MD[3], Jingying Jiang[4], Martin Koci, MD[5], Martin Willemink[5], Jarrett Rosenberg[6], Erika Rubesova, MD[1], Richard Barth, MD[1]; [1]Department of Pediatric Radiology, Lucile Packard Children's Hospital, Stanford University, Stanford, CA, [2]Ultrasonography Unit, Children's Hospital of Fudan University , Shanghai, China, [3]Ultrasound Department, Shandong Provincial Medical Imaging Research Institute, Jinan City, China, [4]Shanghai Medical College, Fudan University, Shanghai, China, [5]Department of Radiology, Stanford University School of Medicine, Stanford, CA, [6]Radiological Sciences Laboratory, Stanford University, Stanford, CA

Disclosures: All authors have disclosed no financial interests, arrangements or affiliations in the context of this activity.

Purpose or Case Report: Ultrasonography (US) is a useful non-invasive test in the workup of neonatal jaundice to rule out biliary atresia (BA). Despite strong US findings that suggest BA, namely fibrotic cord sign and absent gallbladder (GB); accuracy in diagnosing BA from US alone remains difficult. Prior ultrasound studies have evaluated shear wave elastography (SWE) in infants with neonatal jaundice, however cohort size was small. We aim to assess the diagnostic performance of SWE in discriminating BA from other causes of neonatal jaundice in the largest cohort of BA cases to date.
Methods & Materials: Between 11/2017–08/2018, 172 consecutive infants (age 9-93 days at time of US) with jaundice were prospectively evaluated with greyscale US and SWE (Siemens S3000). On greyscale, we recorded liver heterogeneity, fibrotic cord sign (FCD), enlarged HA (>2mm), presence/absence of GB/common bile duct (CBD) and GB size. SWE velocity (meters/second) were performed using 4 different techniques C6 VTQ1 (2.5 cm depth), C6 VTQ2 (3.5cm), L9 VTQ (2.5cm) and L9 VTIQ in hepatic segments V or VI. Normality was assessed with Kolmogorov-Smirnov test. Analysis was assessed with Spearman correlation coefficients, chi-squared, logistic regression models and area under the ROC curve (AUC).
Results: There were 105 BA (biopsy confirmed) and 67 non-BA cases. Median and interquartile range for SWE velocity for BA using C6VTQ1 / C6VTQ2 / L9VTQ / L9VTIQ was 1.94(1.59-2.3) / 1.86(1.66-2.2) / 2.17(1.76-2.52) / 2.19(1.89-2.46), significantly higher (p<0.001) when compared to non-BA 1.45(1.27-1.76) / 1.46(1.28-1.69) / 1.48(1.3-1.9) / 1.77 (1.61-2.01). Stratified by age (≤69 days vs >69 days), SWV difference for both BA and non-BA was statistically significant (p<0.001).

On ROC analysis, AUC was 0.787 for L9VTQ. For a SWV cutoff value of 1.66 m/s, sensitivity/specificity for BA was 80.8%/65.2%. All greyscale US findings were significantly different between BA/non-BA (p<0.001). FCD had the highest sensitivity for BA. Although sensitivity is the same for SWE and FCD (80% vs 80.8%), FCD was markedly more specific (97.1% vs 65.2%). On greyscale, FCD (odds-ratio (OR) 31.5, 95% CI: 5.6-178.6), absent CBD (OR 11.1, CI 1.6-78.6) and enlarged HA (OR 5.5, CI 1.4-21.3) were significant. Combining SWE with US findings improved diagnosis with only absent CBD (OR 12.7).
Conclusions: SWE is feasible in evaluating neonatal jaundice and differentiating BA from non-BA. However, for the majority of greyscale US imaging findings, SWE does not increase diagnostic value.

Paper #: 152

Quantitative assessment of liver stiffness and perfusion using shear wave elastography and dual energy computed tomography in hepatic veno-occlusive disease in rabbit model

Hyun Joo Shin, MD, PhD, *lamer-22@yuhs.ac*; Jaeseung Shin, Yoon Jin Cha, Kyunghwa Han, Myung-Joon Kim, Mi-Jung Lee; Department of Radiology, Severance Hospital, Yonsei University College of Medicine, Seoul, Korea (the Republic of)

Disclosures: All authors have disclosed no financial interests, arrangements or affiliations in the context of this activity.

Purpose or Case Report: To know the usefulness of shear wave elastography (SWE) and dual energy computed tomography (DECT) for the diagnosis of hepatic veno-occlusive disease (VOD) in rabbit model.
Methods & Materials: Among six New Zealand white rabbits (3-4 kg, male), three rabbits had normal saline ingestion throughout 20 days and grouped as normal group. Another three rabbits had 6-thioguanine (6-TG, 5mg/kg/day) ingestion throughout 20 days and grouped as VOD group. Liver stiffness was measured using supersonic shear wave imaging on baseline, 3, 10, and 20th days. Liver perfusion was evaluated using DECT with fast kVp switching (80/140 kVp) on the same days. Three region-of-interests (ROIs) were drawn in liver parenchyma using virtual monochromatic images (VMI) of 55 keV and iodine maps. Morphologic changes of liver including periportal, gallbladder wall edema, or diameter change of hepatic veins were assessed on 20th day using CT. Final pathologic score of VOD was evaluated on the 21st day after sacrifice and compared between two groups using Mann-Whitney U test. Linear mixed model was used to know the differences of liver stiffness and perfusion parameters between two groups. Spearman correlation test was used to know the correlation between liver stiffness, perfusion parameters and pathologic scores.
Results: Final pathologic scores were significantly higher in VOD group than in normal group (median 22, 2, p=0.046). There was no gross morphologic change in the livers in CT. Liver stiffness values using SWE, Hounsfield unit (HU) values using VMI, and iodine concentration values using iodine map were significantly higher in VOD group compared with normal group on 10th and 20th days (all, p≤0.03). Compared to the baseline values, liver stiffness values and iodine concentrations became significantly higher in 20th day in VOD group (p=0.001, <0.001, respectively), while it were not different in normal group. Liver stiffness and iodine concentration showed positive correlation with final pathologic scores (all, r=0.754).
Conclusions: Liver stiffness values from SWE and iodine concentration values from DECT were significantly increased in hepatic VOD model in rabbits. SWE and DECT could aid the diagnosis of hepatic VOD, while morphologic change was not apparent in the liver.

Paper #: 153

Normal Liver and Pancreas Shear Wave Stiffness in Healthy Children

Andrew T. Trout, MD, *andrew.trout@cchmc.org*; Jonathan R. Dillman, MD. MSc, Samantha M. Summers, BS, MA, Paula S. Bennett; Radiology, Cincinnati Children's Hospital Medical Center, Cincinnati, OH

Disclosures: Andrew T. Trout, MD: Consultant, Honoraria: Guerbet Group, Royalty: Elsevier, Wolters-Kluwer, Research Grants: Canon Medical, Siemens Medical Solutions, National Pancreas Foundation, In-Kind Support: ChiRhoClin Inc., Perspectum Diagnostics; **Jonathan R. Dillman, MD, MSc:** Research Grants: Canon Medical Systems; Siemens Healthineers; Perspectum Diagnostics; Bracco Diagnostics, Other: Travel Support (Philips Healthcare, GE Healthcare). All other authors have disclosed no financial interests, arrangements or affiliations in the context of this activity.

Purpose or Case Report: Ultrasound shear wave elastography (SWE) is being increasingly used as a non-invasive means of measuring tissue stiffness which reflects pathologic processes including fibrosis, inflammation and congestion. Consensus guidelines suggest cut-off liver stiffness values for disease in adults but there are limited data on normal values for children. For the pancreas, understanding normal pancreas stiffness might be of value for future detection of diffuse pancreatic disease, including chronic pancreatitis. The purpose of this study was to define normal stiffness values measured in terms of ultrasound shear wave speed (SWS) for the liver and pancreas in the pediatric population and to assess for associations with patient sex, age and size.
Methods & Materials: In this prospective, IRB approved study, 121 healthy children with body mass index (BMI) <85th percentile and without a history of liver disease underwent 2D SWE of the liver and pancreas with a Canon Aplio i800 ultrasound system using a i8CX1 probe. 10 liver stiffness measurements were obtained in the right hepatic lobe and 5 pancreas stiffness measurements were obtained in the pancreatic body or tail, all using a manually placed region of interest (1 cm in the liver, 0.5 cm in the pancreas). Descriptive statistics were utilized to summarize continuous data. T-tests and Pearson correlation were used to define relationships between SWS and predictor variables.
Results: Mean age for the 121 children was 6.56±5.61 years (range: 0.02-17.81 years), mean BMI percentile was 39.7±26.8%, and 62 (51.2%) were female. The majority of children (87.6%, 106/121) were white, non-Hispanic. Mean median liver SWS for the population was 1.29±0.14 m/s. Mean median pancreas SWS for the population was 1.31±0.15 m/s. There were weak but statistically significant correlations between median liver SWS and age (r=0.29, p=0.001), height (r=0.32, p=0.00038), and weight (r=0.31, p=0.00045) but there were no significant correlations between pancreas SWS and any measure of subject size. There was no significant difference in liver or pancreas SWS based on sex and there was no significant correlation between liver and pancreas SWS.
Conclusions: We report normal liver and pancreas stiffness values for healthy children ages 0-17 years. Liver SWS >1.56 m/s and pancreas SWS >1.61 m/s likely reflect abnormal stiffening (>95th percentile) that may be indicative of diffuse disease.

Paper #: 154

Use of Clinical and Quantitative Magnetic Resonance Cholangiopancreatography Parameters for Differentiating Autoimmune Liver Diseases

Leah A. Gilligan, MD, *leah.gilligan@cchmc.org*; Andrew T. Trout, Simon Lam, MD, Alexander G. Miethke, MD, Jonathan R. Dillman, MD. MSc; Radiology, Cincinnati Children's Hospital Medical Center, Cincinnati, OH

Disclosures: Andrew T. Trout, MD: Consultant, Honoraria: Guerbet Group, Royalty: Elsevier, Wolters-Kluwer, Research Grants: Canon Medical, Siemens Medical Solutions, National Pancreas Foundation, In-Kind Support: ChiRhoClin Inc., Perspectum Diagnostics; **Jonathan R. Dillman, MD, MSc:** Research Grants: Canon Medical Systems; Siemens Healthineers; Perspectum Diagnostics; Bracco Diagnostics, Other: Travel Support (Philips Healthcare, GE Healthcare). All other authors have disclosed no financial interests, arrangements or affiliations in the context of this activity.

Purpose or Case Report: Primary/autoimmune sclerosing cholangitis (PSC/ASC) and autoimmune hepatitis (AIH) have overlapping clinical and imaging features but distinct management strategies. The purpose of this study was to assess clinical and novel quantitative magnetic resonance cholangiopancreatography (MRCP) parameters for distinguishing PSC/ASC and AIH in children and young adults.
Methods & Materials: This cross-sectional study was approved by the institutional review board and included participants in our institution's autoimmune liver disease registry who underwent baseline laboratory (ALT, AST, GGT, alkaline phosphatase, total bilirubin) and MRI evaluation with 3D MRCP. The biliary tree was extracted from MRCP images (Perspectum Diagnostics; Oxford, UK) and 15 quantitative parameters were generated (e.g., numbers of visible ducts, strictures, and dilated ducts; total lengths of biliary tree, strictures, and dilated ducts; median and maximum duct diameter; biliary tree volume). Mann-Whitney U test was used to compare patient groups (clinical diagnosis of PSC/ASC vs. AIH). Multivariable logistic regression with receiver operating characteristic curves were used to assess diagnostic performance.
Results: There were 29 patients (mean age=14.7±4.1 years); 14 with PSC/ASC; 15 with AIH. Numbers of bile duct strictures (p=0.0057) and dilations (p=0.007), total length of dilated bile ducts (p=0.004), and maximum common bile duct (CBD) diameter (p=0.046) were significantly different between groups. There was no significant difference between groups in any laboratory value (all p-values >0.05). The best regression model for distinguishing PSC/ASC from AIH was total length of dilated ducts, maximum CBD diameter, GGT, ALT, and age (p=0.014, AUC=0.90).
Conclusions: The combination of laboratory and quantitative MRCP parameters provides good discrimination of PSC/ASC from AIH.

Paper #: 155

How Can Criteria for Interpretation of MRI Examinations of Appendicitis Influence Diagnostic Accuracy?

Eman E. Marie, M.D.- M.Sc., *eezzatmarie@gmail.com*; Ghufran Alhashmi, Angelo Ricci, Carina Man, Andrea Doria, MD; Diagnostic Imaging, The Hospital For Sick Children, Etobicoke, Ontario, Canada

Disclosures: All authors have disclosed no financial interests, arrangements or affiliations in the context of this activity.

Purpose or Case Report: MRI is an imaging modality that provides a paradigm shift in the diagnosis of pediatric acute appendicitis concerning reduced scan time, lack of radiation and avoidance of intravenous contrast. Our study purpose was to compare devised MRI criteria for assessment of pediatric appendicitis with standard criteria.
Methods & Materials: A prospective, IRB approved study, using a non-sedated ultrafast non-enhanced MRI protocol consisting of coronal and axial fast spin echo T2 sequences without fat saturation and axial DWI. Expected maximum scan time was 10 minutes. MRI studies were reviewed independently by two radiologists and were graded as: positive, negative or equivocal for acute appendicitis using devised MRI criteria (based on retrospective review of confirmed positive cases) vs standard criteria (reports) as classifiers. Devised criteria for positive MRI were appendiceal diameter ≥10mm, or periappendiceal signal intensity (SI) on T2-WI, and presence of an appendicolith in the presence of other inflammatory signs. Absence of those criteria was graded as negative. Non-visualized appendix in the presence of RLQ inflammatory changes with no alternate cause was graded as equivocal. Standard criteria for positive test results were appendiceal diameter >7mm, and the presence of appendiceal intraluminal fluid, increased periappendiceal SI on T2-WI and the presence of an appendicolith. Alternate causes of RLQ pain were recorded if present. Final diagnosis was established by review of surgical and pathology reports or 1-month clinical follow up.
Results: 350 children (178 girls, 172 boys), 4-18 years old (mean ± SD age, 9.7±3.5 years old), with clinically suspected acute appendicitis underwent sonography. 86 patients had ultrafast non-sedated, non-enhanced MRI studies performed. 73 out of 350 patients had acute appendicitis, 8 were positive on MRI. Both devised and standard criteria sensitivities were 87.5% (95% CI, 47.3-99.7%); specificities of revised vs standard criteria of MRI were 97.4 % (95% CI, 91.0-99.7%) vs 83.3% (95% CI, 73.2-90.8%) PPV: 77.8 % (95% CI, 46.5-93.4%) vs 35.0% (95%CI,15-59.2%); NPV: 98.7% (95% CI, 92.4-99.8%) vs 98.5 % (95% CI, 91.8-100%), respectively.
Conclusions: Specificity and PPV of MRI varied substantially according to criteria used. Standardization of interpretation criteria of MRI is urgently required to enable comparison of diagnostic performance of MRI studies within institutions over time (upon learning curves) and between institutions for evidence-based purposes.

Paper #: 156

Walk in My Shoes: Interdepartmental Role Shadowing to Develop Workplace Wellness at a Large Pediatric Radiology Department

Tigist Hailu, MPH, *hailut@email.chop.edu*; Abigail Ginader, Alessandria Nigro, Dawnisha Lee, Raymond Sze; Radiology, Children's Hospital of Philadelphia, Philadelphia, PA

Disclosures: All authors have disclosed no financial interests, arrangements or affiliations in the context of this activity.

Purpose or Case Report: Poor relationships, oftentimes based on mere lack of exchange, have a negative impact on employee wellness. Our nearly 500-member department implemented the shadowing program "Walk in My Shoes" to improve interdepartmental relationships and build a stronger sense of community. The program provides both clinical and non-clinical employees an opportunity to shadow colleagues in their various roles and learn more about each other's contribution to the overarching mission of caring for children and their families. This research project aims to understand the impact of such a shadowing program on employees' perceptions of various roles.

Methods & Materials: A preliminary survey distributed to our department in August 2018 assessed the level of interest in the program and covered which role(s) participants were interested in shadowing. Out of 61 employees who completed the preliminary survey, we selected 30 participants and matched them to a coworker in their area of interest. The roles for shadowing included Child Life Specialist, Technologist, Research Staff, Radiologist, Nurse, Administrator, and Information Technologist. Participants were required to complete a pre and post survey to assess their shadowing experience. Individuals who hosted the shadow experience also completed a survey.
Results: Since September 2018, 6 Technologists, 5 Researchers, 5 Administrators, and 2 Nurses participated in the program. The majority of the participants shadowed Radiologists (n=18, 33%) and Research Staff (n=18, 28%).Participant's understanding (44% vs. 61%) and value (50% vs. 78%) of the roles they shadowed changed after the shadowing experience. Preconceived notions about each role (39% vs. 39%) did not change; however, participants' understanding of how their roles relate to each other (44% vs. 61%) increased. Participants showed great interest in shadowing the specific role again (89%) and shadowing another role (94%).Post-shadowing survey comments reveal newfound appreciation for interdepartmental role differences and a heightened sense of collegiality. Responses from the host survey were especially enthusiastic. All hosts would repeat the experience (100%).
Conclusions: Our study shows how interdepartmental shadowing increases a sense of community between clinicians and non-clinicians, which in turn contributes to the broader initiative of workplace wellness. The enthusiasm and openness of the hosts provide evidence that this type of program is practicable in a large busy department.

Paper #: 157

Assessment of Factors Associated with Burnout and Wellness in Pediatric Radiologists

Rama Ayyala, MD[1], *rayyala@gmail.com*; Raymond Sze[2], Brandon P. Brown, MD, MA[3], Grayson Baird[1], George A. Taylor[4]; [1]Radiology, Rhode Island Hospital- Hasbro Children's Hospital, New York, NY, [2]Children's Hospital of Philadelphia, Philadelphia, PA, [3]Indiana University School of Medicine, Indianapolis, IN, [4]Boston Children's Hospital, Boston, MA

Disclosures: All authors have disclosed no financial interests, arrangements or affiliations in the context of this activity.

Purpose or Case Report: An initial survey of Society for Pediatric Radiology (SPR) members in 2017 showed high prevalence of burnout in pediatric radiologists. The purpose of this study is to identify factors associated with burnout to ultimately guide development of departmental interventions for alleviating burnout and promoting wellness.
Methods & Materials: SPR members were sent a survey of questions on institutional factors contributing to burnout, such as call demands, work environment, departmental support and administrative/academic tasks. Questions about wellness resources and mental health were also included. Generalized linear modeling assuming binomial distribution was used for analyses with SAS 9.4.
Results: Response rate was 305/1282 (24%), with 53% female. Most respondents (47%) work at a free standing children's hospital. 35% work at a children's hospital within a large academic medical center, with 48% of those respondents feeling less supported than adult divisions. 60% of respondents feel call is busier than when first started. Frequently performing clinical or academic work outside of working hours was reported by 64% and 50% respectively. 41% feel they are short-staffed frequently or always. Respondents reported both number and complexity of clinical cases have increased since first starting practice, while the days and hours worked did not change, $p<.0001$. Using a scale of 0 (never), 1 (rarely), 2 (sometimes), 3 (frequently), 4 (always), compared to when first practicing, clinical demands have most notably reduced time for research (2.5, $p<.05$). Covering multiple hospitals (2.2) and bureaucratic tasks (2.4) were the most stressful parts of respondents' job, despite reporting a supportive and non-hostile work environment (2.8, $p<.05$). For those in administrative roles, job related tasks decreased satisfaction (2.0) and teaching duties suffered the most (2.0). 52% of respondents have been affected by mental illness due to work stresses. 25% of respondents know a physician who has contemplated or committed suicide. 39% endorsed having resources available to address burnout, with 33% of those respondents utilizing these resources.
Conclusions: Multiple departmental factors have been identified as impacting individual's career perceptions and overall wellness, which can be potential drivers of burnout in pediatric radiology. These results can be used to initiate development of departmental interventions to ultimately alleviate burnout and promote physician wellness in pediatric radiology.

Paper #: 158

Gender Representation in Recent SPR-Sponsored Events

Ami Gokli, MD[2], *goklia@email.chop.edu*; Cory M. Pfeifer, MD[1]; [1]Diagnostic Radiology, University of Texas Southwestern Medical Center, Dallas, TX, [2]Children's Hospital of Philadelphia, Philadelphia, PA

Disclosures: All authors have disclosed no financial interests, arrangements or affiliations in the context of this activity.

Purpose or Case Report: The gender distribution of physicians has emerged as a significant policy issue in diagnostic radiology. While radiology has traditionally experienced female under-representation, pediatric radiology is a rare subspecialty in which men and women are represented similarly. Pediatric radiology is also unique in that approximately half of pediatric radiologists are affiliated with academic centers which renders the subspecialty rich with opportunities for teaching, leadership, and scholarly discovery. This study looks at current trends in male and female participation in recent educational, leadership, and research-based SPR-sponsored activities as a means to define the current state of gender representation within this subspecialty while developing baseline metrics and goals to promote a culture of inclusion.
Methods & Materials: A retrospective review of materials available to SPR members was performed. For the purposes of this study, male and female genders are defined by the most common associations of given names in the United States. In cases where the gender of the individual was in doubt, an Internet search for pronouns used in the physician's profile (he/him/she/her) was used to designate gender for the purposes of this study. Individuals in which determination could not be made were excluded. The 20 largest children's hospitals were defined by using Becker's Hospital Review.
Results: Females are historically under-represented as past presidents of the SPR, but this trend has reversed in recent years. 50% of those scheduled to provide oral scientific presentations at the 2018 SPR Annual Meeting were female, but women represented only 36% of presenters in the Postgraduate Course. As of mid-2018, fewer than 5 of the 20 largest children's hospitals had female radiologists-in-chief. Regarding the 2018 meeting of the Society of Chiefs of Radiology at Children's Hospitals (SCORCH) which may host multiple representatives from a single hospital or include representatives acting in place of sitting chiefs, 37% were female.

Conclusions: Women remain under-represented in some SPR-related roles. SCORCH attendance suggests that women are either more likely to lead smaller pediatric radiology departments or serve as vice-leaders who are interested in improving collaboration with pediatric department chairs. To improve gender diversity, the SPR might consider sponsoring a "50/50" Postgraduate course in which each lecture topic is split between a male and female presenter.

Paper #: 159

Review of Learning Opportunity Rates: Correlation with Radiologist Assignment, Patient Type, and Exam Priority

Marla Sammer, MD[1], *mbsammer@texaschildrens.org*; Marcus Sammer[1], Lane F. Donnelly, MD[2]; [1]Radiology, Texas Children's, The Woodlands, TX, [2]Stanford University, Stanford, CA

Disclosures: All authors have disclosed no financial interests, arrangements or affiliations in the context of this activity.

Purpose or Case Report: Common cause analysis of exams actively submitted as learning opportunities in a peer collaborative improvement (PCI) process can gauge both opportunities to improve and potential risk to patients. Here, rates of learning opportunities were evaluated based on radiologist assignment, patient type, and exam priority.
Methods & Materials: All exams dictated at our pediatric hospital between July 3, 2016 (first full day 24/7 in-house attending) and July 31, 2018, were obtained from RIS including time of dictation, patient type, and exam priority. Exams were categorized based on radiologist assignment, patient type—Inpatient (IP), Outpatient (OP), or Emergency (EC), and exam priority (Stat, Urgent, and Routine). Assignments were defined by institutional rotations of Evenings (5p–10p), Nights (10p-7a), and Daytime (7a-5p, analyzed in two groups as Weekdays and combined Weekends & Holidays). Actively submitted PCI learning opportunities were identified and categorized. Rates were calculated by dividing number of learning opportunities by total number of exams in each category. Chi-square test was used to analyze rate differences. Pairwise comparisons were made for rotations and patient types with Bonferroni method adjusted p-values. Note that the peer learning system studied here focuses primarily on the professional aspects of radiology, and is separate from the hospital incident reporting system which was not evaluated here.
Results: There were 559676 studies. Of these, 1370 were submitted as learning opportunities (overall rate 0.245%). Differences in rates by assignment were statistically significant ($p<0.0001$) with highest rates on exams dictated Evenings (285/91290, 0.313%) and lowest on Nights (157/82467, 0.190%). Daytime Weekends & Holidays (99/37441, 0.264%) and Daytime Weekdays (829/348478, 0.238%) fell in-between. The differences between Evenings and Nights ($p<0.0001$) and Evenings and Weekdays ($p<0.001$) were significant. There were significantly higher rates on IP's (554/169371, 0.327%) than OP's (689/312423, 0.221%, $p<0.0001$) or EC (127/77882, 0.163%, $p<0.0001$). There were no significant differences based on exam priority (Stat 428/182463, 0.235%, Urgent 81/31586, 0.256%, and Routine 861/345627, 0.249%, $p=0.5431$).
Conclusions: In this study, the highest learning opportunity rates occurred on evenings and inpatient studies. These higher rates correspond to increased risk and are likely related to both high volume of studies per radiologist (evening assignment) and exam complexity (inpatients).

Paper #: 160

Teaching File: An Extensive Revision to Optimize Integration and Educational Value

Ami Gokli, *aag298@nyu.edu*; Tara Savage, Janet R. Reid, MD, FRCPC; Children's Hospital of Philadelphia, Philadelphia, PA

Disclosures: All authors have disclosed no financial interests, arrangements or affiliations in the context of this activity.

Purpose or Case Report: Teaching files (TF) are often under-utilized at institutions for various reasons including inefficient software programming, poorly designed user interface, or medical staff resistant to change. We demonstrate how to repurpose a teaching file in order to bolster user acceptance and educational value by optimizing TF integration.
Methods & Materials: Using a pre-existing teaching file in the Primordial® platform which was available but rarely used, we repurposed the program to improve functionality and user interface as well as improve ease of use and encourage integration. We demonstrate an all-encompassing 6 step approach to curriculum development based on Kern including identifying the problems, performing a targeted needs assessment, outlining goals and objectives, providing a vision for the TF, and listing desired features. Multiple 5-minute information sessions were implemented at the start of the new trainee year to reinforce use prior to educational conferences. A hands-on simulation session for all residents and fellows was given by an information technologist specializing in radiology and Primordial®. Finally, we reinforced educational strategies by requiring the TF to be incorporated into interdisciplinary conferences given by attendings and fellows.
Results: Our all-encompassing approach was executed to improve functionality and increase use. Teaching File integration into the program was successful with a significant increase in utilization since its implementation. The number of teaching file entries were recorded at zero in March 2018, and after implementation of the new TF, teaching file entries steadily increased (14 - June 2018, 18 – July 2018, 34 – August 2018) with continued upward trajectory.
Conclusions: Through a deliberate and thorough process, a fully integrated, repurposed Teaching File was created and successfully integrated into the radiologists' daily routine. Radiologists at all training levels now incorporate TF into lectures, teaching file educational lectures, and interdisciplinary conferences and catalogue individual cases.

Paper #: 161

Multifaceted Educational Scaffolding Supports Sub-Specialization in Pediatric Radiology

Ami Gokli, MD, goklia@amail.chop.edu; Brian Hopely, Janet R. Reid, MD, FRCPC; Radiology, Children's Hospital of Philadelphia, Philadelphia, PA

Disclosures: All authors have disclosed no financial interests, arrangements or affiliations in the context of this activity.

Purpose or Case Report: Pediatric radiology is a unique specialty that requires knowledge and skills in all facets of pediatric imaging including body systems, modalities and ages from 0-21 years. Mounting pressure exists in larger academic departments to develop subspecialty service lines in areas such as MSK, fetal, GI and GU imaging among others. Herein we describe our approach to developing an educational scaffolding to support sub-specialization.
Methods & Materials: Our Learning Management System (LMS) was partitioned to house all relevant materials and tools for each of 11 subspecialties. An education steering committee

created breakout groups for each subspecialty to develop and maintain curricula to include a lecture syllabus, assessment questions (to contribute to a question bank) and relevant supportive reference articles. Each subspecialty group collected relevant tools, seminal articles, graphs and suggested protocols used to set up and interpret images. Diagnostic toolboxes were created to house all of the reading tools and references. An intelligent tutor (IT) was created to push relevant toolboxes to the PACS for each examination to support subspecialty level reads. A point of care tool streamlined the creation of "teaching files" that were sorted by subspecialty, with a plan to link back to the toolboxes to serve as reference examples. Assessment included navigation analytics and focus group interview of residents and fellows.
Results: Eleven subspecialty curricula were created in: chest, cardiovascular/lymphatic, fetal, GI, GU, MSK, neonatology, neuroradiology, oncology, emergency, IR. There were 2-25 courses within the curricula (mean 10). Since creation of the toolboxes, LMS was accessed 6605 times per month, 1272 times for toolboxes, with MSK and GI/GU most popular. The IT was used mainly in US, MSK, and plain film for measurements. Focus group of six reported the resources supported their efforts and increased their confidence in image interpretation, teaching, and learning. Teaching cases will be integrated into the LMS and IT in the next iteration.
Conclusions: The drive to subspecialize in pediatric radiology can be supported through an education initiative that develops a scaffolding to include relevant up to date reference resources, instructional materials and reference cases delivered at point of care.

Paper #: 162

RADIAL Learning Management System - One Year Later

Ami Gokli, MD, Brian Hopely, **Janet R. Reid, MD, FRCPC**, *reidj@email.chop.edu*; Radiology, Children's Hospital of Philadelphia, Philadelphia, PA

Disclosures: All authors have disclosed no financial interests, arrangements or affiliations in the context of this activity.

Purpose or Case Report: RADIAL LMS, a tool to manage and increase timely access to educational content that tracks utilization and progress over time, was launched in October 2017 to consolidate valuable resources to enhance radiology education and the quality of work at the PACS. We present the utilization and perceived value of this tool one year later.
Methods & Materials: RADIAL LMS was created following a methodical educational research process that included: needs assessment; inventory of existing resources; analysis and choice of best platform**;** implementation readiness assessment; and roadmap. A timeline for staged rollout and scalability beyond our institution was also developed. The LMS was launched Oct 2017 to all radiology trainees and attending radiologists holding institutional sign-on. Access was also given to administrators, researchers, assistants and incoming fellows. LMS analytics and focus group interview of current fellows and residents were tools used for assessment and evaluation of the LMS including: Navigation: number and time of access, number of users, top resources accessed; Rate of development of courses and curriculum; Appeal: look and feel of user interface, ease of navigation, preferred resources, drawbacks, and future directions for improvement and expansion.
Results: Navigation: 178 registered users with 40-79 logins per day; 1-20 logins per day 2000h-0730h ; 1000 logins per month; average time per resource 2-4 minutes; top "courses": toolboxes and research onboarding. Course Development: 261 courses and 11 curricula; three apps; 51 new objects per month. User Interface: Appealing and intuitive interface but inconsistencies with access related to firewall issues at the institution level. Most helpful for toolboxes, presentation preparation, accessing papers, on-the-go learning. Future directions: Ongoing program assessment with seamless integration with PACS. Process mining using deep learning to generate student modeling algorithms to drive adaptivity and produce true mastery. Inter-institutional collaboration to create a universal resource for pediatric radiology.
Conclusions: RADIAL is a full-service LMS that has gained traction as a resource used for working, teaching and learning at point of care and beyond. The largest drawback related to inconsistencies in access has a manageable solution. It has future promise as a game-changer to support the breadth of subspecialty radiology knowledge to maintain mastery-level image interpretation and promote mastery of the field for trainees.

Paper #: 163

Cost-Effectiveness Analysis in Pediatric Radiology: How the Evidence (or, the Lack Thereof) Can Lead Future Research

Hansel J. Otero, MD[1], *hanselotero@gmail.com*; Andrew J. Degnan, MD, MPhil[1], Nadja Kadom, MD[3], Peter J. Neumann, ScD[2], Tara A. Lavelle, PhD[2]; [1]Children's Hospital of Philadelphia, Philadelphia, PA, [2]Tufts Medical Center, Boston, MA, [3]Children's Healthcare of Atlanta, Atlanta, GA

Disclosures: All authors have disclosed no financial interests, arrangements or affiliations in the context of this activity.

Purpose or Case Report: To systematically review all published cost-effectiveness analyses (CEA) of imaging technologies in children
Methods & Materials: We identified all CEAs involving fetal and pediatric imaging included in the Tufts Medical Center CEA registry, a repository of CEAs published since 1976. Two reviewers with formal training in CEA extracted information from each article on study methods, costs, quality adjusted life years (QALYS, a single measure combining quality of life and survival), quality of life adjustments (i.e., "health utilities"), incremental cost-effectiveness ratios (ICER, a ratio of incremental costs relative to the incremental effectiveness of the new intervention compared to a standard intervention). We recorded imaging modality, organ system of interest, country of study, year and journal of publication
Results: Of 480 diagnostic CEAs, 205 investigated imaging and only 10 focused on fetal and pediatric imaging. The most common imaging modalities studied were CT (n=5) and ultrasound (n=5). Four studies evaluated neuroimaging interventions; while 2 evaluated fetal, 2 other gastrointestinal tract imaging.The 10 studies reported 43 quality of life adjustment measurements (health utilities); of which, 20 (46.5%) used previously published adult quality of life adjustments, 11 (25.6%) were pregnant women perspectives and 12 (27.9%) were treating physician perspectives. No study used quality of life elicited from children nor took into consideration postnatal impact of disease on the quality of life of families.Of 37 ICERs generated, 7 (18.9%) were for cost-saving interventions (i.e., less expensive and more effective than the comparator) and 6 (16.2%) were for more expensive and less effective interventions. The remaining ICERs ranged from $1,400-per-QALY (MRI versus US in newborns with moderate risk of occult spinal dysraphism) to $10,000,000/QALY (CT versus no imaging in children at low risk for craniosynostosis). Using a threshold of $100,000/QALY, 22 (59.5%) of the imaging interventions were cost-effective.
Conclusions: There is a striking paucity of cost-effectiveness studies evaluating imaging technologies in children. Moreover, studies did not incorporate costs from patient and family perspectives (e.g., loss wages, travel, time off) nor utilities (e.g., impact of child's disease on families' quality of life). Our

results indicate a need for more research on the impact of disease on families and an increased understanding of the cost-effectiveness of pediatric imaging interventions.

Paper #: 164

Tackling the "black hole" of encounter specific quality improvement data in imaging

Erin L. Mesi, RT(R), *erin.mesi@nationwidechildrens.org*; Rajesh Krishnamurthy, Nicholas A. Zumberge, MD, Benjamin P. Thompson, Courtney M. Kirby, MBA, Phillip McGonagill, BA, Lean Six Sigma Black Belt; Nationwide Children's Hospital, Columbus, OH

Disclosures: All authors have disclosed no financial interests, arrangements or affiliations in the context of this activity.

Purpose or Case Report: To foster a global quality culture, many hospitals deployed informatics and organizational solutions, including daily readiness huddles to track department operational issues, reporting systems to track enterprise wide safety and near-miss events, and statistical process measures for quality improvement. Radiology visits have a unique daily workflow encompassing Planning, Acquisition, Post-processing, Interpretation, and Communication (PAPIC). Current radiology information systems (RIS) do not capture opportunities for improvement in the above spheres, which are patient encounter-specific. Therefore, error detection and reporting is unreliable. Capturing this detail is critical in identifying and tackling improvement projects that have direct impact on patient care.
Methods & Materials: In the radiology department of a large pediatric center, we created an informatics solution called OPEN (Ongoing Professional Evaluation) within RIS to allow quick 15-30 second capture of real-time encounter-specific opportunities for improvement. Input is categorized based upon imaging workflow (PAPIC), with a free-text comment box for radiology experts to describe issues. Clinical specific data is automatically captured in the hospital information system (HIS). The imaging quality team further augments data collection by categorizing into granular quality elements to evaluate for themes and improvement opportunities, which are then communicated by weekly reports to section leadership for resolution. The collected information is deemed confidential and privileged peer review data.
Results: This new mechanism was envisioned in 2017, built and implemented in the summer of 2018, with staff training and education prior to launch. Engagement and trends are being tracked and evaluated from July-Oct 2018. A total of 385 entries have been reported in OPEN. Of the 385 recorded entries, the largest category was acquisition issues (51%). Acquisition issues include subcategories such as artifacts, motion, technique, wrong exam, equipment errors and missing information. The second largest category was planning. This commonly included issues obtaining correct orders or protocols which lead to delay in patient care.
Conclusions: OPEN is created as a non-punitive, user friendly, quality reporting tool in radiology. It seamlessly integrates with RIS/HIS to provide automatic contextual information, and causes little disruption to patient care, thereby promoting engagement and insight into opportunities for improvement in imaging.

Paper #: 165

Comparison of Different Weight Groups in Pediatric Trauma Using Split-bolus Single-pass Contrast CT protocol.

Martin Koci[1], *martin.koci@fnmotol.cz*; Tomas Melis, Dr[1], Martin Willemink, Dr[2]; [1]Radiology, Motol University Hospital, Prague, Prague, Czechia, [2]Stanford School of Medicine, Stanford, CA

Disclosures: All authors have disclosed no financial interests, arrangements or affiliations in the context of this activity.

Purpose or Case Report: The Royal College of Radiologists (RCR) recommends a split-bolus single-pass CT-protocol for evaluation of pediatric trauma. We assessed the feasibility and enhancement achieved in different patient weight groups.
Methods & Materials: We retrospectively included 117 pediatric trauma-patients who underwent a split-bolus single-pass trauma-CT between August 2015 and August 2018. Contrast-enhancement was measured in the aorta, portal vein, pulmonary trunk, spleen, liver and pancreas. Attenuation, contrast-to-noise ratios (CNR) and subjective evaluation of spleen-enhancement homogeneity were compared among five weight groups with 15 kg increments (W1-W5, respectively).
Results: Median aortic attenuation was significantly higher ($p<0.05$) in low weight-groups of 0-15kg (493[315-583] Hounsfield units (HU)) and 16-30kg (296[238-345] HU) compared to the high weight-groups of 31-45kg (242[218-310] HU), 46-60kg (182[151-248] HU) and >61kg (199[151-223] HU). Similar results were found for portal vein and pulmonary trunk. Optimal enhancement levels (as reported in the literature) were not achieved in 23% of aortas, 38% of livers, 40% of pancreases. Spleen inhomogeneity was observed in 34%; 26%; 21%; 5%; 13% (W1-W5) of cases ($p=0.005$), respectively. Despite similar noise-levels ($p=0.38$, CNR was significantly higher ($p<0.05$) in low weight-groups (W1 15.1; W2 11.1) compared to high weight-groups (W3 9.8; W4 6.7; W5 6.0).
Conclusions: Evaluation of the RCR-adapted pediatric trauma protocol showed relatively poor vascular and solid-organ-enhancement in the highest weight-group and high vascular-enhancement in the lowest weight-group. Spleen-homogeneity and solid-organ-enhancement were insufficient in a substantial number of cases, mainly in higher weight groups. Our study indicates that tailoring unified protocol for different weight groups is challanging and further refining of the split-bolus single-pass CT protocol for children is essential.

SCIENTIFIC PAPERS - TECHNOLOGISTS

(T) indicates an Imaging Technologist Program Submission

Paper #: 001 (T)

Upper gastrointestinal studies indeterminate for malrotation: Are there opportunities for improvement?

Theresa Moore, RT, *tm0021@nemours.org*; Lauren W. Averill, MD, Leslie Grissom, MD, Kathleen Schenker, MD; Medical Imaging, Nemours AI duPont Hospital for Children, Wilmington, DE

Disclosures: All authors have disclosed no financial interests, arrangements or affiliations in the context of this activity.

Purpose or Case Report: A number of upper gastrointestinal (UGI) studies were performed at our institution and interpreted as indeterminate for UGI rotation. These indeterminate cases led to family anxiety and provider uncertainty about the best course of action. We undertook a retrospective case review of all UGI studies performed over a 1 year period as part of a quality improvement initiative. The purpose was to identity the percentage of indeterminate UGI cases and any opportunities for improvement in imaging technique that could reduce this rate.
Methods & Materials: All upper UGI studies from June 2017 to May 2018 were identified using the electronic medical record. All cases were categorized as normal, abnormal, or indeterminate rotation. All indeterminate studies were reviewed by a board certified pediatric radiologist using a list of criteria for optimal UGI technique:1. Avoid over distension of the stomach with air or barium2. With true lateral position, document the retroperitoneal position of the 2nd and 4th portions of duodenum3. Use an unrotated AP view to document the duodenal jejunal junction (DJJ) to the left of the left pedicle of the spine, and at the level of the duodenal bulb4. If there is uncertainty regarding position of the DJJ, follow the barium to cecum or consider contrast enema.
Results: 514 UGI studies were performed over the 1 year period, with 24 dictated as indeterminate for UGI rotation. 6 were excluded because the duodenum did not fill with contrast (2 pyloric stenosis, 2 refusal to drink, 1 small bowel follow-through, 1 duodenal web). The remaining 18 cases (3.5%) were all indeterminate because of low position of the DJJ. With radiologist review for imaging technique, no technical issue was identified in 5/18 cases. Patient rotation in the AP projection (7/18) and/or lateral projection (4/18) was the most common technical factor. Overdistension of the stomach was seen in 4, and duodenal sweep was poorly seen in 2 cases. Contrast was followed to the colon in 4 cases, with normal position of the cecum in 1, abnormal position in 2, and poor visualization in 1.
Conclusions: Over a 1 year period, 3.5% of UGI studies were indeterminate for UGI rotation. Patient rotation was the most common factor that may have contributed to indeterminate impression. To help reduce this rate, future intervention will focus on the radiologist and technolgist working cooperatively to acheive optimal patient positioning and technique using a verbal checklist.

Paper #: 002 (T)

The Importance of Proper Patient Positioning and Immobilization in Suspected Non-Accidental Trauma Cases

Roxanne Munyon, BA, *rmunyon@luriechildrens.org*; Merima Karastanovic, Gina Fanelli, Dawn Whitson, Martha Saker; Radiology, Lurie Children's , Chicago, IL

Disclosures: All authors have disclosed no financial interests, arrangements or affiliations in the context of this activity.

Purpose or Case Report: The purpose of this study is to educate on the importance of proper patient positioning and immobilization techniques for the X-ray technologist while performing suspected non-accidental trauma cases. It will further explain the types of fractures that are typically seen in these cases and the subtlety of such fractures.
Methods & Materials: Non identified case studies, discussion of immobilization devices and discussion of vulnerable population will be utilized. Comparisons of confirmed cases of non-accidental trauma (abuse) to cases where abuse was ruled out. Explanation of techniques technologists can use to properly immobilize patients along with helpful positioning aids. Photographs of these devices will be provided.
Results: Proper immobilization and positioning skills help to improve the diagnosis of non-accidental trauma cases. This allows those children that are most vulnerable to receive the medical care and social work intervention that they require.
Conclusions: When patients are immobilized correctly and optimal positioning is utilized the best images possible can be reviewed by Radiologists. The Radiologists are given the best opportunity to detect very subtle fractures that are often present in non-accidental trauma cases. Proper diagnosis of non-accidental trauma allows for child welfare agencies to utilize protocols to get these children proper care.

Paper #: 003 (T)

Running a Hospital in-house3d printing lab: Challenges and Considerations

Elizabeth Silvestro, MSE, Silvestro@email.chop.edu; Michael L. Francavilla, MD, Raymond Sze; Radiology, Children's Hospital of Philadelphia, Philadelphia, PA

Disclosures: All authors have disclosed no financial interests, arrangements or affiliations in the context of this activity.

Purpose or Case Report: The Children's Hospital of Philadelphia first started additive manufacturing i.e. 3D printing in 2012 and has since renamed its laboratory to the Children's Hospital Additive Manufacture for Pediatrics (CHAMP 3D). CHAMP 3D focuses on the use of 3D printing in surgical planning, educational training, and research. The following provides some operative insights into CHAMP 3D and some tips on starting an AM/3D lab.
Methods & Materials: Setup & LocationDetermining setup and location is a crucial starting point. An in-house lab allows for convenient collaboration within direct workflow of many groups, but this convenience also comes at a cost. The involvement of building operations is essential to ensure space is feasible.Goals & MachinePrinter selection is interlocked with the lab's goals and can set limitations on project scope. The first steps in establishing a 3D lab would be to outline the ideal set of projects and find a machine to match, taking into consideration examining material, cost, applications, and space availability.Team & CollaborationsIt is important to have a dedicated team of radiologists, engineers, administrators, and technologists. Each plays a key role in running the lab, brainstorming projects, segmenting scans, and expanding

opportunities.Cost CenterThe CHAMP lab has introduced an internal billing model. Departments are charged for their prints based on a combination of material used, time processed, and flat overhead rate. The overhead rate has the dual purpose of recouping the cost of running the lab and limiting frivolous printing.OutreachOutreach can greatly extend the possibilities of the lab, ranging from collaboration to education and even recruitment of new team members. Collaborations with AM/3D labs can be an excellent opportunity for resource and knowledge sharing. Education and Maker events provide networking and discussion on the newest methods. Internship for students can expand the team and promote interest in additive manufacturing.
Results: In the last year alone, the CHAMP 3D Lab has supported over twenty-five different groups across the hospital and university. A new metric of success targeting papers, intellectual property, and grants (PIG) has been introduced to drive the focus of the lab and project.
Conclusions: Hospitals around the world continue to establish additive manufacturing labs for research and clinical applications at an ever increasing rate. Strong planning techniques can greatly improve the effectiveness and success of the lab.

Paper #: 004 (T)

Application of 3D Printing and Mold Making to construct custom Phantoms and Task Trainers

Elizabeth Silvestro, MSE, *silvestro@email.chop.edu*; Michael L. Francavilla, MD, Raymond Sze; Radiology, Children's Hospital of Philadelphia, Philadelphia, PA

Disclosures: All authors have disclosed no financial interests, arrangements or affiliations in the context of this activity.

Purpose or Case Report: Phantoms and task trainers are utilized in a variety of training and education purposes. Hands-ontraining with realistic tools allowsfor a controlled learning setting and practice. Unfortunately, these phantoms and trainers can have prohibitive costs and tend to lack pediatric options. The growth of additive manufacturing (3D printing) and other fabrication methods can be used to create pediatric trainers to meet these educational needs unavailable on the market.
Methods & Materials: Additive manufacturing and other fabrication methods, such as silicon molding, are beneficial tools when designing and creating custom phantoms and trainers. Additive manufacturing models can be printed in various types of plastic, rubber, powder, or metal to create a phantom. It can also be used to print molds for silicon pours, therefore allowing for detailed forming. Silicon ranges in a variety of softness, durability, and other certified properties. The design for these models can be generated from a combination of scans that can be generalized and anatomized. By referencing the scans, models can be very realistic in detail. In addition, features can be added to facilitate the use of the models.
Results: Through experiments with designing phantoms, a few tips have been developed to accomplish a variety of effects. First is the use of printed models for embedded structures. A printed bone structure can be encased in soft silicone to give a realistic feel and visualization on imaging. The embedded parts can also be painted to alter the exogeneity. Additives, such as sand or Metamucil, can be mixed into silicon to alter the texture and exogeneity, creating varied regions in scans.Internal cavities can be a challenge when molding but are essential in medical trainers. Break molding and dissolvable materials allow for these cavities to be as detailed as external surfaces. Both processes start by embedding printed cavities and pathways in poured silicon. In break molding, the internal parts are forcibly cracked then pulled and/or poured out. Materials, like PVA, can be used and washed away to clear the cavities.
Conclusions: Additive manufacturing and silicone molding open up new opportunities to design custom phantoms and task trainers to support education and research. Fabrication can be done with simplicity and can greatly improve understanding in education and training.

Paper #: 005 (T)

Innovating Change in Imaging for Patient Care

Georgiena Prevett, Master's,*gprevett@luriechildrens.org*; CT, Ann & Robert Lurie Children's Hospital, Chicago, IL

Disclosures: All authors have disclosed no financial interests, arrangements or affiliations in the context of this activity.

Purpose or Case Report: The purpose of this case is to analyze three main components for MR Appendicitis and MR Brain Ventricles. The first component is to evaluate the reduction of radiation dosage by changing the exams from CT to MRI. The second component is to evaluate the reduction of need for general anesthesia and/sedation. The third and final component is to evaluate the reduction of the overall cost.

Methods & Materials: The research is being conducted by utilizing two types of reporting systems EPIC and mPower. Our time frame for MR Appendicitis is from 3/10/2015- 10/27/2018 and MR Brain Ventricles is from 04/27/2016-10/27/216. Within these time frames we are evaluating three main aspects; reduction of general anesthesia/sedation, reduction of cost and reduction of radiation. Our evaluation is taking the information within the timeframe that has been determined to evaluate the three components and calculate the end results.
Results: 1. Reduction in overall costa. Cost analysis of MR vs CT examsb. Cost analysis of CT contrast and materials2. Reductions in General Anesthesia/Sedation medicationsa. Cost analysis of GA/Seditions vs savings3. Reduction in Radiation Dosagea. Analyzing the estimated reduction of radiation dosage altering the modality to MR
Conclusions: Our evaluation on the improvement of Patient Care has enhanced by utilizing altering imaging methods. This is a substantial change in medical imaging that has been developing over time to have a positive impact on patient care. As we look at our statistical results it will conclusively show that the reduction in radiation dose has increase as well as the cost savings to the patient and the organization. It also will be able to prove that decreased need of general anesthesia/sedation that gives patients the ability to continue their health plan faster and less stressful.

Paper #: 006 (T)

Staff Engagement and the Correlation with Increasing Customer Service

Melissa Goehner, *melissa.goehner@choa.org*; Nikki Butler, BMSc, RT(R)(QM); Diagnostic Radiology, Children's Healthcare of Atlanta, Stone Mountain, GA

Disclosures: All authors have disclosed no financial interests, arrangements or affiliations in the context of this activity.

Purpose or Case Report: To identify that engaging staff to be invested in the workplace and the importance of the work being done will increase the customer service initiatives and develop a more satisfied patient population.
Methods & Materials: There have been many changes implemented to increase staff engagement including changing from 8 hour shifts to 12 hour shifts across all modalities, bringing all modalities to full staff, new phone technology to include texting options throughout the hospital, including staff in decision making, parties and events(some competitive),

leadership rounding and increased communication, staff projects and committees for staff to work together, regular leader meetings, Thank you cards, Dance cards to show patients who have multiple tests in multiple modalities which exams are first and to make sure that all tests are completed prior to leaving the facility, lunch and learns to educate staff and build relationships with the radiologists and administrative staff.
Results: There was a boost in May of 2018 to focus on improving customer service. When improving staff engagement initiatives, customer service scores have been on a slow and steady increase since utilizing the methods and materials. There has been a 3% increase in the departmental customer service scores within the past five months. If staff engagement efforts continue, a steady increase in scores is expected.
Conclusions: When staff are engaged in the work they do and invested in the facility, and believe that the organization is invested in staff, it results in customer satisfaction.

Paper #: 007 (T)

Regulartory Readiness: Preparing Diaganostic Imaging for Joint Commission Accreditation

Rozalon M. Shipp RT(R)MR), *rozalon.shipp@stjude.org*; Mary Freeman, Terry Blancq; Diagnostic Imaging, St. Jude Children's Research Hospital, Memphis, TN

Disclosures: All authors have disclosed no financial interests, arrangements or affiliations in the context of this activity.

Purpose or Case Report: As our institutional technology and standards of care continuously evolve, it is imperative the staff be informed of the institutional and departmental Policies and Procedures. Our objective today is to demonstrate the tools and resources provided to our staff. By utilizing these tools daily, we ensure patient safety, provide quality of care throughout the institution and maintain compliance with The Joint Commission standards for accreditation.
Methods & Materials: This presentation will display communications throughout the institutions intranet. The hospitals intranet provides access to the entire campus to new and updated policies, information on regulatory readiness, missions and goals. Our Departmental Share Point site provides our Diagnostic Imaging staff with a Quality Improvement Dashboard, The Joint Commission updates, Diagnostic Imaging Policies and Procedures and Regulatory Readiness information.
Results: To evaluate the effectiveness of the 8 months regulatory readiness initiative we developed and distributed a survey to Diagnostic Imaging clinical staff. The department consist of technologists, medical physicists, administrative director, radiologists, and biomedical service engineers. The components of the survey consisted of 20 questions covering: medication management 84.61%, patient rights 92.31%, infection control 94.23%, and environment of care 86.54%, medical records 96.15%, and radiology services 94.23%, with an overall score of 94.34%. Based on the results from the survey, the department was confident that the clinical staff was properly prepared for the upcoming Joint Commission Survey.
Conclusions: Upon completion of The Joint Commission survey, the Diagnostic Imaging Department was 100% compliant with the mission of the Joint Commission Accreditation process and the institutional goals. By using the hospital intranet and department Share Point sites, we are continuously staying current with updated Policies and Procedures. All of this again, is to improve the Safety and Quality of Care for our patients, families and related services.

Paper #: 008 (T)

MR Imaging of the Forgotten Circulation: Intrahepatic Dynamic Contrast MR Lymphangiography (IH-DCMRL) to Evaluate the Liver and Central Lymphatics

Justine Wilson, BS, *wilsonj@email.chop.edu*; Yoav Dori, MD, PhD, Christopher L. Smith, MD, PhD, George Englehardt, Brazinski Brian, Mallory Mueller, Dana Allen, Hoffacker Shaun, David M. Biko, MD; Radiology, The Children's Hospital of Philadelphia, Philadelphia, PA

Disclosures: David M. Biko, MD: Financial Interest: Wolters Kluwer - Royalty: Editor of Review Book. All other authors have disclosed no financial interests, arrangements or affiliations in the context of this activity.

Purpose or Case Report: Dynamic contrast enhanced MR lymphangiography (DCMRL) is a described technique of dynamically imaging the central lymphatics following intranodal gadolinium contrast injection. Intrahepatic dynamic contrast enhanced MR lymphangiography (IH-DCMRL) is a new technique which visualizes the central lymphatics via the liver lymphatics. This technique can be advantageous in evaluating pathology and central lymphatic pathways that may be unable to be seen from an intranodal approach, including protein losing enteropathy (PLE) and chylous ascites. We aim to describe the technical aspects of IH-DCMRL.
Methods & Materials: IH-DCMRL involves ultrasound guided injection of a gadolinium contrast agent into the intrahepatic lymphatic ducts followed by MRI of the chest and abdomen with dynamic time resolved imaging. Initially a 25 gauge 3.5 inch spinal needle is placed intrahepatically adjacent to a branch of the portal vein under ultrasound guidance. Needle position is confirmed with fluoroscopy. The patient is then transferred to the MRI suite. Following a heavily weighted 3D T2 weighted sequence, gadolinium is slowly injected into the liver lymphatics and dynamic T1 weighted MR imaging is performed every 5-20 seconds over 6-7 minutes. This is followed by a high resolution respiratory navigated 3D IR inherent gradient echo sequence.
Results: MRI assessment during gadolinium injection of the intrahepatic lymphatics, can be successful technique for evaluation of the liver lymphatics, thoracic duct, and to visualize bowel perfusion as seen in PLE and peritoneal perfusion as seen in chylous ascites.
Conclusions: IH-DCMRL is a promising cross-sectional imaging technique to evaluate liver lymphatic flow and can be helpful for assessment of certain conditions involving abnormal liver lymphatic flow.

Paper #: 009 (T)

Move over wearable and embedded devices there a new MRI safety challenge today call ingestible

Maggie Johnson, RT (R) (MR),
mfjohnson@childrensnational.org; Radiology, Children's National Medical Center, District of Coloumbia, WA

Disclosures: All authors have disclosed no financial interests, arrangements or affiliations in the context of this activity.

Purpose or Case Report: Over the years, the ingestible electronic pill has been shown to be a clinically relevant technology platform, with biomedical applications such as drug delivery, temperature measurements, gastric emptying and transit times. At the same time there is work being done on the next generation of ingestible devices such as those powered by stomach acid or the Capsule Ultrasound device.

Methods & Materials: devices such as those powered by stomach acid or the Capsule Ultrasound device by Arbabian LabThe increase usage of the ingestible devices such as the PillCam, and Smartpill poses a challenge for us in MRI.Families currently have a hard time recognizing or identifying implanted devices but seem to be more challenge with identifying or recognize ingestible devices during our screening process.Most MRI screening process consist of a screening form and or interviewing process that has been designed to detect devices that are either wearables or embedded in the patientsWith the increase use and development of new ingestible devices, we must look at our current screening forms and interviewing process.
Results: When scripting our interviewing process we try using questions that will help trigger for surgical and or wearable devices.As we all know the pressures of getting a diagnosis, as well as being a poor historian can sometimes interfere with how families respond to questions about devices but the connection between an ingestible device that is associated with the word pill becomes even more challenging.We need to continually change our MRI screening and interviewing processes with advancements in technology that can have an effect on being safe in the MRI environmentTo try and meet this challenge we had discussions with MR safety leaders, and decided on the following changes;Added the following change to our screening form, Ingestible(PillCam, SmartPill, etc.) with a Yes or No check boxScreening interviewing process,added these trigger questions;1. Do you or your child have anything in them that he or she was not born with?2. Have you or your child swallowed any devices for medical use?3. Have you or you chld been seen in the Gastro-Interstinal Clinic?
Conclusions: Recent advancement in ingestible devices and advances for next generation devices has become a challenge to us in identifying ingestible devices. Changes in technology bring changes to the MRI safety screening process. Continual updates to both safety screening forms and the interviewing process should be reviewed as new devices are identified

Paper #: 010 (T)

MRI Safety and the MRSO

Robert Carson, B.S.R.T. R,MR,*carsonr@email.chop.edu*; The Children's Hospital of Philadelphia, Philadelphia, PA

Disclosures: All authors have disclosed no financial interests, arrangements or affiliations in the context of this activity.

Purpose or Case Report: The goal of my talk is to present my audience with the obstacles that I faced as an MRSO when implimenting and executing new safety guidlines. I will also outline the safety team and explain their roles in our safety council. I will describe how we changed the over all culture in our department with the help of certain tools to accomplish our safety benchmarks.
Methods & Materials: I will describe the process of implimentation of rules and guidlines that we crrenttly use in our MRI safety process. Show the steps which were taken to update and improve our MRI safety culture.
Results: Explain how our safety process is better know thatn it was two years ago.
Conclusions: MRI safety is a on going process that will constsantly change as a department grows in size and as its patient numbers increase. With that being said the rules and guidelines must change as well.

Paper #: 011 (T)

MRI Safety: Getting the FTEs You Need

Trista Maule, RT (R)(CT)(MR), *trista.raymer@choa.org*; Nikki Butler, BMSc, RT(R)(QM); MRI, Childrens Healthcare of Atlanta, Acworth, GA

Disclosures: All authors have disclosed no financial interests, arrangements or affiliations in the context of this activity.

Purpose or Case Report: Purpose: To document and present data to support the need for additional FTEs to ensure a safe MRI environment.
Methods & Materials: Methods:1. Have a MRI department safety audit performed by a third party.2. Document all accidents, near misses or situations that have the potential to cause harm in a tracking system.3. Compare department staffing to the ACR guidelines.4. Compare patient volume to the number of safety incidents. Note any upward trend.5. Financials-Estimate the cost for the additional staffing. Look into the possibility of extending hours or adding additional exams to help offset the cost.6. Compare your institution's staffing model with similar institutions.7. Create a presentation for the organization using the data to show the cost and need to make your institution compliant with MRI safety.

Results: Results: Additional FTEs granted that allow the institution to meet ACR standards and decrease the number of MRI safety related incidents.
Conclusions: With proper data collection and documentation, gettig the FTEs you need for MRI safety is possible.

Paper #: 012 (T)

Ultrasound Imaging of Orthopedic Magnetically controlled Spinal Rods

Monique Riemann, *mriemann@phoenixchildrens.com*; Smita Bailey, MD, Craig Barnes, MD; Radiology Research, Phoenix Children's Hospital, Phoenix, AZ

Disclosures: All authors have disclosed no financial interests, arrangements or affiliations in the context of this activity.

Purpose or Case Report: One treatment for congenital scoliosis is the use of spine-straightening rods. Previously, the rods that have been surgically implanted were non magnetic and required the patient to undergo additional surgeries (usually every 6 months) to extend the rod length as well as radiographs pre and post surgical to evaluate the distraction. Currently many of the rods in use at our institution
are MAGnetic Expansion Control (MAGEC®) rods that can be extended magnetically with the use of an external remote controller, thereby no longer requiring repeated surgeries every 6 months. As a result, patients have distractions performed every other month. While this is a marvelous improvement, these patients are now receiving an increased number of radiographs to confirm lengthening and interval correction of their condition due to the ability to distract every other month versus every 6 months with non magnetic rods. Several studies investigated whether ultrasound could be used as an alternative to X-ray when measuring rod lengthening in order to reduce radiation exposure. The result showed that ultrasound correlated very well with X-ray measurements and that while X-ray would still be needed, ultrasound could be utilized to eliminate the number of X-rays done and thereby significantly reduce radiation exposure to the patient. We were asked by the orthopedic department to see if we could institute a protocol for ultrasound imaging at our institution for these patients based on Cheung's study. What began as a QI initiative has evolved into

an imaging clinic for these patients. We will show that the implemented standardized protocol and imaging clinic reduced unnecessary radiation, improved time management and increased the quality of care these patients receive. We intend to share the knowledge we have acquired of this successful learning model with other facilities around the country.
Methods & Materials: This study will look at the development of this clinic and evaluate its progression to include the length of exam times and the amount of radiation exposure between the standard x-ray method and the newer ultrasound method.
Results: Our imaging clinic resulted in an 83% reduction in radiation and a 64% reduction in wait time to our patients.

Paper #: 013 (T)

Fabrication and utilization of an Ultrasound Phantom for young patient engagement and understanding

Elizabeth Silvestro, MSE, *silvestro@email.chop.edu*; Casey L. Gregory, BS, RDMS, Marcy L. Hutchinson, AS, Jenelle L. Gardler, BS, RDMS, Suzanne E. DeBari, RDMS, RVT, RT; Radiology, Children's Hospital of Philadelphia, Philadelphia, PA

Disclosures: All authors have disclosed no financial interests, arrangements or affiliations in the context of this activity.

Purpose or Case Report: Ultrasound equipment and transducers can be intimidating to young patients. Many videos and graphics have been made for education, but can be perceived as disconnected from the clinical process. To help address these fears and engage collaboration between sonographers and their patients, a phantom was designed for children to play and learn before their own scan. This phantom would need to be pediatric-friendly, simple use, and educational.
Methods & Materials: The first step was to design an engaging, approachable figure that children would be interested in scanning. The CAD program SolidWorks was used to design a stout, one eye, spiked “monster.” A mold frame was printed on a Fortus 450mc in ABS plastic. The embedded parts to be hidden inside the monster's belly included a crown, a heart, a cat, and a duck; Selected due to their simple shapes that children of all ages and backgrounds should recognize. These shapes were printed on a Connex 500 in VeroWhite plastic.The “monster” was molded out of silicon in a layering process. The silicon can be dyed any color as desired. The initial 0.5 inch-layer of silicon was poured. Once set, the shapes were placed perpendicularly in a pattern within the belly region. A 1.5-inch layer of silicon was poured on, covering the shapes. A fabric face was added and the final 0.5-inch layer was poured on top. Once dry, the “monster” was pushed out of the frame and cleaned up.
Results: Five sonographers were able to scan and find the various shapes using curved array C9-2 MHz and linear array 12-4 MHz transducers under pediatric abdominal and superficial presets. The technologists were challenged and successfully figured out most of the shapes. Notably the cat shape showed some challenge with approximately three misidentifications. The “monster” phantom has since been used as part of the Ultrasound Awareness Day in our institution, as well as in our pediatric ultrasound department. In the clinical setting, this “monster” can be used prior to an exam and allows the pediatric patient to work with sonographers to understand the procedure and potentially help to calm their fears.
Conclusions: In summary, this pediatric-friendly “monster” phantom has been used in our institution to educate children and offers an excellent opportunity for engagement between the sonographer and the patient. The next step will be to work with the child life department to run a larger scale study evaluation of the “monster” phantoms and the potential benefits to pediatric patients.

Paper #: 014 (T)

Design and construction of an infant phantom for hip ultrasound education and training

Elizabeth Silvestro, MSE, *silvestro@email.chop.edu*; Lamont Hill, BS RT(R), RDMS, Mark Boguslavsky, Glenn Bloom, AS, RDMS, Michael L. Francavilla, MD, Raymond Sze; Radiology, Children's Hospital of Philadelphia, Philadelphia, PA

Disclosures: All authors have disclosed no financial interests, arrangements or affiliations in the context of this activity.

Purpose or Case Report: Ultrasound scanning of infant'ship can prove to be a challenge to learn for some sonographer from the precise angling of bones and handling of the not so understanding babies. Phantoms proved a calmer situation to learn and practice skills. To this end, an infant hip phantom with ultrasound visible fat, bones, and femoral head was created. The model will also need to simulate the physical aspect of the scan such as the motion and positioning of the hip and bones.
Methods & Materials: The fabrication of the hip started with the selection of sample patient scan. For this, it was determined to focus on 3-6-month-old patient with pelvis or adnominal CT scans with normal bone structures. The bones and body (skin and contains) were segmented out using Materialise Mimics. A mold was created with a subtraction of the body and pouring hole added. Posting was added to the bones to suspend within the mold and handle extension were placed to the end of the femur to represent the leg. The femoral head was designed geometrically and aligned it to the femur.The bones were printed on a Connex 500 in VeroWhite, which most resembled bone in hand and under ultrasound. The mold and post were printed on Fortus 450mc ABS plastic. To improve the echogenicity of the bones, it was determined to paint them with acrylic paints. The bones with femoral head and posting were assembled in the box and the skin toned dyed Smooth-on Ecoflex 10 silicon was poured.
Results: The hip phantom was tested by several technologist and radiologist. The phantom was placed on the bed and was treated like a normal patient allowing sonographer to apply gel and use traditional set up to practice the procedure as if with a patient. Each user ran through the standard extent angles: transverse neutral, coronal neutral, transverse adduct, transverse abduct, coronal flex and coronal posterior lip.The phantom proved successful in imaging of the spine, pelvic bones and femoral head under scanning with a little noise seen in the silicon that was reduced with degassing process during pouring. Several commented on the realistic feel of manipulating the leg and the click of the joints. During one test a student technologist was even instructed in the probe placement and joint extensions.
Conclusions: Moving forward the next steps will be to fully implement the phantom into the sonographers training and education. This phantom has lead to additional requests for other regions of the body, such as lumbar spine and neuroradiology applications.

Paper #: 015 (T)

Pulmonary Lymphangiectasia (PL) - Diagnosing with Ultrasound Instead of MRI - A Fresh Perspective.

Trudy Morgan, *morgant@email.chop.edu*; David M. Biko, MD, David Saul, Ammie M. White, MD; CHOP, Phila, PA

Disclosures: David M. Biko, MD: Financial Interest: Wolters Kluwer - Royalty: Editor of Review Book. All other authors have disclosed no financial interests, arrangements or affiliations in the context of this activity.

Purpose or Case Report: Purpose: Pulmonary lymphangiectasia (PL) is an uncommon life threatening disorder. Dynamic contrast enhanced MR lymphangiography (DCMRL) is commonly used to diagnose this disorder but it is invasive and often requires sedation. Recently, high resolution chest ultrasound of the lung surface has been proposed as not only less invasive but also as a less stressful and less time constraining bedside method for diagnosing PL.
Methods & Materials: Materials and Methods: The chest ultrasound is performed bedside. High and low frequency transducers used to acquire diagnostic images concentrating on the pleural space and lung surface. While the patient is in supine position, grayscale ultrasound images are obtained bilaterally with the high frequency linear transducer in the anterior and mid-clavicular chest noting the superior, middle, and inferior lung surface bilaterally to evaluate for lung surface irregularity and cystic changes. The final set of images are performed with the lower frequency curved transducer to evaluate for pleural effusions.
Results: Results: By selecting the appropriate transducer, optimizing the image settings, and imaging in the correct plane, ultrasound can be a noninvasive tool in diagnosing PL by focusing on the surface of the lung.
Conclusions: Conclusion: Ultrasound is available as a low cost and noninvasive option imaging modality to evaluate PL. Although DCMRL has become the standard in evaluating the lungs of these infants, ultrasound may be an alternative in diagnosing patients with this disorder. Our hope in the future is to use ultrasound as a screening tool in patients with suspected PL. Future plans may include the use of contrast enhanced ultrasound injected within the lymphatic system to better delineate the lymphatics on the surface of the lung

Paper #: 016 (T)

IVUS for Venous Compression Syndromes

Ashley Brondell, *brondlab02@gmail.com*; Anne Gill, MD, C. Matthew Hawkins, MD; Interventional Radiology, Children's Halthcare of Atlanta Egleston, Atlanta, GA

Disclosures: All authors have disclosed no financial interests, arrangements or affiliations in the context of this activity.

Purpose or Case Report: To describe the logistical and technical aspects of using IVUS (Intra-vascular ultrasound) for the diagnoses and imaging of venous compression syndromes.
Methods & Materials: Interventional radiology procedures are utilized to treat venous compression syndromes including May-Thurner syndrome, Nutcracker syndrome, portal vein stenosis and SVC stenosis. Traditionally, venograms and endovascular pressure measurements have been performed to evaluate the severity of stenosis. Problems arise with accurately evaluating the stenosis of venous structures on two dimensional images (i.e. the flattening of the vein from external compression can be difficult to visualize from one view). In order to better and more accurately diagnose the severity of the venous compression, an intravascular ultrasound (IVUS) allows the operator a full 360 degree view of the vessel. An IVUS catheter has an ultrasound transducer attached to the distal end of the catheter. There are three sizes of IVUS catheters; each size allows a specific viewing diameter based on size of catheter. The catheter is advanced through the area of concern, and the images are recorded and reviewed on a separate workstation. Individual screenshots and diameter measurements can be obtained and saved. If a flow limiting stenosis is present, further treatment such as angioplasty or stent deployment can be pursued. IVUS is particularly helpful in these situations because it allows precise targeting at the area of stenosis as well as post intervention imaging to evaluate the success of angioplasty/stenting.
Conclusions: The use of an IVUS catheter is greatly beneficial in diagnosing, treatment planning, and post-intervention assessment of venous compression syndromes.

ALTERNATE PAPERS

Alt #: 001

Quality Improvement and Patient-Centered Communication: Implementation of NICU Teleradiology Rounds

Susan E. Schmidt[1], *sschmidt916@gmail.com;* Joseph Cao[1]; Jeannie Kwon[1]; Kate Louise Mangona[1], [1]Radiology, UTSW, Fort Worth, TX, United States

Disclosures: All authors have disclosed no financial interests, arrangements or affiliations in the context of this activity.

Purpose or Case Report: Current pediatric radiologists provide daily onsite consultation for two University hospital NICU facilities (CUH and PHHS) at times set by the NICU care teams while also reading studies at the main Children's Hospital (CMC) reading room, a third separate hospital. This required travel to three separate physical locations throughout the day, resulting in wasted time and movement energy expenditure. Additional challenges to the work flow include elimination of campus shuttle route, sprawling multicenter campus. Additionally, similar services for clinical staff are requested at the CMC NICU.
Methods & Materials: The intervention proposed used a cloud based interactive audio/visual platform to facilitate communication between the radiology faculty and NICU treatment teams at their respective off site locations. The software platform was required to provide reliable, user-friendly, and seamless interactivity in order to maintain the same level of service currently provided by onsite consultation. The intended purpose of the intervention was to reduce travel time for pediatric radiologists. Analysis of the travel times was performed and time saved was determined based on pre-intervention travel durations. The preservation of consultation quality following intervention was a primary goal. To that end, the NICU clinical team members as well as pediatric radiologists were surveyed on subjective and objective measures of quality.
Results: Travel times were significantly reduced following implementation of remote consultation at remote NICU facility, estimated to save a potential 4940 radiologist-hours over a six month timeframe. 99% of NICU providers responded very highly to questioning regarding the added value of a radiologist's presence at NICU rounds versus NICU rounds conducted prior to radiology's presence during daily rounds. Satisfaction results were positive after implementing radiologist's presence on NICU rounds.
Conclusions: Feedback from pediatric radiology faculty and NICU treatment teams was widely positive following the implementation of telerounds. We demonstrated the ability to provide a similar level of quality of communication, ability to entertain dialogue regarding exams, timeliness of rounds from both surveyed groups. Survey of pediatric radiologists and NICU providers both show significant increase in satisfaction after implementation across all metrics.

Alt #: 002

Development of ventriculoperitoneal shunt catheter calcifications predicts shunt failure in pediatric patients

M. A. Siddiqui[1], Anna Hardy[1]; Shannon G. Farmakis[1], [1]St. Louis University School of Medicine, St. Louis, MO, United States

Disclosures: All authors have disclosed no financial interests, arrangements or affiliations in the context of this activity.

Purpose or Case Report: To determine whether the presence of calcifications found on radiographic shunt series predicts whether a patient will experience a shunt catheter fracture or complication.
Methods & Materials: An electronic medical record (EMR) search was performed at an academic pediatric hospital to identify patients with shunt series performed from June 1, 2010-July 31, 2017. When available, additional prior shunt series in the patients' picture archiving and communication system (PACS) folder were included. Patients aged 0-21 years with a ventriculoperitoneal, ventriculopleural, or ventriculoatrial shunt and shunt series were included. Pediatric patients with an initial shunt series obtained at 22 years of age were excluded. 2630 shunt series radiographs in 523 pediatric patients (301 male, 222 female) were reviewed to identify the presence and development of calcifications around the catheter. 51 patients were excluded as a result of pre-existing calcifications and/or shunt fracture (48), absence of shunt (2), or advanced age (1). Analysis included descriptive statistics, odds ratio, and Chi square.
Results: Out of 472 patients (473 shunts), 23 of 59 (39%) shunts developed calcifications and fractured. 37 of 414 shunts (8.9%) without calcifications fractured. There is a significant positive association between calcification and fracture ($X2= 42.09$, $p<0.01$). It is 6.51 times more likely that a fractured shunt had calcifications compared to a non-fractured shunt having calcifications. Calcifications appeared within an average of 9 years 3 months (range of 3-19 years) after shunt insertion. Shunt fractures occurred within an average of 5 years 2 months (range of 6 months-9 years 5 months) after the appearance of calcifications. Nearly all fractures were at or adjacent to the calcifications. Shunt fractures occurred within an average of 6.5 cm of calcifications (range 0-13.5cm). The neck was the most common site of fracture (19/23; 82.6%).
Conclusions: Shunt calcification represents a significant risk for catheter fracture in the pediatric population. Early intervention or closer interval follow-up may be indicated in those found to have calcifications.

Alt #: 003

Transient Respiratory Motion with Gadoxetate Disodium Gadolinium-Based Contrast Material in Children and Young Adults Undergoing Liver Magnetic Resonance Imaging

Leah A. Gilligan[1], *leah.gilligan@cchmc.org,* Andrew T. Trout.[1]; Christopher G. Anton[1]; Andrew H. Schapiro[1]; Alexander J. Towbin[1]; Jonathan R. Dillman[1], [1]Radiology, Cincinnati Children's Hospital Medical Center, Cincinnati, OH, United States.

Disclosures: All authors have disclosed no financial interests, arrangements or affiliations in the context of this activity.

Purpose or Case Report: Gadoxetate disodium, a gadolinium-based contrast material utilized in hepatobiliary magnetic resonance imaging (MRI), is associated with transient respiratory motion artifact during the arterial phase in adults. The purpose of this study was to determine if the transient respiratory motion phenomenon is observed in children.
Methods & Materials: This retrospective cohort study was approved by the institutional review board; informed consent was waived. Patients aged 4-18 years who underwent dynamic liver MRI with gadoxetate disodium between October 2010 and January 2018 were identified. 130 exams from 130 patients were selected for review, including patients imaged awake or under general anesthesia. Demographic, medical history, and imaging data were recorded for each patient. Three blinded reviewers scored respiratory motion artifacts on precontrast, arterial, portal venous, and late dynamic phase images using a 5-point Likert scale. Analysis of variance (ANOVA) was used to assess differences in average motion between phases in both the awake and general anesthesia cohorts; significant results were further evaluated using Tukey's multiple comparisons test. Multivariable linear regression was used to identify significant predictors of arterial phase motion in awake patients.
Results: 130 patients (65 boys and 65 girls; mean age: 9.8±3.7 years; awake, n=63; general anesthesia, n=67; gadoxetate disodium dose, 0.05 mmol/kg) were included. The anesthetized cohort was slightly younger than the awake cohort (8.9±4.0 vs. 10.7±3.1 years; $p=0.007$). There were significant differences between phases in average motion scores in the awake cohort ($p<0.0001$) but not in the general anesthesia cohort ($p=0.051$). In the awake cohort the arterial phase motion score (mean score: 3.52±0.83) was significantly higher than the precontrast (mean score: 3.14±0.81; $p=0.0003$), portal venous (mean score: 3.07±0.92; $p<0.0001$), and late (mean score: 3.05±0.89; $p<0.0001$) phase motion scores. Age, sex, body mass index, presence of ascites, presence of pleural effusion, and total contrast dose did not significantly predict arterial phase motion score in the awake cohort.
Conclusions: We observed significantly increased arterial phase respiratory motion artifacts in awake children undergoing dynamic liver MRI using gadoxetate disodium, suggesting that transient respiratory motion artifact does occur in children. A similar finding was not observed in patients imaged under general anesthesia, which may suppress this phenomenon.

Alt #: 004

The Use of Intraoperative Doppler in Pediatric Liver Transplantation: Results of a Survey of SPR Members

Luana A. Stanescu[1]; Ramesh Iyer[1]; Shawn Kamps[1]; Marguerite[1]; Andre A. Dick[1]; **Grace Phillips[1]**, *grace.phillips@seattlechildrens.org* , [1] Radiology, University of Washington, Seattle, WA, United States.

Disclosures: All authors have disclosed no financial interests, arrangements or affiliations in the context of this activity.

Purpose or Case Report: Liver transplantation is a potentially lifesaving treatment for pediatric liver failure. While some elements of perioperative liver transplant Doppler examinations are routine in most practices, there is no standard protocol employed across institutions. To date, no large-scale investigation has been performed to determine best practices based on a consensus of radiologists who perform pediatric liver transplant intraoperative Doppler (IOD) examinations. Our goal is to survey radiologists who perform these studies to better understand variability amongst institutions in the use of IOD in pediatric liver transplant patients.
Methods & Materials: With IRB approval, an online survey was distributed to 1600 members of the Society for Pediatric Radiology (SPR) via the email list serve. To avoid redundancy in responses from the same institution, participants were encouraged to identify one single person from their respective

institution to respond to the survey. The name of the participants' institution was also requested to identify respondents from the same institution. Participants were excluded if pediatric liver transplantation was not performed at their institution, as well as if they were trainees.
Results: Of the 1600 survey recipients, 50 (3%) responded to and completed it, representing 29 of 58 (50%) pediatric liver transplant centers within the United States. IOD was performed at 69% of pediatric transplant centers. In centers performing IOD, 47% performed examinations routinely with every pediatric liver transplant. The hepatic artery was the vessel most commonly routinely interrogated (87%), followed by the portal vein (83%) and hepatic veins (67%), although 50% reported that the exam protocol depended on the area of clinical concern. The surgeon and radiologist operated the transducer with relatively equal frequency. The pediatric radiologist rendered interpretation in 93% of institutions, although frequently in conjunction with the surgeon (30%). Surgeon preference (38%) was identified as the most common barrier to further expansion of IOD programs, followed by radiologist availability (25%). 47% of respondents deemed IOD "extremely useful" in the setting of pediatric liver transplantation.
Conclusions: Despite the perceived utility of IOD in pediatric liver transplantation, there is considerable variability in the use of this technique. Our results support the notion of a team approach between surgeons and radiologists in further expanding the use of IOD in this population.

Alt #: 005

Radiogenomics in Neuroblastoma: Imaging Patterns in Patients with ALK Mutations

Alexandria J. Holroyd[1], *holroyda@email.chop.edu,* Lisa States[1], [1] Radiology, Children's Hospital of Philadelphia, Mount Laurel, NJ, United States

Disclosures: All authors have disclosed no financial interests, arrangements or affiliations in the context of this activity.

Purpose or Case Report: We conducted this study to determine if there is an imaging biomarker associated with ALK mutations in patients with neuroblastoma(NB). MYCN oncogene amplification is identified in 20-25% of all NB cases and portends a poor prognosis. Aberrations of the ALK gene are also characteristic of the disease. Both are located on the p arm of the second chromosome, and are usually associated with aggressive disease and poor prognosis.
Methods & Materials: Data was collected from subjects under 12 years of age diagnosed between July 2008 to February 2018. Clinical, surgical, pathologic and genomic data were extracted from the medical record. Imaging reviewed by a single radiologist included MRI and I123 MIBG scans performed prior to surgical resection. Recorded imaging findings were site of primary lesion (adrenal, neck/thoracic apex, thoracic, lumbar paraspinal, pelvic, midline abdominal retroperitoneal and metastatic disease to lymph nodes, liver, lung, brain, and marrow). MIBG avidity and Curie score were recorded. Inclusion requirements were pathology results from primary specimen at diagnosis or after induction chemotherapy.
Results: 66 subjects with mean age of 2 years, (59% female and 41% male) found 20% (N=13) were ALK positive. Of these, 6 were deceased with 4/6 also MYCN+. Additional mutations were present in all 13. 6 were INRGSS stage L2, 5 were stage M and one was L1. Imaging patterns described as (#ALK positive/total, %) were as follows: Neck/thoracic apex (4/4, 100%), bilateral adrenal (1/3,33%), multicompartmental (2/17, 28.5%), chest/thorax (2/9,22%), midline abdominal retroperitoneal (5/19, 26%), liver metastases (2/9, 22%). Curie scores ranged from 2-27. Of the 6 deceased, 5/6 had additional mutations, including P53 and TERT mutations. Other mutations labeled as having unknown significance were also present. Of all 66 subjects, 86% had other chromosome aberrations.
Conclusions: The strongest association of ALK mutation with a specific primary site was the combined neck/thoracic apex. The lack of a specific imaging biomarker may be related to genomic heterogeneity. Detection of ALK mutations at diagnosis holds promise for personalized therapy with upfront treatment with ALK inhibitors combined with chemotherapy, a current open clinical trial for high risk patients.

CASE REPORT, EDUCATIONAL AND SCIENTIFIC POSTERS

Authors are listed in the order provided. An author listed in bold identifies the presenting author.

Poster #: CR-001

Methicillin-resistant *staphylococus aureus* in Lemierre's syndrome: a rare cause of a rare syndrome in pediatric patients

Donald O. Ibe, M.B.B.S, *church.donaldo@gmail.com*; Maria Navallas Irujo, Michael R. Aquino, MD; Hospital for Sick Children, Toronto, Ontario, Canada

Disclosures: Michael R. Aquino, MD: Royalty Income: Elsevier Co-author. All other authors have disclosed no financial interests, arrangements or affiliations in the context of this activity.

Purpose or Case Report: Lemierre's syndrome is an extremely rare condition characterized by initial oropharyngeal infection with development of septic thrombophlebitis and subsequently disseminated septic microemboli. The syndrome remains a disease of considerable morbidity and mortality. The incidence is approximately 3.6 cases per 1 million per year. It is commonly caused by gram-negative *Fusobacterium necrophorum*. However, less than a third of cases is brought on by other anaerobic bacteria. Here we present a rare case of a Lemierre's syndrome in a child caused by methicillin-resistant *Staphylococcus aureus* (MRSA). A 4-year old male presented to emergency department with unremitting fever, progressive painful submandibular swelling concerning for Ludwig's angina, vesicular lesions on the skin, and decreased level of consciousness. The patient was reported to have fallen onto his chin with resultant lip laceration and tooth avulsion. Fever and neck swelling developed two days later. Computed tomography (CT) of the neck revealed findings in keeping with clinically suspected Ludwig's angina including: soft tissue gas, and diffuse fat stranding involving the sublingual, perioral, and right submandibular spaces with extension to right sternoclavicular muscle, carotid and jugular vessels. No abscess was identified but a focal non-occlusive thrombus was seen in the right internal jugular vein. Additionally, the lung apices demonstrated multiple patchy densities raising concern for Lemierre's syndrome and prompting further evaluation with a contrast-enhanced chest CT. Chest CT confirmed the diagnosis demonstrating multiple, variable-sized, randomly distributed lung nodules with cavitation, and multifocal consolidation consistent with septic emboli. Blood culture and skin swab of vesicular lesions were positive for MRSA. On further discussion, it was revealed that the patient's father was recently treated for MRSA abscess. The patient was placed on intravenous antibiotics (vancomycin, rifampin, meropenem) and anticoagulants (tinazaparin) with improvements in symptoms and imaging findings within six weeks post admission.The learning points include:1) the need to critically evaluate lung apices and vasculature on neck CT in patients with evidence of

soft tissue neck/oropharyngeal infection2) despite the rarity of Lemierre's syndrome, multiple cases caused by MRSA have been described.

Poster #: CR-002

Infantile Myofibromatosis: Prenatal and Postnatal Imaging Features

Ashley Evens[1], *ashleyevens@health.usf.edu*; Ignacio Gonzalez-Gomez, MD[2], Jennifer Neville Kucera, MD[2]; [1]University of South Florida Morsani College of Medicine, Tampa, FL, [2]Johns Hopkins All Children's Hospital, St. Petersburg, FL

Disclosures: All authors have disclosed no financial interests, arrangements or affiliations in the context of this activity.

Purpose or Case Report: Infantile myofibromatosis is a rare condition consisting of benign fibrous tumors typically deposited in the skin, soft tissues, muscles, bones, and visceral organs. The entity can be solitary or multicentric. Although controversial, outcomes are generally worse in cases with visceral organ involvement. The prognosis is generally favorable in cases that lack visceral organ involvement, with a majority of cases showing spontaneous regression. The imaging findings of infantile myofibromatosis will be illustrated using both prenatal and postnatal imaging including ultrasound, MRI, radiography, CT, and bone scintigraphy. We also present gross specimen and pathology images. Our case involves a 33 week 4 day gestational age male fetus that initially revealed dilated loops of bowel on ultrasound. Fetal MRI was performed at 34 weeks and 4 days, which demonstrated the dilated loop was colon in the region of the hepatic flexure. Additionally, multiple solid-appearing lung masses were noted, which had not been visualized on ultrasound. Because of concern for a possible metastatic process, the entire fetus was thoroughly imaged, but no primary source was found. The differential diagnosis that was given on the fetal MRI included metastatic disease from the mother or fetus, infantile myofibromatosis, or infectious etiology. The mother underwent induction of labor at 35 weeks 4 days, and the baby was born via uncomplicated vaginal delivery. To exclude transplacental metastases, the mother underwent dermatologic skin check, mammography, colonoscopy, and head CT, all of which were negative. Postnatal radiographs of the baby revealed a focally dilated loop of bowel, and the patient underwent exploratory laparotomy. In the OR, nodules were noted on the small bowel serosa resulting in a bowel obstruction. Chest radiograph and CT also confirmed the presence of multiple solid lung masses. Bone scintigraphy was negative. Pathology from one of the bowel nodules revealed infantile myofibroma. Our patient has not undergone any therapeutic treatment, and follow up imaging has demonstrated continued spontaneous regression of the lung masses. Although infantile myofibromatosis is a rare entity, it is important to include in the differential diagnosis in a fetus with multiple solid-appearing lung masses. Throughout the clinical course of these patients, imaging plays an imperative role in the assessment of these lesions.

Poster #: CR-003

Peeing Double – A case report of Caudal Duplication

Anna Smyth, *smythannae@gmail.com*; Christina Nowik, Denise Pugash, Daniel Rosenbaum; radiology, BC Children's Hospital, Vancouver, British Columbia, Canada

Disclosures: All authors have disclosed no financial interests, arrangements or affiliations in the context of this activity.

Purpose or Case Report: Caudal duplication syndrome is a rare entity that involves duplication of various structures arising from the embryonic cloaca and notochord. This presentation outlines the case of a 38-year-old G2P1 woman referred to our institution at 21 weeks gestation for anomalies detected on antenatal ultrasound. Antenatal ultrasound demonstrated sagittal duplication of the bladder, duplex phallus, a bifid scrotum and a horseshoe kidney. A subsequent fetal MRI confirmed those findings and also demonstrated apparent duplication of the colon and dysmorphic lumbosacral spine. Following delivery, the baby passed urine via both urethras and meconium via a right-sided anus; there was a left-sided anal dimple with an imperforate anus. VCUG showed no communication between the two bladders. A colovesical fistula was demonstrated between the left bladder and colon, which is likely the redundant duplicated colon with the imperforate anus. MRI of the abdomen and pelvis showed a lipomeningocele with attempted sacral duplication, redemonstrated duplication of the pelvic organs, and confirmed absence of a left-sided rectum and sphincteric complex. Caudal duplication syndrome is a complex malformation, the management of which often requires a multidisciplinary approach involving radiology, general surgery, urology, and neurosurgery. This case illustrates the findings of this rare entity with good correlation between fetal and postnatal imaging. It also highlights respective contributions of the various imaging modalities in guiding management, which usually entails staged surgical correction.

Poster #: CR-004

Systemic Juvenile Xanthogranuloma: A Case Report Involving the Liver

Malik A. Dawoud, MBBS, *malikdawoud@yahoo.com*; Robert F. Buchmann, D.O.; Arkansas Children's Hospital, Little Rock, AR

Disclosures: All authors have disclosed no financial interests, arrangements or affiliations in the context of this activity.

Purpose or Case Report: We report a case of systemic juvenile xanthogranuloma affecting the liver in an 18 month old male.
Methods & Materials: The patient's electronic medical record was reviewed including clinical notes, laboratory data, surgical pathology and treatment. Diagnostic imaging studies reviewed include plain-films, CT, US and MRI.
Results: A previously healthy 18 month old male presented to the emergency department with congestion, fever and abdominal distention. Abnormal labs included pancytopenia and elevation of liver function tests. Initial clinical impression favored a viral illness with secondary pancytopenia. The patient was discharged and returned 1 month later with spiking fevers and abdominal distention. Imaging demonstrated hepatomegaly and numerous solid, oval liver lesions which were hypoechoic on US and hypodense on CT. On MRI with IV Eovist the lesions were T1 & T2 hyperintense and hypointense on hepatocyte phase. A skeletal survey was normal. Differential considerations included infection, neoplasm and metastatic disease. Percutaneous biopsy of two liver lesions was performed and pathology confirmed juvenile xanthogranuloma (JXG). Our patient received chemotherapy (Velban and Prednisone) that is typically used for Langerhans cell histiocytosis. 4 months later the patient's symptoms and labs had normalized and CT demonstrated near complete resolution of liver lesions.
Conclusions: JXG is a rare form of non-Langerhans cell histiocytosis typically diagnosed before the age of 1.95% of cases present as isolated cutaneous disease with yellow, brown skin nodules involving the head, neck and trunk. Prognosis is favorable and skin lesions remain stable or gradually regress without treatment. Organ involvement is rare, occurring in only 5% of all cases and can present with or without cutaneous

disease. Organs commonly involved include the orbit, lung, muscle, CNS, liver, spleen and heart. Systemic JXG is associated with an increased risk of serious complications requiring aggressive medical therapy. Our patient presented with multiple liver lesions, but lacked cutaneous disease. Imaging findings on CT, US and MRI were non-specific, but critical to assess sites and extent of disease. Percutaneous biopsy was necessary to establish the diagnosis of systemic JXG. Chemotherapy led to a favorable response. This rare histiocytic disorder should be considered in a young child presenting with imaging findings of multiple liver lesions, and when present, skin lesions are helpful to establish the correct diagnosis.

Poster #: CR-005

Mimicker or a sinister lesion- Inflammatory myofibroblastic tumour, a diagnostic enigma unveiled.

Sreekumar Muthiyal, MBBS DMRD DNB M Med FRCR, *kumardr6@hotmail.com*; Viswanatha Kini, MD DNB FRCR, Sheeja M. Koshy, MD; Hamad General Hospital , Doha, Doha, Qatar

Disclosures: All authors have disclosed no financial interests, arrangements or affiliations in the context of this activity.

Purpose or Case Report: Inflammatory myofibroblastic tumour is a rare quasineoplastic lesion in the gatrointensitnal tract ; often present with variable and nonspecific imaging features, which may mimic other more common lesions, including malignancy. Occurrence in early infancy involving mesentery has been only sparsely reported in literature. We present such a paradigm in a 4 months old infant with clinical, radiological and histopathological features and corroborative overview of literature.On Ultrasound abdomen, a mass lesion measuring about 6x4cm with irregular lobulated margin in the left lumbar–iliac fossa regions , involving the mesenteric planes and contigous descending colonic wall, having heterogeneous echotexture was seen . No calcification or cystic component was evident . Left kidney and spleen were seen separately . On Doppler it showed a few areas of vascularity.On MRI ,It measured about 6.1x5.1x5.2 cm in CC, TR and AP dimensions with lobulated margins, involving the mesentery. It was heterogeously hypo intense on T1 W images and hyper intense on T2W images. On DW sequences, a few areas of restricted diffusion , predominantly along the periphery of the lesion, while the central areas showed minimal/non-restriction ; which also reflected in ADC map. On post contrast, the lesion showed moderate heterogeneous enhancement corresponding to the areas of restricted diffusion and dominant non enhancing components, suggesting areas of necrosis. Apart from contiguous colonic wall involvement , no other evidence of loco regional infiltration or metastasis was seen. Based on these, a diagnosis of Inflammatory myofibroblastic tumor was made.with differential diagnosis of non Hodgkin's lymphomaThe patient subsequently underwent laparotomy. On Histopathology, it showed myofibroblastic spindle cells and inflammatory infiltrates of lymphocytes with no evidence of nuclear pleomorphism or atypical mitosis ; suggesting the diagnosis of inflammatory myofibroblastic tumour ; which matched the MRI diagnosis.
Conclusions: Inflammatory myofibroblastic tumour is a rare quasineoplasm with a myriad of radiological features, vary from that of a dormant benign lesion to an aggressive malignant neoplasm. The indexed case is unique as its occurrence is in early infancy with mesenteric involvement and similar cases have been only sparsely reported in the literature. Awareness of this entity is imperative in evaluation of pediatric abdominal mass lesions; which may be a mimicker than a sinister lesion.

Poster #: CR-006

Fatty Falciform Ligament Appendage Torsion: Diagnosis and Management in a Pediatric Patient.

Richard D. Horak, DO[1], *horakrd@gmail.com*; James Mega, MD[1], Phillip Tanton[2], Erik Criman, MD[1], Benjamin Tabak, MD, FACSI MAJ, MC, USAI[1], Veronica J. Rooks, MD[1]; [1]Radiology, Tripler Army Medical Center, Honolulu, HI, [2]University of Illinois Urbana-Champaign, Champaign, IL

Disclosures: All authors have disclosed no financial interests, arrangements or affiliations in the context of this activity.

Purpose or Case Report: Fatty falciform ligament appendage torsion (FFLAT) is a rare phenomenon as there are only two reported pediatric cases of falciform ligament fatty appendage torsion in the literature. In this case, the diagnosis was established via ultrasound (US) and confirmed with computed tomography (CT). US showed an echogenic, ill-defined mass in the epigastric region that extending into the falciform ligament. CT showed the "hyperattenuating rim" sign. This report is the first reported female pediatric case of FFLAT that was diagnosed with US and CT, given a trial of analgesics, and definitively cured via minimally invasive surgical excision. A 13-year-old female presented to the emergency department with episodic waxing and waning abdominal pain for three days. The pain had localized to the mid-epigastrium and worsened with deep inspiration. On examination, vital signs were within normal limits. Focal tenderness was elicited upon palpation of the epigastrium. Laboratory evaluation revealed a mild leukocytosis 14.2 x 109/L, normal range (3.9-10.6 x 109/L).
Results: Ultrasound demonstrated an irregularly marginated hyperechoic mass in the epigastric region that extended into falciform ligament. Confirmatory CT scan of the abdomen/pelvis with IV and oral contrast revealed mass-like stranding of the intraperitoneal fat in the epigastric region with a classic ovoid hyperattenuating rim sign. The vessels extending into the falciform ligament did not demonstrate contrast enhancement further raising concern for torsion. Surgical consultation was obtained. Conservative management was recommended via a trial of non-steroidal anti-inflammatory medication. Despite several weeks of treatment, the patient's pain persisted without significant improvement. Transumbilical laparoscopic excisional findings strongly suggested an acute on chronic inflammatory process confined to the fatty appendage of the falciform ligament. The pathologist described the resected mass as fibrofatty rubbery tissue. The pre-operative diagnosis of FFLAT was confirmed. The patient was found to have complete resolution of pain at her two-week post-operative follow-up.
Conclusions: This case reiterates the clinical multidisciplinary team approach required to diagnose the rare case of FFLAT in a pediatric patient. It also demonstrates careful observation of conservative management, and optional minimally invasive surgical resection for patients with persistent symptoms.

Poster #: CR-007

Reactive Appendicitis Associated with Abdominal Solid Organ Injury

Jane Tong[2], **Yu Luo**[1], *yu.luo@vanderbilt.edu*; [1]Vanderbilt University, Nashville, TN, [2]Drexel University, Philadelphia, PA

Disclosures: All authors have disclosed no financial interests, arrangements or affiliations in the context of this activity.

Purpose or Case Report: Although acute appendicitis is thought to be result from luminal obstruction of the appendix, rarely it may develop following abdominal trauma. Traumatic

appendicitis is thought to occur through direct injury to the appendix, or as a response to other abdominal organ injury. On the other hand, in patients with other organ injury, some distension of the appendix can occur with surrounding free fluid secondary to trauma, mimicking appendicitis. While the clinical presentation of traumatic appendicitis is similar to that of traditional appendicitis, differentiation between reactive appendiceal changes in the setting of traumatic injury to other intra-abdominal organs is important, as the latter will not require appendectomy. We present two pediatric patients in whom following initial suspicion of acute appendicitis, ultrasonography (US) identified mildly enlarged fluid-filled and hyperemic appendix with out of proportion complex fluid, raising the suspicion of previously unsuspected abdominal trauma. Upon further examination, injury to other abdominal solid organs was discovered as the primary cause of patient's presentation and appendiceal findings were reactive to abdominal solid organ injury. In cases of suspected appendicitis, visualization of significant free fluid with dense debris on ultrasonography (US) calls for more careful examination to assess clues of other abdominal injury.

Poster #: CR-008

Reflux of contrast during voiding cystourethrogram to the peritoneum in an otherwise healthy female patient

Abraham Noorbakhsh, MD[1], *anoorbak@ucsd.edu*; Jeffrey Koning[2], Peter Kruk[2]; [1]Radiology, University of California, San Diego, San Diego, CA, [2]Rady Children's Hospital, San Diego, CA

Disclosures: All authors have disclosed no financial interests, arrangements or affiliations in the context of this activity.

Purpose or Case Report: We report a case of a 7 year old female who presented to urology clinic due to recurrent urinary tract infections that had started 4 years ago. The patient also reported symptoms of urge incontinence and nocturnal enuresis beginning at the same time. She previously consulted an adult gynecologist, which showed no physical exam evidence of genitourinary abnormalities. An MRI of the abdomen and pelvis was also ordered at that time which reported a normal exam except for a small left renal cyst. At our institution she underwent DMSA renal scan, which was normal. She underwent a voiding cystourethrogram (VCUG), which showed no vesicoureteral reflux. However, during the VCUG, an incidental note was made of large amounts of vaginal reflux extending into the cervix, uterus, and with spillage into the peritoneal cavity presumably via the salpinges.
Conclusions: Extension of contrast into the peritoneal cavity via vaginal reflux on VCUG has previously been reported only in patients with genitourinary anomalies. However, this patient had prior workup demonstrating no definite genitourinary abnormalities. This case suggests that reflux of contrast to the peritoneal cavity may be possible in patients with otherwise normal genitourinary anatomy.

Poster #: CR-009

Extramedullary Hematopoiesis Masquerading as Metastases in Liver in a Known Case of Neuroblastoma with Opsoclonus-Myoclonus Syndrome

Abhijeet Taori, MD, DNB, EDiR, *ataori@cheo.on.ca*; Nazih Shenouda; Medical Imaging, CHEO, University of Ottawa, Ottawa, Ontario, Canada

Disclosures: All authors have disclosed no financial interests, arrangements or affiliations in the context of this activity.

Purpose or Case Report: Extramedullary hematopoiesis (EH) is defined as hematopoiesis occurring in organs outside of the bone marrow. It occurs in diverse conditions, including fetal development, normal immune responses, and pathological circumstances. These sites of extramedullary hematopoiesis may present as masses mimicking malignancy or produce symptoms due to pressure effects. In the setting of an existing malignancy they may appear as metastatic deposits signifying progression of disease. It is essential to confirm this due to its prognostic and treatment implications.We report a 2-year-old little girl who presented initially with an acute history of ataxia, nystagmus, tremor, mydriasis and bruises on her left forehead. A solid left suprarenal mass was detected and a diagnosis of Stage 4 Neuroblastoma and Opsoclonus-Myoclonus syndrome was established. Subsequently she was on treatment which included chemotherapy, IVIG and stem cell transplant. On an MRI of the abdomen done a year later, a single lesion was detected in the right lobe of the liver. On subsequent short term follow up, innumerable scattered lesions were seen in the hepatic parenchyma and were thought to represent metastases. A liver biopsy showed that these hepatic lesions represented sites of extramedullary hematopoiesis.Extramedullary hematopoiesis has been uncommonly seen in the cranium and sacrum in the setting of Neuroblastoma. We believe this is a unique presentation with extramedullary hematopoiesis presenting as solid liver masses masquerading as metastases in a known case of Neuroblastoma.

Poster #: CR-010

Role of diagnostic and interventional radiology in a successful separation of conjoined thoraco-omphalopagus twins

Christopher J. Yen, MD[1], *cjyen@bcm.edu*; Kamlesh Kukreja, MD[2], Prakash M. Masand, MD[2]; [1]Radiology, Baylor College of Medicine, Houston, TX, [2]Texas Children's Hospital, Houston, TX

Disclosures: Prakash M. Masand, MD: Consultant, Honoraria: Canon Medical Systems, Phillips MRI Users Meeting 2018, Daiichi Sankyo, Speakers Bureau: Canon Medical Systems, Royalty: Amirsys. All other authors have disclosed no financial interests, arrangements or affiliations in the context of this activity.

Purpose or Case Report: Female conjoined throraco-omphalopagus twins were delivered via cesarean section at 35 weeks 5 days gestational age to a 38-year-old mother who received standard prenatal care. After resuscitation, the twins were transferred to the neonatal ICU, where they remained for monitoring and growth as they were assessed for potential separation.CT angiography was performed at 3-4 months of life using a staged approach. Selective IV and oral contrast administration was used over two visits to delineate shared and non-shared structures. Most significantly, there was a single shared liver with anomalous hepatic venous drainage. Twin A had three normal caliber hepatic veins draining into a normal IVC, but a large branch of the middle hepatic vein traversed midline into Twin B and received hepatic venous drainage from Twin B via numerous anomalous vessels. Twin B had a normal IVC but three diminutive hepatic veins, thought to be due to reduced venous drainage as a result of the anomalous shared vasculature.After multidisciplinary discussion, interventional radiology was consulted for hepatic venogram and intervention as needed. The anomalous communicating vessels were identified on hepatic venogram via Twin A femoral approach. Occlusion of the anomalous branches was achieved with serial embolization of the primary draining vessel on the Twin A side using Amplatzer vascular plugs. Successful occlusion was confirmed on venography after the final embolization

procedure.Follow-up Doppler ultrasound exams confirmed improved hepatic venous outflow in Twin B, initially with reversal of flow in the anomalous veins back toward the IVC of Twin B, followed by nonvisualization of the anomalous veins on later exams. CT angiography later showed enlarged caliber of the native Twin B hepatic veins. Following the optimization of hepatic venous outflow, the multispecialty surgical team proceeded with separation. The twins were separated at 13 months of age without complication. In addition to restoring venous outflow to allow for a successful surgical outcome, it was noted that the Amplatzer devices were used as surgical landmarks during separation for identification of shared anatomy. Through careful planning and execution, diagnostic and interventional radiology techniques played a critical role in this successful outcome.

Poster #: CR-011

BioPlug Utilized for Closure of Esophagocutaneous Fistula

Brittany Johnson, MD, *bxjohns7@texaschildrens.org*; Sudhen Desai, MD, Paul Minifee, MD; Pediatric Surgery , Texas Children's Hospital , Houston , TX

Disclosures: All authors have disclosed no financial interests, arrangements or affiliations in the context of this activity.

Purpose or Case Report: Introduction: The management of gastrobronchial fistula (GBF) is not well defined in the literature. First line management is non-operative, allowing time for the fistula to close naturally. Surgical intervention is implemented when non-operative management fails. In medically complex patients, who often fail non-operative management, surgical procedures for closure remain high risk for complications.Case: We present a 2 year-old female with congenital esophageal atresia, duodenal atresia and annular pancreas. Beginning October 2015, she underwent multiple surgical procedures resulting in a multitude of complications. In August 2017, she transferred to our institution for management. Additional immediate operative intervention was pursued given the presence of the GBF. Despite two attempts at operative repair, the fistula recurred. Interventional radiology, consulted March 2018, developed a plan to place a percutaneous pigtail catheter in the esophagus through the dehiscent stomach wall from an external chest tube entry site, creating an iatrogenic enterocutaneous fistula (ECF). Diversion of flow from the GBF to the ECF was hypothesized to allow a conservative alternative for closure and tissue healing to occur. Initially, a 12 French (F) pigtail catheter was placed through the gastric wall into the esophageal pouch allowing the formation of the ECF tract. The patient returned for catheter downsizing to 8F three weeks later. A third intervention was performed to reposition the catheter to ensure that the tissues remained as dehydrated as possible. In May 2018, a 7 mm Cook Biodesign SIS fistula plug was placed. The 8F catheter was used to place a guide wire through the tract, then removed. The AFP bioplug, soaked in contrast to facilitate use of fluoroscopy, was placed through the mouth to seal the gastric wall. Placement was confirmed with a rigid esophagoscope and fluoroscopy. One week later, esophogram confirmed no leak. At 1 month follow-up the patient had no evidence of right pleural fluid and remains without evidence of fistula at five months. The skin site is well-healed.Discussion: In this case, an ECF was closed with a Cook Biodesign SIS fistula plug allowing for a successful non-operative strategy after multiple failed operative revisions. The plug has FDA approval for the treatment of anal fistula, but given the positive outcome in this case, its use in esophagocutaneous fistulas may be a viable off-label option for other patients.

Poster #: CR-012

Leptomeningeal Melanocytosis: A Lethal Cause of Pediatric Seizures

Sophia Xie, MD, *sophia.xie@phhs.org*; Cory M. Pfeifer, MD; Radiology, University of Texas Southwestern, Dallas, TX

Disclosures: All authors have disclosed no financial interests, arrangements or affiliations in the context of this activity.

Purpose or Case Report: Leptomeningeal melanocytosis is a rare proliferation of melanocytes in the arachnoid and pia mater that presents as diffuse leptomeningeal enhancement. Findings in a rare case of this disorder are discussed along with differential considerations and diagnostic implications.
Methods & Materials: A 9-year-old male presented to the emergency department after hitting his head on the door of a car. CT of the head performed at that time showed minimal high attenuation material throughout the right parietal cortical reported as a small amount of subarachnoid hemorrhage. After it became clear that the patient was having uncontrolled seizures that may have contributed to the original trauma, he was placed on anti-epileptic medication and referred for MRI.
Results: Multiple MRI's were performed with and without contrast over the next 6 months. The findings on the CT were found to be due to thickening of the leptomeninges which exhibited robust contrast enhancement, greatest in the right parietal lobe. Multifocal hemorrhages were observed in the left cerebral hemisphere over the course of the exams. A diagnosis of Sturge-Weber Syndrome was assigned. Since the leptomeningeal enhancement showed progression over 5 months, a surgical biopsy was performed. Upon entry into the calvarium, the surface of the brain was found to be dark brown in color. Biopsy revealed the diagnosis of leptomeningeal melanocytosis.
Conclusions: Leptomeningeal melanocytosis is a rare disorder that can be confused with infectious, inflammatory, and/or vascular abnormalities. The disease is typically fatal with a short life expectancy following diagnosis. Careful attention on follow-up of leptomeningeal enhancement is essential to exclude a proliferative or neoplastic process.

Poster #: CR-013

Rest assured, it's benign: Intrathyroidal thymic rests

Adina Alazraki, MD, *adina.alazraki@choa.org*; Sarah Milla, MD; Children's Healthcare of Atlanta, Atlanta, GA

Disclosures: All authors have disclosed no financial interests, arrangements or affiliations in the context of this activity.

Purpose or Case Report: Ectopic thymic tissue may be found in the neck in up to 20% of the general population. Intrathyroidal thymic rest has been described as a rare entity, present in as many as 1% of children. The course of thymic migration parallels the thyroid and parathyroid glands, which explains their similar ectopic locations. While the natural history of these lesions has not been well studied, it is likely that there is involution of thymic rests with age. A few individual case reports have described the imaging features of intrathryoidal thymic rests confirmed by histopathology and flow cytometry. The aim of this case series is to raise awareness of the characteristic sonographic appearance of this entity to the radiology community.
Methods & Materials: This case series will review clinical and imaging features of 4 biopsy-proven intrathyroidal thymic rests. Characteristic imaging features will be elucidated. Differences between this entity and more concerning thyroid nodules that require biopsy and perhaps excision will be highlighted.

Results: The presence of dot-dash echogenic foci within a focal hypoechoic nodule are characteristic for thymic rests but can be mistaken for more worrisome calcifications in a thyroid nodule. Additionally, the border can be lobulated and somewhat irregular, which is another significant feature of suspicious thyroid nodules by TiRADS criteria.
Conclusions: The sonographic appearance of thymic rests within the thyroid gland is very characteristic and should be suggested in the differential diagnosis of an incidentally found characteristic nodule in an otherwise healthy child. These nodules do not follow TiRADS criteria for benignity, however, radiologists should be aware of this entity. When patients have this classic appearance , conservative management should be considered, with less invasive sampling with fine needle aspiration favored over surgical excision if there remains clinical concern.

Poster #: CR-014

In the Chest, the Abdomen, and the Pelvis: 3 Cases of Inflammatory Myofibroblastic Tumors in Children in Varied Locations

Jane B. Lyon, M.D., *jlyon@uwhealth.org*; Hau D. Le, M.D.; Department of Radiology, University of Wisconsin School of Medicine and Public Health, Madison, WI

Disclosures: All authors have disclosed no financial interests, arrangements or affiliations in the context of this activity.

Purpose or Case Report: Inflammatory Myofibroblastic Tumor (IMT) is now considered a distinct entity and a true neoplasm within the heterogeneous group of inflammatory mass-forming tumors. It is now recognized as a fibroblastic/myofibroblastic neoplasm with intermediate biological potential. It occurs predominantly in children. Abnormalities on Chromosome 2p23 with a rearrangement of the ALK (anaplastic lymphoma kinase) locus causes abnormal tyrosine kinase receptor expression. Chromosomal abnormalities suggest a clonal origin and not just a reactive process or "pseudotumor," as these masses have been categorized in the past. Up to sixty percent of inflammatory myofibroblastic tumors express ALK which may help establish the diagnosis of the inflammatory mass as an IMT. The masses can occur in a variety of locations and have non-specific imaging findings, which will be reviewed.We present three cases, each in a different location:Case 1: 7 year old female presents with chronic cough and persistent right middle lobe abnormality on chest x-ray with concern for pneumonia or inhaled foreign body. She was found to have a soft tissue mass in her right mainstem bronchus with extra-luminal extension. CT, MR and gross surgical photos of the endobronchial IMT will be presented.Case 2: 20 month old male presents with hepatomegaly, jaundice and elevated bilirubin, alkaline phosphatase and liver function tests. Ultrasound and MR images of the pancreatic head IMT causing biliary obstruction will be presented.Case 3: 13 year old male presents with back, leg and pelvic pain. MR, CT and gross surgical photos of the right posterior pelvic sidewall IMT, which had evidence of nerve entrapment at biopsy, will be presented.The imaging, pathological and surgical findings from these patients, where available, will be presented and reviewed.We suggest that the radiologist consider Inflammatory Myofibroblastic Tumor in the differential diagnosis for inflammatory and fibrous lesions in children.

Poster #: EDU-001

Born To Be Wide: Aortopathy and Thoracic Aortic Aneurysm in Children

Andrew B. Wallace, *wallaceab@wustl.edu*; Demetrios Raptis, MD, Sanjeev Bhalla, MD; Mallinckrodt Institute of Radiology, Saint Louis, MO

Disclosures: All authors have disclosed no financial interests, arrangements or affiliations in the context of this activity.

Purpose or Case Report: This case-based, pictorial, educational exhibit will:1. Examine the predisposing conditions of thoracic aortic aneurysm (TAA) in children2. Illustrate the histopathologic and imaging features of these conditions3. Demonstrate proper technique for measuring and reporting aortic dimensions in children4. Review treatment options for TAA and how treatment depnds on the underlying disease and imaging findings
Methods & Materials: There are several inherited disorders and congenital defects that predispose to progressive dilation of the thoracic aorta in childhood. Well known disorders like Marfan syndrome and bicuspid aortic valve have long served as clinical models but many, seemingly disparate, disorders result in similar abnormalities of the aorta. As knowledge about the genetic and histopathologic underpinnings of TAA grows, management will be guided by multidisciplinary teams. In order to maintain value in these teams, the pediatric radiologist must understand the varied causes of TAA, the underlying histopathology, and the treatment implications. This exhibit will introduce these predisposing conditions, review the similarities and differences, and review treatment options.
Results: The following conditions that predispose to aortic aneurysm will be reviewed:I. Extracellular Matrix Proteins1. Marfan Syndrome2. Ehlers-Danlos Syndrome3. Alport Syndrome4. Cutix Laxa5. MFAP5 Gene MutationII. TGF-ß Signaling Pathway1. Loeys-Dietz Syndrome2. Osteoarthritis-Aneurysm Syndrome3. Sphrintzen-Goldberg Syndrome4. Arterial Tortuosity Syndrome5. SMAD2 and SMAD4 Gene MutationsIII. Nonsyndromic Familial Thoracic Aortic Aneusysms and Dissections Gene Mutations1. ACTA22. MYH113. MLK4. PRKG15. FLNA6. MAT2AIV. Congenital Heart Disease1. Bicuspid Aortopathy2. Aortic Coaractation3. Tetralogy of Fallot4. Truncus Arteriosus5. Hypoplastic Left Heart Syndrome6. Ross Procedure7. Arterial Switch Procedures
Conclusions: Seemingly disparate conditions converge to cause similar aortopathies, resulting in TAA. As knowledge about aortopathy expands, pediatric radiologists must maintain knowledge about the defects and disorders linked to TAA, understand expected patterns of aortic dilation in the different conditions, and provide meaningful information to colleagues in cardiology and surgery. In doing so, radiologists will maintain value in the multidisciplinary approach these conditions warrant.

Poster #: EDU-002

Unpacking the trunc: Imaging of Truncus Arteriosus

Erin Romberg, MD, *erin.romberg@seattlechildrens.org*; Sadaf Bhutta, MD; Radiology, Seattle Children's Hospital, Seattle, WA

Disclosures: All authors have disclosed no financial interests, arrangements or affiliations in the context of this activity.

Purpose or Case Report: Truncus arteriosus is a rare congenital cardiac anomaly characterized by failure of conoseptal separation resulting in a single arterial trunk supplying both the pulmonary and systemic circulation.

Diagnosis has historically been made with fetal echocardiography, and palliative surgery performed frequently in the neonatal period. Cross-sectional imaging is typically reserved for post-operative complications. However, due to lower dose radiation and faster scanners, preoperative CT angiography imaging is becoming more common with the increasing use of cardiac EKG-gated CT angiograms, requiring pediatric imagers to be familiar with the diagnosis of the truncus arteriosus spectrum.
Methods & Materials: This retrospective imaging review will describe the imaging features of truncus arteriosus, including the 2-D multiplanar reformatted images and 3-D volume rendered images. Various anatomical types of Truncus Arteriosus detailed in the widely used Van Praagh classification will be demonstrated. Illustrative examples will also detail variants not clearly defined by the current classification systems. Important imaging distinctions between truncus arteriosus and other similar appearing congenital cardiac anomalies, such as Tetralogy of Fallot or pulmonary atresia with major aorto-pulmonary collateral arteries, will be described.
Conclusions: This educational exhibit will provide viewers with a framework to recognize and classify truncus arteriosus, as well as provide vital distinction between truncus arteriosus and other similar appearing conotruncal anomalies.

Poster #: EDU-003

Practical Use of Compressed Sensing in Clinical Pediatric Cardiovascular MRI: The Low Hanging Fruit.

Taylor Chung, MD[1], *taylorchung12@gmail.com*; Mariya Doneva, PhD[3], Quin Lu, PhD[2], Dave Hitt[2], Jonathan I. Tamir[4]; [1]UCSF Benioff Children's Hospital Oakland, Oakland, CA, [2]Philips Healthcare, Gainesville, FL, [3]Philips Research, Hamburg, Germany, [4]University of California Berkeley, Berkeley, CA

Disclosures: Mariya Doneva, PhD: Salary: Philips Research; **Quin Lu, PhD:** Salary: Philips; **Dave Hitt:** Salary: Philips HealthTech; **Jon Tamir, PhD:** Consultant, Honoraria & Equity Interest/Stock Option: Subtle Medical, Research Grants: GE Healthcare. All other authors have disclosed no financial interests, arrangements or affiliations in the context of this activity.

Purpose or Case Report: This electronic educational poster will first introduce the concept behind Compressed Sensing - a very powerful MR technique (that has just become commercially available in 2018) allowing for, amongst many different applications, acceleration of MR data acquisition beyond parallel imaging (SENSE, GRAPPA, ASSET). Then, the poster will show comparative clinical examples of application of Compressed Sensing onto commonly used cardiovascular MR sequences such as 1) cine balanced SSFP, both breath-hold and non-breath-hold examinations, 2) cine phase contrast in free-breathing, and 3) respiratory-navigated 3D Whole-Heart examination using T1-weighted fast gradient echo sequence with DIXON technique. In these clinical examples, Compressed Sensing, in addition to parallel imaging, can further accelerate the acquisition time to allow for less number of breath-holds for patients to complete a stack of cine images through the ventricles without sacrificing spatial or temporal resolution or signal-to-noise ratio. The acquisition time of free-breathing cine phase contrast can be reduced and yield accurate flow quantification. The increased speed of acquisition can be traded off to achieve higher spatial resolution in young patients who may not be able to achieve long breath-hold times otherwise needed when high spatial resolution is necessary. These clinical examples were accumulated since January 2017 with a Compressed Sensing software patch made available by the scientific research group of the MR vendor under research agreement and the clinical use was approved by Institutional Review Board.

Poster #: EDU-004

Pediatric congenital arterial switches: on or off?

Jennifer Wu[1], *jjw386@gmail.com*; Ross A. Myers, MD[1], David Sadowsky, MD[1], Tianyang Li, MD[1], Edison Tsui[2], Pierre-Yves Sonke[1]; [1]Westchester Medical Center, Valhalla, NY, [2]Columbia University, New York, NY

Disclosures: All authors have disclosed no financial interests, arrangements or affiliations in the context of this activity.

Purpose or Case Report: Congenital heart diseases often occurs secondary to a variety of insults and rotational errors during development in utero. These can range from a spectrum of simple to more complex pathologies including arterial switches. It is important for radiologists to recognize the embryology and complications of arterial switches to further management. Today largely secondary to new advances in technology both corrected and uncorrected arterial switches are diagnosed more commonly; previously many patients with arterial switches may not have survived into adulthood.In utero, the primitive truncus is normally positioned anterior and midline. It eventually divides into the aorta and the pulmonary artery, which then rotates clockwise 150 degrees such that the pulmonary artery lies anterior to and left of the aorta. When variations occur it can result in a congenitally corrected transposition such as L- transposition of the great arteries (L-TGA) where the two ventricles are morphologically switched in position. With L-TGA, the truncus rotates 30-degrees clockwise which results in the aorta being anterior and leftward in relation to the pulmonary artery.In uncorrected transposition (R-TGA) the aorta arises from the right ventricle and the pulmonary artery arises from the left ventricle, secondary to a 30-degree counterclockwise rotation of the primitive truncus, the aorta is then located rightward and anterior to the pulmonary artery. This condition needs to be corrected surgically due to cyanosis resulting from the right ventricle not being able to supply the systemic circulation. Other variations of arterial switches that can occur is situs inversus where the rotation of the aorta and pulmonary artery is completely opposite of that which would be considered normal. Lastly in truncus arteriosus, the primitive truncus does not divide into a separate aorta and pulmonary artery. We will provide several cases from our institution of arterial switches on imaging as well as diagramatic representative models describing the embryology of how arterial switches and rotations occur. We also discuss the repairs and complications of these cases.
Conclusions: Congenital arterial switches and complications from repairs can be confusing but are becoming more commonplace. It is thus important for radiologists to understand the embryology and identify the imaging characteristics.

Poster #: EDU-005

RASA1 mutations associated with capillary malformation-arteriovenous malformation: imaging findings

Frederic Thomas-Chausse, MD[1], *frederic.thomas-chausse.hsj@ssss.gouv.qc.ca*; Maïa Proisy, M.D[1], Catherine McCuaig, MD[2], Francoise Rypens, MD[1], Chantale Lapierre, MD[1], Josée Dubois, MD[1]; [1]CHU Sainte-Justine, Medical Imaging Department, Montreal, Quebec, Canada, [2]CHU Sainte-Justine, Department of Pediatrics, Montreal, Quebec, Canada

Disclosures: Maïa Proisy, M.D.: Research Grants: Société Francaise de Radiologie, Région Bretagne (France). All other authors have disclosed no financial interests, arrangements or affiliations in the context of this activity.

Purpose or Case Report: Capillary malformation-arteriovenous malformation (CM-AVM) is an autosomal dominant disorder with variable phenotype caused by heterozygous inactivating mutations in the RASA1 gene located on chromosome 5. Clinical manifestations are variable with cutaneous multifocal capillary malformation associated with fast-flow lesions. Most of them are located in soft tissues (intramuscular, intraosseous, spinal or cerebral). Many authors reported the clinical spectrum or the genetic association but few data are available on the imaging characteristics or criteria to establish the diagnosis of AVM. The goal of this poster is to review the imaging characteristics in the RASA1 series of our institution and in particular to evaluate the distribution of patients having true AVMs versus capillary hypervascularity. **Methods & Materials**: A retrospective study of clinical and imaging files was conducted for all patients seen in our vascular anomalies group with a genetic diagnosis confirmation of RASA1 mutation. Institutional approval was obtained from the IRB and all patients (or parents) signed an informed consent. We reviewed 9 cases (8F, 1M) with RASA1 mutations. Cutaneous capillary malformation aspect, color Doppler ultrasound and MR findings will be described. Lung AVM has never been reported in RASA1 except in our series. **Conclusions**: Patients with RASA1 mutations have a wide spectrum of clinical manifestations. CM is the clue for the diagnosis, particularly if the CM has the pale halo. However, the AVM criterion for extracranial lesions has to be clarified. Most lesions in our series behave more like a capillary hypervascularization without AV shunting. Thus, the presence of extracranial/spinal true AVMs seems to be rare. The integration of genetic, clinical and imaging findings is important to have a better understanding of the disease and to offer the best treatment.

Poster #: EDU-006

Thinking Outside The Heart-Shaped Box- A Pictorial Review of Extracardiac Complications of Congenital Heart Disease in Infants.

Jamie Frost, DO,*j_mel46@yahoo.com*; Michigan State University, Grand Rapids, MI

Disclosures: All authors have disclosed no financial interests, arrangements or affiliations in the context of this activity.

Purpose or Case Report: Congenital heart disease (CHD) is the most common type of birth defect; affecting ~1% of the births per year in the U.S. Advancements in medical and surgical treatment have markedly improved survival and even infants with complex CHD survive into adulthood. However, extracardiac complications in the newborn period can cause increased morbidity and mortality. These complications can relate to alteration in flow dynamics, treatment changes, and/or sequelae of associated syndromes (Trisomy 21, 22q deletion syndrome, Heterotaxy, PHACES). The purpose of this exhibit is to highlight extracardiac complications of CHD and to review their imaging findings. Imaging findings to be reviewed will include catheter thromboses, necrotizing enterocolitis, arterial ischemic strokes, infections, malrotation, pulmonary complications related to prematurity, prolonged intubations, and associated syndromes, and complications of extracorporeal membrane oxygenation. The goal of this exhibit is to familiarize radiologists with the multiplicity of extracardiac complications in infants with CHD and to review the common imaging findings.

Poster #: EDU-007

The Varied Manifestations of Cystic Renal Disease on Fetal MRI: What the Radiologist Needs to Know

Nicole P. Steinhardt[1], *nsteinha@iu.edu*; Mariana L. Meyers, MD[2], Brandon P. Brown, MD, MA[1]; [1]Radiology and Imaging Sciences, Indiana University School of Medicine, Indianapolis, IN, [2]Children's Hospital Colorado - CFCC, Aurora, CO

Disclosures: All authors have disclosed no financial interests, arrangements or affiliations in the context of this activity.

Purpose or Case Report: Fetal MRI is now an important adjunct imaging modality in the evaluation of complex fetal anomalies, including cystic renal disease. The improved resolution and anatomic detail of the renal parenchyma offered by MRI can assist with identification, localization, and characterization of cystic lesions which are less clearly visualized on ultrasound. Advanced imaging adds value through enabling prenatal prognostication and patient counseling. In this presentation, we evaluate the spectrum of renal cystic abnormalities at the microscopic and macroscopic scale, and review the patterns of disease by cyst location, effect on parenchymal integrity, and obstruction of the collecting system. A clearer understanding of the diverse appearances and broad spectrum of outcomes of these fetal anomalies can contribute to more detailed treatment planning and more precise, family-centered care.In this presentation, we review the varied patterns of cystic renal disease as identified on fetal MRI, highlighting those forms known to be more associated with perinatal morbidity and mortality. Further, we correlate their appearance on MRI with pre- and post-natal US imaging, as well as pathologic findings. Finally, we will describe secondary prenatal imaging biomarkers that may be valuable in counseling and also with both definitive and palliative surgical planning.

Poster #: EDU-008

Contrast-enhanced ultrasound for the evaluation of the neonatal brain: Diagnostic methods and scanning protocol

Kayla Cort, DO, *kayla.cort12@gmail.com*; Maciej Piskunowicz, MD, Misun Hwang, MD; Children's Hospital of Philadelphia, Philadelphia, PA

Disclosures: All authors have disclosed no financial interests, arrangements or affiliations in the context of this activity.

Purpose or Case Report: Contrast-enhanced ultrasound (CEUS) for the evaluation of the neonatal brain provides additional diagnostic information when compared to conventional gray scale ultrasound through the detection of perfusion abnormalities associated with injury. When compared to cross-sectional imaging, CEUS has many advantages given its relative low cost and ability to be performed at the bedside, without the need for sedation or exposure to ionizing radiation. Diagnostic information is yielded through the qualitative

evaluation of parenchymal enhancement patterns as well as quantification of microbubble perfusion kinetics from which time intensity curves are derived and additional perfusion parameters can be extrapolated. Given the 2-dimensional nature of the modality, a strategically designed scanning protocol is necessary to obtain the aforementioned quantitative values. The purpose of this exhibit is to demonstrate the current understanding of brain CEUS and educate on the brain CEUS protocol used for the diagnosis of neonatal brain pathology.

Poster #: EDU-009

Spotlight on the Fetal Eye: A Review of Prenatal Orbital Malformations

Eman S. Mahdi, M.D.[1], *dremansm81@gmail.com*; Matthew Whitehead, MD[2], Mohannad Al-Samarraie, M.D.[1], Dorothy Bulas, MD[2]; [1]Radiology department, University of Missouri Hospital, Columbia, MO, [2]Children's National Health System, Washington, DC

Disclosures: All authors have disclosed no financial interests, arrangements or affiliations in the context of this activity.

Purpose or Case Report: Congenital eye malformations are relatively rare. However, they are often associated with complex clinical syndromes that require extensive prenatal evaluation and counseling. The purpose of this study is to provide a review of various congenital ocular anomalies that can be detected on prenatal ultrasound and/or MRI in isolation or as part of a syndromic findings and to address the importance of the prenatal genetic evaluation and parental counseling.
Methods & Materials: A retrospective review of the radiology database at our institution is performed. Various congenital orbital malformations are reviewed using prenatal ultrasound and/or multiplanar fetal MRI images.
Results: Presented orbital pathologies are:hypo/hypertelorism, micro/anophthalmia, cataract, coloboma, optic nerve hypoplasia, persistent hyperplastic primary vitreous and orbital masses with discussion on the associated clinical syndromes.
Conclusions: Early prenatal diagnosis of ocular malformations has an important role in appropriate genetic counseling and postnatal management.The identification of orbital anomalies can help in the search for associated cerebral or systemic anomalies.

Poster #: EDU-010

The Extremely Low Gestational Age Infants: Neuro Sonography of Normal Brain and Complications.

Abhijeet Taori, MD, DNB, EDiR, *ataori@cheo.on.ca*; Emanuela Ferretti, MD, FRCPC, Elka Miller, MD, Claudia Martinez-Rios; CHEO, University of Ottawa, Ottawa, Ontario, Canada

Disclosures: All authors have disclosed no financial interests, arrangements or affiliations in the context of this activity.

Purpose or Case Report: Advances in Neonatal Intensive Care have led to substantial improvement in survival of preterm infants of extremely low gestational age (ELGA) between 22+0 and 23+6 weeks gestation. ELGA newborns are more susceptible to several complications of prematurity. Recognition of the sonographic features of the normal brain and identification of potential short and long-term complications of these infants is paramount.High resolution transfontanellar ultrasonography is the baseline “gold standard” of care imaging modality to assess the integrity of the neonatal brain and potential complications encountered in ELGA newborns. Color and spectral Doppler US allows high reliability and precision in the evaluation of the intracranial vasculature.The purpose of this exhibit is1. To illustrate a spectrum of the sonographic features of the normal developing brain in ELGA infants.2. To characterize the sonographic findings of short and long-term brain anatomical complications.3. To describe common pitfalls when imaging these infants.

Poster #: EDU-011

Prenatal Imaging Evaluation of Disorders of Sexual Development

Tara Cielma, *tcielma@cnmc.org*; Anna Blask, Eva Rubio, Judyta Loomis, Meg Menzel, Dorothy Bulas, MD; Children's National Medical Center, Washington, DC

Disclosures: All authors have disclosed no financial interests, arrangements or affiliations in the context of this activity.

Purpose or Case Report: Background: Disorders of sexual development (DSD) resulting in ambiguous genitalia are a rare spectrum of anomalies that have the potential to be diagnosed prenatally using a combination of genetic testing and imaging. The incidence of prenatal detection is rising with the increased use of noninvasive prenatal testing, which can reveal discordance between genotype and phenotype.Sonographic and MR imaging contribute to prenatal assessment of disorders of DSD and may narrow the differential diagnosis and facilitate prenatal testing and postnatal evaluation.The goals of this exhibit are:1. Review imaging features of normal prenatal male and female genitalia.2. Review imaging patterns of ambiguous genitalia.3. Discuss changes in appearance with various pathologies, providing imaging examples.4. Review different categories of disorders of sexual differentiation and see how imaging may narrow the differential diagnosis.
Methods & Materials: Fetal ultrasound and MR studies at our institute were reviewed retrospectively with selected representative cases chosen to illustrate technical aspects and to demonstrate the imaging features in cases of ambiguous genitalia. Correlation was made with NIPT, amniocentesis, and CVS results in conjunction with follow up radiology studies, and clinical or surgical outcomes.Categorical disorders of sexual development, such as 46 XX, 46 XY, ovotesticular DSD and sex chromosome will be described.
Results: Prenatal findings in the normal fetus and in disorders of sexual development fetal will be illustrated with postnatal correlation.
Conclusions: DSD is a complex group of disorders requiring an understanding of anatomical variations of genitalia and the diseases within each group. US and MR contribute to the prenatal detection of DSD, help narrow the differential diagnosis and help direct prenatal and postnatal genetic testing and imaging.

Poster #: EDU-012

A Review of Cystic Pediatric Presacral Masses: Sacrococcygeal Teratoma and Beyond

Ryan Murphy, MD, *murp1066@umn.edu*; Michael A. Murati, Tara Holm, Kelly Dietz, MD; Department of Radiology, University of Minnesota, Plymouth, MN

Disclosures: All authors have disclosed no financial interests, arrangements or affiliations in the context of this activity.

Purpose or Case Report: The presacral space is composed of multiple tissue types, including osteochondral, mesenchymal, neurogenic, vascular and lymphatic. The presence of these tissues leads to a long and complex differential for a presacral mass in a pediatric patient. Specifically, the differential also

includes anterior sacral meningocele, enteric cyst, vascular malformations, neuroblastoma, ganglioneuroma, schwannoma, neurofibroma, rhabdomyosarcoma, lymphomatous masses, giant cell tumor, aneurysmal bone cyst, osteosarcoma, Ewing sarcoma, and chordoma. Imaging plays a key role in characterizing these masses and treatment planning. Familiarity with the common presacral masses of infancy and childhood is therefore necessary for the pediatric and general radiologist.Once an osteochondral or neurogenic mass is excluded, and a predominantly cystic presacral mass is present, the primary differential consists of a collection of developmental or congenital masses including sacrococcygeal teratoma, anterior meningocele, low flow vascular malformation, and an enteric duplication cyst. We will review the common imaging features and associations of these cystic masses by presenting a series of cases. Additional examples of solid and osteochondral presacral masses will be included where appropriate for comparison in order to avoid characterization pitfalls and highlight teaching points.

Poster #: EDU-013

Prenatal three-vessel and trachea view: the rationale behind doing it.

Julie Dery, MD, *julie.dery.hsj@ssss.gouv.qc.ca*; Francoise Rypens, MD, Juliette Garel, MD, Marie-Josee Raboisson, MD, Chantale Lapierre, MD; Medical Imaging Department, CHU Sainte-Justine, Montreal, Quebec, Canada

Disclosures: All authors have disclosed no financial interests, arrangements or affiliations in the context of this activity.

Purpose or Case Report: Prenatal screening and diagnosis of fetal anomalies rely upon ultrasound studies (US). US is generally considered safe during pregnancy. It is estimated that 1% of all neonates are born with a congenital heart defect that makes careful standardized examination of the fetal heart a mandatory step during all fetal US exams. US examination of the fetal heart requires at least analysis of the fetal situs, the four-chamber (4CH) view and the three-vessel view (3V). In the evaluation of the fetal heart, it is now worldwide accepted that the three-vessel trachea (3VT) view should be obtained, if technically feasible, in supplement of the other classical fetal cardiac views (4CH, 3V).The relevance of adding the 3VT view is that some congenital cardiovascular abnormalities, potentially significant for fetal outcome, can only be diagnosed with this view; these malformations include vascular rings and right aortic arches.
Methods & Materials: We conducted a retrospective review of prenatal US and cardiac US data of fetuses with abnormal 3VT view, with correlation with postnatal imaging (CTA) and outcome. The most frequent abnormalities detectable will be illustrated and discussed: right aortic arch with retroesophageal diverticulum of Kommerell, mirror-image right aortic arch, right aortic arch with aberrant left subclavian artery, right circumflex aorta, double aortic arch and left aortic arch with aberrant right subclavian artery.The goals of this exhibit are:- To review the normal appearance of the fetal 3VT view;- To review the embryological development of aortic arches explaining the malformations that can be observed;- To understand the significance of abnormal appearance of the fetal 3VT view by correlation with postnatal CT-scan imaging;- To propose a practical algorithm and work-up regarding detection of an abnormal 3VT view in a foetus;- To help radiologists provide appropriate counselling to parents when discovering an abnormal 3VT view in routine fetal screening.

Poster #: EDU-014

Assessment of Lower Extremity Anomalies in the Fetus

Richard Becker, MD, *karatmanek@hotmail.com*; Eva I. Rubio, MD, Dorothy Bulas, MD, Anna Blask, MD, Judyta Loomis, MD, Matthew Oetgen, MD; Radiology, Childrens National Medical Center, Indianapolis, IN

Disclosures: All authors have disclosed no financial interests, arrangements or affiliations in the context of this activity.

Purpose or Case Report: Congenital anomalies causing lower extremity shortening can result from dysgenesis or agenesis of the bones of the thigh, leg or foot; they are generally a very uncommon occurrence, with an incidence on the order of one case per 1,000,000 to one case per 100,000 births. These conditions result in varying degrees of morbidity, ranging from gait dysfunction to complete lack of the ability to ambulate. The accurate characterization of such an anomaly may be challenging prenatally, but can have significant impact on prognosis and treatment planning.We present a collection of cases depicting the spectrum of prenatally diagnosed anomalies of limb development, including proximal focal femoral deficiency, multiple cases of varying degrees of fibular and tibial hemimelia, amniotic band syndrome, benign uterine packing, neurofibromatosis, clubfoot anomaly and rocker bottom foot, all of which were evaluated on prenatal ultrasound and/or fetal MRI. Accurate prenatal diagnosis is extremely important for prognosis, treatment planning and risk-stratification for associated congenital anomalies. The purpose of this poster will be to highlight the imaging features by both fetal MRI and prenatal US, discuss potential diagnostic pitfalls and review the clinical implications of this interesting spectrum of congenital disorders. We will describe a methodical approach to assessment of these patients. Our recommendations include: prenatal US to include a complete set of bilateral long bone and foot length measurements; lateral and footprint views of the fetal foot; views of both tibiae and fibulae bilaterally; views of the spine and upper extremities, a thorough search for other abnormalities; fetal MRI for complex cases or when US findings are limited; and a complete family and maternal history, including notation of family stature.Examples of the classic appearance of these conditions will be presented. Several missed diagnoses and the lessons learned will also be discussed. Counseling points addressed by the orthopedic surgeon will be included. Outcome management will be reviewed.

Poster #: EDU-015

Fetal MRI of Multiple Gestations at 3 Tesla: A Double-Edged Modality

Matthew Bauer, *matthew.p.bauer6.mil@mail.mil*; Matthew Burgess, MD, Mark Heitzmann, DO; Naval Medical Center San Diego, San Diego, CA

Disclosures: All authors have disclosed no financial interests, arrangements or affiliations in the context of this activity.

Purpose or Case Report: This educational exhibit will demonstrate the strengths and weakness of Fetal MRI at 3 Tesla in the evaluation of multiple gestations.
Methods & Materials: Employing a case series of multiple gestation pregnancies evaluated via 3 Tesla MRI, this educational exhibit will highlight the strengths and weaknesses of imaging obtained at a higher magnetic field strength when compared the more routinely available 1.5 Tesla field strength. Findings and pathology will be correlated with prenatal ultrasounds as well as post-natal imaging as applicable.

Results: Although the superior resolution obtained at higher field strengths can be advantageous in identifying and further characterizing fetal pathology, the sequences are more susceptible to artifact accentuation, particularly dielectric effect and motion.
Conclusions: The continued advancement of MR imaging technology has made higher field strength imaging available at a growing number of medical centers. Although imaging at 3 Tesla affords improved spatial resolution to visualize and define pathologic entities, the increased prevalence of artifacts at these higher field strengths, particularly in the setting of multiple gestations, requires familiarization on the part of both the technologist and radiologist to ensure diagnostic images are successfully obtained.

Poster #: EDU-016

Spectrum of Midface Anomalies on Fetal MRI

Arielle VanSyckel, MD, MS, *aresvans@iu.edu*; Brandon P. Brown, MD, MA; Radiology and Radiological Sciences, Indiana University, Indianapolis, IN

Disclosures: All authors have disclosed no financial interests, arrangements or affiliations in the context of this activity.

Purpose or Case Report: Midface anomalies in the fetus can present with a range of severity and corresponding neonatal morbidity, on a spectrum from cosmetic disturbance to airway obstruction. Immediate postpartum complications include life-threatening hypoxia and feeding disturbances. These anomalies not only present immediate difficulties but also often exist within a variety of syndromes with long-term consequences, affecting various organ systems. While screening ultrasound frequently can identify deviations from normal, fetal MRI may provide more detailed and high-resolution imaging for the characterization of midface anomalies and associated prenatal disease.The identification of facial anomalies in utero should prompt further investigation for associated abnormalities, and will also allow for improved prenatal counseling, which can prepare parents for the immediate postpartum management including surgical planning and resource allocation. It furthermore provides a foundation to shape family expectations and to begin to frame psychosocial support, allowing parents to engage mentally and emotionally with the medical and surgical course that awaits.In this presentation, we highlight the normal fetal midface as seen on MRI at various stages of development, and outline a systematic approach for evaluation of the fetal midface structures. Recognition of this typical appearance will allow the radiologist to identify the range of possible abnormalities that can occur and which can shape prognosis when properly identified. Various cases of midface anomalies will be reviewed and linked to their clinical significance, including cases with associated intracranial anomalies and deficiencies in swallowing and respiration.

Poster #: EDU-017

Neuronal migrational anomalies and cortical malformations in Fetal MRI - Embryological perspective and avoiding pitfalls

Shankar S. Ganapathy, MD[1], *sganapathy@akronchildrens.org*, Kyle Hunter[2], Emily Janitz[1], Gayathri Sreedher[1]; [1]Pediatric Radiology , Akron Children's Hospital , Akron, OH, [2]Aultman Hospital, Canton, OH

Disclosures: All authors have disclosed no financial interests, arrangements or affiliations in the context of this activity.

Purpose or Case Report: Neuronal migration and cortical organization takes place primarily during the second trimester and early third trimester. Therefore, detection of cortical malformations and migrational anomalies on a fetal MRI in a maturing brain is difficult and may not be evident in some cases, if performed early.Familiarity with normal sulcation pattern in a fetus at various ages of gestation and a basic understanding of the embryogenesis of neuronal migration is essential to be able to make a diagnosis of these entities.**Goals of the exhibit** -Understand development of cerebral cortex and normal fetal MRI appearance at various stages of gestation.-Using this knowledge, be able to recognize various cortical malformations in a fetus and provide a comprehensive diagnosis regarding etiology, whenever feasible or when the appearance is typical or when there are ancillary findings- Avoid certain pitfalls and improve accuracy without overcalling or undercalling migrational anomalies in a fetal MRI**Outline of the exhibit**Embryology of neuronal migration (during second and third trimesters)Normal sulcation pattern during mid and late trimestersEtiology of neuronal migration and cortical malformations-Multifactorial- Infectious- Genetic mutation/chromosomal- Ischemic insult- Metabolic disorders like Zellweger**Appearance of various migrational anomalies and cortical malformations in a fetal brain**Polymicrogyria – subtle and extensive forms, appearance during various stages of gestation, correlation with post-natal imaging, typical appearance in certain genetic mutations, TORCH infections etcSchizencephaly – associations with absence of septum pellucidum and other abnormalitiesGray matter heterotopia – How to differentiate from subependymal nodules and hemorrhage?Lissencephaly – How to identify a true lissencephaly/pachygyria in a developing brain with immature sulcal pattern?Hemimegalencephaly, Microcephaly with simplified gyral pattern and other cortical malformations. Evolution of cortical malformations on imaging-Comparison between early and late gestation fetal MRIs in the same patient when available- Prenatal and post-natal MRI correlation of migrational anomalies, when availableAncillary CNS and extra-CNS abnormalities identified in fetuses with migrational anomaliesPitfalls and false positive/ false negative cases and how to avoid them.

Poster #: EDU-018

Radiological findings in nutritional deficiencies and eating disorders in children: A pictorial review

Christian A. Barrera, M.D., *barreracac@email.chop.edu*; Savvas Andronikou, MBBCh, FCRad, FRCR, PhD (UCT), PhD (Wits), Hansel J. Otero, MD; The Children's Hospital of Philadelphia, Philadelphia, PA

Disclosures: All authors have disclosed no financial interests, arrangements or affiliations in the context of this activity.

Purpose or Case Report: Nutritional deficiencies in children are prevalent both in the US and abroad often under-diagnosed unless symptomatic. Some nutritional deficiencies have conspicuous imaging findings that might help with diagnosis and/or follow up in a timely manner. Similarly, imaging might be needed to diagnose or follow complications related to malnutrition and eating disorders such as bulimia, anorexia nervosa, binge eating and pica. This educational exhibit will review radiographic, CT and MR imaging of nutritional deficiencies and complications of malnutrition and eating disorders in children

Poster #: EDU-019

Pediatric Emergency Gastrointestinal Ultrasonography: Pearls and Pitfalls

Moshe Meister, MD[1], *moshe.meister1@gmail.com*; Jane Kim, MD[2], Jennifer K. Son[2]; [1]University of Maryland Medical Center, Baltimore, MD, [2]University of Maryland School of Medicine, Baltimore, MD

Disclosures: All authors have disclosed no financial interests, arrangements or affiliations in the context of this activity.

Purpose or Case Report: Ultrasonography (US) is an essential tool in pediatric imaging, particularly in the emergency setting. Although US is often the favored initial modality for abdominal imaging in children, it is a highly operator-dependent modality prone to misinterpretation which can lead to false positive or negative exams, or even a different, incorrect diagnosis. Conditions discussed in this series include ileocolic intussusception, hypertrophic pyloric stenosis, appendicitis, and foreign bodies. We will review diagnostic criteria, highlight crucial findings, as well as illustrate commonly-encountered difficulties and mimics.

Poster #: EDU-020

Do we need to differentiate between different types of intestinal rotational abnormalities in asymptomatic children?

Boaz Karmazyn, MD, *bkarmazy@iupui.edu*; Megan B. Marine, MD, Matthew R. Wanner, Deborah Billmire, MD; Indiana University School of Medicine, Riley Hospital for Children, Indianapolis, IN

Disclosures: All authors have disclosed no financial interests, arrangements or affiliations in the context of this activity.

Purpose or Case Report: Intestinal rotation abnormality (IRA) can lead to catastrophic events from midgut volvulus. In a child that presents with bilious vomiting, urgent surgery should be performed. Ladd's surgery is associated with complications in 10% to 20% of the patients. In this review we will show that in selected asymptomatic children with IRA, imaging can help decide if observation should be considered rather than surgery.
Methods & Materials: We reviewed upper gastrointestinal contrast studies, small bowel follow through contrast studies (SBFT), and colon enemas of children with a diagnosis of IRA who had surgery. We evaluated location of the duodenal jejunal junction (DJJ), position of the duodenum in the lateral view, and the anatomy of the colon. Location of the DJJ to the right of the left pedicle on the anterioposterior view or anterior in the lateral view was defined as IRA. We evaluated three types of IRA based on current literature: nonrotation (entire colon in the left abdomen, cecum in the left lower quadrant and the small bowel in the right abdomen), atypical malrotation (DJJ between midline and left pedicle), and typical malrotation (IRA that cannot be defined as nonrotation or atypical malrotation).
Results: We will present an imaging algorithm for evaluation of malrotation and show imaging findings of all types of IRA as well as challenging cases. We will show cases with nonrotation when there was no need for surgery and other cases when Ladd bands were found. We will show cases of atypical malrotation. We found that if the duodenum is posterior and the entire colon is normal, the mesenteric root is broad and there is no need for surgery. We will also show indeterminate cases, when laparoscopy was necessary.We will show how anatomy of the colon helps to define the types of IRA. We will show cases where SBFT did not demonstrate the entire colon and was misleading. Enema should, therefore, be considered to evaluate the anatomy of the colon for definitive diagnosis.
Conclusions: We suggest considering a more stringent definition of atypical malrotation when there is also posterior position of the duodenum and normal colon. In asymptomatic children, especially at older ages, findings of nonrotation or atypical malrotation can provide an option for observation rather than surgery.

Poster #: EDU-021

Eovist in Pediatric MR: What Can and Can't It Do?

Narendra S. Shet, MD[1], *narendras@gmail.com*; John F. Flynn, MD[1], Ezekiel Maloney, MD[2], Ramesh Iyer, MD[2]; [1]Children's National Medical Center, Washington, DC, [2]Seattle Children's Hospital, Seattle, WA

Disclosures: All authors have disclosed no financial interests, arrangements or affiliations in the context of this activity.

Purpose or Case Report: The purpose of this review is to provide an overview of applications of Eovist in the pediatric population, as well as pitfalls. We will begin with an introduction on the origins of Eovist and how it and other hepatocyte specific contrast agents (HSCAs) differ from conventional gadolinium based contrast agents (GBCAs). We will then provide a sample of imaging protocols when Eovist is used for hepatic mass evaluation and for biliary indications. We will review benefits of Eovist in characterizing a variety of pediatric hepatic neoplasms, including hepatoblastoma, hepatocellular carcinoma, focal nodular hyperplasia, hepatic adenomas, and regenerative nodules, with mention of pathologies that do not follow traditional patterns (i.e., inflammatory adenomas). After this, we will cover biliary applications, including choledochal cysts, biliary obstruction, and postoperative bile leak. Finally, we will review some limitations of Eovist; notably, we will mention several scenarios where the hepatobiliary phase could not be achieved, and recommendations for how to approach these cases.

Poster #: EDU-022

Mimics of appendicitis on pediatric appendicitis protocol MRI

Ryne Dougherty, M.D. M.B.A., *dryne@med.umich.edu*; Timothy Alves, MD; University of Michigan, Ann Arbor, MI

Disclosures: All authors have disclosed no financial interests, arrangements or affiliations in the context of this activity.

Purpose or Case Report: Abdominal pain is common presentation to the pediatric emergency department, and appendicitis remains the most common pediatric surgical emergency. While the imaging workup of pediatric appendicitis typically begins with ultrasound, MRI is increasingly being used for problem-solving and to further evaluate equivocal ultrasound results. With increased utilization, more and more mimics of appendicitis are being encountered on MRI. The purpose of this educational exhibit is to familiarize the practicing pediatric radiologist with these mimics through a case-based review in order to improve diagnostic accuracy and patient care.
Methods & Materials: We will present a series of common and uncommon mimics of appendicitis on MRI in the pediatric patient based on over 5 years of experience with limited pediatric protocol MRI for appendicitis. While the exhibit will focus on MRI findings, correlative US and CT findings will be included.

Results: This case-based educational exhibit will cover multiple mimics of appendicitis encountered in clinical practice, including but not limited to: omental infarct, Meckel's diverticulitis, pyelonephritis, ovarian torsion, tubo-ovarian abscess, isolated fallopian tube torsion, intussusception, and psoas myositis.
Conclusions: Abdominal pain with concern for appendicitis is a common pediatric clinical presentation which relies heavily on imaging for diagnosis. The utilization of MRI for the evaluation of possible appendicitis continues to rise, and familiarity with common and uncommon mimics of appendicitis which may be encountered on MRI will help the practicing pediatric radiologist with interpretation of these studies and improve patient care.

Poster #: EDU-023

Radiologic Manifestations of Epidermolysis Bullosa

Samar Sheriff, MBA, *samarsheriff@gmail.com*; Anne Lucky, MD, Niekoo Abbasian, MD, Alexander J. Towbin, MD; Cincinnati Children's Hospital Medical Center, Cincinnati, OH

Disclosures: All authors have disclosed no financial interests, arrangements or affiliations in the context of this activity.

Purpose or Case Report: Epidermolysis bullosa (EB) is a group of rare genetic disorders that arise from at least 19 gene mutations for proteins that are involved in skin integrity. EB affects 1 out of 20,000 births in the United States and results in fragile skin that easily blisters from any minor friction or mechanical trauma. Other organ systems can also be seriously affected. The chronic skin inflammation and infections also places patients at risk for developing squamous cell carcinoma. Unfortunately, there is currently no cure for EB. The standard of care is supportive therapy and includes daily wound care, specialized dressings, and pain control.Because of the wide spectrum of systemic symptoms, there are numerous imaging findings that can be seen in patients with EB. These radiologic features can be categorized by body system including: 1) cardiac; 2) respiratory; 3) gastrointestinal; 4) genitourinary; 5) musculoskeletal; and 6) prenatal/fetal.There are various precautions that must be taken when performing any type of imaging study or anesthetic procedure for a patient with EB. These include but are not limited to: avoiding adhesives on the skin, providing special care when moving a patient, supporting pressure points on the imaging table, using large amounts of sterile water-based gel for ultrasound probes, and taking special care to protect the patient's skin, airway and oral cavity during anesthesia or sedation events.The purpose of this poster is to: 1) review the various clinical presentations, pathologies, and associated imaging findings involved in EB, 2) examine imaging and anesthetic concerns when dealing with patients with EB, and 3) discuss the imaging and anesthesia approach used when evaluating EB patients.

Poster #: EDU-024

Pediatric total pancreatectomy and islet autotransplant: an introduction for the radiologist

John J. Groene, MD, *groene.johnj@gmail.com*; Minna M. Wieck, MD, Seng Ong, Mario F. Zaritzky, MD, Kate A. Feinstein; Radiology, University of Chicago, Chicago, IL

Disclosures: All authors have disclosed no financial interests, arrangements or affiliations in the context of this activity.

Purpose or Case Report: In this exhibit we will describe a fairly new surgical procedure - total pancreatectomy and islet autotransplant (TPIAT). TPIAT is an uncommon procedure performed in children who suffer from chronic or recurrent acute pancreatitis. The purpose of the exhibit is to learn about the selection criteria, the surgery itself, and the imaging features of surgical complications. Candidates are selected for surgery based on a multitude of factors including severity and chronicity of pain, laboratory evaluation of pancreatic exocrine and endocrine function, and imaging features of chronic pancreatitis on MRCP and/or endoscopic ultrasound. In the surgical procedure, the pancreas and duodenum are resected, islet cells are isolated and then infused through the portal vein into the liver. A splenectomy is performed and continuity of the GI tract restored. Patients may spend three weeks in the hospital after surgery. Months after the infusion, the islet cells will be embedded within the liver and begin to produce insulin. The primary goal of this procedure is to relieve debilitating pain and improve quality of life, for which this procedure is around 90% successful. The secondary goal of the procedure is to retain islet cell function. In this regard, approximately 40% of the pediatric patients will regain complete islet cell function, 30% will regain partial function while 30% will have no islet cell function. Follow up imaging may also be performed on these patients for evaluation of complications such as delayed gastric emptying, small bowel obstruction, surgical site infections, bile leak, and intra-abdominal hemorrhage. Complications seen in our hospital, including small bowel obstruction, delayed gastric emptying, and prolonged ileus will be highlighted.

Poster #: EDU-025

Is the new ultrasound technology affecting the way radiologists are interpreting studies for Hypertrophic Pyloric Stenosis?

Juan S. Calle Toro, MD, *ctjuans@gmail.com*; Savvas Andronikou, MBBCh, FCRad, FRCR, PhD (UCT), PhD (Wits); Radiology, Children's Hospital of Philadelphia, Philadelphia, PA

Disclosures: All authors have disclosed no financial interests, arrangements or affiliations in the context of this activity.

Purpose or Case Report: To retrospectively review the imaging planes performed, the number pyloric layers visible and the location of measurements taken, in infants with suspected (HPS).
Methods & Materials: 103 pyloric ultrasound studies referred for suspected HPS were included. One pediatric radiologist with 20 years of experience and one medical doctor reviewed the studies. For each individual study, it was recorded whether longitudinal or transverse views were performed, the layers that could be visualised. A schematic was developed to categorise the interfaces of the anatomic layers of the pylorus visualised and position of the internal measurement cursor. Categories for the anterior wall were: a deep aspect of the muscularis propria; b superficial aspect of the muscularis mucosa; c deep aspect of the muscularis mucosa; d superficial aspect of the mucosa interfacing with the muscularis mucosa from a mucosal fold; e deep aspect of the muscularis mucosa from a mucosal fold. Categories for the posterior wall were: 1 deep aspect of the muscularis propria; 2 superficial aspect of the muscularis mucosa; 3 deep aspect of the muscularis mucosa; 4 deep aspect of the mucosa interfacing with muscularis mucosa from a mucosal fold; 5 deep aspect of the muscularis mucosa from a mucosal fold. Descriptive analysis was made for the categorical variables using STATA 15 software.
Results: A total of 100 studies (97 patients) were reviewed. Studies recorded longitudinal (99%) and transverse (69%) views of the pylorus. For the longitudinal view, measurements included muscle thickness in 95%, length in 97% and 0% for the pyloric diameter. For the transverse view, measurements included muscle thickness in 16% and the diameter in 3%.

Pyloric layer interfaces (as defined above) were visible as follows: a in 64%, b in 64%, c in 66%, d in 30% and e in 26%. The internal (deep) reference point of cursor placement for measuring the muscle wall thickness in the longitudinal view was as follows: a in 46%, b in 27%, c in 30%, d in 1% and e in 2% of the studies.
Conclusions: New US technology provides more detailed anatomy and this affects measurements for muscle wall thickness. Considering that a millimetre can make a measurement fall into the abnormal category resulting in surgical treatment such differences in practice must be highlighted and recommendations need to be clarified. We believe that the largely abandoned diameter measurement, in the transverse or longitudinal views, may offer a solution as it is not defined by any internal layers.

Poster #: EDU-026

Optimizing Your Evaluation of Contrast Enemas for Distal Bowel Obstruction in Neonates: Protocol, Technique, Imaging Findings and Differential Diagnoses

Austin Dillard, MD, *raustindillard@gmail.com*; Steve Kraus, MD; Cincinnati Childrens, Cincinnati, OH

Disclosures: All authors have disclosed no financial interests, arrangements or affiliations in the context of this activity.

Purpose or Case Report: Bowel obstruction in the neonate is common. When neonatal intestinal obstruction is suspected, initial workup may include abdominal radiographs or ultrasound; however, in most busy pediatric radiology practices fluoroscopy is indicated to diagnose the cause, which helps the surgeon make management decisions. Accurate diagnosis is key to the successful management of these neonates. The fluoroscopist should be mindful of the methods and techniques which make evaluation of distal bowel obstruction straightforward and efficient. This exhibit will detail the rationale and protocol to perform the optimal contrast enema, which is essential to have a chance to reliably distinguish the several causes of distal bowel obstruction in neonates. Will include examples with imaging findings and differential diagnoses.

Poster #: EDU-027

Traumatic Handlebar Injuries

Joseph McCrary, MD, *jmccrary@alumni.nd.edu*; Jennifer Talmadge, MD; Maine Medical Center, Portland, ME

Disclosures: All authors have disclosed no financial interests, arrangements or affiliations in the context of this activity.

Purpose or Case Report: Direct impact upon the bicycle handlebars is an especially harmful mechanism of injury in children. Pediatric patients who present following direct impact of the bicycle handlebars upon the abdomen are much more likely to suffer internal organ injury and require operative intervention than those who present following a bicycle accident without direct impact upon the handlebars.Unfortunately, bicycle handlebar trauma is not only a damaging mechanism of injury, but also a treacherous one. Physical exam findings can be subtle; these children often appear misleadingly well. Many such children are initially misdiagnosed and sent home prematurely only to re-present. Delays in definitive diagnosis are typical.The radiologist, therefore, by aiding in the timely identification of injuries and determination of any need for surgery, can make a valuable contribution to patient care.Our cases include a 9-year-old girl with a puncture wound and abscess in the medial thigh musculature, a 13-year-old male with a penetrating wound to the left lower abdominal quadrant with extensive retroperitoneal and extraperitoneal hematoma and other injuries, a 14-year-old male with a hematoma in the right lower abdominal quadrant, and a 7-year-old boy with a liver laceration, each of whom suffered a bicycle handlebar impact to the abdomen.As companion cases, we also present a 12-year-old boy with a transected pancreas following an ATV rollover which involved impact of the handlebars upon the abdomen, and a 49-year-old man who sustained a shattered kidney in a bicycle accident.

Poster #: EDU-028

Acute, emergent and post-surgical disorders involving the pediatric jejunum.

Deborah Brahee, *Deborah.Brahee@cchmc.org*; Alexander J. Towbin, MD; Cincinnati Children's Hospital Medical Center, Cincinnati, OH

Disclosures: All authors have disclosed no financial interests, arrangements or affiliations in the context of this activity.

Purpose or Case Report: Pediatric pathology involving the jejunum is more common than one might initially expect. Early recognition of the important imaging characteristic, atypical findings, and useful imaging tools/techniques in the evaluation of jejunal pathology is important in prompt diagnosis and management of these patients.In this educational exhibit we will present a series of cases involving pathology of the jejunum encountered in the pediatric population. We will focus on important pathologies affecting a difficult to image and sometimes forgotten portion of the intestine.A range of acute, emergent and post-surgical cases are presented. Using an interactive, quiz based approach we will discuss the following pediatric pathologies that may affect the jejunum of pediatric patients from neonates to teenagers with multimodality imaging and pathologic examples:AtresiaMeconium plug syndromePneumatosisEnteritisForeign bodySmall bowel intussusceptionLymphomaIschemia/shockHerniaGraft versus host diseaseTraumaVasculitis

Poster #: EDU-029

The Belly Button: Imaging of Pediatric Umbilical Disorders

Arushi Devgan, MD, *devganarushi@gmail.com*; Amy Rowell, MD; Diagnostic Radiology, University of Arkansas for Medical Sciences (UAMS), Little Rock, AR

Disclosures: All authors have disclosed no financial interests, arrangements or affiliations in the context of this activity.

Purpose or Case Report: This poster aims to educate about the radiographic findings of pediatric umbilical disorders by presenting a case series, and to correlate the pathology with embryogenesis.
Methods & Materials: A retrospective review of our database was performed to select cases of umbilical disorders in children that required imaging. Imaging findings, pathological reports, and electronic medical records of these cases were reviewed.
Results: Radiographic, surgical, and pathologic findings of 6 cases of pediatric umbilical disorders were reviewed from our database. Patient age ranged from 10 weeks to 11 years old. The cases included patent omphalomesenteric duct, infected urachal cyst, patent urachus, and Meckel's diverticulum.
Conclusions: Umbilical disorders are classified according to embryonic remnants in the umbilicus and its associations with the urinary bladder and the bowel, which is why imaging can be useful in understanding the anatomy and differential diagnoses in such cases. These abnormalities can also have nonspecific

clinical manifestations. Therefore, imaging can help in identifying and correctly diagnosing umbilical disorders, which is key to appropriate and timely patient management.

Poster #: EDU-030

Pediatric Spleen: Anatomic Variants and Pathology

James Davis, *jdavi@umich.edu*; Kathleen Gebarski, Peter Strouse; University of Michigan, Ann Arbor, MI

Disclosures: All authors have disclosed no financial interests, arrangements or affiliations in the context of this activity.

Purpose or Case Report: While the most common abnormalities of the spleen are splenomegaly and trauma, many additional disease states can be manifested in the spleen which should be considered when evaluating the abdomen on cross sectional imaging. We composed a pictorial guide of a wide variety of variants and diseases for education and reference.
Methods & Materials: Illustrative cases of congenital, developmental, infectious, and neoplastic processes involving the spleen were chosen from the last fifteen years of abdominal sonography at our institution along with CT, MRI and pathologic correlation. Case examples include polysplenia, storage diseases, wandering spleen, torsed spleen, various cysts, siderotic nodules, splenic complications of sickle cell disease including autolysis, islands of residual splenic tissue and echogenic foci, hamartoma, various infections, hemangioma, and infiltrative diseases such as leukemia and lymphoma.
Results: Reviewing these cases provides an experience of a wide variety of splenic anatomic variants and pathology and improves the accuracy of interpretation.
Conclusions: A pictorial review of a wide variety of splenic anatomy and pathology improves the accuracy of interpretation.

Poster #: EDU-031

Imaging Findings and Clinical Manifestations of Pancreatic Neoplasms in Children

Reem Haswegh, dr_*reemnh@hotmail.com*; Andrew T. Trout, Alexander J. Towbin, MD; Department of Radiology, Cincinnati Children's Hospital Medical Center Cincinnati, OH

Disclosures: Andrew T. Trout, MD: Consultant, Honoraria: Guerbet Group, Royalty: Elsevier, Wolters-Kluwer, Research Grants: Canon Medical, Siemens Medical Solutions, National Pancreas Foundation, In-Kind Support: ChiRhoClin Inc., Perspectum Diagnostics. All other authors have disclosed no financial interests, arrangements or affiliations in the context of this activity.

Purpose or Case Report: Pancreatic neoplasms are rare in children and young adults, with an incidence of 0.46 per million under 30 years of age. Fortunately, children with a pancreatic neoplasm have a better prognosis than adults. The better prognosis and rarity of disease both contribute to the fact that pancreatic malignancies account for less than 0.2% of cancer-related deaths.Ultrasound is often the initial imaging modality to identify a pancreatic neoplasm due to its use for evaluation of symptoms such as upper abdominal pain, a palpable epigastric mass, or jaundice. Known pancreatic masses, or those detected initially by ultrasound should be imaged with CT or MRI to best characterize the mass and its relationship to adjacent structures, particularly the vasculature. Nuclear medicine plays a role in imaging of some pancreatic neoplasms depending on histology.Once a pancreatic neoplasm is identified, the radiologist is tasked with making a diagnosis from a differential diagnosis list of rare tumors. Primary pancreatic neoplasms are divided into epithelial and nonepithelial types. The epithelial tumors are more common and may be further subdivided into exocrine or endocrine subtypes. Epithelial exocrine tumors are the most common in children. Examples of these tumors include the two most common pediatric pancreatic neoplasms pancreatoblastoma and solid-pseudopapillary neoplasms. Endocrine tumors are uncommon. While functioning endocrine tumors can occur, non-functioning tumors are more common and are associated with syndromes such as von Hippel Lindau, multiple endocrine neoplasia type 1, and tuberous sclerosis. Nonepithelial tumors are also rare and include a number of different entities such as lymphoma, neurofibroma, and teratomas. Finally, the pancreas is an extremely rare site of metastasis. Pancreatic metastases can occur with multiple primary malignancies including neuroblastoma, rhabdomyosarcoma, and osteosarcoma.This exhibit will describe the imaging work-up of pancreatic tumors in children. We will illustrate the different clinical manifestations and imaging appearances of the various pediatric pancreatic neoplasms.

Poster #: EDU-032

To Spleen, with Love

Anne K. Misiura, MD, *annekmisiura@gmail.com*; Jacqueline Urbine, MD, Erica Poletto, MD, Archana Malik, MD, Mea Mallon; Radiology, St. Christopher's Hospital for Children, Philadelphia, PA

Disclosures: All authors have disclosed no financial interests, arrangements or affiliations in the context of this activity.

Purpose or Case Report: The spleen is rarely the first organ to come to mind in discussing pathology of the abdomen, and indeed may often be the last. However, there are a multitude of splenic processes and abnormalities that should be kept in mind when discussing the pediatric abdomen. Additionally, splenic abnormalities, or lack thereof, can also be clues to diagnosis in more difficult cases.
Methods & Materials: A retrospective analysis of multimodality imaging in pediatric patients demonstrating splenic imaging abnormalities, who presented to an urban children's hospital since 2005 is performed. Imaging and clinical history are correlated with laboratory findings where applicable. A variety of splenic abnormalities are selected for imaging review.
Results: Review of splenic abnormalities is provided with imaging examples. Examples include metabolic, malignancy, trauma, and other disorders, including, but not limited to abnormalities in splenic size, cystic and solid splenic lesions, infiltrative/consumptive processes, and situs disorders.
Conclusions: The spleen is often the forgotten organ of the pediatric abdomen, but there are many exciting things to be found in the left upper quadrant. Clinicians and pediatric radiologists alike should not disregard the spleen in abdominal cases, for there are many pathologies and clues to be found.

Poster #: EDU-033

Spectrum of imaging abnormalities in patients with eating disorders in the pediatric population

Karuna Shekdar, MD, *shekdar@email.chop.edu*; Sudha Anupindi, MD, Janet R. Reid, MD, FRCPC; Radiology, Children's Hospital of Philadelphia, Philadelphia, PA

Disclosures: All authors have disclosed no financial interests, arrangements or affiliations in the context of this activity.

Purpose or Case Report: To describe the spectrum of imaging abnormalities seen in eating disorders such as anorexia nervosa in the pediatric population.
Methods & Materials: Patients who were diagnosed with anorexia nervosa and had imaging studies for indications related to their eating disorder at our institution were included in this review. The imaging studies reviewed included chest, abdomen and pelvis radiographs, fluoroscopy studies of the upper gastrointestinal tract, studies, ultrasound studies of the abdomen, Computed Tomography of the brain, abdomen and pelvis and Magnetic resonance imaging studies of the brain.
Results: A variety of imaging findings were identified in these patients including mild morphological findings to sequelae of multi-organ failure which will be illustrated with case examples on this review.
Conclusions: Eating disorders can affect multiple organ systems with a spectrum of morbidity. Eating disorders manifest usually in teen age females and can be challenging to diagnose. Awareness among pediatric radiologists about imaging findings in eating disorders is crucial to the diagnosis and management.

Poster #: EDU-034

Where are We Exactly?: Navigating the Complex Roadmap of Müllerian Duct Anomalies

Ross A. Myers, MD[1], *ross.myers@wmchealth.org*; Tianyang Li, MD[1], Jennifer Wu, MD[1], David Sadowsky, MD[1], Mary Paul, MS4[2], Perry Gerard, MD[1], Adele Brudnicki, MD[1], Lesli LeCompte, MD[1]; [1]Westchester Medical Center, Valhalla, NY, [2]New York Medical College, Valhalla, NY

Disclosures: All authors have disclosed no financial interests, arrangements or affiliations in the context of this activity.

Purpose or Case Report: Müllerian Duct Anomalies (MDA) are a broad category of congenital deformities of the urogenital structures due to abnormal development, fusion, or resorption of the fetal Müllerian Ducts. By definition, the Müllerian Ducts are the paired fetal structures that are located medially to the Wolffian Ducts and develop into the Fallopian Tubes, uterus, cervix, and upper two-thirds of the vagina. The multitude of symptoms associated with MDAs vary broadly in severity, ranging from patients with no symptoms and incidentally discovered MDAs to patients with primary infertility, recurrent pregnancy loss and other reproductive problems.There are well documented associations of MDAs with other genitourinary malformations. The most commonly reported is renal agenesis, which accounts for up to 30% of all associated renal anomalies in the setting of MDA, however abnormalities including ureteral remnants with ectopic insertion or collecting system duplication have been reported as well. The overall incidence of MDAs varies, but have been estimated to be approximately 1-5% within the general population and up to 13-25% in patients with recurrent pregnancy loss.The most commonly accepted system of classification of the various types of MDAs is that of the American Fertility Society, which divides MDAs into seven categories. However, there is often confusion as to how to categorize MDAs demonstrating characteristics of more than one class. Medical imaging is of essential importance for both this reason and for appropriate planning of therapy. The imaging of suspected MDAs involves the implementation of a combination of 3D Ultrasound, Magnetic Resonance Imaging, Sonohysterography, Hysterosalpingraphy and/or laparoscopy. Sonography and MRI have the benefits of being the least invasive methods of diagnosis.The goal of our educational exhibit will provide an overview of the embryology and pathophysiology related to a broad variety Müllerian Duct Anomalies. We will discuss the common imaging techniques employed in the workup of patients with Müllerian Anomalies. In addition, we provide a plethora of interesting cases from our home institution including a case of Mayer-Rokitansky-Küster-Hauser Syndrome, Obstructed Hemivagina and Ipsilateral Renal Anomaly (OHVIRA), cloacal abnormality, bicornuate uterus and other complex cases utilizing a variety of imaging modalities.

Poster #: EDU-035

Rapid MRI as accurate one-stop imaging for adnexal torsion

S Pinar Karakas, MD[1], *pkarakasrothey@mail.cho.org*; Unni K. Udayasankar, MD, FRCR[2], Ellen S Park[3], Bamidele Kammen[1], Wendy Su[1], Sunghoon Kim[1], Thomas Hui[1], Taylor Chung, MD[1]; [1]Pediatric Radiology, Benioff Children's Hospital at Oakland, CA, Oakland, CA, [2]university of Arizona, Tuscon, AZ, [3]Cleveland Clinic, Cleveland, OH

Disclosures: All authors have disclosed no financial interests, arrangements or affiliations in the context of this activity.

Purpose or Case Report: Adnexal torsion is a common emergency room query in young girls and teenagers presenting with pelvic pain. It is a consequence of an underlying adnexal lesion or to anatomical laxity of the suspensory/anchoring ligaments. Clinical symptoms at presentation can be confusing and nonspecific, yet prompt diagnosis and surgical intervention are essential to save the adnexa. Radiology plays a crucial role in the diagnosis of adnexal torsion. Our exhibit will review and promote the rapid MRI as the first line, one-stop imaging in the diagnosis of adnexal torsion and other causes of pelvic pain. Some cases will be presented with initial ultrasound images and demonstrate how MRI increased the confidence in the diagnosis. All presented cases have pathology correlation and or operative reports and follow-up imaging. We will show various cases of ovarian and tubal torsions and their mimickers. In particular, we include torsions due to anatomical laxity of the suspensory ligaments, resulting from tubo-ovarian cysts and solid adnexal masses as well as cases of isolated tubal torsions.**Table of Contents/Outline:**Review of the embryology and anatomy of adnexa including suspensory/ anchoring ligaments.Review pathophysiology and progression of ovarian torsionReview rapid motion insensitive high-resolution MRI protocol for adnexal torsionReview hallmark imaging findings of adnexal torsion with MRI (with accompanying ultrasound comparison in some cases)Review MRI findings of adnexal viability and demiseReview multiple MRI examples of adnexal torsion and its mimickers

Poster #: EDU-036

Twisted Pelvic Pathology: Overview of pelvic torsions in the pediatric population

Brianna Oliver,*broliver@med.umich.edu*; Radiology, University of Michigan, Ann Arbor, MI

Disclosures: All authors have disclosed no financial interests, arrangements or affiliations in the context of this activity.

Purpose or Case Report: Pelvic and scrotal pain are common emergent presenting symptoms in the pediatric population, and these patients are commonly imaged to evaluated for gonadal torsion. In this educational exhibit we will review the entire spectrum of gonadal and paragonadal torsions in the pediatric population, focusing on clinical presentations, key imaging findings, possible pitfalls in diagnosis, and next steps in management. It is essential for the pediatric radiologist to be familiar with this range of pathology in order to render an accurate and timely diagnosis, particularly given that some (but not all) of these diagnoses require emergent surgery.

Methods & Materials: Illustrative cases of gonadal and paragonadal torsions were selected from the past 5 years at our tertiary-case academic medical center with a dedicated pediatric hospital. Cases include, but are not limited to, the spectrum of ovarian torsion (from subtle findings of torsion in a previously normal ovary to cases of ovarian torsion with an underlying mass), the spectrum of testicular torsion (from a twisted spermatic cord with preserved testicular flow to more severe torsion with testicular infarction), isolated fallopian tube torsion, paratubal cyst torsion, and paratesticular appendage torsion.
Results: A case-based review of pediatric pelvic (gonadal and paragonadal) torsions covering the entire range of presentation of common entities and classic presentations of rare entities will allow the pediatric radiologist to become more confident and competent in the interpretation of ultrasonography performed for these indications, and well as the interpretation of MRI performed for problem-solving.
Conclusions: Suspected gonadal and paragonadal torsions are relatively common indications for imaging, particularly ultrasonography, in the pediatric population. Familiarity with these entities and the entire spectrum of imaging findings will improve diagnostic accuracy and efficiency of interpretation. This is extremely important as the pediatric radiologist plays a key role in making the ultimate diagnosis and distinguishing surgical emergencies from benign self-limited conditions.

Poster #: EDU-037

Pediatric urodynamics: a radiologist's primer

Emily Sellers, MD, *emily.sellers@uchospitals.edu*; Katherine L. Stahoviak, Seng Ong, MD, Kate A. Feinstein, MD; Radiology, University of Chicago, Chicago , IL

Disclosures: All authors have disclosed no financial interests, arrangements or affiliations in the context of this activity.
Purpose or Case Report: In this exhibit, we will describe the synergistic effect of urodynamics and imaging. Bladder dysfunction, a common problem in children, accounts for up to 40 percent of pediatric urology clinic visits. Urodynamics is a key study to determine the etiology of bladder dysfunction yet, many radiologists are unfamiliar with this exam. Urodynamics is a fluoroscopic evaluation of the bladder with contrast during which abdominal and bladder pressures are measured while the bladder fills and empties. It uses a combination of electromyogram to evaluate pelvic floor contractions, cystometrogram to evaluate bladder pressures and capacity, and voiding cystourethrography to evaluate lower urinary tract anatomy. This exhibit will explain the indications for urodynamics, the basics of its interpretation including detrusor function and pressure flow studies, and the types of pathologies which may be diagnosed. Neurogenic bladder, congenital abnormalities, and how to differentiate between subsets of overactive bladder and underactive bladder will be explained. We will show imaging findings which correlate with these urodynamic diagnoses and describe ways to enhance voiding cystourethrograms and sonograms to better evaluate children with lower urinary tract dysfunction.

Poster #: EDU-038

Implementing a contrast enhanced Voiding Ultrasonography (ceVUS) Program at a Large Children's Hospital: How our experience can help you

Kate Louise M. Mangona, MD, *katelouise.mangona@utsouthwestern.edu*; Matthew R. Hammer, MD, Jeannie Kwon, MD; UTSW/ Children's Health, Dallas, TX

Disclosures: All authors have disclosed no financial interests, arrangements or affiliations in the context of this activity.

Purpose or Case Report: Voiding cystourethrography (VCUG) has long been utilized in the diagnosis of vesicoureteral reflux in children with urinary tract infections. Sonographic techniques have been developed to make the same diagnosis without exposing the child to ionizing radiation. This presentation describes the implementation steps of a new service including: pharmacy approval and formulary addition; sonographer training and coordination with fluoroscopy technologists; referring clinician education and outreach. This exhibit educates the reader on how ceVUS can be performed, how it can be established at a children's hospital, and the benefits it provides.Correct technique and acquisition of images is shown using clinical case examples. Relevant anatomy is reviewed. Correlation of ultrasound abnormalities with VCUG results is provided. The process of training technologists and radiologists is highlighted. Pitfalls and tips to improve imaging are described. We will present results on how our new service has been accepted and utilized by the urologists and referring physicians. We have now performed over 50 ceVUS studies this year.

Poster #: EDU-039: *Withdrawn*

Poster #: EDU-040

A Customized Virtual Reality Experience for Simulating Magnetic Resonance Imaging Exams

Yungui Huang, PhD, *yungui.huang@nationwidechildrens.org*; John Luna, Ramkumar Krishnamurthy, PhD, Lacey J. Lubeley, BS, Tricia Buskirk, Master of Science in Child and Family Studies, Arleen Karczewski, Whitney Garrett, Simon Lin, MD, Aaron S. McAllister, MD, Rajesh Krishnamurthy, Houchun Hu, PhD; Nationwide Children's Hospital, Columbus, OH

Disclosures: **Aaron S. McAllister, MD:** Equity Interest/Stock Option: GE, MMM, CHD, JNJ. All other authors have disclosed no financial interests, arrangements or affiliations in the context of this activity.

Purpose or Case Report: **Background:** Image quality in MRI is often degraded by patient motion. To reduce the need for repeat exams, sedation or general anesthesia is used in pediatric patients. This requires additional clinical staff, and leads to increased scheduling wait times and overall procedure times that impact workflow. Many institutions prepare children for MRI using mock-up replicas. While effective in acclimating patients to the MRI environment, the availability of mock-up practices are often limited. Mock-ups also require physical space and do not simulate the full MRI environment and exam experience.**Purpose:** We build an affordable, scalable, and portable immersive virtual reality (IVR) platform for simulating MRI exams. Specifically, we designed an IVR environment that accurately mimics a Siemens 3 Tesla suite within our Radiology practice, including intricate details such as room size, color, lighting, ancillary equipment, pulse sequence audio, and background noise. The IVR platform also attempts to simulate the complete sequence of events and environments a child will experience during an exam, including the check-in process, interactions with staff (e.g., nurses, technologists), the waiting area and changing rooms, the positioning and motion of the MRI table, placement of coils, and within-exam instructions, such as breath-holds. Our platform also allows the patient to move around in the VR space and interact with the environment. Additionally, the platform can be easily converted to mimic any other MR suite. We hypothesize that our platform can be easily adopted by Child Life and hospital staff to quickly acclimate a

patient and assess whether he/she can suitably undergo an MRI exam without sedation or general anesthesia.We believe the IVR platform can overcome the limitations of mock-up replicas. First, IVR has a smaller footprint and is scalable and portable across the hospital. This allows multiple IVR sessions to be held in parallel. Second, IVR can give the patient a hospital-specific and scan-specific first-person experience. The patient can interact with realistic 3D representations of the MRI environment and processes. Our current implementation of IVR was developed using HTC VIVE headsets with a dedicated laptop for control. To further improve portability, the IVR setup can be adopted using simple goggles and handheld devices. This will enable future IVR sessions to be conducted at the bedside, in patient's homes, and in referring physician offices.:

Poster #: EDU-041

Speeding Up Pediatric MRI: Making Sense of the Alphabet Soup of Acceleration Techniques

Eric Loken, Joo Cho, David Bessom, Frank Corwin, Brent Metts, **Gregory Vorona, MD**, *gregory.vorona@vcuhealth.org*; Radiology , Virginia Commonwealth University , Richmond, VA

Disclosures: All authors have disclosed no financial interests, arrangements or affiliations in the context of this activity.

Purpose or Case Report: Magnetic resonance imaging (MRI) is a robust imaging modality. However, the necessity for patients to hold still commonly requires pediatric patients to be sedated (which carries its own risks), or limits the useful scan time window in some nonsedated pediatric patients. In some circumstances, there is no way to control the movement of the imaging target (i.e. fetal MRI).MRI is also very customizable, and there are number of options currently available to accelerate MR imaging. It is important for pediatric radiologists supervising pediatric MRI examinations to have a broad understanding of the technology that is currently available, in order to optimize imaging quality and mitigate sedation use.In this educational exhibit, we will briefly review a number of acceleration techniques available on the Siemens platform, noting that other vendors have very similar options available for their customers. These techniques will include single-shot fast spin echo , balanced steady-state gradient echo, parallel imaging, radial imaging, and simultaneous multislice imaging. Our review will focus on the relative advantages and disadvantages of these techniques, rather than on the physics of image generation.

Poster #: EDU-042

Creation of a Multi-Institutional Registry Framework

Erin Payne, BSN[1], *epayne@cmh.edu*; Juan S. Martin-Saavedra, MD[2], Teresa Victoria, MD, PhD[2], Amie L. Robinson, BSRT(R)(MR)[1], Kristin Fickenscher, MD[1], Sherwin S. Chan, MD PhD[1]; [1]Radiology, Children's Mercy Hospital, Kansas City, MO, [2]Children's Hospital of Philadelphia, Philadelphia, PA

Disclosures: Sherwin S. Chan: Consultant, Honoraria: Jazz Pharmaceuticals, Research Grant: GE Healthcare. All other authors have disclosed no financial interests, arrangements or affiliations in the context of this activity.

Purpose or Case Report: Many diseases in pediatrics are relatively uncommon and imaging of these diseases is difficult to study due to small patient numbers at a single site. This limits the ability of single institutions to adequately power a study. Thus, there is a pressing need for a multi-site structure to combine data for rare diseases to appropriately power outcome studies. Our goal is to create an infrastructure to support pooling of imaging and clinical data across institutions to facilitate multi-institutional studies.
Methods & Materials: For multi-site studies, a centralized IRB structure is necessary to efficiently perform the study. The site establishing the centralized IRB will be considered the 'primary' site. The primary site is also responsible for IRB regulatory, data management, including imaging, and facilitation of project overall. The centralized IRB will establish reliance agreements with participating sites, enabling the sites to utilize the central IRB as the IRB of record. Once IRB approval is obtained, a centralized REDCap, or data entry system, at the primary site will grant access to participating institutions for data entry. Centralized data collection allows all data to be housed in one location, allowing for quicker analysis. For studies requiring imaging transfer, a standard operating procedure (SOP) for image de-identification, naming convention, and image transfer to centralized PACS system should be followed.
Results: Our site has established three multi-site clinical imaging trials to date. First, we have an 11-site imaging repository for pleuropulmonary blastoma through the Midwest surgical consortium. All images have been uploaded to our site and pediatric radiologists at three different institutions are viewing de-identified images and inputting data in REDCap. Second, we have a three-site retrospective study evaluating the use of grayscale and Doppler imaging in veno-occlusive disease. Each site has access to centralized REDCap and data entry is performed on local subjects. Third, we have a two-site retrospective and prospective fetal MRI registry. Data collection and image upload to centralized PACS is being used to combine data between institutions.
Conclusions: We have successfully created infrastructure to support multi-institution clinical imaging trials. We hope that SPR members can use this resource for future studies on rare conditions where we can pool data to see how imaging affects patient outcomes.

Poster #: EDU-043

3D Printed Training Simulation for Assessment of Pathology in Pediatric Upper GI Fluoroscopy

Neil Lall, *nulall@gmail.com*; Jack McGee, BSE, Korak Sarkar, MD; Radiology, Ochsner Health System, Orleans, LA

Disclosures: All authors have disclosed no financial interests, arrangements or affiliations in the context of this activity.

Purpose or Case Report: Fluoroscopy of the upper GI tract (UGI) can be difficult to master given the time-sensitive nature of the examination, the necessary hand-eye coordination, the complex button layout and broad featureset of the fluoroscopic equipment, the desire for minimizing radiation dose, and the required understanding of normal anatomy. Additionally, encountering abnormal findings for the first time, particularly before one is familiar with normal findings, can lead to confusion and increased difficulty in performing the examination. The use of 3D printed models of normal anatomy in pediatric fluoroscopic UGI training simulation has previously been demonstrated as a viable alternative to learning on live patients; however, such a technique has not previously been used with known pathological anatomic configurations.
Methods & Materials: A freely-available computer generated 3D model of the normal anatomy of the esophagus, stomach, and duodenum was downloaded and modified using Blender™ and Autodesk Fusion 360™. The model was edited to create 4 alternative models corresponding to the 4 classic patterns of abnormal UGI configuration: Malposition of the duodenal-jejunal junction (DJJ), corkscrew duodenum, complete duodenal obstruction, and partial duodenal obstruction with normally

positioned DJJ. Additionally, known normal variants of anatomy (such as duodenum inversum) were modeled as well.Inexpensive reusable simulator models were printed using a waterproof photo-reactive resin to allow residents to practice UGI fluoroscopy on both normal and abnormal patients. Residents were tested on their performance and interpretation of UGI fluoroscopy on these models to enhance their comfort with performing the examination and to increase their familiarity with these important variants/abnormalities.
Results: Though the models were entirely reliant on gravity-dependent flow of contrast, they behaved similar to real neonates when filled with contrast and placed in different positions.
Conclusions: 3D printed models of the UGI tract can serve as adequate training tools for both general examination performance as well as education of normal anatomic and pathological variants.

Poster #: EDU-044

Fabrication and application of realistic three-dimensional (3D) printed pediatric static and dynamic airway training models for bronchoscopy and foreign body removal

Pia Maier, *maierp@email.chop.edu*; Elizabeth Silvestro, MSE, Samuel B. Goldfarb, MD, Joseph Piccione, MD, Pelton A. Phinizy, MD, Savvas Andronikou, MBBCh, FCRad, FRCR, PhD (UCT), PhD (Wits); Children's Hospital of Philadelphia, Philadelphia, PA

Disclosures: All authors have disclosed no financial interests, arrangements or affiliations in the context of this activity.

Purpose or Case Report: Successful bronchoscope handling requires the skill to orient bronchoscope position and direction in response to the intraluminal view provided by the bronchoscope camera. Additional challenges for pediatric physicians are smaller airways and the physiologically higher breathing frequency and airway collapsibility in babies and toddlers. We aimed to create a set of anatomically accurate 3D printed pediatric static and dynamic airway models that can be further used to teach and train residents/fellows in bronchoscopy and foreign body removal.
Methods & Materials: Three versions of 3D printed models were designed: a static tree model, a dynamic tree model, and translucent airway box model. CT patient data of three different ages (1, 5, 18) was selected for segmenting in Materialise Mimics. For the tree methods, the airway was then wrapped with a 2mm offset and hollowed out to create a lumen-like model and then was printed in the soft Tango+ material on Connex 500 or J750 printers. The branches were open for the static model and closed for the dynamic. The box was created by subtracting the airway from a box around its extents. This was then printed in VisoClear on a Project 6000HD printer. A y-connector and air sucking pump was attached to the dynamic model to simulate breathing and airway collapsibility.Three pediatric pulmonology attendings evaluated the models for physiologic accuracy and usefulness for teaching and training.
Results: All models were evaluated to have an excellent intraluminal accuracy (branching and angles of bronchi, appearance of the lumen) and usefulness for teaching and training. The translucent box was favored for presenting and the static model to learn basic handling of the bronchoscope in bronchoscopy and foreign body removal. The dynamic model provided the most realistic cartilage consistency and endoscopic simulation of the physiologic breathing patient.Next steps planned are automatization of breathing simulation with different age-adjusted breathing frequencies and prospective enrollment of residents/fellows to formally assess technical skill development.
Conclusions: By fabricating three different 3D printed airway models, which enable visualization of bronchoscope handling and simulation of realistic intraluminal as well as physiological conditions in different age groups, we created a promising tool for teaching, training and testing pediatric residents/fellows in bronchoscopy and foreign body removal.

Poster #: EDU-045: ***Withdrawn***

Poster #: EDU-046

Estimation of Peak Skin Dose with Dose Structure Reports in a Radiation Data Management System

Xiaowei Zhu, M.S., *zhuw@email.chop.edu*; Jayme Whitaker, Sphoorti Shellikeri, Master's in Biomedical Engineering, Anne Marie Cahill; The Children's Hospital of Philadelphia, Philadelphia, PA

Disclosures: All authors have disclosed no financial interests, arrangements or affiliations in the context of this activity.

Purpose or Case Report: It is important for radiologists to recognize and discuss with patients and families the potential risks and clinical manifestations of high Peak Skin Dose. In children undergoing complex Interventional procedures accurate Peak Skin Dose estimates are complicated and time consuming despite reference point doses being available. The availability of the Dose Structure Report (SR) on modern fluoroscopic equipment allows such estimates to be timely and consistent. The process of creating a Peak Skin Dose estimate using a validated radiation data management system (RDMS), capable of collecting detailed acquisition data and modeling will be discussed.
Methods & Materials: Interventional fluoroscopic equipment is configured to transfer the SR to the hospital PACS system (PACS). PACS sends SR to a RDMS, which interprets SR reports and provides details of each study acquisition including: dose area product, reference point dose, beam on time, pulse rate, pulse width and height, table positions, collimation, preliminary and secondary angulations, distances of source to table and receptor. Acquisition protocols, timeline, and angulation maps are generated for each study. A Peak Skin Dose estimate for each study is performed using the detailed acquisition data, with manual adjustments made for table offsets in lateral and longitudinal directions, patient orientation and skin model (i.e. patient size). The skin dose map can be captured and used for initial and follow-up discussions with patients and families.
Results: For all studies, a default Peak Skin Dose estimate and a color skin dose map are automatically generated. With a pre-set institutional threshold (1 Gy) for Peak Skin Dose evaluation, RSMS automatically alerts the lead staff members of IR and physicist if the threshold level is exceeded upon completion of the study. The Peak Skin Dose estimate is then re-calculated with minor adjustments as described above. The skin dose map can be captured and used for initial and follow-up evaluations with patients and families.Two cases are selected for demonstration: 1) >1Gy Reference Point Dose, < 2Gy Peak Skin Dose; 2) >1Gy Reference Point Dose, > 2Gy Peak Skin Dose.
Conclusions: Using SR in RDMS for estimates of Peak Skin Dose can provide clinicians with timely Peak Skin Dose data to inform clinical patient follow up. This technology can also be a useful tool in the investigation of a potential sentinel event and in planning future similar interventions

Poster #: EDU-047

Instituting an Interventional MRI program at a pediatric institution

Sphoorti Shellikeri, Master's in Biomedical Engineering[1], *sphoortishellikeri@gmail.com*; Randolph M. Setser, PhD[2], Michael Acord, MD[1], Abhay Srinivasan, MD[1], Seth Vatsky[1], Fernando Escobar, MD[1], Jayme Whitaker[1], Anne Marie Cahill[1]; [1]Radiology, Children's Hospital of Philadelphia, Philadelphia, PA, [2]Siemens Healthineers, Hoffman Estates, IL

Disclosures: Randolph M. Setser, PhD: Salary: Siemens Healthineers. All other authors have disclosed no financial interests, arrangements or affiliations in the context of this activity.

Purpose or Case Report: Percutaneous interventions are increasingly being performed under MR-guidance due to the absence of ionizing radiation, the ability to visualize target lesion and the capability to monitor real-time treatment effect. Here we outline our experience with developing an interventional MRI (iMRI) service at a pediatric institution.
Methods & Materials: Subjects of discussion include: education, interventional use of diagnostic MR suites, coil types, MR-compatible supplies, billing and scheduling codes, MR safety training, creation and optimization of procedure specific MR protocols, building/simulation of procedural workflow, initial procedure selection, and role assignments for MR and IR personnel.
Results: Site visits to a well established interventional MR program for procedural and workflow observation informs the initial education and training. The choice of a 1.5T/3T scanner is institution specific with consideration for more needle artifact with 3T field strength. Appropriate fast imaging sequence protocols and installation of a slave monitor for in-suite visualization of procedures is required. Sequences should be tailored so that the visibility of saline, gadolinium and/or needles is optimized and artifacts are minimized. Protocols can be tested using basic gel or other phantoms.MRI coils are tailored to the intervention, including surface, flex and shoulder coils. MR-compatible interventional equipment is required but limited in availability. Coil choice to enable needle placement and appropriate protection of coil during sterile procedures requires planning and ideally phantom testing. Billing and scheduling codes can be created with the expertise of IR specific coding personnel. Most importantly the entire interventional team needs to complete MRI safety training.Roles assignments need to be clearly defined. In our institution this is a follows; IR technologist manages the MR-compatible supplies stocked on an MR-compatible rolling table, and assist the IR physician during the intervention; the IR nurse monitors the patient; the MR technologist controls the MR host; and the IR physician performs the intervention. It is ideal to start the program with a relatively non-complex non sedated intervention, as in our institution MRI-guided shoulder arthrography.
Conclusions: Conventional MRI suites can be adapted for interventional procedures. Collaborating with experienced institutions and thoughtful proactive planning are keys to a safe and successful iMRI program.

Poster #: EDU-048

An Overview of Techniques for Intrathecal Administration of Nusinersen in Children with Spinal Muscular Atrophy

Carlos B. Ortiz[1], *carlos.ortiz@bcm.edu*; Alex Chau, MD[2], Sudhen Desai[2], Kamlesh Kukreja, MD[2]; [1]Department of Radiology, Baylor College of Medicine, Houston, TX, [2]Texas Children's Hospital, Houston, TX

Disclosures: All authors have disclosed no financial interests, arrangements or affiliations in the context of this activity.

Purpose or Case Report: 1) Reviewing the pathology and outcomes of children with spinal muscular atrophy (SMA)2) Learning the procedures available for intrathecal access3) Understanding the indications for choosing more advanced techniques to deliver nusinersenSpinal muscular atrophy is an autosomal recessive disease affecting motor neurons and is the most common genetic cause of death in infants. Nuinersen (Spinraza) was recently approved by FDA for intrathecal administration in SMA patients. Commonly administered by lumbar puncture in the clinic or with imaging guidance, this is the initial method of administering nusinersen. Deformities and spinal instrumentation from orthopedic surgeries are common in SMA patients, preventing traditional intrathecal access by lumbar puncture for nusinersen delivery. Transforaminal lumbar sac access, ultrasound or fluoroscopy guided cervical spine access, or subcutaneous catheter placement can be the alternative approaches with failed/difficult lumbar access. Given the potential benefit of nusinersen, understanding all methods to obtain intrathecal access is essential for a pediatric interventional radiology (IR) practice.
Methods & Materials: We intend to review the technique, indications, complications, tips and tricks for each of these techniques and their relevance to an IR practice.1) Ultrasound guided lumbar puncture2) Fluoroscopy guided lumbar puncture3) Ultrasound guided cervical puncture4) Fluoroscopy guided cervical puncture (C1-C2)5) Transforaminal delivery using cone-beam computed tomography6) Transosseous access via drill7) Subcutaneous Intrathecal Catheter System
Conclusions: Nusinersen administration for SMA is providing a novel treatment for a previously untreatable condition and the number of patients requiring these procedures is expected to increase. Pediatric interventional radiologists can provide the safest approach for delivering nusinersen by being aware of the options.

Poster #: EDU-049

Eliminating Radiation and Decreasing Sedation Time For Pediatric Peripherally Inserted Central Catheter (PICC) Placement: A Technical Review

Malay Bhatt, MD, *malay.bhatt@beaumont.edu*; Alyssa Kirsch, Terrence Metz, MD; Diagnostic Radiology, Beaumont Hospital-Royal Oak, Royal Oak, MI

Disclosures: All authors have disclosed no financial interests, arrangements or affiliations in the context of this activity.

Purpose or Case Report: To familiarize the audience with our institution's technique utilizing ultrasound (US) and electrocardiogram (ECG) for anatomic localization and technical guidance for PICC placement in a pediatric intensive care unit (PICU) procedure suite utilizing intravenous (IV) sedation without general anesthesia to eliminate patient and operator radiation exposure and decrease sedation specifically in a pediatric population.

Methods & Materials: A majority of our institutions pediatric (newborn to 18 years) PICC placements are performed in our PICU procedure suite under IV sedation only, administered by qualified attending pediatric intensivists. The procedure is performed with US and ECG guidance which is described.
Results: Initial procedural suite preparation is described including patient and operator positioning. Patient preparation and localizing ECG device placement as well as ECG interpretation for final PICC placement is explained. Finally, troubleshooting techniques and complication management is reviewed.
Conclusions: Although ECG-guided PICC placement is currently used in the adult population, it is a newer and unique technique used for the pediatric population at our institution allowing decreased sedation times and anesthetic use as well as eliminating patient and operator radiation exposure. The technique is described to the audience.

Poster #: EDU-050

Imaging Essentials of Congenital Foot Deformities

Elizabeth P. Wellings, MD[1], Monica Epelman, MD[2], Tushar Chandra, MD[2], Jason Malone, DO[3], John F. Lovejoy, MD[3], **Arthur B. Meyers, MD[2]**, *arthurbmeyers@yahoo.com*; [1]Orthopedic Surgery, Mayo Clinic, Rochester, MN, [2]Department of Radiology, Nemours Children's Hospital and Health System, Orlando, FL, [3]Department of Orthopedics, Nemours Children's Hospital and Health System, Orlando, FL

Disclosures: Arthur B. Meyers, MD: Royalty: Author/Editor for Amirsys, Elsevier. All other authors have disclosed no financial interests, arrangements or affiliations in the context of this activity.

Purpose or Case Report: This education exhibit will provide a general review of radiographic techniques of the foot followed by a section identifying clinical and radiographic findings for specific foot deformities. Learning objectives for this exhibit include: (a) recognize the imaging needed for specific foot deformities, (b) measure critical angles from different radiographic views and interpret their meanings, (c) recognize radiographic identifying features for specific foot deformities, (d) identify what views are necessary when trying to differentiate between similar deformities, and (e) interpret post-operative/post-procedural imaging and recognize possible complications.

Poster #: EDU-051

Algorithm-based approach to the evaluation and diagnosis of congenital skeletal dysplasia

Marcus I. Hook, MD, *marcus.hook@uvmhealth.org*; Timothy Higgins, MD, Andrea Hildebrand, MD, Betsy Sussman, MD, Leah Burke, MD; Radiology, University of Vermont Medical Center , Burlington, VT

Disclosures: All authors have disclosed no financial interests, arrangements or affiliations in the context of this activity.

Purpose or Case Report: **Objectives:**1. Present the use of a published algorithm for the evaluation and diagnosis of the pediatric patient with congenital skeletal dysplasia and abnormal skeletal survey.2. Review usefulness of accurate, narrowed differential diagnosis or suspected single diagnosis in terms of confirmatory testing, treatment implications, and genetic counseling.3. Demonstrate the utility of the algorithm when applied to recent, rare cases of congenital skeletal dysplasia at our institution, a tertiary trauma center and children's hospital in the Northeastern United States.**Content:**We present a refined, algorithm-based approach to the evaluation and diagnosis of the pediatric patient with congenital skeletal dysplasia and abnormal skeletal survey. The algorithm optimizes evaluation of the skeletal survey in cases of congenital skeletal dysplasia, aiding in timely, accurate diagnosis. The utility of the refined algorithm is demonstrated as it was applied to recent, confirmed cases of rare skeletal dysplasias at our institution, including metatropic dysplasia and cleidocranial dysplasia.**Teaching Message:**Evaluation of the pediatric patient with congenital skeletal dysplasia and abnormal skeletal survey can be challenging, even for the subspecialty-trained radiologist. By assessing the presence or absence of discriminating imaging features and findings on skeletal survey, the interpreting radiologist can significantly shorten the differential diagnosis or in many cases suggest a single, most-likely primary diagnosis. Narrowing the differential diagnosis is helpful in guiding confirmatory molecular or genetic testing. Timely, accurate diagnosis may have significant treatment and prognostic implications for patients and their families.

Poster #: EDU-052

When soft tissues turn hard - ossifying soft tissue lesions.

Anna Smyth, *smythannae@gmail.com*; Rosemond N. Aboagye, BSc Med Sci, MB ChB, Anna Lee, MD, Heather Bray, MD; radiology, BC Children's Hospital, Vancouver, British Columbia, Canada

Disclosures: All authors have disclosed no financial interests, arrangements or affiliations in the context of this activity.

Purpose or Case Report: The purpose of this educational exhibit is to illustrate the radiological appearance of various ossified soft tissue lesions. The differential diagnosis is wide, with entities ranging from benign to malignant. Using instructive and interesting cases encountered at our department, this presentation will outline an approach to forming a differential diagnosis. Various teaching points will be highlighted. Pathological correlation will be included where available.The cases to be presented include:Myositis ossificansFibrodysplasia ossificans progressivaTenosynovial osteochondromatosisDysplasia Epiphysealis HemimelicaPseudohypoparathyroidism - Albright's hereditary osteodystrophyPhlebolith in a vascular malformationPilomatrixomaHeterotopic ossificationSynovial SarcomaThis presentation will highlight the distinguishing imaging characteristics of each entity and help narrow the differential diagnosis for a radiologist when faced with a pediatric ossified soft tissue lesion.

Poster #: EDU-053

Don't Be Nervous About the Nerves!: A Sonographic Review of the Normal Appearance of Peripheral Nerves and the Spectrum of Disease Pathology That Can Affect Them

Jillian R. Krauss, MD, *jillianrose.k@gmail.com*; Jonathan Samet, MD; Northwestern Feinberg School of Medicine Ann & Robert H. Lurie Children's Hospital of Chicago, Chicago, IL

Disclosures: All authors have disclosed no financial interests, arrangements or affiliations in the context of this activity.

Purpose or Case Report: At our institution and in general practice, we have observed that ultrasound is an underutilized modality in the field of pediatric musculoskeletal imaging, particularly when compared to its body imaging counterparts and the adult population. Within the spectrum of musculoskeletal radiology, ultrasound can be an especially

helpful tool in evaluating the peripheral nervous system (PNS), which can often be challenging to assess on other imaging modalities. For instance, ultrasound offers the ability to carefully trace small nerves and easily allows for comparison to the other, often unaffected or normal extremity, as well as dynamic imaging. This advantage is often not possible on magnetic resonance imaging (MRI), which is currently the primary modality being utilized to assess for nerve pathology. In small children, nerves are often difficult to visualize on MRI, which can be limited by artifact and motion and may require sedation. Due to its superior axial resolution, ultrasound can better visualize the intra-neural architecture, sometimes better than MRI, especially in the case of small nerves. Also, as was demonstrated by one of the cases at our institution, ultrasound was superior in evaluation when there was adjacent surgical hardware which resulted in artifact on MRI. Additionally, we as radiologists, can aid our peripheral nerve surgeon colleagues intra-operatively with ultrasound.Some of the hesitance in using the modality may be a reflection of a lack of familiarity on the part of both radiologists and technologists with respect on how to image the PNS and uncertainty about the normal and abnormal appearance of these structures. The objective of this educational exhibit is to provide the knowledge necessary to successfully acquire and interpret ultrasound images of the PNS. The topics addressed in the review will include an introduction on how to appropriately obtain images of the major peripheral nerves, how to distinguish between the normal and abnormal appearance of nerves on ultrasound, and the spectrum of pathology affecting the peripheral nervous system. The exhibit will feature a variety of cases from our institution, including examples of neuropathy, post-traumatic focal neuroma, nerve laceration resulting in transection, ulnar nerve subluxation/dislocation, and nerve sheath tumors, among others, with some intraoperative and pathologic correlation.

Poster #: EDU-054

Clinical update on high resolution magnetic resonance imaging of small joints in children and adolescents using 3D proton density fat suppressed turbo spin echo imaging accelerated with compressed sensing

Eric Padua, MD[1], *epadua@mail.cho.org*; Bamidele Kammen[1], S Pinar Karakas, MD[1], Dave Hitt[2], Chau Tai, MD[1], Nirav Pandya[1], Quin Lu[2], Taylor Chung, MD[1];[1]Diagnostic Imaging, UCSF Benioff Children's Hospital Oakland, Oakland, CA, [2]Philips Healthcare North America, Gainesville, FL

Disclosures: Dave Hitt: Salary: Philips HealthTech; **Nirav Pandya, MD:** Consultant/Honoraria: Orthopediatrics; **Quin Lu, PhD:** Salary: Philips. All other authors have disclosed no financial interests, arrangements or affiliations in the context of this activity.

Purpose or Case Report: Current musculoskeletal MR imagiing utilizes multiple imaging planes and multiple weightings of two-dimensional turbo spin echo (2D TSE) to precisely delineate and characterize intra-articular abnormalities. Three-dimensional (3D) TSE sequences are currently available on most MRI vendor platforms. High resolution isotropic 3D imaging of the small joints reduces partial volume artifacts and allows for the reconstruction in any orientation, thus eliminating the need to acquire additional scans of different orientations with identical tissue contrast. However, the typical trade off of achieving very high resolution (under 0.5mm isotropic) is long acquisition time. Scan time reduction can be achieved with parallel imaging at the expense of reducing the signal-to-noise ratio (SNR) and with increasing the echo train length at the expense of image blurring. The addition of compressed sensing (CS), a recently commercially available acceleration technique, allows for decrease in acquisition time without the significant loss of SNR experienced with identical acceleration factors achieved with parallel imaging alone. CS exploits (1) image data sparsity via application of a sparsity transform of the image data; (2) pseudo-random-type of k-space sampling; (3) non-linear iterative reconstruction. We utilized CS to decrease scan time (range 4:55 to 5:35 minutes) of 3D PD FS TSE sequences to obtain high resolution (voxel size 0.45 x 0.45 x 0.45) imaging of the fingers, toes, wrist and feet. In this educational exhibit, we will review the normal anatomy and pathology of small joints

Poster #: EDU-055

Behind closed doors. Detecting Posterior Acetabular Fractures in Adolescence.

Kevin P. Boyd, DO, *kboyd@chw.org*; Pooja Thakrar, MD; Pediatric Imaging , Medical College of Wisconsin, Milwaukee, WI

Disclosures: All authors have disclosed no financial interests, arrangements or affiliations in the context of this activity.

Purpose or Case Report: The purpose of the exhibit is: 1. Illustrate the presence of multiple and accessory ossification centers about the hip that can make it challenging to diagnosis fractures on radiographs in adolescence. 2. Demonstrate that posterior acetabular fractures are typically hidden behind the femoral head on radiographs. 3. Review variant os acetabuli that are commonly encountered in patients with hip pain and demonstrate that the orientation of the fragments compared with posterior acetabular fractures can help to make a distinction. 4. Highlight that a complete pelvis radiograph (AP or AP/Frog leg lateral) in trauma patients or hip pain NOS can aid in the detection of fractures and assess for asymmetry of normal variants.

Poster #: EDU-056

Beyond a Lesionable Doubt: An Algorithmic Approach to Pediatric Soft Tissue Lesions on Ultrasound

Sarah Eliades, MD, *sarahkeliades@gmail.com*; Christy B. Pomeranz, MD, Michael Baad, MD, Michelle Roytman, MD, Arzu Kovanlikaya, MD; Radiology, NewYork Presbyterian-Weill Cornell Medical Center, New York, NY

Disclosures: All authors have disclosed no financial interests, arrangements or affiliations in the context of this activity.

Purpose or Case Report: Ultrasound is typically the first-line imaging modality for the evaluation of superficial soft tissue masses in the pediatric population. While certain superficial soft tissue masses have a classic appearance on ultrasound, others may have a nonspecific appearance and may vary in their sonographic characteristics. This can make a definitive diagnosis and follow-up recommendations difficult, especially for trainees.We aim to provide a basic overview of some of the common and less common superficial soft tissue masses that may be encountered in pediatric imaging, and introduce a novel, structured algorithmic approach for evaluating these lesions on ultrasound. The algorithm will assist the radiologist in reaching a definitive diagnosis or narrowing the differential such that a helpful recommendation for further workup can be made. For example, the algorithm will include internal vascularity, border distinctness, cystic or solid components, presence or absence of calcifications, and location in the body and within the superficial soft tissue layers. Pictorial examples of each sonographic feature in the algorithm will provide further assistance.Pathologies will include but not be limited to: pilomatricoma, glanuloma annulare, epidermal inclusion cyst,

ganglion cyst, abscess/infection, lipoma, hematoma, lymph nodes, vascular anomalies, and soft tissue sarcomas. When a definitive diagnosis is not achievable, this algorithm will help the radiologist determine the likelihood of benignity, a short differential diagnosis, and a recommendation for any further imaging workup.

Poster #: EDU-057

Imaging of Gaucher Disease in Children: Advances in Comprehensive Assessment of Disease Involvement

Andrew J. Degnan, MD, MPhil, *degnana@email.chop.edu*; Suraj Serai, Victor Ho-Fung, MD, Christian A. Barrera, M.D., Dah-Jyuu Wang, Rebecca Ahrens-Nicklas, Can Ficicioglu; Radiology, Children's Hospital of Philadelphia, Philadelphia, PA

Disclosures: All authors have disclosed no financial interests, arrangements or affiliations in the context of this activity.

Purpose or Case Report: Gaucher disease is an inherited metabolic disorder due deficiency of the lysosomal enzyme β-glucocerebrosidase that results in the accumulation of abnormal macrophages (“Gaucher cells”) within multiple organs, most conspicuously affecting the liver, spleen and bone marrow. As the diagnosis is increasingly made during childhood and young adulthood, pediatric radiologists should be familiar with imaging features of Gaucher disease and its complications.Visceromegaly consisting of hepatosplenomegaly is a hallmark of Gaucher disease and uniformly present in cohorts of pediatric patients. In addition, bone marrow involvement with ‘Erlenmeyer flasks’ have been long recognized as part of this disease, although the classic radiographic finding is not present until adulthood. Marrow involvement confers significant morbidity for these patients with pain, bone infarcts and pathologic fracture.Traditionally, imaging of disease severity has been based on hepatic and splenic visceral organ enlargement and/or qualitative assessment of bone marrow involvement. However, advances in the understanding of Gaucher disease and observations of elevated ferritin levels and increased risk of hepatic fibrosis emphasize the importance of more comprehensive assessment of liver involvement beyond simple enlargement. Moreover, quantitative MRI assessment of bone fat-fractions also may have a role in assessing marrow involvement. These methods of disease assessment are important in addressing management decisions regarding enzyme replacement and substrate reduction therapy.
Conclusions: This presentation summarizes the imaging evaluation of Gaucher disease as it pertains to pediatric patients. We review multimodal conventional imaging manifestations of Gaucher disease from radiographic manifestations to MRI appearances. Semi-quantitative marrow scoring methods are discussed. This exhibit also discusses newer quantitative approaches to assessment of liver and bone marrow involvement with an emphasis on future applications of advanced methods including spectroscopy, elastography, fat-fraction and iron quantification in guiding therapy decisions and monitoring treatment response.

Poster #: EDU-058

Skeletal Ciliopathy: A Primer on a Major Bone Dysplasia Family

Atsuhiko Handa[1], *atsuhiko-handa@uiowa.edu*; Gen Nishimura, Dr.[2]; [1]Radiology, University of Iowa, Iowa City, IA, [2]Saitama Medical University, Saitama, Japan

Disclosures: All authors have disclosed no financial interests, arrangements or affiliations in the context of this activity.

Purpose or Case Report: A term “ciliopathy” represents a diverse group of genetic disorders caused by mutations in genes coding for components of the primary cilia. Primary cilia have a pivotal biological role in the cell surface of nearly every organ system of the body. "Skeletal ciliopathy" is a subset of ciliopathy mainly affecting the skeleton and shares common radiological findings such as short ribs, short limbs, and short digits with or without polydactyly. Pattern recognition approach is thus useful to diagnose skeletal ciliopathy. Skeletal ciliopathy includes (1) Jeune asphyxiating thoracic dysplasia, (2) Ellis-van Creveld syndrome (chondroectodermal dysplasia), (3) Sensenbrenner syndrome (cranioectodermal dysplasia), and (4) Short rib-polydactyly syndromes. Clinically, affected patients commonly present with thoracic hypoplasia with respiratory failure and disproportional stature with a normal trunk and short limbs most severe in the distal segments. Brachydactyly is conspicuous. Patients may have extra-skeletal anomalies such as retinopathy, cardiac anomalies, cerebellar malformations, and hepatorenal failures.Radiological diagnosis of bone dysplasia might be regarded as something complex. We aim to highlight a pattern recognition approach to diagnose skeletal ciliopathies, one of the major bone dysplasias, by providing many cases. We will also review a general concept of "bone dysplasia family" which refers to a grouping of radiologically similar skeletal disorders into a “family.” This concept has been widely accepted now after we found that phenotypic similarities usually indicate the same/similar pathogenetic mechanisms, and it supports the use of a pattern recognition approach. Imaging diagnosis can guide genetic testing, interpretation, and possibly identify new genes or mutations.

Poster #: EDU-059

In-phase and opposed-phase evaluation of bone marrow lesions in the pediatric population.

Mariangeles Medina Perez, MD, *medinapm@upstate.edu*; Saurabh Gupta, MBBS, Ninad Salastekar, MBBS, MPH, Zain Badar, MD, Anand Majmudar, MD; Radiology, SUNY Upstate Medical University, Syracuse, NY

Disclosures: All authors have disclosed no financial interests, arrangements or affiliations in the context of this activity.

Purpose or Case Report: Bone marrow is composed of fat and cellular elements supported by the trabecular bone. Pathological lesions of the bone marrow usually replace its normal constituent to a variable degree. Differentiation among traumatic, neoplastic, and inflammatory processes of the bone marrow is often not possible with MRI, which commonly requires the patient to undergo additional invasive diagnostic procedures to obtain an accurate diagnosis.In-phase and opposed-phase imaging has been used extensively in imaging of the liver and adrenal glands. However, recently it has been introduced into the evaluation of the bone marrow. The technique takes advantage of different excitation frequencies of water and fat protons due to differences in their molecular environments. The main concept is that the presence of normal bone marrow would result in suppression of signal intensity on

the opposed-phase images. In the presence of infiltration lesions of the bone marrow, normal fat-containing marrow will be replaced with neoplastic cells and result in lack of suppression on the opposed-phase images.The main teaching purpose of this exhibit will be to demonstrate, by a pictorial case-based review, the appearance of multiple cases of biopsy-proven infiltrating lesions of the bone marrow, and emphasize how they can be differentiated from other traumatic or inflammatory processes.

Poster #: EDU-060

Congenital fibular deficiency. Diagnosis, Image-based Classification, and Follow-up

Eman E. Marie, M.D.- M.Sc., *eezzatmarie@gmail.com*; Manuela Perez, MD, Michael R. Aquino, MD, Jennifer Stimec; The Hospital For Sick Children, Toronto, Ontario, Canada

Disclosures: Michael R. Aquino, MD: Royalty Income: Elsevier Co-author. All other authors have disclosed no financial interests, arrangements or affiliations in the context of this activity.

Purpose or Case Report: Although rare, fibular hemimelia or congenital fibular deficiency (CFD), is the most common congenital long bone deficiency, with an approximate incidence of 7.4- 20 per 1 million live births. The clinical presentation of CFD represents a broad spectrum of manifestations, ranging from mild fibular deficiency with limb length discrepancy to a significantly short limb with multiple associated foot, ankle and knee deformities.Traditional FH classification such as Achterman and Kalamchi described the amount of fibular deficiency, which is today known to be unrelated to length discrepancy and foot deformity. Current classifications are based on the associated deformities of the ankle and subtalar joint, as the foot deformity is the main prognostic factor.Treatment should be tailored for each patient to maximize the lower limb function - this involves predicting the limb length discrepancy and then coming up with a surgical plan to correct these in the fewest number of surgeries spread out as much as possible throughout the child's growing years, so that by skeletal maturity the child has achieved equal leg length, a functional plantigrade foot, excellent alignment of the hip, knee and ankle and, as needed, a stable knee joint.Multimodal imaging provides detailed evaluation of the osteochondral and extraosseous malformations. In-utero identification can be accomplished with prenatal ultrasonography. After birth, radiographs often show striking bony anomalies. Detailed information regarding associated crucial cartilaginous, articular, soft tissue, and vascular abnormalities required for preoperative planning necessitates the use of magnetic resonance (MR) imaging.The purpose of this poster is to: 1) review the various types of osteochondral and extra-osseous abnormalities of CFD as depicted by different imaging modalities, 2) describe the limitations of each of these modalities, 3) outline the image-based classification of CFD, 4) describe the options for treatment, and 5) discuss the post-operative imaging evaluation of CFD.

Poster #: EDU-061

Preliminary Definitions for Sacroiliac Joint Pathologies in the OMERACT Juvenile Idiopathic Arthritis MRI Score (OMERACT JAMRIS-SIJ)

Tarimobo M. Otobo, MD[1], *otobopanebi@gmail.com*; Philip G. Conaghan[2], Walter P. Maksymowych[3], Desiree van der Heijde[4], Pamela F. Weiss[5], Iwona Sudol-Szopinska[6], Nele Herregods[7], Jacob L. Jaremko[8], Arthur B. Meyers, MD[9], Dax Rumsy[10], Emilio C. Inarejos[11], Eva Kirkhus[12], Jennifer Stimec[1], Jyoti Panwar, MD, FRCR[1], Kevin Thorpe[13], Lennart Jans[7], Marion A. van Rossum[14], Mirkamal Tolend[1], Manuela Perez, MD[1], Nikolay Tzaribachev[15], Pulukool Sandhya[16], Shirley Tse[1], Appenzeller Simone[18], Vimarsha G. Swami[19], Zahi Touma[17], Robert Lambert[8], Andrea Doria, MD[1]; [1]Diagnostic Imaging , Hospital for Sick Children , Toronto, Ontario, Canada, [2]Leeds Institute of Rheumatic and Musculoskeletal Medicine, University of Leeds & NIHR Leeds Biomedical Research Centre, Leeds Teaching Hospitals NHS Trust, Leeds, United Kingdom, [3]Department of Rheumatology, University of Alberta, 562 Heritage Medical Research Building, Edmonton, Alberta, Canada, [4]Department of Rheumatology, Leiden University Medical Center, Leiden, Netherlands, [5]University of Pennsylvania Perelman School of Medicine, Division of Rheumatology, Children's Hospital of Philadelphia, Philadelphia, PA, [6]Department of Radiology, National Institute of Geriatrics, Rheumatology and Rehabilitation, Warsaw, Poland, [7]Department of Radiology and Medical Imaging, Ghent University Hospital, De Pintelaan 185, Ghent, Belgium, [8]Department of Radiology and Diagnostic Imaging, University of Alberta, Edmonton, Alberta, Canada, [9]Nemours Children's Hospital, Orlando, FL, [10]Division of Pediatric Rheumatology, Department of Pediatrics, University of Alberta, Edmonton, Alberta, Canada, [11]Department of Radiology; Hospital Sant Joan de Deu, Passeige de Sant Joan deDeu, Esplugues de Llobregat, Barcelona, Spain, [12]Department of Radiology, Rikshospitalet, Oslo University Hospital, Oslo, Norway, [13]Dalla Lana School of Public Health, University of Toronto, 155 College Street, Toronto, Toronto, Ontario, Canada, [14]Reade | Emma Children's Hospital / Academic Medical Center, Amsterdam, Netherlands, [15]Pediatric Rheumatology Research Institute, PRI Achtern Dieck 9, Bad Bramstedt, Germany, [16]Department of Clinical Immunology and Rheumatology, Christian Medical College, Vellore, India, [17]Department of Rheumatology, Center for Prognosis Studies in Rheumatologic Diseases, Toronto Western Hospital, Toronto, Ontario, Canada, [18]Department of Medical Imaging, University of Toronto, Toronto, Ontario, Canada

Disclosures: Arthur B. Meyers, MD: Royalty: Author/Editor for Amirsys, Elsevier. All other authors have disclosed no financial interests, arrangements or affiliations in the context of this activity.

Purpose or Case Report: Clinical assessment of the Sacroiliac Joint (SIJ) is limited due to the location and anatomy of the joint. Magnetic Resonance Imaging is a sensitive, non- invasive tool in detecting early SIJ inflammatory changes and structural damage in Juvenile Idiopathic Arthritis (JIA). The quantification of interval change of pediatric SIJs using MRI based scoring methods will serve as an important objective outcome measure for the assessment of disease severity and treatment effectiveness in JIA.
Methods & Materials: The OMERACT consensus-driven methodology consisting of iterative surveys and focus group meetings within an international group of pediatric rheumatologists and radiologist was utilized to decide the measurement construct, items, and definitions. Consensus was deemed to have been achieved if greater than 70% agreement was reached among voting attendees at the session in the

absence of greater than 15% present or more in strong disagreement.
Results: Twenty-eight international multidisciplinary experts from North America, Europe, South Asia and South America participated in the study. Two domains, inflammation and structural, were identified. Definitions for bone marrow edema, joint space inflammation, capsulitis, and enthesitis were derived for joint inflammation; sclerosis, erosion, fatty lesion and ankylosis were defined for assessing structural joint changes.
Conclusions: Preliminary consensus-driven definitions for inflammation and structural elements have been drafted, underpinning the ongoing development of the Juvenile arthritis MRI scoring system for SIJ (JAMRIS-SIJ).

Poster #: EDU-062

Proximal humeral epiphyseal fracture-separation in infants

Edward P. Fenlon, MD[1],*ef2599@cumc.columbia.edu*
Andrew J. Degnan, MD, MPhil[2], Alexis B. Maddocks, MD[1], Susie Chen, MD[1], Diego Jaramillo, MD MPH[1]; [1]Radiology, Columbia University Medical Center, New York, NY, [2]Children's Hospital of Philadelphia, Philadelphia, PA

Disclosures: All authors have disclosed no financial interests, arrangements or affiliations in the context of this activity.

Purpose or Case Report: Proximal humeral epiphyseal fracture-separation is a rare fracture pattern in infants often associated with birth-related or non-accidental trauma, representing a Salter-Harris type I or type II fracture. Lack of a proximal humeral epiphyseal ossification center in most newborns or only subtle displacement of a small epiphyseal ossification center in older infants, makes this injury difficult to diagnose on plain radiographs, potentially leading to delayed diagnosis or misdiagnosis. Ultrasound and MRI are therefore useful imaging modalities in indeterminate cases.Clinical findings of infant proximal humeral epiphyseal fracture-separation such as shoulder swelling, tenderness, and decreased active motion, overlap with more common entities including clavicular fracture, brachial plexus injury and osteomyelitis. Radiographs are often the first diagnostic study ordered to evaluate these symptoms but are insensitive due to minimal ossification of the proximal humeral epiphysis. Radiographs may be normal or show subtle displacement of the epiphyseal ossification center, apparent joint space widening, small metaphyseal fracture fragments or displacement of the proximal humeral metaphysis in relation to the scapula. These findings can be misdiagnosed as shoulder dislocation or pseudosubluxation due to a joint effusion. Careful review of the medical record may elucidate a history of difficult delivery with shoulder dystocia or suspected shoulder trauma.Ultrasound and MRI are useful in indeterminate cases due to their ability to resolve the cartilaginous physis and proximal humeral epiphysis, and to resolve their relationship to the humeral shaft and cartilaginous labrum. Ultrasound has higher anatomic resolution and offers the flexibility to quickly image the asymptomatic contralateral shoulder and image in planes that best show the relationship between the non-ossified epiphysis and the humeral shaft. Doppler ultrasound demonstrates epiphyseal perfusion without the need for contrast administration, and serial ultrasound imaging can be used to evaluate healing and remodeling. MRI is more useful in evaluating cases where osteomyelitis and/or septic arthritis are being considered, or in cases of an inconclusive history suspicious for non-accidental trauma to evaluate for additional osseous and soft tissue injuries.Several examples of typical proximal humeral epiphyseal fracture-separations in infants will be presented and the relevant imaging findings discussed.

Poster #: EDU-063

AVID: A Cause of Mistaken Diagnoses

Megan Albertson[1], *megan.albertson@unmc.edu*; Andria M. Powers, MD[2], Angela Beavers, MD[2]; [1]University of Nebraska Medical Center, Omaha, NE, [2]Children's Hospital & Medical Center, Omaha, NE

Disclosures: All authors have disclosed no financial interests, arrangements or affiliations in the context of this activity.

Purpose or Case Report: Background:AVID is an acronym describing a triad of findings including 1) asymmetric ventriculomegaly, 2) interhemispheric cyst, and 3) dysgenesis of the corpus callosum. This entity accounts for one of the presentations of callosal dysgenesis along a wide spectrum. Because midline anomalies occur with many processes, including holoprosencephaly and aqueductal stenosis, it may appear to have overlapping features on initial glance. However, by focusing attention on the secondary findings, a specific diagnosis may be determined.Objectives:By the end of this presentation the learner will: 1) Become familiar with the imaging characteristics of AVID. 2) Describe the differential diagnosis of AVID and the important distinguishing features. 3) Understand the clinical implications of interhemispheric cysts and similar diagnoses.Cases/Differential Diagnosis:Through several case examples of mistaken diagnoses, we will describe key findings to differentiate brain disorders with midline anomalies including AVID, holoprosencephaly, and aqueductal stenosis. Holoprosencephaly creates a monoventricle, but may also be associated with a dorsal midline cyst which can be confused for an interhemispheric cyst. Features that differentiate holoprosencephaly from AVID are the presence of fused cerebral hemispheres, thalamic fusion, and a true monoventricle. Aqueductal stenosis may also show severe hydrocephalus, but lacks the cystic component which is seen with the other mentioned entities. Aqueduct stenosis usually causes symmetric ventriculomegaly of the lateral and 3rd ventricles as well as upward displacement of anterior cerebral arteries and inferior displacement of internal cerebral veins. The hydrocephalus from all of these entities may be treated with ventricular shunt placement, but AVID is an important diagnosis to consider because the wall of the interhemispheric cyst could be imperceptible by imaging and may not improve if the tip of the drainage catheter is not within the cyst. Conclusion: When evaluating cases of true ventriculomegaly it is important to consider a differential including AVID, holoprosencephaly, aqueductal stenosis, among other less common congenital syndromes. Careful attention to additional imaging findings is necessary to distinguish the correct diagnosis from look-alikes. Making an accurate diagnosis is important as there are differences in medical decision making, treatment outcomes, and long-term prognosis.

Poster #: EDU-064

Acquired non-traumatic temporal bone lesions in children: A Pictorial Review.

Ashok Mithra Karuppiah Viswanathan, *ashokmithrakv@gmail.com*; Nagwa Wilson; CHEO, University of Ottawa, Ottawa, Ontario, Canada

Disclosures: All authors have disclosed no financial interests, arrangements or affiliations in the context of this activity.

Purpose or Case Report: A number of acquired non-traumatic diseases of myriad aetiologies involve the temporal bone in children. While some of these are also noted in adults, many diseases are specific to the pediatric age group. These can be

grouped into infectious/inflammatory, neoplastic, vascular and other miscellaneous disorders.Anatomy of the temporal bone is complex. It forms the lateral aspect of skull base and comprises of five osseous parts viz. squamous, mastoid, petrous, tympanic and styloid segments. Specific disease processes afflict each part of the temporal bone, largely dictated by its anatomy and constituent structures. Hence a structured approach to image interpretation and reporting is especially useful in this region to localise the lesion and subsequently generate differential diagnoses.Traditionally CT has been the imaging modality of choice in assessing temporal bone lesions. However, currently, CT and MRI are deemed complimentary. CT provides exquisite details of anatomy, characterises osseous lesions, determines bony involvement/destruction and extension while MRI is highly useful in assessing intrinsic lesion characteristics due to its superior contrast resolution. In certain aetiologies such as cholesteatoma MRI is diagnostic.This poster aims to review the anatomy of temporal bone and various common, uncommon acquired non traumatic temporal bone lesions in children.The lesions that will be discussed in this poster are listed below:**Infectious / Inflammatory:** 1. Otitis externa2. Otitis media3. Coalescent mastoiditis with orbital involvement4. Bell's Palsy5. Guillain-Barre' syndrome with facial palsy**Neoplastic Lesions:** 1. Vestibular schwannoma2. Rhabdomyosarcoma3. Ewing's sarcoma4. Langerhan's cell histiocytosis5. Osteoblastoma6. Osteoma7. Aggressive Myofibromatosis**Vascular:** 1. Carotid vasculitis secondary to petrous abscess**Miscellaneous Lesions:** 1. Cholesteatoma (congenital and acquired)2. Cholesterol granuloma

Poster #: EDU-065

Radiographic manifestations and clinical relevance of central nervous system complications of leukemia in children

Yan Sun,*sunyan.xwz@163.com*; Shanghai Children's Medical center, Shanghai, China

Disclosures: All authors have disclosed no financial interests, arrangements or affiliations in the context of this activity.

Purpose or Case Report: To investigate the radiological findings of central nervous system complications of leukemia (CNSCL） in children.

Methods & Materials: The CT and MR findings and clinical features of 49 pediatric patients with CNCSL were retrospectively analyzed.

Results: (1) Cerebrovascular abnormalities in 23 cases included hemorrhage(n=20), infarction(n=2) and sinus thrombosis(n=1). 1 case of epidural hematoma and 19 cases of intracerebral multiple bleeding were seen in the hemorrhage group, which demonstrated high-density on CT and different signal on MR as time went by. Microhemorrhage displayed as low signal on susceptibility weighted imaging (SWI). (2) Among 23 cases of leukemic infiltration, dura and/or skull were involved in 18 cases, which presented as fusiform or mass, with high density on CT, low signal on T1WI, intermediate signal on T2WI and strong enhancement. 6 leptomeningeal infiltration demonstrated as meningeal thickening and enhancement. 2 parenchymal involvement manifested with high-density mass. 2 oculomotor nerve and 1 optic nerve infiltration demonstrated thickening and enhancement .(3)White matter disease were seen in 2 case, with hyper-intensity on T2WI.(4) one case of secondary tumor is glial tumor of brainstem.

Conclusions: The radiographic manifestations of CNCSL in children are various. CT and MR are of important diagnostic values. SWI is suggested as routine modality because of sensitivity of hemorrhage, which is of practical significance to clinical politics.

Poster #: EDU-066

Introduction to the Technical Aspects of PET/MRI with Clinical Applications to Pediatric Neuroradiology for Residents and Fellows

Alex Chan, D.O.[1], *alchan@christianacare.org*; Brady Laughlin, D.O.[1], Rachael Latshaw, DO[1], Waqas Abid[1], Alberto Iaia, M.D.[1], Parham Moftakhar, M.D.[1], Vinay V. Kandula, M.D.[2], Rahul Nikam, M.D.[2], Arabinda Choudhary, M.D.[2]; [1]Diagnostic Radiology, Christiana Care Health System, Bear, DE, [2]Nemours/Alfred I. duPont Hospital for Children, Wilmington, DE

Disclosures: Arabinda Choudhary, M.D.: Consult, Honoraria: Child Abuse Lectures, Equity Interest/Stock Options: GE Shares. All other authors have disclosed no financial interests, arrangements or affiliations in the context of this activity.

Purpose or Case Report: PET/MRI has recently become a clinical realization after overcoming complex hardware and image reconstruction issues. The goal of this educational exhibit is to provide a comprehensive, yet understandable, introduction to these aspects of PET/MRI along with displaying a pictorial assay of different normal and abnormal metabolic findings within the field of Pediatric Neuroradiology.The first part of this presentation will begin by highlighting the basic hardware components of the PET/CT contrasting with the interactions between the main components of the PET/MRI scanner along with their associated solutions. In general, these issues include how MRI can affect PET in terms of their magnetic field and RF properties and how PET affect MRI due to the scintillator/electronic components.The second part will begin by discussing some soft tissue and hardware attenuation correction techniques that are currently in use, such as: Segmentation and atlas-based methods along with attenuation map generation and coil localization methods. Additionally, we will show the consequence of field-of-view (FOV) mismatch between the PET and MRI acquisitions and partial volume effects along with their solutions.The final part will showcase clinical applications of PET/MRI to Pediatric Neuroradiology, featuring imaging protocol details and a pictorial guide of normal distributions and pathologic conditions. Clinical examples range from seizure localization, cortical malformations, manifestations of Phakomatoses, perinatal stroke, tumor recurrence, and Flutriciclamide (^{18}F-GE180) imaging in the setting of neuroinflammation.

Poster #: EDU-067

CT and MRI of pediatric skull base

Rukya Masum, MD, *rukya.ali@northwestern.edu*; Chanae Dixon, MD, Maura Ryan, MD, Alok Jaju, MD; Radiology, Lurie Children's Hospital, Chicago, IL

Disclosures: All authors have disclosed no financial interests, arrangements or affiliations in the context of this activity.

Purpose or Case Report: This review describes the CT and MRI features of developmental variants and pathological lesions that involve the skull base, excluding those centered in the nasal cavity, nasopharynx, sinuses and orbits.Normal anatomy of developing bony skull base will be illustrated. The lesions are categorized by pathology rather than locations, and the following entities will be covered.Congenital and developmental lesions - arrested pneumatization, aberrant arachnoid granulations, dermoid/epidermoid cysts, ecchordosis physaliphora, encephaloceles, persistent craniopharyngeal canalInflammatory/Infectious lesions - skull base osteomyelitis, petrous apicitis, cholesterol granulomaBenign lesions - Fibrous

dysplasia, aneurysmal bone cyst, osteoma, osteochondroma, meningiomaMalignant lesions - Langerhans cell histiocytosis, lymphoma, neuroblastoma metastasis, Ewing's sarcoma, osteosarcoma, chordoma, chondrosarcoma

Poster #: EDU-068

Inclusion of the Transfontanelle Doppler as a Staple of Neonatal Head Ultrasound

Michael Collard, MD, *mdcollard@gmail.com*; Jeannie Kwon, Kate Louise M. Mangona, MD, Cory Pfeifer; Children's Medical Center, Dallas, TX

Disclosures: All authors have disclosed no financial interests, arrangements or affiliations in the context of this activity.

Purpose or Case Report: Head ultrasound has long been utilized in the first few months of life to screen neonates for hemorrhage, assess midline anatomy, characterize extra-axial fluid collections, elucidate causes for suspected ventriculomegaly, and serially evaluate parenchymal echotexture without exposing the child to ionizing radiation or the expense of MRI. Less commonly utilized in a routine fashion is Doppler interrogation of the midline vasculature as part of the inpatient routine head ultrasound protocol. This exhibit will educate the reader on how and when transfontanelle Doppler can be utilized and the benefits it can provide.
Methods & Materials: The routine use of transfontanelle Doppler interrogation of the intracranial vasculature is described. Using medical illustrations and relevant images from patient exams, the correct positioning and acquisition of images is shown. A review of the relevant anatomy is performed. Correlation of ultrasound abnormalities with MRI results is provided. Use in patients undergoing ECMO is highlighted. Pitfalls and tips to improve imaging are described. Comparisons to transcranial Doppler are made using correlational diagrams.
Results: The transfontanelle Doppler can provide valuable clues to diagnosis. Abnormal resistive indices can have prognostic value in the setting of hypoxic ischemic encephalopathy and for patients on extracorporeal membrane oxygenation. Specifically, abnormally low resistive indices in the perinatal period have been shown to have a positive predictive value of 71% for adverse outcomes. Doppler has also been shown to add value to ultrasound evaluation of patients with known brain damage, whether due to ischemia, infection, or hemorrhage. Extra-axial fluid collections can affect Doppler values. Interestingly, in patients who have had recent cardiac surgery, elevated resistive indices have been shown to be associated with improved neurodevelopmental outcomes.
Conclusions: Transfontanelle Doppler has been shown to add valuable information in multiple clinical scenarios. Transfontanelle Doppler evaluation is feasible with little additional training and should be performed as part of the routine head ultrasound protocol on inpatient neonates.

Poster #: EDU-069

Imaging spectrum in pediatric focal cortical dysplasia (FCD) on MR and FDG-PET imaging with correlation to surgical pathology based on ILAE classification.

Pankaj Watal, *pankajwatal@gmail.com*; Sarv Priya, MD, T. Shawn Sato, Girish Bathla, DMRD FRCR; University of Iowa Hospitals and Clinics, Iowa City, IA

Disclosures: All authors have disclosed no financial interests, arrangements or affiliations in the context of this activity.

Purpose or Case Report: 1. Review of structural and metabolic imaging findings across various classes of FCD based on recent ILAE classification.2. Review of correlation between imaging findings and pathologic features in different FCD groups.
Methods & Materials: The review is based on retrospective evaluation of pediatric patients who underwent surgery for treatment of medical refractory epilepsy at our institution between 2000 and 2018. The inclusion criteria were presence of at least one pre-operative optimal quality MR imaging (1.5T or 3T) exam of brain dedicated to epilepsy evaluation and interictal FDG-PET brain study within past 1 year of surgery. Patients with presence of mMCD (mild malformation of cortical development) including microdysgenesis and neuronal heterotopia were also included. Patients with pathology proven isolated epileptogenic neoplastic lesions, isolated hippocampal sclerosis or nonspecific gliosis were excluded.
Results: The search of institutional radiology database showed 20 patients who met our criteria. 2 patients were excluded because of suboptimal imaging exam (either MRI or FDG-PET brain). Out of the 18 patients, no patients were noted under ILAE pathologic Class Ia, IIIb and IIIc. The ILAE class with most number of patients was IIIa (FCD with hippocampal sclerosis), MR imaging in all of them demonstrated hippocampal sclerosis but was negative or equivocal for FCD; the FDG-PET in this group appeared to correlate better with distribution of FCD on surgical pathology. No transmantle sign was noted in this pediatric population, although this could be due to small sample size. 2 patients had underlying tuberous sclerosis evident on MR imaging and showing diffuse hypometabolism reflecting global pathology. 2 patients had mMCD with unremarkable MRI exams and focal abnormalities on FDG-PET corresponding to area of pathology.
Conclusions: The use of information from both MRI and FDG-PET can help in identifying the epileptogenic zone better in FCD. The FDG-PET appears more sensitive than MRI in type I FCD. The structural imaging has higher specificity and can characterize FCD lesions of type II and III better.

Poster #: EDU-070

Dermoid cysts in the suprasternal notch: focus on initial sonographic diagnosis

Jose Molto, *josemolto85@gmail.com*; Judyta Loomis, Tara Cielma, Matthew Whitehead, MD; Radiology, Children's National Medical Center, Washington, DC

Disclosures: All authors have disclosed no financial interests, arrangements or affiliations in the context of this activity.

Purpose or Case Report: Dermoid cysts are a sequestration of ectoderm containing secondary skin structures, usually at characteristic locations of embryologic fusion lines. The midventral suprasternal fusion line is one such location in the developing embryo with both simple and complicated dermoids of this region reported in the literature. We reviewed our academic pediatric institutional experience with dermoid cysts of the suprasternal notch, focusing on the initial presentation as a palpable nodule referred for sonographic evaluation.The purpose of this educational exhibit is to depict the ultrasound imaging features of suprasternal notch dermoid cysts in the pediatric population.Secondary purposes are to describe the anatomy of the suprasternal notch, demonstrate CT and MR correlates of the these dermoids, and depict regional inflammatory complications.
Methods & Materials: 47 retrospective cases aged from 2 months to 13 years were collected utilizing an electronic database of radiology reports at our academic children's hospital from January 2008 to July 2018. Many cases were confirmed either with typical MR appearance or excisional biopsy.

Results: Suprasternal notch dermoid cysts demonstrate specific sonographic findings:(1) circumscribed ovoid mass located between the sternornohyoid muscles in the midline(2) longitudinal orientation(3) homogeneously echogenic with some of them showing small internal anechoic areas(4) posterior acoustic enhancement(5) absence of internal Doppler blood flow
Conclusions: Characteristic location of a nodule in the suprasternal notch and specific sonographic findings allow for a confident radiologic diagnosis of a dermoid cyst without the need for additional imaging.

Poster #: EDU-071

Basic Physics of ASL with Clinical Applications to Pediatric Neuroradiology

Alex Chan, D.O.[1], *alchan@christianacare.org*; Brady Laughlin, DO[1], Waqas Abid[1], Rachael Latshaw, DO[1], Alberto Iaia, M.D.[1], Parham Moftakhar, M.D.[1], Rahul Nikam, M.D.[2], Vinay V. Kandula, M.D.[2], Arabinda Choudhary, M.D.[2]; [1]Diagnostic Radiology, Christiana Care Health System, Bear, DE, [2]Nemours/Alfred I. duPont Hospital for Children, Wilmington, DE

Disclosures: Arabinda Choudhary, M.D.: Consult, Honoraria: Child Abuse Lectures, Equity Interest/Stock Options: GE Shares. All other authors have disclosed no financial interests, arrangements or affiliations in the context of this activity.

Purpose or Case Report: The goal of this educational exhibit is to use a graphical and image heavy Powerpoint presentation to familiarize the reader with the background necessary to understand common clinical ASL-PWI imaging techniques along with displaying a pictorial assay of different normal and abnormal ASL perfusion findings within the field of Pediatric Neuroradiology.To introduce our topic, we will briefly discuss the physiology of cerebral blood flow and how it is measured with and without an exogenous tracer. Next, to serve as an overview, we will show the general ASL experiment, namely, labeling, post label delay, and readout. Following, we will discuss each of the above components, beginning with showing the different main labeling methods, CASL, PCASL, and PASL. Finally, the concept of post label delay will be illustrated respective to each of the main labeling methods.In the second section, we will discuss the image acquisition component by first describing and illustrating two common readout methods, such as 2D-EPI and 3D-GRASE methods along with their advantages and disadvantages. Additionally, we will illustrate the process of background suppression along with its significance. Finally, we will review the process of obtaining perfusion weighted images through the subtraction between tagged and control images.The third section will illustrate an assortment of clinical examples beginning with showing normal physiological hyper- and hypoperfusion and newborn perfusion characteristics. Following, we will highlight a spectrum of clinical cases including: moyamoya, HIE, medullary infarct with luxury perfusion, arteriovenous malformation, PRES, infections (intracerebral abscess, toxoplasmosis, cerebellitis), characteristics of headache, intracranial tumors (juvenile astrocytoma, hemangioblastoma, ATRT, and choroid plexus papilloma), cortical dysplasia, tuberous sclerosis with seizures, and variations presentations of methotrexate toxicity. Lastly, we will discuss cerebral blood reserve imaging utilizing acetazolamide challenge. All cases will contain pertinent clinical information and images from other sequences/modalities that aid in the diagnosis of disease.

Poster #: EDU-072

Congenital structural MRI findings in epilepsy

Amy Farkas, MD, *afarkas@umc.edu*; Niki Patel, David Joyner; University of Mississippi Medical Center, Jackson, MS

Disclosures: All authors have disclosed no financial interests, arrangements or affiliations in the context of this activity.

Purpose or Case Report: Epilepsy can be a progressive and debilitating illness in the pediatric population. There is a large range of congenital conditions that present with seizures in neonatal patients, which are essential for the radiologist to accurately characterize on imaging. Accurately diagnosing the cause of epilepsy can not only allow appropriate treatment, but also provide important information on prognosis and associated abnormalities.The goal of this educational poster is to provide an overview of different congenital etiologies of epilepsy. This case based review includes congenital malformations of the brain such as focal cortical dysplasia, schizencephaly, heterotopias, hemimegalencephaly, and polymicrogyria. Cases highlighting neurocutaneous conditions associated with epilepsy including tuberous sclerosis and Sturge-Weber are reviewed. Cortical injuries from insults such as congenital infection, hypoxic-ischemic injury, or hemorrhage are also included.Familiarity with the imaging findings of epilepsy is essential for the radiologist, especially the trainee and those with less experience with pediatric neuroimaging. After reviewing this educational poster, viewers will be able to describe the imaging features of congenital causes of epilepsy and understand the treatment and prognoses of these conditions.

Poster #: EDU-073

Imaging of Pediatric olfactory system anomalies

Schoenbrun Lori, MD[1], *schoenbrunle@upmc.edu*; Subramanian Subramanian[1], Deepa S. Rajan, MD[1], Jenna Gaesser, MD[1], Cecilia W. Lo, PhD[2], Vincent Schmithorst, PhD[1], Ashok Panigrahy, MD[1]; [1]Radiology, Children's Hospital of Pittsburgh, Pittsburgh, PA, [2]University of Pittsburgh, Pittsburgh, PA

Disclosures: All authors have disclosed no financial interests, arrangements or affiliations in the context of this activity.

Purpose or Case Report: Understanding anatomy and embryology is crucial for evaluation of olfactory epithelium, olfactory nerve, olfactory bulb and olfactory cortex pathology. We will discuss various imaging modalities available to evaluate olfactory system and discuss role of fMRI and Diffusion tensor imaging of olfactory system. Fetal MRI can identify olfactory bulb and olfactory sulci after 30weeks of gestation consistently and can be helpful in diagnosis of charge syndrome. Various congenital CNS malformations associated with olfactory system abnormalities like CHARGE, Holoprosencephaly, Kallmann syndrome, Acrocallosal syndrome, frontal encephalocele and sphenoidal encephalocele will be presented. Traumatic injury to cribriform plate of ethmoid can result in transection of olfactory nerve resulting in anosmia. Primary tumors of olfactory epithelium, esthesioneuroblastoma and secondary involvement of olfactory epithelim by rhabdomyosarcoma will be presented. Various tumors that can involve olfactory cortex namely DNET, ganglioglioma and pilocytic astrocytoma will be presented.References:Booth TN, Rollins NK. Spectrum of clinical and associated MR findings in children with olfactory anomalies. Am J Neuroradiol.2016; 37:1541-48Blustajn J, Krisch CFE, Panigrahy A, Netchine I. Olfactory anomalies in CHARGE syndrome: Imaging findings of a potential major

diagnostic criterion. Am J Neuroradiol.2008; 29:1266-69.

Poster #: EDU-074

Imaging Transcranial Doppler in the Pediatric Neurocritical Care Unit: Principles and Applications

Chen Yin, M.D., *chen.yin@phhs.org*; Cory Pfeifer, Rebekah Clarke; Radiology, University of Texas Southwestern Medical Center, Dallas, TX

Disclosures: All authors have disclosed no financial interests, arrangements or affiliations in the context of this activity.

Purpose or Case Report: There are 2 types of transcranial Doppler ultrasound. In the non-imaging technique, vessels are identified and interrogated based on sound, waveform, and sample depth, often using a transorbital window. The imaging technique involves the use of color Doppler to visualize the vessels themselves, commonly via a transtemporal window. Non-imaging transcranial doppler has long been used as diagnostic tool to assess for intracranial vasospasm in critically ill adults. Imaging transcranial Doppler is a common tool used in the surveillance of children with sickle cell anemia to evaluate for risk of stroke. This presentation describes the use of the imaging transcranial Doppler technique to monitor the intracranial circulation in critically ill children in neurocritical care setting.
Methods & Materials: A review of the limited available literature is performed. Indications for the exam are detailed. The technique used to acquire images and the protocol used are described. Velocities, direction of flow, and waveforms are discussed. The template used to report the results is reviewed. The relationship of the major vessels to the probe is depicted graphically. Recommendations in the use of this technique to determine brain death are noted.
Results: A 3V sector probe is used with transtemporal and transforaminal approach to interrogate the Circle of Willis including the middle cerebral artery, anterior cerebral artery, posterior cerebral artery, distal internal carotid artery, basilar artery and vertebral arteries. Mean velocities and pulsatility indices are recorded. Detection and evaluation of the hemodynamic effects of severe stenosis or occlusion of the extracranial (greater than or equal to 60% diameter reduction) and major basal intracranial arteries (greater than or equal to 50% diameter reduction) are possible. Transcranial Doppler has the advantage of providing real-time evaluation of cerebral vasculature without the use of contrast agents, ionizing radiation, or sedation.
Conclusions: Imaging transcranial Doppler can be a useful diagnostic aid in the approach to managing treatment in the pediatric neurocritical care unit.

Poster #: EDU-075

Ultrasonographic approach of neck masses in the pediatric population.

Mariangeles Medina Perez, MD, *medinapm@upstate.edu*; Saurabh Gupta, MBBS, Zain Badar, MD, Ninad Salastekar, MBBS, MPH, Anand Majmudar, MD; Radiology, SUNY Upstate Medical University, Syracuse, NY

Disclosures: All authors have disclosed no financial interests, arrangements or affiliations in the context of this activity.

Purpose or Case Report: Neck masses are commonly seen in the pediatric population and are a frequent reason for pediatric consults and can represent a diagnostic challenge. Although there is a broad spectrum of differentials, the vast majority of these lesions are benign, however malignant etiologies can also be encountered. Ultrasonography has become the first-line imaging modality in the evaluation of neck masses, given the ability to avoid radiation, wide availability and cost-effectiveness. Also, ultrasound represents an option when trying to avoid contrast administration or sedation.The main teaching points of this exhibit will be:1. Review variety of congenital and acquired neck masses in the pediatric patients.2. Discuss imaging features and approach to various vascular, congenital abnormalities, benign and malignant tumors and other acquired abnormalities with Ultrasound.3. Discuss the role of anatomic imaging in management.A case-based pictorial review will be used to demonstrate:1. Approach to vascular tumors and malformations based on clinical and imaging features including congenital, infantile hemangioma, low flow, various types of vascular malformations, locally aggressive lesions like kaposiform hemangioendothelioma, malignant tumors likely angiosarcoma and hemangioendothelioma.2. Reviewing salient features of various congenital and acquired abnormalities including branchial cleft cysts, thyroglossal duct cysts, congenital goiter and midline frontal masses.3. Discuss imaging features of other benign and malignant masses including teratomas, primary cervical neuroblastomas, soft tissue tumors (myofibroblastic), lipoblastoma. Also malignant tumors like fibrosarcoma, rhabdomyosarcoma.4. Describe masses which mimic tumors such as fibromatosis coli and ectopic thymus.5. Treatment and prognosis.

Poster #: EDU-076

When Poland Met Mobius: a Hyperlucent Hemithorax Should Prompt MRI of the Brain

Xiaozhou Liu, MD, *liaoliaojiao@gmail.com*; Akshita Mehta, MD, Cory Pfeifer; Radiology, University of Texas Southwestern, Coppell, TX

Disclosures: All authors have disclosed no financial interests, arrangements or affiliations in the context of this activity.

Purpose or Case Report: Poland Syndrome is a classic differential consideration for a unilateral hyperlucent hemithorax on chest radiograph due to pectoralis aplasia or hypoplasia. Additional associations include brachysyndactyly, simian crease, dextrocardia, and liver/biliary abnormalities. Isolated pectoral hypoplasia or aplasia without limb involvement is generally cosmetic and can be corrected with plastic surgery, but Mobius syndrome should be ruled out due to its association. Children with Mobius syndrome can exhibit an expressionless affect, excessive drooling, and/or eye paralysis due to cranial nerve deficiencies. This educational exhibit discusses the pediatric radiologist's role in the imaging approach to these supposedly separate diseases which may represent a continuum of one pathology.
Methods & Materials: The epidemiological, clinical, genetic, and imaging findings of both Poland syndrome and Mobius syndrome are described. A discussion of the appropriate protocol required to aid in the diagnosis of Mobius syndrome is included. Differential diagnoses are explored. Radiologic examples of additional associations such as morning glory syndrome and Pierre-Robin syndrome are also depicted.
Results: Poland syndrome can occur sporadically, but some familial associations have been observed. It is more common in males and more commonly affects the right side of the body. Mobius does not appear to exhibit a gender predominance. Like Poland syndrome, the disease commonly occurs sporadically, though associated genetic mutations have been characterized. Imaging findings include cranial nerve hypoplasia or aplasia. Due to the association between these diseases, the name Poland-Mobius syndrome is sometimes uses. In the child presenting with Poland syndrome, MRI of the brain with high resolution imaging of the cranial nerves is indicated.

Conclusions: Poland syndrome and Mobius syndrome, though both rare, can occur in tandem. The pediatric radiologist should be aware that the diagnosis of either disease should prompt assessment for the other. High resolution imaging of the cranial nerves is indicated when Poland syndrome is diagnosed.

Poster #: EDU-077

The Imaging Saga of Growth Disturbances in the Pediatric Population

Aayushi Rai, *aayushi.rai07@gmail.com*; Rachita Gupta, Medical Student, Bindu Setty, MD; Boston Medical Center, Boston, MA

Disclosures: All authors have disclosed no financial interests, arrangements or affiliations in the context of this activity.

Purpose or Case Report: The pituitary gland, the epicenter of various regulatory hormones, plays an unquestionably important role in determining timely growth and sexual maturation. Indeed, multiple studies have examined the role of Growth Hormone (GH) and Gonadotrophic Releasing Hormone (GnRH) in treating delayed and precocious puberty respectively.[1]Research has shown the importance of imaging the pituitary gland in patients with growth disturbances and/or documented endocrine abnormalities, in differentiating and classifying disorders based on etiology, prognosis and management.[2] Currently, data are limited in identifying a correlation between bone age abnormalities and pituitary findings via MRI, in children diagnosed with deviations in pubertal development. We present a comprehensive review of common structural abnormalities affecting the pituitary as seen on MRI – including developmental (dysgenesis/hypoplasia), traumatic, and neoplastic processes (both benign and malignant) – and how those pituitary lesions correlate with bone age and endocrine function in patients with growth failure and precocious puberty. Establishing a correlation between a patient's endocrine profile, bone age and pituitary morphology on MRI imaging can be extremely useful in the judicious management of patients, in terms of patient selection, early diagnosis and treatment. Moreover, our review aims to highlight the importance of imaging in the workup of patients with known or suspected growth disturbances, illustrated via concept maps. The concordance of endocrine abnormalities and clinical information (including age, sex and ethnicity demographics) with imaging data will also be reviewed to demonstrate various patterns of disease presentation and diagnosis.**References:**[1] Du X.F., Yang X.H., Li J., Hao M., Guo Y.H. Growth hormone co-treatment within a gnrh agonist long protocol improves implantation and pregnancy rates in patients undergoing IVF-ET. Arch. Gynecol. Obstet. 2016;294:877–883. doi: 10.1007/s00404-016-4163-1.[2] Di Iorgi N, Iorgi ND, Allegri AEM et al (2012) The use of neuroimaging for assessing disorders of pituitary development. Clin Endocrinol 76:161–176

Poster #: EDU-078: ***Withdrawn***

Poster #: EDU-079

The Many Faces of Brainstem Anomalies

Sean Creeden, MD, *creeden@stanford.edu*; Hisham M. Dahmoush, MD, Carolina Guimaraes, MD; Stanford University, Stanford, CA

Disclosures: All authors have disclosed no financial interests, arrangements or affiliations in the context of this activity.

Purpose or Case Report: Brainstem anomalies pose a diagnostic challenge for trainees to even the most advanced in their practice. Our exhibit aims to provide a comprehensive review of these rare disorders which are being diagnosed earlier and more frequently utilizing advanced imaging and genetic sequencing techniques. Representative images of these disorders with key distinguishing features will be presented. Familiarity with these conditions will benefit practicing radiologists, radiologists in training, and our clinical colleagues.
Methods & Materials: A diagnostic imaging approach to brainstem anomalies using high quality representative images with emphasis on MRI, including fetal MRI, will be presented.
Results: 1) Review the appropriate stages of brainstem development.2) Highlight a number of cases demonstrating brainstem anomalies including tubulinopathies, dystroglycanopathies, ciliopathies, cri-du-chat syndrome, pontocerebellar hypoplasia, Aicardi-Goutieres syndrome, patterning defects, pontine tegmental cap dysplasia and other rare disorders.3) Provide key distinguishing imaging features for these malformations.
Conclusions: This review aims at familiarizing radiologists with complex and challenging cases of brainstem maldevelopment from in-utero to post-natal presentation. Early and accurate diagnosis are key to meaningful outcomes and future planning. It is important for neuroradiologists and pediatric radiologists alike to retain a wide range of differential diagnoses thus providing diagnostic confidence when potential future cases are encountered.

Poster #: EDU-080

Imaging of Conductive Hearing Loss in Children: A Pictorial Review

Diana Rodriguez, MD,*dprodrigu@gmail.com*; Nationwide Children's Hospital, Columbus, OH

Disclosures: All authors have disclosed no financial interests, arrangements or affiliations in the context of this activity.

Purpose or Case Report: To review the embryology and anatomy of the temporal bone, with emphasis in the external and middle ear.To describe the imaging findings of common and rare pathology of conductive hearing loss within the pediatric population.
Methods & Materials: We retrospectively reviewed CT and MR examinations between Jan 2010 and Oct 2018 of patients undergoing imaging for evaluation of conductive hearing loss. We identified subjects with normal temporal bones, as well as subjects with various pathology causing conductive hearing loss.
Results: Normal anatomy of the external and middle ear. Diverse pathology of the external and middle ear was encountered.Cases were categorized into the following groups:A. Congenital: External auditory canal atresia, oval window atresia, congenital ossicular anomalies and fixation, congenital cholesteatoma, fenestral otosclerosis, persistent stapedial artery, fibrous displasia, and osteopetrosis.B. Acquired: External auditory canal exostosis, otitis externa, otitis media, cholesteatoma, trauma, and neoplasm such as Langerhans Cell Histiocytosis.
Conclusions: We have demonstrated the normal anatomy of the temporal bone, with emphasis in the external and middle ear, as well as pertinent imaging findings of both common and more rare causes of conductive hearing loss in children.

Poster #: EDU-081

Pictorial Review of Pitfalls in SPECT-CT I-123 MIBG Imaging of Neuroblastoma

Lillian Lai, MD, *lmlai@chla.usc.edu*; Rachel Berkovich, Fariba Goodarzian; Children's Hospital Los Angeles, Los Angeles, CA

Disclosures: All authors have disclosed no financial interests, arrangements or affiliations in the context of this activity.

Purpose or Case Report: The purpose of this exhibit is explore pitfalls in our experience with SPECT-CT Iodine-123 (I-123) MIBG imaging in patients with neuroblastoma. SPECT-CT can more specifically localize areas of uptake over planar imaging and mitigate false-positive results with correlative anatomic information. We will review cases of false-positive MIBG uptake in nonmalignant sites, cases of false-negative MIBG uptake in neuroblastoma/neural crest tumors, and cases of secondary tumors/malignancies occurring in the setting of known neuroblastoma, with variable uptake on MIBG.
Methods & Materials: Pictorial, retrospective review of key false positive and false negative cases of I-123 MIBG uptake in neuroblastoma imaging.-Review of normal MIBG uptake and excretion-Significance of SPECT positive but planar negative findings on Curie score-Imaging artifacts (misalignment/mis-coregistration, etc.)-Physiologic cases of false positive increased uptake in benign/non-malignant sites (glomerulonephritis/pyelonephritis, renal vein thrombosis, remaining unilateral adrenal gland, brown fat, thyroid gland, skeletal muscles, lungs, liver. Additional false positive uptakes localizing to previously treated neuroblastoma and representing post-surgical changes.-Explore false negative MIBG uptake in neuroblastoma or neural crest tumors (i.e. ganglioneuroma and metastatic neuroblastoma liver lesions showing little to no uptake.) *Key Point:* Non-MIBG avid neuroblastoma may require troubleshooting with 18F-DOPA or 18F-FDG PET-CT.-Review cases of secondary tumors/malignancies occurring in the setting neuroblastoma, with variable uptake on MIBG (Increased MIBG uptake in renal cell carcinoma and medullary thyroid carcinoma; no MIBG uptake in myofibroma of the jaw and a mucoepidermoid salivary gland tumor.) *Key Point:* Suggest further dedicated imaging and correlation with tissue sampling if a lesion is suspected clinically.
Results: A pictorial review of false positive and false negative cases at SPECT-CT I-123 MIBG imaging of neuroblastoma patients will be discussed. SPECT-CT may help localize areas of uptake and minimize false-positive results.
Conclusions: Recognizing pitfalls during SPECT-CT I-123 MIBG imaging of neuroblastoma patients will help radiologists correctly interpret findings and help guide proper treatment and management.

Poster #: EDU-082

All that's hot is not malignant: A review of non-malignant pathology on pediatric PET/MRI

Akash Patel, M.D., *patela22@email.chop.edu*; Lisa States; Children's Hospital of Philadelphia, Philadelphia, PA

Disclosures: All authors have disclosed no financial interests, arrangements or affiliations in the context of this activity.

Purpose or Case Report: With the increased demand and utilization of PET/MRI in oncologic imaging, there is an ever increasing database of non-malignant pathology that has not yet been described on PET/MRI. Furthermore, the pediatric population provides an even more unique breadth of pathology that is often only seen in this age group. It is important to be able to accurately identify these common pathologies so as to not mistake them for malignancy and to prevent unnecessary follow up imaging studies and further invasive diagnostic procedures.For this educational exhibit we review over 200 clinical pediatric 18F-FDG PET/MRs performed at our institution and highlight the most common and most interesting cases of FDG-avid non-malignant pathology.Listed below are some of the cases to be included in the poster:-Benign FDG avid bone tumors including non-ossifying fibromas-Benign causes of FDG avid lymphadenopathy including cat scratch disease-Benign causes of FDG avid lung lesions including aspiration pneumonia-Benign causes of gastro-intestinal FDG uptake including pseudomembranous colitis-Benign FDG avid infectious pathologies including a liver abscess

Poster #: EDU-083

Imaging of Post-Transplant Lymphoproliferative Disease and its Complications

Alexis B. Maddocks, MD, *ar3684@cumc.columbia.edu*; Edward P. Fenlon, MD, Susie Chen, MD, Carrie Ruzal-Shapiro, MD, Diego Jaramillo, MD MPH; Columbia University Medical Center-Morgan Stanley Children's Hospital, New York, NY

Disclosures: All authors have disclosed no financial interests, arrangements or affiliations in the context of this activity.

Purpose or Case Report: Post-Transplant Lymphoproliferative Disease (PTLD) is a polyclonal and monoclonal lymphoid proliferation which occurs in 1-20% of solid organ transplant recipients. It is most common in multivisceral organ transplants followed by small bowel transplants, heart and lung transplants and less commonly in liver and kidney transplants. PTLD has a bimodal distribution of occurrence with the largest peak occurring within 1 year after transplantation and a second peak at approximately 4-5 years after transplantation. The Epstein Barr virus (EBV) is associated in 50-70% of cases. EBV seronegativity in the recipient at the time of transplant predicts a 2-4 times increased risk of PTLD especially if they receive a donor organ which is positive for EBV. This may explain the higher incidence in the pediatric population who tend to be seronegative for EBV. The World Health Organization (WHO) identifies four pathologic categories of PTLD: early lesions, polymorphic type, monomorphic type and classic Hodgkins lymphoma. The majority of PTLD cases are caused by B-lymphocyte proliferation in a T-cell depleted environment in the setting of immunosuppression. However, there is a subset of cases that are caused by T-cell or natural killer cells as well as cases that occur in the setting of negative EBV. Multiple clones of proliferating B-cells can be seen in a single patient. 2/3 of cases have diffuse expression of CD20 which is an important target for therapy.PTLD may be focal or diffuse and can manifest in a variety of different organ systems or even in the allograft itself. There is a higher percentage of extranodal disease in PTLD as compared to immunocompetent patients with lymphoma. The GI tract and liver are most commonly involved. Isolated lymph node involvement in comparison is less common in patients with PTLD. Central nervous system (CNS) involvement is relatively rare in PTLD.This educational exhibit will provide a pictorial review of PTLD and illustrates cases from one of the busiest transplant centers in North America to highlight the major imaging findings as well as complications seen on imaging of this disease. Extranodal and nodal disease will be demonstrated on multiple modalities as well as complications of this disease including intussusception and biliary obstruction. CNS disease will also be shown. The clinical manifestations, imaging characteristics, prognosis and treatment will be discussed and depicted.

Poster #: EDU-084

Pediatric Oncologic Emergencies: Recent Updates in Pediatrics that the Radiologist Needs to Know

Atsuhiko Handa[1], *atsuhiko-handa@uiowa.edu*; Taiki Nozaki[2;] [1]Radiology, University of Iowa, Iowa City, IA, [2]St Luke's International Hospital, Tokyo, Japan

Disclosures: All authors have disclosed no financial interests, arrangements or affiliations in the context of this activity.

Purpose or Case Report: Children with cancer are at increased risk of life-threatening emergencies, either from cancer itself or related to cancer treatment. These conditions need to be assessed and treated as early as possible to minimize their morbidity and mortality. Cardiothoracic emergencies encompass a variety of pathologies, including (1) pericardial effusions and cardiac tamponade, (2) massive hemoptysis, (3) superior vena cava syndrome, (4) pulmonary embolism, and (5) pneumonia. Abdominal emergencies include (6) bowel obstruction, (7) intussusception, (8) perforation and tumor rupture, (9) intestinal graft-versus-host disease, (10) acute pancreatitis, (11) neutropenic colitis, and (12) obstructive uropathy. Radiological imaging plays a vital role in the diagnosis of these emergencies. Although imaging features have been described in most of these conditions, recent advancement in clinical pediatrics is fast-paced. In this educational exhibit, we aim to review the clinical and imaging features of pediatric oncologic emergencies including a review of the recently published literature. Key radiological images are presented to highlight the radiological approach to the diagnosis. Pediatricians, pediatric surgeons, and pediatric radiologists need to work together to arrive at the correct diagnosis and to ensure prompt and appropriate treatment strategies.

Poster #: EDU-085

An Updated Approach to Pediatric Abdominal Tumors

LeAnn M. Shannon, MD, *leann.m.shannon@vumc.org*; Sudha Singh, MD; Radiology, Vanderbilt University Medical Center, Mount Juliet, TN

Disclosures: All authors have disclosed no financial interests, arrangements or affiliations in the context of this activity.

Purpose or Case Report: With research pushing ever onward, it is often difficult to keep pace with the dynamic landscape of pediatric abdominal tumors and their classification systems. However, it is imperative that we, as radiologists, remain vigilant of these changes, as our initial and follow-up imaging assessments often have the potential to drive clinical intervention in widely differing directions.In this educational poster, we will review the most up-to-date risk stratification and staging criteria for neuroblastoma, hepatoblastoma, and Wilms tumor in order to:1. Educate about the most recent criteria for categorizing pediatric abdominal tumors such as neuroblastoma, hepatoblastoma, and Wilms tumor.2. Provide imaging examples of these pediatric abdominal tumors and describe how the above-mentioned criteria might change radiology reports and patient management.3. Encourage accurate risk stratification of these tumors so that radiologists are better equipped to assist in directing appropriate patient care.

Poster #: EDU-086

Breaking Ondine's Curse: The Pediatric Radiologist's Role in Congenital Central Hypoventilation Syndrome

Elisabeth Moredock[2], *Elisabeth.Moredock@BSWHealth.org*; J. M. Fulmer, MD[2], Michael Collard, MD[1], Cory M. Pfeifer, MD[1]; [1]Diagnostic Radiology, University of Texas Southwestern Medical Center, Dallas, TX, [2]Baylor University Medical Center, Dallas, TX

Disclosures: All authors have disclosed no financial interests, arrangements or affiliations in the context of this activity.

Purpose or Case Report: Congenital Central Hypoventilation Syndrome (CCHS) is a rare disorder that can cause respiratory arrest during sleep. It is sometimes referred to as "Ondine's Curse" in reference to a fictional character who had to remember to breathe based on a spell cast by a jilted lover. The number of cases has been reported to be near 1,000. The purpose of this educational exhibit is to describe CCHS and emphasize its implications for pediatric radiology.
Methods & Materials: The molecular basis and incidence of CCHS are described. Neoplastic associations and additional abnormalities are emphasized. The effects on multiple organ systems are discussed.
Results: CCHS is caused by a mutation in PHOX2B. The product of this gene is found in neural crest cells and promotes neuron formation and differentiation. Most cases of CCHS occur from spontaneous mutation, but the disease can be inherited in an autosomal dominant fashion. Due to its neural crest involvement, CCHS predisposes patients to neuroblastoma which prompts regular screening by oncologists. Likewise, neural developmental failure can result in Hirschsprung disease requiring barium enema for evaluation. Patients often have a short wide face. Treatment sometimes involves the use of a diaphragmatic pacer which may be unfamiliar to radiologists.
Conclusions: CCHS is rare, but the diagnosis prompts screening for neuroblastoma which is more common in this disease. Barium enema is indicated early in life to exclude Hirschsprung disease.

Poster #: EDU-087

Dicey DNA: DICER1 Syndrome and its Implications for Pediatric Radiologists

Jay R. Coleman, MD, *jay.coleman@phhs.org*; Michael Collard, MD, Cory M. Pfeifer, MD; Diagnostic Radiology, University of Texas Southwestern Medical Center, Dallas, TX

Disclosures: All authors have disclosed no financial interests, arrangements or affiliations in the context of this activity.

Purpose or Case Report: Molecular biology has come to the forefront of modern oncology. Knowledge of specific genetic mutations within tumors drives prognostic information and can guide therapy. Keeping up with new terminology in oncology can be difficult for pediatric radiologists who often host oncology conferences and present regularly at grand rounds. The purpose of this educational exhibit is to describe DICER1 syndrome and discuss its implications for pediatric radiology.
Methods & Materials: Basic information regarding the molecular basis for tumor promotion is presented. The DICER1 gene and its product are described. Neoplastic associations with DICER1 are emphasized. The effects on multiple organ systems are discussed.
Results: The DICER1 gene encodes a protein that controls production of micro RNA molecules (miRNA). miRNA serves a regulatory role in gene expression by binding messenger RNA (mRNA). Messenger RNA is the intermediary between the

genetic information encoded by DNA and the proteins and enzymes that eventually produce phenotypes. The DICER1 product thus serves as a policeman of sorts, and common DICER1 mutations result in a dysfunction and loss of regulation which increases the likelihood that a neoplastic process will ensue. Most individuals with a DICER1 mutation do not develop cancer, but the risk is increased. Pleuropulmonary blastoma is a primary concern in DICER1 syndrome. Cystic nephroma is also a common association. Sertoli-Leydig cell tumors and multinodular goiter are seen in patients with DICER1syndrome. Pineoblastoma and pituitary blastoma are seen with specific DICER1 abnormalities.
Conclusions: DICER1 syndrome is a cancer predisposition condition that can affect multiple organ systems. Understanding the function of this gene is essential to appreciating its associated disease processes.

Poster #: EDU-088

PET/MR of pediatric bone tumors: What the radiologist needs to know

Crystal R. Farrell, MD, *cfarrell@stanford.edu*; Anuj Pareek, MD, Anne M. Muehe, MD, Allison Pribnow, MD, Robert Steffner, MD, Raffi S. Avedian, MD, Heike E. Daldrup-Link, MD, PhD; Stanford University, Palo Alto, CA

Disclosures: All authors have disclosed no financial interests, arrangements or affiliations in the context of this activity.

Purpose or Case Report: PET/MR is a valuable and growing imaging method for the assessment and management of pediatric bone tumors. Although plain radiography remains the first line modality for initial evaluation, cross sectional imaging is often required for further characterization of indeterminate or aggressive appearing lesions. Due to its superior soft tissue contrast resolution compared to CT, MR has become the mainstay in tissue characterization, locoregional staging, and surgical planning of pediatric bone tumors. By adding functional and metabolic information, FDG-PET imaging is useful for “one stop” local tumor and whole-body staging, evaluating response to therapy and surveillance. 18F-FDG PET/MR scans have the benefit of lower radiation and increased patient convenience compared to 18F-FDG PET/CT scans. However, due to the relatively recent development of this technology, many radiologists may be unfamiliar with the technical considerations and interpretation pearls and pitfalls of PET/MR. This educational exhibit reviews the imaging technique, reporting requirements, and imaging characteristics of the most common pediatric bone tumors with 18F-FDG PET/MR.
Methods & Materials: We conducted a comprehensive literature search on 18F-FDG PET/MR of pediatric bone tumors and have included the most current evidence-based information for review. We also present our institutional approach and experience with performing 18F-FDG PET/MR scans of pediatric bone tumors.
Results: We describe the imaging technique and reporting criteria for conducting 18F-FDG PET/MR scans of bone tumors in children and young adults. We review the epidemiology, pathology, 18F-FDG PET/MR imaging characteristics, and treatment monitoring approaches for the most common pediatric bone tumors, including osteosarcoma, Ewing sarcoma, primary bone lymphoma, bone and bone marrow metastases, and Langerhans cell histiocytosis. We also discuss various potential “false positive” bone lesions, and some important similarities and differences between 18F-FDG PET/MR and 18F-FDG PET/CT. Finally, we provide insight into the future directions and developments of this new technology.
Conclusions: Familiarity with 18F-FDG PET/MR in the evaluation of pediatric bone tumors is of growing importance. This review covers the 18F-FDG PET/MR imaging features of the most common pediatric bone tumors, as well as technical considerations, reporting methods, and future possibilities for performing “one stop” 18F-FDG PET/MR cancer staging of children and young adults.

Poster #: EDU-089

PET/CT Evaluation of Pediatric Lymphoma: A Classification System Review

James Leake, MD, *jim.leake@u.northwestern.edu*; Cory Pfeifer; Radiology, UT Southwestern, Dallas, TX

Disclosures: All authors have disclosed no financial interests, arrangements or affiliations in the context of this activity.

Purpose or Case Report: Lymphoma (including both Hodgkin’s and non-Hodgkin’s) is the third most common pediatric malignancy. Treatment requires distinct definitions of bulky disease, response to therapy, and organ involvement. In this way, pediatric radiologists form a center role in the medical care of affected children. This educational exhibit examines pediatric lymphoma diagnosis and response to therapy by detailing the varying classification systems, including the newer PET-related Deauville and Lugano classification systems.The Ann Arbor staging classification system for Hodgkin’s lymphoma was initially developed in the 1970’s and anatomically classifies lymphoma by site and number of lymph nodes affected, cross-diaphragmatic disease, and extralymphatic organ dissemination. More recently, after the introduction of PET/CT, newer classification systems which incorporated tumor metabolism were developed - including Deauville and Lugano. Notably, these systems are commonly applied to both Hodgkin’s and non-Hodgkin’s lymphoma. This educational exhibit includes a discussion of these various systems as well as annotated examples. Additionally, risk stratification is discussed using strata defined by the Children’s Oncology Group (COG), EuroNet, and Pediatric Hodgkin Consortium.After review, the pediatric radiologist should feel more comfortable staging and classifying response to treatment of lymphoma using PET assessment principles.

Poster #: EDU-090

Childhood Interstitial (Diffuse) Lung Disease: A Pattern Recognition Approach to Diagnosis in Infants

Teresa Liang, MD BSc, *teresaliang86@gmail.com*; Edward Lee, MD, MPH; Boston Children's Hospital, Boston, MA

Disclosures: All authors have disclosed no financial interests, arrangements or affiliations in the context of this activity.

Purpose or Case Report: Childhood interstitial (diffuse) lung disease (chILD) in infants consists of a rare and heterogeneous group of disorders previously classified with clinical, radiologic, and pathologic features. The purpose of this article is to discuss imaging techniques and provide a pattern-based approach for chILD in infants.
Methods & Materials: 1. Review the current American Thoracic Society (ATS) guidelines for diagnosis and classification of chILD2. Discuss the utility and limitations of imaging modalities including radiographs, CT and MRI for diagnosis and follow up of chILD in infants3. Review a CT pattern-based approach with imaging examples for chILD in infants

Results: After reviewing the exhibit, the reader will be aware of the spectrum of chILD in infants, and be able to use the discussed imaging based algorithm to assist in efficient and accurate diagnosis of various chILD entities in the infant population.
Conclusions: chILD in infants constitutes a diverse group of lung abnormalities which can be complex and challenging to diagnose. Aside from the infants with diffuse development disorders, whom typically are only imaged with chest radiographs, the remainder of the diseases in the chILD spectrum presenting in infants can be approached with a CT algorithm utilizing the stepwise assessment of lung volumes, ground glass, and cysts. In conjunction with the patient's demographics and clinical presentation, this algorithm can aid the radiologist in making an accurate and timely diagnosis.

Poster #: EDU-091

Standardization of Postnatal CT Imaging and Interpretation of Bronchopulmonary Malformations (BPM)

Beverley Newman, MD,*bev.newman@stanford.edu*; Stanford University, Stanford, CA

Disclosures: All authors have disclosed no financial interests, arrangements or affiliations in the context of this activity.

Purpose or Case Report: BPM's are often identified prenatally; while some have more detailed imaging and description, many are loosely called congenital pulmonary airway malformations (CPAM). A chest radiograph is usually obtained at birth, but CT imaging is often deferred until 3-6months of age in asymptomatic babies, when surgical removal is being considered. Participation in a presurgical conference has indicated that there is poor standardization of both performance and interpretation of CT for BPM's. High quality studies are most often hampered by poor timing of imaging, poor vascular opacification and obscuration of pathology due to atelectasis. There are four key internal feature of BPM's that help with lesion characterization, differential diagnosis and management decisions. These include: systemic arterial supply; bronchial mucoid impaction; overinflated lung and macroscopic cysts. Reliable recognition and description of these features in all cases is essential for guiding surgical decisions since some lesions can be treated conservatively, especially those with just hyperinflation and mucoid impaction. A feature that tends to be overlooked is mucoid impaction, indicative of bronchial atresia. Cystic changes and overinflated lung may be mischaracterized. Small systemic arteries can be missed. Multiplanar reconstructions and interaction with maximum intensity projections and a 3D dataset are very helpful. This poster aims to educate by providing multiple illustrative imaging examples and a standardized report template useful for radiologists, clinicians, research and registries.

Poster #: EDU-092

There is MAGEC going on in Ultrasound

Amy Winer,*amy.weiner@cchmc.org*; Ultrasound, Cincinnati Children's Hospital, Cincinnati, OH

Disclosures: All authors have disclosed no financial interests, arrangements or affiliations in the context of this activity.

Purpose or Case Report: 1.To identify what are MAGEC rods and how ultrasound is utilized in the lengthening procedure to reduce the number of x-rays that they are exposed to.2. To describe the use of Ultrasound to aid with lengthening the MAGEC rods in Scoliosis patients.3. Decscribe the pros and cons of Ultrasound use.

Methods & Materials: Scoliosis is a sideways bending or curvature of the spine. At times, surgical intervention is required to help correct or stop the curvature from getting worse. By using the MAGEC rods, this can reduce the number of surgeries and radiation from xrays that a patient is exposed to.Ultrasound is used to help measure the growth of the growing rods at each lengthening and reduce the number of xrays that the patient is getting. In this poster, I will discuss the procedure of performing an lengthening of the MAGEC rods and the benefits and downfalls of ultrasound.
Results: What is scoliosisTreatment of scoliosisMAGEC rods-what is it?How do they workAnatomy of the rodsUsing Ultrasound as a measuremen toolBenefit of Ultrasound usageDownfalls of Ultrasound usage
Conclusions: Using Ultrasound to help with the lengthening MAGEC rods can save a patient from the exposure or xrays along with reducing the number of surgeries that a patient will need in their lifetime.

Poster #: EDU-093

The Pediatric Breast: When to Worry

Rimpi Saini, MD[1], *Rimpi.Saini26@gmail.com*; Joshua D. Wermers, DO[1], Shelby Larson[1], Grace Mitchell, MD[2], Amy Patel, MD[1]; [1]Radiology, University of Missouri Kansas City, Kansas City, MO, [2]Children's Mercy Hospital, Kansas City, MO

Disclosures: All authors have disclosed no financial interests, arrangements or affiliations in the context of this activity.

Purpose or Case Report: With an incidence of 3.25%, breast masses in the pediatric population are a relatively rare phenomenon. Despite this, breast masses are a substantial source of anxiety and concern for parents and patients alike, largely due to the increased awareness of breast cancer in the adult population. Fortunately, the vast majority of masses are benign, and pediatric breast malignancies constitute less than 1% of all pediatric malignancies. Moreover, malignancy tends to be secondary to metastatic disease from lymphoma, leukemia, or rhabdomyosarcoma, as primary breast carcinoma is exceedingly rare. Although initial sonographic characteristics of breast masses may be nonspecific, recommendation for further evaluation with biopsy and/or excision of the mass is usually not recommended due to the rarity of malignancy, and avoidance of disrupting immature breast parenchymal tissue. In adults, the Breast Imaging-Reporting and Data System classification is quite accurate for dictating management recommendations. However, this system grossly over-emphasizes the risk of malignancy in pediatric patients, as imaging findings are usually discordant with histology. Currently, there are no standardized guidelines for management recommendations of pediatric breast masses, and short-term follow-up ultrasound is usually recommended to evaluate for malignant potential. The purpose of this educational exhibit is to compare the sonographic abnormalities of breast pathologies arising from normal breast development, including but not limited to gynecomastia, mastitis, and abscesses, from those arising from neoplastic processes including fibroadenomas, hemangiomas, arterio-venous malformations, and phyllodes tumors. In addition, the current literature on management recommendations, including indications for MRI and biopsy/excision of breast masses, will be reviewed. Finally, this exhibit will discuss the important role pediatric radiologists play in understanding the epidemiology and natural history of breast pathologies, enabling accurate characterization of masses and appropriate treatment recommendations to further guide patient management.

Poster #: EDU-094

Imaging Findings in Pleuropulmonary Blastoma and the DICER1 Mutation

Rosario Carrasco, MD, *rcarrasco@wustl.edu*; Rebecca Hulett-Bowling, MD; Pediatric Radiology, St. Louis Children's Hospital, St. Louis, MO

Disclosures: All authors have disclosed no financial interests, arrangements or affiliations in the context of this activity.

Purpose or Case Report: Pleuropulmonary blastoma (PPB) is a rare, intrathoracic, malignant tumor in the pediatric population with approximately 500 cases reported worldwide. Over 90% of these cases are in patients below the age of 6. The spectral morphology of PPB is used to classify the lesions along a continuum from the least malignant to the most malignant: type I (cystic) 14%, type II (solid and cystic) 48%, and type III (solid) 38%. Congenital lung cysts are not known to degenerate to become PPB, but the cystic type I PPB may progress to the more aggressive type II or type III PPB. In addition, PPB is associated with cystic nephroma in 30% of cases, and has been linked to the DICER1 mutation which puts these patients at risk for other tumors. For example, the genetic basis of the PPB familial syndrome (which is the heterozygous loss of function mutation of DICER1) includes PPB, cystic nephroma, ovarian Sertoli-Leydig cell tumors, ciliary body medulloepithelioma, nodular hyperplasia and differentiated carcinoma of the thyroid gland, pituitary blastoma, pineoblastoma, nasal chondromesenchymal hamartoma, and cervical embryonal rhabdomyosarcoma.The purpose of this educational report is to demonstrate various presentations and identify distinguishing features of each type of PPB as seen on initial radiographs with correlation on subsequent CT scans. Only cases where the PPB and type were confirmed by pathology are included. At least one case of the PPB familial syndrome will also be presented. Positive DICER1 mutations will be provided when available, as this information is increasingly used to aid in the treatment decisions. Early recognition of PPB with timely investigation for cystic nephroma and DICER1 mutations can lead to improved patient outcomes.

Poster #: EDU-095

TB or not TB: The Pediatric Radiologist's Role in Diagnosing Mycobacterial Infections

Ali Alian, M.D., *afaramar@gmail.com*; Cory Pfeifer; University of Texas Southwestern Medical Center, Dallas, TX

Disclosures: All authors have disclosed no financial interests, arrangements or affiliations in the context of this activity.

Purpose or Case Report: In 2017, children under the age of 15 accounted for only 10% of the 10 million Mycobacterium tuberculosis (TB) infections estimated by the World Health Organization. Child carriers of TB pose health risks to their adult caregivers, and children can exhibit greater susceptibility to significant health risks from the infection. Nontuberculous mycobacterial (NTM) infection presents disparate health risks and can generate imaging specific findings. This presentation addresses radiologic manifestations of mycobacterial disease as a means to educate pediatric radiologists given the medical significance of mycobacterial infection.
Methods & Materials: This exhibit will discuss how children may manifest TB infections differently than adults and describe imaging findings of pulmonary and extra-thoracic TB infection in children. Contrasting findings in multi-system NTM infection will also be detailed. The presentation will provide radiologic manifestations of verified mycobacterial infection and emphasize unique characteristics of mycobacterial infection.
Results: Pulmonary TB in children may present with diffuse pulmonary disease and/or pleural effusions that can appear more impressive than the clinical presentation seemingly suggests. Extra-pulmonary TB can cause brain abscesses, osteomyelitis, and intra-abdominal infection which have distinct appearances compared to typical bacterial infections. Pathogenic NTM organisms include Mycobacterium avium-intracellulare, Mycobacterium kansasii, Mycobacterium xenopi, Mycobacterium fortuitum, and Mycobacterium chelonae. MTB commonly infect the soft tissues and cervical lymph nodes as well as the lungs. The radiologic and clinical presentation of mycobacterial infection often depends on the immune status of the child. Mycobacterial recovery is often complicated by inability to obtain a sufficient biologic specimen and lack of growth on routine contrast media. For this reason, pediatric radiologists play a key role in raising appropriate management-guiding concerns for disease.
Conclusions: Mycobacterial infection can present differently in children. Radiographic findings suggestive of pediatric TB should prompt testing in relevant contacts.

Poster #: EDU-096

Big bubbles, little bubbles, bubbles everywhere: A review of macro and microcystic lymphatic malformations in less common anatomical locations.

Marian Gaballah, D.O., *mgaballah@northwell.edu*; Rachelle Goldfisher, MD; Zucker School of Medicine at Hofstra/Northwell, New Hyde Park, NY

Disclosures: All authors have disclosed no financial interests, arrangements or affiliations in the context of this activity.

Purpose or Case Report: Lymphatic malformations (LMs) are low-flow vascular malformations which are composed of dilated lymphatic channels, forming septated cyst-like structures (2). LMs are the second most common type of vascular malformation, second to venous malformations (1). The most common locations are in the neck, followed by the axillary region. On MRI, LMs are multiloculated, T2 hyperintense lesions, which may have fluid-fluid levels, and are without flow voids (1, 2). They can involve multiple tissue planes and do not regard anatomical and fascial boundaries (2). Cystic lymphatic malformations are further divided into microcystic, macrocystic, or mixed, based on the size of their cystic components. Macrocystic LMs are composed of larger cysts, while microcystic LMs are composed of smaller cysts and may appear solid on imaging.We present ten cases of microcystic, macrocystic, and mixed lymphatic malformations in a variety of anatomical locations. In addition to demonstrating the imaging findings, we present a review of the literature in regards to each anatomical region. Lymphatic malformations in this presentation include right orbit (n=1), mediastinum (n=2), pulmonary bronchovascular bundles/pleural space (n=1), retroperitoneum (n=1), mesentery (n=2), perirectal and scrotal (n=1), lower extremity (n=2). 6 of these children also had additional sites of T2 hyperintense disease involving the bones or spleen, suggestive of additional lymphangiomas.This presentation summarizes ten cases of lymphatic malformations in a variety of less common anatomical locations and a review of the pertinent literature.**References:**1. Flors L, Leiva-Salinas C, Maged IM et al. (2011) MR Imaging of Soft-Tissue Vascular Malformations: Diagnosis, Classification, and Therapy Follow-up. Radiographics 31:1321-1340.2. White CL, Olivieri B, Restrepo R et al. (2016) Low-flow vascular malformation pitfalls: from clinical examination to practical imaging evaluation- part 1, lymphatic malformation mimickers. AJR 206: 940 – 951.

Poster #: SCI-001

Pediatric Dose Evaluation of 4D Dynamic CT Protocol

Mohammed H. Aljallad, PhD,
mohammed.aljallad1@yahoo.com; Brian S. Dunoski, MD; Children's Mercy Hospital, Kansas City, KS

Disclosures: All authors have disclosed no financial interests, arrangements or affiliations in the context of this activity.

Purpose or Case Report: Balancing PEEP settings in mechanically ventilated premature infants to maximize air exchange while minimizing barotrauma is typically evaluated using bronchography. A 4D dynamic airway computerized tomography protocol (4D CT) was developed as a less invasive method to evaluate large and small airways collapse at variable PEEP settings. Our purpose was to evaluate the radiation dose from 4D CT and to demonstrate the number of cycles impact on the radiation dose.
Methods & Materials: 39 pediatric patients <5 years who underwent imaging as part of routine clinical care between 1/1/16-10/1/18. Dynamic sequential CT scan was performed on Siemens Flash, fixed 70 kVp, fixed 10 mAs. One 4D CT imaging cycle was defined as the time required for one full inspiratory-expiratory cycle at a given PEEP, which ranged between 2-8 seconds. Each cycle contained 7 rotations. The body and skin effective radiation doses were estimated using two methods: (1) the body effective dose is calculated using Monte Carlo simulations of a library of male and female anthropomorphic size and age-specific phantoms. (2) NanoDots optically stimulated luminescent dosimeters were used to measure the peak skin dose (PSD) by placing them on the chest of a newborn phantom for a different number of cycles.
Results: Increasing the number of cycle/rotations increased the PSD, dose length product (DLP), effective dose, and the lung organ dose. The estimated effective dose varied depending on the patient's DLP value, patient's gender, and age weighting factors. The average effective dose was higher for female patients. From the simulation's results, the highest organ dose was received by the lungs. The average value for lung dose was 0.9 mSv.
Conclusions: Irradiation over the same anatomic region by 4D CT results in accumulation of radiation dose and raising the concern for the potential deterministic effect of skin injury. The maximum measured entrance skin exposure by the 4D CT was orders of magnitude lower than the threshold dose for early transient erythema (2000 mGy). As the PSD increased by increasing the number of rotations, reducing the number of imaging cycles may reduce the overall patient radiation exposure. A differential effective dose in female patients is due to higher end-organ risk from radiation scatter. Extra caution to limit cycles should be exercised when using 4D CT technique in children under 1 year. In addition, DLP would be a better dose metric than CTDI because of DLP metric account for the total irradiated area.

Poster #: SCI-002

Delayed Phase Imaging in Pediatric Trauma: A review of the literature and experience in a Level I Trauma Center

Zachary E. Stewart, MD[1], *zestewart90@gmail.com*; Kate Elmore[2], Allison Thompson, MD[1], Huy Pham[1]; [1]Diagnostic Radiology, Memorial Health University Medical Center, Savannah, GA, [2]Mercer University School of Medicine, Savannah, GA

Disclosures: All authors have disclosed no financial interests, arrangements or affiliations in the context of this activity.

Purpose or Case Report: Delayed phase imaging increases the sensitivity of detection of injuries to the urinary tract and also assists in characterizing solid visceral organ injuries at the expense of doubling the radiation dose to the patient. If institutions can lower the rate of these examinations, the cumulative radiation exposure reduction would be substantial. Here we evaluate the rate of delayed phase imaging in the pediatric trauma population at our Level I trauma center as well as the frequency with which these patients demonstrate an indication on portal venous imaging for delayed phase acquisition. Finally, there are minimal guidelines dictating the appropriateness of delayed imaging in pediatric trauma. We include a review of the literature in order to elucidate appropriate indications and help guide clinicians to make evidenced based decisions.
Methods & Materials: A retrospective chart review was performed analyzing data of pediatric (0-18 years) trauma activations at our institution with a CT chest/abdomen/pelvis, between January 1 2016-January 1 2018. The primary variable analyzed was acqusition of delayed imaging. Indications for delayed imaging on portal venous phase imaging, including solid organ injury, pelvic fracture, and free fluid, were also reviewed. Given the potential for physiologic free fluid in post-pubescent girls, data was also analyzed excluding free fluid as an indication in girls older than 12 years old.
Results: 134 patients met the inclusion criteria. Delayed imaging was acquired in the majority of patients (91%, n=122). There was a near even split for presence/abscence of an indication for delayed imaging on the portal venous phase imaging. There was no statistical correlation with an indication for delayed imaging and the acquisition of delayed imaging ($p=0.475$). When accounting for each indication independently, there was no statistical correlation between a specific indication and acquisition of delayed imaging.
Conclusions: We found no correlation between indication for delayed-phase imaging and its acquisition in pediatric trauma patients at our Level I trauma center. Delayed phase imaging was obtained in the vast majority of these patients, irrespective of indication. Improving referral education and adoption of a protocol in which delayed imaging is only obtained in pediatric patients with appropriate indications could reduce the effective radiation dose to the pediatric trauma patients at our instition by 25%. Review of the literature corroborates these findings.

Poster #: SCI-003

Improving Collimation in Pediatric Chest Radiographs

Cory Pfeifer, MD,*cpfeifer2018@gmail.com*; Diagnostic Radiology, University of Texas Southwestern Medical Center, Dallas, TX

Disclosures: All authors have disclosed no financial interests, arrangements or affiliations in the context of this activity.

Purpose or Case Report: Given the relative sensitivity of pediatric patients to radiation, the need to limit exposure to the region of interest is of the utmost importance in pediatric radiography. This study assesses the practice of acquiring pediatric chest radiographs at a community hospital in which the imaging contract was acquired by a radiology practice with subspecialty-certified pediatric radiologists. Pediatric radiologists in the new radiology practice saw a need for improved collimation of pediatric chest radiographs at the community hospital. Many radiographs exhibited poor collimation and included much of the abdomen. This study examines an initiative to measure and improve radiograph quality.
Methods & Materials: All pediatric chest radiographs (n = 50, average age 5.6 years) obtained at the community hospital during 4 consecutive weeks were reviewed. The following

method was employed to assess collimation: a horizontal line was drawn across the image at the level of the inferior border of the lower hemidiaphragm, an "optimal" vertebral body level was assigned by allowing 1 vertebral body height below the line for patients 5 years and younger (0.5 vertebral body heights for patients older than 5 years), and comparing this to the actual lowest vertebral level included in the film. After analysis of the control group was complete, an in-service was provided at the community hospital in which the proper and expected technique was reviewed with the technologists.
Results: In the initial analysis of films in the pre-intervention group, an average of 1.72 extra vertebral levels were included on 49 frontal radiographs analyzed. A single film was excluded due to over-collimation meaning that both costophrenic angles were not included. Of the 39 lateral films obtained in the control period, an average of 1.33 extra vertebral levels were included. Of the lateral films, 2 were excluded due to over-collimation.
Conclusions: Reducing unnecessary x-ray exposure to children through the use of an inservice program is achievable.

Poster #: SCI-004

A More Reasonable Approach to ALARA: Emergent Contrast-Enhanced CT Results in Lower SSDE at an Academic Children's Hospital

Joseph Cao, *joseph.cao@phhs.org*; Cory Pfeifer; Radiology, UT Southwestern, Dallas, TX

Disclosures: All authors have disclosed no financial interests, arrangements or affiliations in the context of this activity.

Purpose or Case Report: The principle of ALARA and its application in the pediatric population serves as the focus of the Image Gently campaign. Tertiary care institutions dedicated to the care of children are well situated to be regional leaders in maximizing the ALARA concept. This study compares the size-specific dose estimates of computed tomography (CT) studies performed at our institution to those from outside facilities referring patients for emergent care.
Methods & Materials: Our institution, a major pediatric referral center, is a large academic pediatric hospital that performs approximately as many CT exams of the abdomen and pelvis with contrast for acute abdominal pain as it receives consult requests for CT exams performed at referral centers. The SSDE of 20 consecutive contrast enhanced CT exams of the abdomen and pelvis performed at our institution were calculated and compared to 20 consecutive CT exams of the abdomen and pelvis with contrast submitted from outside referral facilities over the same time period. Size specific dose estimates (SSDE) of CTs of the abdomen and pelvis were calculated using established reference ranges based on patient size as defined by the AAPM[1].
Results: The mean SSDE for patients scanned at our institution was 10.31 (95% CI: 9.49-11.13). The mean SSDE for exams performed on studies at outside referral facilities was 28.12 (95% CI: 17.15-39.10). The average age and patient body size of our patient population were statistically similar.
Conclusions: These findings demonstrate that there is a significant decrease in SSDE of CT studies performed at our institution compared to outside referral institutions. This finding is important in highlighting the successful application of the optimization principle of ALARA at our institution. Furthermore, the degree of SSDE variability among referral institutions is important in showing that the choice of facility is likely a major determinant in radiation dose to children in the region. Outside facilities may benefit from additional training regarding dose optimization techniques in the pediatric population.

Poster #: SCI-005

Bismuth breast shields for pediatric patients undergoing CT chest, abdomen, and pelvis: the benefits

Joshua H. Finkle, MD[1], *jfinkle@luriechildrens.org*; Emily Marshall, PhD[2], Ingrid Reiser[2], Yue Zhang, PhD[2], Zheng Feng Lu, PhD[2], Anji Jones, BS, RT(C)[2], Kate A. Feinstein[2]; [1]Medical Imaging, Ann & Robert H. Lurie Children's Hospital of Chicago, Chicago, IL, [2]University of Chicago Medicine, Chicago, IL

Disclosures: All authors have disclosed no financial interests, arrangements or affiliations in the context of this activity.

Purpose or Case Report: Global mAs reduction is accepted as being superior to bismuth breast shields in reducing breast organ dose for children undergoing CT of the chest. However, in imaging of chest, abdomen, and pelvis (CAP), globally reducing mAs degrades image quality in the abdomen and pelvis. This study compares bismuth shields to global mAs reduction including a region-specific boost feature to maintain abdominal image quality.
Methods & Materials: CT CAP was performed on three phantoms of varying sizes, using three different techniques. First, each phantom was scanned with a bismuth breast shield. To establish dose savings, a control scan was performed with the same technique as the shielded scan but with the breast shield removed. Each phantom was scanned a third time without a shield but with global mAs reduction enabled to match image quality at the heart established during the shielded scan. Parameters for the third scan included a liver region boost feature to improve image quality in the abdomen. Entrance skin exposure was measured at the anterior and posterior chest, with the anterior measurement representing breast organ dose. Image quality was assessed using standard deviation measurements in the heart and liver regions.
Results: In the smallest phantom (water-equivalent diameter, WED 16.6 cm), the breast shield provided greater breast dose savings (14%) than global mAs reduction (7.6%) at the same image quality. In the larger two phantoms (WED 23.5 and 28.9 cm, respectively), breast dose savings with the breast shield (20.6% and 18.7%) were comparable to those when using global mAs reduction with the liver boost enabled (18.6% and 18.9%), with similar image quality in the heart and liver.
Conclusions: For small patients and for scanners without region-specific boost features, breast shields provide the best dose savings while maintaining abdominal image quality and therefore should be used for all CT CAP protocols. In larger patients with access to scanners with these advanced dose modulation methods, global mAs reduction can be used to achieve similar results to breast shields.

Poster #: SCI-006

Improved Understanding of Radiologic Appropriateness Among Pediatric Residents via Radiologist-Driven Didactics

Cory Pfeifer, **Samantha Castillo, MD**, *samantha.castillo@phhs.org*; Radiology, University of Texas Southwestern Medical Center, Hurst, TX

Disclosures: All authors have disclosed no financial interests, arrangements or affiliations in the context of this activity.

Purpose or Case Report: This study evaluates the value of radiologist-driven imaging education in a pediatric residency program. The primary goals of this educational program were to provide pediatric residents with resources such as the American College of Radiology Appropriateness Criteria, support optimal

resource utilization and patient care, increase resident understanding of radiation risk, and determine the value of integrating radiologists into pediatric education.
Methods & Materials: A needs assessment was performed in which the chief residents of a large pediatrics program were surveyed. The consensus of chief residents was that a 4-part lecture series delivered by a pediatric radiologist would be beneficial to pediatric residents. Topics included general radiation risk as well as basic imaging topics in the chest, abdomen, neurologic system, extremities, and vasculature. Each lecture integrated appropriate ordering, ALARA/Image Gently, and basic image interpretation. Pediatric residents were given a 10-item quiz before and after the lecture series assessing their knowledge regarding the best test to order in clinical scenarios. Residents were also asked, using a Likert scale, to rate their understanding of radiation risk, the ACR Appropriateness Criteria, and other topics of interest before and after each lecture.
Results: A total of 79 unique surveys were collected from a program of 92 residents. Chief residents reported that most residents were able to attend at least 2 lectures. The average pre-lecture score for knowledge of radiation risk was 3.27 (95% CI: 3.02-3.51) out of 5 which improved to 4.27 (95% CI: 4.09-4.57) post-lecture. There was a further increase in understanding of ACR appropriateness, with pre-lecture rating of knowledge increasing from 1.91 (95% CI 1.54-2.29) out of 5 to 3.61 (95% CI 3.33-3.90) post-lecture. Other areas of notable improvement included understanding of appropriate imaging orders for neurologic pathology (2.61 to 4.06 pre- and post-lecture) and in the abdomen/pelvis (2.78 to 4.17 pre- and post-lecture). Residents also provided positive subjective feedback upon conclusion of the program and reported a beneficial effect on their education.
Conclusions: A radiologist-driven lecture series in a pediatric residency can improve resident understanding of appropriate ordering practices and radiation risk. Radiologist participation in pediatric residency training is well-received. Future directions for research could include evaluation of the rate of appropriateness compliance.

Poster #: SCI-007

Right ventricular pulmonary regurgitation and two dimensional right ventricular strain in repaired Tetralogy of Fallot in children

Rong-Zhen Ouyang, Master, *oyrongzhen@163.com*; Yumin Zhong, Chen Guo, Li-Wei Hu, master; Radiology, Shanghai Children's Medical Center, Shanghai Jiao Tong University, School of Medicine, Shanghai, China

Disclosures: All authors have disclosed no financial interests, arrangements or affiliations in the context of this activity.

Purpose or Case Report: Many patients with repaired Tetralogy of Fallot (TOF) have right ventricular (RV) volume overload due to pulmonary regurgitation (PR)and would have ventricular deformation as time goes by after repaired surgery. We studied the effect of pulmonary regurgitation on global and regional right ventricular (RV) deformation, and their relationships with conventional diagnostic parameters.
Methods & Materials: Cases of repaired Tetralogy of Fallot with the duration time of 5-15years between surgery and cardiac magnetic resonance(CMR) were enrolled. The main pulmonary regurgitation fraction(PRF), RV volume and RV ejection fraction(RVEF), RV three segments (basal, mid, apical) of radial, circumferential and longitudinal strain were analyzed on CVI[46](Circle Vascular Imaging, Canada). Independent Sample t test and Pearson correlation were used to analyze the parameters. RVEF is equal or greater than 54% was considered as normal value.
Results: Twenty repaired Tetralogy of Fallot were enrolled in this study, 8 girls and 12 boys, duration time is 10.27±3.52 years. RV basal, mid and apical radial strain were 19.71±9.54（%）, 19.39±6.84(%)and 37.28±14.92(%) respectively. RVbasal, mid and apical circumferential strain were -11.39±3.89(%), -12.00±3.65(%) and –18.10±4.90(%) respectively. RV global longitudinal strain was -11.18±3.29(%). There was no correlation between PRF and RV strain but RV end diastolic volume (RV EDVi) and stroke volume(RVSVi). Duration time had obvious negative correlation with LVEF but positive correlation with RV EDVi and RV end systolic volume (RV ESVi). Each segment radial and circumferential strain had obvious correlation.
Conclusions: Pulmonary regurgitation fraction will cause right ventricular volume overload and ventricular deformation. RV strain was not found to have correlation with right ventricular volume overload and ventricular deformation in this small group study, but more cases need to be enrolled and control group should be include to compare which will be continued to study.

Poster #: SCI-008

Clinical Applications of Coronary CT Angiography in Preclinical Coronary Abnormalities in Children

Sharon W. Gould, MD, *Sharon.Gould@nemours.org*; M. P. Harty, MD, John W. Ostrowski, MD, Takeshi Tsuda, MD; Medical Imaging, Nemours/A.I. duPont Hospital for Children, Wilmington, DE

Disclosures: All authors have disclosed no financial interests, arrangements or affiliations in the context of this activity.

Purpose or Case Report: Diseases of the coronary arteries are rare in children, but can present as unexpected catastrophic events without preceding symptoms. It is essential to identify patients at risk to prevent potentially serious cardiovascular events. Coronary CT angiography (CCTA) has been widely studied in adults, but its clinical applications are not well established in children.
Methods & Materials: Retrospective chart and image review of coronary artery computed tomographic angiography from 2016 - 2018 was conducted to assess 1) image quality, 2) unexpected events, and 3) radiation dose.
Results: A total of 32 cases of CCTA were performed in our hospital from January 2016 to May 2018 (from 0.5 to 30 years of age; median 12). Indications for CCTA include 1) congenital coronary anomalies (n = 12), 2) after arterial switch operation (n = 10), 3) other congenital heart disease (n = 6), and 4) miscellaneous (n = 4). All patients had a diagnostic echocardiogram. Although a few, initial studies were performed on a 64 slice scanner, most of the studies were performed using a 2 x 128 slice dual source scanner. High-pitch, prospectively gated, adaptive, prospectively gated, and dose modulated, retrospectively gated techniques were utilized depending upon the patients' heart rhythms. Exposure parameters, kilovolt peak (kVp) and milliampere-seconds (mAs) were adjusted according to patient size and body habitus, as well as due to the presence of metallic chest implants. Three had suboptimal CT images due to an ectopic beat (1), hiccups (1), and a limited injection rate (1). Twenty nine cases (91%) showed expected diagnostic quality: 97% for coronary ostia and 91% for distal segments, superior to echocardiogram. Average/median radiation dose was 2.83/1.97 mSv, which was improved in 2018 (1.53/1.62 mSv) after protocol revision.
Conclusions: Coronary CTA provides more reliable image quality of the coronary ostia and distal segments than echocardiogram and delineates a distinct spatial relationship with extravascular structures that angiography cannot. The

radiation dosage has been significantly reduced with proactive heart rate control by pre- and intra-procedural use of beta-blockers, as well as implementation of aggressive protocol dose reduction techniques. CCTA is a reliable and safe diagnostic modality in analyzing coronary anatomy in children.

Poster #: SCI-009

Acute Chest Pain and Troponin Leak in Duchenne Muscular Dystrophy: Comparison with Acute Myocarditis Using Parametric Mapping

Simon Lee, MD, *simon.lee@nationwidechildrens.org*; Rajesh Krishnamurthy, Ramkumar Krishnamurthy, PhD, Thomas P. Johnston, Kan Hor, M.D.; Pediatric Cardiology, Nationwide Children's Hospital, Columbus, OH

Disclosures: All authors have disclosed no financial interests, arrangements or affiliations in the context of this activity.

Purpose or Case Report: Duchenne muscular dystrophy (DMD) is a myopathy with a natural history of progressive cardiomyopathy and vasogenic edema, fatty infiltration, and myocardial fibrosis. We recently identified a group of patients with DMD who presented with acute onset of chest pain (ACP), troponin leak (TL), and new late gadolinium enhancement (LGE), similar in presentation to acute viral myocarditis (AM). It is unclear if these patients have suffered an episode of AM or if this is a different disease process. Given the presumed acute myocardial necrosis in both processes, we hypothesize that native T1 and T2 values would be elevated in AM and DMD patients with ACP compared to asymptomatic DMD patients.
Methods & Materials: This was a retrospective study of three groups: Group 1: DMD, LV ejection fraction (LVEF) > 55%, and no LGE; Group 2: DMD presenting with ACP, TL, and new LGE; Group 3: clinical diagnosis of AM. All patients from January 2016 to June 2018 with native T1 and T2 mapping performed during a clinically indicated cardiac MRI study were included. T1 and T2 mapping was performed at a single mid-ventricular short axis slice. The slice was divided into a septal, anterior, and inferior region. All images were post-processed by a single observer.
Results: LVEF was lower in the Group 3 ($p < 0.05$) compared to Group 1, with no difference between Group 2 and 3 ($p = 0.99$). Native T1 values were elevated in Group 2 ($p < 0.01$) and Group 3 ($p = 0.02$) compared to Group 1 with no difference between Group 2 and 3 ($p = 0.41$). However when comparing T2 values for Group 1 and Group 2, this did not reach statistical significance ($p=0.72$) despite their similar age. T2 values for Group 3 were statistically higher for all segments when compared to Group 1 ($p < 0.01$) and approached statistical significance when compared to Group 2 ($p = 0.07$). Regional differences were identified in the native T1 maps, particularly in the inferior segment.
Conclusions: Patients with DMD who present with ACP, TL, and new LGE have increased T1 values compared to asymptomatic DMD patients, and similar to patients with AM. Increased signal is particularly noted in the inferior and anterior segments. However their T2 values are similar to the asymptomatic DMD patients and lower than AM patients. Although the presentation and clinical course of the DMD patients with ACP and TL has many similarities to AM, the T2 values suggest a lack of significant myocardial edema. This may represent a unique and unusual disease process in the natural history of DMD.

Poster #: SCI-010

Young Becker Muscular Dystrophy patients with Late Gadolinium Enhancement Demonstrate Left Ventricular Ejection Fraction Decline in Short Term Follow Up

Thomas P. Johnston,*pace.johnston@nationwidechildrens.org*; Simon Lee, MD, Ramkumar Krishnamurthy, PhD, Rajesh Krishnamurthy, Kan Hor, M.D.; Nationwide Children's Hospital, Columbus, OH

Disclosures: All authors have disclosed no financial interests, arrangements or affiliations in the context of this activity.

Purpose or Case Report: Cardiomyopathy is the leading cause of mortality for Becker Muscular Dystrophy (BMD).Risk stratification is challenging due to the wide variation of cardiomyopathy onset, progression, and severity; with cardiomyopathy developing independent of skeletal myopathy progression. Current guidelines recommend “complete cardiac evaluation” at ten years of age, but do not specify the type of imaging modality. We have been performing cardiac magnetic resonance imaging (CMR) routinely by 10 years of age. We sought to determine the progression of BMD cardiomyopathy during the adolescent years among patients who have evidence of fibrosis by late gadolinium enhancement(LGE).
Methods & Materials: At our center, all BMD patients undergo CMR when sedation is no longer necessary by age 10 years. We retrospectively reviewed the CMR studies performed between June 2013 and June 2018. Statistical analysis was performed using Student’s t-test.
Results: There were 43 BMD patients who underwent 98 CMR studies with LGE assessment. The average age of the first CMR study was 15.5±4.8 (range 7-25) years. Of these 27/43 (63%) patients had negative LGE and 14/43 (33%) had positive LGE on the first study. The LGE positive group was significantly older ($p<0.001$) with average age 19.5±3.1 years (range 16-25 years) compared to 13.5±4 years (range 7-22 years). Patients who were LGE positive had a lower mean LVEF compared with LGE negative patients (53.9±11.7% vs 62.6±5.3% p-value < 0.005). 31 patients had serial studies for a total of 72 CMR studies. Of the LGE negative patients 2/27 (7%) became positive over a 12 month period. In serial follow up, LGE positive patients showed a statistically significant decline in LVEF. Over an interval of 2.6± 1.7 years, LGE positive patients had a decline in LVEF from 53.9±11.7% to 48.5 ± 10.9 % (p-value < 0.005).
Conclusions: Our study demonstrates a large number of BMD patients with occult cardiomyopathy identified by LGE at a younger age than previously described. Serial studies demonstrated a significant decline in LVEF and increase in $LVEDV_i$ over an interval of 2.6± 1.7 years. CMR studies should be considered in BMD patients when sedation is no longer required. Escalation of medical therapy should be considered for patients who demonstrate evidence of fibrosis. Larger longitudinal studies should be considered to better isolate independent risk factors of cardiomyopathy progression.

Poster #: SCI-011

Fetal MRI in the Prognostication of Prenatally-diagnosed Omphalocele

Rachel Wise[1], *rwise2011@gmail.com*; Jessica H. Belchos, MD[2], Brian W. Gray, MD[1], Lava R. Timsina[1], Brandon P. Brown, MD, MA[1]; [1]Indiana University School of Medicine, Indianapolis, IN, [2]St. Vincent Hospital of Indianapolis, Indianapolis, IN

Disclosures: All authors have disclosed no financial interests, arrangements or affiliations in the context of this activity.

Purpose or Case Report: Frequently diagnosed on prenatal imaging, including fetal MRI, omphalocele has highly variable morbidity and mortality. Few prenatal prognostic indicators have been previously identified. We propose that features found on fetal MRI can predict morbidity and mortality in patients diagnosed with omphalocele.
Methods & Materials: We performed a retrospective review of all patients prenatally diagnosed with omphalocele who received fetal MRI from 2006-2017 at a single institution. Thirty neonates met study criteria. Imaging biomarkers identified on fetal MR included observed-to-expected total fetal lung volume (O/E TFLV); herniation of stomach, spleen, or liver; omphalocele size; and number of umbilical cord vessels. The primary outcome was survival, whether to birth or to discharge. Bivariate and multivariable regression analyses were performed.
Results: Seventy percent of patients survived to birth, and 45.2% survived to discharge. On bivariate analysis, observed/expected total fetal lung volume (O/E TFLV) correlated with survival to discharge (69 ± 29% vs 39 ± 25% for survivors vs. non-survivors, respectively ($p = 0.007$)). 23.1% of patients with stomach herniation ($p = 0.021$) and no patients with a herniated spleen survived to discharge ($p<0.001$). Liver herniation on MRI approached, but did not reach, significance for survival to discharge (53% vs. 81% for survivors vs. non-survivors, respectively ($p=0.06$)).On multivariable regression analysis after controlling for gestational age and gender, stomach herniation on MRI predicted lower likelihood of surviving at discharge (Adjusted Odds Ratio: 0.04 [CI: 0.004, 0.557], $p=0.016$).
Conclusions: Utilizing one of the largest reported series, this advanced imaging series of omphalocele demonstrates the value of organ-specific characterization to prognostication. While identifying liver position has long been recognized as valuable in predicting outcome, our analysis found predictive value for spleen and stomach position as well. These markers should be examined in a larger patient cohort with the goal of creating a validated set of prognostic imaging biomarkers.

Poster #: SCI-012

Fetal MRI findings in congenital high airway obstruction syndrome: comparison with the normal fetus

Hidekazu Aoki[1], *hdkz0706@gmail.com*; Osamu Miyazaki, Chief[1], Saho Irahara[1], Reiko Okamato[1], Yoshiyuki Tsutsumi[1], Mikiko Miyasaka[1], Haruhiko Sago[2], Yutaka Kanamori[3], Yasuyuki Suzuki[4], Shunsuke Nosaka[1]; [1]Department of Radiology, National Center for Child Health and Development, Setagaya-ku, Tokyo, Japan, [2]Center for Maternal-Fetal, Neonatal and Reproductive Medicine, Nationcal Center for Child Health and Development, Setagaya-ku, Tokyo, Japan, [3]Division of Surgery, Department of Surgical Specialties, National Center for Child Health and Development, Setagaya-ku, Tokyo, Japan, [4]Department of Anesthesiology and Critical Care, National Center for Child Health and Development, Setagaya-ku, Tokyo, Japan

Disclosures: All authors have disclosed no financial interests, arrangements or affiliations in the context of this activity.

Purpose or Case Report: Congenital high airway obstruction syndrome (CHAOS) is a rare life-threatening disease and prenatal diagnosis is essential. Some characteristic features seen on fetal MRI are well-known: primary lesion (upper airway obstruction) and secondary changes (dilated trachea, flattened/inverted diaphragm, enlarged and hyperintense lung). It is also reported that these secondary changes may be reduced if tracheoesophageal fistula (TEF) is present. The aim of this study is to evaluate the accuracy of fetal MRI in the prenatal diagnosis of CHAOS by comparing results with those of normal fetuses.
Methods & Materials: The MRI images from eight fetuses with CHAOS (29±6 weeks' gestation [mean±SD]) and 37 fetuses with no thorax abnormalities (32±2 weeks) were assessed retrospectively. The fetuses with CHAOS were selected from among those who were diagnosed at our institution from 2006 to 2018 (four CHAOS fetuses with TEF were also included), and the normal fetuses were selected from consecutive fetal MRI performed in 2017 and 2018. Identification of the upper airway was evaluated in both groups (false negative rate [FNR] in the CHAOS group and false positive rate [FPR] in the control group). Measurement of tracheal diameter (TD), craniocaudal/antero-posterior ratio in the right diaphragm (CC/APR), cardiothoracic ratio (CTR), and lung-to-liver signal intensity ratio (LLSIR) were also carried out in both groups. For comparison between the CHAOS group and the control group, a t-test was used. Also, CHAOS fetuses with TEF were evaluated in the same way as described above.
Results: Upper airway obstruction could be detected in all fetuses with CHAOS (FNR=0%), while the upper airway could not be clearly identified in five fetuses in the normal group (FPR=13.5%). There was no statistical difference in TD (3.6±1.0 mm, 3.2 mm±0.5 mm, $p=0.13$) and LLSIR (2.64±0.68, 2.54±0.66, $p=0.35$) between the CHAOS group and the control group. However, CC/APR (4.4±14.1%) and CTR (45.9±7.2%) in the CHAOS group were significantly lower than those of the control group (23.3±4.5%, 57.1±3.8%, [$p<0.05$]). Also, the same statistical results were obtained for the CHAOS fetuses with TEF (TD [3.2±1.0 mm, $p=0.48$], CC/APR [14.5±7.4%, $p<0.05$], CTR [50.5±4.0%, $p<0.05$], and LLSIR [2.74±0.39, $p=0.20$]) as well as in all CHAOS patients.
Conclusions: CC/APR and CTR may reflect distension of the lungs and are more reliable predictors than TD and LLSIR for prenatal diagnosis of CHAOS, even where airway obstruction is incomplete (CHAOS accompanied by TEF).

Poster #: SCI-013

Prenatal MR Imaging as a Predictor of Respiratory Symptoms at Birth for Congenital Lung Malformations

Alexis B. Maddocks, MD[1], *ar3684@cumc.columbia.edu*; Rama Ayyala, MD[2], Shimon Jacobs[1], Russell Miller[1], Vincent Duron, MD[1]; [1]Columbia University Medical Center-Morgan Stanley Children's Hospital, New York, NY, [2]Rhode Island Hospital-Hasbro Children's Hospital, Providence, RI

Disclosures: All authors have disclosed no financial interests, arrangements or affiliations in the context of this activity.

Purpose or Case Report: Congenital pulmonary airway malformations (CPAM), bronchopulmonary sequestrations (BPS), and hybrid lesions are the most common congenital lung lesions. They are primarily diagnosed prenatally via ultrasound and further characterized by MRI. While most affected neonates are asymptomatic at birth, some may experience varying severities of respiratory distress requiring intervention. We seek to develop a prognostic model for prediction of post-natal outcomes in patients with congenital lung lesions using fetal MRI calculated observed to expected normal lung volume (O/E NLV).
Methods & Materials: We did an IRB approved, retrospective study of patients with congenital lung lesions who underwent fetal MRI and received pre- and post-natal care at our institution from 2006 to 2016. 163 cases were referred to our institution for prenatal diagnosis of CPAM, BPS, or hybrid lesion. 68 of these patients had prenatal MRI performed at our institution. 8 patients were excluded due to "disappearing" lesion at the time of MRI or non diagnostic study. Statistical analysis was performed using Chi-square and Student's t-test. MRI was reviewed by 2 pediatric radiologists to determine volume of

normal lung (NLV), defined as the difference between total lung volume (TLV) and the volume of the lesion. NLV was normalized against published lung volumes by gestational age (O/E NLV). Imaging parameters were correlated with respiratory outcomes at birth including respiratory symptoms at birth, need for oxygen supplementation, mechanical ventilation, and delay in feeding.
Results: Mean gestational age at fetal MRI was 23.3 ± 3.0 weeks with a mean O/E NLV of 0.74 ± 0.26. Mean gestational age at birth was 38.4 ± 2.7 weeks. 14 of those neonates who had prenatal MRI had respiratory distress at birth. Requirement for oxygen supplementation at birth was observed in 12 of those patients and mechanical ventilation was necessary in the remaining 2 patients. O/E NLV did not significantly correlate with symptomatology at birth (p=0.15) or delay in feeding (p=0.14). O/E NLV did significantly correlate with requirement for supplementary oxygen (p=0.05) and requirement for mechanical ventilation (p=0.05) with a mean O/E NLV of 0.62 ± 0.17 and 0.4 ± 0.005 respectively.
Conclusions: Fetal MRI calculated O/E NLV ratio may be helpful in predicting respiratory prognosis at birth in patients with congenital lung lesions.

Poster #: SCI-014

Prenatal diagnosis of fetal skeletal dysplasias with 3DCT: Dose evaluation using a custom-made phantom that matches characteristics of pregnant women

Osamu Miyazaki, Chief[1], *miyazaki-o@ncchd.go.jp*; Hideaki Sawai, Dr.[3], Takahiro Yamada, Dr.[5], Jun Murotsuki, Dr.[4], Tetsuya Horiuchi[1], Gen Nishimura, Dr.[2]; [1]Dept. of Radiology, National Center for Child Health and Development, Setagaya-ku, Tokyo, Japan, [2]Center for Intractable Disease, Saitama Medical University Hospital., Omiya, Saitama, Japan, [3]Department of Genetics, Hyogo Medical University, Nishinomiya, Hyogo, Japan, [4]Department of Maternal and Fetal Medicine, Miyagi Children's Hospital, Sendai, Miyagi, Japan, [5]Clinical Genetics Unit, Kyoto University Hospital, Sakyoku, Kyoto, Japan

Disclosures: All authors have disclosed no financial interests, arrangements or affiliations in the context of this activity.

Purpose or Case Report: Fetal CT has almost the same utility as a postnatal skeletal survey. Despite this benefit, the associated radiation exposure is disadvantageous and radiation dose reduction is mandatory. It is however impossible to measure the actual radiation dose to the fetus directly. Several previous reports have described the CT dose index (CTDI) volume and dose length product (DLP) as representing an imagined fetal dose. The actual fetal radiation dose needs to be confirmed using a phantom that practically corresponds to a pregnant woman.
Methods & Materials: We created a custom-made phantom that corresponds to a pregnant woman, using acrylic resin (Polymethyl methacrylate: PMMA; 340 (Width) x 260 (Height) x 300 (Length)). It could contained three artificial fetal skeletons with different densities of calcium fluoride (300 HU: 1.90 mol/L, 500 HU: 3.63 mol/L, 700 HU: 5.37 mol/L). Dose measurements were obtained using four CT scanners (GE, TOSHIBA, SIEMENS, PHILIPS) at three different institutions with the same scan parameters (CTDIvol: 3.0 mGy; tube voltage: 80, 100, 120 kV) at four measurement points (distance from skin surface: 4 cm, 7 cm, 10 cm, and center). We compared the radiation dose for each tube voltage, at the different measurement points. The differences in dose between CTDIvol and measured data were assessed.
Results: The mean measured dose was 2.3 mGy at the center, and 3.73 mGy, 4 cm from the skin surface, across all vendors and tube voltages, corresponding to doses between 76% and 124% of the displayed CTDIvol (3 mGy). The maximum deviation was 1.58 fold (at 120 kV, distance from skin surface: 4 cm). Doses in the peripheral part of the pelvis showed 1.5–1.8 fold greater exposure in comparison with the central position. Doses increased in proportion to tube voltage settings and mean doses at 120 kV were 1.03–1.18 fold greater than at 80 kV. There were discrepancies in the measured dose among four CT scanners that ranged from 61 to 120% (around the mean of 120 kV).
Conclusions: Fetuses undergoing CT for suspected skeletal dysplasia may be exposed to approximately 0.8–1.2 times the displayed CTDIvol on the CT console. We suggest that the CTDIvol roughly represents fetal dose. There is however heterogeneity and the wide range of fetal doses depends on the position of the fetus, the selection of tube voltage, and CT units. As pediatric radiologists, we should be aware of these characteristics so that we can prevent excess radiation.

Poster #: SCI-015

Does Early Cerebral Blood Flow in Asphyxiated Neonates Indicate Degree of Neural Injury?

Ann Hill[1], *hilae@musc.edu*; Leslie E. Hirsig, MD[3], Milad Yazdani, M.D.[3], Heather Collins, Ph.D.[4], Dorothea Jenkins, M.D.[2]; [1]Medical University of South Carolina - College of Medicine, Charleston, SC, [2]Medical University of South Carolina - Department of Pediatrics, Charleston, SC, [3]Medical University of South Carolina - Department of Radiology, Charleston, SC, [4]Medical University of South Carolina - Department of Psychiatry & Behavioral Sciences, Charleston, SC

Disclosures: Leslie Hirsig, MD: Other: SealCath. All other authors have disclosed no financial interests, arrangements or affiliations in the context of this activity.

Purpose or Case Report: MRS is the best prognostic indicator for hypoxic-ischemic encephalopathy (HIE) but is difficult to obtain early after injury. We investigated whether cerebral blood flow measures of resistive indices (RI) and time average maximum velocities (TAMx) shortly after birth would relate to later degree of neural injury by MRI in hypothermic HIE newborns. We predicted that abnormally high/low blood flow would be associated with poor outcomes.
Methods & Materials: We retrospectively investigated 81 infants born between 2012 and 2018, ≥34 weeks gestation, treated with hypothermia, who received a transcranial Doppler ultrasound within 24 hours after birth, and MRI at 3-10 days. Cerebral blood flow measures (RI, TAMx) in anterior cerebral (ACA), middle cerebral (MCA) and basilar (BA) arteries were correlated with MRS ratios of neuronal health (N-acetylaspartate, NAA) in the basal ganglia (BG) and frontal white matter (WM). As both high and low RI and TAMx are abnormal, we divided our data into quartiles (Q) to find linear correlations between blood flow and NAA.
Results: As resistance in MCA increased above normal (Q3), NAA ratios in WM decreased (r^2 = -0.574, p=0.02), reflecting a decrease in neuronal integrity. Also, as blood flow velocity in BA (Q4) increased above normal, NAA ratios decreased in BG (r^2 = -0.550, p =0.012). Conversely, as velocity in the BA approached normal (Q2), NAA ratios increased in WM (r^2 = +0.618, p=0.011) indicating greater preservation of axons.
Conclusions: In this largest reported sample of cerebral blood flow in hypothermic HIE neonates, increased resistive index in the MCA and cerebral blood flow velocity in BA in the first 24h after HIE birth are associated with more injury, and worse NAA ratios. Transcranial doppler US can be performed at bedside shortly after birth and might prove useful for earlier prognosis in neonates with HIE.

Poster #: SCI-016: ***Withdrawn***

Poster #: SCI-017

Midgut Volvulus without Malrotation: Value of the Superior mesenteric artery (SMA) cut-off sign - A report of 2 cases.

Mostafa Youssfi, MD, *myoussfi@phoenixchildrens.com*; Deepa R. Biyyam, MD, Smita Bailey, MD; Phoenix Children's Hospital, Phoenix, AZ

Disclosures: All authors have disclosed no financial interests, arrangements or affiliations in the context of this activity.

Purpose or Case Report: To share these uncommon but important cases of Midgut Volvulus (MGV) without malrotation.
Methods & Materials: - 15-day-old Male presented with bilious emesis. An Ultrasound was perfomed.- 9-year-old Female with History of cerebral palsy, Gastro-jejunostomy tube fed. Presented with abdominal pain and hematemesis. A CT scan was obtained.
Results: - The 15-day-old patient Ultrasound showed: SMA Cut-off as well as Superior mesenteric vein (SMV) Cut-off. In addition, congestion of the mesenteric venous vasculature and a subtle swirling of the bowel around the SMA. The diagnosis of Midgut Volvulus was made. No UGI examination was performed. At Surgery, MGV without malrotation were found.- The 9-year-old CT showed: SMA Cut-off as well as (SMV) Cut-off. In addition, a subtle swirling/kinking of the bowel around the SMA. The diagnosis of Midgut Volvulus was made. No UGI examination was performed. At Surgery, MGV without malrotation were found in addition to midgut infarction.
Conclusions: These 2 cases illustrate the fact that a typical MGV can occur in the absence of malrotation. Although, no UGI was performed, we speculate that UGI examination to the ligament of Treitz may have been negative in these cases since there was no malrotation at surgery.SMA cut-off sign was important to make the diagnosis at Ultrasound and CT.

Poster #: SCI-018

The Value of MSCT in guiding staging and treatment of hepatoblastoma in Children based on PRETEXT staging system

Chen Guo, *guochen0028@163.com*; Yumin Zhong, Ying Zhou, Li-Wei Hu, Master; Radiology, Shanghai Children's Medical Center affiliated with Shanghai Jiao Tong University Medical School, Shanghai, China

Disclosures: All authors have disclosed no financial interests, arrangements or affiliations in the context of this activity.

Purpose or Case Report: To apply the Couinaud' system of segmentation and PRETEXT staging system of the liver to the tumor staging, combined with MSCT for evaluate the effectiveness in pre or post therapy of hepatoblatoma.
Methods & Materials: We retrospectively reviewed the outcomes of 67 cases that were diagnosed as hepatoblastoma in our hospital between July of 2012 and September of 2017. The patient ages ranged from 4 months and 5 years old (median age 3.2 years old). Couinaud' system of segmentation of the liver and PRETEXT staging system in MSCT were used to evaluate hepatoblastoma. According to the staging system results and imaging features, received the therapy relatively. We evaluate the patient's response to the therapy of these 67 cases. All cases were confirmed by pathology, diagnostic accuracy was calculated.
Results: Among the 67 cases: (1) The density of tumors were heterogeneous and lower than hepatic tissues, 22/67 had calcifications. (2) MSCT PRETEXT staging results: Stage I 7 cases, Stage II 31 cases, Stage III 26 cases, Stage IV 3 cases; PRETEXT staging was used again according to the results of operation: Stage I 7 cases, Stage II 27 cases, Stage III 31 case, Stage IV 2 cases, the accuracy was 73.1%(49/67). (3) Therapy evaluation: According to the PRETEXT staging and CT features, 7 cases of Stage I and 24/27 of Stage II were underwent the operation directly; As 3/27 of Stage II had ascites or portal vein tumor thrombus, with 31 cases of Stage III and 2 case of Stage IV, were underwent tumor biopsy. 31 cases who underwent the operation directly, 7 cases were followed up and had no recurrence, 24 cases were underwent chemotherapy and had no recurrence too. 36 cases were received 2 durations of chemotherapy, all 36 tumors were reduced in size, but the PRETEXT staging had no change, then the tumors were received resection.
Conclusions: PRETEXT staging system combined with MSCT is valuable for evaluaton the hepatoblastoma and conduting the timing of surgery and the chemotherapy protocols.

Poster #: SCI-019

Ultrasound has limited diagnostic utility in children with acute lymphoblastic leukemia developing pancreatitis.

Rebecca Richardson, MD[1], *rweller@uthsc.edu*; Cara Morin, MD, PhD[1], Charles Wheeler[1], Seth Karol[2], Sima Jeha[2], Hiroto Inaba[2], Beth McCarville, MD[1]; [1]Diagnostic Imagin, St. Jude Children's Research Hospital, Memphis, TN, [2]St. Jude Children's Research Hospital, Memphis, TN

Disclosures: All authors have disclosed no financial interests, arrangements or affiliations in the context of this activity.

Purpose or Case Report: Acute lymphoblastic leukemia (ALL) is the most common childhood malignancy. Children with ALL are at risk for developing acute pancreatitis (AP) during treatment, most commonly related to asparaginase. According to the American College of Radiology guidelines, ultrasound (US) should be the first line imaging modality in the diagnosis of AP. However, AP in children with ALL is thought to be due to direct pancreatic injury rather than ductal obstruction, and thus US may not be the optimal imaging modality for this diagnosis.
Methods & Materials: This retrospective study was approved by the institutional review board. Protocol databases were searched for ALL patients who were diagnosed with AP during therapy, according to Common Terminology Criteria for Adverse Events (CTAE) version 3. This list was cross-referenced with the diagnostic imaging database to identify patients who had undergone abdominal US or CT within 10 days of AP diagnosis. Chemotherapy dosing, amylase/lipase levels, clinical symptoms, and dates of imaging studies were recorded. All CT and US studies were overread by a radiology trainee blinded to the original imaging report, for findings of AP according to the CT Severity Index (CTSI) and the Revised Atlanta Classification. Discrepancies in the diagnosis of AP were adjudicated by a pediatric radiologist.
Results: 69 patients, ranging from 2-21 years, experienced 88 episodes of AP (between 2008-2018) and underwent 98 US and 44 CT exams. 72/88 (82%) events occurred within 30 days of asparaginase administration. 69 events (69/88, 78%) were diagnosed clinically by the presence of abdominal pain and amylase/lipase levels greater than 3 times the upper limit of normal. No imaging was obtained in 18 (20%) of events. The pancreas was completely obscured in 12/98 (12%) of US exams and was never visualized in entirety by US. The overall sensitivity for the detection of AP was 47% by US. Although obtained less frequently, CT detected AP in all but one case (98% sensitivity). CTAE Grade 4 events had the highest CTSI

scores, highest percentage of necrotizing pancreatitis, and highest US sensitivity (83%).
Conclusions: Most cases of AP in children being treated for ALL can be diagnosed with clinical history and labs. When imaging is used, US is much less sensitive in detecting AP than CT, except in the most severe cases (CTAE Grade 4). Imaging to diagnose AP in this patient population should be limited to clinically equivocal cases.

Poster #: SCI-020

Feasibility of a scoring system to predict reducibility and surgical outcomes of ileocolic intussusceptions in children.

Edward Richer, MD, *richerej@gmail.com*; Dhruv Patel, MD, Kiery Braithwaite, MD, Sarah Milla, MD, Jonathan M. Loewen, MD; Radiology, Emory University, Atlanta, GA

Disclosures: All authors have disclosed no financial interests, arrangements or affiliations in the context of this activity.

Purpose or Case Report: Determine if a simple scoring system can accurately predict the reducibility of ileocolic intussusceptions with therapeutic enema, and eventual surgical outcomes in those patients failing reduction.
Methods & Materials: An IRB approved, retrospective study was performed. In previous, unpublished research, the authors identified several imaging findings associated with a significantly decreased success rate of therapeutic enema, including presence of bowel obstruction on plain film, trapped fluid and poor blood flow on ultrasound, and location of the leading edge of the intussusception at or beyond the splenic flexure. A scoring system was devised assigning 1 point to each of these findings. This scoring system was then retrospectively applied to the cases of ileocolic intussusception at our institution between September 2012 – August 2017 in which plain films and ultrasounds were both available. The cases were then stratified according to their scores, and correlated with enema results and surgical outcomes. Complicated surgical cases were defined as those that required more extensive surgery than a standard laparoscopic reduction, such as conversion to open laparotomy.
Results: 191 cases were reviewed. Following point assignment, the following categories were generated: Category 0 (114 cases), Category 1 (35 cases), Category 2 (32 cases), Category 3 (8 cases), and Category 4 (2 cases). Category 0 had the highest enema success rate (86%) and lowest rates of complicated surgery (3%) and bowel resection (3%). Lower rates of enema success, and higher rates of complicated surgery and bowel resection, were seen in higher categories. In grouped analysis, there was a statistically significant decrease in enema success rate between Categories 0-1 and Categories 2-4 (83% vs 19%, $p < 0.0001$), and increase in complicated surgeries (4% vs 40%, $p < 0.0001$) and bowel resections (3% vs 29%, $p < 0.0001$).
Conclusions: A simple scoring system based on imaging findings obtained in most cases of ileocolic intussusception can predict reducibility by therapeutic enema, as well as surgical outcomes in cases of failed reductions. This information can be useful to radiologists, surgeons, and emergency physicians when determining patient management, as some patients may be better served by proceeding to surgery rather than enema. Further research to validate the scoring system in a prospective fashion is planned.

Poster #: SCI-021

The bottom line on air enemas: Does "door to catheter" time affect outcomes?

Kiery Braithwaite, MD, *kiery.braithwaite@choa.org*; Dhruv Patel, MD, Jonathan M. Loewen, MD, Sarah Milla, MD, Edward Richer, MD; Radiology, Emory University, Atlanta, GA

Disclosures: All authors have disclosed no financial interests, arrangements or affiliations in the context of this activity.

Purpose or Case Report: Determine if the length of time between diagnosis of an intussusception and therapeutic enema, or reported length of symptoms, is associated with lower enema success rates or higher rates of complicated surgery and bowel resection.
Methods & Materials: An IRB approved, retrospective study was performed. The radiology information system at our institution was queried for the keyword "intussusception" in fluoroscopic reports from September 2012 – August 2017. The length of time ("time to catheter") between diagnosis of intussusception, defined as the end time stamp of the ultrasound or CT on which it was first identified, and the start of therapeutic enema, defined as the first time stamp on images from the enema, was then calculated. In addition, the medical record was reviewed for overall length of symptoms (LOS) as documented in the emergency department note. Correlation with enema results, and surgical outcomes in patients failing reduction, was then performed. Complicated surgical cases were defined as those that required more extensive surgery than a standard laparoscopic reduction, such as conversion to open laparotomy.
Results: 209 cases were reviewed. There were 148 successful enemas and 61 failures. No significant difference was found in mean overall LOS between the 2 groups (1.44 days vs 1.58 days, $p = 0.44$) or in mean "time to catheter" (1 hour 53 minutes vs 1 hour 54 minutes, $p = 0.3$). Using grouped analysis, in patients with "time to catheter" of 0 – 4 hours versus those > 4 hours, no significant difference was identified in enema success rates (71% vs 65%, $p = 0.6$), rates of complicated surgery (11% vs 12%, $p = 0.9$), or rates of bowel resection (8% vs 12%, $p = 0.56$). Similarly, there was no significant difference among groups with the shortest and longest LOS. In patients with LOS 0 – 1 days versus those > 2 days, enema success rates (73% vs 68%, $p = 0.5$), complicated surgery rates (9% vs 15%, $p = 0.25$), and bowel resection rates (6% vs 13%, $p = 0.14$) were not significantly different.
Conclusions: Air enemas for intussusception performed within 4 hours of diagnosis did not show a difference in rates of enema success, complicated surgery, or bowel resection compared to those performed greater than 4 hours after diagnosis. Additionally, overall length of symptoms does not show a difference in rates.

Poster #: SCI-022

Development of a 3D Ultrasound Bowel Phantom for Trainee Education.

Rebecca A. Dennis, DO, *dennis.rebecca.ann@gmail.com*; E lizabeth Silvestro, MSE, Lamont Hill, BS RT(R), RDMS, Savvas Andronikou, MBBCh, FCRad, FRCR, PhD (UCT), PhD (Wits), Sudha Anupindi, MD, Misun Hwang, MD; Radiology, Children's Hospital of Philadelphia, Philadelphia, PA

Disclosures: All authors have disclosed no financial interests, arrangements or affiliations in the context of this activity.

Purpose or Case Report: To create a three dimensional (3D) ultrasound (US) bowel phantom that simulates bowel sonographic characteristics to aid in education for bowel scanning techniques and for microbubble contrast utilization in bowel.
Methods & Materials: A pliable 3D bowel US model composed of silicone (Ecoflex® 00-35, Smooth-On) was made containing a central lumen and a false lumen within the wall. Multiple materials of various consistencies for simulating bowel content including Play-Doh®(Hasbro), Play-Doh® in water, Kinetic Sand™ (Spin Master), Kinetic Sand™ in water, Flarp Putty® (Ja-Ru), polyvinyl acetate in water (Elmer's® glue), support material in water (Support 705®, Connex 500) and Metamucil® in water were tied-off into nitrile gloves separately. These were placed individually into the central lumen of the synthetic bowel in a tub of water and a sonographer with 17 years experience scanned the bowel using a Philips EpiQ-7G to evaluate the sonographic characteristics. Microbubbles (Lumason®, Bracco Diagnostics Inc) were then injected into the false lumen and rescanned. A numerical grading system was developed ranging from 4 to 12 to determine the optimal material. The criteria assessed on US included: visualization and imaging quality of the bowel wall(s), ± sonographic artifact and presence of echogenicity on B-mode and signal intensity on contrast mode. The luminal material with the highest score was deemed the optimal material.
Results: Materials ranged from a score of 6 to 12. The Play-Doh®, support material and Elmer's® glue each had the lowest scores of 6 due to poor image quality, extensive artifact and poor visualization of the bowel walls and Lumason® on contrast mode. The Kinetic Sand™ had a score of 7 and was better at visualizing the lateral bowel wall. The Metamucil® and Flarp Putty® had scores of 8 and 9 respectively, with complete visualization of the bowel wall and little artifact but both materials had increased echogenicity on B-mode. Play-Doh® in water and Kinetic Sand™ in water had the highest scores, 12 and 11 respectively. These materials demonstrated no artifact from luminal content with optimal image quality of the bowel wall. Yet, the Play-Doh® in water scored the highest due to best Lumason® visualization in the bowel wall.
Conclusions: The preliminary data shows Play-Doh® dissolved in water results in optimal sonographic characteristics for use in a 3D US bowel phantom. Such a phantom model will serve as a valuable training tool for grayscale and contrast enhanced bowel US evaluation.

Poster #: SCI-023

Incidence and Findings of Genitourinary Involvement in Pediatric Patients with Klippel-Trenaunay Syndrome

Nimai Patel[1], *npatel9@knights.ucf.edu*; Hubert Swana[2], Craig Johnson[3]; [1]UCF College of Medicine, Orlando, FL, [2]Arnold Palmer Hospital for Children, Orlando, FL, [3]Nemours Children's Hospital, Orlando, FL

Disclosures: All authors have disclosed no financial interests, arrangements or affiliations in the context of this activity.

Purpose or Case Report: To assess the incidence, scope, clinical findings and imaging characteristics of GU pathology due to underlying KTS in pediatric patients with the goal of improved diagnosis and outcomes for children with this potentially fatal disorder.
Methods & Materials: Using a retrospective data analysis design, the charts and imaging studies of 58 patients with confirmed diagnosis of KTS within a single tertiary care pediatric health care system were studied for insight into the degree of GU involvement in pediatric patients.
Results: 17% of patients (10) were noted to have GU findings, with 5% (3) having extensive GU involvement (defined as greater than 1 finding). The overall scope of GU involvement was diverse and varied with more than 9 different findings identified spanning 6 unique organs. Kidney, bladder and scrotum had the most common findings. Hematuria was the most common presenting symptom in 30% (3/10). Findings included those discussed in the literature along with previously unreported lymphatic findings. The importance of early recognition of GU involvement due to KTS was confirmed as the average age of GU complication was 7.6 years, less than 3 years after the average age of KTS diagnosis in this patient population.
Conclusions: Significant GU complications due to KTS can occur in the pediatric population with pathologies manifesting at an early age and with delayed recognition. Early clinical and imaging characterization of these conditions is important for expectant management and early intervention strategies, thereby playing a central role in improving patient education, patient outcomes and reducing costs, morbidity and mortality.

Poster #: SCI-024

Post-mortem imaging assessment of endotracheal tube, nasogastric tube and intraosseous trocar placement in pediatric patients in the Emergency setting

Laura A. Fitzpatrick[2], *laura.fitzpatrick@dal.ca*; Dominic Allain[1], Pierre Schmit[1]; [1]Department of Diagnostic Imaging , IWK Health Centre, Halifax, Nova Scotia, Canada, [2]Dalhousie University Department of Radiology, Halifax, Nova Scotia, Canada

Disclosures: All authors have disclosed no financial interests, arrangements or affiliations in the context of this activity.

Purpose or Case Report: Accurate placement of lines and tubes is essential in pre-hospital emergent care of pediatric patients, to ensure that lifesaving measuring can be initiated in an effective and timely manner. Malpositioned pediatric tubes can lead to failed resuscitation efforts. The purpose of this study is to determine the prevalence of misplaced endotracheal tubes (ETT), nasogastric tubes (NGT) and intraosseous trocars (IOT) in the pediatric acute care setting using post-mortem imaging.
Methods & Materials: The post-mortem imaging for 87 patients under the purview of the Medical Examiner Office performed between June 2007-May 2017 was retrospectively reviewed by a Pediatric Radiologist as part of a quality review in conjunction with the Nova Scotia Medical Examiner Service and Emergency Health Services (EHS). Of these 87 patients, 27 patients were excluded as no tubes were placed. For the remaining patients (N=61), ETT, NGT and IOT placement was assessed using a combination of radiographs and multiplanar CT, and characterized as "satisfactory position" or "malpositioned". For the malpostioned devices, the exact location was also documented.
Results: Of the 45 patients with an ETT, the tube was in satisfactory position in 9 (20%) patients and malpositioned in 36 (80%) patients. Of the malpositioned tubes, 5 were at the carina, 20 in the right main bronchus, 9 in the esophagus and 5 in other locations (at T2, T4, nasopharynx, etc.). The NGT was in satisfactory position in 13 (76%) patients and malpositioned in 4 (24%) patients, with tubes in the pharynx (two cases) and distal esophagus (2 cases). Of the 58 IOTs inserted, 15 (26%) were in satisfactory position and 43 (74%) were malpositioned, including 10 that had been completely removed but with CT evidence of prior incorrect positioning, 8 were through and through bone and 6 in the superficial soft tissues.
Conclusions: Malpositioning of the ETT, NGT and IOTs in this study is likely multifactorial. Tube placement is less common in the pediatric emergency setting compared to adult medicine,

possibly resulting in decreased experience and comfort level among pediatric EHS teams. There may be a role for further specialized training, with more frequent recertification. Use of a laryngeal airway mask could also be considered as an alternative to ETT in pediatric patients with difficult airways. The results of study will help to inform future training of pediatric EHS teams at our institution, with ongoing review of post-mortem imaging as a means of quality assurance.

Poster #: SCI-025

Optimizing Imaging Clinical Decision Support: Perspectives of Pediatric Emergency Department Physicians

James Hogan, MD[1], *jrhogan7@gmail.com*; Rosemary Frasso, Ph.D.[2], Tigist Hailu, MPH[1], Alyssa Tate, B.A.[2], Robert Martin[2], Raymond Sze[1]; [1]Children's Hospital of Philadelphia, Philadelphia, PA, [2]Thomas Jefferson University, Philadelphia, PA

Disclosures: All authors have disclosed no financial interests, arrangements or affiliations in the context of this activity.

Purpose or Case Report: To explore the imaging clinical decision support (ICDS) needs of pediatric emergency department physicians (PEDP's) prior to the implementation of imaging clinical decision support software (ICDSS).
Methods & Materials: Following institutional review board approval, through semi-structured interviews, researchers explored perspectives of 30 PEDP's on how they seek and obtain imaging consultation and the potential impact of ICDSS on practice. Open-ended questions were designed to elicit a range of responses rather than quantifiable data. The team employed a directed content analysis approach and codes were developed and explicitly defined through team evaluation. Coding and analysis was facilitated by NVivo 12 Software. Two research assistants independently coded all transcripts and discrepancies were addressed through consensus (mean k = 0.99). Codes were arranged into thematic categories to inform an explanatory model that illustrates the PEDP's priorities and needs related to the imaging decision process.
Results: Data analysis revealed three thematic categories: (1) Common Influences on the Decision Process (these include patient factors, PEDP's experience, the specialist perspective, and logistics), (2) Radiology Consultation Experience, (3) PEDP Perspectives on ICDSS which includes perspectives on how implementation of an ICDS system at our institution may impact practice. PEDP's described consultation as a valuable component of ICDS but reported difficulty in coordinating an imaging strategy with radiologists and other physician consultants. PEDP's described the exchange of ideas as especially worthwhile for clinical scenarios that do not fit neatly into ICDS pathways. Significant barriers to radiologist consultation included: time, access to radiology attendings, limited confidence in trainees, and not wanting to disrupt radiologist workflow. PEDP's expressed a belief that ICDSS could potentially improve their workflow and augment effective interaction with the radiology department.
Conclusions: PEDP's predict that radiologist consultation will continue to be an essential component of ICDS following the implementation of ICDSS. These results present an opportunity for radiologists to improve in-person radiologist consultation in clinical and didactic settings. Additionally, these findings will inform the development and implementation of an ICDSS system that meets the needs of the PEDP's and ultimately improves patient outcomes.

Poster #: SCI-026

Distinguishing between stable buckle fractures and other distal radius fractures: improved accuracy utilizing a measurement guideline

Lynne Ruess, *lynne.ruess@nationwidechildrens.org*; Julie B. Samora, MD, PhD; Nationwide Children's Hospital, Columbus, OH

Disclosures: Julie B. Samora, MD, PhD: Consultant, Honoraria: Globus. All other authors have disclosed no financial interests, arrangements or affiliations in the context of this activity.

Purpose or Case Report: To test radiographic diagnostic accuracy for distinguishing between stable distal radius buckle fractures (BF) from other distal radius fractures (DRF) after introducing a measurement guideline.Background: Management of pediatric forearm fractures has become fracture specific, as treatment of the common stable BF is trending toward home management with a removable wrist splint while other potentially unstable, DRF require immobilization and orthopaedic follow-up. Diagnostic accuracy between BF and DRF is therefore imperative. We developed and suggested our radiologists use a measurement guideline to aid diagnosis with this general rule: an isolated distal radius fracture in a child $\geq$ 7y is not likely to be a BF if the fracture-to-physis distance is < 1 cm.
Methods & Materials: This study was part of a quality improvement project between the Departments of Radiology and Orthopaedic Surgery. Medical record search identified children $\geq$3y with closed distal radius fractures diagnosed after all of our 26 pediatric radiologists received explanation of the measurement guideline. The radiology reports for the initial forearm and/or wrist series were compared to the final diagnosis (BF or DRF) as determined by consensus of 1 pediatric radiologist and 1 pediatric hand surgeon. The fracture-to-physis distance was measured for all fractures on the AP and LAT views by 1 author.
Results: Results: Before introducing the measurement guideline, radiologists received training to differentiate BF from DRF, but diagnostic accuracy was only 54% in a patient group with 148 BF and 55 DRF, and agreement was 'slight' (κ=0.120, SE=0.058, n=203). In the first 6 months after introducing the measurement guideline, there were 153 children $\geq$3y (range 4-16y) with isolated distal radius fractures: 64 (42%) stable BF and 89 (58%) potentially unstable DRF. Report diagnostic accuracy = 84%. Agreement for the diagnosis in this patient group was 'moderate' (κ=0.592, SE=0.066, n=153). Eleven DRF were misdiagnosed as BF (sensitivity 83%). Thirteen BF were misdiagnosed as DRF (specificity 86%). No patient $\geq$ 7y had a BF less than 1 cm from the physis. Only 1 false positive BF misdiagnosis was made in an older patient with a fracture-physis distance of < 1cm.
Conclusions: Conclusion: Diagnostic accuracy for distinguishing stable buckle fractures versus potentially unstable isolated distal radius fractures by our group of pediatric radiologists improved after introduction of a measurement guideline.

Poster #: SCI-027

'LogServer': A Novel Customizable Tool to Automatically Track MRI Scan Efficiency

Ramkumar Krishnamurthy, PhD[1], *ramkumar.krishnamurthy@nationwidechildrens.org*; Roy Wiggins[2], Houchun Hu, PhD[1], Rajesh Krishnamurthy[1], Tobias Block, Ph.D.[2]; [1]Radiology, Nationwide Children's Hospital, Columbus, OH, [2]NYU-Medical Center, New York, NY

Disclosures: All authors have disclosed no financial interests, arrangements or affiliations in the context of this activity.

Purpose or Case Report: MRI scans are long, and scan durations are unpredictable. Combined with challenges of inter-departmental coordination, this leads to poorer operational efficiency, increased need for sedation (especially in a pediatric population), increased wait time, and overall poorer patient care. There is a need for active, automatic tracking of scan log in a MRI machine to 1) determine operational efficiency, 2)disease specific scan information, 3) identifying patient specific scan metrics.Currently, there exist no customizable open-source solution that can automatically obtain information from MRI scanners. The purpose of this study is to demonstrate implementation of a novel, customizable QI tool that can automatically extract scan log data from a MRI scanner in a pediatric setting.
Methods & Materials: 'LogServer' (https://yarra.rocks/doc/server/yarralogserver/) was developed for use in Siemens MRI machines. This uses the 'Yarra' framework – an open source framework for complex MRI reconstructions. 'LogServer' monitors sequences, parses MRI sequences into discrete exams, generates 'EPIC-formatted' patient names, monitors scanner health, and tags exams with body region information. All extracted data were stored in 'PostgreSQL' - an open source database. 'ReDASH', an open source dashboard, was used to create customizable dashboards. In this study, for a clinical MRI scanner, we looked at 1) Daily scanner efficiency, defined as ratio of total hours scanner unused time to total hours (8am-7pm workday), and 2) Scan efficiency, defined as time when scanner was running to total time when the patient was on table.
Results: 'LogServer' was successfully able to automatically extract scan logs from MRI machines on an hourly basis, extract all relevant information, and visualize them in needed format using a remote PHI secure web browser. Figure 1 (https://drive.google.com/open?id=1fvyrSjq96EcHaAv9GenX1v4b070tFP3l) demonstrates the scanner schedule for any given day. Figure 2 (https://drive.google.com/open?id=1O7fxAIhWrAeqFVr3qRW5QyMGaN3F0mnX) shows the scan metrics for a selected patient, including total scan time, idle time during a scan session, as well time for adjustments in scanner. Our daily scanner efficiency for a week was 64% while scan efficiency was 76.3 ± 10%.
Conclusions: We demonstrated a robust customizable QI tool that lets continuous automatic monitoring of MRI scanner. This is a useful tool for hospital administrators, clinical managers, clinical leaders in their informed decision making.

Poster #: SCI-028

Beyond the numbers: favorable perceptions of a scoreless peer review pilot program.

A. Luana Stanescu, MD, *stanescu@u.washington.edu*; Randolph K. Otto, MD, Ramesh Iyer, MD; Radiology, Seattle Children's Hospital, Seattle, WA

Disclosures: All authors have disclosed no financial interests, arrangements or affiliations in the context of this activity.

Purpose or Case Report: Peer review is an essential component of quality improvement in radiology departments. Over the last years, several papers described a shift towards peer learning, emphasizing that feedback in the form of comments and peer learning conferences creates a more productive environment for reviewing and understanding perceptual or interpretive errors of peer radiologists, with improved diagnostic performance as the objective.At our institution, we instituted a three-month scoreless peer review pilot period. Radiologists' impressions regarding the current comment-enhanced numerical system and the pilot scoreless, comments-only period were collected through an online survey.
Methods & Materials: The survey containing 17 questions was distributed twice to the radiologists in our group to evaluate and compare their perceptions regarding the numerical scoring and the scoreless peer review systems. A Likert-style rating scale of 1-5 was used for the survey, ranging from strongly disagree (1) to strongly agree (5). The first survey, administered at the inception of our pilot period, was applied towards the numerical scoring system. The second survey, administered at the end of the pilot period, targeted the scoreless peer review system. Responses from both surveys were compared.
Results: 16 out of 20 radiologists in our group responded to both surveys. Overall satisfaction was slightly higher (weighted average of 3.64 versus 3.5) for the scoreless peer review compared to the numerical scoring system. Our colleagues felt more likely to underreport while reviewing a case with the numerical system as compared to the scoreless one. Reported negative emotional impact from discordances was slightly higher with the scoring system. Radiologists felt more inclined to provide a comment for educational purposes when agreeing with the interpretation while using the scoreless system. Comments were felt to be important in both systems.
Conclusions: A scoreless comments-only peer review system shows promise in providing more educational opportunities than a comment-enhanced numerical system, with less negative emotional impact on participant radiologists. This benefit may be even greater in practices in which radiologists are prone to underscore their colleagues.

Poster #: SCI-029

Value of specialist interpretation of cross-sectional pediatric imaging studies

Summit H. Shah, MD, MPH, *summitshah@gmail.com*; Ramkumar Krishnamurthy, PhD, Sean Kelleher, Rajesh Krishnamurthy; Radiology, Nationwide Children's Hospital, Columbus, OH

Disclosures: All authors have disclosed no financial interests, arrangements or affiliations in the context of this activity.

Purpose or Case Report: Two major insurance companies have recently enacted policies requiring outpatient advanced imaging at free-standing imaging facilities for adults. Examining the potential clinical and economic implications of non-subspecialized interpretations in children is important. We evaluated the rate of major discrepancies and changes in

management arising from second interpretations by a dedicated pediatric facility.
Methods & Materials: A retrospective and prospective analysis of CTs and MRs presenting for over-read by a pediatric radiologist was performed. For the prospective review, a standardized dictation template was implemented to track disagreements. A board-certified radiologist identified cases with major discrepancies as defined by those that were likely to change surgical or medical management. A chart review was performed to identify changes in clinical course and outcomes based on the second interpretation.
Results: 1397 patients were referred to our pediatric hospital for second interpretation following an outside facility interpretation. 3.6% of all patients (18/574 patients from retrospective review and 32/823 patients from prospective analysis) had major discrepancies between the outside report and the pediatric subspecialty interpretation. Of all major discrepancies, 31 were body cases (chest, abdomen, or pelvis), 13 were neuroradiology cases (head or neck), and 6 were musculoskeletal cases (spine or joint). Second interpretations changed surgical management for 14 patients, with 4 patients receiving a necessary surgery and 10 patients avoiding an unnecessary surgery. Medical management changed for 36 patients. Eleven of the cases with major discrepancies involved an incorrect diagnosis related to appendicitis. Examples of other serious missed findings included secondary reads that lead to diagnoses of meningoencephalitis, Crohn's disease, herpes encephalitis, intracranial hemorrhage, pulmonary embolism, and ovarian teratoma.
Conclusions: Pediatric subspecialty interpretations altered the surgical or medical management in 3.6% of referrals, which compares with a 0.4% rate of level 3 and 4 errors from the ACR RADPEER database. This supports the case for performing and interpreting these studies at a facility with dedicated pediatric radiologists. Since changes in reimbursement related to hospital-based cross-sectional imaging are driven by costs, the potential long-term adverse economic impact of non-subspecialized interpretations suggested by our study needs to be carefully considered.

Poster #: SCI-030

Clinical quality and cost effectiveness of a pediatric MRI simulator program

Summit H. Shah, MD, MPH, *summitshah@gmail.com*; Phillip McGonagill, BA, Lean Six Sigma Black Belt, Houchon Hu, Akila Sankaran, Rajesh Krishnamurthy, Ramkumar Krishnamurthy, PhD; Radiology, Nationwide Children's Hospital, Columbus, OH

Disclosures: All authors have disclosed no financial interests, arrangements or affiliations in the context of this activity.

Purpose or Case Report: The likelihood of sedation for an MRI exam in a patient under 8 years is high. Disadvantages of sedation usage include direct complications, suspected long-term effects, and higher costs. Sedation reduction techniques include the use of an MRI simulator, accelerated MRI scans, abbreviated protocols, and swaddle and sleep techniques. We evaluated the clinical image quality and cost effectiveness associated with an MRI simulator training program.
Methods & Materials: An MRI simulator program was created, and all patients going through the program from Aug 2014 and Oct 2018 were analyzed. To assess clinical image quality, 20 brain MRIs of age-matched patients were randomly selected including 10 patients who avoided sedation after the simulator program and 10 patients who received sedation for a brain MRI. A blinded pediatric radiologist scored the same 3 sequences on each study on a 4-point quality scale (1=significant limitations for clinical use, 2=moderate limitations, 3=minimal limitations, 4=no limitations). To assess cost effectiveness, success rate of avoiding sedation after simulation was calculated along with average differential cost to payer for a sedated MRI vs. a non-sedated MRI after MRI simulator training.
Results: 592 patients (mean age: 7.9 ± 3.0 years) were enrolled in the MRI simulator program over 4 years with the majority scheduled for a brain MRI (71%). The mean image quality score for sedated brain MRIs was 3.50 ± 0.51, and the mean quality score for non-sedated brain MRIs after successfully completing the MRI simulator program was 3.37 ± 0.49. All examined sequences demonstrated minimal to no limitations for clinical use. No sequence was found to have moderate or significant limitations for clinical use in either group. The success rate of children avoiding sedation after MRI simulation was 87%. The average differential cost to payer was $963 higher for a sedated MRI than an MRI that avoided sedation after MRI simulator training. Factoring in the success rate, the total payer cost savings over 4 years was estimated to be $495,984 for our simulator program.
Conclusions: In addition to reducing sedation rates, our study validates the clinical image quality of non-sedated pediatric MRIs obtained after successful simulator training and demonstrates the cost effectiveness of a simulator program over 4 years. The clinical quality and large payer cost savings should be considered when evaluating future reimbursements and investments for MRI simulator programs in pediatric patients.

Poster #: SCI-031

Distinguishing Button Batteries from Other Foreign Bodies: Specialized Skill or Flip of a Coin?

Jennifer L. Nicholas, MD, MHA,
jenniferlynn444@gmail.com; Michael Marrocco, MD, Peter Shelton, MD, Amy Killeen, MD, Steven Don, MD; Mallinckrodt Institute of Radiology, Saint Louis, MO

Disclosures: All authors have disclosed no financial interests, arrangements or affiliations in the context of this activity.

Purpose or Case Report: A button battery lodged in the esophagus is a medical emergency. This study evaluated how accurately button batteries can be distinguished from other ingested foreign bodies on radiographs and how this influences clinical management.
Methods & Materials: 71 cases of ingested foreign bodies were compiled, anonymized, and randomized. 49 were clinical cases and 22 were created using a chest phantom *(italics)*. Fifteen cases were button batteries *(6)*; 2 were hearing aid batteries *(1)*; 20 were a single penny *(1)*, 3 were 2 pennies stacked on each other, 4 were a nickel *(1)*, 1 was a dime *(1)*, 2 were a single quarter *(1)*, and 2 were a quarter with at least one other coin. Remaining cases were identified only as "coin", were foreign coins, or other round objects.12 clinicians ranging from PGY-2 to 30 years of experience participated in the study: 5 radiology residents, 2 radiology fellows, 2 radiology attendings, 1 ED fellow, 1 ED attending, and 1 pediatric attending. The cases were presented in Synapse PACS. The participants indicated the likelihood the object was a button battery using a Likert scale: 5 (definitely), 4 (probably), 3 (equal likelihood), 2 (probably NOT), 1 (definitely NOT); to decide how urgently the object needed to be removed (4=within 2 hrs regardless of NPO status, 3=within 24 hrs, 2=electively, 1=does not need to be removed); and were asked how comfortable they were identifying button batteries on radiographs before and after viewing the cases and after reviewing the answers.
Results: The average score for cases containing a button battery was 4.62 (Rads 4.67; ED 4.34; Peds 4.06). The average score for a single penny was 2.09 (Rads 1.87; ED 2.63; Peds 2.90). The average level of urgency for removal of button batteries

was 3.89 (Rads 3.86; ED 4.00; Peds 4.00). The average level of urgency for removal of a single penny was 2.93 (Rads 2.89; ED 3.50; Peds 3.27). The average degree of confidence before the cases were reviewed was 64%, 70% after viewing, and 85% after reviewing the answers.
Conclusions: Button batteries are readily distinguishable from other foreign bodies on radiographs, which helps to guide appropriate clinical management. Radiologists more accurately distinguish between button batteries and coins and clinicians are more likely to recommend emergent removal. This exercise increased the participants' levels of confidence in identifying button batteries on radiographs and could serve as a valuable teaching tool.

Poster #: SCI-032

Clinical Usefulness of MR Lymphangiography in Pediatric Patients

Seunghyun Lee, *seunghyun.lee.22@gmail.com*; Saebeom Hur, Young Hun Choi, Yeon Jin Cho, Jung-Eun Cheon, Woo Sun Kim, In-One Kim; Radiology, Seoul National University Hospital, Seoul, Korea (the Republic of)

Disclosures: All authors have disclosed no financial interests, arrangements or affiliations in the context of this activity.

Purpose or Case Report: The recent advances of the lymphatic intervention, has prompted progress in imaging of the lymphatic system. We would describe the clinical usefulness of the dynamic contrast-enhanced (DCE) magnetic resonance (MR) lymphangiography for imaging of the lymphatic system in pediatric patients.
Methods & Materials: A retrospectively evaluation of experience with DCE MR lymphangiography in four patients (Mean age 11.3 ± 5.5 years) was performed. The access needle was placed in the central part of both inguinal lymph nodes (LNs) under ultrasound guidance. CT contrast agent was injected into the LNs to confirm proper access under fluoroscopic guidance. After moving patients into the MR imaging room, MR contrast material was injected into the inguinal LNs for DCE MR imaging by using T1-weighted 3D gradient sequence with VIBE in the coronal plane that can be acquired in 15-30 seconds was repeated every other minute to study lymphatic transit into the cisterna chyli and thoracic duct and ultimately into the confluence of the left internal jugular vein and subclavian vein.
Results: Three patients were suspected to have protein-losing enteropathy. Two of these patients had a history of Fontan operation and liver transplantation, and one patient had no underlying disease. Another one patient was suspected to have chylothorax with unknown cause. The DCE MR lymphangiographic findings confirmed the presence of relatively normal thoracic duct in one patient, and abnormal thoracic duct dilatation in three patients. We could identify the retroperitoneal lymph system through DCE MR, though it did not provide evidence of the direct lymphatic leak to the retroperitoneal space associated with the symptoms in all patients. However, DCE MR showed an abnormal lymphatic leakage draining into the pleural space in one patient having chylothorax. The DCE MR lymphangiographic finding led to a help in management in all patients, continuation of conservative treatment in two patients, and intervention treatment in two patients. Image quality for visualizing the lymphatic system was considered good by both radiologists in all cases. There were no known adverse effects related to the DCE MR lymphangiography.
Conclusions: DCE MR lymphangiography is a recently developed technology, and its clinical application is feasible in pediatric patients. The application of DCE MR lymphangiography would significantly increase in pediatric patients as the lymph-based understanding of many diseases increases.

Poster #: SCI-033

Evaluation of the Experience with Implanted Venous Port-a-Caths in Children with Medical Complexity and Neurologic Impairment

Paymun Pezeshkpour, B. Sc.,
paymun.pezeshkpour@mail.utoronto.ca; Nicholas Armstrong, Sanjay Mahant, Prakash Muthusami, Joao Amaral, Dimitri Parra, Michael Temple, Bairbre Connolly; Hospital for Sick Children, Toronto, Ontario, Canada

Disclosures: All authors have disclosed no financial interests, arrangements or affiliations in the context of this activity.

Purpose or Case Report: To analyze the use of implanted port-a-caths in Children with Medical Complexity (CMC), neurological impairment and difficult venous access.
Methods & Materials: REB approved retrospective single centre observational study of port-a-caths placed by Interventional Radiology (IR), in CMC with neurological impairment, to meet their general vascular access needs. Details of peripheral intravenous (PIV) attempts, PIV successful starts, PIV complications, alternative devices, port-a-cath insertions, dwell times, times accessed, and port-a-cath-related complications were analyzed. Information for the year pre-port-a-cath was compared to the year post-port-a-cath in 21 patients (10M; 11F). The Wilcoxon signed ranks test were performed by SPSS.
Results: 21 patients underwent 26 port-a-cath insertions (median age 3 years; median weight 12.7 kg). The median port-a-cath dwell time was 26.5 months, total number of port-a-cath dwell days was 31,632 and total number of days accessed was 1,066 (median 21/pt). There was a significant reduction ($p<0.05$) in number of PIV attempts, PIV starts, needle pokes, ED visits and admissions in year the post-port-a-cath compared to pre-port-a-cath. There was no severe adverse events, 6 moderate and 18 mild adverse events. Limitations of the study include its retrospective design, lack of scores for difficult IV access or scales for IV infiltration and extravasation.
Conclusions: Port-a-cath placement in CMC significantly reduced the number of PIV attempts, needle pokes and admission requirements with no major added complications. These results provide useful information for parents and health care providers considering port-a-cath placement in this population.

Poster #: SCI-034

Embolization of the Lateral Marginal Vein in Klippel-Trenaunay Patients: Early Experience with Clarivein™

Daniel Ashton, *djashton@texaschildrens.org*; Texas Children's Hospital, Houston, TX

Disclosures: All authors have disclosed no financial interests, arrangements or affiliations in the context of this activity.

Purpose or Case Report: The lateral marginal vein, a persistent embryonic vein found in Klippel-Trenaunay (KT) patients, can be a major cause of morbidity such as venous hypertension and venous thromboembolism. Our purpose is to report our experience embolizing the lateral marginal vein using the Clarivein™ device, a pharmacomechanical embolization system.
Methods & Materials: Retrospective review of PACS and EMR for KT patients undergoing treatment of their lateral marginal vein using the Clarivein™ device. Patient

demographics, technical details of the procedure, and follow up imaging was collected.
Results: Four KT patients underwent four procedures to embolize the lateral marginal venous system. Technical success was 100% and there were no complications related to the embolization. Two of the four patients underwent additional therapies at the same time including sclerotherapy for venous and lymphatic malformations. Three of the four patients had ultrasound follow up that demonstrated complete occlusion of the treated venous segment. One patient had partial recanalization on further follow up one month after the procedure and underwent laser ablation which was also only partially successful.
Conclusions: Embolization of the lateral marginal venous system with the Clarivein™ device may be a good option for effective treatment.

Poster #: SCI-035

Fabrication of a custom pediatric phantom for pediatric interventional radiology endovascular simulation and training. Technical aspects.

Elizabeth Silvestro, MSE, *silvestro@email.chop.edu*; Sphoorti Shellikeri, Master's in Biomedical Engineering, Sean Trahan, BSE, Raymond Sze, Anne Marie Cahill; Radiology, Children's Hospital of Philadelphia, Philadelphia, PA

Disclosures: All authors have disclosed no financial interests, arrangements or affiliations in the context of this activity.

Purpose or Case Report: 3D printing technology presents a unique opportunity for the creation of custom phantoms for training and simulation for pediatric interventional procedures that are complex and/or uncommonly performed. The purpose of this study was to describe the elements of designing a 3D phantom for simulation of pediatric abdominal intra -vascular procedures.
Methods & Materials: In order to create a phantom design considerations such as the consistency of the "soft tissues", vascular system, creation of flow simulation and visibility of the vascular components using fluoroscopy, needed to be considered.
Results: Silicone was the chosen material poured into 3D printed molds with break-away and dissolvable internal cavities to create the anatomic vein and atrial system. The phantom design was also divided into three main regions of interest: chest, neck, and thigh. Rubber tube connections between the regions and pumps allowed for circulatory flow.The design process of the phantom consisted of incorporating several 15-year-old patient CTA exams to create the atrial and venous pathways. The pathways were then aligned with regions (chest, neck, thigh) segmented from CT exams in *MaterialiseMimics* and*3-Matic*. Connection ports between regions were added. Access points covered with a replaceable “skin patch” were added to the neck and thigh regions for reusability. The mold and breakaway cavities were 3D printed on a *StratasysFortus450mc*in ABS plastic. *Smooth-On Ecoflex30*was selected for molding to simulate the body and *DragonSkin10*for the skin patch based off the ShoreValue.Phantom feasibilityfor fluoroscopic visibility, contrast visibility, angiography, venography and device placement and removal was assessed and was successful in this prototype.
Conclusions: Phantom creation for pediatric interventional radiology simulation and training is an exciting prospect in pediatric IR for complex and/uncommonly performed procedures both for attending staff skill maintenance and initial training for fellows and residents. Going forward subsections of this phantom will be removable for repeat procedures such as stent placement.

Poster #: SCI-036

Percutaneous Treatment of Aneurysmal Bone Cysts in the Pediatric and Adolescent Population

Alexander M. Dabrowiecki, MD[1], *adabrow@emory.edu*; Anne Gill, MD[2], C. Matthew Hawkins, MD[2]; [1]Emory University School of Medicine, Atlanta, GA, [2]Children's Healthcare of Atlanta, Atlanta, GA

Disclosures: All authors have disclosed no financial interests, arrangements or affiliations in the context of this activity.

Purpose or Case Report: Aneurysmal bone cysts (ABCs) are expansile lytic lesions and can cause significant disability and pain most commonly seen in patients 10-30 years old. This study evaluates the technical feasibility, safety, and efficacy of percutaneous management of ABCs in pediatric and adolescent patients.
Methods & Materials: In this Institutional Review Board approved retrospective study, 11 consecutive ABCs treated with doxycycline sclerotherapy and/or percutaneous ablation from December 2015 to October 2018 were evaluated. Demographics, clinical presentation, procedural details, and safety/efficacy outcomes were assessed.
Results: A total of 11 ABCs in 11 patients (average age = 13.4 yrs; range: 8-17) were treated with 22 total procedures (range: 1-4 treatments/patient). 7/11 (63.6%) ABCs presented with recurrence following surgical resection. ABC location included spine 3/11 (27.3%), pelvis 4/11 (36.4%), lower extremity 2/11 (18.1%), humerus 1/11 (9.1%), and rib 1/11 (9.1%). Doxycycline sclerotherapy alone was used in 10 procedures in 4 (36.4%) patients, cryoablation alone was used in 7 procedures in 4 (36.4%) patients, and a combination of percutaneous ablation and doxycycline was used in 5 procedures in 3 patients (27.3%). All 22 (100%) procedures were technically successful. Clinically, 10/11 (91%) showed clinical improvement including cessation of pain and improved range of motion. Mean follow-up time= 9 months (range: 1-20 months). On imaging, 9/10 (90%) ABCs decreased in size with increasing sclerosis on follow-up imaging. 1/10 (10%) ABC did not respond to percutaneous treatment and required repeat surgical resection. One patient is awaiting imaging follow-up. 1/11 (9.1%) patient experienced a major complication of left lower-extremity paralysis, bowel incontinence, and fecal incontinence following treatment of an L4 ABC that resolved. 1/11 (9.1%) patient experienced a minor complication of transient numbness of the lateral thigh.
Conclusions: Percutaneous treatment of ABCs is a safe and efficacious treatment option in the pediatric and adolescent population.

Poster #: SCI-037

Posteriorly Tunneled Central Lines in Children: Does it decrease rates of dislodgement?

Michael Acord, MD[1], *mra0305@gmail.com*; Carl A. Termine[2], Anne Marie Cahill[1], Fernando Escobar, MD[1]; [1]Radiology, Children's Hospital of Philadelphia, Philadelphia, PA, [2]Monmouth Medical Center, Long Branch, NJ

Disclosures: All authors have disclosed no financial interests, arrangements or affiliations in the context of this activity.

Purpose or Case Report: To assess the rate of dislodgement of posteriorly tunneled central lines, over-the-shoulder, in children.
Methods & Materials: This was a single center, IRB-approved retrospective study of all children with a posteriorly tunneled central line placed in pediatric interventional radiology over a 12-year period. The following parameters were reported;

indication for posterior line placement, type of catheter, number of catheter days, rates and reasons for replacement, and infections. Mechanical complications were also assessed, which were defined as catheter fracture, occlusion, cuff exposure, or tip migration. For each patient, time between dislodgement or removal with a posterior line was compared to time to dislodgement or removal of that patient's most recently placed anterior line.
Results: 17 patients (4 female, 13 male) underwent 68 posterior line placements during the study period, most commonly for total parenteral nutrition administration (58.8%). Median age at posterior line placement was 12.5 months (IQR= 10.3-19.5). Lines were most commonly single lumen (73.9%), silicone (86.6%), and placed via the right IJ (76.7%). The most common indication for posterior line placement was to avoid patient line manipulation (76.4%). The total number of catheter days was 10,699. The median number of days between catheter replacements was 80 (IQR= 18-150); however, only 9 (13.2%) lines were replaced due to pulling by the patient. The most common reason for replacement was for mechanical complications (47.1% or 2.99 per 1000 catheter days), which included 11 fractured catheters and 11 unintentional cuff exposures. There were 20 catheters (1.86 per 1000 catheter days or 29.0%) that were removed for infection. When compared to the most recently placed anterior line, posteriorly lines remained in place for significantly longer duration (mean 66.2 ± 15.5 (SEM) days vs 31.3 ± 5.6 days, p=0.04).
Conclusions: Posterior tunneled central line placement is a potential longer-lasting option in children at risk for intentional catheter dislodgement but is associated with a high mechanical complication rate.

Poster #: SCI-038

Sharp recanalization provides restoration of patency across stenosed hepatic venous circulation in pediatric patients.

Thomas Shum, PhD, *shum@bcm.edu*; Heather Cleveland, BSRS, PA-S, Alex Chau, MD, Daniel Ashton, Alberto j. Hernandez; Texas Children's Hospital, Houston, TX

Disclosures: Thomas Shum, PhD: Financial Interest: Translate Bio - Intellectual property rights for a licensed patent: Patent co-author. All other authors have disclosed no financial interests, arrangements or affiliations in the context of this activity.

Purpose or Case Report: Stenosis of the inferior vena cava or the hepatic veins is an underlying cause for hepatic compromise in liver transplant patients and in patients with inflammatory diseases of the liver, leading to considerable morbidity. CT-guided or ultrasound-guided minimally invasive vessel recanalization procedures can reverse liver failure in these patients by restoring vessel patency. However, it can be difficult to employ these techniques using traditional guidewire tips against fibrotic obstructions associated with vessels that have undergone repeated stenosis. Sharp recanalization offers an alternative strategy to gain access through these obstacles by utilizing needles or the sharp end of the guidewire tip to penetrate the vessel obstruction. This technique has been well-described and employed successfully in adult patients, but has not yet been reported in the pediatric setting.
Results: Here, we present 3 cases of image-guided hepatic vein sharp recanalization in pediatric patients, one of whom required stent placement for recurrent venous stenotic obstructions of the inferior vena cava and hepatic veins. We were able to restore hepatic vein patency in all three patients with no acute or long-term complications. Two of the patients had undergone previous liver transplants, and in following the durability of the venous recanalization in these patients, we observed long-term extension of liver graft life to the extent of at least 18 months and 38 months, respectively.
Conclusions: To the best of our knowledge, we present the first application of sharp recanalization in pediatric patients, and demonstrate evidence that it can be used safely and effectively to restore IVC and HV patency and prolong liver function in this patient population.

Poster #: SCI-039

Multimodality image fusion for guiding pediatric interventional radiology procedures: Preliminary evaluation

Karun Sharma[1], *KVsharma@childrensnational.org*; Bhupender Yadav[1], Ranjith Vellody[1], William Plishker[2], Raj Shekhar[1]; [1]Children's National Health System, Washington, DC, [2]IGI Technologies, College Park, MD

Disclosures: William Plishker: Ownership/partnership /principal & Officer, Director or other fiduciary role: IGI Technologies**; Raj Shekhar:** Ownership/partnership/principal: IGI Technologies. All other authors have disclosed no financial interests, arrangements or affiliations in the context of this activity.

Purpose or Case Report: Percutaneous CT-guided biopsy and ablation are established techniques to diagnose and treat solid tumors. However, some tumors are not adequately visualized with CT, even after IV contrast administration, because of transient enhancement. Many of these "CT-occult" tumors are optimally seen on preprocedural MRI or PET scans. To enable targeting of such tumors, we developed software that fuses MRI/PET images to intraprocedural CT in real time. The software corrects for soft-tissue deformations which occur due to differences in patient positioning or motion. The fusion imaging is generated after each intraprocedural CT scan and takes advantage of all available imaging data. We report retrospective evaluation of this fusion method for pediatric interventional radiology procedures.
Methods & Materials: The software was tested on four patients with CT-occult tumors undergoing biopsy. Two patients had bone lesions (Salmonella osteomyelitis and Ewing Sarcoma) that were optimally visualized on preprocedural MRI and PET. Two patients with neurofibromatosis had soft-tissue lesions with regions that were suspicious for malignant transformation best seen on preprocedural MRI and PET. During biopsy, CT images were pushed from the scanner to the workstation and fused with the corresponding MRI or PET. The time and accuracy of image fusion were measured. Accuracy was measured as target registration error (TRE) at anatomic landmarks identified by an expert in individual images while blinded to the fusion images.
Results: Clinical experts reviewed the fusion images after the procedures and judged them to be visually adequate and accurate. The mean TRE of 4.1 mm supported this finding. The TRE data further showed that the algorithm achieved subvoxel registration accuracy (registration error < voxel size) of 0.85 voxels, averaged over all four cases. The mean time of image data transfer from CT scanner to the fusion workstation was 2.0 s for volumetric and 0.4 s for fluoroscopic scans. The mean time to perform image fusion was 35.7 s for volumetric scans and 7.0 s for fluoroscopic scans.
Conclusions: The image fusion software was fast and allowed accurate visualization of MRI/PET visible tumors on the intraprocedural CT images. When fully integrated in the IR workflow, this tool has the potential to provide improve targeting of CT-occult tumors and improve efficiency and efficacy for CT-guided biopsy and ablation. A prospective clinical trial is planned to quantify the anticipated clinical benefits.

Poster #: SCI-040

Imaging and Clinical Findings of Aneurysmal Bone Cysts Post-Percutaneous Cryoablation

Jonathon Weber, MD, *jon.weber7@gmail.com*; Jonathan Samet, MD, Jared Green, MD, James Donaldson, MD, Shankar Rajeswaran, MD; Radiology, Ann and Robert H. Lurie Children's Hospital of Chicago, Chicago, IL

Disclosures: All authors have disclosed no financial interests, arrangements or affiliations in the context of this activity.

Purpose or Case Report: Aneurysmal bone cysts are benign expansile osseous lesions which may behave locally aggressively, leading to growth plate destruction, angular deformity, and pathologic fracture. Current treatments such as curettage and bone graft reconstruction, sclerosis, and intra-arterial embolization have high recurrence rates and morbidity. Percutaneous cryoablation is a promising new treatment modality. Three patients with ABCs underwent cryoablation at our institution and follow-up MRIs over the span of a year were obtained. This is the first study of its kind to elucidate the imaging findings post-cryoablation of ABCs, which may help the radiologist interpret response to treatment.
Methods & Materials: In this HIPAA compliant, IRB-approved study, three children with ABCs were treated using IcePearl percutaneous cryoablation needles (Galil Medical). Patients included an 11-year girl with a clavicular lesion, a 16 year-old girl with a femoral lesion, and a 14-year old boy with a femoral lesion. Clinical and imaging follow up with MRI occurred at 3, 6, and 12 months.
Results: Common imaging findings after cryoablation include resolution of fluid-fluid levels, decreased size of a T2-hyperintense core, appearance of a sclerotic rim of bone, and a cryoablation burn zone. All patients reported markedly decreased pain and return to normal activity by 6 months post treatment, including one patient able to play a full hockey game at 3 months. No major complications were reported. No clinical or imaging indicators were present to suggest recurrence.
Conclusions: ABCs are a difficult entity to treat with high recurrence rates and morbidity with current treatment options. After percutaneous cryoablation, ABCs may show common imaging findings which may help radiologists monitor treatment efficacy. All three patients treated at our institution showed excellent clinical results. Percutaneous cryoablation is a promising treatment modality for ABCs which in our series confers exceptional benefit to patient symptomatology without serious morbidity.

Poster #: SCI-041

Sonoelastography in the Evaluation of Cutaneous Fibrosclerotic Conditions

Maria Manuela Perez Matta, MD, *manuelitalinda@gmail.com*; Jennifer Zuccaro, Arun Mohanta, Joel Fish, MD, FRCSC, Elena Pope, MD, Ronald Laxer, MD, Andrea Doria, MD; Diagnostic Imaging, Hospital for Sick Children, Hamilton, Ontario, Canada

Disclosures: All authors have disclosed no financial interests, arrangements or affiliations in the context of this activity.

Purpose or Case Report: Acoustic radiation force imaging (ARFI) is a type of quantitative sonoelastography (SE) that has been used to determine tissue stiffness in many disorders including liver fibrosis, breast cancer, thyroid nodules and more recently, cutaneous scleroderma. However the use of this technology for the assessment of skin lesions in the paediatric population has not yet been investigated. The purpose of this study is to test the feasibility of using ARFI SE to quantify the stiffness of morphea or localized scleroderma (LS) and hypertrophic burn scars (HTS), two skin conditions in which there is excessive deposition of collagenous and non-collagenous extracellular matrix causing fibrosis.
Methods & Materials: We employed conventional ultrasound (US) and ARFI SE to characterize changes in the skin of pre-assigned LS and HTS lesions and compared them to the normal contralateral sites as controls. The inclusion criteria was clinical diagnosis of the corresponding skin condition by a specialist. For each participant, a "target lesion" was selected and marked by the clinician as well as a section of contralateral matched normal skin for US and ARFI measurements. The Wilcoxon signed-rank test was used to compare scar and control sites.
Results: 26 patients from the outpatient Morphea (n = 13) and Burn (n = 13) clinics at our tertiary pediatric hospital were prospectively recruited (age range: 4 to 16; 12 females, 14 males). Lesions varied in location and severity. As expected LS lesions and HTS were significantly stiffer than normal skin (E means of 17.61 for LS and 41.11 kPa for HTS respectively, versus 10.32 and 10.05 kPa for the normal controls).Skin thickness of the LS lesions was 30.7% thinner than the respective healthy skin, but the difference between means was only significant for the dermal layer. HTS were significantly thicker than the control sites ($p < 0.05$). Mean thickness values for the scar and control sites were 4.06 mm and 1.43 mm respectively. Variable changes in echogenicity and vascularity were seen in both group of lesions.
Conclusions: This study demonstrated the feasibility of using ARFI SE to discriminate between normal skin and fibrosclerotic skin conditions (LS and HTS) by measuring skin stiffness. In addition, the findings show that both these types of lesions are significantly stiffer than normal skin. Future research should focus on establishing reference data and determining the technology's ability to detect scar changes over time and evaluate response to treatment.

Poster #: SCI-042

Pediatric Sacroiliac Joint Infection on MRI: Are There Age-Specific Imaging Features?

Sara Cohen, MD, *cohens10@email.chop.edu*; David M. Biko, MD, Summer Kaplan, MD MS, Christian A. Barrera, M.D., Suraj Serai, Jie C. Nguyen; Children's Hospital of Philadelphia, Philadelphia, PA

Disclosures: David M. Biko, MD: Financial Interest: Wolters Kluwer - Royalty: Editor of Review Book. All other authors have disclosed no financial interests, arrangements or affiliations in the context of this activity.

Purpose or Case Report: To investigate magnetic resonance (MR) imaging features of sacroiliac joint infections in children with respect to age and with clinical correlation.
Methods & Materials: This IRB-approved, HIPPA compliant study included 40 MR studies with sacroiliac joint infections from 40 children (mean age 8.62 +/- 6.1 years; 19 boys and 21 girls) performed between December 1, 2002 and July 31, 2018. Infections were established using a combination of positive cultures, elevated inflammatory markers, clinical assessment, and response to antibiotic treatment. MR studies were retrospectively reviewed by 2 radiologists in consensus for the presence of bone marrow edema, bony erosions, joint effusion, extracapsular edema, soft tissue abscess, and sciatic neuritis. Pre-treatment radiography was reviewed for the presence of radiographically visible osseous change. Clinical chart review was performed for clinical history and outcomes. Descriptive data is presented as mean ± SD. The inter-observer agreement was evaluated with weighted-kappa. Kappa scores (k) of 0.41–0.60, 0.61–0.80 and ≥0.80 were regarded to be indicative of

moderate, good, and excellent agreement, respectively. Non-parametric, Chi-square and Fisher tests were used, $p < 0.05$ was considered significant.
Results: A bimodal age distribution for infectious sacroiliitis was identified with 40% (16/40) from children ≤ 5 and 60% (24/40) from children ≥ 8 years of age. No difference was found between the groups in the presence of bone marrow edema, bony erosions, joint effusion, and soft tissue abscess. Although anterior extracapsular edema was present in all patients, posterior extracapsular edema was more common in the younger age group (p=0.006, k=0.923). Radiographically visible osseous changes were often not present at the time of diagnosis. 80% of patients had diagnostically adequate radiography within a month prior to MRI (3.6 ± 4.6 days between studies). The ability to identify infection using radiography was poor, at 31%. Clinically, the mean duration of symptoms was 8.6 ± 7.4 days and length of hospital stay was 7.8 ± 4.1 days, which did not differ between the age groups (p=0.28 for symptom duration, p=0.24 for hospital stay).
Conclusions: Clinical findings and many of the MR imaging features of infectious sacroiliitis in children did not significantly differ with respect to age. Posterior extracapsular edema was more common in younger children, which suggests regional ligamentous and capsular laxity and immaturity.

Poster #: SCI-043

Dynamic Contrast-Enhanced MRI Using a 3D Radial Acquisition: Potential Applications in Musculoskeletal and Bone Marrow Assessments

Mitchell Rees, *mitch.rees@nationwidechildrens.org*; Kathryn S. Milks, MD, Ramkumar Krishnamurthy, PhD, Rajesh Krishnamurthy, Houchun Hu, PhD; Radiology, Nationwide Children's Hospital, Columbus, OH

Disclosures: All authors have disclosed no financial interests, arrangements or affiliations in the context of this activity.

Purpose or Case Report: There is limited understanding and utilization of dynamic contrast enhancement MRI of marrow, periosteum and cartilage for diagnosis of musculoskeletal (MSK) disease in children. This is partly due to limited availability of pediatric disease models of marrow inflammation, infection, infiltration, or involvement by tumor. Herein we explore signal intensity time curves of relevant MSK targets using a 3D Golden-angle RAdial Sparse Parallel (GRASP) MRI technique. GRASP is an accelerated, free-breathing dynamic acquisition that has been shown to reduce the need for sedation. We aim to establish a baseline for normal enhancement characteristics of marrow, cartilage, synovium and periosteum of the growing skeleton in a sheep model as a precursor to translation to children.
Methods & Materials: GRASP data were acquired in 4 sheep using standard dose gadobutrol at 3 mL/sec. All studies were performed on a 3T system. GRASP data are acquired with consecutive radial spokes that are rotated by the golden angle. The data can be reconstructed into time-resolved dynamic frames with user-selectable temporal resolution during contrast passage (https://cai2r.net/research/radial-vibe-sequence). We reconstructed at a temporal resolution of 4.5s. Signal intensity curves were generated from regions-of-interests in: marrow of diaphysis, metaphysis, and epiphysis of the humerus, proximal humeral physis, periosteum of the proximal humerus, a thoracic vertebral body and an adjacent intervertebral disc.
Results: A sample data set is here https://www.dropbox.com/s/zmh5dakn847s6w0/20180727.mov All structures exhibited onset of contrast-enhancement within approximately the same time frame after contrast administration, with a time to peak signal of <10s and with little washout over 180 seconds. There was no difference in the slope of wash-in and wash-out. However, the peak signal varied by anatomy. Specifically, signal in the diaphyseal marrow increased from 16% to 31% above baseline; metaphyseal marrow: 56% to 246%; physis: 155% to 206%; epiphyseal marrow: 54% to 96%; periosteum: 62% to 339%; intervertebral disc: 65% to 118%; and vertebral body: 155% to 321%.
Conclusions: GRASP allows rapid free-breathing characterization of contrast ehancement in the growing skeleton. It provides excellent anatomic delineation and can potentially demonstrate difference in peak signal between relevant MSK targets. We hope to translate our technique to children, and utilize it for qualitative and quantitative diagnosis of pediatric MSK disease.

Poster #: SCI-044

Capitellar-radial distance (CRD): a new standardized measurement for determining developmental maturity in younger pediatric patients.

Dustin G. Roberts, M.D. Candidate, 2019[1], *dgroberts@mednet.ucla.edu*; Soni Chawla, M.D.[2]; [1]David Geffen School of Medicine at UCLA, Los Angeles, CA, [2]Olive View-UCLA Medical Center, Sylmar, CA

Disclosures: All authors have disclosed no financial interests, arrangements or affiliations in the context of this activity.

Purpose or Case Report: To date, a standard for CRD has not been established. Plain radiographs are a cost-effective, low-risk option for studying osseous structures in great detail. It is well known that bone age is superior to chronological age for determining biological and structural maturity; for decades, pediatricians have relied on plain films of the wrist and hand for assessing bone age in children (e.g. Greulich & Pyle Atlas, Tanner Whitehouse Method). However, some have proposed new approaches with greater accuracy and reliability across all ages and ethnic groups. Here, we present a new standardized radiographic dimension, CRD, as a tool to assess developmental maturity, which can be readily obtained from standard medical imaging platforms.
Methods & Materials: X-rays of the elbow were systematically searched in the electronic medical record at a single institution from a 15-month period (June 1, 2017 – Sept 30, 2018). Inclusion criteria included patients <18 years of age with plain films in anteroposterior (AP) and lateral views. Patients with radial head dislocation, displaced supracondylar fractures, or a history of dysplasia were excluded. Follow up images were also excluded. CRD values, measured as closest linear distance from the humeral capitellum to the radial head, were measured by a staff radiologist. P-values <0.5 using a two-tailed Student's t-test were deemed to be statisticallysignificant.
Results: 75 patients ages 3 months to 18 years were included in the study. 45 were male (mean age=10 yrs, range=24 mo-18 yrs) and 29 were female (mean age=9 yrs, range=3 mo-17 yrs).CRD decreased with age, with the most significant drop off observed after age 5, when most patients developed a radial head ossification center. Mean AP CRD for ages 5 and below was 7.25 mm [SD ±1.54 mm], while mean AP CRD for ages 6 and above was 3.41 mm [SD ±0.81 mm] (P <0.0001).
Conclusions: The standard for determining developing skeletal maturity has historically involved X-rays of the hand and wrist. However, these methods have shown inconsistency across certain age groups and ethnic groups. Here, we present another radiographic measurement to aid in the determination of skeletal maturity. CRD proves to have a strong negative curvilinear relationship with increasing age, particularly from ages 3 months to 5 years, before many healthy patients have developed a radial head ossification center and thus demonstrate largest CRD values. Knowledge of this measurement will aid diagnosis of radial head subluxation.

Poster #: SCI-045

Mycobacterium bovis osteitis following immunization with Bacillus Calmette-Guérin (BCG): Clinical and Imaging Characteristics

Jung-Eun Cheon, *cheonje@snu.ac.kr*; Eun Hwa Choi, MD, Won Joon Yoo, MD, Young Hun Choi, In-One Kim, Woo Sun Kim; Radiology, Seoul National University College of Medicine, Seoul, Korea (the Republic of)

Disclosures: All authors have disclosed no financial interests, arrangements or affiliations in the context of this activity.

Purpose or Case Report: Mycobacterium bovis BCG osteitis, a rare complication of BCG vaccination. The aims of this study were to evaluate the clinical and imaging characteristics of BCG osteitis.
Methods & Materials: Twenty children with BCG osteitis at the Seoul National University Children's Hospital from January 2007 to March 2018 were included [M:F=13:7, median age at symptom onset:15 months (range: 7-34 months)]. M. bovis BCG osteitis was confirmed by multiplex PCR in the affected bone. BCG immunization status, clinical information, radiological findings [plain radiography and MRI (all), ultrasonography (n=9), and CT (n=1)] were reviewed retrospectively.
Results: Most common presenting symptoms were soft tissue swelling and pain (n=13, 65%) while fever was accompanied only in three patients (15%). Median duration of symptom was 1 month (range: 2 days-3 months). Leukocytosis and elevation of C-reactive protein (CRP, > 0.5 mg/dL) were depicted in three (15%) and seven patients (35%), respectively. Sixteen children (80%) received Tokyo-172 vaccine by percutaneous multiple puncture method, three (15%) and one (5%) received intradermal Tokyo-172 and Danish strain, respectively. Distal femur (n=7) was the most frequently involved site followed by tarsal bones (n=4), proximal tibia (n=2), distal humerus (n=1), distal radius (n=1), sternum (n=1), rib (n=1) and proximal phalanx of big toe (n=1). Epiphyseal involvement of the long tubular bones were seen in seven patients (35%). Multiple bone lesions were depicted in two patients. Plain radiography showed ill-defined osteolytic lesion with cortical disruption in 13 patients. MRI showed central necrosis in the involved marrow cavity with cortical destruction and cold abscess formation in 14 patients (70 %). Surgical drainage was performed in 19 patients (95%), and half of them required repeated surgical interventions due to recurrent infection. Antituberculosis medications were administered for a median duration of 12 months (range, 12-31 months).
Conclusions: BCG osteitis in immunocompetent children is a rare but serious complication of BCG immunization. High level of suspicion of BCG osteitis based on clinical and radiological manifestations is important for early diagnosis and prompt management.

Poster #: SCI-046

Automated analysis of bone health and bone age from hand radiograph in children with Duchenne muscular dystrophy

Jonathan Bowden, *bowdenjon01@gmail.com*; Sasigarn Bowden, Brent Adler, MD, Houchun Hu, PhD, Rajesh Krishnamurthy, Ramkumar Krishnamurthy, PhD; Radiology, Nationwide Children's Hospital, Columbus, OH

Disclosures: All authors have disclosed no financial interests, arrangements or affiliations in the context of this activity.

Purpose or Case Report: Children with Duchene muscular dystrophy (DMD) have increased risk for osteoporosis and fragility fractures due to progressive muscle weakness with eventual loss of ambulation and chronic corticosteroid therapy. Their fracture prevalence is 40-60%, and increases with age. Bone Mineral Density (BMD) is not reflective of fracture risk. Recent studies showed that cortical thickness and area were associated with increased facture risk. Digital X-ray measurement of the cortical thickness of the metacarpal bones can be used as a marker for metacarpal cortical health. To our knowledge, this marker of bone health has not been evaluated in DMD patients. The purpose of this study was to assess bone age (BA), cortical thickness and area of metacarpal bones in relation to age in children with DMD.
Methods & Materials: In this retrospective IRB approved study, 47 boys (age range: 3-17 years; mean:11.9 ± 4.5 years) with DMD who had a bone age radiograph was included. Automated determination of bone age, and cortical bone density expressed as Bone Health Index (BHI) were performed using BoneXpert (Visiana, Holte, Denmark). Validation of bone age from Bonexpert has been performed extensively before. Z-scores were computed for bone age and BHI, and age-related changes were noted. Pearson's correlation coefficient (r) was calculated for each metric in comparison to age.
Results: The mean z scores of bone age and BHI reduced significantly with age. Z-scores for BA and BHI were: 1) 5-8 years (n=7), BA:-0.51; BHI: -1.17; 2) 8-11 years (n=14), BA: -1.17; BHI: -1.78; 3) 11-15 years (n=21), BA: -2.36; BHI: -1.745; 4) 15-17 years (n=4), BA:-3.77, BHI:-2.46. The Pearson's r = -0.47 for BA and r = -0.36 for BHI (reduces with age, $p<0.005$). The actual BHI with age was: 1) 5-8 years BHI: 3.86 ± 0.38; 2) 8-11 years; BHI: 3.83 ± 0.35; 3) 11-15 years BHI: 3.76 ± 0.95; 4) 15-17 years ; BHI: 3.84 ± 0.32
Conclusions: We showcase a new metric that looks at bone health in DMD children, and demonstrate a worsening BHI with age in DMD patients. BHI may have values in assessment of bone health in children with DMD. The worsening BHI with increasing age may correlate with increased fracture risk that is known to increase over time due to disease progression and longer corticosteroid exposure. Future study is needed to determine the association of BHI and fracture risk.

Poster #: SCI-047

3D Printed Patient Specific Surgical Guides for Pediatric Orthopedic Tumor Resection

Jayanthi Parthasarathy, B.D.S, MS, PhD.D.S., *Jayanthi.Parthasarathy@NationwideChildrens.org*; Thomas Scharschmidt, MD, FACS, MBOE, Mitchell Rees, Bhavani Selvaraj, MS; Radiology, Nationwide Children's Hospital, Columbus, OH

Disclosures: Thomas Scharschmidt, MD, FACS, MBOE: Consultant, Honoraria: Stryker Orthopaedics. All other authors have disclosed no financial interests, arrangements or affiliations in the context of this activity.
Purpose or Case Report: We describe a process for pre-operative virtual surgical planning and creation of patient specific surgical guides for bony tumor resection in pediatric orthopedic surgery and demonstrate a case in which this process was used for successful surgical guidance.
Methods & Materials: Herein we describe the general process for creating a virtual surgical plan (VSP) and show an example of a scapula tumor resection aided by a 3D printed surgical guide.First, a virtual 3D model of the bony anatomy is reconstructed using pre-operative CT scan images.MRI sequences that clearly delineate the tumor margins then are chosen to reconstruct the tumor.Using segmentation, region growing and 3D modeling algorithms of MIMICS™ (Materialise,Belgium), 3D models of the region of

interest (ROI) are created.The CT and MRI sequences are fused using the image registration algorithms in MIMICS™.VSP and creation of patient specific surgical guides:The registered 3D models are imported into Geomagic Freeform (3D systems,SC,USA).The program has a force feedback haptic phantom and tools for cutting, moving, rotating, and creation of offsets, etc. Resection(osteotomy)planes are created on the model after due consideration of the safety margin required for the type of tumor,blood vessels in the line of osteotomy, preservation of musculoskeletal function, and any other clinical requirements of the surgeon.The planes are then used to cut the models, simulating the surgical procedure.Open type or closed guides are created depending on the anatomical location,tumor type,surgical plan and surgeon's preferences.Guides are designed as an offset of the remaining normal bone along the osteotomy plan. Screw holes for fixing the guide to the anatomical region of resection are provided.Bone thickness in the ROI is provided ahead of surgery for appropriate planning and preparedness.3D Printing:Designed guides are 3D printed with autoclavable materials such as DentalSG™resin,ULTEM 9085, and Polyamide or with MED610–Sterrad sterilization.Patient specific surgical guides so produced are used in the sterile field and fitted on the ROI.The VSP resection plan is transferred to the OR and executed precisely.
Results: We utilized this procedure for successful resection of Ewing's Sarcoma of the scapula in a 12-year-old, preserving as much of the patient's native scapula as safely feasible.
Conclusions: This process can lead to better safety and quality procedures, eventually leading to better clinical outcomes.

Poster #: SCI-048

Can zone of provisional calcification (ZPC) imaging predict physeal outcome after fracture?

Deborah Brahee, *Deborah.Brahee@cchmc.org*; Andrea Chan, Kathleen H. Emery, Roger Cornwall, Thomas Maloney; Cincinnati Children's Hospital Medical Center, Cincinnati, OH

Disclosures: All authors have disclosed no financial interests, arrangements or affiliations in the context of this activity.

Purpose or Case Report: Physeal injuries can result in premature physeal fusion. MR imaging is useful for mapping these bony physeal bridges. Resection of the bony bridge does not reliably restore normal physeal function. We have observed subtle loss of the normal low signal intensity line of the zone of provisional calcification (ZPC) extending beyond areas of physeal bar formation in some patients with prior growth plate fractures. This loss is a marker of disrupted endochondral ossification and likely reflects a more extensive region of physeal damage that might be used to better predict treatment outcomes. Given the subjectivity of visual ZPC assessment, we sought to develop a quantitative 3D map of the periphyseal area of the distal radius using a high resolution 3D fast/turbo spin echo sequence.
Methods & Materials: Evaluation of two patients' wrist MRI was performed retrospectively with IRB approval. One patient had a prior Salter–Harris type II fracture of the distal radius with a bony bar while the second had a normal wrist MRI performed for non-traumatic reasons.We developed a program to quantify the MRI signal intensity of the periphyseal region in cross section using a semi-automated approach to provide a more accurate assessment of loss of the ZPC. The normally continuous higher signal band of healthy distal radial physeal cartilage adjacent to the normal low signal intensity ZPC was assessed and compared to the normal distal ulnar periphyseal region. Signal metrics and periphyseal 3D signal maps were obtained. These were evaluated and compared.
Results: Four signal metrics were calculated producing associated signal maps that were color coded: Difference in signal minimums, peak minus minimum ratio, slope of minimums and voxel distance from ZPC to peak. Comparisons were made between the distal radius and ulna and between the 2 subjects with fracture and normal wrist. Signal maps demonstrated visually detectable differences that correlate with loss of the ZPC surrounding the physeal bridge versus normal radius and ulna.
Conclusions: Quantifiable changes in the ZPC can be demonstrated with this model. The model will be applied to MRI's in patients with prior growth plate fractures and compared with clinical outcomes to determine its utility in providing a more complete assessment of physeal function.

Poster #: SCI-049

Quantitative MRI for Bone Marrow Fat Fraction to Differentiate Malignant versus Non-Malignant Marrow

Jonathan Samet, MD[1], *jsamet@luriechildrens.org*; Kristian Schafernak[2], Nicoleta Arva[1], Jie Deng[3]; [1]Medical Imaging, Ann & Robert H. Lurie Children's Hospital of Chicago, Chicago, IL, [2]Phoenix Children's Hospital, Phoenix, AZ, [3]Rush University Medical Center, Chicago, IL

Disclosures: All authors have disclosed no financial interests, arrangements or affiliations in the context of this activity.

Purpose or Case Report: MRI interpretation of pediatric bone marrow is a challenging task due to the highly variable appearance. The bone marrow composition, especially the cellularity, changes with age, benign and malignant hematologic conditions, medications, among other etiologies. Detection of a marrow replacement process on MRI can be missed even by experienced radiologists. Normal hematopoietic bone marrow from birth to 9 years ranges from 20-40% fat (inversely related to cellularity). In malignant marrow replacement processes such as leukemia, bone marrow is highly cellular and fat percentage is low. Currently, no technique is routinely used in clinical practice to quantify bone marrow fat percentage on MRI.
Methods & Materials: A pilot study of patients with suspected malignant marrow replacement recruited by convenience sampling. MRI and bone marrow biopsy were performed within 8 days of one another. Bone marrow biopsy fat % was averaged between two blinded pathologists. MRI obtained from the suspected area of symptoms and core bone marrow biopsy obtained (as standard of clinical care) from the iliac crest. The MRI technique used was the Dixon technique with fat and water separation. Fat fraction is calculated based on the ratio of fat and water proton density. MRI was considered predictive of malignancy if fat fraction % was less than 20.
Results: Six cases of patients (mean age 7.5y (range 3-14y)) were recruited. Pathologic diagnoses included: leukemia (n=5) or rhabdomyosarcoma (n=1). MRI was performed and analyzed from the: pelvis (n=4), spine (n=1), and elbow (n=1). MRI fat% correlated with pathology, but due to the small sample size was not significant ($r=0.6$, $p=.20$). Inter-pathologist correlation was high ($r= 0.9$, $p<0.05$). Elbow MRI fat% correlated with pathology (76 v. 67.5%), but was falsely negative in predicting leukemia. Of all other locations, mean fat percentage calculated by MRI versus pathology was similar (average± standard deviation, 3.7± 1.3 v 3.0± 3.0).
Conclusions: MRI can help radiologists detect a malignant marrow replacement process with more confidence using the fat fraction technique. Studies are ongoing to compare these cases to control patients.

Poster #: SCI-050

Pediatric Osteomyelitis (OM) Assessment using a Fat Suppressed Dynamic 3D Radial Acquisition: Preliminary Experience

Kathryn S. Milks, MD, *ks.mueller@gmail.com*; Mitchell Rees, Ramkumar Krishnamurthy, PhD, Houchun Hu, PhD, Rajesh Krishnamurthy; Radiology, Nationwide Children's Hospital, Columbus, OH

Disclosures: All authors have disclosed no financial interests, arrangements or affiliations in the context of this activity.

Purpose or Case Report: To determine if a 3-minute Golden-angle RAdial Sparse Parallel (GRASP) dynamic contrast enhanced (DCE) MRI sequence with 8-10 second temporal resolution is equivalent in diagnostic performance to a conventional MR sequences (CS) in the assessment of osteomyelitis (OM) in children.
Methods & Materials: 6 subjects (9m – 23y) with suspected OM were imaged at 3T as part of an IRB-approved study. The scans included both conventional sequences (T1, IR, PD, T2-weighted and T1 fat suppressed postcontrast) for osteomyelitis as well as a 3-minute GRASP DCE sequence that we have been concurrently evaluating in a sheep model. CS were interpreted per clinical standards. GRASP was interpreted independently by 3 radiologists, blinded to CS, and scored with binary (y/n) answers for reporting elements in OM including marrow signal abnormality, synovitis, subperiosteal abscess, intraosseous abscess, soft tissue or muscle hypoenhancement, myositis, and cellulitis.
Results: Average total exam time for CS protocol was 46.2 ± 15.1 minutes. Average additional time for GRASP was 8 ± 5.1 minutes including prescription and scanning. Average slice thickness was 3.2 mm for CS and 1.5 mm for GRASP. CS demonstrated marrow signal abnormality in 4 of 6 cases, attributed to OM in 3, with one case being posttraumatic. Synovitis (n=3), soft tissue hypoenhancement (n=3), myositis (n=2), and cellulitis (n=4) were also identified. There were no cases of intraosseous or subperiosteal abscess. Based on the average sensitivity and specificity of the 3 readers, GRASP was relatively sensitive (83%) and highly specific (100%) in detection of marrow signal abnormality, highly sensitive (100%) and specific (89%) for soft tissue or muscle hypoenhancement, and 100% sensitive and 67% specific for cellulitis. GRASP was less sensitive than CS for detection of synovitis (50%) and myositis (50%), with high specificity (100% and 92% respectively). Locations of disease were concordant across readers and consistent with CS.
Conclusions: Based on preliminary data in this ongoing study, GRASP holds promise for replacing CS in the diagnosis of OM and ultimately reducing sedation. Further analysis is necessary to determine if the addition of a single precontrast fluid sensitive sequence and quantitative DCE curves may provide additional diagnostic benefit.

Poster #: SCI-051

Characterization of T2 Map of Healthy Children and Adolescent Ankle Cartilage Under Altered Magnetic Resonance Image Protocols

Haris Majeed, BSc[1], Marshall Sussman, PhD[2], Brian Feldman[1], **Carina Man[1]**, *carina.man@sickkids.ca*; Victor Blanchette[1], Andrea Doria, MD[1]; [1]Diagnostic Imaging, The Hospital for Sick Children, Toronto, Ontario, Canada, [2]Toronto General Hospital, Toronto, Ontario, Canada

Disclosures: All authors have disclosed no financial interests, arrangements or affiliations in the context of this activity.

Purpose or Case Report: To evaluate the T2 map relaxation times in healthy male children and adolescent ankle cartilage under altered magnetic resonance image (MRI) protocols and to document trends in these T2 relaxation times with varying ages and body mass index (BMI).
Methods & Materials: This cross sectional study recruited 11 healthy male children and adolescents (median age of 14 years; range 8-17 years), who each underwent 3.0 Tesla T2 map MRI examinations of ankle (tibia-talus) using three protocols. Protocol 1 – a single echo spin echo constant TR/TE (TE = 13, 19, 28 ms; TR = 513, 519, 528 ms). Protocol 2 – a multi-echo spin echo (TE = 9.6, 19.2, 28.8 ms; TR = 1000 ms). Protocol 3 (high spatial resolution) – a multi-echo spin echo (TE = 11.1, 22.2, 33.3 ms; TR = 1690 ms). Images were analyzed at sagittal lateral and medial MRI slices using a house-made MATLAB software. A P value less than 0.05 was considered statistically significant.
Results: We found statistically significant negative associations between age and T2 relaxation times of ankle cartilage, ranging from -0.91 ($P < 0.001$) to -0.66 ($P = 0.03$) for all image protocols. Furthermore, statistically significant negative trends of T2 relaxation times for ankle cartilage were found with increasing age, ranging from -2.08 ms/year ($P = 0.006$) to -0.80 ms/year ($P < 0.01$) for all image protocols. Similarly, mean T2 relaxation times were found upon using a constant TR/TE to other image protocols, thus enforcing the generalizability of the protocol. In contrast, weak associations were found between BMI and ankle cartilage T2 relaxation times.
Conclusions: Age plays an important role in understanding cartilage T2 relaxation times. Additionally a TR/TE protocol can be used to help optimize scanning time for children and adolescents.

Poster #: SCI-052

The Role of MR Susceptibility-Weighted Imaging in Acute Pediatric Seizures: in Relation to Electroencephalographic Activities

Yongwoo Kim, *kyw47914@gmail.com*; Jae- Yeon Hwang; Radiology , Pusan National University Children's Hospital, Yangsan, Korea (the Republic of)

Disclosures: All authors have disclosed no financial interests, arrangements or affiliations in the context of this activity.

Purpose or Case Report: To evaluate the relationship between cortical venous signal and electrographic activity in children with seizure using magnetic resonance imaging with susceptibility weighted imaging (SWI) and electroencephalogrphy (EEG).
Methods & Materials: Children presented with seizures, who underwent both SWI and EEG within 12 hours after seizure onset were retrospectively reviewed. An increased signal of cortical veins (SWI+) was assessed using SWI, while abnormal activities such as slowing or epileptiform discharges (EEG+) were investigated on EEG. We defined three groups of patients in accordance to the topographic correlation between SWI+ and EEG+: (A) no increased venous flow and no abnormal discharges, (B) discordant finding between the SWI+ and EEG+ area, (C) concordant distribution between the SWI+ and EEG+ area.
Results: We identified 297 children (194 in group-A, 76 in group-B, and 27 in group-C). The mean age among the three groups was similar (group-A =3.5±4.5 years; group-B = 3.1±3.5 years; group-C = 5.2±5.4 years, p=0.079). Multiple seizures were revealed more frequently in group-C (51.9%) than in group-A (23.7%) or group-B (39.5%, p=0.002). The incidence of newly-diagnosed epilepsy was significantly higher in group-C (20/27, 74.1%, p=0.001) than in group-A (45/194, 23.2%) or group-B (17/76, 22.4%). By contrast, there were no significant

differences in seizure duration and seizure types among the three groups.
Conclusions: Patients with concordant distribution of the findings between SWI and EEG had significantly frequent multiple or epileptic seizures. SWI may be helpful to discover the epileptic focus localization in children with acute seizures.

Poster #: SCI-053

Corpus callosum morphology in children on mid-sagittal MR imaging

Lauren A. Raubenheimer, MBChB[1], *laraubs@gmail.com*
Savvas Andronikou, MBBCh, FCRad, FRCR, PhD (UCT), PhD (Wits)[2], Tracy Kilborn[1]; [1]Radiology, University of Cape Town, Cape Town, Western Cape, South Africa, [2]University of Bristol, Bristol, United Kingdom

Disclosures: All authors have disclosed no financial interests, arrangements or affiliations in the context of this activity.

Purpose or Case Report: There is little published research on the wide variation of corpus callosum (CC) morphology in children, the assessment of which is made difficult by the complex alteration of its appearance in childhood. The purpose of our study was to assess the morphology of the CC on mid-sagittal T1-weighted magnetic resonance imaging (MRI) in a large number of children and correlate the findings with demographic and clinical criteria.
Methods & Materials: We reviewed all mid-sagittal T1-weighted brain MRI's performed from July to December 2015 and obtained relevant demographic and clinical information from the accompanying report and laboratory system. The CC morphology was analysed by three radiologists and compared using cross tabulation with the chi-square test and ANOVA. Interobserver correlation was assessedusing Kappa coefficient of conformance.
Results: 257 children (mean age 72±60 months) were included, (142 male; 55%). In abnormal MRI's the CC was less likely to have an identifiable isthmus and more likely to be convex, thin and have separation of the fornix insertion (all $p<0.01$). In young children (< 5 years) the CC was also less likely to have an identifiable isthmus ($p=0.01$) and was more likely to be convex ($p=0.04$) but the fornix was more likely to insert normally ($p<0.01$).
Conclusions: There is a distinct pathological appearance of the CC. The immature appearance of the corpus callosum can mirror this but is distinguished by normal insertion of the fornix and normal quantitative measurements.

Poster #: SCI-054

Evaluation of lymphocytic thyroiditis in children with quantitative gray-scale ultrasound using a PACS-based tool

Aneliya Maleeva, *aneliyamaleeva@yahoo.com*; Jennifer E. Lim-Dunham, MD, Iclal E. Toslak, MD, Brendan Martin, Phd, Davide Bova, Aishe I. Kilic, Guliz Barkan; Radiology, Loyola Medical Health Care System, Vernon Hills, IL

Disclosures: All authors have disclosed no financial interests, arrangements or affiliations in the context of this activity.

Purpose or Case Report: To evaluate diagnostic performance of quantitative gray-scale ultrasound as an objective method in evaluation of pediatric thyroiditis.
Methods & Materials: In this retrospective study of 37 children with tissue proven diagnosis, two radiologists independently reviewed thyroid ultrasounds twice and subjectively classified images according to presence or absence of thyroiditis. A consensus session was performed for patients for which there was disagreement. Unweighted kappa coefficients were calculated to assess intra- and inter-observer reliability. Pearson chi-square and Fisher's exact tests were used to compare categorical measures by final pathology.A third radiologist performed quantitative measurements of echo-intensity level of the thyroid and adjacent strap muscles from US images using a PACS-based tool. Thyroid /muscle ratio (TMR) was obtained by dividing thyroid mean by muscle mean values. Heterogeneity index (HI) for thyroid was calculated by dividing thyroid SD by thyroid mean values. Wilcoxon Rank Sum tests were used to assess distribution of continuous risk factors by final pathology.
Results: Patient group comprised 29 females and 8 males, with median age 17 years (interquartile range 15-18). By pathology, 19 (51.3%) patients had lymphocytic thyroiditis and 18 (48%) had normal thyroid. For subjective assessment, there was fair inter-observer agreement (kappa .36 (95% CI .14-.57), $p=.004$) and slight intra-observer agreement for each radiologist (kappa .13 and .17, $p>.05$). A large proportion of patients for whom consensus review indicated thyroiditis were confirmed with pathology (12/19 (63%), $p=.03$). For quantitative assessment, no significant difference between thyroiditis and normal thyroid groups was found for either TMR (1.51 and 1.62, respectively, $p=.82$) or HI (.23 and .23, respectively, $p=.37$).
Conclusions: Quantitative gray-scale ultrasound did not accurately diagnose thyroiditis. However, subjective consensus evaluation showed significant correlation with the condition, suggesting that multiple radiologists performing more than one review may be beneficial for accurate diagnosis of thyroiditis in children.

Poster #: SCI-055

Does a decrease in hematocrit predict intracranial hemorrhage on neonatal head ultrasound?

Matthew O. Thompson, MD[1], *matthewthomp@gmail.com*; Joseph Davis, MD[1], Atalie C. Thompson, MD[1], Nathan Hull, MD[2], Gary Schooler, MD[1]; [1]Pediatric Radiology, Duke University, Durham, NC, [2]May Clinic, Rochester, MN

Disclosures: All authors have disclosed no financial interests, arrangements or affiliations in the context of this activity.

Purpose or Case Report: The purpose of this study is to determine whether a decrease in hematocrit is predictive of an intracranial hemorrhage (ICH) on neonatal head ultrasound (HUS).
Methods & Materials: This is a retrospective study of 136 neonatal HUS between 2005 and 2017 at a single institution. The indication for the HUS was categorized as being related to hematocrit (e.g. "drop in hematocrit") or unrelated to hematocrit. The medical record was also reviewed for the change in hematocrit in the 48 hours prior to HUS, a decrease in hematocrit, gestational age, number of days since birth, prematurity, and abnormal neurologic exam. The association between these variables and the presence or absence of hemorrhage on the HUS was analyzed using STATA 12.1.
Results: Twenty-one percent (N=29/136) of neonates had an ICH on their HUS. Studies that were ordered with an indication related to hematocrit were less likely to have an ICH on HUS compared to those with alternative indications for the study (odds ratio 0.35, $p=0.018$). The mean change in hematocrit ($p=0.95$), a decrease in hematocrit ($p=0.30$), and an abnormal neurological examination ($p=0.25$) were not associated with ICH on HUS. However, a lower gestational age (mean difference 4.47, $p<0.001$) and number of days since birth (mean difference 25.1, $p=0.01$) were both significantly predictive of ICH. Those with an ICH were also three times more likely to be premature, though this association was only borderline significant (odds ratio 3.03. $p=0.09$).

Conclusions: A decrease in hematocrit in the preceding 48 hours is not predictive of an ICH on neonatal HUS. Those with ICH on HUS had a significantly lower gestational age and were more likely to be born premature.

Poster #: SCI-056

Regional Differences in Paranasal Sinus Mucosal Thickening: Implications For Neutropenic Febrile Children

Susan E. Schmidt, MD, *sschmidt916@gmail.com*; Joseph Cao, Cory Pfeifer; Radiology, UTSW, Fort Worth, TX

Disclosures: All authors have disclosed no financial interests, arrangements or affiliations in the context of this activity.

Purpose or Case Report: The diagnostic approach to fever of unknown origin (FUO) in a neutropenic child is challenging. Recommendations of the Children's Oncology Group and the ACR provide some guidance, but evidence basis for use of sinus CT in the acutely febrile neutropenic child is poorly established. This presentation assesses baseline paranasal sinus mucosal thickening in children in 2 separate cities and compares them to children with neutropenia undergoing sinus CT in the work-up of FUO.
Methods & Materials: Data collected from 2 large children's hospitals in major metropolitan cities in the southern US. Hospital A is in a desert climate, Hospital B is in a humid subtropical climate. 18 consecutive sinus CTs were reviewed in neutropenic children undergoing diagnostic evaluation for FUO at Hospital A. Bone marrow transplant patients were excluded. All children were oncology patients undergoing treatment. Control groups used include 18 consecutive patients at hospital A and 18 consecutive patients at hospital B who presented to the ED requiring CT of the face. Control patients with a history of sinusitis, patients with a facial bone fracture, and patients with any oronasal support devices were excluded. No exams of neutropenic fever patients at hospital B were available, hospital B uses nasal endoscopy to assess for sinus disease in this population. Lund-Mackay (L-M) and modified Lund-Mackay scores were applied to all CT scans.
Results: The mean age in the neutropenic fever group was 9.86 years. The mean ages of hospital A and B control groups were 8.16 and 8.34 years, respectively. Age differences were not significantly different using a Student t-test. LM scores in the hospital A control group exhibited a mean of 5.50 with a mean modified-LM score of 6.92. Corresponding values in the hospital B control group were 3.11 and 4.00, respectively. In the neutropenic fever group of hospital A, the mean LM and modified-LM scores were 4.17 and 4.59, respectively. Findings viewed as "positive" in the neutropenic fever group resulted in 2 infectious disease and 2 ENT consults. All 4 consults concluded that fever was unlikely to be due to paranasal sinus disease, no intervention recommended.
Conclusions: Mucosal sinus thickening is omnipresent in children and can vary based on region. Baseline paranasal sinus mucosal thickening is greater among children living in a desert climate. The description of paranasal sinus mucosal thickening in neutropenic children may be of little value in the approach to fever without source.

Poster #: SCI-057

Variation In Conspicuity Of Focal Cortical Dysplasias And Its Effect Upon Ease Of Detection

John Vu, MD, MPH, *johntdvu@gmail.com*; Matthew Parsons, Markus Zei, MD, Aseem Sharma, MD; Mallinckrodt Institute of Radiology, Saint Louis, MO

Disclosures: All authors have disclosed no financial interests, arrangements or affiliations in the context of this activity.

Purpose or Case Report: Detection of focal cortical dysplasias (FCDs) can be challenging. Our aim was to evaluate quantitative contrast differences between FCDs and the mirror-location normal gray matter, and the effect thereof on the ease of detection by radiologists.
Methods & Materials: Coronal FLAIR and T1WI of 20 pathology proven cases of FCD, including 11 cases where the diagnosis was missed on the initial review, were analyzed. CNR and conspicuity differences between gray matter within FCDs and contralateral mirror image locations were calculated using manually drawn ROIs. Similar calculations were made in 20 age and gender matched controls for lateralized differences in normal gray matter at locations equivalent to those of FCDs.
Results: On FLAIR images, median (25^{th} percentile, 75^{th} percentile) CNR and conspicuity for FCD was 11.3 (8.5, 20.9) and 10.2 (7.1, 15.4), significantly higher than corresponding CNR of 1.0 (-0.2, 5.5) and conspicuity of 0.8 (-0.2, 2.8) for controls ($p<0.0001$ for both). Similarly, CNR and conspicuity for FCD was also higher than controls on T1WI ($p<0.0001$). Subgroup analysis showed that these differences from normal were maintained irrespective of FCD detection or lack thereof at the initial review. Median CNR and conspicuity on FLAIR ($p = 0.79$ and 0.07 respectively) and T1WI ($p = 0.64$ and 0.76 respectively) were not significantly different for FCD cases that were detected and those that were missed on the initial review.
Conclusions: Focal cortical dysplasia lesions have significantly higher CNR and conspicuity relative to mirror-location gray matter when compared to age and sex matched controls. These differences exist even in cases that were missed at the time of initial review. Accentuation of such differences may serve as a means to improve detection of FCDs.

Poster #: SCI-058

Fidelity of 3DPrinted patient specific functional brain models from multi sequence MRI and their clinical utility in pediatric epileptic patients with focal lesions

Jayanthi Parthasarathy, B.D.S.,M.S.,PhD, *Jayanthi.Parthasarathy@NationwideChildrens.org*; Satya Gedela, Adam Ostendorf, Jonathan Pindrik, jeremy Jones, MD, Aaron S. McAllister, MD, Bhavani Selvaraj, MS, Alexander Long, Bachelors; Radiology, Nationwide Children's Hospital, Columbus, OH

Disclosures: Aaron S. McAllister, MD: Equity Interest/Stock Option: GE, MMM, CHD, JNJ. All other authors have disclosed no financial interests, arrangements or affiliations in the context of this activity.

Purpose or Case Report: Establish and evaluate a process for 3DPrinting (3DP) patient specific functional anatomical models of the brain from multiple MRI sequences in patients with epileptic focal lesions.The second objective was to evaluate the clinical utility of the models.
Methods & Materials: Eight patients with intractable epilepsy and focal lesions in the brain were selected for the study.**Data acquisition:**T1 and T2 weighted MR images with DTI fiber

Tractography were acquired on GE Medical systems, Siemens Prisma and Skyra MRI scanners with a field strength of 3 TESLA.Slice thickness range-1.00-1.6mm and the slice increment was 0.5-1mm.**Image data processing:**Using the segmentation,region growing and 3D modeling algorithms of MIMICS™(Materialise, Belgium)3D virtual models of the structural anatomy of the affected hemisphere and the lesion were created. DTI fiber tracts and the vasculature were segmented from Dynasuite™(InvivoInternationalUSA)and exported as DICOM data.3D models of the vasculature and the DTI FIBERs were created and integrated into the structural model of the brain.**3DPrinting:**After preprint preparation the with Geomagic Freeform(3Dsystems,SC,USA)the model were printed with Stratasys PolyjetCONNEX 3 Objet 350 multicolor printer.Models were post processed with high-pressure waterjet.**Model verification:The 3DP models were scanned with** Toshiba Aquilion CT scanner with a slice thickness and slice increment of 0.5mm.The Dicom image data was imported into MIMICS™ and a 3D model created.The model so created was overlayed on the virtual model created from the MRI data. Surface variation of the 3DP model and the virtual model created from MRI data was mapped with 3Matics™.Models were resliced into 2D contours and overlayed on the MRI image dataset for verification.3DP models of the brain were used for team discussion,resident and fellows and patient education of the specific neuro anatomy.
Results: Comparative analysis of the CT 3DP model and the 3D models created from 2D MRI image data showed a mean difference of -0.36 mm with STD Dev.+/-0.5mm.
Conclusions: Precise patient specific functional anatomic brain models can be created from multiple MRI sequences using 3D modeling and Polyjet printing. 3DP patient specific models are a valuable adjunct to neurosurgical planning. Brain models help surgeons to educate the patients, parents, residents and fellows to understand neuroanatomy better.Parents understand the clinical situation and suggested treatment implications better and give better informed consent.

Poster #: SCI-059

Complex-Valued Convolutional Neural Networks for MRI Reconstruction

Elizabeth Cole, *ekcole@stanford.edu*; John Pauly, PhD, Shreyas Vasanawala, MD/PhD, Joseph Y. Cheng, PhD; Electrical Engineering, Stanford University, Stanford, CA

Disclosures: Shreyas Vasanawala, MD/PhD: Arterys, Royalty: Arterys, GE Healthcare, Siemens, Philips, Research Grants: GE Healthcare; **Joseph Y. Cheng, PhD:** Consultant, Honoraria: HeartVista, Inc., Research Grant: GE Healthcare. All other authors have disclosed no financial interests, arrangements or affiliations in the context of this activity.

Purpose or Case Report: Convolutional neural networks (CNNs) have proven to be valuable in the fields of image processing and computer vision. Our work applies complex-valued CNNs to magnetic resonance imaging (MRI) to reduce scan times. The reduction of scan times has widespread pediatric benefits. A typical scan requires that patients remain still for up to an hour to produce a clear image, which is difficult for children without inducing anesthesia, which carries risks. A need exists for greatly improved MRI scan times without the loss of diagnostic accuracy. This scan time can be reduced by subsampling in k-space. We use CNNs to reconstruct images from these undersampled acquisitions. Our work investigates complex-valued CNNs for image reconstruction in lieu of two-channel real-valued CNNs.
Methods & Materials: Recent work suggests complex-valued CNNs could be more accurate than real-valued CNNs when dealing with complex-valued data. Typically, complex-valued data is fed into CNNs by using a 2-channel architecture where the channels contain the real and imaginary components of the data. This does not preserve phase information, which is valuable for many MRI applications. Recent work in applying complex-valued CNNs to music transcription and speech prediction tasks demonstrates complex-valued models are highly competitive with their real two-channel counterparts (Trabelsi et al., 2018). Complex-valued neural networks have been applied to MRI fingerprinting with improvements in accuracy in comparison to real models (Virtue et al., 2017).We apply complex-valued CNNs to subsampled image reconstruction by modifying components of our current CNN within our deep unrolled architecture to be complex-valued. We perform complex convolution and explore various complex-valued activation functions which keep the pre-activated phase intact, as well as activation functions which are based on the phase component. We evaluate the performance in terms of accuracy of this complex model compared to its real counterpart.
Results: We trained two otherwise identical CNNs with real-valued convolution and complex-valued convolution, and approximately 900K trainable parameters each. The validation loss was 0.693 and 0.639, respectively. This shows complex-valued networks have the potential to be much more accurate than their real-valued counterparts.
Conclusions: Our work shows potential for reducing MRI scan times by more accurately reconstructing images from subsampled data acquisitions using complex-valued CNNs.

Poster #: SCI-060

Impact of diffusion-weighted sequences in ^{18}F-FDG PET/MR whole-body pediatric oncologic imaging

Vanessa Sanders, *vrsanders@wustl.edu*; Geetika Khanna, Joyce Mhlanga, MD, Maria R. Ponisio, MD; Mallinckrodt Institute of Radiology, St. Louis, MO

Disclosures: Geetika Khanna, MD, MS: Financial Interest: Elsevier - Royalty: Independent contractor. All other authors have disclosed no financial interests, arrangements or affiliations in the context of this activity.

Purpose or Case Report: To determine if diffusion weighted imaging (DWI) adds value to PET/MRI in pediatric solid tumors.
Methods & Materials: After obtaining IRB approval, all pediatric simultaneous PET/MR studies with DWI performed between April 2015 and August 2017 were concurrently interpreted by 2 blinded readers (board certified pediatric and nuclear medicine radiologists) in 2 sessions. In session 1, the 2 readers had access to whole body PET, Dixon, and HASTE images. Images were assessed for quality, number and location of lesions, designation as malignant or not. After 6 weeks, in session 2 the above images were re-reviewed by same readers with DWI added, for the above assessment with the added value of DWI. The results of the two sessions were compared by an independent reviewer.
Results: PET/MR with DWI was available in 20 cases (10 boys), age range: 5 months-18 years (median 10.7 years). Tumors included: rhabdomyosarcoma (6), Ewing sarcoma (4), neurofibromatosis-1 (5), post-transplant lymphoproliferative disease (2), clear cell renal carcinoma (1), squamous cell carcinoma (1), and neuroblastoma (1). A total of 44 lesions were identified in session 1; 23 designated malignant and 21 benign. DWI did not detect any additional distant foci of disease in session 2. No change in final diagnosis or local extent of disease was noted in 19/20 cases. In one patient with Ewing sarcoma the local extent of osseous tumor was greater with DWI than with PET.

Conclusions: Diffusion weighted imaging had no impact on distant staging in our pediatric cohort, but may add value in local staging. Routine performance of whole body DWI can be eliminated and limited to the region of interest in pediatric patients undergoing PET/MRI to improve patient throughput.

Poster #: SCI-061:

Ultrasensitive detection of translocations in the cell free DNA of pediatric sarcoma patients

Heike E. Daldrup-Link, MD, PhD[1], Avanthi Shah, MD[2], **Frederick M. Wittber, MD[1]**, *fwittber@stanford.edu*; Tej Azad[1], Jake Chabon[1], Stan Leung[2], Aviv Spillinger[2], Heng-Yi Liu[2], Marcus Breese[2], Maxamilian Diehn[1], Ash Alizadeh[1], Alejandro Sweet-Cordero[1]; [1]Radiology, Stanford, Palo Alto, CA, [2]UCSF, San Francisco, CA

Disclosures: All authors have disclosed no financial interests, arrangements or affiliations in the context of this activity.

Purpose or Case Report: Currently, biopsy serves as the gold standard to accurately diagnose disease in pediatric sarcoma patients, but the risks of anesthesia and surgery, along with a failure to characterize the true heterogeneity of disease make this method less than ideal. Progression and response to therapy are monitored by radiologic exams which lack the sensitivity to detect early relapse. Cell free DNA (cfDNA) is released into the plasma as they undergo apoptosis and necrosis. ctDNA represents a small fraction of cfDNA in cancer patients and contains tumor specific alterations. It holds promise as a highly sensitive and specific biomarker. A limitation in applying liquid biopsy in clinical practice is the need to develop PCR or other DNA analysis methods to detect alterations specific to a single patient. We have developed a more widely applicable off the shelf test that does not involve a patient specific design.
Methods & Materials: Our CAPP Seq technique involves designing a selector comprised of custom designed oligonucleotide probes that tile across genomic regions of interest. These oligonucleotide probes are used to enrich for the relevant ctDNA via hybrid capture, followed by ultra deep sequencing to analyze alterations in the selected regions. Our selector was applied to pretreatment plasma samples from newly diagnosed or newly relapsed pediatric sarcoma patients. Plasma samples were analyzed at key timepoints over the course of treatment.
Results: Pediatric sarcoma patients had higher levels of cfDNA when compared to published levels in adult cancer patients. Canonical translocations were detected in the plasma of 13/14 (93%) pediatric sarcoma patients. This was confirmed by analysis of matched tumor samples, when available. Patients with metastatic disease had higher ctDNA levels compared to nonmetastatic patients. ctDNA levels correlated with clinicalcourse and, in some cases, rising ctDNA levels predicted relapse, earlier than was clincally apparent by imaging studies.
Conclusions: ctDNA analysis holds promise as an ultrasensitive and specific tool for monitoring tumor burden. Our assay was able to detect ctDNA in the plasma of metastatic and nonmetastatic pediatric sarcoma patients at diagnosis. Furthermore, we demonstrated that ctDNA levels correlated with clinical response to therapy. In some cases, ctDNA levels proved more sensitive than imaging, detecting minimal residual disease andpredicting relapse.

Poster #: SCI-062

Pediatric Nuclear Medicine After Hours: Exploring the Need for On-Call Nuclear Medicine Training

Jennifer Gillman[1], *jennifer.gillman@uphs.upenn.edu*; Janet R. Reid, MD, FRCPC[2], Sabah Servaes[2], Hongming Zhuang[2], Lisa States[2]; [1]Diagnostic Radiology, Hospital of the University of Pennsylvania, Philadelphia, PA, [2]Children's Hospital of Philadelphia, Philadelphia, PA

Disclosures: All authors have disclosed no financial interests, arrangements or affiliations in the context of this activity.

Purpose or Case Report: Experience in pediatric nuclear medicine is limited and not uniform across residency and pediatric fellowship training programs. At our tertiary care pediatric hospital, emergent nuclear medicine exams performed after hours are currently read by radiologists with expertise in pediatric nuclear medicine. A decision to shift this responsibility to in-house faculty has prompted creation of a continuing medical education (CME) learning module as part of an institutional comprehensive learning management system (LMS). The goal of this module is to train faculty, fellows and residents in the indications, protocols, diagnostic criteria, potential pitfalls and problem-solving techniques when reading emergent pediatric nuclear medicine exams. The purpose of this study is to better understand the volume of nuclear medicine cases on-call and the potential need for a dedicated pediatric nuclear medicine curriculum.
Methods & Materials: All nuclear medicine gastrointestinal bleeding scans, Meckel's scans, hepatobiliary scans for biliary leak or acute cholecystitis, brain death scans and renal transplant evaluations performed between July 1, 2017 and June 30, 2018 were reviewed. Exams ordered after 4:30 PM on weekdays or performed on weekends were considered call studies. Faculty were surveyed to assess length of time since reading each type of scan, as well as their level of comfort protocolling and interpreting studies.
Results: Case review revealed 54 emergent pediatric nuclear medicine studies with 13 (24.1%) read after hours. Of all studies performed, 28.6% of gastrointestinal bleeding studies (n= 2/7), 16.7% of Meckel's scans (n= 5/30), 22.2% of brain death studies (n = 2/9), 33.3% renal transplant scan (n=1/3), 75.0% of acute cholecystitis scans (n=3/4) and 0% of biliary leak scans (n=0/1), were read on-call. 19 (70.4%) of 27 faculty members who take call completed the survey. At least 63.2% have not read any of these types of nuclear medicine study since residency/fellowship or not at all. The percentage of those uncomfortable protocoling studies ranges from 73.7% to 89.5%, greatest with renal scans. The percentage of those uncomfortable interpreting studies ranges from 47.4% to 84.2%, greatest with renal scans.
Conclusions: Even in large academic centers, there is a limited number of radiologists with expertise in pediatric nuclear medicine, making call coverage challenging. There is a need for continued training to provide important emergent nuclear medicine studies for patients after hours.

Poster #: SCI-063

Does a skeletal survey detect additional bone lesions of Langerhans Cell Histiocytosis in children undergoing 18F-FDG Positron Emission Tomography-Computed Tomography?

Rosemond N. Aboagye, BSc Med Sci, MB ChB, *rosemondhammond@yahoo.com*; Lydia M. Bajno, MD, Helen R. Nadel, MD FRCPC, James E. Potts, PhD, Heather Bray, MD; Radiology, BC Children's Hospital, Vancouver, British Columbia, Canada

Disclosures: All authors have disclosed no financial interests, arrangements or affiliations in the context of this activity.

Purpose or Case Report: **Purpose:** ^{18}F-FDG Positron Emission Tomography (PET-CT) has been shown to be superior to other imaging modalities in assessment of soft tissue involvement with Langerhans Cell Histiocytosis (LCH) and is now commonly included in the staging workup of LCH. Our purpose is to analyze the utility of skeletal survey in addition to PET-CT scan for detecting bone lesions in children with LCH and to evaluate if skeletal survey can be eliminated from the staging workup of LCH in order to reduce radiation exposure.
Methods & Materials: This is a retrospective study of patients with biopsy-confirmed LCH diagnosed and treated at a tertiary care children's hospital between 2013 and 2018. The medical records, skeletal survey and PET-CT imaging records for staging and follow-up studies were reviewed. The distribution and number of LCH lesions on both skeletal survey and PET-CT were documented from our institution's PACS. Any reports with insufficient information or ambiguity were re-evaluated by a Pediatric Radiologist. Demographic information was recorded and the concordance between lesions seen on the skeletal survey and/or PET-CT scan was calculated.
Results: Data from 10 children (60% female) with a median age of 4.6 years (range from 1 year 7 months to 15 years, 1 month) are reported. A total of 53 lesions in 40 different bones were evaluated. Forty-nine per cent of all lesions were identified on both PET-CT and skeletal survey. PET-CT identified an additional 34% of lesions not seen on skeletal survey, while skeletal survey identified 17% of lesions not seen on PET-CT. There were 9 calvarial lesions, all identified on skeletal survey while only 4/9 were identified on PET-CT scan. The median interval between the skeletal survey and PET-CT scan was 2.5 days (1-15 days).
Conclusions: Skeletal survey continues to be important in the evaluation of LCH patients, especially when assessing lesions involving the calvarium. This may, in part, be due to the thickness of the PET-CT slices reducing lesion conspicuity and the marked avidity of the brain parenchyma on PET-CT obscuring lesions within the calvarium.

Poster #: SCI-064

mIBG optimized SPECT/CT improves interpretation and Curie score assignment

Melissa C. Kong, James E. Potts, **Helen R. Nadel, MD FRCPC**, *hnadel@stanford.edu*; BC Children's Hospital, Vancouver, British Columbia, Canada

Disclosures: All authors have disclosed no financial interests, arrangements or affiliations in the context of this activity.

Purpose or Case Report: In the past, neuroblastoma patients frequently had mIBG and diagnostic CT scans performed at separate times. This practice sometimes caused issues in correlating findings from the two imaging modalities. A retrospective review of our entire experience aimed to confirm the added value of optimized co-registered contrast-enhanced diagnostic CT to I-123 mIBG SPECT/CT protocol in children with neuroblastoma. An additional objective was to identify if SPECT/CT improved Curie score assignment vs planar imaging.
Methods & Materials: We previously reported on a limited recent experience of optimized mIBG SPECT/CT. We have now completed a retrospective review of 384 SPECT/CT scans of pediatric neuroblastoma patients (aged 0 to 18 years) performed from April 2007 to June 2018. Added value of the co-registered CT was categorized as providing: increased sensitivity, improved localization, improved tumour delineation, improved differentiation between malignant and physiological or benign findings, detection of additional incidental findings, and/or no additional value when fused with the I-123 mIBG scintigraphy. Chi-square tests were performed to assess differences between diagnosis vs follow-up scans with added value from the co-registered CT. Curie score evaluation was performed using planar and SPECT/CT imaging.
Results: Of all assessed scans, 70% of co-registered contrast-enhanced diagnostic CT studies performed as part of the SPECT/CT scan provided added value (87% of staging scans at diagnosis (n=47), 67% in follow-up (n=337)). Overall, use of co-registered CT enhanced diagnostic sensitivity, tumour localization and delineation, and differentiation of malignant versus benign findings in many cases, and also identified additional incidental findings. Curie score assessment was improved in areas of equivocal lesions involving mainly the torso and particularly on follow-up examinations.
Conclusions: Optimized mIBG SPECT/CT can reduce the need for additional imaging studies by improving accuracy of disease characterization and Curie score.

Poster #: SCI-065

The value of physical and psychological distraction methods in reducing pain in paediatric nuclear medicine procedures.

Mandy L. Kohli, BASc, M.R.T(N), *mandy.kohli@sickkids.ca*; Reza Vali, Afsaneh Amirabadi, Caroline Frankfurter Frankfurter, Ontario, Amer Shammas; Nuclear Medicine, The Hospital for Sick Children, Toronto, Ontario, Canada

Disclosures: All authors have disclosed no financial interests, arrangements or affiliations in the context of this activity.

Purpose or Case Report: In paediatric nuclear medicine the majority of the scans require intravenous (IV) access to deliver the radiotracers. Children and parents often cite procedural pain as the most distressing part of their child's hospitalization. In our department, various pain management strategies including physical and psychological distraction methods and pharmacological intervention have been implemented for the reduction of procedural pain. The purpose of this study was to evaluate and compare different pain reduction strategies used in the paediatric Nuclear Medicine department.
Methods & Materials: The chart of 155 children (85 female) were reviewed retrospectively. Patients were categorized into 4 groups of 1. Maxiline (topical liposomal lidocaine) (n=17), 2. Pain Ease (vapocoolant) (n=71), 3. oral sucrose (n=48), and 4. no pharmacological intervention (n=19). Physical and psychological distraction were used in all patients. Therefore, group 4 only received physical and psychological strategies. Physical methods included supportive positioning, deep breathing, temperature considerations, massage Pressure or vibration and neonatal development strategies (e.g. non-nutritive sucking, facilitated tucking, swaddling, rocking). Psychological strategies included education, distraction with movies, books or storytelling, relaxation techniques. The pain perceived by the children after the IV access were compared in these 4 groups. Two types of pain assessment were used in this study: 1- Self reporting pain scale, and behavioural observational pain rating scale. Pain was reported on a scale 1 to 10. The average pain was also compared between patients who had one or two, and those who had more than two attempts for IV access.
Results: The average pain score was relatively low in all 4 groups (Maxiline=2.8, pain ease=2.1, sucrose=2.7, and no pharmacology=3.4). There was no statistically significant difference between the 4 groups. In particular, although the average pain was slightly more in patients who didn't receive pharmacological intervention, it was not statistically significant. The average pain was 2.2 with one or two attempts, and 4.8 with

more than two attempts.
Conclusions: Physical and psychological distraction methods are useful to reduce the pain in paediatric patients who cannot receive pharmacological intervention.

Poster #: SCI-066

Evaluation of 3 Tesla Lung Magnetic Resonance Imaging in children with Allergic Bronchopulmonary Aspergillosis: Pilot Study

Kushaljit S. Sodhi, MD, PhD, FICR[1], *sodhiks@gmail.com*; Pankaj Gupta[1], Akshay Saxena[1], Joseph Mathew[2], Ritesh Agarwal[1]; [1]Radiodiagnosis & Imaging, Pgimer,Chandigarh, Chandigarh, India, [2]Pgimer, Chandigarh, India

Disclosures: Ritesh Agarwal: Consultant, Honoraria: Pulmatrix Inc., USA, Research: Cipla, India. All other authors have disclosed no financial interests, arrangements or affiliations in the context of this activity.

Purpose or Case Report: To evaluate the diagnostic performance of 3 Tesla lung magnetic resonance imaging (MRI) in children with allergic bronchopulmonary aspergillosis (ABPA).
Methods & Materials: This study protocol was approved by the institutional ethics committee and written informed consent was obtained from parents/ guardians. From October 2015 to January 2018, we prospectively evaluated twenty-seven consecutive children with ABPA. The diagnosis of ABPA was made on the ISHAM-ABPA working group criteria. High resolution computed tomography (HRCT) and 3T MRI of the chest was performed on the same day. Bronchiectasis, consolidation, nodules, and mucus impaction were assessed in all segments. The sensitivity, specificity, positive predictive value (PPV) and negative predictive value (NPV) of MRI were calculated using HRCT findings as the reference standard. Interobserver agreement was calculated using the kappa statistic.
Results: The mean age of the patients was 9.89 years (range: 5–16 years). There were 20 males and 7 females. The sensitivity, specificity, PPV, and NPV for bronchiectasis was 68%, 100%, 100% and 71.43% respectively. The sensitivity, specificity, PPV, and NPV for consolidation was 80%, 100%, 100% and 96% respectively. For detection of nodules, the sensitivity, specificity, PPV, and NPV was 75%, 100%, 100% and 88.46% respectively. There was 100% sensitivity, specificity, PPV and NPV for mucus impaction. There was a high degree of interobserver agreement for MRI findings (k=0.9-1) as well as agreement (k=0.7-1) between CT and MRI for all the four findings.
Conclusions: With the currently available routine MR sequences, MRI demonstrates high specificity but less sensitivity and negative predictive value to HRCT scan in children with ABPA. Newer MR sequences need to be explored and validated to enhance the potential of lung MRI in ABPA.

Poster #: SCI-067

Diagnostic accuracy of ultrasound for identifying metastatic cervical adenopathy in pediatric patients with differentiated thyroid carcinoma at presentation

Mara Navallas Irujo, MD, *maria.navallasirujo@sickkids.ca*; Alan Daneman, Afsaneh Amirabadi, Jonathan Wasserman; Hospital for Sick Children, Toronto, Ontario, Canada

Disclosures: All authors have disclosed no financial interests, arrangements or affiliations in the context of this activity.

Purpose or Case Report: To evaluate the diagnostic accuracy of US and the most useful sonographic features for diagnosing metastatic cervical adenopathy in pediatric patients with thyroid carcinoma
Methods & Materials: IRB-approved retrospective study in a tertiary children's hospital. Eligiblity for inclusion were all consecutive children with pathologically proven thyroid carcinoma from 2008 to 2017. Patients with no preoperative US or no resected lymph nodes were excluded. Pathology report of lymphadenopathy was used as the gold standard. Size, shape, echotexture and vascularity of the lymph nodes were analyzed and compared to the pathology findings
Results: We reviewed preoperative US and histology reports of resected lymph nodes in 52 children with proven thyroid carcinoma (33F,19M; age range 5-18y; mean 13y). Metastatic cervical lymph node disease was documented on US in 29 children and on histology in 33. Sensitivity of US was 79%, specificity 84%, PPV 90%, NPV 70% and accuracy 81%. A significant association was seen between round shape, echotexture, vascularity and lymph node histology. The measurements in short axis for the metastatic nodes was significantly higher than benign nodes (U=168.5,P=0.005, Mann-Whitney U test). No significant difference was noted between the groups in long axis. Logistic regression Univariate analysis showed that round shape (OR=0.054,95%CI=0.006–0.466), echotexture (OR=0.048,95%CI=0.01-0.234), vascularity (OR=0.025,95%CI=0.003–0.225) and short axis measurement (OR=1.473,95%CI=1.019–2.130) contribute significantly to make a positive diagnosis. Multiple logistic regression analysis showed only vascularity contributed significantly to explain the disease probability when adjusting for the other variables. Importantly, 11 patients (38% of children with metastatic disease documented on US) had US diagnosis of abnormal lymph nodes based solely on abnormal echogenicity and vascularity, with normal size and shape
Conclusions: Neck US showed high accuracy, sensitivity and specificity for identifying malignant adenopathy in children with thyroid carcinoma. Most of the abnormal lymph nodes were round in shape and had abnormal echogenicity and vascularity. However, this paper emphasizes that metastatic nodes may be normal in size and shape and the abnormality may be based solely on abnormal echogenicity and vascularity. Size, particularly long axis measurement, is not a reliable criterion to differentiate between malignant and benign lymph nodes. This has not been reported previously in pediatrics

Poster #: SCI-068

Prospective Comparison of MRI and Enhanced MDCT for Evaluation of Pediatric Pulmonary Hydatid Disease: Added Diagnostic Value of MRI

Kushaljit S. Sodhi, MD, PhD, FICR[1], *sodhiks@gmail.com*; Anmol Bhatia[1], Joseph Mathew[1], Ram Samujh[1], Edward Lee, MD, MPH[2]; [1]Radiodiagnosis & Imaging, Pgimer,Chandigarh, Chandigarh, India, [2]Boston Children Hospital, Boston, MA

Disclosures: All authors have disclosed no financial interests, arrangements or affiliations in the context of this activity.
Purpose or Case Report: To prospectively investigate the diagnostic accuracy and added value of lung MRI for evaluating pulmonary hydatid disease in children by comparing MRI findings with MDCT findings.
Methods & Materials: 28 consecutive children with clinically suspected of having pulmonary hydatid disease were enrolled in this prospective research study from October, 2012 to July, 2018. In all 28 pediatric patients (24 boys, 4 girls; mean age, 8.93 +/- 3.1 years; range, 5 to 17) were included in this study, MRI without contrast and enhanced MDCT of the chest were performed within 48 hours of each other. Two pediatric radiologists independently evaluated the lungs for the presence

of consolidation, nodule, and mass (solid versus cyst). Cyst was further evaluated for the presence of fluid, air, and internal membrane. The accuracy of MRI and MDCT for detecting pulmonary hydatid disease was obtained and compared between them. Interobserver agreement was measured with the kappa coefficient.
Results: Final diagnosis of pulmonary hydatid cyst was established in 25 children. Post-surgical histopathological confirmation was available in 12/25 patients (48%), while a positive hydatid serology was confirmed in 8/25 patients (32%). Remaining five patients (20%) were diagnosed to have pulmonary hydatid cyst based on the epidemiological setting and typical radiological findings. The accuracy of MRI and MDCT for detecting pulmonary hydatid cyst was 92.86%. There was no difference between MRI and MDCT for accurately detecting pulmonary hydatid cyst ($p < 0.001$). Internal membranes were detected in 11/28 patients (39.28%) with MRI and 3/28 patients (10.71%) with MDCT. Almost perfect interobserver agreement was present between two independent reviewers ($k = 1$).
Conclusions: Lung MRI without contrast is comparable to enhanced MDCT for accurately detecting lung cyst in pediatric patients with pulmonary hydatid disease. However, MRI provides an added diagnostic value by demonstrating internal membranes which is specific to pulmonary hydatid disease.

Poster #: SCI-069

Combining chest radiographic findings and genomic scores to improve assessment of disease severity in pediatric community acquired pneumonia (CAP).

Julie C. O'Donovan, MD[1],
julie.odonovan@nationwidechildrens.org; Becky Murray, MD[1], Houchun Hu, PhD[1], Rebecca Wallihan, MD[2], Asuncion Mejias, MD, PhD[2], Octavio Ramilo, MD[2], Rajesh Krishnamurthy[1]; [1]Department of Radiology, Nationwide Children's Hospital, Columbus, OH, [2]Division of Infectious Disease, Nationwide Children's Hospital, Columbus, OH

Disclosures: Asuncion Mejias, MD, PhD: Consultant, Honoraria & Research Grant: Janssen, CME Lectures: Abbvie. **Octavio Ramilo, MD:** Consultant, Honoraria: Merck, Pfizer, Sanofi, Janssen, Research Grants: Janssen. All other authors have disclosed no financial interests, arrangements or affiliations in the context of this activity.

Purpose or Case Report: CAP is a worldwide contributor to morbidity and mortality in children. Radiogenomics is an emerging specialty which correlates imaging features to gene expression to predict disease severity, therapeutic response and clinical outcomes. A genomic score termed Molecular Distance to Health (MDTH) is a biomarker that measures the global transcriptional perturbation in blood and has been shown to correlate with disease severity in pediatric CAP (Wallihan R, Front. Cell. Infect. Microbiol. 2018). This study was undertaken to determine whether abnormalities on chest radiographs correlate with genomic and clinical markers of disease severity.
Methods & Materials: Initial chest radiographs of children (age 2 months - 18 years) admitted to a single institution between February 1, 2011, and May 10, 2012 for CAP were reviewed retrospectively. An experienced pediatric radiologist blinded to the clinical data recorded abnormalities including peribronchial thickening, adenopathy, pleural effusion, and pulmonary opacities (characterized as band-like, streaky, consolidative, round or other). Clinical and laboratory data were collected including length of hospitalization (LOS), days of respiratory support (DOS), days of fever (DOF), blood culture, CBC, procalcitonin, C-reactive protein (CRP), and nasopharyneal/oropharyngeal swabs for viral and bacterial pathogen detection, and whole blood for transcriptional analysis and MDTH calculation. We used chest radiographic findings to classify patients according to clinical variables and the genomic MDTH score. We performed two-tailed unpaired t-test to compare groups stratified by radiological findings.
Results: 144 chest radiographs were reviewed. Patients with pleural effusion (right or left) (n=43, 30%) showed significantly longer LOS, DOS, DOF, CRP and higher MDTH scores (all $p < 0.05$) compared with those patients without pleural effusion (n=101). Likewise, patients with consolidative opacity (air space opacity) (n=82, 57%) showed significantly longer LOS, DOF, and higher MDTH scores (all $p < 0.05$) compared with those patients without a consolidative opacity (n=62).
Conclusions: In a cohort of children hospitalized with CAP, we identified chest radiographic findings that classified patients according to: 1) clinical markers of disease severity and 2) the MDTH genomic score. Combining radiographic and genomic markers should contribute to a more precise clinical disease severity classification in pediatric CAP.

CASE REPORT, EDUCATIONAL AND SCIENTIFIC POSTERS - TECHNOLOGISTS

(T) indicates an Imaging Technologist Program Submission

Poster #: CR-001 (T)

SMA Syndrome: An Obscure but Clinically Relevant Condition

Parker T. Stanley, MHA, BSRST[1],
parker.stanley.us@gmail.com; Charles T. Stanley, BSRT[2]; [1]Ultrasound, VCU Health, Charlottesville, VA, [2]Guerbet LLC, Trenton, NJ

Disclosures: All authors have disclosed no financial interests, arrangements or affiliations in the context of this activity.

Purpose or Case Report: Superior mesenteric artery (SMA) syndrome, or Wilkie's syndrome, is an obscure condition in which an acute angulation between the aorta and SMA leads to compression of the third part of the duodenum. Subsequently, patients typically present with a constellation of gastrointestinal findings that closely resemble small bowel obstruction, early satiety, and anorexia. SMA syndrome is most often observed in the setting of rapid weight loss, wasting conditions, and corrective spinal surgeries, where a decrease in retroperitoneal fat diminishes the cushion between the aorta and SMA, causing vascular compression of the duodenum. Diagnosis of SMA syndrome is one of exclusion and is based on the combination of highly suspicious clinical findings and confirmatory diagnostic imaging evidence of obstruction. Upper GI Fluoroscopy can demonstrate a dilated first and second portion of the duodenum, with compression of the third portion, and delayed passage of contrast past midline. Ultrasound and computed tomography (CT)/magnetic resonance imaging (MRI) enable measurement of the aortomesenteric angle and distance, with normal values ranging from 25-60° and 10-28mm, respectively, and values indicative of SMA syndrome ranging from 6-15° and 2-8mm, respectively.We present a classic case of SMA syndrome in a 15-year-old patient. The patient presented with clinical symptoms consisting of scoliosis, chronic nausea and vomiting, weight loss, and anorexia. The patient then underwent Upper GI Fluoroscopy which demonstrated duodenal dilatation and delayed contrast transit past midline, achieved only after prolonged decubitus and prone positioning. Subsequently, abdominal ultrasound demonstrated an aortomesenteric angle of 10-18° and an aortomesenteric distance of 5 mm. Lastly, abdominal MRI demonstrated an aortomesenteric angle of 15° and an aortomesenteric distance of

3 mm, corroborating the ultrasound findings and confirming the diagnosis of SMA syndrome. The patient was initiated on nutritional support and at most recent follow-up was responding well to conservative treatments.
Conclusions: Knowledge of the imaging findings of this rare disorder can provide early diagnostic capabilities and lead to more effective treatment plans.

Poster #: CR-002 (T)

MRI Non-Contrast Images of the Great Vessels in Pediatric Cardiac Patients

Audrey Bryant, Advanced Medical Imaging Technology, *audrey.bryant@cchmc.org*; Ali Kandil; MRI, Cincinnati Children's Hospital, Ludlow, KY

Disclosures: All authors have disclosed no financial interests, arrangements or affiliations in the context of this activity.

Purpose or Case Report: Gadolinium, a type of MRI contrast is typically used when imaging pediatric cardiac patients. Gadolinium enhances the images to give more clarity to the radiologists when distinguishing normal tissue from abnormal tissue. Further, contrast also allows for better visualization of the great vessels.Gadolinium alters the magnetic properties of nearby water molecules in the tissue. While contrast itself does not alter the tissue composition, it does affect how the scanner takes the picture. Accordingly, images can differ between pre- and post-contrast administration. While IV contrast can be administered safely, it is not without logistic implications and/or risks.MRI contrast can be given to pediatric cardiac patients intravenously, but IV access is oftentimes challenging in pediatric cardiac patients. In an effort to reduce the number of unsuccessful IV attempts and quantity of contrast administered, a novel non-contrast MR sequences is being utilized to better depict the great vessels in these children. If IV access is unsucessful or the patient cannot complete the MRI, this modality is employed to obtain more information on the patient's cardiact vasculature.This purpose of this case report paper is to show the MR imaging when using a non-contrast sequence to identify cardiac vessels in pediatric patients who cannot recieve IV contrast.

Poster #: CR-003 (T)

Scrotal Complication or Inflammation: Case Study of Pediatric Epididymitis

Teela M. Durfee, AAS, *teela13@hotmail.com*; Tara Cielma; Ultrasound, Children's National Medical Center, Silver Spring, MD

Disclosures: All authors have disclosed no financial interests, arrangements or affiliations in the context of this activity.

Purpose or Case Report: Pediatric scrotal ultrasound pathology can be difficult because of the similar presentation of different pathology such as scrotal torsion, epididymitis, inguinal hernia, epididymal appendix torsion, and trauma. Identifying key factors of each condition is paramount to providing a clear diagnostic picture in the setting of an atypical presentation of any pathology.Epididymitis is an inflammatory process precipitated by bacterial or viral infections. Symptoms typically present as increasing scrotal pain with swelling of the epididymis. Depending on degree of severity imaging presentation can mimic other pathology.A 5 year old male transferred to a pediatric facility from an area hospital to assess suspected incarcerated hernia with outside CT and ultrasound images.
Methods & Materials: Outside diagnostic imaging shows complex, hyperemic mass-like structure in the superior aspect of the right scrotal sac with surrounding edema and preserved flow to both testicles.Outside CT exam, upon second read, shows an enlarged, edematous right epididymis and small hydrocele with overlying soft tissue thickening and stranding tissue extending from the right scrotum through the inguinal canal. Examination shows no evidence of hernia or incarceration.
Results: Additional diagnostic sonography imaging demonstrated progression of inflammatory condition within the right scrotal and inguinal area. The right epididymis presented edematous, hyperemic, and heterogenous with surrounding soft tissue edema and scrotal wall thickening. Flow to the right testical was preserved however, the inflammation affected the orientation of the right testical in the scrotal sac.
Conclusions: This case highlights the difficulty in clearly identifying pathology for acute testicular pain in a pediatric patient without known trauma.

Poster #: EDU-001 (T)

EDI: a friendly interactive tool to guide the pediatric health professional in ordering the correct radiograph

Caroline Boileau, Medical Radiation Technologist[1], *caboileau@cheo.on.ca*; Lee Treanor, Medical Student (MS2)[2], Cassandra Kapoor[1], Kerri Highmore, MD[1], Elka Miller, MD[1]; [1]Medical Imaging, CHEO, Ottawa, Ontario, Canada, [2]University of Ottawa, Ottawa, Ontario, Canada

Disclosures: All authors have disclosed no financial interests, arrangements or affiliations in the context of this activity.

Purpose or Case Report: Imaging requisitions are the legal documents that health professionals use to communicate to radiologists and Medical Radiation Technologists (MRT(R)s) the relevant clinical information to guide their requested radiographic examination. Inadequate or incomplete information may have a substantial impact on patient care.Since the implementation of our electronic medical record system, EPIC (Epic Systems Corp.), we have the ability to track the number of errors on requisitions; the most common error is having the incorrect body parts selected or multiple unnecessary exams being ordered. The MRT(R)'s identify these errors and correct the inconsistencies following departmental protocols. Without such vigilance on the MRT(R)'s part, inappropriate radiographs could have been performed and could lead to additional, unnecessary radiation exposure. To help select the most appropriate protocol, educate and guide the health professionals at our hospital, an electronic software tool, "EDI" has been created.**EDI** (**E**xamine the patient, **D**etermine the correct radiograph, **I**nput the order with pertinent and relevant clinical information) is an interactive tool that includes the exam protocol with the associated views per body part. Each exam also includes EDI with the field of view that will be exposed to radiation during the exam.Our goal is that EDI will serve health professionals to better understand what order needs to be selected in the electronic system and which radiographs will be provided. Ultimately, this will reduce any unnecessary exams and reduce pediatric radiation exposure.

Poster #: EDU-002 (T)

Non-contrast MRA to decrease gadolinium-based contrast agent administration in children and young adults

Kathleen A. Rendon, A.A.S., *kathyhorn123@yahoo.com*; Cynthia K. Rigsby, MD; Medical Imaging , Ann and Robert H. Lurie Chidlren's Hopsital of Chicago, Chicago, IL

Disclosures: All authors have disclosed no financial interests, arrangements or affiliations in the context of this activity.

Purpose or Case Report: Purpose: The long-term effects from gadolinium tissue deposition in organs and the brain is unknown especially in children who may need repeated contrast studies for necessary follow-up of cardiovascular abnormalities. We aim to show the utility of a non-contrast MRA sequence in older children and young adults undergoing chest and/or abdominal MRA.
Methods & Materials: Methods: We retrospectively review the utility of non-contrast navigator-triggered and ECG-gated 3D steady-state free precession (SSFP) imaging of the chest and abdomen generally acquired in the coronal plane performed for evaluation of cardiovascular abnormalities.
Results: Results: When acquired during diastole to limit the amount of turbulent flow, non-contrast 3D SSFP imaging is successful in all patients who are able to remain still with regular breathing rates. The studies are diagnostic in over 90% of all older children and young adults with non-diagnostic imaging only occurring when there is substantial flow turbulence related to vascular or valve stenosis. The pulmonary veins are also occasionally not well visualized. There can be substantial artifact in younger children. A contrast-enhanced study should be performed following a non-diagnostic non-contrast study which will occur in a small percentage of older children and young adult patients.
Conclusions: Conclusions: Gadolinium based contrast can be eliminated for most chest and abdomen MRA studies in older children and young adults.

Poster #: EDU-003 (T)

Bowel Sonography: Technical approach and challenging diagnoses

Tara Cielma[1], *tcielma@cnmc.org*; Teela Durfee[1], Dorothy Bulas, MD[1], Judyta Loomis, MD[1], Adebunmi Adeyiga[2], Anjum Bandarkar[2]; [1]Children's National Medical Center, Washington, DC, [2]Mid-Atlantic Permanente Medical Group, Rockville, MD

Disclosures: All authors have disclosed no financial interests, arrangements or affiliations in the context of this activity.

Purpose or Case Report: Bowel ultrasound is a critical component of gastrointestinal evaluation. Serial examination allows real-time assessment of disease progression or improvement, and assists the clinician in therapeutic decision making and clinical management.The goals of this exhibit are:1. Describe the technical approach of performing bowel ultrasound.2. Review tips, and up to date technology that assist in optimizing studies.3. Discuss sonographic appearance of various pathologies.4. Review future potential techniques and applications including utility of Doppler flow and contrast enhanced ultrasound.
Methods & Materials: Bowel ultrasound studies at our institute were reviewed retrospectively with selected representative cases chosen to illustrate technical aspects and clinical indications for this procedure. Correlation was made with follow up radiology studies, clinical and/or surgical outcomes.Necrotizing enterocolitis, inflammatory bowel disease, infectious colitis, neutropenic enterocolitis, malrotation, short bowel syndrome, appendicitis, intussusception, Meckel's diverticulitis, intestinal polyp, vascular malformations, graft versus host disease, intestinal hemorrhage, perforation, and obstruction will be discussed.
Results: Typical findings in normal and abnormal pediatric bowel exams will be illustrated. Emphasis on appropriate technique and methodology for serial examinations will be described.
Conclusions: Through this exhibit, participants will learn to utilize bowel ultrasound as a powerful tool in evaluating pediatric gastrointestinal diseases and understand how to optimize their technique.

Poster #: EDU-004 (T)

Abdominal distention in a Newborn: Is it NEC?

Libby Schneeman, *dorfeld@email.chop.edu*; Asef Khwaja, MD, Glenn Bloom, AS, RDMS, Hansel J. Otero, MD; Children's Hospital of Philadelphia, Clayton, NJ

Disclosures: All authors have disclosed no financial interests, arrangements or affiliations in the context of this activity.

Purpose or Case Report: Ultrasound has become a powerful tool for the evaluation of bowel pathology in the children. In the newborn, ultrasound (US) can be used to diagnose, stage, and follow up necrotizing enterocolitis (NEC) and its complication. US has excellent sensitivity and specificity for the identification of bowel wall thickening, peristalsis, pneumatosis, portal venous gas and free air and has become an integral evaluation tool for the newborn with abdominal distention. Our educational poster will:1. Summarize proper US equipment, technique and protocol for diagnosing and following up NEC2. Discuss advantages and benefits of incorporating US in the evaluation of bowel in newborns3. Illustrate the sonographic findings of mild, moderate and severe NEC through cases
Methods & Materials: Pictorial review of US findings of NEC including grayscale and color Doppler. Comparison is made to similar findings in radiographs and clinical correlation.
Results: The spectrum of normal and abnormal neonatal bowel US findings are presented. Abnormal findings are presented using illustrative cases.
Conclusions: Ultrasound is a powerful tool that supplements and at times can replaced more traditional diagnostic methods in the assessment of NEC. This educational exhibit provides a practical guide for systematic evaluation of bowel in the newborn and how to diagnose, stage and follow up NEC and its complications.

Poster #: EDU-005 (T)

Reliable Projectile Hazard Reduction in MRI

Katherine Bushur, BSRS RT(R)(MR), MRSO (MRSC™), *katherine.bushur@childrenscolorado.org*; MRI, Children's Hospital Colorado, Aurora, CO

Disclosures: All authors have disclosed no financial interests, arrangements or affiliations in the context of this activity.

Purpose or Case Report: In 2016, we focused on MRI safety and the inherent cultural barriers to reduce the risk of undetected or misplaced metal objects causing MRI accidents. We successfully addressed this opportunity using a coordinated approach with Patient Safety, Performance Improvement and Radiology Leadership to provide a multi-faceted solution.Despite implementation of ferromagnetic detection systems (FMDS) technology, numerous gaps in screening effectiveness were identified. Three primary improvement objectives were established involving place, people and process leading to 42 new practice changes that were implemented, and 68 existing process improvements instituted. Alarm fatigue was one among many identified risks. Variables included the physical location of the projectile on the transport person, as well as the horizontal or vertical orientation of potential hazard while being carried were identified during a series of nine standardized PDSA testing sessions that were completed in the clinical setting.

Methods & Materials: A series of ten standardized PDSA testing sessions were completed in the clinical setting and included the use of a *pre-screened* ferrous-free person who transported a "control" projectile through the FMDS at separate intervals. The control consisted of either a 4.5" straight scissors or a 5" curved forceps divided into two groups; exposed and non-exposed. All controls were deemed a "projectile hazard", according to the ASTM deflection test (Ref).
Results: Significant gaps in effectiveness and programmatic variables were identified within the expected performance of the FMDS installed. With the current settings and modifications made, we discovered a gap that exists at the center region of each door passageway where detection was minimal.Through our project, 42 new practice changes were implemented and 68 existing process improvements were achieved. A 78% reduction in alarm rates was achieved and a 100% reduction of incidents where hazardous projectiles entered zone IV was realized. These reductions were achieved via optimization and customization of the latest FMDS technology and various process changes and improvements.

Conclusions: Institutions where these devices have been installed may not be able to reliably detect metallic objects classified as projectile hazards. Validation of installed systems can and should be accomplished in order to optimize the level of sensitivity and effectiveness of each FMDS installed *in situ*.

Poster #: EDU-006 (T): *Withdrawn*

Poster #: EDU-007 (T)

Challenges of Pediatric DEXA

Melissa Goehner, *melissa.goehner@choa.org*; Mary E. Anderson, Associates of Applied Science, Monica C. Pinson, B.S, CNMT, Stephen Simoneaux; Diagnostic Radiology, Children's Healthcare of Atlanta, Stone Mountain, GA

Disclosures: All authors have disclosed no financial interests, arrangements or affiliations in the context of this activity.

Purpose or Case Report: To describe and discuss some of the challenges of performing DEXA scans on pediatric patients including positioning, technical obstacles, reference data and post-processing and describing how to overcome some of these challenges.1. Positioning: Many patients with syndromes, have scoliosis, para or quadriplegia, or contractures that make placing the patient on the table difficult. In these patients, imaging has to be adapted to the patients' abilities and some components may need to be eliminated. With cerebral palsy and muscular dystrophy for example, the whole body and AP spine might have to be deferred and only a hip and forearm obtained.2. Technical obstacles: There are many technical obstacles that can present challenges when performing DEXA scans on pediatric patients. Patients who have prostheses or metal rods present technical obstacles. There is no way to remove the metal artifacts in a whole body scan on these patients, so a hip or forearm might be the most accurate way to obtain the patient's bone density due to this technical factor.3. Reference Data: The reference data for pediatrics is limited in national data bases. For example, a total Z-score will not be factored for children under the age of 5 because there is not enough information in the national database for comparison. There is also not enough information on children of certain ethnicities. This presents a problem when diagnosing and treating children with abnormal bone density.4. Post-processing could be different for each user. It can also be different for machines manufactured by different companies. For example, a machine made by Hologic might produce different numbers than a machine made by General Electric. Also, if the user does not place the post-processing tools the exact same way the prior user did, the results can vary.Overcoming some of these challenges has presented opportunities to grow. Sedation is used for children who may not be able to be perfectly still for a Dexa and positioning tools help on some of the more challenging patients. Learning how to work around prostheses and working with the ordering physicians and radiologists with the limited amount of reference data are a few ways of growing from these challenges. Placement of post-processing tools are the key to providing key information in comparing Dexa scans for patients who have them regularly for evaluations. Staff Education is the largest challenge to overcome.

Poster #: EDU-008 (T)

Optimization of PET/MR Scan Protocol With Introduction of a 3D T2 Dixon Sequence

Elad Nevo, MS, RT(MR)(N)(CT), CNMT, *Nevoe@email.chop.edu*; Lisa States, Ralph Magee, RT(R)(MR)(CT); Children's Hospital of Philadelphia, Philadelphia, PA

Disclosures: All authors have disclosed no financial interests, arrangements or affiliations in the context of this activity.

Purpose or Case Report: PET/MRI is a relatively new imaging modality whose efficacy is still being determined. One of the major draws to PET/MR over PET/CT is the reduction in radiation exposure to patients. This is especially desirable in the pediatric population due to the likelihood of multiple exposures during their lifetime, and the increased sensitivity they have to radiation. A typical whole body PET/CT exam can take about 30 minutes, whereas a typical whole body PET/MR exam takes about 90 minutes at our institution. The introduction of a new 3D T2 Dixon technique sequence for PET/MR has the potential of decreasing total scan time significantly, however maintaining current image quality and diagnostic value is critical. Our objective is to test out this new sequence to see whether scan times are reduced and if it is a viable diagnostic replacement for our current T2 sequence.

Poster #: EDU-009 (T)

Discussion over speed stitching in the pediatric world

Amal Baida, *amal.baida@choa.org*; Stephen Simoneaux; Children's Healthcare of Atlanta, Duluth, GA

Disclosures: All authors have disclosed no financial interests, arrangements or affiliations in the context of this activity.

Purpose or Case Report: The purpose of this study is to outline the benefit of speed stitching and recognize it as one of the best stitching tools available for the pediatric population. Looking at the history of stitching, we started by using the CR for scoliosis and long bones stitching. The time of exposure, the radiation dose, and image quality were not optimal. Moving to automatic DR stitching was a good step in the right direction. However, there was still a frustration from having to repeat so many exams because of the high possibility of motion captured between exporsures. That's when speed stich came to play with fast acquisation and less operator interference while doing the exam.
Methods & Materials: Recognizing the challenges of doing scoliosis or long film stitching in the pediatric world led us to start this conversation. Motion and exposure factors were big topics.CR's low bone resolution has been posing a challenge with the risk of overexposure; DR's auto stitching brought the fast image acquisition with better quality and high volume capacity, still posing some issues with manual stitching and the overlap of vertebras. Discussions were conducted on several

scoliosis and example cases were identified. Most importantly, the accuracy of the images for optimum diagnosis was our priority at CHOA. Speed stitching was identified as a solution for many of the inefficiencies in other technologies. With Speed stitching, we were able to reduce a scoliosis exam from 15 minutes to about 4 minutes with lower radiation and better quality.
Results: A case- based education for speed stitch vs other ways of stitching was developed and comparison cases with other methods of stitching were demonstrating for comparison and contrast. Reviews by the radiologists determine the advantages of speed stich and full transition to that technology is in process for the whole system at CHOA.
Conclusions: Beside the higher initial cost, using speed stitch was faster. It demonstrated better image quality, less dose and better accuracy.Technologists moving from CR/DR to speed stitch had no challenges or issues learning the new technology. Mostly everyone thought it was more efficient and easier to use.

Poster #: EDU-010 (T)

An Imaging Technologist's Guide to Artificial Intelligence

Parker T. Stanley, MHA, BSRST[1], **Charles T. Stanley, BSRT[2]**, *ctstan@gmail.com*; [1]Ultrasound, VCU Health, Charlottesville, VA, [2]Guerbet LLC, Trenton, NJ

Disclosures: All authors have disclosed no financial interests, arrangements or affiliations in the context of this activity.

Purpose or Case Report: In 2017, roughly 2 trillion (2,000,000,000,000) medical images were produced, reviewed, reported, archived, and used in the detection and management of disease. Based on historical trends, this number has doubled every 5 years and is accelerating. This explosive growth in imaging data has created major opportunities for the use of Artificial Intelligence (AI). The question is less whether radiologists, and technologists, will be replaced by AI (they will not) and more about whether we could survive without AI. Although intelligent algorithms have been used for some time in segments of the imaging field, new methods of machine learning, based particularly on “deep learning”, are much more powerful. Many of the deep learning publications today point to the promise of significant advances in efficiency, precision, reproducibility, and prognostic abilities.If AI will not replace radiologists/technologists but rather augment them with tools to meet the rising demands for diagnostic imaging, then it is imperative that we have a basic understanding of the concepts and language that defines this area of knowledge. In the not so distant past the average technologist understood the basics of film processing but wouldn’t even recognize the words DICOM or EMR; we are now at that point of change with AI. Deep learning, machine learning, neural networks, ground truth, the list goes on. The goal of this presentation is to provide a basic framework of the concepts, terminology, and references to how AI has, and likely, will be employed in medical imaging, thus making us better practitioners and partners with this technology.

Poster #: EDU-011 (T)

What is a Pediatric Trigger Thumb?

Falguni Patel, Associates,*fpatel0807@yahoo.com*; Medical Imaging (Ultrasound), Lurie Children's Hospital of Chicago, Chicago, IL

Disclosures: All authors have disclosed no financial interests, arrangements or affiliations in the context of this activity.

Purpose or Case Report: My purpose is to teach my audience about a congenital condition called Pediatric Trigger Thumb. My educational poster will include anatomy, causes, and symptoms associated with Trigger thumb and a pediatric ultrasound case that relate with a finding of Trigger thumb.
Methods & Materials: 3 years old girl presented as an outpatient with a history of bump or nodule to the base of her Left thumb for about a year. The ultrasound of left thumb was order to rule out the nodule and any structure anomaly.
Results: Musculoskeletal ultrasound of the left thumb was performed using Musculoskeletal (MSK) superficial setting. The series of longitudinal and transverse images were documented of the nodule area. Based on the sonographic evaluation of the palmar base of the left thumb demonstrated a well-defined ovoid predominantly hypoechoic lesion superficial to the flexor pollicis longus tendon (FPL). The lesion measures 6x1x5mm without vascularity on the color Doppler ultrasound. It did not exert mass effect on the underlying tendon but definitely demonstrated A1 pulley thickening. Dynamic scanning during passive flexion and extension showed difficult tendon gliding underneath the abnormal A1 pulley. This may represent the condition called Pediatric Trigger thumb.
Conclusions: In conclusion, Ultrasound should be an initial imaging study of choice for condition such as pediatric trigger thumb. Ultrasound can show varying degrees of flexor pollicis longus(FPL) tendinosis with a distinct nodule, A1 pulley thickening, and tenosynovitis. With ultrasound dynamic scanning is so beneficial to rule our Trigger thumb. Even color Doppler ultrasound plays a huge role in evaluating hyper vascularity in the region of the pulley and surrounding soft tissues. Thus, Ultrasound plays an important role in diagnosis congenital condition such as Pediatric Trigger thumb.

Poster #: EDU-012 (T)

Importance of medical imaging and radiographic findings in skeletal manifestations of Langerhans Cell Histiocytosis

Ewelina Ulikowska,*eulikowska@luriechildrens.org*; Medical Imaging, Ann and Robert Lurie Childresn Hospital , Des Plaines, IL

Disclosures: All authors have disclosed no financial interests, arrangements or affiliations in the context of this activity.

Purpose or Case Report: Langerhans Cell Histiocytosis (LCH), is a disorder that primarily affects children, but can affect individuals of all ages. Langerhans cells are cells that are responsible for regulating immune system in our bodies. They are mostly found in the skin, spleen, lymph nodes, liver and bone marrow. In patients who have LCH, these cells grow and multiply excessively. The abnormal growth of the Langerhans cells causes a formation of tumors called granulomas. LCH can affect different areas of the body: skin, nails, lymph nodes, gastrointestinal tract, central nervous system, pituitary and thyroid gland, liver, lungs and bones. The severity and symptoms of the disease vary in individual patients and are dependent on the organs and systems affected. Oftentimes, LCH can be found in multiple areas of the body and when that happens, the disease becomes a multisystem disease. The most common system affected by LCH, seen in about 80 % of individuals affected, is the skeletal system. Granulomas, which develop most commonly in the flat bones such as skull and long bones of arms and legs, cause sclerotic and lytic lesions that can in turn become the cause of pathologic fractures. Therefore it is crucial, to recognize the radiographic signs of skeletal manifestations of LCH. Radiography is the preliminary imaging of choice and skeletal surveys are oftentimes the best assessment of the status of LCH prior and post treatment. The purpose of this abstract is to describe radiographic appearances associated with Langerhans Cell

Histiocytosis. In order to confirm the importance of follow up skeletal surveys, I will present cases and associated radiographs that show signs of LCH prior to treatment and post treatment.

Poster #: EDU-013 (T)

Imaging Juvenile Idiopathic Arthritis with Ultrasound

Parker T. Stanley, MHA, BSRST[1], *parker.stanley.us@gmail.com*; Erika Rubesova, MD[2]; [1]Virginia Commonwealth University Health, Charlottesville, VA, [2]Lucile Packard Children's Hospital, Palo Alto, CA

Disclosures: All authors have disclosed no financial interests, arrangements or affiliations in the context of this activity.

Purpose or Case Report: Introduction: Juvenile Idiopathic Arthritis (JIA) is the most common rheumatic entity in children and the second most common cause of musculoskeletal symptoms in pediatric patients. Treatment of JIA largely depends on frequently managing inflammation within the joints, and as such, ultrasound is a prime imaging modality that can be used for detection and monitoring of inflammation. Ultrasound is more sensitive than plain films in the early detection of JIA, and ultrasound is more sensitive than clinical examinations alone. As a low-cost, high-resolution imaging modality, ultrasound allows visualization of the joint spaces, can be used to detect joint effusions, and can monitor synovial proliferation and joint hyperemia, all while not exposing the patient to radiation. We will present ultrasound images of various joints in children such as knees, ankles, wrists, hands and feet. Ultrasound technique, imaging planes, choice of probes frequencies and ultrasound settings are analyzed for optimization of the images. This presentation will highlight the diagnostic imaging findings of JIA on ultrasound, such the presence of joint effusions, synovial proliferation, capsular thickening, tendinitis as well as provide information on common pitfalls associated with age-specific appearances of pediatric musculoskeletal structures on ultrasound. Familiarity with JIA and musculoskeletal ultrasound findings will allow timely diagnosis and implementation of appropriate treatment strategies.

Poster #: EDU-014 (T)

Ultrasound Utilization to Measure Spinal Lengthening with Magnetic Expansion Control (MAGEC System)

Allison Lombardi, Associates*,lombardia1@email.chop.edu*; Children's Hospital of Philadelphia, Philadelphia, PA

Disclosures: All authors have disclosed no financial interests, arrangements or affiliations in the context of this activity.

Purpose or Case Report: The MAGEC System is a surgical treatment for children with severe spinal deformities. The system utilizes surgically implanted rods, which are periodically extended by an External Remote Control (ERC). The traditional method to measure lengthening progression involved radiation exposure. Ultrasound provides an immediate evaluation with no bio-effects. Additionally, soft tissue changes incurred by rod implantation can be seen, which is difficult to assess with a radiograph. The sonographer acquires both pre- and post-lengthening measurements before and after the ERC is applied to the child's skin at the level of the rods. The entire process can be completed in minutes within a single outpatient room, for the ease of both patient and parent.
Methods & Materials: Children with scoliosis too severe for bracing or casting and too young for spinal fusion, have been traditionally managed with growing rods. This involves repeated surgical elongation, often requiring ten or more surgeries before the child reaches skeletal maturity.MAGEC rods require initial implantation surgery and are expanded with the use of an externally applied ERC. The sonographer scans each rod, measuring the pre-lengthening measurement. The physician utilizes the ERC to externally manipulate the MAGEC rods. The sonographer scans the child again, and can determine if the rods have been sufficiently extended. Additional ERC applications, if necessary, can then be employed.
Results: Ultrasound has proven to be a useful tool in the measurement of MAGEC rod extension in patients with severe spinal deformities. It can easily be performed within the examination room in conjunction with the application of the ERC.
Conclusions: The use of ultrasound to measure the lengthening of MAGEC rods minimizes radiation exposure, decreases the need for repeated surgeries, and allows for soft tissue evaluation. It streamlines the process of obtaining measurements and can be utilized in one room within an outpatient setting, simplifying the encounter for patient and family.

Poster #: EDU-015 (T)

Dynamic Sonographic Evaluation of the Glenohumeral Joint in Children with Brachial Plexus Birth Injury (BPBI) – A Practical Approach

Marcy L. Hutchinson, AS[1], *hutchinsonm@email.chop.edu*; Brandi Kozak, BSDI[1], Victor Ho-Fung, MD[1], Nancy Chauvin, MD[2]; [1]Children's Hospital of Philadelphia, Philadelphia, PA, [2]Penn State Hersey Radiology, Hersey, PA

Disclosures: All authors have disclosed no financial interests, arrangements or affiliations in the context of this activity.

Purpose or Case Report: **Background:**Sonographic techniques are simple and safe. The utility and clinical value of dynamic sonographic evaluation of the glenohumeral joint in infants with brachial plexus injury (BPBI) has been described since the late 1990's. However, this technique remains an underutilized tool in most imaging practices. Brachial plexus injury during the birthing process can lead to glenoid dysplasia, posterior shoulder subluxation and significant morbidity if left untreated. Imaging evaluation of the degree of deformity is paramount to guide clinical treatment and the follow-up of complicated cases. Imaging techniques include MRI, CT and US. Shoulder ultrasound provides a dynamic, noninvasive method of evaluation. It has also been our experience that this imaging technique can be mastered by the Sonographer and supported with accurate interpretation by the Radiologist.**Purpose:**Describe the imaging features of glenohumeral joint dysplasia due to BPBI with emphasis on ultrasound technique.Review step-by-step dynamic sonographic evaluation of the glenohumeral joint in BPBI with emphasis on correct positioning of the patient to ensure consistency and reproducible quality imaging.Improve both confidence and independent evaluation of patients through this presentation by the sonographer.
Methods & Materials: Proper technique will be demonstrated utilizing multiplanar dynamic imaging techniques performed with high frequency linear transducers. Tips for proper patient positioning in the abducted and adducted shoulder positions will be included. The normal glenohumeral joint anatomy will be shown as well as cases of varying degrees of shoulder dysplasia.
Results: Knowledge of proper patient positioning and imaging planes is crucial in order to accurately evaluate for pathology. With proper technique, ultrasound can evaluate the severity of shoulder dysplasia and help guide treatment.
Conclusions: Dynamic ultrasound can be used successfully to evaluate the infant shoulder for evaluation of BPBI. The

techniques can be mastered by a sonographer and radiologist in the setting of clear concise practical techniques, resulting in broader scopes of practice.

Poster #: EDU-016 (T)

Imaging of Pediatric Airways: You Might Get Winded, Take a Deep Breath First

Kathleen Ksiazek, Bachelor's of Science
kksiazek@luriechildrens.org; Medical Imaging, Ann & Robert H. Lurie Children's Hospital of Chicago, Chicago, IL

Disclosures: All authors have disclosed no financial interests, arrangements or affiliations in the context of this activity.

Purpose or Case Report: Medical imaging of the soft tissue of the neck or airway is one of the most common, and sometimes challenging, exams performed at a pediatric hospital. Imaging of the airway can help identify enlarged adenoids, the presence of a foreign body, an abscess, pathology or anatomical abnormality. It is crucial to understand the proper technique, breathing instructions and positioning in order to obtain optimal imaging for correct diagnosis. Different radiographic findings will be presented with examples of incorrect positioning, grid usage, exposure factors, artifacts and ways to improve the image quality. This poster will also provide technologists with tips and recommendations to help them to feel prepared and confident to work with all pediatric patients.

Poster #: EDU-017 (T)

DXA! DXA!! Read All About It!!!

Sara Turner, Associates of Applied Science, Radiography, *saturner@childrensnational.org*; Radiology, Children's National Medical Center, Frederick, MD

Disclosures: All authors have disclosed no financial interests, arrangements or affiliations in the context of this activity.

Purpose or Case Report: The goal of this presentation is to provide a review of the important role Dual Energy X-ray Absorptiometry (DXA) plays in treating pediatric patients with low bone density. It also aims to educate on the different DXA machines used today, give a review of the official positions for pediatric DXA scans determined by the International Society for Clinical Densitometry (ISCD), give a brief history of the lateral distal femur (LDF) scan and why it was developed, and touch on the other modalities that can be used to asses bone density..Osteoporosis is commonly thought of as an adult bone health issue; however recently it has gained more attention as being an issue for pediatric patients. Different factors affect bone health, such as genetics and family history, diet and exercise, certain medications, and whether a patient is ambulatory or non-ambulatory. It is important to conduct the proper testing to determine a patient's fracture risk and trying to prevent further bone deterioration. A DXA Scan is the gold standard across all age groups in providing vital bone health information as it provides a look into the body with minimal radiation exposure to evaluate the bones to determine how much at risk a patient may be.
Methods & Materials: We will look at examples of properly positioned scans and what the results can look like. We will also look at the difference between ambulatory and non-ambulatory lateral distal femurs scans and compare the Z-Scores of those scans.

Poster #: EDU-018 (T)

Transcranial Doppler – How to successfully perform an optimal TCD on our younger patient demographic (ages 2-5 years)

Brandi Kozak, BSDI,*kozakb@email.chop.edu*; Ultrasound, Children's Hospital of Philadelphia, Philadelphia, PA

Disclosures: All authors have disclosed no financial interests, arrangements or affiliations in the context of this activity.

Purpose or Case Report: Transcranial Doppler examinations are crucial in the care and treatment of patients in the Sickle cell population. The earlier we are able to obtain diagnostic studies on these patients the more effective treatment is and can reduce the risk of the patient suffering from a life altering stroke.
Methods & Materials: This procedure while not invasive can be very frightening for a younger patient. We employ several different techniques and distractions tools to help the patient cope soundly through the exam. We work closely with the Hematology department staff and have developed a TCD task force specifically focused for this age group to increase our success rate. Some of the strategies we employ are as follows: arranging the ultrasound room so that the patient is able to view the television to watch a favorite show or program, letting the child play games on smart phones or tablets (without too much patient movement), having a parent or guardian lying with or holding the patient, sitting the patient up slightly, blowing bubbles, singing, having hand held musical or light up toys available and/or arranging to have a child life specialist present for the duration of the exam to help distract the patient. We have also produced a short informational video for new patients to view prior to coming to their first TCD exam so they can see what to expect.
Results: By having several options in place and available, by planning ahead and having resilient, dedicated sonographers we are able to successfully perform TCDs on younger and younger patients thereby facilitating more positive outcomes for this patient population.
Conclusions: Transcranial Doppler ultrasound is a low cost, easy to perform with dedicated practice, portable, radiation-free modality that with set parameters in place can be extremely successful in imaging younger patients. This exam gives immediate, important information to the Hematologist that will improve long term outcomes in the Sickle cell population.

Poster #: EDU-019 (T)

Pediatric Considerations for Y-90 TARE

Joseph MacLean, MHA, CNMT,
joseph.maclean@cchmc.org; Nuclear Medicine, Cincinnati Children's Hospital Medical Center, Cincinnati, OH

Disclosures: All authors have disclosed no financial interests, arrangements or affiliations in the context of this activity.

Purpose or Case Report: To communicate important information to technologists about the challenges associated with performing Y-90 transarterial radio embolization (TARE) therapy on pediatric patients. This "how to" poster will include discussion of: coordination of services, pre-treatment Tc-99m MAA mapping, preparing the dose calibrator for accurate measurement of Y-90 activity, ideal hot lab set-up for dose preparation, and imaging options for post Y-90 therapy scanning.

Poster #: SCI-001 (T)

Analyzing the Effects of Giraffe Beds on Radiation Dose during Neonatal Digital Radiography

Jesse Green, *jesse.green@choa.org*; Nikki Butler, BMSc, RT(R)(QM), Kimberly M. Riegert, BS, Stephen Simoneaux; Children's Healthcare of Atlanta, Atlanta, GA

Disclosures: All authors have disclosed no financial interests, arrangements or affiliations in the context of this activity.

Purpose or Case Report: To compare the radiation doses that result from different digital radiography imaging methods on neonatal patients in Giraffe Beds using phantom imaging and radiation measurement devices. The lowest dose options will be considered to design an imaging process.
Methods & Materials: Using technical factors of 0.63 mAs and 60 kVp as a constant, test images were taken on a phantom in a Giraffe Bed using the following methods:1) Cassette placed in the bed tray and image taken with the hood down at 40" SID (Source-to-Image Distance)2) Cassette placed directly under phantom on bed mattress (not in tray) and image taken with the hood down at 40" SID3) Cassette placed in the bed tray and image taken with the hood up at 36.5" SID4) Cassette placed directly under phantom on bed mattress (not in tray) and image taken with the hood up at 32" SID5) Cassette placed directly under phantom on bed mattress (not in tray) and image taken with the hood down at 32" SIDFor each imaging method, the radiation dose and EI (Exposure Index) number were recorded.
Results: The range of radiation dose recorded was 2.045-4.163 mR. The range of EI numbers collected was 78-318. The results of the above methods are as follows:1. 2.045 mR, 78 EI2) 2.146 mR, 121 EI; 2.153 mR, 122 EI3) 3.874 mR, 99 mR; 3.941 mR, 101 EI4) 4.107 mR, 192 EI; 4.163 mR, 1915) 3.629 mR, 318 EIThe radiolucent bed hood caused a decrease of approximately 13% of the radiation reaching the image detector. Utilizing the imaging tray in the Giraffe Bed caused a decrease of approximately 5% of the radiation reaching the image detector. Images taken at the shortest SID resulted in the highest doses and least optimal EI numbers as anticipated. Please note Image 1 had an inconsistant EI measurement.
Conclusions: During the study**,** varying the SID had the most significant impact on radiation doses and EI numbers compared to the other factors caused by the Giraffe Bed. The maximum SID allowed when the bed hood is raised is only 32" which produces higher radiation doses and EI numbers compared to imaging through the bed hood in the down position at a greater SID. When designing an imaging process, the primary consideration should compensate for a greater SID to reduce the radiation dose and EI number. Imaging at a greater SID also allows the technologist to select a wider range of technical factors and avoid over exposure of the smallest neonatal patients.

Poster #: SCI-002 (T)

Anesthesiology Challenges in MRI

Chris Harris, RT[1], *harrisc_57@hotmail.com*; Elizabeth Drum[2]; [1]Radiology, Childrens National Medical Center, Philadelphia, PA, [2]Children's Hospital of Philadelphia, Philadelphia, PA

Disclosures: All authors have disclosed no financial interests, arrangements or affiliations in the context of this activity.

Purpose or Case Report: Anesthesiologists face challenges in practicing in locations outside of the operating room. In particular when working in the MRI environment there may be unfamiliarity of the physiologic monitors and other equipment, MRI safety policies and procedures, limited access to expected equipment or additional anesthesia providers, unsure imaging protocols and positions as well as inability to rescue patients in the MRI scanner room.
Methods & Materials: Radiology must also understand how lengthy or unpredictable imaging times, positioning, and monitoring and equipment issues challenges anesthesia providers as they care for patients in the MR environment.Therefore anesthesiology and radiology must recognize possible risk factors while caring for patients in MRI and they must familiarize themselves with policies and procedures of both departments to ensure safe practice for the anesthetized children.
Results: To understand the risk of both anesthetizing patients and the risk MR safety, radiology and anesthesiology must partner to form a structure where anesthesiology, radiology and nursing collaborate to ensure that the needs for patient safety and the needs of MRI are met but ensuing that the priorities are first to the patient, next to the enterprise and third to the individual departments and division in order to provide the safest environment for our patients.The structure has two committees:**Radiology, Anesthesia and Sedation (RAS) Committee** and is an active working group to improve patient care and flow with ongoing initiatives that utilize appropriate metrics to measure improvement. Issues that cannot be solved in committee are escalated to the Operational Governance Oversight Committee.**Operational Governance Oversight Committee (meets quarterly):** Provides oversight to ensure that the needs of all constituents are considered and met to the best degree possible. Overriding priorities are first to the patient, next to the enterprise, and third to the individual departments and divisionsChairs from Anesthesiology, Pediatrics, Radiology, Chief Operating Officer, Chief Nursing Officer
Conclusions: The MRI environment can be challenging to anesthesiologists as they care for patients outside of their usual environment. Collaboration between both radiology and anesthesiology can improve the experience and safety of anesthetized patient during MRI exams.

2019 AUTHOR INDEX BY ABSTRACT

C

H

L

M

N

O

S

T

U

2019 KEYWORD INDEX BY ABSTRACT

Q

R

U

V